

Marijuana and Cannabinoid Research

Methods and Protocols

Edited by

Emmanuel S. Onaivi, PhD



Marijuana and Cannabinoid Research

METHODS IN MOLECULAR MEDICINE™

John M. Walker, SERIES EDITOR

125. **Myeloid Leukemia: Methods and Protocols**, edited by Harry Iland, Mark Hertzberg, and Paula Marlton, 2006
124. **Magnetic Resonance Imaging: Methods and Biological Applications**, edited by Pottumarthi V. Prasad, 2006
123. **Marijuana and Cannabinoid Research: Methods and Protocols**, edited by Emmanuel S. Onaivi, 2006
122. **Placenta Research Methods and Protocols: Volume 2**, edited by Michael J. Soares and Joan S. Hunt, 2006
121. **Placenta Research Methods and Protocols: Volume 1**, edited by Michael J. Soares and Joan S. Hunt, 2006
120. **Breast Cancer Research Protocols**, edited by Susan A. Brooks and Adrian Harris, 2006
119. **Human Papillomaviruses: Methods and Protocols**, edited by Clare Davy and John Doorbar, 2005
118. **Antifungal Agents: Methods and Protocols**, edited by Erika J. Ernst and P. David Rogers, 2005
117. **Fibrosis Research: Methods and Protocols**, edited by John Varga, David A. Brenner, and Sem H. Phan, 2005
116. **Interferon Methods and Protocols**, edited by Daniel J. J. Carr, 2005
115. **Lymphoma: Methods and Protocols**, edited by Timothy Illidge and Peter W. M. Johnson, 2005
114. **Microarrays in Clinical Diagnostics**, edited by Thomas O. Joos and Paolo Fortina, 2005
113. **Multiple Myeloma: Methods and Protocols**, edited by Ross D. Brown and P. Joy Ho, 2005
112. **Molecular Cardiology: Methods and Protocols**, edited by Zhongjie Sun, 2005
111. **Chemosensitivity: Volume 2, In Vivo Models, Imaging, and Molecular Regulators**, edited by Rosalyn D. Blumethal, 2005
110. **Chemosensitivity: Volume 1, In Vitro Assays**, edited by Rosalyn D. Blumethal, 2005
109. **Adoptive Immunotherapy: Methods and Protocols**, edited by Burkhard Ludewig and Matthias W. Hoffman, 2005
108. **Hypertension: Methods and Protocols**, edited by Jérôme P. Fennell and Andrew H. Baker, 2005
107. **Human Cell Culture Protocols, Second Edition**, edited by Joanna Picot, 2005
106. **Antisense Therapeutics, Second Edition**, edited by M. Ian Phillips, 2005
105. **Developmental Hematopoiesis: Methods and Protocols**, edited by Margaret H. Baron, 2005
104. **Stroke Genomics: Methods and Reviews**, edited by Simon J. Read and David Virley, 2004
103. **Pancreatic Cancer: Methods and Protocols**, edited by Gloria H. Su, 2004
102. **Autoimmunity: Methods and Protocols**, edited by Andras Perl, 2004
101. **Cartilage and Osteoarthritis: Volume 2, Structure and In Vivo Analysis**, edited by Frédéric De Ceuninck, Massimo Sabatini, and Philippe Pastoureau, 2004
100. **Cartilage and Osteoarthritis: Volume 1, Cellular and Molecular Tools**, edited by Massimo Sabatini, Philippe Pastoureau, and Frédéric De Ceuninck, 2004
99. **Pain Research: Methods and Protocols**, edited by David Z. Luo, 2004
98. **Tumor Necrosis Factor: Methods and Protocols**, edited by Angelo Corti and Pietro Ghezzi, 2004
97. **Molecular Diagnosis of Cancer: Methods and Protocols, Second Edition**, edited by Joseph E. Roulston and John M. S. Bartlett, 2004
96. **Hepatitis B and D Protocols: Volume 2, Immunology, Model Systems, and Clinical Studies**, edited by Robert K. Hamatake and Johnson Y. N. Lau, 2004
95. **Hepatitis B and D Protocols: Volume 1, Detection, Genotypes, and Characterization**, edited by Robert K. Hamatake and Johnson Y. N. Lau, 2004
94. **Molecular Diagnosis of Infectious Diseases, Second Edition**, edited by Jochen Decker and Udo Reischl, 2004
93. **Anticoagulants, Antiplatelets, and Thrombolytics**, edited by Shaker A. Mousa, 2004
92. **Molecular Diagnosis of Genetic Diseases, Second Edition**, edited by Rob Elles and Roger Mountford, 2004
91. **Pediatric Hematology: Methods and Protocols**, edited by Nicholas J. Goulden and Colin G. Steward, 2003
90. **Suicide Gene Therapy: Methods and Reviews**, edited by Caroline J. Springer, 2004
89. **The Blood–Brain Barrier: Biology and Research Protocols**, edited by Sukriti Nag, 2003
88. **Cancer Cell Culture: Methods and Protocols**, edited by Simon P. Langdon, 2003
87. **Vaccine Protocols, Second Edition**, edited by Andrew Robinson, Michael J. Hudson, and Martin P. Cranage, 2003
86. **Renal Disease: Techniques and Protocols**, edited by Michael S. Gligorsky, 2003

METHODS IN MOLECULAR MEDICINE™

Marijuana and Cannabinoid Research

Methods and Protocols

Edited by

Emmanuel S. Onaivi, PhD

*Department of Biology
William Paterson University, Wayne, NJ*

HUMANA PRESS  TOTOWA, NEW JERSEY

© 2006 Humana Press Inc.
999 Riverview Drive, Suite 208
Totowa, New Jersey 07512

www.humanapress.com

All rights reserved.

No part of this book may be reproduced, stored in a retrieval system, or transmitted in any form or by any means, electronic, mechanical, photocopying, microfilming, recording, or otherwise without written permission from the Publisher. Methods in Molecular Medicine™ is a trademark of The Humana Press Inc.

All papers, comments, opinions, conclusions, or recommendations are those of the author(s), and do not necessarily reflect the views of the publisher.

This publication is printed on acid-free paper. 
ANSI Z39.48-1984 (American Standards Institute) Permanence of Paper for Printed Library Materials.

Production Editor: Robin B. Weisberg

Cover design by Patricia F. Cleary.

Cover illustrations from (background) Fig. 2, Chapter 5, "Morphometric Study on Cytoskeletal Components of Neuronal and Astroglial Cells After a Chronic CB₁ Agonist Treatment," by Patricia Tagliaferro, Alberto J. Ramos, Emmanuel S. Onaivi, Sergio G. Evrard, Maite Duhalde Vega, and Alicia Brusco; (foreground) Figs. 1 and 2, Chapter 1, "Molecular Neurobiological Methods in Marijuana-Cannabinoid Research," by George R. Uhl, Hiroki Ishiguro, Emmanuel S. Onaivi, Zhicheng Lin, B. Emmanuel Akinshola, Bruce Hope, Claire M. Leonard, and Qing-Rong Liu.

Photocopy Authorization Policy:

Authorization to photocopy items for internal or personal use, or the internal or personal use of specific clients, is granted by Humana Press Inc., provided that the base fee of US \$30.00 per copy is paid directly to the Copyright Clearance Center at 222 Rosewood Drive, Danvers, MA 01923. For those organizations that have been granted a photocopy license from the CCC, a separate system of payment has been arranged and is acceptable to Humana Press Inc. The fee code for users of the Transactional Reporting Service is: [1-58829-350-5/06 \$30.00].

Printed in the United States of America. 10 9 8 7 6 5 4 3 2 1

eISBN: 1-59259-999-0

ISSN: 1543-1894

Library of Congress Cataloging-in-Publication Data

Marijuana and cannabinoid research : methods and protocols / edited by Emmanuel S. Onaivi.

p. cm. -- (Methods in molecular medicine ; 123)

ISBN 1-58829-350-5 (alk. paper)

1. Cannabinoids--Laboratory manuals. 2. Marijuana--Laboratory manuals.

I. Onaivi, Emmanuel S. II. Series.

QP801.C27M35 2005

615'.7827--dc22

200546133

Dedication



*To Dr. Patricia Tagliaferro for her unwavering love, companionship,
and support throughout the preparation of this book.*

Preface

Marijuana has remained one of the most widely used and abused drugs in the world. Research on the biological basis of the effects of marijuana, and therefore its usefulness as medicine, may have been hampered by several decades of irrational prejudice and also by the lack of specific molecular tools and technology. But the discovery of specific genes coding for cannabinoid receptors (CBRs) that are activated by smoking marijuana, and that the human body and brain makes its own marijuana-like substances called endocannabinoids that also activate CBRs, has transformed marijuana–cannabinoid research into mainstream science. An overwhelming body of scientific evidence now indicates the existence of an elaborate, and previously unknown but ubiquitous, endocannabinoid physiological control system (EPCS) whose fundamental role in human development, health, and disease is unfolding. This system appears to exert a powerful modulatory action on retrograde signaling associated with cannabinoid inhibition of synaptic transmission. The promiscuous action and distribution of CBRs in most biological systems provides the EPCS limitless signaling capabilities of crosstalk within, and possibly between, receptor families that may explain the numerous behavioral effects associated with smoking marijuana. Advances in marijuana–cannabinoid research have already resolved the issue that marijuana use can be addicting in vulnerable individuals and that a missense in human fatty acid amide hydrolase, which inactivates endocannabinoids (anandamide) and related lipids, is associated with drug and alcohol dependence problems. These and other remarkable advances in understanding the biological actions of marijuana and cannabinoids have provided a much richer than previously appreciated cannabinoid genomics and raised a number of critical issues on the molecular mechanisms of cannabinoid-induced behavioral and biochemical alterations. Although these advances have enhanced our understanding of the molecular mechanisms associated with the behavioral effects of marijuana use, the molecular identity of other cannabinoid receptor subtypes and transporters (if any), along with the growing number of endocannabinoids, will allow specific therapeutic targeting of different components of the EPCS in health and disease.

The major focus of marijuana–cannabinoid research is to develop better understanding of the seemingly limitless signaling capabilities and endless complexity of the EPCS in the human body and brain with the expectation that new knowledge will contribute to elucidating this naturally occurring regulatory mechanism in health and disease. The primary goal of *Marijuana and*

Cannabinoid Research: Methods and Protocols is to provide experimental protocols for scientists interested in marijuana–cannabinoid research from genes to behavior. Although the effects of marijuana use and its medicinal applications may be influenced by multiple genetic factors, the role of environmental factors in the behavioral and psychological effects should not be overlooked, although these may be difficult to replicate in animal models. Nevertheless, animal models are widely used to study the physiological and behavioral correlates of human disorders. Of course, where applicable, humans have been used to study the biochemical, physiological, and behavioral effects of marijuana–cannabinoids as documented here.

The methods and protocols found useful in marijuana research are described here by experts using their specialized techniques to resolve issues from genes to behavior: the molecular neurobiology methods we present outline analysis of the structure, polymorphisms, molecular genomic, and expression studies of the CB1r gene and haplotypes, and the association with polysubstance abuse. Other chapters describe methods to study the role of CBrs in immune function, to localize cannabinoid receptors in different systems, to study morphometric cytoskeletal components of neuronal and astroglial cells after cannabinoid treatment, to visualize cannabinoid effects using brain slice imaging and electrophysiological approaches, to assay anandamide hydrolysis and transport in synaptosomes, to conduct CBr and stimulated [^{35}S]GTP γ S binding to membrane homogenates or intact cultured cells, to assay cannabinoids using the mouse-isolated vas deferens, to design and synthesize cannabinoids and endocannabinoids, and to study in vitro and in vivo effects of cannabinoids in animals including humans. It is difficult to include all the relevant techniques and expanding interests in the recent explosion of new knowledge in marijuana–cannabinoid research. A number of the methodologies described here will find application far beyond marijuana–cannabinoid research and may be extended to studying mental and neurological disorders, especially because the EPCS is intricately involved in almost all the biological processes of the human body and brain. We embrace with euphoria and excitement the current explosion of new information from marijuana–cannabinoid research in the hope that it will unravel the specific mechanisms of marijuana–cannabinoid actions, which are of potentially central importance in biology and therapeutics. *Marijuana and Cannabinoid Research: Methods and Protocols* should whet our appetites for further groundbreaking research that will lead to deeper understanding of these interesting genes, their variants, and roles in the vulnerability to addictions and other disturbances caused by deficiencies in the endocannabinoid physiological control system.

Emmanuel S. Onaivi

Acknowledgments

Many thanks to Dr. John Walker, the editor of the Humana Press *Methods in Molecular Biology* and *Methods in Molecular Medicine* series, for suggesting this book and to the staff at Humana Press for their patience and support throughout the process of this book project. I am indebted to my colleagues in the Biology Department, to Dr. Sandra DeYoung, the Dean of the College of Science and Health, Center for Research, and to William Paterson University's Provost Office for their continuous support and release time. We are also enormously thankful to Mary Pfeiffer, Chief, Library services, National Institute on Drug Abuse-National Institutes of Health for her editorial assistance and patience. Thanks to Doug Hansen for the Dedication photograph.

Emmanuel S. Onaivi

Contents

Dedication	v
Preface	vii
Acknowledgments	ix
Contributors	xiii
1 Molecular Neurobiological Methods in Marijuana–Cannabinoid Research <i>George R. Uhl, Hiroki Ishiguro, Emmanuel S. Onaivi, Ping-Wu Zhang, B. Emmanuel Akinshola, Zhicheng Lin, Bruce Hope, Claire M. Leonard, and Qing-Rong Liu</i>	1
2 Experimental Methods to Study the Role of the Peripheral Cannabinoid Receptor in Immune Function <i>Nancy E. Buckley, Diep Burbridge, Manop Buranapramest, Tanya Ferguson, and Renee Y. Paau</i>	19
3 Localization of Cannabinoid Receptors Using Immunoperoxidase Methods <i>Guy A. Cabral</i>	41
4 Localization of Cannabinoid CB ₁ Receptor mRNA Using Ribonucleotide Probes: <i>Methods for Double- and Single-Label In Situ Hybridization</i> <i>Andrea G. Hohmann</i>	71
5 Morphometric Study on Cytoskeletal Components of Neuronal and Astroglial Cells After a Chronic CB ₁ Agonist Treatment <i>Patricia Tagliaferro, Alberto J. Ramos, Emmanuel S. Onaivi, Sergio G. Evrard, Maite Duhalde Vega, and Alicia Brusco</i>	91
6 Visualizing Cannabinoid Effects Using Brain Slice Imaging and Electrophysiological Approaches <i>Alexander F. Hoffman and Carl R. Lupica</i>	105
7 Methods for the Synthesis of Cannabinergic Ligands <i>Ganesh A. Thakur, Spyros P. Nikas, Richard I. Duclos, Jr., and Alexandros Makriyannis</i>	113
8 Cannabinoid Receptor Binding to Membrane Homogenates and Cannabinoid-Stimulated [³⁵ S]GTPγS Binding to Membrane Homogenates or Intact Cultured Cells <i>Chris Breivogel</i>	149

9	Methods to Assay Anandamide Hydrolysis and Transport in Synaptosomes Filomena Fezza, Natalia Battista, Monica Bari, and Mauro Maccarrone	163
10	Methods Evaluating Cannabinoid and Endocannabinoid Effects on Gastrointestinal Functions Nissar A. Darmani	169
11	The Bioassay of Cannabinoids Using the Mouse Isolated Vas Deferens Adèle Thomas and Roger G. Pertwee	191
12	Assessment of Cannabis Craving Using the Marijuana Craving Questionnaire Stephen J. Heishman and Edward G. Singleton	209
13	Methods for Studying Acute and Chronic Effects of Marijuana on Human Associative Processes and Memory Robert I. Block	217
14	Methods for Clinical Research Involving Cannabis Administration David A. Gorelick and Stephen J. Heishman	235
15	Neurological Assessments of Marijuana Users Jean Lud Cadet, Karen Bolla, and Ronald I. Herning	255
16	Behavioral Methods in Cannabinoid Research Ester Fride, Alex Perchuk, F. Scott Hall, George R. Uhl, and Emmanuel S. Onaivi	269
17	Methods to Study the Behavioral Effects and Expression of CB ₂ Cannabinoid Receptors and Its Gene Transcripts in Chronic Mild Stress Model of Depression Emmanuel S. Onaivi, Hiroki Ishiguro, Patel Sejal, Paul A. Meozzi, Lester Myers, Patricia Tagliaferro, Bruce Hope, Claire M. Leonard, George R. Uhl, Alicia Brusco, and Eileen Gardner	291
Index	299

Contributors

- B. EMMANUEL AKINSHOLA • *Department of Pharmacology, Howard University College of Medicine, Washington DC*
- NATALIA BATTISTA • *Department of Biomedical Sciences, University of Teramo, Teramo, Italy*
- MONICA BARI • *Department of Experimental Medicine and Biochemical Sciences, University of Rome, "Tor Vergata," Rome, Italy*
- ROBERT I. BLOCK • *Department of Anesthesia, University of Iowa, Iowa City, IA*
- KAREN BOLLA • *Molecular Neuropsychiatry Branch, Intramural Research Program, National Institute on Drug Abuse-National Institutes of Health, Baltimore, MD*
- CHRIS BREIVOGEL • *Department of Pharmaceutical Sciences, Campbell University School of Pharmacy, Buies Creek, NC*
- ALICIA BRUSCO • *Instituto de Biología Celular y Neurociencias, Universidad de Buenos Aires, Buenos Aires, Argentina*
- NANCY E. BUCKLEY • *Biological Sciences Department, California State Polytechnic University, Pomona, CA*
- JEAN LUD CADET • *Molecular Neuropsychiatry Branch, Intramural Research Program, National Institute on Drug Abuse-National Institutes of Health, Baltimore, MD*
- GUY A. CABRAL • *Department of Microbiology and Immunology, Virginia Commonwealth University, Richmond, VA*
- NISSAR A. DARMANI • *Department of Basic Medical Sciences, College of Osteopathic Medicine of the Pacific, Western University of Health Sciences, Pomona, CA*
- RICHARD I. DUCLOS, JR. • *Center for Drug Discovery, Department of Pharmaceutical Sciences, Northeastern University, Boston, MA*
- SERGIO G. EVRARD • *Instituto de Biología Celular y Neurociencias, Universidad de Buenos Aires, Buenos Aires, Argentina*
- FILOMENA FEZZA • *Department of Experimental Medicine and Biochemical Sciences, University of Rome, "Tor Vergata," Rome, Italy*
- ESTER FRIDE • *Department of Behavioral Sciences and Department of Molecular Biology, College of Judea and Samaria, Ariel, Israel*
- EILEEN GARDNER • *Department of Biology, William Paterson University, Wayne, NJ*

- DAVID A. GORELICK • *Intramural Research Program, National Institute on Drug Abuse-National Institutes of Health, Baltimore, MD*
- F. SCOTT HALL • *Molecular Neurobiology Branch, National Institute on Drug Abuse-National Institutes of Health, Baltimore, MD*
- STEPHEN J. HEISHMAN • *Clinical Pharmacology and Therapeutics Branch, National Institute on Drug Abuse-National Institutes of Health, Baltimore, MD*
- RONALD I. HERNING • *Molecular Neuropsychiatry Branch, Intramural Research Program, National Institute on Drug Abuse-National Institutes of Health, Baltimore, MD*
- ALEXANDER F. HOFFMAN • *Cellular Neurobiology Research Branch, National Institute on Drug Abuse-National Institutes of Health, Baltimore, MD*
- ANDREA G. HOHMANN • *Neuroscience and Behavior Program, Department of Psychology, University of Georgia, Athens, GA*
- BRUCE HOPE • *Behavioral Neuroscience, National Institute on Drug Abuse, National Institutes of Health, Baltimore, MD*
- HIROKI ISHIGURO • *Molecular Neurobiology Branch, National Institute on Drug Abuse-National Institutes of Health, Baltimore, MD*
- CLAIRE M. LEONARD • *Department of Biology, William Paterson University, Wayne, NJ*
- ZHICHENG LIN • *Molecular Neurobiology Branch, National Institute on Drug Abuse-National Institutes of Health, Baltimore, MD*
- QING-RONG LIU • *Molecular Neurobiology Branch, National Institute on Drug Abuse-National Institutes of Health, Baltimore, MD*
- CARL R. LUPICA • *Cellular Neurobiology Research Branch, National Institute on Drug Abuse-National Institutes of Health, Baltimore, MD*
- MAURO MACCARRONE • *Department of Biomedical Sciences, University of Teramo, Teramo, Italy*
- ALEXANDROS MAKRIYANNIS • *Center for Drug Discovery, Department of Pharmaceutical Sciences, Northeastern University, Boston, MA*
- PAUL A. MEOZZI • *Department of Biology, William Paterson University, Wayne, NJ*
- LESTER MYERS • *Department of Biology, William Paterson University, Wayne, NJ*
- S. P. NIKAS • *Center for Drug Discovery, Department of Pharmaceutical Sciences, Northeastern University, Boston, MA*
- EMMANUEL S. ONAIVI • *Department of Biology, William Paterson University, Wayne, NJ and Molecular Neurobiology Branch, National Institute on Drug Abuse-National Institutes of Health, Baltimore, MD*
- ALEX PERCHUK • *Department of Biology, William Paterson University, Wayne, NJ*

ROGER G. PERTWEE • *Institute of Medical Sciences, School of Medical Sciences, University of Aberdeen, Foresterhill, Aberdeen, Scotland UK*

ALBERTO J. RAMOS • *Instituto de Biología Celular y Neurociencias, Universidad de Buenos Aires, Buenos Aires, Argentina*

PATEL SEJAL • *Department of Biology, William Paterson University, Wayne, NJ*

EDWARD G. SINGLETON • *Clinical Pharmacology and Therapeutics Branch, National Institute on Drug Abuse, National Institutes of Health, Baltimore MD*

PATRICIA TAGLIAFERRO • *Cellular Neurophysiology, National Institute on Drug Abuse-National Institutes of Health, Baltimore, MD*

GANESH. A. THAKUR • *Center for Drug Discovery, Department of Pharmaceutical Sciences, Northeastern University, Boston, MA*

ADÈLE THOMAS • *School of Medical Sciences, Institute of Medical Sciences, University of Aberdeen, Foresterhill, Aberdeen AB25 2ZD, Scotland UK*

GEORGE R. UHL • *Molecular Neurobiology Branch, National Institute on Drug Abuse-National Institutes of Health, Baltimore, MD*

MAITE DUHALDE VEGA • *Instituto de Biología Celular y Neurociencias, Universidad de Buenos Aires, Buenos Aires, Argentina*

PING-WU ZHANG • *Molecular Neurobiology Branch, National Institute on Drug Abuse-National Institutes of Health, Baltimore, MD*

Molecular Neurobiological Methods in Marijuana–Cannabinoid Research

George R. Uhl, Hiroki Ishiguro, Emmanuel S. Onaivi, Ping-Wu Zhang,
B. Emmanuel Akinshola, Zhicheng Lin, Bruce Hope, Claire M. Leonard,
and Qing-Rong Liu

Summary

Recent aggregation of evidence for the roles of endogenous agonist and receptor systems that are mimicked or activated by cannabinoid ligands has provided a focus for work that has elucidated details of some of the multiple physiological roles and pharmacological functions that these systems play in brain and peripheral tissues. This chapter reviews some of the approaches to improved elucidation of these systems, with special focus on the human genes that encode cannabinoid receptors and the variants in these receptors that appear likely to contribute to human addiction vulnerabilities.

Key Words: Arachidonic acid; addiction; endocannabinoid; haplotypes; pain; CB1; CB2.

1. Introduction

Research on the molecular and neurobiological basis of the physiological and neurobehavioral effects of marijuana and cannabinoids lagged behind that of other natural addictive products like opium and tobacco because of the lack of specific molecular tools and several decades of irrational prejudice. Now significant and rapid progress has transformed marijuana–cannabinoid research into mainstream science with the cloning of the gene that encodes cannabinoid receptors (CBRs) and generation of cannabinoid knockout mice. Furthermore, these advancements in marijuana and cannabinoid research indicate the existence of a previously unknown, but elaborate and ubiquitous endocannabinoid physiological control system (EPCS) in the human body and brain, the role of which is unfolding. This remarkable progress includes identification of genes encoding CB₁ (1–3), isolation of endocannabinoids (4–8) and entourage lig-

ands (9), and functional identification of transporters and enzymes for the biosynthesis and degradation of these endogenous substances, which thus represent the EPCS (for review, *see* ref. 10). Taken together, the CBr and the endocannabinoids (eCBs) along with the systems involved in their synthesis, uptake (if any), and degradation, form this previously unknown yet ubiquitous complex system. Although the CB₁ receptors are among the most abundant neuromodulatory receptors in the brain, both CB₁ and CB₂ receptors are widely distributed in peripheral tissues, with CB₂ particularly enriched in immune tissues (11,12) and perhaps present in the brain as physiologically needed. Despite this wealth of information and major advances, little information is available at the molecular level about CBr gene structure, regulation, function, and polymorphisms. Consequently, the contribution of CBr genes and how they are regulated in the manifestation of the behavioral and physiological effects is poorly understood. We describe here molecular neurobiological methods applied to study the structure, regulation and some molecular neurobiological actions of marijuana–cannabinoids using *in vitro* and *in vivo* systems.

2. Materials

1. Endocannabinoid ligands.
2. ³H-endocannabinoid.
3. Cos-7 cell line.
4. AM 404.
5. Polymerase chain reaction (PCR) reagents and PCR.
6. Human DNA and cDNA (lymphocyte, brain).
7. Animal brain tissues.
8. Autosequencer (ABI3100, etc.), TaqMan real-time PCR system (ABI 7900).
9. Primers, probes, and restriction enzymes that are unique for single-nucleotide polymorphism (SNP), single-sequence length polymorphism (SSLP) genotyping and for gene-expression study.
10. Primer extension reagents, real-time PCR reagents.
11. H-endocannabinoid, [γ -³²P]ATP, [α -³²P]dCTP.
12. Cos-7, NG108-15, N1E-115, SK-N-SH, and CHO-K1 cell lines.
13. PCR and reverse transcriptase (RT)-PCR, real-time PCR reagents.
14. Human genomic DNA, brain RNA and poly A RNA.
15. Reagents for rapid amplification of cDNA ends (RACE), primer extension, Northern blotting.
16. Dual-luciferase reporter system (Promega, Madison, WI).
17. Other reagents for DNA manipulation, molecular cloning.

3. Methods

The methods described here outline analysis of the structure of the CBr gene, protein expression, molecular genomic and expression studies, polymorphisms, haplotypes, and association with polysubstance abuse.

3.1. Analysis of CB1r Gene and Genetic Variation in Polysubstance Abuse

1. Cannabinoid receptor gene variation in polysubstance abusers can be studied using bioinformatics, resequencing, and other genotyping methods, such as restriction fragment length polymorphism (RFLP), primer extension methods, and/or 5' nuclease assay.
2. Genotyping information is used for further analysis to evaluate haplotype blocks and associations/linkages with the phenotypes.
3. cDNA analysis demonstrates the isoforms, RNA editings, and genetic expression patterns in tissue samples.
4. In addition, in animal studies the expression of CB₁ can be evaluated following drug treatment regimen, e.g., chronic treatment with morphine, and CB₁ gene expression can be analyzed.

3.1.1. Bioinformatics

1. Genomic databases can be accessed from the National Center for Biotechnology Information (NCBI) <http://www.ncbi.nlm.nih.gov/> (open for public access) and Celera database. However Celera database was closed June, 2005.
2. The genomic sequences from bacterial artificial chromosomes (BACs), expressed sequence tags (ESTs), and cDNA sequence of RNA transcript can be aligned to find the genetic variations, as well as the haplotype blocks and epigenetic modifications on RNA.

3.1.2. Human Subjects

1. Polysubstance abusers and controls are collected from research volunteers of each population recruited from the same area. This reduces the risk of stratification problems in each group of subjects. Postmortem brain subjects are obtained from Brain Bank for RNA/cDNA analysis, with careful evaluation for their quality that depend on postmortem interval (PMI), pH and 28S/18S, as well as their age, sex, ethnicity, cause of death, etc.
2. Subjects should be under informed consent agreed upon by the ethics committee of the research institutes.
3. The phenotypes are characterized using quantity-frequency and Diagnostic and Statistical Manual of Mental Disorders (DSM)-III-R, IV, and International Classification of Diseases and Related Health Problems (ICD)-10 criteria obtained from interviews by skilled clinicians.

3.1.3. Resequencing and Genotyping

The genotyping for variations/polymorphisms in the cannabinoid gene of interest can be evaluated by using different methods.

1. Resequencing at region of interest directly shows the sequence variations.
2. Indirect methods for genotyping, RFLP, primer-extension methods (e.g., SnapShot, Applied Biosystems Inc. (ABI), matrix-assisted laser desorption ionization-time of flight (MALDI-TOF), primer extension method to assay allele-

specific expression levels (SEQUENOME), and TaqMan 5' nuclease assay in real-time PCR machine (ABI) are common.

3. Fluorescent-labeled primers are used for PCR, amplifying the region containing single-sequence length polymorphism (SSLP), and PCR product lengths are measured with autosequencing to determine the number of repetitive sequences.

3.1.4. Linkage Study

Linkage studies are performed in family samples that have an inherited pattern of polysubstance abuse phenotype.

1. Linkage studies require the use of SSLP and single nucleotide polymorphism (SNP) markers across the region of the chromosomes.
2. Genotyping data for individuals in families are analyzed with computer linkage software (e.g., GENEHUNTER) to evaluate linkages to chromosomal regions that contribute genetically to polysubstance abuse.

3.1.5. Haplotype Determination

1. Haplotypes can be seen in actual sequences, such as BACs, and in sequences from cloning of PCR products that amplify the region of interest.
2. Haplotype frequencies in a population can be estimated by HAPLOVIEW program and computer programs, such as EH, ASSOCIAT, or Arlequin (<http://lgb.unige.ch/arlequin/>).
3. Maximum-likelihood haplotype frequencies are estimated from the observed data using an expectation-maximization (EM) algorithm and standardized linkage disequilibrium values ($D' = D/D_{\max}$), and D' values are shown as graphic maps (<http://www.well.ox.ac.uk/asthma/GOLD/docs/ldmax.html>) and HAPLOVIEW program.

3.1.6. Association Study of CB1 Gene and Polysubstance Abuse

The fine mapping of the CB₁ gene improves the understanding of CB₁ gene association with polysubstance abuse.

1. Genetic markers are chosen to satisfy the marker(s) in each haplotype.
2. The allelic frequencies between the control and abuser populations are compared.

3.1.7. Statistics

The deviations of genotype frequencies from Hardy-Weinberg values are tested.

The differences in observed allele and genotype frequencies and estimated haplotype frequencies between groups are tested using analogs of Fisher's exact test on 2×2 or $2 \times$ (number of genotypes or haplotypes) contingency tables. p Values of < 0.05 are considered nominally significant.

3.1.8. RNA Analysis

1. Total and poly A⁺ RNAs are extracted from frozen brain regional samples using oligo-dT cellulose (Fastrack, Invitrogen) and RNazol B (Tel-Test Inc., Friendswood, TX).

2. Single-stranded cDNA is synthesized from mRNAs from individuals using oligo-dT priming and Thermoscript reverse transcriptase reactions (Invitrogen, Carlsbad, CA).
3. Allele-specific expression levels can be assessed in two ways. Expression of mRNA and cDNA with different alleles at heterozygote SNPs is assessed using oligonucleotides and TaqMan/real-time PCR 5′ nuclease assays (ABI, Foster City, CA) or the primer extension method (SnapShot, ABI, Foster City, CA and MALDI TOF, Sequenom).
4. C_t values (TaqMan) and peak heights (primer extension) are compared to allelic expression signals from standards constructed by pooling DNA from individuals with known genotypes and normalized allelic ratios are calculated. Comparison of gene expression between individuals may have more variables based on the cause of death, general conditions and medications before death, and overall quality of tissue samples.

3.1.9. Regulation of CB1 by Opiates

1. Selected strains of animals are injected acutely or chronically with 20 mg/kg morphine subcutaneously.
2. For chronic treatment, groups of mice are injected with morphine or saline every day for a week and subgroups of mice are injected morphine or saline on d 8 for acute treatment.
3. Mice are sacrificed 4 h after final injections, and brains are removed immediately to extract RNA or protein.
4. The expression of CB1 RNA can be compared by real-time PCR (TaqMan, ABI) using gene-specific probe and primers. **Figure 1** shows the reduced expression of CB₁ gene transcripts in the striatum, midbrain, and hippocampus following acute and chronic treatment of mice with morphine.

3.2. Microarray Analysis

3.2.1. SNP Genome Scanning

1. Multiplex PCR reactions are performed as 24 separate reactions in 96-well microtiter plates (Affymetrix mapping assay manual).
2. DNA from individuals or pools is amplified in 24 separate reactions containing 6 ng of DNA from each individual and 84 multiplex PCR primer pairs.
3. Primary PCR products are subjected to labeling PCR as described by Affymetrix. The 24 labeled PCR samples corresponding to each genomic DNA sample are then pooled, diluted in hybridization buffer, heated to 95°C, cooled to 4°C, then hybridized with Affymetrix HuSNP GeneChip microarrays at 45°C for 18 h.
4. Arrays are washed with two changes of 6X SSPE/0.01% Triton at 25°C and then with six changes of 4X SSPE/0.01% Triton at 35°C. DNA hybridized to the washed microarrays is stained using 2 µg/mL phycoerythrin-conjugated streptavidin in 6X SSPE, 0.01% Triton, 0.5 mg/mL BSA at 25°C for 30 min. Stained arrays are washed with four changes of 6X SSPE/0.01% Triton at 25°C and then scanned using a GeneArray Laser Scanner (Hewlett Packard).

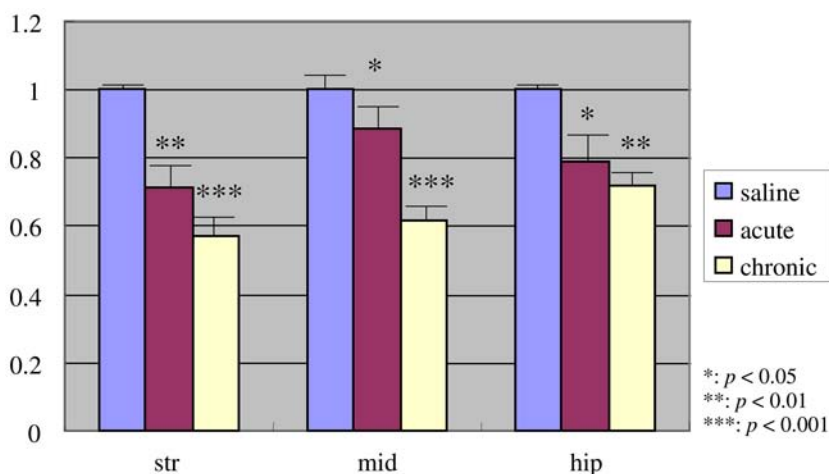


Fig. 1. C57BL/6 mice were acutely treated with 20 mg/kg morphine subcutaneously and separate sub groups treated chronically with either the same dose of morphine daily or saline. Mice were sacrificed 4 h after final injections and the brains quickly dissected to extract RNA for CB₁R gene expression study. The expression of CB₁R RNA was compared by real-time PCR using the gene-specific probe and primers. Acute and chronic treatment with 20 mg/kg morphine produced a reduction in the expression of CB₁R gene transcripts in the striatum (str), midbrain (mid), and hippocampus (hip).

3.2.2. SNP Genome Scanning Analysis

With genotyping, individual DNAs are made using Affymetrix GeneChip software. Allelic frequencies in pooled DNA samples are assessed based on data from the “cell” files and an algorithm averaging the hybridization intensity signals from the 8–16 features per chip that provided perfectly complementary hybridization to the alleles termed A or B for each SNP.

1. The background, determined as the average of the lowest 5% of intensity values on each microarray, is subtracted from the fluorescence intensity of each cell of that microarray.
2. Background-corrected values are normalized by dividing each value by the average of the highest 5% of intensity values on each microarray.
3. Normalized hybridization intensities from the microarray elements that corresponded to the perfect match A and perfect match B alleles for each SNP are each averaged.
4. A/B ratios are determined by dividing average normalized A values by average normalized B values.
5. Arctangent transformations are applied to each ratio to improve combination of data from experiments with different absolute intensity values.

6. Arctan A/B ratios for abusers are then divided by arctan A/B ratios for controls to form an abuser/control ratio, in our primary analysis.
7. Means of three replications for each experiment identified SNPs with abuser/control hybridization ratios in the top and bottom 5% of the distribution for the European-American abuser vs control comparisons.
8. Reproducibility of these “candidate-positive” SNPs was sought by asking if they were also in the upper or lower 7.5% of the distribution of hybridization ratios in data from two replications in African American abuser vs control samples. Physical locations of these reproducibly positive SNPs and of markers linked to alcohol or nicotine dependence in previous studies were sought in Mapviewer build 22 (5/01) and related NCBI programs by two independent investigators. Additional locations were sought in Mapviewer build 24 (9/01).
9. Allele calls from individual DNA samples are also compared to results from pooled DNAs from the same individuals. Regression analyses compared allele frequencies for SNPs in most of the individuals studied ([Fig. 2](#)).
10. Test–retest variability was studied in replicated microarray results from DNA pools prepared in duplicate or triplicate from the same DNA stocks from the same individuals.
11. Results are compared to those expected by chance using Monte Carlo simulations, using the C computer language. For the initial results of SNPs that were positive in both Caucasian and African-American samples, 100,000 Monte Carlo trials were carried out. In each trial, 148 markers (5% + 5% of 1493) were sampled with replacement, and subsequently 222 (7.5% + 7.5% of 1493) were sampled with replacement from the all of the 1493 markers. The number of markers common to both samples were then determined. In only 11 of these trials did we find at least 42 markers in common ($p = 0.00011$).
12. To model the chance probabilities of obtaining positive markers as close to each other as the three closest pairs identified here, we used 1 million simulation trials in which 42 markers were randomly positioned on a 3.2 billion bp genome and pairwise distances between each marker pair were determined.
13. We assessed the number of simulations in which the smallest distance was <0.7 Mbp, the second smallest distance was <1.5 Mbp, and the third smallest distance was <2.2 Mbp (Mapviewer build 22 distances modeled corresponding to build 24 distances are 0.2, 2.8, and 6.6 Mb).
14. To model the chance probabilities of obtaining positive markers as close to markers previously reported to be linked to ethanol or nicotine addiction, we used more than 100 million simulation trials in which 61 markers were randomly positioned on a 3.2 billion bp genome, then 31 markers randomly placed on the same genome and pairwise distances between each marker pair, consisting of one member of the first set and one member of the second set, were determined.
15. We assessed the number of simulations in which at least seven of the distances were <1 Mbp (Mapviewer 22 distances modeled; corresponding build 24 distances are 0, 0.1, 0.4, 0.4, 0.4, 2.3, and 2.7 Mb). Linkage disequilibrium was assessed for data from individual genotypes determined for 20 control subjects using Arlequin.

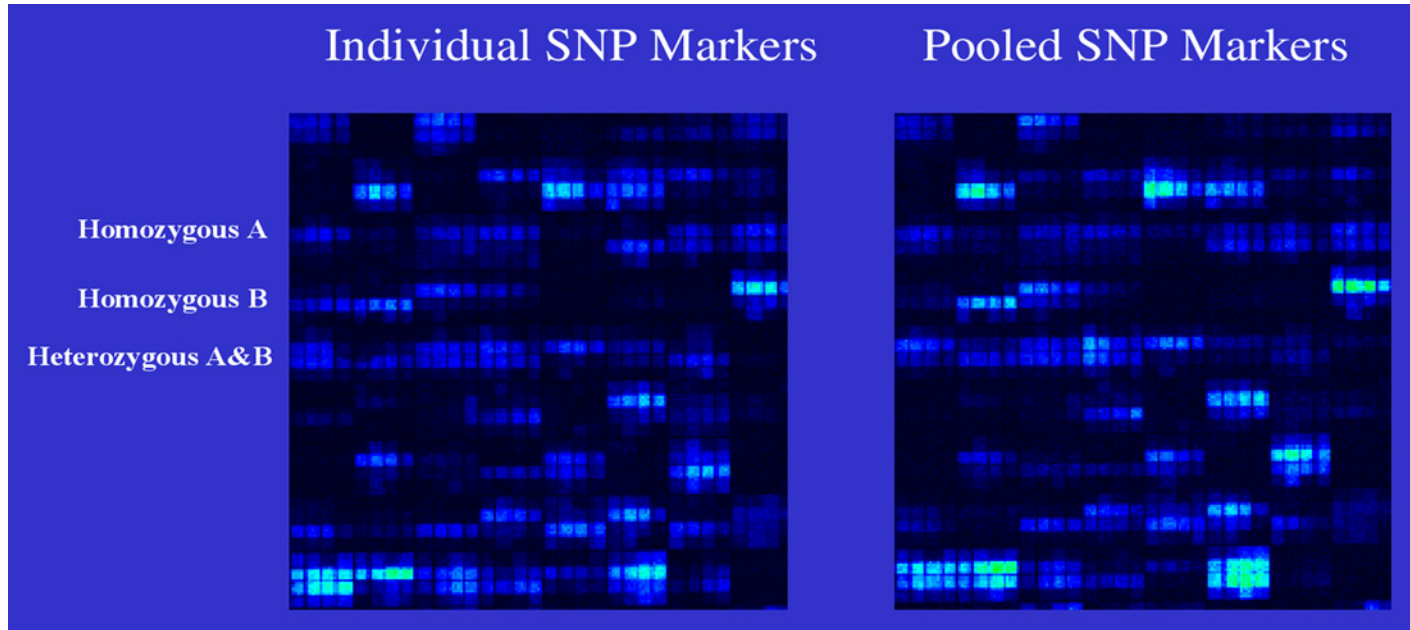


Fig. 2. Hybridization of Affymetrix HuSNP GenChips using biotinylated PCR probes synthesized from individual or pooled DNA samples. A SNP marker is represented by four oligomer “quartets” in which two perfect matches (PM) correspond to allele A and B, respectively, and two mismatches (MM) correspond to homomeric bases of the respective SNP. As shown in the individual SNP markers and pooled SNP markers, individual genotypes could be called according intensities of allele A, B, or AB. Pooled allele frequencies could be derived from intensity ratio of allele A and B using arctangent transformation.

3.2.3. Gene Expression Array

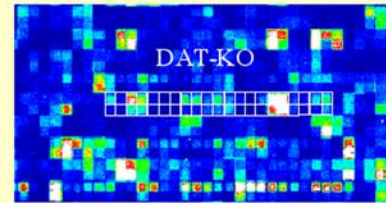
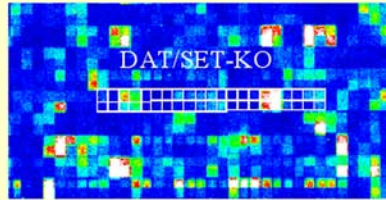
1. Male mice (age: 14–16 wk and weight: 20–30 g) are kept under 12-h light/dark cycle with free access to water and food. A slow-releasing morphine pellet (25 mg) or placebo pellet (25 mg) (NIDA, Rockville, MD) was implanted subcutaneously in each mouse under isofluorene anesthesia. Mice with morphine pellets developed withdrawal syndrome after 4 d. On d 5, mice were sacrificed by cervical dislocation. Mu knockout mice and wild-type littermates in the experiments were described previously. The mouse brain was dissected rapidly and frozen immediately in liquid nitrogen.
2. Total RNA was extracted from mouse whole brain using RNeasy (Qiagen, Valencia, CA) protocol. mRNA was isolated from total RNA using RNeasy (Qiagen, Valencia, CA) protocol.
3. Double-stranded cDNA was synthesized using SuperScript™ Choice System protocol (GIBCO/BRL, Rockville, MD) with (dT)₂₄-T7 primer. In order to amplify cDNA linearly, cRNA probes were transcribed in vitro in the presence of biotin-11-CTP and biotin-16-UTP (Enzo, Farmingdale, NY) using MEGAscript T7 protocol (Ambion, Austin, TX). Biotin-labeled cRNA was purified with RNeasy Mini Kit (Qiagen, Valencia, CA) and fragmented with alkaline to 100–300 bases before hybridization.
4. Mu6500 GeneChips (Affymetrix, Santa Clara, CA) are hybridized with biotin-cRNA overnight at 45°C according to the manufacturer's protocol and stained with R-phycoerythrin conjugated streptavidin (Molecular Probes, Eugene, OR). After wash, Mu6500 chips were scanned with the Hewlett Packard GeneArray Scanner.
5. The expression levels of various genes are analyzed with Affymetrix Microarray Suite 5.0 software. The experiments for chronic morphine treatment and mu knockout mice are repeated independently three times with the Mu6500 GeneChip.
6. The data from Affymetrix analysis were transferred into Microsoft Access database, and the reproducible gene expression changes were extracted by linking data from separate experiments.
7. Hybridization of Affymetrix Mu6500 GenChip using biotinylated cRNA probes synthesized from brain cDNAs of dopamine (DAT) and serotonin (5-HT) transporter gene knockout mice or double (DAT/5-HT) knockout mice is shown in [Fig. 3](#). A gene transcript is represented by matches of 11–16 oligomers. The hybridization intensities of the perfect matches from separate knockout mouse brains are compared as shown.

3.3 Gene Structure and Expression Studies

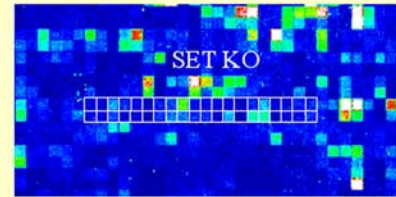
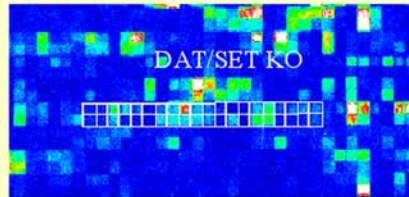
3.3.1. Identification of CB₁ Receptor Novel Exons, mRNA Isoforms and Nested RACE, RT-PCR, and Northern Blotting

1. Database searches reveal sequences of (BAC) clones that provide a genomic contig that includes CB₁ sequences.
2. ESTs with >93% homology with the relevant 80 kb of these BAC clone sequences were also used for CB₁ DNA sequence assemblies.

3.2 fold decrease of androgen regulated gene RP2 in DAT/SET-KO vs DAT-KO



6.0 fold increase of protein tyrosine phosphatase delta in DAT/SET-KO vs SET-KO



5.3 fold increase of single strand CRE-BP/Pur alpha in DAT-KO vs SET-KO

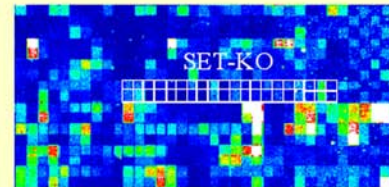
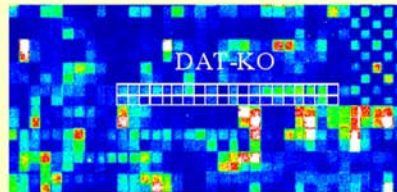


Fig. 3. Hybridization of Affymetrix Mu6500 GenChip using biotinylated cRNA probes synthesized from brain cDNAs of dopamine (DAT) and serotonin (SET) transporter gene knockout mice or double (DAT/SET) knockout mice. A gene transcript is represented by 11–16 oligomers in perfect matches (PM, upper squares) and mismatches (MM, lower squares). The hybridization intensities of the perfect matches from one knockout mouse brain are compared.

3. Two gene-specific reverse primers that corresponded to sequences in the CB1 coding region were used for nested RACE. Product bands were cloned into pCR.2.1-TOPO (Invitrogen, Carlsbad, CA) and sequenced using an ABI capillary sequencing instrument.
4. Single-strand cDNA that was reverse-transcribed from human hippocampal poly A⁺ RNA was used for RT-PCR reactions.
5. Partial RT-PCR products are used as Northern blotting probes. Probes are hybridized to nylon membranes that had been blotted with 40 µg of human brain total RNA or 10 µg of human hippocampal poly A⁺ RNA (Clontech, Palo Alto, CA).
6. After hybridization, membranes are washed twice for 20 min with 0.1X SSC/0.1% SDS at 25°C, rinsed once with water, exposed to phosphoimaging plates, stripped of hybridization probe by boiling in 0.1X SSC/0.1% SDS solution for 5 min, and rehybridized. Blots are hybridized serially with different hybridization probes.

3.3.2. Transcription Start Site and Candidate Promoter Region of CB₁

1. An oligonucleotide complementary to exon 1 sequences was labeled with [γ -³²P]ATP (ICN Biomedicals, CA) and T4 polynucleotide kinase (Invitrogen, Carlsbad, CA) and allowed to hybridize to sequences in 5 µg human hippocampal poly A⁺ RNA.
2. Primer extension was performed as described by the manufacturer (Promega, Madison, WI). Radiolabeled primer extension products were separated using 6% polyacrylamide gels containing 8 M urea and co-electrophoresed size standards and detected by autoradiography.
3. Promoter activities of 5'-flanking regions were analyzed by fusing regions of different lengths to luciferase in pGL3-Enhancer (Promega, Madison, WI) to generate recombinant plasmids.
4. The promoterless negative control (pGL-blank), the positive SV-40 promoter-containing control vector pGL-SV40, and the transfection-efficiency control plasmid pRL-TK are transfected into NG108-15, N1E-115, SK-N-SH cells and CHO-K1 cells, respectively (ATCC, Manassas, VA), grown to 80% confluence in 6-well plates in Dulbecco's modified Eagle medium (DMEM) (Invitrogen, Carlsbad, CA) or F12K (Sigma, Germany) by 18 h, 37°C incubation using SuperFect transfection reagent as described by the manufacturer (Qiagen, Valencia, CA).
5. Cells were incubated for another 48 h to allow expression, then collected, and lysed. Lysate luciferase activities were quantitated using the dual-luciferase

reporter system (Promega, Madison, WI) and TD-20/20 (Turner Designs, Fresno, CA) as described by the manufacturer.

3.3.3 Brain-Region-Specific CB_1 Isoform Expression Pattern Analysis

Human brain RNAs from different region were used as quantitative RT-PCR templates. The ratio between RT-PCR products corresponded to that of isoforms.

3.4. Endocannabinoid Uptake Studies: In Vitro Assay of Endocannabinoid Uptake

1. COS cells (10^7) grown to confluence in flasks in DMEM (Life Technologies, Gaithersburg, MD) containing 10% FCS (Life Technologies) were split 1:2, harvested the next day using trypsin/EDTA, centrifuged (200g) for 10 min at 4°C, washed with sterile HEBS (20 mM HEPES, 137 mM NaCl, 5 mM KCl, 0.7 mM Na_2HPO_4 , and 6 mM dextrose), recentrifuged, and resuspended at 10^7 cells/mL in 4°C HEBS. Then, 0.9 mL of suspended cells was transfected by electroporation at 300 V and 1100 μ F in 400-mm Gene Pulser cuvettes (Bio-Rad) containing 20 μ g of plasmid DNA and 500 μ g of fish sperm DNA (Boehringer-Mannheim, Mannheim, Germany) using a geneZAPPER 450/2500 (IBI, New Haven, CT).
2. The transfected cells were suspended in DMEM, followed by distribution into 6-well plates. Cells were grown for 3 d and then assayed for their abilities to accumulate tritium-labeled anandamide [arachidonyl-5,6,8,9,11,12,14,15- 3H]-, 160 Ci/mmol (New England Nuclear Research Products, Boston, MA).
3. Kinetic and saturation analyses were used to determine K_m , V_{max} values. For uptake assays, 1 nM tritium-labeled anandamide [arachidonyl-5,6,8,9,11,12,14,15- 3H]-, 25 μ Ci (925 kBq), and 0.1, 1, 2, 4, 10, and 20 μ M unlabeled anandamide concentrations were used.
4. COS cells transfected with pcDNA3.1/V7-3 and the vector pcDNA3.1 served as positive and negative controls, respectively. Parallel incubations with 30 μ M of unlabeled anandamide allowed estimation of nonspecific uptake and binding. Uptake assays were carried out for 5 min at 37°C, followed by two washes each with 2 mL of Krebs–Ringer–Henseleit buffer.
5. Cells were solubilized in 0.5 mL of 1% SDS, and radioactivity was determined using a Beckman Instruments (Palo Alto, CA) LS 6000 liquid scintillation counter at approx 50% efficiency. Cells from parallel wells were solubilized in 0.5 mL of 1 N NaOH for protein amount measurements using a Bio-Rad Protein Assay solution (Bio-Rad) (see Fig. 4 and Note 1).

3.5. Immunoblotting of Cannabinoid Receptors

3.5.1. Protein Extraction From Blood or Tissue Samples

1. Blood or tissue samples are obtained for CBr protein determinations from the subjects.

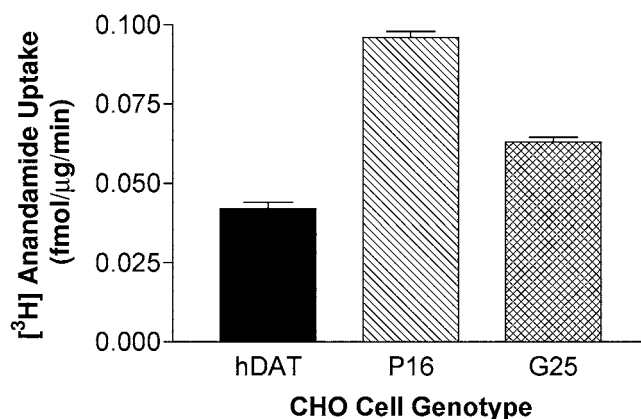


Fig. 4. [³H]Anandamide uptake by CHO cells expressing hDAT (black bar) and two unidentified transporters (P16, slashed bar and G25, hatched bar). Uptake was carried out for 5 min at 37°C in KRH buffer (*see Subheading 3.*). These CHO cells are stable cell lines. Data are mean \pm SEM from three experiments.

2. Two mL of blood or tissue sample was centrifuged at 5000 rpm at 4°C for 5 min and the supernatant discarded.
3. The pellet was resuspended in 400 μ L of lysis buffer containing protease inhibitors and homogenized. After rinsing with 200 μ L lysis buffer into a tube, the homogenate was centrifuged at 15000 rpm at 4°C for 15 min. The supernatant can be aliquoted and stored at -80°C for immunoblotting.
4. Samples are then prepared for immunoblotting using 50 μ L of the homogenate and 2X Laemilli's buffer and boiled for 10 min. After cooling, the mixture was centrifuged at 1500 rpm at 4°C and the supernatant used for Western blotting.

3.5.2. Western Blotting

1. Equal amounts of protein were loaded and separated by 10% SDS-PAGE and then transferred to nitrocellulose. The blots were blocked in freshly prepared PBS containing 3% nonfat milk for 20 min at 20–25°C with constant agitation.
2. After incubation with a rabbit-anti-human CB1 antibody (Calbiochem, Cambridge, MA) for overnight at 4°C, a goat anti-rabbit IgG linked to horseradish peroxidase (Amersham Life Science products, Arlington Heights, IL) was added for an additional 1.5 h.
3. Blots are developed using enhanced chemiluminescence (Amersham Life Science products, Arlington Heights, IL).
4. Films are scanned in Pharmacia LKB Ultrosan XL enhanced laser densitometer and the results reported in relative units. (*See Notes 2 and 3 for additional discussions on localization of CBs and Fig. 5.*)

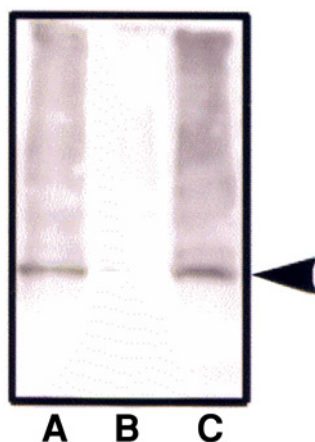


Fig. 5. CB1r immunoblots from whole brains of mice following chronic treatment with vehicle A, metanandamide B (10 mg/kg), and rimonabant C (3 mg/kg). Each lane represents a pooled sample of six mice.

3.6. Modification of Gene Expression in *Xenopus laevis* Oocytes

3.6.1. cRNA Synthesis and Oocyte Expression

Complementary RNAs (cRNAs) are synthesized from corresponding complementary DNAs (cDNAs) coding for the receptor gene of interest such as the glutamate receptor and are individually injected into *Xenopus laevis* oocytes individually or in desired receptor subunit combinations of 16–20 ng per subunit using a microinjector and prepared for electrophysiological recording.

3.6.2. Electrophysiological Recording

1. After detecting receptor expression, oocytes were placed in a 100- μ L recording chamber perfused with modified Barth's solution and voltage-clamped using two microelectrodes at a holding potential of -70 mV.
2. Agonist-activated receptor currents were measured and recorded in response to known agonist concentrations such as 200 μ M kainic acid used to measure AMPA receptor currents in oocytes.
3. Cannabinoids, endocannabinoids, alcohol, and other abused substances of interest are either co-applied or preapplied for a measured period of time such as 30–60 s with a period of about 5 min between applications to allow for drug washout and receptor recovery from desensitization. A schematic illustration of the expression system and electrophysiological recording is presented in [Fig. 6](#).

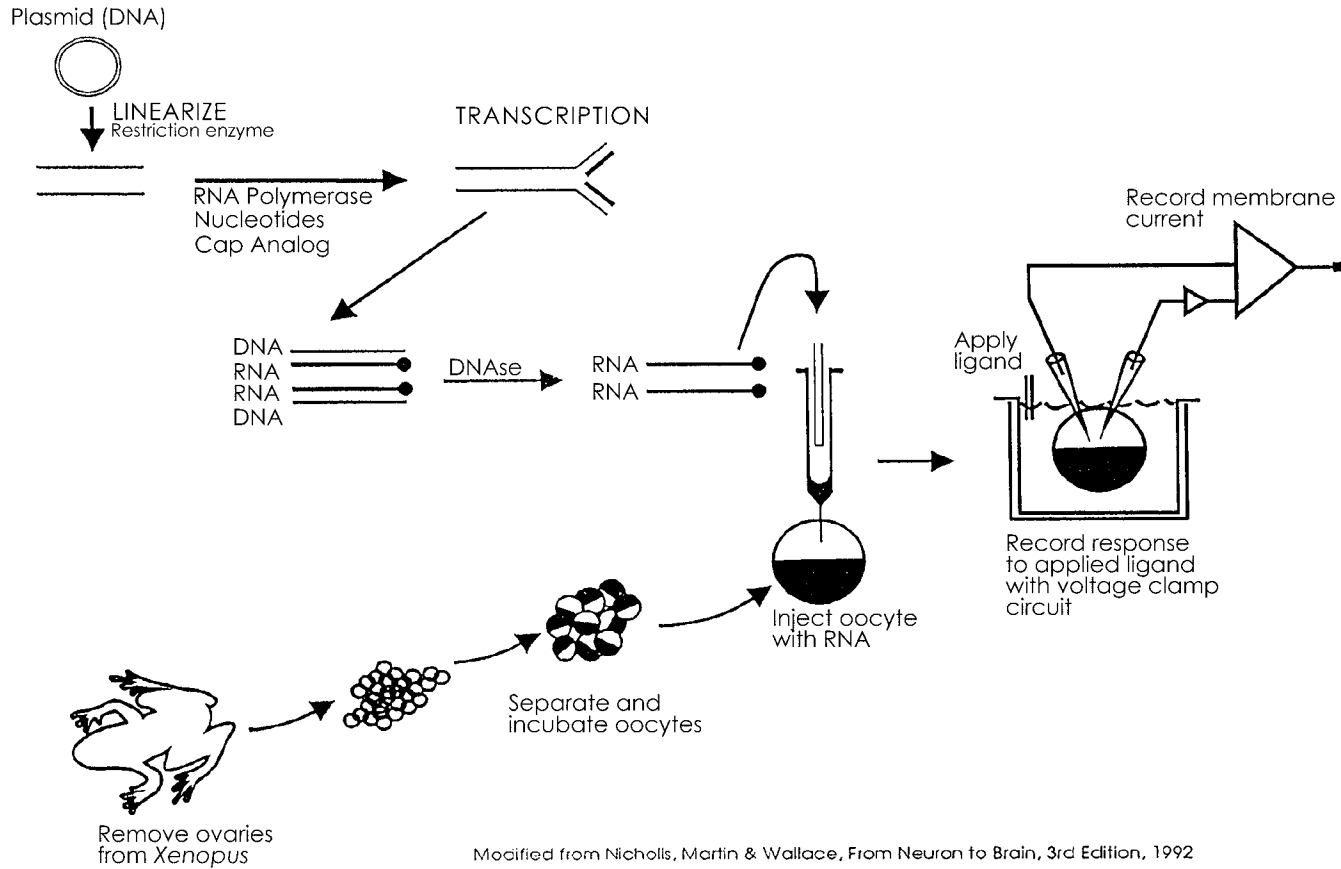


Fig. 6. Schematic illustration of receptors and ion channels in expressed *Xenopus laevis* oocytes for the study of the modification of receptors or ion channels by application of cannabinoids, endocannabinoids, or alcohol following current activation by 200 μ M kainic acid in the two-microelectrode voltage-clamp setup.

4. Notes

1. A number of studies indicate the functional existence of an anandamide transporter, but at this time its molecular identity is unknown. The methods reported here demonstrate that CHO cells carrying different transporters display different capacities for taking up anandamide.
2. Marijuana is frequently used to achieve euphoria, relaxation, and sensory changes. There has been increased attention to the medicinal properties of marijuana and its use for a number of disorders. Serious consideration and clinical evaluation of cannabinoid ligands in obesity and substance dependence and traumatic brain injury have reached advanced stages.
3. Numerous studies have shown the absence of CB₂ receptors in the brain. However, the presence and overexpression of CB₂ receptors and fatty acid amide hydrolase in neuritic plaque-associated glia in Alzheimer's disease brains has been reported (13). The availability of cannabinoid receptor antibodies has allowed for analysis of the expression of cannabinoid receptors in human and various animal model systems. The methodology for the analysis of the expression of CBRs is similar in different species and using a variety of samples, from blood to brain tissue.

Acknowledgments

Drs. Uhl's and Hope's laboratories are supported by NIDA–NIH intramural program, while ESO and CML acknowledges support from William Paterson University and the Center for Research. ESO also acknowledges continued Guest Scientist support by NIDA/NIH. BEA acknowledges the support of grant AA13415 from NIAAA.

References

1. Matsuda, L. A., Lolait, T. I., Brownstein, M. J., Young, A. C., and Bonner, T. I. (1990) Structure of a cannabinoid receptor and functional expression of the cloned cDNA. *Nature* **346**, 561–564.
2. Chakrabarti, A., Onaivi, E. S., and Chaudhuri, G. (1995) Cloning and sequencing of a cDNA encoding the mouse brain-type cannabinoid receptor protein. *DNA Sequence* **5**, 385–388.
3. Munro, S., Thomas, K. L., and Abu-Shaar, M. (1993) Molecular characterization of a peripheral cannabinoid receptor. *Nature* **365**, 61–65.
4. Devane, W. A., Hanus, L., Breuer, A., Pertwee, R.G., Stevenson, L. A., Griffin, G., Gibson, D., Mandelbaum, A., Etinger, A., and Mechoulam, R. (1992) Isolation and structure of a brain constituent that binds to the cannabinoid receptor. *Science* **258**, 1946–1949.
5. Hanus, L., Abu-Lafi, S., Frider, E., Breuer, A., Vogel, Z., Shalev, D.E., Kustanovich, I., and Mechoulam, R. (2001) 2-Arachidonyl glyceryl ether, an endogenous agonist of the cannabinoid CB1 receptor. *Proc. Natl. Acad. Sci. USA* **98**, 3662–3665.
6. Mechoulam, R. and Parker, L. (2003) Cannabis and alcohol – a close friendship. *Trends Pharmacol. Sci.* **24**, 266–268.

7. Porter, A. C., Sauer, J. M., Knierman, M. D., et al. (2002) Characterization of a novel endocannabinoid, virodhamine, with antagonist activity at the CB1 receptor. *J. Pharmacol. Exp. Ther.* **301**, 1020–1024.
8. Sugiura, T., Kondo, S., Sukagawa, A., et al. (1995) 2-Arachidonoylglycerol: a possible endogenous cannabinoid ligand in brain. *Biochem. Biophys. Res. Commun.* **215**, 89–97.
9. Ben-Shabat, S., Fride, E., Sheskin, T., et al. (1998) An entourage effect: inactive endogenous fatty acid glycerol esters enhance 2-arachidonyl-glycerol cannabinoid activity. *Eur. J. Pharmacol.* **353**, 23–31.
10. Onaivi E. S., Leonard C. M., Ishiguro H., et al. (2002) Endocannabinoids and Cannabinoid receptor genetics. *Prog. Neurobiol.* **66**, 307–344.
11. Wilson, R. I. and Nicoll, R. (2001) Endogenous cannabinoids mediate retrograde signaling at hippocampal synapses. *Nature* **410**, 588–592.
12. Sugiura, T. and Waku, K. (2000) 2-Arachidonoylglycerol and cannabinoid receptors. *Chem. Phys. Lipids* **108**, 89–106.
13. Benito, C., Nunez, E., Tolon, R. M., et al. (2003) Cannabinoid CB2 receptors and fatty acid amide hydrolase are selectively overexpressed in neuritic plaque-associated glia in Alzheimer's disease brains. *J. Neurosci.* **23**, 11136–11141.

Experimental Methods to Study the Role of the Peripheral Cannabinoid Receptor in Immune Function

Nancy E. Buckley, Diep Burbridge, Manop Buranapramest,
Tanya Ferguson, and Renee Y. Paau

Summary

Marijuana components, such as Δ -9-tetrahydrocannabinol, and endogenous cannabinoids, such as anandamide and 2-arachidonoylglycerol, alter diverse immune functions. Two cannabinoid receptors have been discovered to date, the central cannabinoid receptor (CB₁R) and the peripheral cannabinoid receptor (CB₂R). The CB₁R is expressed predominantly in the central nervous system. The CB₂R is expressed mainly in cells of the immune system, suggesting that the CB₂R is involved in immunoregulatory events. Cannabinoids have been shown to modulate diverse immune functions including cytokine production, lymphocyte proliferation, and humoral and cell-mediated immune responses. In addition, cannabinoids have been shown to induce different signal transduction pathways. However, the role of cannabinoids and their receptors in the immune system remains unclear. The objective of the experimental methods described herein is to investigate the role of CB₂R activation in specific splenocyte and macrophage functions using a mouse lacking the CB₂R. Interestingly, our findings, thus far suggest that basal CB₂R activation modulates lymphocyte proliferation and cytokine secretion and macrophage phagocytic activity. Therefore, data obtained using the methodology described in this chapter will help us elucidate the role of cannabinoids and the CB₂R in the immune system.

Key Words: Cannabinoids; immune function; splenocytes; T cells; lymphocyte proliferation; macrophages; cytokines; mitogen-activated kinase; CB₂R knockout mouse.

1. Introduction

Cannabinoids are marijuana components known to modulate immune functions. Δ -9-tetrahydrocannabinol (Δ^9 -THC), the major psychoactive compound of marijuana, has been the most widely studied cannabinoid. However, synthetic cannabinoids and the recently discovered endogenous cannabinoids

arachidonoyl ethanolamine (anandamide) and 2-arachidonoyl glycerol are also known to have immunoregulatory effects. THC and other exogenous cannabinoids affect lymphocytes, macrophages, and natural killer cells in a variety of functions such as cellular proliferation, cytokine activity, and cell and humoral immunity (reviewed in refs. 1–13).

1.1. Cannabinoid Receptors

Although the observations described here have suggested a role for cannabinoids in immunomodulation, the mechanisms by which cannabinoids induce these immunomodulatory effects remain elusive. To date, two receptors with high affinity for cannabinoid ligands are known (14–16). The central cannabinoid receptor (CB₁R) was first cloned in 1990 by Matsuda et al. (14). This receptor is predominantly found in the central nervous system (CNS) (17–19) and to a much lesser degree in cells of the immune system (20–23). Because of its high expression in the CNS, the CB₁R is thought to mediate most, if not all, of the effects of the cannabinoids in the CNS. The peripheral cannabinoid receptor (CB₂R), cloned by Munro et al. in 1993 (15), is predominantly expressed in cells of the immune system (15,22,23). Therefore, the immunomodulatory effects of cannabinoids are thought to be mediated by the CB₂R. Human blood cell subpopulations have different degrees of CB₂R expression with the following rank order: B cells > natural killer cells > monocytes > neutrophils > T8 cells > T4 cells. CB₂R has been demonstrated in rat spleen, mouse spleen and thymus, and a number of immune-system-derived cell lines (20,22). Thus, several immunoregulatory effects of cannabinoids may be mediated by CB₂R present on immune cells.

1.2. Cannabinoid Receptors and Cell Signaling

Cannabinoid receptors are G protein-coupled receptors. Besides the modulation of adenylate cyclase (23–26), G proteins link cannabinoid receptors to the mitogen-activated protein kinase (MAPK) signaling cascade. Activation of the MAPK cascade is independent of regulation of adenylate cyclase (5,27–30). The CB₂R, specifically, is known to be coupled through a G_i. Thus, the CB₂R is a G protein-coupled receptor that is both positively and negatively coupled to MAPK and cAMP pathways, respectively, through a *Bordetella pertussis* toxin-sensitive G protein.

1.3. CB₂R Knockout Mouse

To investigate the role of the CB₂R in immunomodulation, we created a mouse deficient for the CB₂R using homologous recombination (CB₂R knockout or CB₂R^{-/-} mouse) (31). The CB₂R^{-/-} gene is encoded by a single exon. Upon homologous recombination, 341 bp from the coding region's 3' end was

replaced by the neomycin gene. This mouse model as well as cell lines derived from these mice have been successfully used to answer questions regarding the role of the CB₂R^{-/-} in the immune system (32). In addition, a CB₂R antagonist, SR144528 (33), has provided several investigators with a tool to study the role of the CB₂R in immune function (35). However, the CB₂R antagonist is also an inverse agonist (35–37). The CB₂R has a basal activity in the absence of ligand. This basal activity is reduced or blocked by SR144528 (37).

In our CB₂R^{-/-} mouse model, the CB₂R gene has been mutated to render the receptor incapable of binding cannabinoids and coupling to G proteins. Therefore, this animal model is unique in that it can provide us with different information from that obtained by using the CB₂R antagonist. The CB₂R^{-/-} mice have been backcrossed to c57BL/6 mice more than 12 times to ensure c57BL/6 genetic background strain. Therefore, the control (wild-type, CB₂R^{+/+}) mice are c57BL/6.

1.4. Conclusions

It is now known that the cannabinoid system includes at least two receptors and several endogenous ligands widely distributed throughout the body (16). Despite these findings, the role of the cannabinoid system in immune function remains unclear. It is very tempting to speculate that the cannabinoid system has a role in immunity due to the diverse effects of cannabinoids on immune functions and the reversion of some of these effects using cannabinoid receptor antagonists. However, we have yet to show direct evidence implicating cannabinoid receptor activation in immune events and specifically on immune cells.

The primary objective of the experimental methods described herein is to help us determine the role of CB₂R activation in cannabinoid-induced immune responses; specifically, the role of CB₂R activation on cell proliferation and cytokine production from lymphocytes, macrophage phagocytic activity, and putative signal transduction pathways mediating the immune responses to cannabinoids. To do this we use a mouse lacking a functional CB₂R receptor, the CB₂R knockout mouse (31).

2. Materials

2.1. Cell Cultures

2.1.1. Splenocyte Cell Cultures

1. Complete media: RPMI-1640 medium (stored at 4°C, wrapped in aluminum foil to protect it from light) supplemented with a 100 U/mL penicillin, 100 µg/mL streptomycin mixture, 4 mM L-glutamine and 7.5% heat-inactivated fetal calf serum (FCS) (all from BioSource International, Camarillo, CA). Allow the RPMI medium and the reagents to reach 37°C in a warm water bath before the reagents are added to the media. This complete media can be stored at 4°C for a maximum of 2 wk.

2. Concanavalin A (ConA): 5 mg powder stock of ConA lectin from *Canavalia ensiformis*, 5-mg powder vial (Sigma, St. Louis, MO). ConA was reconstituted in 1 mL RPMI medium (5 mg/mL stock), aliquotted into 50- μ L fractions, and stored at -20°C .
3. Sterile 70-m nylon mesh filter screen (Falcon, Becton Dickinson Labware, Franklin Lakes, NJ).
4. Red blood cell lysis buffer (ACK lysing buffer from BioSource International, Camarillo, CA): 156 mM NH_4Cl , 10 mM KHCO_3 , and 1 mM Na_2EDTA .
5. Trypan blue: 0.4% stock concentration of trypan blue (Sigma, St. Louis, MO).
6. Sterile flat-bottom, tissue-culture grade 24-well plates (Corning Inc., Corning, NY).
7. Sterile flat-bottom, tissue-culture-grade 96-well microtiter plates (Corning Inc., Corning, NY).

2.1.2. T-Cell Cultures

1. RPMI-1640 medium: RPMI-1640 medium (BioSource International, Camarillo, CA) supplemented with 100 units/mL penicillin, 100 $\mu\text{g/mL}$ streptomycin, and 4 mM L-glutamine.
2. Complete media: RPMI-1640 medium (stored at 4°C , wrapped in aluminum foil to protect it from light) supplemented with a 100 U/mL penicillin, 100 $\mu\text{g/mL}$ streptomycin mixture, 4 mM L-glutamine and 7.5% heat-inactivated FCS (all from BioSource International, Camarillo, CA). Allow the RPMI medium and the reagents to reach 37°C in a warm water bath before the reagents are added to the media. This complete media can be stored at 4°C for a maximum of 2 wk.
3. ConA: 5 mg powder stock of ConA lectin from *Canavalia ensiformis*, 5 mg powder vial (Sigma, Saint Louis, MO). Con was reconstituted in 1 mL RPMI medium (5 mg/mL stock), aliquoted into 50- μ L fractions and stored at -20°C .
4. Plate-bound anti-CD3 antibody: Purified hamster anti-mouse CD3e (145-2C11, 0.5 mg/mL (BD Biosciences, San Diego, CA) is plated 5–0 $\mu\text{g/mL}$ in PBS. For proliferation assays, 50 μL are plated in 96-well plates. For cytokine assays, 250 μL are added to 24-well plates.
5. Sterile 70- μm nylon mesh filter screen (Falcon, Becton Dickinson Labware, Franklin Lakes, NJ).
6. Red blood cell lysis buffer (ACK lysing buffer from BioSource International, Camarillo, CA): 156 mM NH_4Cl , 10 mM KHCO_3 , and 1 mM Na_2EDTA .
7. Phosphate-buffered saline (PBS): Prepare 10X stock with 1.37 M NaCl, 27 mM KCl, 100 mM Na_2HPO_4 , 18 mM KH_2PO_4 , adjust to pH 7.4 with HCl. Autoclave before storing at room temperature. Before using, dilute to 1X PBS.
8. Trypan blue: 0.4% stock concentration of trypan blue (Sigma, St. Louis, MO).
9. Sterile flat-bottom, tissue-culture-grade 24-well plates (Corning Inc., Corning, NY).
10. Sterile flat-bottom, tissue-culture-grade 96-well microtiter plates (Corning Inc., Corning, NY).
11. Pan T-Cell Isolation Kit (Miltenyibiotec, Auburn, CA).

- a. MidiMACS Separation Unit.
 - b. MACS MultiStand.
 - c. MACS High Gradient Magnetic Separation Columns of type LS.
 - d. Biotin-Antibody Cocktail.
 - e. Anti-Biotin MicroBeads.
12. Column buffer: PBS, pH 7.2 supplemented with 0.5% FBS and 2 mM EDTA. Degas by applying vacuum and maintain at 4–8°C.

2.1.3. Macrophage Cell Cultures

1. Thioglycolate broth: 3% thioglycolate broth (Becton Dickinson, Franklin Lakes, NJ) in sterile glass-distilled water. The bottle is placed in a boiling water bath to ensure complete dissolution of the powder. Autoclave the solution at 15 psi, 121°C for 15 min. Store at room temperature and use within 1 d.
2. Lavage medium: 0.95% NaCl in glass-distilled H₂O. Autoclave the solution at 15 psi, 121°C, 15 min, following dissolution.
3. Macrophage complete media: RPMI-1640 medium (stored at 4°C, wrapped in aluminum foil to protect it from light) supplemented with a 100 units/mL penicillin, 100 µg/mL streptomycin mixture, 4 mM L-glutamine and 5% heat-inactivated FCS (all from BioSource International, Camarillo, CA). Allow the RPMI medium and the reagents to reach 37°C in a warm water bath before the reagents are added to the media. This complete media can be stored at 4°C for a maximum of 2 wk.
4. Sterile 70-µm nylon mesh filter screen (Falcon, Becton Dickinson Labware, Franklin Lakes, NJ).
5. Red blood cell lysis buffer (ACK lysing buffer from BioSource International, Camarillo, CA): 156 mM NH₄Cl, 10 mM KHCO₃, and 1 mM Na₂EDTA.
6. Trypan blue: 0.4% stock concentration of trypan blue (Sigma, St. Louis, MO).
7. Sterile flat-bottom, tissue-culture-grade 12-well plates (Corning Inc., Corning, NY).

2.2. Splenocyte and T-Cell Proliferation Assay

1. BrdU cell proliferation ELISA kit from Roche Molecular Biochemicals (Indianapolis, IN):
 - a. BrdU labeling reagent (1000X) (10 mM 5'-bromo-2'-deoxyuridine in PBS, pH 7.4) (provided in kit).
 - b. FixDenaturant (ready to use) (provided in kit).
 - c. Anti-BrdU-POD lyophilisate, stabilized. Monoclonal antibody from mouse-mouse hybrid cells (clone BMG 6H8, Fab fragments) conjugated with peroxidase (POD) (provided in kit).
 - d. Antibody dilution solution (ready to use) (provided in kit).
 - e. Washing buffer (10X) in PBS (provided in kit).
 - f. Substrate solution TMB (tetramethyl-benzidine) (provided in kit).
2. SpectraMax Plus Microplate Spectrophotometer plate reader (Molecular Devices, Sunnyvale, CA).

2.3. Cytokine Assays

2.3.1. Splenocyte Cytokine Assay

1. Bio-Plex cytokine assay kit (Bio-Rad Laboratories, Hercules, CA).
 - a. Anti-cytokine conjugated beads (25X), 2.5×10^6 beads/mL per cytokine (provided in kit).
 - b. Cytokine detection antibody 8-plex (50X) = 0.05 mg/mL per cytokine (provided in kit).
 - c. Cytokine standard (lyophilized), 25 ng per cytokine (provided in kit).
 - d. Bio-Plex assay buffer A (provided in kit).
 - e. Bio-Plex wash buffer A (provided in kit).
 - f. Bio-Plex detection antibody diluent A (provided in kit).
 - g. Streptavidin-PE (100X) (provided in kit).
 - h. Sterile filter plate (96-well) with cover, tray, and sealing tape (provided in kit).
2. Luminex 100 microplate platform (Luminex Corporation, Austin, TX).

2.3.2. T-Cell Cytokine Assays

1. Mouse interleukin (IL)-2 ELISA set from BD Biosciences (San Diego, CA).
 - a. Anti-mouse IL-2 monoclonal capture antibody (provided in kit).
 - b. Biotinylated anti-mouse IL-2 detection antibody (provided in kit).
 - c. Streptavidin-horseradish peroxidase conjugate enzyme reagent (provided in kit).
 - d. Lyophilized recombinant mouse IL-2 standards (provided in kit).
2. Mouse IL-4 ELISA set from BD Biosciences (San Diego, CA).
 - a. Anti-mouse IL-4 monoclonal capture antibody (provided in kit).
 - b. Biotinylated anti-mouse IL-4 detection antibody (provided in kit).
 - c. Streptavidin-horseradish peroxidase conjugate enzyme reagent (provided in kit).
 - d. Lyophilized recombinant mouse IL-4 standards (provided in kit).
3. Coating buffer: 0.1 M sodium carbonate, pH 9.5. 8.40 g NaHCO_3 , 3.56 g Na_2CO_3 , to 1.0 L; pH to 9.5. Freshly prepare or use within 7 d of preparation, stored at 2–8°C.
4. Assay diluent: PBS: 80.0 g NaCl, 11.6 g Na_2HPO_4 , 2.0 g KH_2PO_4 , 2.0 g KCl, to 10 L; pH to 7.0. with 10% FBS (Sigma, St. Louis, MO), pH 7.0. Freshly prepare or use within 3 d of preparation, with 2–8°C storage.
5. Wash buffer: PBS: 80.0 g NaCl, 11.6 g Na_2HPO_4 , 2.0 g KH_2PO_4 , 2.0 g KCl, to 10 L; pH to 7.0. with 0.05% Tween-20. Freshly prepare or use within 3 d of preparation, stored at 2–8°C.
6. Substrate solution: Tetramethylbenzidine (TMB) and hydrogen peroxide (BD Pharmingen™ TMB Substrate Reagent Set).
7. Stop solution: 2 N H_2SO_4 .

8. Immulon 2HB 96-well flat-bottom microtiter plates (Thermo Labsystems, Franklin, MA).
9. SpectraMax Plus Microplate Spectrophotometer plate reader (Molecular Devices, Sunnyvale, CA).

2.4. Phagocytosis Assay

2.4.1. Foreign Antigens

2.4.1.1. MICROSPHERES

1. Red-dyed polystyrene latex particles (0.8 μm) (Bangs Laboratories, Fishers, IN): 2.5% solids in 5% heat-inactivated FCS and incubated at 37°C for 30 min immediately prior to use. Incubation with FCS allows optimal opsonization.
2. Fluorescent microspheres: Yellow-green Fluoresbrite polystyrene latex particles (1 μm) (Polyscience, Inc., Warrington, PA): 1% solids in 5% heat-inactivated FCS and incubated at 37°C for 30 min immediately prior to use. Incubation with FCS allows optimal opsonization.

2.4.1.2. *ESCHERICHIA COLI*

1. Bacteria expressing a fluorescent marker: *E. coli* transformed and induced to express green fluorescent protein (GFP) using EDVO-kit no. 223 (Edvotek, Bethesda, MD) kit reagents.
2. Opsonization of bacteria: Incubate *E. coli* expressing GFP in 5% heat-inactivated FCS for 30 min at 37°C, immediately prior to use.

2.4.2. Cell Fixation and Permeabilization

1. Fixative: 4% formaldehyde in PBS containing 4% sucrose. Filter-sterilize and store at room temperature. For best results, the fixing medium should be prepared fresh or used within 1 wk of preparation.
2. Permeabilization solution: 0.25% Triton-X (BioRad Laboratories, Hercules, CA) in PBS. Filter-sterilize and store at room temperature. For best results, the fixing medium should be prepared fresh or used within 1 wk of preparation.

2.4.3. Microscopy

1. Mounting media: 13.3% polyvinyl alcohol (PVA, elvanol), 33% glycerol, and 0.5% 1,4-diazabicyclo-2,2,2-octane (DABCO) in 0.132 *M* Tris. Gradually dissolve 8 g PVA (J.T. Baker) in a beaker containing 30 mL 0.2 *M* Tris, pH 8.5 at 50°C, with stirring, over a 1- to 2-h period. Following complete dissolution of the PVA, turn off the heat and gradually add 20 mL glycerol in a thin stream over 5 min while stirring (see **Note 1**). In a separate container, dissolve 0.3 g DABCO (Sigma) in 10 mL 0.2 *M* Tris, pH 8.5. Once completely dissolved, add the DABCO solution to the PVA/glycerol stock. Cover the viscous solution with foil to protect it from ambient light and wrap with parafilm. Allow to stand overnight to remove bubbles. Finally, aliquot the solution and centrifuge in a microcentrifuge at 6000g for 20 min to

eliminate all bubbles. Immediately store at -20°C . Because of its viscosity, elvanol is kept in a 60°C heating block while in use.

2. Light microscope with 40X magnification capability to visualize the red-dyed microspheres.
3. Phase-contrast microscopy with a green fluorescent filter (Nikon Eclipse TE300 microscope): Fluorescent-dyed microspheres and GFP-expressing *E. coli* can be viewed under 20X or 40X magnification.
4. Metamorph Imaging Software, version 6.2r2 (Universal Imaging Corporation).
5. Microscope slides double frosted ($75\text{ mm} \times 25\text{ mm} \times 1.2\text{ mm}$) (Fisher, Pittsburgh, PA).
6. Round microscope cover glass (18 mm diameter) (Fisher, Pittsburgh, PA).

2.5. Mitogen-Activated Protein Kinase Assay

2.5.1. Cell Lysis and Treatment

1. RPMI-1640 medium: RPMI-1640 medium (BioSource International, Camarillo, CA).
2. Red blood cell lysis buffer (ACK lysing buffer from BioSource International, Camarillo, CA): $156\text{ mM NH}_4\text{Cl}$, 10 mM KHCO_3 , and $1\text{ mM Na}_2\text{EDTA}$.
3. Sterile $70\text{-}\mu\text{m}$ nylon mesh filter screen (Falcon, Becton Dickinson Labware, Franklin Lakes, NJ).
4. Sterile flat-bottom, tissue-culture-grade 12-well plates (Corning Inc., Corning, NY).
5. Lipopolysaccharide (LPS): LPS derived from *E. coli* 055:B55 (Sigma, St. Louis, MO), 1 mg/ml in complete media. Special precaution should be taken when handling LPS as it is highly pyrogenic. Stored at -20°C .
6. Myelin basic protein (Sigma, St. Louis, MO) is dissolved in deionized water at a concentration of 1 mg/mL and stored in aliquots at -70°C .
7. Cell lysis buffer and Mg^{2+} /ATP cocktail: 20 mM HEPES-NaOH at pH 7.2, 1% (v/v) Triton X-100, 10% glycerol (v/v), 1 mM [ethylene-bis-(oxyethylenenitrilo)]-tetraacetic acid (EGTA), 50 mM sodium fluoride, 75 mM magnesium chloride, 1 mM sodium orthovanadate, $100\text{ }\mu\text{g/mL}$ leupeptin, 1 mM dithiothreitol (DTT), 0.05 mM phenyl methylsulfonyl fluoride (PMSF), 0.5 mM adenosine triphosphate (ATP). Store at room temperature (see **Note 2**).

2.5.2. Enzyme-Linked Immunosorbent Assay (ELISA)

1. Blocking buffer (10X): 10X PBS , 20% bovine serum albumin (BSA) (w/v), 0.1% Tween-20 (v/v), 0.02% sodium azide. Store at 4°C .
2. Dilution buffer (5X): 100 mM HEPES-NaOH at pH 7.2, $125\text{ mM } \beta\text{-glycerophosphate}$, 25 mM EGTA , 5 mM sodium orthovanadate, 5 mM DTT . Store at 4°C .
3. Wash buffer (10X): 10X PBS , 0.5% Tween-20 (v/v). Store at room temperature.
4. Capture and primary antibody: Mouse anti-human phosphorylated myelin basic protein (MBP) (US Biological, MA) (see **Note 3**).
5. Detection antibody: Affinity-purified sheep anti-mouse IgG conjugated to alkaline phosphatase (Sigma, St. Louis, MO).

6. Substrate for alkaline phosphatase: Alkaline phosphatase yellow *p*-nitro-phenylphosphate (pNPP) substrate system for ELISA (Sigma, St. Louis, MO). Stored at 4°C (see **Note 4**).
7. Custom-made peptide, standard: MBP phosphorylated at Thr98, FFKNIVTPRpTPPPSQGK, (City of Hope, Duarte, CA) is dissolved in PBS at a concentration of 1 mg/mL with 0.02% sodium azide (w/v) and stored at 4°C. Lyophilized peptide is stored at -70°C (see **Note 5**).
8. Immulon 2HB 96-well flat-bottom microtiter plates (Thermo Labsystems, Franklin, MA).

2.6. Cannabinoids

1. (-)-*trans*- Δ^9 -Tetrahydrocannabinol (THC) (NIDA-Research Triangle Institute) 5 mg/mL in absolute ethanol, MW 314.45. Prepare THC aliquots in silica-coated vials. Purge vials containing THC with N₂ gas and store in a locked freezer at -20°C. Do not use the cannabinoid solutions if there is suspicion of oxidation. After aliquotting, use within 6 mo. Working solutions are prepared by dilution in absolute ethanol.
2. *R*-(+)-[2,3-Dihydro-5-methyl-3-(4-morpholynylmethyl)pyrrolo[1,2,3-DE]-1,4-benzoxazin-6-yl]-1-naphthalenylmethanone mesylate (WIN55,212-2) (Tocris, Ellisville, MO) 10 mM in absolute ethanol, MW 531.62. Prepare WIN55,212-2 aliquots in silica-coated vials. Purge vials containing WIN55,212-2 with N₂ gas and store at -70°C. Do not use the cannabinoid solutions if there is suspicion of oxidation. After aliquotting, use within 6 mo. Working solutions are prepared by dilution in absolute ethanol.
3. 2-Arachidonyl ethanolamide (2-AG) (NIDA-Research Triangle Institute) 26.4 mM in absolute ethanol, MW 378.5. Prepare 2-AG aliquots in silica-coated vials. Purge vials containing 2-AG with N₂ gas and store at -70°C. Do not use the cannabinoid solutions if there is suspicion of oxidation. After aliquotting, use within 6 mo. Working solutions are prepared by dilution in absolute ethanol.

3. Methods

3.1. Cell Cultures: Splenocyte Cell Cultures

1. First, sacrifice the mice by CO₂ asphyxiation. Working in a sterile hood, cut into the animal's skin below the front legs, and pull away the skin to expose the peritoneum and the underlying internal organs. Make a sterile incision into the peritoneal membrane on the animal's left side. Then remove the spleen with forceps. Pool together three spleens from CB₂R^{+/+} and CB₂R^{-/-} mice groups and process them for primary splenocyte culture preparations.
2. Transfer the three spleens to a sterile 70- μ m nylon mesh filter screen covering a 50-mL conical centrifuge tube containing 5 mL of complete media. Release the splenocytes from the spleens by gently massaging the spleens with the end of a 3-cc tuberculin syringe.

3. Carefully rinse the cell suspension in the filter screen with 15 mL of complete media to harvest all the spleen cells.
4. Centrifuge the cell suspension at 150g for 10 min at 15–18°C (CRU-500 Centrifuge, International Equipment Co., Neeham Heights, MA).
5. Discard the supernatant and add 5 mL of ACK lysing buffer to the cell pellet to lyse all red blood cells. Swirl the solution gently and place the tube on ice for 5 min with occasional swirling.
6. At the end of the 5 min, add 10 mL of complete media to the solution to stop cell lysis and centrifuge the cell suspension again at 150g for 10 min.
7. Discard the supernatant and add 20 mL of complete media to the cell pellet to remove any remaining lysis buffer. Gently resuspend the cells thoroughly.
8. To perform a cell count, a 1:20 dilution of the cell solution is needed. This is done by making a 1:10 dilution with complete media and then a 1:2 dilution with 0.4% stock concentration of trypan blue.
9. Count the cells using a hemacytometer. Then centrifuge the cell suspension at 150g for 5 min. Resuspend the cell pellet in 5 mL of serum-free media and dilute to 2×10^6 cells/mL in complete media.
10. For proliferation studies, plate the cells in complete media at 2×10^5 cells/0.1 mL/well into sterile flat-bottom, tissue-culture-grade 96-well microtiter plates. For cytokine studies, plate the cells in complete media at 2×10^6 cells/mL/well into sterile flat-bottom, tissue-culture-grade 24-well plates.
11. Treat specified wells with various final concentrations of the cannabinoid agonists (0, 0.01 μ M, 0.1 μ M, 1 μ M, 5 μ M). Using a repeater pipetor, treat the 24-well plates with 10- μ L aliquots of the cannabinoid reagents (or 10 μ L absolute EtOH as the non-cannabinoid-treated control), and treat the 96-well plates with 1 μ L of the cannabinoid reagents (or 1 μ L absolute EtOH as the non-cannabinoid-treated control). Set up the wells in the 24-well plates in triplicates. Set up the wells in the 96-well plates in quadruplicates.
12. After cannabinoid treatment, incubate the plates for 1 h in a humidified 5% CO₂ incubator at 37°C. After 1 h of incubation, treat specified wells with the T-cell mitogen ConA at a final concentration of 2.5 μ g/mL. Treat each well of the 24-well plates with 10 μ L of ConA (or 10 μ L RPMI as the non-ConA-treated control). And treat every well of the 96-well plates with 1 μ L of ConA (or 1 μ L RPMI as the non-ConA-treated control).
13. Incubate the plates at 37°C in a humidified 5% CO₂ incubator for 72 h.

3.1.2. T-Cell Cultures

1. After obtaining the CB₂R^{+/+} and CB₂R^{-/-} transfer the spleens to a sterile 70- μ m nylon mesh filter screen covering a 50-mL conical centrifuge tube containing 5 mL of RPMI medium. Release the splenocytes from the spleens by gently pressing the spleens with the end of a 3 cc tuberculin syringe.
2. Carefully rinse the cell suspension in the filter screen with 15 mL of serum-free media to harvest all the spleen cells.

3. Perform a cell count using a hemacytometer by making a 1:10 dilution of the splenocyte suspension with serum-free media and then a 1:2 dilution with 0.4% stock concentration of trypan blue.
4. Transfer 5×10^8 total cells to a fresh 50-mL conical centrifuge tube.
5. Centrifuge the cell suspension at 300g for 10 min at 4–8°C.
6. Pipette off supernatant completely and resuspend cell pellet in 2 mL of column buffer.
7. Add 500 μ L of biotin-antibody cocktail and incubate for 10 min at 4–8°C.
8. Add 1.5 mL of buffer and 1000 μ L of anti-biotin microBeads and incubate for an additional 15 min at 4–8°C.
9. Wash cells with 10 mL of column buffer and centrifuge at 300g for 10 min.
10. Pipette off supernatant completely and resuspend cell pellet in 2500 μ L of column buffer.
11. Place an LS column in the magnetic field of a suitable MACS Separator.
12. Prepare column by rinsing with 3 mL of column buffer.
13. Apply cell suspension onto the column. Allow the cells to pass through and collect effluent as fraction with unlabeled cells, representing the enriched T-cell fraction.
14. Wash the column with 12 mL of column buffer. Collect entire effluent in the same tube as effluent of previous step.
15. Perform a cell count by making a 1:10 dilution of the T-cell suspension with serum-free media and then a 1:2 dilution with 0.4% stock concentration of trypan blue.
16. Count the cells using a hemacytometer and determine the total number of T cells.
17. Centrifuge the cell suspension at 300g for 10 min at 4–8°C.
18. Resuspend pellet in a suitable volume of warm complete media to obtain a 2×10^6 cell/mL T-cell suspension.
19. Prepare a 5–10 μ g/mL solution of anti-CD3 in sterile PBS.
20. Dispense 50 μ L of the antibody solution in each well of the sterile flat-bottom, tissue-culture grade 96-well microtiter plates or 250 μ L in each well of the sterile flat-bottom, tissue-culture-grade 24-well plates.
21. For the control unstimulated wells, add sterile PBS.
22. Tightly cover the plate with Parafilm to avoid sample evaporation and incubate at 4°C overnight.
23. Just before adding cells, remove the antibody solution with a multichannel pipettor.
24. Rinse each well two times with sterile PBS and discard PBS.
25. For proliferation studies, plate the cells in complete media at 2×10^5 cells/0.1 mL/well into sterile flat-bottom, tissue-culture-grade 96-well microtiter plates. For anti-CD3 stimulation, plate the cells in complete media at 2×10^5 cells/0.1 mL/well into the anti-CD3 prebound plates. For cytokine studies, plate the cells in complete media at 2×10^6 cells/mL/well into sterile flat-bottom, tissue-culture-grade 24-well plates for ConA stimulation. For anti-CD3 stimulation, plate the cells in complete media at 2×10^6 cells/mL/well into the anti-CD3 prebound plates.
26. Treat specified wells with various final concentrations of cannabinoids (0 μ M, 0.01 μ M, 0.1 μ M, 1 μ M). Using a repeater pipettor, treat the 24-well plates with 10- μ L

aliquots of the cannabinoid reagents (or 10 μ L absolute EtOH as the non-cannabinoid-treated control), and treat the 96-well plates with 1 μ L of the cannabinoid reagents (or 1 μ L absolute EtOH as the non-cannabinoid-treated control). Set up the wells in the 24-well plates in triplicates. Set up the wells in the 96-well plates in quadruplicates.

27. After cannabinoid treatment, incubate the plates for 1 h (in the case of ConA stimulation) in a humidified 5% CO₂ incubator at 37°C. After 1 h of incubation, treat specified wells with ConA to a final concentration of 2.5 μ g/mL. Treat each well of the 24-well plates with 10 μ L of ConA (or 10 μ L RPMI as the non-ConA treated control). And treat every well of the 96-well plates with 1 μ L of ConA (or 1 μ L RPMI as the non-ConA-treated control).
28. Incubate the plates at 37°C in a humidified 5% CO₂ incubator 24, 48, and 72 h.

3.1.3. Macrophage Cell Cultures

1. A 3% thioglycolate broth is prepared by dissolving 1.5 g Bacto-Thioglycollate dehydrated medium (Becton Dickinson, Franklin Lakes, NJ) in a 100-mL sterile glass bottle containing 50 mL of deionized water. The bottle is placed in a boiling water bath to ensure complete dissolution of the powder. Autoclave the solution at 15 psi, 121°C, for 15 min. Allow the thioglycolate broth to cool to 37°C. Upon cooling, inject 3 mL of the broth intraperitoneally using a 5 mL syringe and 27-gauge needle. Injections should be administered in the lower left section of abdominal area to avoid intestinal or internal organ puncture.
2. Four days following injection, sacrifice the animals via CO₂ asphyxiation. Peritoneal macrophages are obtained by peritoneal lavage with 9 mL of cold, sterile 0.95% NaCl. For experimental purposes, put the solution on ice in order to minimize macrophage activity prior to culturing. To do the lavage, make a slight cut in the abdominal area and pull back the fur to expose the peritoneum. Inject the cold lavage medium with a 20-gage needle at the fatty spot on the left side of the animal. Massage the inflated abdominal area and incubate for 5 min to obtain a maximum yield of macrophages. Place the animal on a 50-cc centrifuge tube and use a 20-gage needle to pierce the right ventral lateral section of the peritoneum, allowing the fluid to drain directly into the tube. Pool macrophages from CB₂R^{+/+} and CB₂R^{-/-} genotypes in order to obtain higher cell counts.
3. Pooled cells are then filtered through a 70- μ m nylon mesh filter screen to remove chunks of tissue and cell debris. Gently centrifuge for 5 min at 327g and 4°C. Pour off the supernatant and lyse the red blood cells for 1 min with 1 mL ACK lysing buffer. After 1 min add 19 mL of PBS to stop the lysis of red blood cells and to maintain macrophage integrity. Pellet cells for 5 min at 327g and 4°C. Pour off the supernatant and resuspend in complete medium.
4. Determine cell viability using trypan blue exclusion dye.
5. Prior to plating the thioglycolate-elicited macrophages, round cover slips are sterilized with ethanol and flamed. Subsequently, the cover slips are added to the bottom of Costar 12-well cluster microplates (Corning, Inc., Acton, MA).

Macrophages are then plated, 1 mL per well, at $0.5\text{--}1 \times 10^6$ cells per well and allowed to adhere to the topside of the cover slips for 1–2 h.

6. Adherent cells are then rinsed with 1 mL of complete medium for enrichment. Cannabinoids (0, 0.01 μM , 0.1 μM , 1 μM) are then added to plated macrophages for 1 h.

3.2. Splenocyte and T-Cell Proliferation Assays

1. The protocol described in the BrdU cell proliferation ELISA kit is used to assess cell proliferation.
2. Forty-eight hours after the cells were stimulated with ConA or plate-bound anti-CD3 antibody, treat each well in the 96-well microtiter plates with 10 μL of bromodeoxyuridine (BrdU)-labeled stock solution. Return the plates to the same 5% CO_2 incubator as described in the kit. After incubating for 24 h more, remove the 96-well microtiter plates containing the BrdU-labeled cells from the incubator. Centrifuge the plates in a plate centrifuge (Heraeus Model no. Megafuge 2.0 R table-top centrifuge) at 300g for 10 min to pellet the cells.
3. Remove the supernatant by suction using a sterile cannula and dry the plates containing the cell pellets in a 60°C oven for 30 min. Proceed as the kit protocol describes to fix the cells, detect the denatured BrdU containing DNA with anti-BrdU-peroxidase antibody, and visualize the BrdU incorporation by the colorimetric reaction. The colorimetric reaction is stopped by adding 25 μL of 1 M H_2SO_4 to each well. Gently tap the plates to allow the H_2SO_4 to mix thoroughly with the contents of the wells.
4. Within 5 min of adding the stop solution, quantify the colorimetric reaction product by measuring the absorbance of the samples at 450 nm (reference wavelength 690 nm) using the SpectraMax Plus Microplate Spectrophotometer plate reader (Molecular Devices, Sunnyvale, CA). The developing color and the corresponding absorbance values directly correlate to the amount of DNA synthesis, which is an indicator of the number of proliferating cells in the cell culture samples.
5. As seen in [Fig. 1](#), cell proliferation is enhanced in the presence of THC (10–100 nM) in $\text{CB}_2\text{R}^{+/+}$ cells, but not in $\text{CB}_2\text{R}^{-/-}$ cells. Interestingly, cell proliferation in $\text{CB}_2\text{R}^{-/-}$ cells is greater than in $\text{CB}_2\text{R}^{+/+}$ cells ([Fig. 1](#)). Effects similar to those of THC were observed with WIN55,212-2 and 2-AG on splenocyte proliferation (data not shown).

3.3. Cytokine Assays

3.3.1. Splenocyte Cytokine Assay

3.3.1.1. BIORAD ASSAYS

1. Seventy-two hours postculture, remove the 24-well plates from the incubator and collect 120 μL of supernatant from each well and place into a sterile, flat-bottom, non-tissue-culture-treated 96-well microtiter plate. Store the plate containing the supernatant in the -70°C Revco freezer until it is assayed for specific cytokines using the Bio-Plex cytokine assay as indicated in the kit. The protocol included in

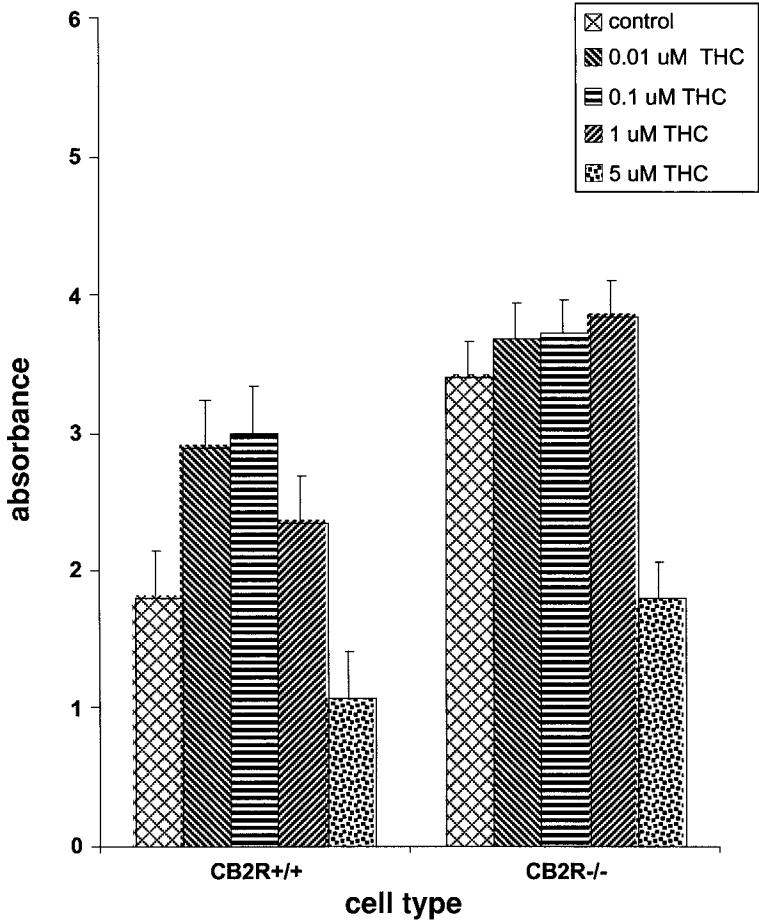


Fig. 1. Δ^9 -THC enhances CB₂R^{+/+} splenocyte proliferation, but not CB₂R^{-/-} splenocyte proliferation. Splenocyte proliferation was determined by BrdU incorporation assay as described in the text. Cells were plated at 2×10^5 cells/0.1 mL/well in complete media. Cells were treated with 2.5 μ g/mL ConA and the indicated Δ^9 -THC concentration for 72 h. Data are expressed as the mean of quadruplicate samples \pm standard deviation. Vehicle is absolute ethanol.

the kit is followed to assess the concentration of IL-1 β , IL-2, IL-4, IL-5, IL-10, granulocyte-macrophage colony-stimulating factor (GM-CSF), interferon (IFN)- γ and tumor necrosis factor (TNF)- α in the supernatant.

2. The Luminex 100 microplate reader (Luminex Corporation, Austin, TX) is used to determine cytokine concentration using the Bio-Plex cytokine kit.

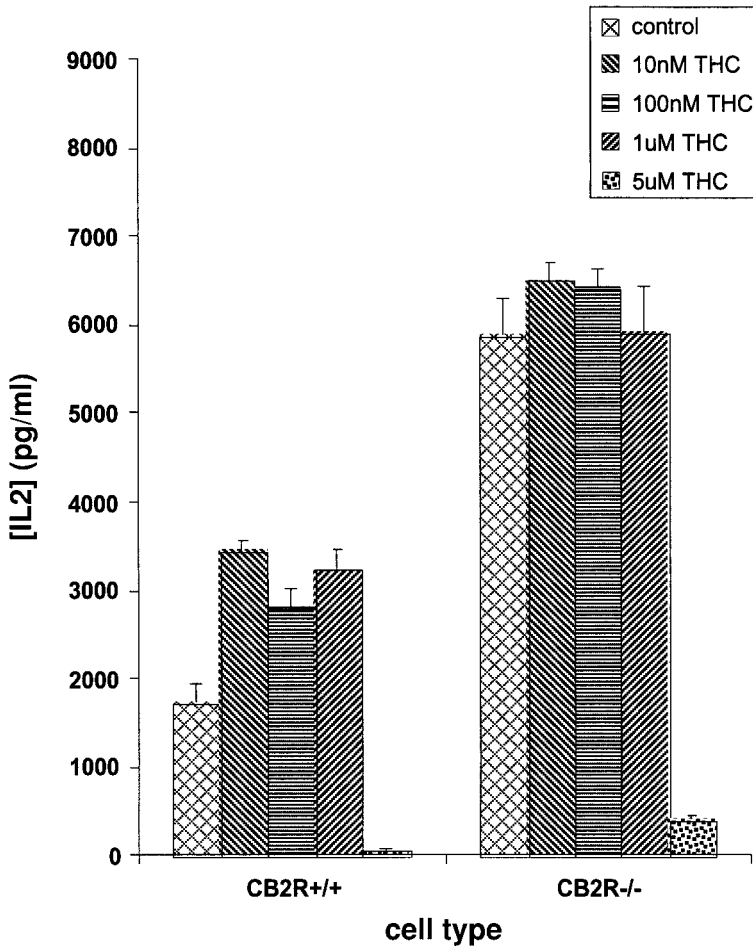


Fig. 2. Δ^9 -THC enhances CB₂R^{+/+} splenocyte IL-2 cytokine secretion, but not CB₂R^{-/-} splenocyte IL-2 secretion. Splenocyte proliferation was determined by BrdU incorporation assay as described in the text. Cells were plated at 2×10^5 cells/0.1 mL/well in complete media. Cells were treated with 2.5 μ g/mL ConA and the indicated Δ^9 -THC concentration for 72 h. Data are experiments and are expressed as the mean of quadruplicate samples \pm standard deviation. Vehicle is absolute ethanol.

- As seen in Fig. 2, the CB₂R mediates THC-induced splenocyte IL-2 cytokine secretion, because this effect is not seen in the CB₂R^{-/-} cells. Perhaps more interesting is the finding that in CB₂R^{-/-} splenocytes IL-2 secretions are enhanced over those of CB₂R^{+/+} cells (Fig. 2). Effects similar to those of THC were observed with WIN55,212-2 and 2-AG on splenocyte cytokine secretion (data not shown).

3.3.2. T-CELL CYTOKINE ASSAYS

1. Twenty-four, 48, and 72 h after the cells are stimulated with ConA or plate-bound anti-CD3 antibody, remove 225 μ L of supernatant from each well and place into a sterile, flat-bottom, non-tissue-culture-treated 96-well microtiter plate. Store the plate containing the supernatant in the -70°C Revco freezer until it is assayed for specific cytokines using IL-2 and IL-4 BD Bioscience kits. The protocol included in the kit is followed to assess the concentration of IL-2 or IL-4 in the supernatant.
2. Quantify the colorimetric reaction product by measuring the absorbance of the samples at 450 nm (reference wavelength 570 nm) using the SpectraMax Plus Microplate Spectrophotometer plate reader (Molecular Devices, Sunnyvale, CA).
3. As seen in [Fig. 3](#), the CB₂R mediates WIN55,212-2-induced IL-2 cytokine secretion, because this effect is not seen in the CB₂R^{-/-} cells. Furthermore, in CB₂R^{-/-} T-cell IL-2 secretions are enhanced over those of CB₂R^{+/+} cells ([Fig. 3](#)).

3.4. Phagocytosis Assay

Phagocytosis is one of the first lines of defense against invading microorganisms. Macrophages play a central role in this process as a host defends against intruding foreign bodies. This phagocytosis assay was developed in order to further elucidate the level at which macrophage function is compromised, if at all, in the presence of cannabinoids.

3.4.1. Macrophage Treatment With Foreign Antigen

1. Thioglycolate-elicited peritoneal macrophages from CB₂R^{+/+} or CB₂R^{-/-} are plated and treated with cannabinoids as indicated in **Subheading 3.1.3**. After incubating with cannabinoids for 1 h, in order to reduce cannabinoid interference, media is removed and 1 mL of fresh complete media is added prior to the addition of the foreign particles. Ten to 25 μ L of opsonized microspheres or 100:1 bacteria to macrophage are added and allowed to incubate for 1 h at 37°C .
2. Following the 1-h incubation, decant the complete medium to remove non-phagocytized particles. Phagocytosis is stopped by applying several rinses of 0.5-mL cold PBS to each well.
3. Next, fix macrophages onto the coverslips with 0.25 mL warm fixing medium and incubate for 15 min at 55°C . Rinse cells several times with 0.5 mL warm PBS.
4. Permeabilize macrophages with 0.25 mL of warm permeabilization medium for 10 min at 37°C . Wash cells two times with 0.5 mL of warm PBS, with a 5-min incubation step between washes, to ensure complete elimination of the detergent, Triton X-100. Do a final wash with 0.25 mL of sterile distilled water in order to remove all the salts prior to mounting.
5. To mount the cover slips, one drop of warm mounting medium is dropped onto a clean slide. Immediately pry the cover slip from the bottom of the well using an 18-gage needle and sterile tweezers. Flip the cover slip so that the adherent macrophages are preserved and mounted directly on top of the mounting medium.

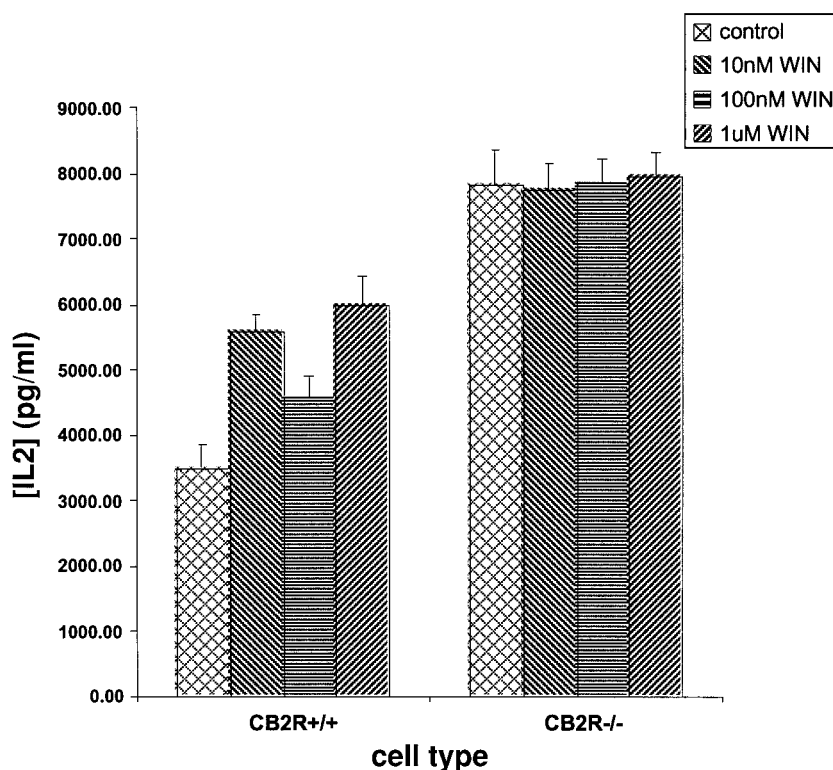


Fig. 3. WIN55-212,2 enhances CB₂R^{+/+} T cell IL-2 secretion, but not CB₂R^{-/-} T cell IL-2 secretion. IL-2 secretion was determined using the IL-2 kit from BD Biosciences as indicated in **Subheading 3**. Cells were plated at 2×10^5 cells/0.1 mL/well in complete media. Cells were treated with 2.5 μ g/mL ConA and the indicated Δ^9 -THC concentration for 72 h. Data are expressed as the mean of quadruplicate samples \pm standard deviation. Vehicle is absolute ethanol.

Finally, secure the cover slips with nail polish and allowed to dry overnight prior to viewing under the microscope.

3.4.2. Microscopic Analysis

1. The red-dyed latex beads are viewed with light microscopy under 40X magnification. The percent phagocytosis is determined by comparing the number of phagocytosing macrophages vs total macrophages present in the field. Macrophages with 5 or more red-dyed microspheres are considered positive for phagocytosis. A total of 200 macrophages are counted per mount.
2. Phagocytosis of microspheres and bacteria is determined using phase-contrast microscopy with a green fluorescent filter. Fluorescent-dyed microspheres and

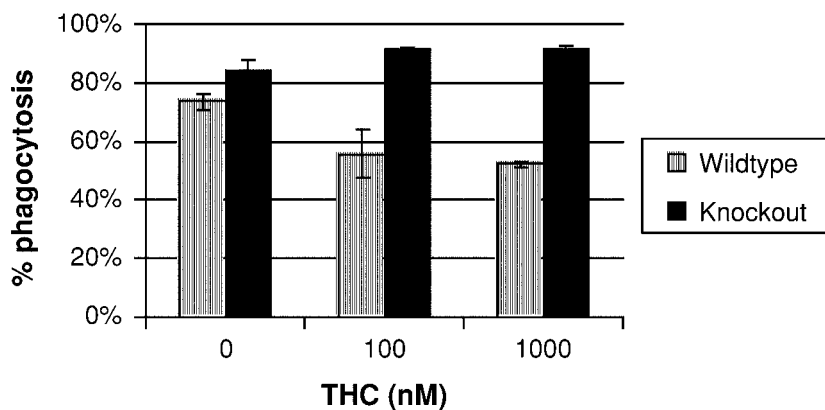


Fig. 4. Δ^9 -THC inhibits phagocytosis by $CB_2R^{+/+}$ macrophages, but not of $CB_2R^{-/-}$ macrophages. Thioglycolate-induced peritoneal macrophages were plated at a density of $0.5\text{--}1 \times 10^6$ cells/well as indicated in text and treated with the indicated concentrations of THC or 1% ethanol as vehicle control for 1 h. After 1 h, the cells were challenged with opsonized red-dyed microspheres. The cells were then processed for light microscopy as indicated in the text. Phagocytic activity, expressed at % phagocytosis, was determined by counting cells that had engulfed five or more red-dyed microspheres out of a field of 200 cells. Data are representative of three experiments and are expressed as the mean of triplicate samples \pm standard deviation.

GFP-expressing *E. coli* can be viewed under 20X or 40X magnification using a Nikon Eclipse TE300 microscope.

3. A field of interest is first visualized and photographed with the fluorescent filter. The same field is then photographed with the fluorescent filter. Resulting photographs are digitally overlaid using Metamorph Imaging Software, version 6.2r2 (Universal Imaging Corporation). An acceptable threshold of fluorescence inside and outside of the cell is then established using Metamorph. Based on the established parameters, quantification of phagocytosis is possible.
4. As seen in [Fig. 4](#), THC inhibits phagocytic activity of thioglycolate-induced peritoneal $CB_2R^{+/+}$ macrophages, but not of $CB_2R^{-/-}$ macrophages, suggesting that THC is, at least partially, acting through the CB_2R . Similar results are obtained when using WIN55-212-2 (data not shown).

3.5. Mitogen-Activated Protein Kinase Assay

3.5.1. Cell Lysis and Treatment

1. After obtaining the $CB_2R^{+/+}$ and $CB_2R^{-/-}$ spleens, transfer the spleens to a sterile 70 μ m nylon mesh filter screen covering a 50-mL conical centrifuge tube containing 5 mL of RPMI medium. Release the splenocytes from the spleens by gently pressing the spleens with the end of a 3-cc tuberculin syringe.

2. Carefully rinse the cell suspension in the filter screen with 15 mL of RPMI medium to harvest all the spleen cells.
3. Perform a cell count using a hemacytometer by making a 1:10 dilution of the splenocyte suspension with serum-free media and then a 1:2 dilution with 0.4% stock concentration of trypan blue.
4. Resuspend cells at a starting working concentration of 0.9×10^7 cells/mL. Further serially dilute into 0.6×10^7 cells/mL and 0.3×10^7 cells/mL. Plate two sets, in a total volume of 500 μ L, into a 24-well plate in triplicates.
5. Add 20 μ g/mL LPS, in the presence or absence of cannabinoids (0, 0.01 μ M, 0.1 μ M, 1 μ M), for 4 min at 37°C. LPS stimulates the MAPK pathway in B cells.
6. Lyse splenocytes by adding 500 μ L of cell lysis buffer and Mg^{2+} /ATP cocktail plus 4 μ g MBP and incubating for 20 min at 37°C with agitation.
7. Add 200 μ L of cell lysate to mouse anti-human phosphorylated MBP antibody-coated 96-well microtiter plates (*see below*) at 4°C, overnight.

3.5.2. Enzyme-Linked Immunosorbent Assay

1. In triplicates, bind 100 ng/well, at a final volume of 100 μ L, mouse anti-human phosphorylated MBP to a 96-well microtiter plate at 4°C, overnight. Include wells for 5 standards in triplicates and an extra triplicate set for the detection of background signal.
2. Using an immuno-wash, wash twice with 1X wash buffer.
3. Add 100 μ L of blocking buffer for 60 min at room temperature.
4. Wash twice with 1X wash buffer.
5. Add 200 μ L of cell lysate to mouse anti-human phosphorylated MBP antibody-coated 96-well microtiter plates at 4°C overnight. For the standards, add 0, 1, 2, 4, and 8 μ g of the custom-made peptide (phosphorylated MBP). Add 1X PBS to wells for background signal detection.
6. Wash five times with 1X wash buffer.
7. Add 100 μ L of mouse anti-human phosphorylated MBP, diluted 1:1000 in dilution buffer, for 60 min at room temperature.
8. Wash five times with 1X wash buffer.
9. Add 100 μ L of affinity-purified sheep anti-mouse IgG conjugated to alkaline phosphatase, diluted 1:1000 in dilution buffer, for 60 min at room temperature.
10. Wash five times with 1X wash buffer.
11. Add 100 μ L of the pNPP substrate system for ELISA and wait until a yellow color develops. The reaction is normally completed within 10 min. Read absorbance at 405 nm with a microplate reader.

4. Notes

1. The viscosity of the mounting media will decrease if PVA is dissolved over longer periods of time (i.e., 8 h).
2. It is strongly recommended that leupeptin, DTT, PMSF, and ATP be freshly added before usage.
3. This antibody can be used for both immunoblots and ELISAs. It should be stored at 20°C for prolonged usage, although it also can be stored at 4°C for a short peri-

od of time. Numerous competitive reagents are available from other commercial sources.

4. *p*-Nitrophenyl phosphate is the preferred substrate for enzyme immunoassays using microtiter plates because the reaction product is water-soluble, whereas substrates that form precipitates are not recommended.
5. Custom-made peptides can be purchased from various commercial sources. Storage conditions are dependent on the characteristics of the peptide. Low concentrations of sodium azide are sufficient to prevent fungal contamination. At high concentrations the enzymatic activity of alkaline phosphatase will be inhibited.

References

1. Berdyshev, E. V., et al. (1997) Influence of fatty acid ethanolamides and delta-9-tetrahydrocannabinol on cytokine and arachidonate release by mononuclear cells. *Eur. J. Pharmacol.* **330**, 231–240.
2. Klein, T. W., Friedman, H., and Specter, S. (1998) Marijuana, immunity and infection. *J. Neuroimmunol.* **83**, 102–115.
3. Klein, T. W., Newton, C., and Friedman, H. (1998) Cannabinoid receptors and immunity. *Immunol. Today* **19**(8), 373–381.
4. Srivastava, M. D., B.I.S. Srivastava, B. I. S., and Brouhard, B. (1998) Delta-9-tetrahydrocannabinol and cannabidiol alter cytokine production by human immune cells. *Immunopharmacology*. **40**, 179–185.
5. Berdyshev, E. V. (2000) Cannabinoid receptors and the regulation of immune response. *Chem. Phys. Lipids* **108**, 169–190.
6. Gonsiorek, W., et al. (2000) Endocannabinoid 2-arachidonyl glycerol is a full agonist through human type 2 cannabinoid receptor: antagonism by anandamide. *Mol. Pharmacol.* **57**, 1045–1050.
7. Gardner, B., et al. (2002) Autocrine and paracrine regulation of lymphocyte CB2 receptor expression by TGF- β . *Biochem. Biophys. Res. Commun.* **290**, 91–96.
8. Parolaro, D., et al. (2002) Endocannabinoids in the immune system and cancer. *Prostaglandins, Leukotrienes Essential Fatty Acids* **66**(2&3), 319–332.
9. Yuan, M., et al. (2002) Delta-9-tetrahydrocannabinol regulates Th1/Th2 cytokine balance in activated human T cells. *J. Neuroimmunol.* **133**(1–2), 124–131.
10. Ihenetu, K., et al. (2003) Pharmacological characterisation of cannabinoid receptors inhibiting interleukin 2 release from human peripheral blood mononuclear cells. *Eur. J. Pharmacol.* **464**, 207–215.
11. Klein, T., et al. (2004) Cannabinoid receptors and T helper cells. *J. Neuroimmunol.* **147**, 91–94.
12. Lopez-Rodriguez, M L., et al. (2005) Involvement of cannabinoids in cellular proliferation. *Mini Rev. Med. Chem.* **5**(1), 97–106.
13. Rodriguez de Fonseca, F., et al. (2005) The endocannabinoid system: physiology and pharmacology. *Alcohol*, **40**(1), 2–14.
14. Matsuda, L., et al. (1990) Structure of a cannabinoid receptor and functional expression of the cloned cDNA. *Nature*. **346**, 561–564.

15. Munro, S., Thomas, K. L., and Abu-Shaar, M. (1993) Molecular characterization of a peripheral receptor for cannabinoids. *Nature*. **365** 61–65.
16. Felder, C. C. and. Glass, M. (1998) Cannabinoid receptors and their endogenous agonists. *Annu. Rev. Pharmacol. Toxicol.*, **38**, 179–200.
17. Herkenham, M., Lynn A. B., Johnson, M. R., Melvin, L. S., de Costa, B. R., Rice, K. C. (1991) Characterization and localization of cannabinoid receptors in rat brain: a quantitative in vitro autoradiographic study. *J. Neurosci.* **11**(2), 563–583.
18. Glass, M., Dragunow, M. and. Faull, R. L. M. (1997) Cannabinoid receptors in the human brain—a detailed anatomical and quantitative autoradiographic study in the fetal, neonatal and adult human brain. *Neuroscience* **77**(2), 299–18.
19. Buckley, N. E., Hansson, S., Harta, G., Mezey, E. (1998) Expression of the CB1 and CB2 receptor mRNAs during embryonic development in the rat. *Neuroscience* **82**(4), 1131–1149.
20. Bouaboula, M., Rinaldi, M., Carayon, P., et al. (1993) Cannabinoid-receptor expression in human leukocytes. *Eur. J. Biochem.* **214**, 173–180.
21. Daaka, Y., Klein, T. W., and Friedman, H. (1995) Expression of cannabinoid receptor mRNA in murine and human leukocytes. *Adv. Exp. Med. Biol.* **373**, 91–96.
22. Galiegue, S., et al. (1995) Expression of central and peripheral cannabinoid receptors in human immune tissues and leukocyte subpopulations. *Eur. J. Biochem.* **232**, 54–61.
23. Schatz, A. R., Lee, M., Condie, R. B., Pulaski, J. T., Kaminski, N. E. (1997) Cannabinoid receptors CB1 and CB2: a characterization of expression and adenylylate cyclase modulation within the immune system. *Toxicol. Appl. Pharmacol.* **142**, 278–287.
24. Kaminski, N. E., Abood, M. E., Kessler, F. K., Martin, B. R., Schatz, A. R. (1992) Identification of a functionally relevant cannabinoid receptor on mouse spleen cells that is involved in cannabinoid-mediated immune modulation. *Mol. Pharmacol.* **42**, 736–742.
25. McAllister, S. D. and Glass, M. (2002) CB1 and CB2 receptor-mediated signalling: a focus on endocannabinoids. *Prostaglandins, Leukotrienes Essential Fatty Acids*, **66**(2&3), 161–171.
26. Howlett, A. C., Breivogel, C. S., Childers, S. R., Deadwyler, S. A., Hampson, R. E., Porrino, L. J. (2004) Cannabinoid physiology and pharmacology: 30 years of progress. *Neuropharmacology* **47**, 345–358.
27. Bouaboula, M., Poinot-Chazel, C., Marchand, J. et al. (1996) Signaling pathway associated with stimulation of CB2 peripheral cannabinoid receptor. Involvement of both mitogen-activated protein kinase and induction of Krox-24 expression. *Eur J. Biochem.* **237**, 704.
28. Ellert-Miklaszewska, A., Kaminska, B., and. Konarska, L. (2005) Cannabinoids down-regulate PI3K/Akt and Erk signalling pathways and activate proapoptotic function of Bad protein. *Cell Signal* **17**(1), 25–37.
29. Karanian, D. A., Brown, Q. B., Makriyanis, A., Bahr, B. A. (2005) Blocking cannabinoid activation of FAK and ERK1/2 compromises synaptic integrity in hippocampus. *Eur. J. Pharmacol.* **508**(1–3), 47–56.

30. Powles, T., te Poele, R., Shamash, J., et al. (2005) Cannabis-induced cytotoxicity in leukemic cell lines: the role of the cannabinoid receptors and the MAPK pathway. *Blood* **105**(3), 1214–1221.
31. Buckley, N. E., McCoy, K. L., Mezey, E., et al. (2000) Immunomodulation by cannabinoids is absent in mice deficient for the cannabinoid CB2 receptor. *Eur. J. Pharmacol.* **396**, 141–49.
32. Chuchawankul, S., Shima, M., Buckley, N. E., Hartmann, C. B., McCoy, K. L. (2004) Role of cannabinoid receptors in inhibiting macrophage costimulatory activity. *Int. Immunopharmacol.* **4**(2), 265–278.
33. Rinaldi-Carmona, M., Barth F., Millan, J., et al. (1998) SR 144528, the first and selective antagonist of the CB2 cannabinoid receptor. *J. Pharmacol. Exp. Ther.* **284**(2), 644–650.
34. Carayon, P., Marchand, J., Dussossoy, D., et al. (1998) Modulation and functional involvement of CB2 peripheral cannabinoid receptors during B-cell differentiation. *Blood* **92**(10), 3605–3615.
35. Bouaboula, M., Desnoyer, N., Carayon, P., Combes, T., Casellas, P. (1999) Gi protein modulation induced by a selective inverse agonist for the peripheral cannabinoid receptor CB2: implication for intracellular signalization cross-regulation. *Mol. Pharmacol.* **55**, 473–480.
36. Bouaboula, M., Dussossoy, D., and Casellas, P. (1999) Regulation of peripheral cannabinoid receptor CB2 phosphorylation by the inverse agonist SR 144528. implications for receptor biological responses. *J. Biol. Chem.* **274**(29), 20397–20405.
37. Portier, M., Rinaldi-Carmona, M., Pecceu, F., et al. (1999) SR144528, an antagonist for the peripheral cannabinoid receptor that behaves as an inverse agonist. *J. Pharmacol. Exp. Ther.* **288**(2), 582–589.

Localization of Cannabinoid Receptors Using Immunoperoxidase Methods

Guy A. Cabral

Summary

Two cannabinoid receptors have been identified to date. The first of these, designated CB₁, is localized primarily in the central nervous system but is also present at lower levels in other tissues. The second receptor, CB₂, has been found natively in cells of the immune system. Both receptors have an extracellular amine-terminal domain, seven transmembrane domains, an intracellular carboxy-terminal domain, and are coupled through G proteins to adenylate cyclase and mitogen-activated protein kinase. In this chapter, a series of experimental protocols is presented that allows for the systematic identification and localization of cannabinoid receptors in tissues and cells. Immunoperoxidase staining for light microscopy is complemented with correlative application for electron microscopy. This approach is followed by that using immunogold labeling for high-resolution definition of cannabinoid receptor distribution at the ultrastructural level.

Key Words: Cannabinoid receptors; CB₁ receptor; CB₂ receptor; electron microscopy; immunocytochemistry; immunoelectron microscopy; immunogold; immunohistochemistry; immunoperoxidase.

1. Introduction

It is now recognized that at least two cannabinoid receptors exist. The first of these, designated CB₁, was the first to be identified and is present at high levels in brain and testis (1–4), although it has been identified at relatively low levels in other tissues and cells of the immune system (5). The second cannabinoid receptor, designated CB₂, is found primarily in cells of the immune system (5–9). The CB₁ is highly conserved among mammalian species, as exemplified by the greater than 97% sequence identity shared between mice, rats, and humans (10). In contrast, the CB₂ exhibits greater mammalian interspecies variation. For example, cloning of the murine CB₂ has indicated that it shares 82%

sequence identity with the human CB₂ (11). Both receptor types are coupled through G proteins to adenylate cyclase and mitogen-activated protein kinase. The CB₁ also is coupled to several types of calcium and potassium channels. Structurally, both receptors have an extracellular amine-terminal domain, seven transmembrane domains, and an intracellular carboxy-terminal domain. The CB₁ and CB₂ share 48% amino acid sequence identity overall but greater than 80% homology for transmembranal regions constituting the putative ligand-binding site.

Consideration of the structure and distribution of cannabinoid receptors is critical to the successful application of immunocytochemical approaches to the identification of cannabinoid receptors in cells and tissues. CB₁ and CB₂ receptors exhibit greatest type specificity at their extracellular amine-terminal domains. Thus, experiments designed for identification of cannabinoid type-specific receptor expression at the protein level should entail use of affinity-purified antibodies directed against the amine-terminal domains. Use of such antibodies is also critical for the identification of cell surface expression of cannabinoid receptors. On the other hand, if assessment of expression of fully processed receptor protein is required, then antibodies directed against carboxy-terminal domains of the CB₁ or CB₂ should be considered. Immunocytochemical methods in which such antibody preparations are considered should include a limited cell/tissue solubilization so as to allow for adequate antibody penetration. A list of commercially available antibodies to domains of CB₁ and CB₂ receptors is included in Table 1. In addition, various laboratories have applied these commercially available antibodies (or have developed their own antibodies) to the identification of cannabinoid receptors at the fluorescence, light, and electron microscopy levels. Table 2 lists references in which immunocytochemical approaches have been utilized for the identification of cannabinoid receptors in a variety of tissues and cell types.

A second consideration to be applied to the immunocytochemical or histochemical identification of cannabinoid receptors is recognition of receptor tissue distribution and levels at which these receptors are expressed within the respective tissues. Expression of the CB₁ protein is highest in brain, at relatively moderate levels in testis, and at low levels in other tissues including cells of the immune system. In contrast, native expression of the CB₂ has been reported to be limited to cells of the immune system with a rank order of expression of highest levels for B lymphocytes followed in order by natural killer cells, cells of macrophage lineage (e.g., monocytes, macrophages, and microglia), and T lymphocytes. However, Carlisle et al. (12) have demonstrated in vitro that the CB₂ undergoes differential expression in murine peritoneal macrophages and neonatal rat cerebrocortical microglia in relation to cell activation state, although a similar series of events has yet to be demonstrated definitively in

Table 1
List of Commercially Available Cannabinoid Receptor Immunological Reagents
Applicable to Cytochemical and/or Histochemical Procedures

Reagent	Comments	Company/cat. no.
Anti-cannabinoid CB ₁	Polyclonal antibody (affinity-purified IgG)	Cayman Chemical Co., Ann Arbor, MI (cat. no. 101500)
Anti-cannabinoid CB ₁	Affinity-purified rabbit IgG directed against first 77 amino acids of the receptor N-terminus of CB ₁	Calbiochem-Novabiochem Corp., La Jolla, CA (cat. no. 209550)
Anti-cannabinoid CB ₁	Affinity-purified rabbit IgG directed against amino acids 1–14 of the receptor N-terminus of CB ₁ ; reacts with human, mouse, and rat	Calbiochem-Novabiochem Corp., La Jolla, CA (cat. no. 216401)
Anti-cannabinoid CB ₁	Affinity-purified rabbit antibody directed against the N-terminal region; reacts with human	Sigma, St. Louis, MO (cat. no. C8985)
Anti-cannabinoid CB ₁	Affinity-purified rabbit antibody directed against amino acids 1–99 of the N-terminal region; reacts with human	Sigma, St. Louis, MO (cat. no. C1108)
Anti-cannabinoid CB ₁	Affinity-purified rabbit antibody directed against amino acids 1–77 of the N-terminal region; reacts with rat	Sigma, St. Louis, MO (cat. no. C1233)
Anti-phospho-cannabinoid CB ₁ (pSer ³¹⁶)	Affinity-purified rabbit antibody directed against polypeptide derived from region of CB ₁ containing serine 316; conserved in human, mouse, and rat	Sigma, St. Louis, MO (cat. no. C9980)
Anti-cannabinoid CB ₂	Polyclonal antibody (affinity-purified IgG)	Cayman Chemical Co., Ann Arbor, MI (cat. no. 101550)
Anti-cannabinoid CB ₂	Affinity-purified rabbit IgG directed against first 33 amino acids of the receptor N-terminus of CB ₂ ; reacts with human	Calbiochem-Novabiochem Corp., La Jolla, CA (cat. no. 209552)

(continues)

Table 1
(Continued)

Reagent	Comments	Company/cat. no.
Anti-cannabinoid CB ₂	Affinity-purified rabbit IgG directed against amino acids 20–33 at the amine terminus of CB ₂ ; reacts with human	Calbiochem-Novabiochem Corp., La Jolla, CA (cat. no. 216407)
Anti-cannabinoid CB ₂	Affinity-purified rabbit IgG directed against the first 32 amino acids at the amine terminus of CB ₂ ; reacts with rat	Calbiochem-Novabiochem Corp., La Jolla, CA (cat. no. 209554)
Anti-cannabinoid CB ₂	Affinity-purified rabbit antibody directed against amino acids 1–33 at the amine terminus of CB ₂ ; reacts with human	Sigma, St. Louis, MO (cat. no. C1358)
Anti-cannabinoid CB ₂	Affinity-purified rabbit antibody directed against amino acids 1–32 at the amine terminus of CB ₂ ; reacts with mouse	Sigma, St. Louis, MO (cat. no. C1483)
CB ₁ receptor blocking peptide	Blocking peptide for use with anti-cannabinoid CB ₁ (Cayman no. 101500)	Cayman Chemical Co., Ann Arbor, MI (cat. no. 301500)
CB ₂ receptor blocking peptide	Blocking peptide for use with anti-cannabinoid CB ₂ (Cayman no. 101550)	Cayman Chemical Co., Ann Arbor, MI (cat. no. 301550)
(pSer ³¹⁶) - cannabinoid CB ₁	Positive control peptide of anti-phospho-cannabinoid CB ₁ (pSer ³¹⁶)	Sigma, St. Louis, MO (cat. no. C9110)
(Ser ³¹⁶) - cannabinoid CB ₁	Negative control peptide of anti-phospho-cannabinoid CB ₁ (pSer ³¹⁶)	Sigma, St. Louis, MO (cat. no. C9360)

vivo. Thus, at least as relates to assessment of expression in immune cells, the state of activation should be considered. Immunofluorescence techniques lend themselves to the identification of receptors in tissues or cells, such as brain or cultured cells stably transfected or infected with a variety of expression constructs in which they are expressed at high levels. However, for tissues in which cannabinoid receptors are expressed at modest or low levels, immunocyto-

Table 2**Select References of Studies in Which Immunocytochemical Methods Have Been Used to Localize Cannabinoid Receptors**

-
- Bridges, D., Rice, A. S., Egertová, M., Elphick, M. R., Winter, J., and Michael, G. J. (2003) Localization of cannabinoid receptor 1 in rat dorsal root ganglion using in situ hybridization and immunohistochemistry. *Neuroscience* **119** (3), 803–812.
- Casu, M. A., Porcella, A., Ruiu, S., et al. (2003) Differential distribution of functional cannabinoid CB1 receptors in the mouse gastroenteric tract. *Eur. J. Pharmacol.* **459** (1), 97–105.
- Egertová, M., and Elphick, M. R. (2000) Localization of cannabinoid receptors in the rat brain using antibodies to the intracellular C-terminal tail of CB. *J. Comp. Neurol.* **422** (2), 159–171.
- Harkany, T., Hartig, W., Berghuis, P., et al. (2003) Complementary distribution of type 1 cannabinoid receptors and vesicular glutamate transporter 3 in basal forebrain suggests input-specific retrograde signaling by cholinergic neurons. *Eur. J. Neurosci.* **18** (7), 1979–1992.
- Hernandez, M., Berrendero, F., Suarez, I., et al. (2000) Cannabinoid CB(1) receptors colocalize with tyrosine hydroxylase in cultured fetal mesencephalic neurons and their activation increases the levels of this enzyme. *Brain Res.* **857** (1-2), 56–65.
- Kulkarni-Narla, A., and Brown, D. R. (2000) Localization of CB1-cannabinoid receptor immunoreactivity in the porcine enteric nervous system. *Cell Tissue Res.* **302** (1), 73–80.
- Lu, X. R., Ong, W. Y., and Mackie, K. (1999) A light and electron microscopic study of the CB1 cannabinoid receptor in monkey basal forebrain. *J. Neurocytol.* **28** (12), 1045–1051.
- McDonald, A. J., and Mascagni, F. (2001) Localization of the CB1 type cannabinoid receptor in the rat basolateral amygdala: high concentrations in a subpopulation of cholecystokinin-containing interneurons. *Neuroscience* **107** (4), 641–652.
- McIntosh, H. H., Song, H., and Howlett, A. C. (1998) CB1 cannabinoid receptor: cellular regulation and distribution in N18TG2 neuroblastoma cells. *Brain Res. Mol. Brain Res.* **53** (1-2), 163–173.
- Moldrich, G., and Wenger, T. (2000) Localization of the CB1 cannabinoid receptor in the rat brain. An immunohistochemical study. *Peptides* **21** (11), 1735–1742.
- Nowell, K. W., Pettit, D. A., Cabral, W. A., Zimmerman, Jr., H. W., Abood, M. E., and Cabral, G. A. (1998) High-level expression of the human CB2 cannabinoid receptor using a baculovirus system. *Biochem. Pharmacol.* **55** (11), 1893–1905.
- Ong, W. Y., and Mackie, K. (1999) A light and electron microscopic study of the CB1 cannabinoid receptor in the primate spinal cord. *J. Neurocytol.* **28** (1), 39–45.
- Ong, W. Y., and Mackie, K. (1999) A light and electron microscopic study of the CB1 cannabinoid receptor in primate brain. *Neuroscience* **92** (4), 1177–1191.
- Pettit, D. A., Harrison, M. P., Olson, J. M., Spencer, R. F., and Cabral, G. A. (1998) Immunohistochemical localization of the neural cannabinoid receptor in rat brain. *J. Neurosci. Res.* **51** (3), 391–402.
- Straiker, A., and Sullivan, J. M. (2003) Cannabinoid receptor activation differentially modulates ion channels in photoreceptors of the tiger salamander. *J. Neurophysiol.* **89** (5), 2647–2654.
- Straiker, A. J., Maguire, G., Mackie, K., and Lindsey, J. (1999) Localization of cannabinoid CB1 receptors in the human anterior eye and retina. *Invest. Ophthalmol. Vis. Sci.* **40** (10), 2442–2448.
- Tsou, K., Brown, S., Sanudo-Pena, M. C., Mackie, K., and Walker, J. M. (1998) Immunohistochemical distribution of cannabinoid CB1 receptors in the rat central nervous system. *Neuroscience* **83** (2), 393–411.
- Tsou, K., Mackie, K., Sanudo-Pena, M. C., and Walker, J. M. (1999) Cannabinoid CB1 receptors are localized primarily on cholecystokinin-containing GABAergic interneurons in the rat hippocampal formation. *Neuroscience* **93** (3), 969–975.
- Waksman, Y., Olson, J. M., Carlisle, S. J. and Cabral, G. A. (1999) The central cannabinoid receptor (CB1) mediates inhibition of nitric oxide production by rat microglial cells. *J. Pharmacol. Exp. Ther.* **288** (3), 1357–1366.
- Yang, Z. M., Paria, B. C., and Dey, S. K. (1996) Activation of brain-type cannabinoid receptors interferes with preimplantation mouse embryo development. *Biol. Reprod.* **55** (4), 756–761.
-

chemical procedures that entail the use of horseradish peroxidase (HRPO) linked to antibody are recommended owing to the sensitivity of these methods.

A third consideration centers around the application of immunocytochemical or histochemical methods for detection of cannabinoid receptors at the light microscopy vs the electron microscopy levels. A critical issue in ultrastructural analysis is the maintenance of tissue and cellular integrity while retaining antigenicity of target molecules and permitting access of cognate antibody probes. Unfortunately, fixatives classically used for optimizing ultrastructural integrity also destroy most antigens and preclude entrance of antibody probes into cells. Thus, any immunoelectron microscopic approach to be applied constitutes a compromise between application of measures that permit specific antibodies to target specific antigenic sites while maintaining recognizable tissue and cellular ultrastructure. For immunoelectron microscopy two general approaches may be applied. The first of these is through the exposure of cells and tissues to primary anti-cannabinoid receptor antibody followed by treatment with a secondary HRPO-conjugated antibody probe, the species specificity of which is directed against that of the primary antibody. Limitations of this approach are that (1) fine features of intracellular and cytoplasmic components such as rough endoplasmic reticula and other membranous compartments may not be retained as a consequence of treatment of tissues or cells with solubilization agents and (2) resolution of targeted antigenic sites may be limited since product from the immunoperoxidase reaction may diffuse. However, under carefully designed probing and incubation conditions, these potential confounding issues can be minimized. The second approach to ultrastructural analysis is to first embed the cells or tissues in resin, section the resin-embedded material, and then expose thin sections to anti-cannabinoid receptor antibody followed by exposure to a secondary antibody conjugated to gold. This immunogold approach has the advantage of allowing for better ultrastructural preservation of cellular structures and greater resolution of labeling for specific antigenic sites. A disadvantage, however, is that immunogold labeling is generally less sensitive than that in which immunoperoxidase labeling is applied. Thus, a reasonable approach to be applied to the identification and localization of cannabinoid receptors is to first apply correlative light and electron microscopy immunoperoxidase labeling. If higher ultrastructural resolution of immunolabeling is required, this approach can be followed by that using immunogold labeling.

In this chapter we outline a general approach for the identification and localization of cannabinoid receptors within cells and tissues using correlative light and electron microscopy immunoperoxidase procedures. This approach, then, is followed by that using immunogold at the ultrastructural level, which can be applied to high-resolution localization of cannabinoid receptors.

2. Materials

1. Isopentane.
2. Liquid nitrogen.
3. Model Minotome Microtome Cryostat (Damon/IEC Division) or comparable instrument.
4. Coplin staining jar or a glass slide rack (Fisher Scientific, Pittsburgh, PA).
5. Glass slides.
6. Subbed slides: Dissolve gelatin (1 g) in 1 L of hot distilled water. Cool and add 0.1 g chromium potassium sulfate. Store in refrigerator. Dip slides two to three times in the solution. Drain and dry in a vertical position. Store in a dust-free box.
7. Humidified chamber: Falcon no.1058 polystyrene Petri dish (150 × 15 mm). Line inside of dish with Parafilm and place six droplets (50 μ L each) of 0.85% saline onto the Parafilm along the inner rim of the dish so as to circumscribe it. Placing the Petri dish cover on the bottom half of the Petri dish creates a humidified container.
8. Endogenous peroxidase activity blocking solution: Acid alcohol (add 1.0 mL HCl to 100 mL of 70% ethyl alcohol) or 0.1% phenylhydrazine in phosphate-buffered saline (PBS).
9. Blocking buffer: SuperBlock blocking buffer in PBS (Pierce, Rockford, IL); alternatively, use a blocking buffer consisting of 1% normal goat serum (NGS) and 1% bovine serum albumin (BSA) in PBS.
10. 10X PBS: NaCl (80 g), KCl (2 g), $\text{Na}_2\text{HPO}_4 \cdot 7\text{H}_2\text{O}$ (11.5 g), KH_2PO_4 (2 g) in a final volume of 1 L.
11. Primary antibody: Rabbit antibodies to cannabinoid receptors (*see* [Table 1](#)).
12. Secondary antibody: HRPO-conjugated IgG goat anti-rabbit IgG (heavy and light chains, Organon Teknika Cappel, Durham, NC).
13. Antibody controls: Normal rabbit IgG control (Organon Teknika Cappel, Durham, NC) or preimmune serum from rabbit used to make the anti-cannabinoid receptor antibody; antigen added in excess to primary antibody (*see* [Table 1](#)).
14. Staining dishes.
15. Plastic slide box.
16. 0.2% Triton X-100/PBS: Add 200 μ L Triton X-100 to 1X PBS.
17. Hanker-Yates reagent (Polysciences, Warrington, PA): Hanker-Yates mixture (7.5 mg), Tris-HCl buffer, 0.05 M, pH 7.6 (10 mL), hydrogen peroxide, 1% (0.1 mL).
18. Cresyl violet acetate (0.1%): Add 100 mg cresyl violet acetate to distilled water to make a final volume of 100 mL. Filter with a Whatman no. 2 filter paper.
19. Light microscopy aqueous mounting medium: Aquamount Aqueous Mountant (Lerner Laboratories, Pittsburgh, PA); Crystal/Mount Permanent Aqueous Mounting Medium (Biomeda Corp., Foster City, CA).
20. Permout Histological Mounting Medium (Fisher Scientific, Company, Pittsburgh, PA).
21. Large glass cover slips (No.1, 22 X 50 mm; Arthur H. Thomas Co., Philadelphia, PA).
22. 0.05 M Tris-HCl buffer, pH 7.6 (store at room temperature): Trizma HCl (6.06 g), Trizma base (1.39 g). Bring to 1 L with distilled water.

23. 2% Formalin in PBS (50 mL): Weigh 1 g of paraformaldehyde and add to 25 mL reagent-grade water. Heat the solution to 60°C on a heating-stir plate in a chemical hood. Once the temperature has reached 60°C, immediately remove from the heat. Transfer to another stir plate and add 10 *N* NaOH (approximately two to three drops) until the cloudy solution clears. Allow the solution to cool. Add 20 mL of reagent-grade water and 5 mL of 10X PBS. Filter and store at 4°C for no more than 1 wk.
24. 12-mm No.1 round glass cover slips (Arthur H. Thomas Co., Philadelphia, PA), sterilized by autoclaving or soaking in 70% ethanol.
25. 150-mm Petri dishes.
26. Ethanol.
27. Xylene.
28. Equipment and facilities for paraffin embedding and tissue sectioning.
29. Slide warmer (GCA Precision Scientific, Chicago, IL).
30. Liquid release agent (Electron Microscopy Sciences, Fort Washington, PA).
31. Acetone.
32. Vibratome (Vibratome Series 2000, Technical Products International Inc., St. Louis, MO) or similar instrument.
33. Hemostat.
34. Blunt 13 G and 15 G hypodermic needles.
35. Ultramicrotome for cutting thin plastic sections.
36. Tools for removing brain (Fine Science Tools (USA), Inc., Foster City, CA): 17-cm standard tough cut scissors (no. 14110-17), spring scissors angled to side with a 10-mm cutting edge (no. 15006-09), 14.5-cm straight forceps (no. 11000-14), 16-cm angled forceps (no. 11080-02), Dumont forceps (no. 11295-51), standard scalpel handle (no. 10003-12).
37. Anesthesia: Administer sodium pentobarbital intraperitoneally to mouse or rat at 60 mg/kg. Verify animal death by absence of cardiac pulse and presence of fixed/dilated pupils. Pinch animal in foot to verify absence of response.
38. Rotary mixer (Penetron Mark IIIB, Sunkay Laboratories, Inc., Tokyo, Japan).
39. Perfusion instruments.
40. Tygon tubing.
41. Peristaltic pump.
42. Avidin/Biotinylated Enzyme Complex (ABC) kit (Vector Laboratories, Burlingame, CA).
43. Glass vials with caps (Fisher Scientific, Pittsburgh, PA).
44. Camel's hairbrush.
45. Poly-L-lysine: Add 25 μ L of 1 mg/mL to each sterilized no.1 cover slip in a hood and allow to stand (10 min). Rinse cover slips three times with sterile distilled water and air dry.
46. Perfusion fixative (4% paraformaldehyde and 0.1% glutaraldehyde in 0.1 *M* phosphate buffer): Add 20 g paraformaldehyde to 200 mL distilled water and heat to 60°C. Add 1 *N* NaOH until solution clears and allow solution to slightly cool. Add 125 mL 0.4 *M* standard phosphate buffer and cool to 20°C on ice. Add 2 mL puri-

- fied 25% glutaraldehyde and 2 mL 0.5% calcium chloride and adjust pH to 7.2. Add distilled water to make 500 mL.
47. Perfusion prewash solution (mouse, rat): Add in the following order: 0.4 M standard phosphate buffer (50 mL), NaCl (1.8 g), 0.5% calcium chloride (0.8 g), and heparin sodium (1000 IU/mL). Adjust pH to 7.2. Add distilled water to make 200 mL.
48. 0.4 M Standard phosphate buffer, pH 7.2: Add in order sodium phosphate, monobasic (10.6 g); potassium phosphate, dibasic (56 g); distilled water (800 mL). Adjust pH to 7.2 with NaOH or HCl. Add distilled water to make 1 L.
49. 0.1 M Sodium phosphate buffer: To 100 mL distilled water add sodium phosphate (Sigma-Aldrich S-0876) (3.55 g) and 0.5 % calcium chloride (1 mL). Adjust pH to 7.2 using HCl and add distilled water to make 250 mL.
50. Double strength buffer for osmium tetroxide (0.2 M phosphate buffer with 0.04 mM CaCl_2 and 14% dextrose): Dextrose (14 g), 0.4 M standard phosphate buffer (50 mL), 0.5% calcium chloride, anhydrous (0.8 mL).Add distilled water to make 100 mL.
51. Osmium solution (1.0% osmium tetroxide in 0.1 M phosphate buffer with 7% dextrose and 0.02 mM CaCl_2 and 1.5% potassium hexacyanoferrate): Double strength buffer (5 mL), 2% osmium tetroxide solution (5 mL) (0.5 g OsO_4 /25 mL distilled water), potassium hexacyanoferrate (0.15 g).
52. 2% Osmium: Distilled water (25 mL, osmium tetroxide (0.5 g). Pour liquid nitrogen into a plastic cup and immerse vial of osmium to crystallize. Score the vial of osmium using a file and place into a white silicon holder. Snap vial open and put crystallized osmium into 25-mL Erlenmeyer flask with a stopper. Add distilled water to osmium under a chemical hood. Wrap Parafilm tightly around flask and stopper. Store in refrigerator. It will take at least 24 h to dissolve.
53. Sodium hydrogen maleate–NaOH buffer solutions (Sodium hydrogen maleate, $\text{NaHC}_4\text{H}_2\text{O}_4 \cdot 3\text{H}_2\text{O}$, MW 192.11): 0.2 M solution is prepared by dissolving in distilled water 23.2 g maleic acid (requires heating), and mixing with 200 mL 1 N NaOH and diluting to 1 L with distilled water. Prepare for appropriate pH as follows: to 25 mL 0.2 M NaH maleate add x mL 0.1 M (N) NaOH and dilute to 100 mL with distilled water.

pH at 25°C	x
5.2	7.2 mL
6.0	26.9 mL

54. 0.5% Uranyl acetate (Sigma-Aldrich, St. Louis, MO): Uranyl acetate powder (50 mg), 0.05 M sodium hydrogen maleate–NaOH buffer, pH 6.0 (10 mL).
55. TAAB 812 Embedding resin: TAAB 812 (12.00 g), dodecyl succinic anhydride (4.75 g), nadic methyl anhydride (8.25 g), DMP-30 (0.50 g). Weigh first three components into 50-mL disposable beaker using Pasteur pipets. Mix thoroughly first with stirring rod and then with magnetic stirrer for 30 min covered tightly with Parafilm. Before use, add DMP-30 to mixture, and mix thoroughly and slowly with magnetic stirrer for 30 min. Place under vacuum in a desiccator to remove air

before use. Mixture may be stored in desiccator in freezer indefinitely, but allow desiccator to reach room temperature before removing.

56. Resin stubs: Place resin into size 00 BEEM capsules (Ted Pella, Redding, CA). Place capsules with pointed side up in a 60°C oven for 2–3 d to harden.
57. 10% Phosphate-buffered formalin: Made up fresh from (powdered) paraformaldehyde (Sigma-Aldrich, St. Louis, MO). Add 20 g to 50 mL distilled water. Heat to 60°C with stirring and then add drops of 1 *N* NaOH (usually about 12 drops) until solution clears. Cool. Add 10 mL 10X PBS. Bring final volume to 100 mL with distilled water.
58. Glutaraldehyde (Polysciences, Warrington, PA): Bought as 25% solution. Wear gloves and dispense in a fume hood.
59. 4% Paraformaldehyde, 0.25% glutaraldehyde in 0.1 *M* sodium cacodylate/HCl buffer: 10% formaldehyde (40 mL), 25% glutaraldehyde (1 mL), 0.2 *M* sodium cacodylate buffer (100 mL). Bring to 200 mL with distilled water.
60. 0.1 *M* Sodium cacodylate/HCl: Add 2.12 g sodium cacodylate to 50 mL distilled water. Adjust pH to 7.4 with 1 *N* HCl and bring to a final volume of 100 mL with distilled water. Store at 4°C for as long as 6 mo.
61. 0.2 *M* Sodium cacodylate/HCl: Prepare as described for 0.1 *M* sodium/cacodylate except that 4.24 g of sodium cacodylate are added.
62. Uranyl acetate, aqueous (Polysciences, Warrington, PA): Make up from powder as 0.5% aqueous solution then thoroughly mix and filter.
63. LR gold resin (Polysciences, Warrington, PA): Purchased as liquid resin and separate catalyst (benzoin methyl ether). The 0.1% benzoin methyl ether is added to the resin for the complete mixture.
64. Lead citrate (Polysciences, Warrington, PA): Made up from three stock solutions, which are: solution A) trisodium citrate (37.7g/100 mL); (solution B) lead nitrate (31g/100 mL); (solution C) NaOH (4 g/100 mL). Make up in a 1.5-mL Eppendorf tube: To 0.64 mL distilled water, add 0.12 mL solution A. Mix, then add 0.08 mL solution B and mix. To the mixture then add 0.16 mL solution C and mix. Centrifuge and dispense from top. *Note*: Do not exhale over lead citrate mixture, as CO₂ will result in formation of lead carbonate precipitate.
65. Modified phosphate-buffered saline (MPBS): BSA 10.0 g/L; Na₂HPO₄ (anhydrous) 0.524 g/L, KH₂PO₄ (anhydrous) 0.092 g/L; NaCl 8.76 g/L; NaEDTA 0.372 g/L; NaN₃ 0.2 g/L, Tween-20 500 µL/L. Mix thoroughly and adjust pH to 8.2. Filter immediately before use (0.22 µm). *Note*: Use as diluent for all antisera and gold probe as well as for all buffer rinsing steps.
66. Methanol.
67. Propylene oxide (Polysciences Inc., Warrington, PA).
68. Benzoin methyl ether (Polysciences Inc., Warrington, PA).
69. Nickel grids (300 mesh) (Polysciences Inc., Warrington, PA; Ted Pella, Redding, PA).
70. Gelatin capsules (Polysciences Inc., Warrington, PA; Ted Pella, Redding, PA).
71. Goat anti-rabbit IgG-polygold (10 nm) (Nanoprobes Inc., Stony Brook, NY; Aurion, 6702 AA Wageningen, The Netherlands; BBI International: distributed in United States by Vector Laboratories Inc., Burlingame, CA).

72. Formvar (Polysciences Inc., Warrington, PA).
73. Near-ultraviolet lamp set-up (Thorn projector lamp, A1/209 FDX, 12 V 100 W).
74. 0.85% Saline: Add NaCl (8.5 g) to 100 mL distilled water and mix. Bring to a final volume of 1 L with distilled water.
75. Vecastain STAIN ABC kit (Vector Laboratories, Burlingame, CA).
76. DAB substrate kit for peroxidase (Vector Laboratories, Burlingame, CA).

3. Methods

3.1. Processing of Cells and Tissues for Light Microscopy

3.1.1. Procedure for Preparation of Cryostat Tissue Sections

1. Precool isopentane in liquid nitrogen. Dip freshly dissected tissue block (5 × 5 mm pieces) into cold isopentane. Frozen tissue blocks can be stored in sealed vials at -70°C in the presence of a few drops of isopentane to prevent drying. *Caution:* Do not allow either isopentane or liquid nitrogen to come in contact with skin! Do not inhale vapors!
2. Transfer frozen tissue blocks to a cryostat and allow temperature to equilibrate to -20°C for 30 min.
3. Mount the tissue block on the cryostat stub with embedding medium such as Tissue-Tek O. C. T. Compound (Sakura Finetek U.S.A. Inc., Torrance, CA) or TBS Tissue Freezing Medium (Triangle Biomedical Sciences, Durham, NC).
4. Trim surface of block.
5. Cut sections (5–20 μm) of unfixed tissue in a cabinet cryostat (-20°C) directly onto subbed slides. Allow the sections to air dry overnight at room temperature in a dark, dust-free place. Alternatively, sections on slides may be stored at -70°C to -80°C (2–3 mo) in a sealed plastic slide box. Stored slides should be allowed to warm to room temperature before use.
6. Pretreat slides with Triton X-100 to increase permeability of tissue sections: Place slides in a rack and insert rack in PBS containing 0.2% Triton X-100. Incubate for 20 min at room temperature.
7. Wash slides in PBS (four times, 5 min each, room temperature). Make certain to remove all of the detergent.
8. Rinse slides with distilled water and allow to air dry. Do not include Triton X-100 or any other detergent in any of the subsequent steps.
9. Treat tissue sections with endogenous peroxidase inhibitor solution (4 min).
10. Rinse tissue sections in reagent quality water (5 min).
11. Treat tissue sections with 150–200 μL blocking solution (e.g., SuperBlock) for 1 h at room temperature. If processing immune cells or tissues, include 1% NGS in the blocking buffer to block Fc receptors present on the surface of some immune cells.
12. Drain off excess blocking solution by touching edge of slide to a paper towel. Transfer slides to a humidified chamber.
13. Cover tissue slice with the primary anti-cannabinoid receptor antibody (see [Table 1](#)). It is preferable initially to use at least four dilutions of affinity purified antibody (1:10, 1:25, 1:50, 1:100) in blocking buffer. Use a 1:25 dilution of normal rabbit

- IgG (1 mg/mL) in blocking solution as a control. Incubate for 1 h at room temperature in a humidified chamber. Do not let the sections dry out in this or subsequent steps.
14. Gently drain the primary antibody solution off the slides. Wash slides (five times, 5 min each) at room temperature in PBS. Use a large volume for the wash (e.g., 50 mL per slide).
 15. Cover tissue slice with the secondary antibody. Initially, use a 1:32 dilution of goat IgG anti-rabbit IgG-HRPO diluted in blocking solution. Subsequent experiments may require titration of the HRPO-conjugated secondary antibody. Dilutions of 1:32–1:64 work well if the primary antibody used is directed against extracellular amine terminal domains of cannabinoid receptors, while dilutions of 1:100–1:1000 work well for antibodies directed against the entire receptors. Incubate for 1 h at room temperature in a humidified chamber at room temperature.
 16. Gently drain the secondary antibody solution off the slides by touching the edge of the slide to a paper towel. Wash the slides (five times, 5 min each) at room temperature in PBS.
 17. Incubate slides in 0.05 M Tris-HCl buffer, pH 7.6 for 2–3 min.
 18. Develop with Hanker-Yates reagent (Polysciences, Warrington, PA) in the dark by placing a sheet of tin foil over the humidified incubation chamber. Development usually is complete by 15 min. However, intensity of development may vary depending on the primary antibody used and the amount of cannabinoid receptor present in tissue. A general approach is to place a negative control (e.g., tissue slice treated with normal rabbit IgG as the primary antibody) side by side with a positive control (e.g., tissue slice known to contain the cannabinoid receptor at a relatively high concentration such as a brain slice that contains high levels of CB₁). The development reaction is terminated when the positive control qualitatively exhibits a twofold level of staining at the macroscopic level. *Note:* A metallic layer may appear on the surface of the reaction solution. If this occurs at the termination of the reaction period, gently flush this layer off the surface with 0.05 M Tris-HCl buffer, pH 7.6. Do not allow the metallic layer to come in contact with the tissue, as it will form precipitate.
 19. Wash slides in 0.05 M Tris-HCl buffer, pH 7.6, for 2–3 min.
 20. Rinse slides briefly in distilled water. *Note:* Slides may be counterstained with 0.1% cresyl violet acetate (2–3 min for cells on a cover slip; 10–20 min for a tissue section) at this point.
 21. Remove excess water around the tissue section by touching edge of slide to a paper towel. Proceed below to **step 22** for mounting in aqueous mounting medium or to **step 23** for mounting in inorganic medium.
 22. Aqueous medium mounting: Mount with Aquamount under a large coverslip. Allow to harden overnight in a refrigerator. If using Crystal/Mount, do not add a coverslip. Instead, add three drops of the Crystal/Mount directly onto the tissue section. Rotate the slide so as to distribute the medium over the entire tissue. Place in a horizontal position in an oven at 40–50°C (30 min). Remove slides and allow to cool. Examine directly under the light microscope.

23. Organic medium mounting: Dehydrate the sections by 5-min washes with graded concentrations of ethanol (70%, 95%, and two changes of absolute ethanol). Immerse slides in 100% xylene (two changes, 5 min each). Apply a large cover slip (22 × 50 mm) using a few drops (e.g., 25–50 μ L) of permanent mounting medium suitable for light microscopy such as Permount (Fisher Scientific, Pittsburgh, PA).

3.1.2. Procedure for Processing Formalin-Fixed and Paraffin-Embedded Tissue

3.1.2.1. PROCESSING OF BRAIN TISSUE

The following protocol is designed for either murine or rat brain but can be adapted for other tissues.

1. Store tissue in 10% phosphate-buffered formalin (freshly prepared from paraformaldehyde at room temperature for 7 d, after which the formalin is removed and replaced with 70% ethanol. Tissue may be stored in 70% ethanol for several weeks. *Note:* Transfer to 70% ethanol is recommended to minimize loss of antigenicity in tissues owing to prolonged exposure to formalin.
2. Antecedent to processing for paraffin embedding, transfer tissue to fresh 10% phosphate-buffered formalin (two times, 45 min each).
3. Dehydrate tissue by immersion through the following series of solutions (30 min each): 80% ethanol (once), 95% ethanol (two times), 100% ethanol (three times).
4. Immerse tissue in xylene (two 45-min incubations) in order to clear the tissue and allow paraffin infiltration.
5. Immerse tissue four times in hard paraffin (melting point = 56–57°C), which is heated and maintained at 60°C. Embed in paraffin.

3.1.2.2. PROCESSING OF PARAFFINIZED TISSUE SECTIONS FOR IMMUNOPEROXIDASE STAINING

1. Cut sagittal sections from the right or left hemispheres for each brain starting from the center (middle) out. Alternatively, coronal sections may be cut. Seven sections 3 μ m thick are mounted onto clean subbed glass slides. Number the slides sequentially according to the tissue label (coded). The first and last slides are processed further and stained using hematoxylin and eosin to serve for histological assessment and for orientation of brain sections.
2. Make certain that slides containing tissue sections are dry.
3. Immerse slides in the following solutions for the indicated periods of time. Slides can be inserted into a Coplin jar for each treatment. Move slides gently up and down two to three times after immersing into each solution.
 - a. Xylene (2–3 min or longer).
 - b. Xylene (2–3 min).
 - c. Absolute ethanol (2–3 min).
 - d. 95% ethanol (2–3 min).
 - e. 70% ethanol (2–3 min).

- f. 50% ethanol (2–3 min).
 - g. 30% ethanol (2–3 min).
 - h. PBS (two times, 10 min each).
4. Wipe excess PBS from slides by touching edge of slide to a paper towel.
 5. Treat tissue sections with endogenous peroxidase inhibitor solution (4 min).
 6. Rinse sections in reagent-quality water (5 min).
 7. Transfer slides to a humidified chamber and treat with 150–200 μ L blocking solution (e.g., SuperBlock) for 1 h at room temperature. If processing immune cells or tissues, supplement blocking buffer with 1% NGS in order to block Fc receptors present on the cell surface of some immune cells.
 8. Drain off excess blocking solution.
 9. Cover tissue slice with the primary rabbit IgG anti-cannabinoid receptor antibody. It is preferable initially to use at least four dilutions of each affinity-purified antibody (1:10, 1:25, 1:50, 1:100) in blocking buffer. Use a 1:25 dilution of normal rabbit IgG (1 mg/mL) in blocking solution as a negative control. Incubate for 1 h at room temperature in a humidified chamber. Do not let the sections dry out in this or subsequent steps. Ideally, a negative control should consist of preimmune IgG derivative from the same rabbit which was used to produce the anti-cannabinoid receptor antibody. However, when using commercially available anti-cannabinoid receptor antibodies, such preimmune IgG may not be available and normal rabbit IgG can be used as a control.
 10. Gently drain the primary antibody solution off the slides. Wash slides (five times, 5 min each) at room temperature in PBS. Use a large volume for the wash (e.g., 50 mL/slide).
 11. Cover tissue slice with secondary antibody. Use a 1:32 dilution of goat IgG anti-rabbit IgG-HRPO (Organon Teknika Cappel, Durham, NC) diluted in blocking solution. Incubate for 1 h at room temperature in a humidified chamber at room temperature.
 12. Gently drain the secondary antibody solution off the slides by touching the edge of the slide to a paper towel. Wash the slides (five times, 5 min each) at room temperature in PBS.
 13. Transfer slides to a Coplin jar and incubate with 0.05 M Tris-HCl buffer, pH 7.6 for 2–3 min.
 14. Transfer slides to a humidified chamber and develop with Hanker-Yates reagent in the dark. This can be achieved by placing paper towels over the humidified incubation chamber. Development usually is complete by 15 min. However, intensity of development may vary depending on the primary antibody used and the amount of cannabinoid receptor present in tissue. A general approach is to place a negative control (e.g., tissue slice treated with normal rabbit IgG as the primary antibody) side by side with a positive control (e.g., tissue slice known to contain the cannabinoid receptor at a relatively high concentration). The development reaction is terminated when the positive control qualitatively exhibits a twofold level of staining at the macroscopic level. *Note:* The intensity of reaction

product also can be monitored by placing a positive control slide on an inverted microscope.

15. Wash the slides in 0.05 M Tris-HCl buffer, pH 7.6, for 2–3 min.
16. Rinse the slides briefly in distilled water.
17. Immerse the slides sequentially in the following solutions for the indicated periods of time:
 - a. 50% ethanol (2–3 min).
 - b. 70% ethanol (2–3 min).
 - c. 95% ethanol (2–3 min).
 - d. Absolute ethanol (2–3 min).
 - e. Xylene–absolute ethanol (1:1) (2–3 min).
 - f. Xylene (2–3 min).
 - g. Xylene (2–3 min).
18. Mount in Permount Organic Medium (Fisher Scientific, Pittsburgh, PA). Apply a large cover slip (22 × 50 mm) using a few drops (25–20 µL) of Permount. Allow Permount to harden on a slide warmer.
19. Examine under the light microscope and photograph using Kodak Elite Chrome 160T Tungsten 35-mm film (Eastman-Kodak Company, Rochester, NY). Alternatively, images may be obtained using a digital camera system such as the Spot RT Slider Digital Camera (Diagnostic Instruments Inc., Sterling Heights, MI). **Figure 1** shows results obtained for identification of the CB₁ cannabinoid receptor in rat brain fixed in formalin and embedded in paraffin.

3.1.3. Procedure for Processing of Cells Maintained in Culture for Demonstration of Intracellular Cannabinoid Receptors

1. Seeding of cells and cell culture:
 - a. For adherent cells, grow cells on sterile coverslips which have been placed (four cover slips/well) in 6-well tissue culture dishes (Falcon No. 3046, Becton Dickinson Labware, Franklin Lakes, NJ). Allow cells to reach approx 90% confluency. Alternatively, place coverslips in a 60-mm Petri dish. Add a 100-µL volume of cell suspension (1×10^6 cells/mL in culture medium) to each cover slip so as to form a bubble confined to the cover slip. Place cover on Petri dish and place in a humidified CO₂ incubator maintained at 37°C for 2 h or until cells attach to the cover slip. Attachment of cells can be monitored by screening the Petri dish with its contained cover slips on an inverted microscope.
 - b. For nonadherent cells, apply 10–20 µL of cell suspension (1×10^6 cells/mL) to each coverslip which has been precoated with poly-L-lysine. Allow to sit 10 min, then proceed with fixation. Alternatively, cells in suspension can be attached to cover slips using a cytocentrifuge according to the manufacturer's instructions. A StatSpin Cytofuge 2 Cytocentrifuge (StatSpin Technologies, Norwood, MA) works well. Typically, one adds 100 µL of a cell suspension

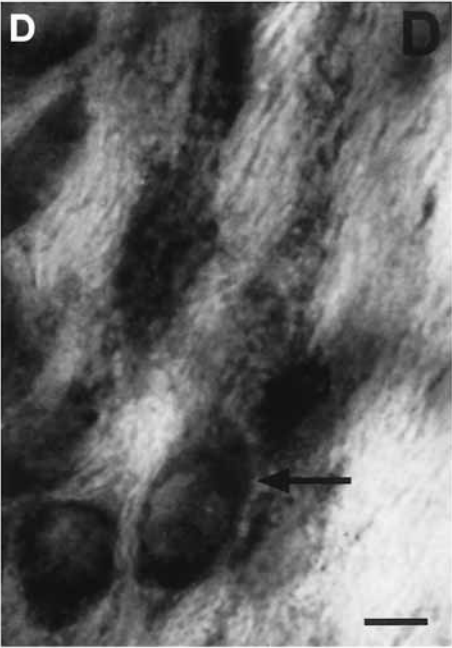
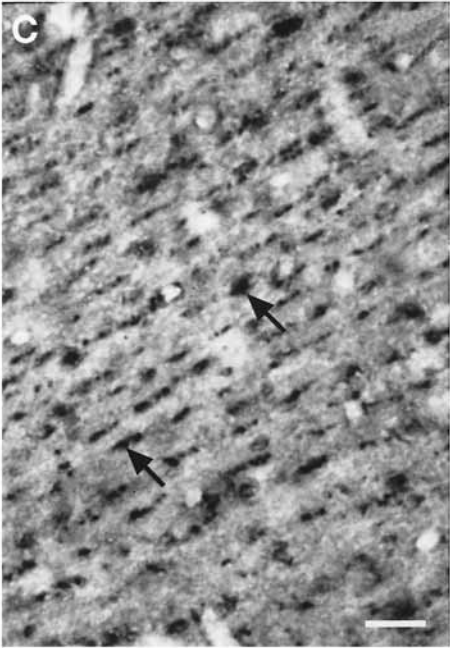
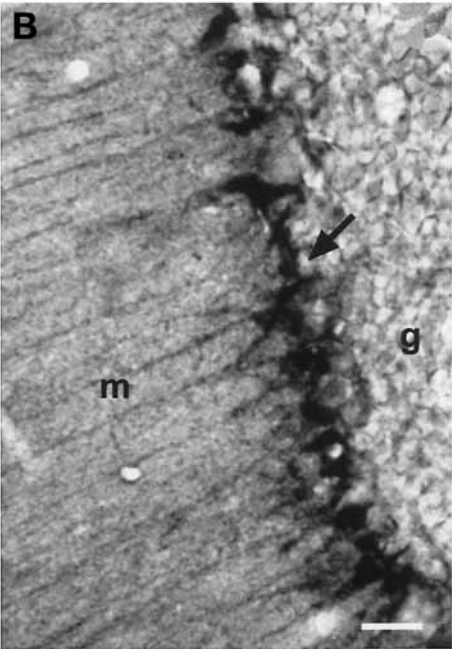
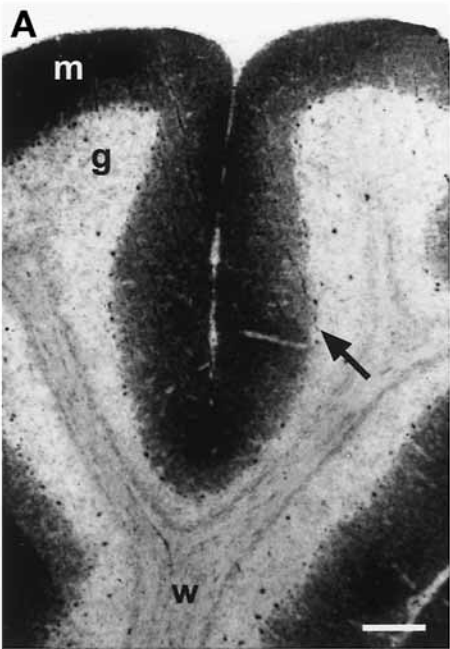


Fig. 1. Light micrographs depicting the distribution of CB₁ cannabinoid receptor immunoperoxidase staining in rat brain. **(A)** Immunoreactive labeling in the cerebellum is concentrated in the molecular (m) layer while minimal labeling is identified in the granular (g) layer. Immunoreactive product is absent also from the white matter (w). The arrow denotes the Purkinje cell layer. **(B)** Localization of immunoreactive labeling in the Purkinje cell layer. Intense labeling is localized within areas (*arrow*) that form arborizations into the molecular layer (m). Cells with morphology consistent with that of basket cells show intense immunoreactivity for the CB₁. **(C)** Immunoreactive labeling for the CB₁ receptor is localized as intense clusters (*arrows*) within processes forming parallel arrays extending through the molecular layer. **(D)** Localization of immunoreactive product for the CB₁ receptor within the cytoplasm of individual cells (*arrow*) within the amygdala. Scale bars: **A**, 100 μ m; **B**, 50 μ m; **C**, 25 μ m; **D**, 10 μ m.

- ($1 \times 10^5 - 1 \times 10^6$ cells/mL) to each cell concentrator unit for spinning down onto a glass slide.
2. Remove cover slips from tissue culture well and drain off excess medium by touching edge of cover slip to a paper towel.
 3. Rinse gently (three times) in PBS (room temperature) and air dry for 30 min.
 4. Fix cover slips in absolute acetone for 5 min.
 5. Air dry cover slip cultures for 30 min.
 6. Store cover slips in a Petri dish in a desiccator (with desiccant) at 41° C long term (e.g., up to 2 yr) or leave in Petri dish at room temperature short term (e.g., up to 6 mo).
 7. Prewet cover slips by immersion in PBS (5 min).
 8. Treat cover slips with endogenous peroxidase inhibitor solution (4 min).
 9. Rinse cover slips in reagent-quality water (5 min).
 10. Treat cover slips with 50 μ L blocking solution (e.g., SuperBlock) for 1 h at room temperature. *Note:* Supplement blocking solution with 1% NGS if processing immune tissues or cells in order to block for Fc receptors that are present on surfaces of some immune cells.
 11. Drain off excess blocking solution by touching edge of cover slip to a paper towel.
 12. Cover cover slips with the primary rabbit anti-cannabinoid receptor antibody. It is preferable initially to use at least four dilutions of each affinity purified antibody (1:10, 1:25, 1:50, 1:100) in blocking buffer. Use a 1:25 dilution of normal rabbit IgG (1 mg/mL) in blocking solution as a negative control. Incubate for 1 h at room temperature in a humidified chamber. Do not allow the sections to dry out in this or subsequent steps.
 13. Gently drain the primary antibody solution off the cover slips by touching the edges to a paper towel. Wash cover slips (five times, 5 min each) at room temperature in PBS. Use a large volume for the wash (e.g., 50 mL).
 14. Add 25 μ L secondary antibody goat IgG anti-rabbit IgG (heavy and light chains)–HRPO to cover slips. Use a 1:32 dilution of goat anti-rabbit HRPO (1

- mg/mL) diluted in blocking solution. Incubate for 1 h at room temperature in a humidified chamber at room temperature.
15. Gently drain the secondary antibody solution off the cover slips by touching edge to a paper towel. Wash the cover slips (five times, 5 min each) at room temperature in PBS.
 16. Immerse cover slips in 0.05 M Tris-HCl buffer, pH 7.6 for 2–3 min.
 17. Develop with Hanker-Yates reagent. Development usually is complete by 15 min. However, intensity of development may vary depending on the primary antibody used and the amount of cannabinoid receptor present in tissue. A general approach is to place a negative control (e.g., cells on a cover slip treated with normal rabbit IgG as the primary antibody) side by side with a positive control (e.g., cells transfected with a cannabinoid receptor expression construct). The development reaction is terminated when the positive control qualitatively exhibits a twofold level of staining at the macroscopic level. Alternatively, the staining reaction can be monitored under an inverted cell culture microscope.
 18. Wash cover slips in 0.05 M Tris-HCl buffer, pH 7.6, for 2–3 min.
 19. Rinse cover slips briefly in distilled water.
 20. Remove excess water by touching edge of cover slip to a paper towel. Proceed to **step 21** for mounting in aqueous mounting medium or to **step 22** for mounting in inorganic medium. *Note:* Mounting with AquaMount requires a small amount of residual water to allow medium to harden. Do not air dry for Permount or AquaMount. If mounting in Permount, must go from water to alcohols to xylene without interruption.
 21. Aqueous medium mounting: Mount (25 μ L) with AquaMount under a 12-mm circular cover slip if cells have been spun down onto a glass slide. If cells are adherent to the cover slip, add 25 μ L directly onto a glass slide and place the cover slip cell-side down onto the droplet.
 22. Organic medium mounting: Dehydrate the cells on the cover slips by 5-min washes with graded concentrations of ethanol (70%, 95%, and two changes of absolute ethanol). Transfer to 100% xylene (two changes, 10 min each). If cells have been spun down onto a glass slide, apply a cover slip using a few drops (e.g., 25 μ L) of permanent mounting medium suitable for light microscopy such as Permount (Fisher Scientific, Pittsburgh, PA). If cells are adherent to the cover slip, add 25 μ L directly onto a glass slide and place the cover slip cell side down onto the droplet.

3.1.4. Procedure for Processing of Cells Maintained in Culture for Demonstration of Cell Surface Cannabinoid Receptors

1. Prepare cell cultures on cover slips and harvest for immunoperoxidase staining as described in **steps 1–3** in **Subheading 3.1.3**. *Note:* Trypsinization of cell monolayers should not be considered since this process may remove cannabinoid extracellular domains from cell surfaces.
2. Fix in 2% formalin in PBS for 20 min.
3. Rinse cover slips in four to five changes of PBS for 10 min each. Do not allow cells on cover slips to dry out at any point.
4. Proceed with **steps 10–22** as described in **Subheading 3.1.3**.

3.2. Processing of Cells and Tissues for Electron Microscopy

3.2.1. Detection of Cannabinoid Receptors by Immunoperoxidase Staining

3.2.1.1. PERFUSION OF MOUSE/RAT AND REMOVAL OF BRAIN WITH 4% PARAFORMALDEHYDE, 0.1% PURIFIED GLUTARALDEHYDE FIXATIVE IN 0.1 M PHOSPHATE BUFFER

1. Prepare separate flasks containing cold (4°C) saline (0.9%) and room-temperature fixative solution.
2. Prepare peristaltic pump, Tygon tubing, and perfusion instruments according to manufacturer's instructions. Arrange such that saline will be drawn through the tube first by configuring the tubing with a valve to allow for selection of solution to be drawn.
3. Attach Tygon tubing primed with saline to a blunt 15 G hypodermic needle.
4. Administer a lethal dose of anesthesia to mouse or rat. Make certain that the animal is unresponsive before proceeding. Lack of responsiveness can be determined by pinching the animal's foot.
5. Make an incision through the abdomen just below the rib cage and expose the diaphragm. Make incision through the diaphragm and expose the heart.
6. Open the thoracic cavity with two horizontal cuts through the rib cage on either side of the heart. Clamp the sternum with a hemostat and fold the cut rib flap headward to expose the heart
7. Make a small incision at the bottom apex of the left ventricle. Insert a blunt 13 G hypodermic needle upward through the ventricle past the aortic valve so that it can be visualized at approx 5 mm inside the ascending aorta. Clamp the needle in place with a hemostat across the ventricle.
8. Begin perfusion by slowly (i.e., 20–40 mL/min) introducing perfusion prewash solution. Immediately after the peristaltic pump starts pumping saline, cut the right atrium to allow for an escape route for blood and perfusion fluid. Keep saline on ice so as to minimize coagulation of blood
9. Continue to perfuse with perfusion prewash solution (approx 40 mL/min) until the effluent runs clear. Perfusion may require up to 500 mL of saline.
10. Stop the peristaltic pump and begin the flow of fixative. Perfuse at approx 20 mL/min such that approx 500 mL of fixative is perfused over a 10- to 20-min period.
11. Remove the brain and immerse it overnight in 0.1 M sodium phosphate buffer.

3.2.1.2. SECTIONING OF MOUSE/RAT BRAIN AND INCUBATION OF BRAIN SECTIONS WITH THE PRIMARY ANTI-CANNABINOID RECEPTOR ANTIBODY

1. Cut brain (embedded in 4% agar, 50–100 μ m sections) using a Vibratome according to the manufacturer's instructions. Place sections into glass vials with caps filled with 0.1 M sodium phosphate buffer. *Note:* Sections can be transferred from one solution to another with a camel hair's brush. Subsequent steps can be performed by treating sections within the glass vials under gentle agitation by placing vials on a rotator mixer.

2. Rinse sections with PBS three times (10 min each) at room temperature.
3. Treat sections with 0.1% phenylhydrazine (endogenous peroxidase activity inhibitor) at room temperature for 30 min.
4. Rinse sections with PBS three times (10 min each) at room temperature.
5. Preincubate sections (30 min) in 5 mL of blocking solution of PBS supplemented with 4% NGS, 0.3% Triton X-100, 0.1 M lysine (0.146 g/10 mL), and 1% BSA
6. Rinse (5 min) sections in 1% NGS.
7. Incubate sections overnight in a refrigerator (4°C) on a shaker with affinity-purified primary rabbit anti-cannabinoid receptor antibody (*see Table 1*). Use the affinity-purified antibody at a 1:1000–1:5000 dilution of a stock antibody preparation (1 mg/mL) in a final volume of 5 mL PBS supplemented with 1% NGS. *Note:* For immunoelectron microscopy it is recommended that affinity-purified antibody be used (*see Note 1*).

3.2.1.3. INCUBATION OF VIBROTOME SECTIONS IN SECONDARY ANTIBODY, IMMUNOPEROXIDASE DEVELOPMENT, AND INITIAL SCREENING BY LIGHT MICROSCOPY

1. Rinse sections three times (10 min each) in 1% NGS.
2. Incubate sections (1 h at room temperature) in biotinylated goat anti-rabbit IgG (1 mg/mL stock solution). Prepare by adding 50 μ L per 10 ml 1% NGS.
3. Rinse sections three times (10 min each) in PBS. *Note:* At this time prepare the ABC solution (Vector Laboratories, Burlingame, CA). Add 50 μ L of solution A (Avidin DH) to 10 mL PBS. Then add 50 μ L of solution B (biotinylated horseradish peroxidase H). Mix immediately. Let stand for 30 min before use.
4. Incubate tissue sections in ABC solution for 1 h at room temperature (*see Note 2*).
- 5 Rinse sections three times (10 min each) in PBS.
6. Rinse sections twice (10 min each) in 0.1 M sodium phosphate buffer.
7. Preincubate sections (10 min) in DAB substrate with nickel (Ni) solution without hydrogen peroxide (H_2O_2). To prepare, use the DAB substrate kit (Vector Laboratories, Burlingame, CA). Add two drops buffer stock to 5 mL of distilled water and mix. Add four drops DAB stock solution and mix. Add two drops of nickel solution and mix.
8. Incubate sections in DAB substrate with nickel plus H_2O_2 . Prepare from the DAB substrate kit (Vector Laboratories) as in **step 7** and add two drops of H_2O_2 solution. Mix well. *Note:* Determination of the optimal time for development of reaction product for electron microscopy assessment is achieved best by monitoring the development process under a light microscope. Ideally, sections are obtained for three development periods. The first of these is allowed to over-develop so as to allow for definition of which sites within the tissue section are positive for immunoprodut. The second section, then, is monitored for development just to the point where product is first observed. Finally, the third section is allowed to develop for a time period which is just under that obtained for the second section. The latter two sections are examined under the electron microscope. Using this approach, it is possible to obtain sections for observation under the electron micro-

scope for which diffusion of immunoelectron dense product from antigenic sites is limited.

9. Rinse sections (10 min) in 0.1 *M* sodium phosphate buffer.
10. If required, rinse sections (5 min) with fixative solution to clear background.
11. Rinse sections twice (10 min each) in 0.1 *M* sodium phosphate buffer.
12. Mount a representative number of tissue sections out of 0.1 *M* sodium phosphate buffer for initial assessment by light microscopy. For light microscopy, proceed to **step 13**. For electron microscopy, proceed to **Subheading 3.2.1.4**.
13. Dehydrate and coverslip and screen by light microscopy according to the following schedule:
 - a. 50% ethanol (2–3 min).
 - b. 70% ethanol (2–3 min).
 - c. 95% ethanol (2–3 min).
 - d. Absolute ethanol (2–3 min).
 - e. Xylene–absolute ethanol (1:1) (2–3 min).
 - f. Xylene (2–3 min).
 - g. Xylene (2–3 min).
 - h. Mount in Permount Organic Medium (Fisher Scientific, Pittsburgh, PA). Allow Permount to harden on a slide warmer.

3.2.1.4. *EN BLOC* STAINING OF TISSUE WITH URANYL ACETATE AND PROCESSING FOR TRANSMISSION ELECTRON MICROSCOPY

1. Place vials on ice in a chemical fume hood. Remove buffer and add 300 μ L of cold (4°C) 1% osmium solution. Snap on cap of vial and incubate for 1 h at 4°C with gentle agitation on a rotary mixer. *Note:* OsO₄ is highly toxic and volatile. Perform all steps in a chemical hood. Do not breathe in vapors and do not allow contact with skin. Dispose of all used solutions in a chemical waste bottle that is maintained in the chemical hood. Dispose of all waste using procedures mandated by your institutional biohazardous waste/safety officer.
2. After postfixation with osmium tetroxide, wash tissue sections thoroughly in cold (4°C) sodium hydrogen maleate–NaOH buffer, 0.05 *M*, pH 5.2 (three changes, 5 min each).
3. Immerse tissue sections in 0.5% uranyl acetate (Sigma-Aldrich, St. Louis, MO) dissolved in 0.05 *M* sodium hydrogen maleate–NaOH buffer, pH 6.0 (50 mg/10 mL) for 2 h at 4°C in the dark.
4. Rinse tissue sections in cold (4°C) sodium hydrogen maleate–NaOH buffer, 0.05 *M*, pH 5.2 (two changes, 5 min each).
5. Proceed with dehydration and embedding according to the schedule below. *Note:* All steps are performed on ice with frequent agitation. Tissue sections are placed in glass vials with caps, which, in turn, are placed in a rotary mixer (Penetron Mark IIIB, Sunkay Laboratories Inc., Tokyo, Japan).
 - a. 50% methanol (5 min).
 - b. 70% methanol (5 min).

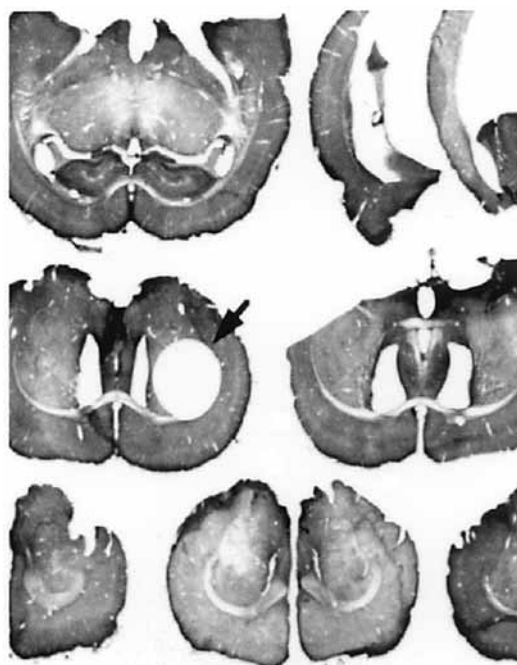


Fig. 2. Brain serial cross-sections which have been subjected to immunoperoxidase preembedding immunoperoxidase reaction for localization of the CB₁ receptor and oriented on a glass microscope slide coated with liquid release agent. An area of interest has been identified as having intense labeling under the light microscope and has been excised (*arrow*) using a sharpened cork borer for mounting on resin stubs.

- c. 80% methanol (5 min).
 - d. 95% methanol (5 min).
 - e. 100% (absolute) methanol (two changes of 10 min each).
 - f. Propylene oxide (two changes of 10 min each).
 - g. Propylene oxide, TAAB resin (1:1 mixture) (1 h on a rotary mixer).
 - h. Straight TAAB resin for 4–8 h on rotatory shaker. During the last hour, remove caps from tissue vials and place under vacuum in a desiccator to remove air.
6. Using an applicator stick (broken to make flat tapered tip), transfer each section with a small amount of TAAB to a glass microscope slide coated with liquid release agent (Electron Microscopy Sciences, Fort Washington, PA). The size of the sections will determine how many can be arranged on a single glass slide. Sections should be properly oriented with at least 5-mm separation (**Fig. 2**). Place another coated glass microscope slide over each group of sections. Do not overlap the sides and ends of the two slides. Press lightly over each section to spread resin

and clamp slides together with clothespins. Place slides with sections on flat surface and polymerize in oven at 60°C for 48–72 h to harden resin.

7. Pry the two slides apart carefully using a single-edged razor blade. Identify the area of interest or intense labeling under the light microscope. Under a dissecting microscope, use a scalpel or a sharpened cork borer (approx 2–3 mm in diameter) and cut out area of interest for mounting on resin stubs (Fig. 2, arrow).
8. Place embedded tissue sample on glass microscope slide coated with liquid release agent. Place a drop of liquid TAAB resin onto one flat end of a hardened resin stub. Place same end of stub on top of tissue sample. Place a small drop of resin on the other end of the stub and affix a small piece of paper with a label identifying the sample. A circular piece of paper resulting from using a hole puncher will suffice.
9. Place slide with stubbed tissue in a 60°C oven for 2–3 d.
10. Trim the surface of the tissue block and subject to thin-sectioning on an ultramicrotome.
11. Examine in an electron microscope. Figure 3 illustrates the comparative application of light and electron microscopy for the localization of the CB₁ cannabinoid receptor in rat brain. Figure 4 illustrates high-resolution localization of the CB₁ receptor within rat brain.

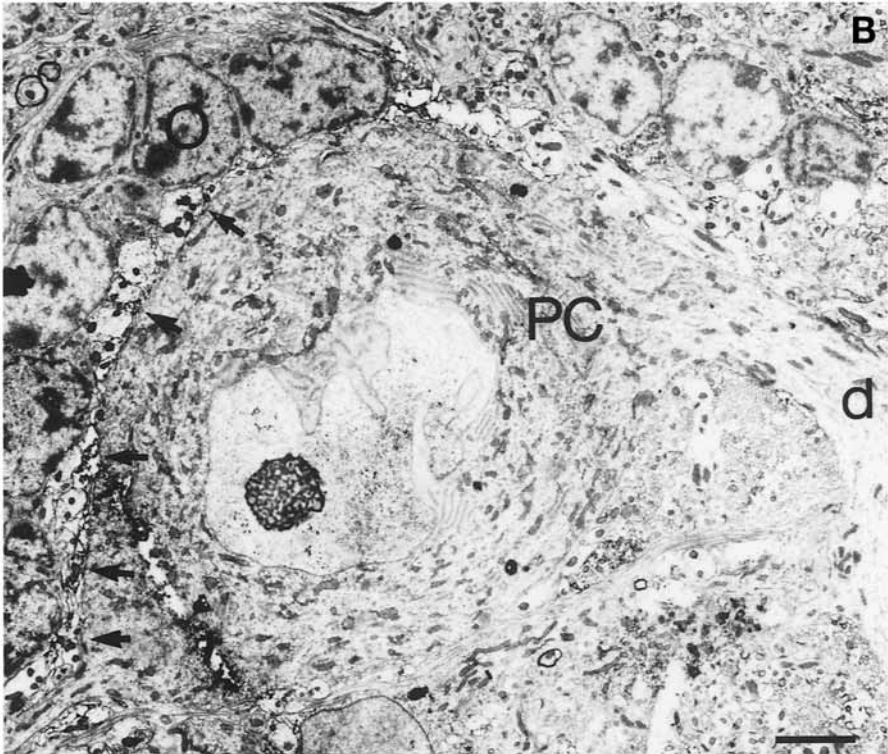
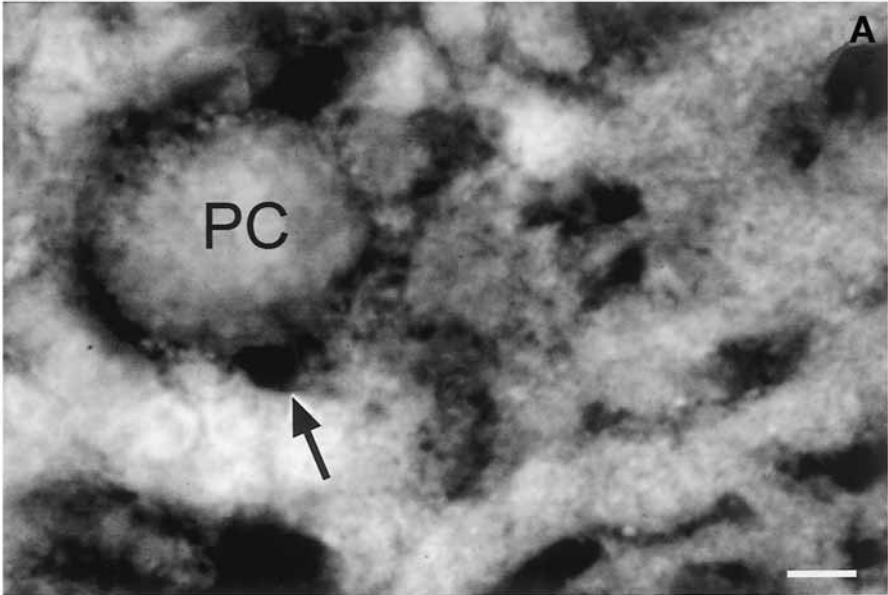
3.2.2. Detection of Cannabinoid Receptors by Immunogold Labeling

3.2.2.1. PREPARATION OF TISSUE (NOTE: ALL STEPS ARE PERFORMED AT 4°C UNLESS OTHERWISE INDICATED)

1. Immerse 2-mm³ pieces of tissue in fixative consisting of 4% paraformaldehyde and 0.25% glutaraldehyde in 0.1 M sodium cacodylate/HCl buffer for 3–4 h.
2. Rinse tissue in 0.1 M sodium cacodylate/HCl buffer. Use four to five changes over a 4-h minimum. It is preferable to leave tissue samples overnight in buffer (on a rotator in a cold room maintained at 4–10°C).
3. Dehydrate tissue samples in a graded series of ethanol: 50% (20 min), 75% (20 min), and 100% (three times, 20 min each with rotation).

3.2.2.2. Embedding in Resin

1. Remove the final absolute ethanol and add LR gold resin (Polysciences Inc., Warrington, PA). Note: Depending on the size of the sample, allow to infiltrate in resin for at least 5 d (up to 7 d for larger samples). Change the resin every 2 d. For the last two changes of the LR gold include 0.1% benzoin methyl ether (the light-activated catalyst).
2. Polymerization: Pipet the samples into gelatin capsules so that they are filled with LR Gold resin (supplemented with 0.1% benzoin methyl ether) and replace the cap on the capsule because the light-activated polymerization is anaerobic. Place the gelatin capsules in a 96-well microtiter plate on a plate of glass held approx 25 cm above a near ultraviolet lamp set-up in a cold room (4°C). Allow to polymerize for 48 h.



←

Fig. 3. Comparative light and electron microscopy for the localization of the CB₁ cannabinoid receptor in the rat cerebellum. **(A)** Light microscopy immunoperoxidase staining showing immunoreactive product in an area "cradling" or apposed (*arrow*) to the basal soma of a Purkinje cell (PC). **(B)** Transmission electron micrograph illustrating similar immunoreactivity for the CB₁ receptor (*arrows*) in areas apposed to the basal portion of a nonimmunoreactive Purkinje cell (PC) body. Note absence of reaction product from Purkinje cell proximal dendrite (d). Scale bars: **A**, 10 μ m; **B**, 5 μ m. O, oligodendrocyte.

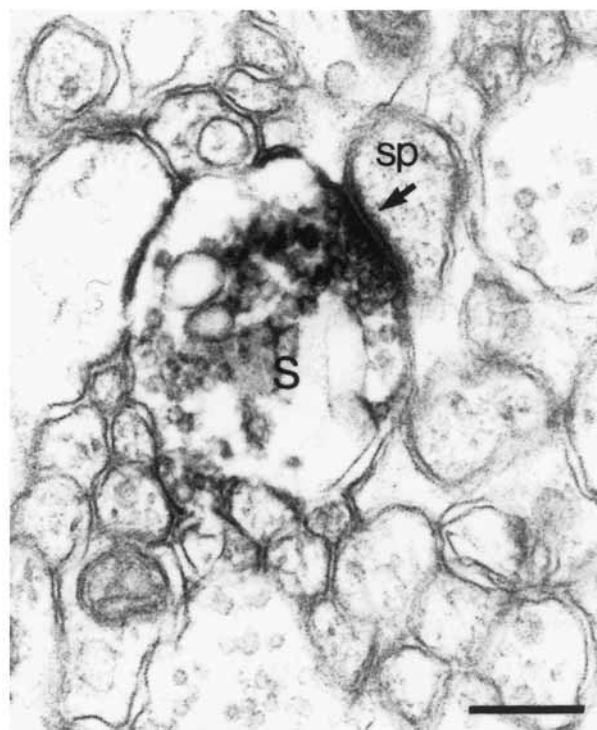


Fig. 4. Transmission electron micrograph illustrating a small immunoperoxidase-reactive synaptic ending (s) establishing contact (*arrow*) with a spine-like profile (sp). Note the presence of dense immunoreactive product associated with the presynaptic membrane and encompassing adjacent synaptic vesicles. Scale bar, 0.25 μ m.

3. Sectioning: Ultrathin sections of LR gold-embedded specimens are cut as for standard (epoxy) electron microscopy resins. Cut sections fresh for any immunolabeling experiment. *Note:* Collect sections on nickel grids (300 mesh). Grids may be used with or without Formvar coating.

3.2.2.3. IMMUNOLABELING OF PLASTIC SECTIONS FOR CANNABINOID RECEPTORS

1. For all incubations place grids on 20- μ L droplets on Parafilm within a Petri dish. Rinses in buffer are performed by floating grids section side down on droplets. Transfer grids from one solution to another with fine forceps using care to not to wet the opposite face of the grid that is being labeled.
2. Blocking step: Incubate grids in MPBS containing 1% BSA for 30 min at room temperature. If immune tissue or cells are being examined, add 1% NGS to the blocking buffer in order to block Fc receptors, which are present on the surface of some immune cells.
3. Incubate in affinity-purified rabbit anti-cannabinoid receptor IgG overnight at 4°C (in a humidified chamber). A first immunolabeling should include a titration series of the specific affinity-purified antibody at dilutions of 1:5–1:20 to establish the optimal dilution. This titration series is required to optimize the signal-to-noise ratio of immunolabeling. Concurrent incubations should be carried out in non-immune rabbit IgG (at similar dilutions) from the primary antibody donor species to serve as negative controls.
4. Rinse the grids in MPBS (three times, 2 min each).
5. Incubate the grids in goat anti-rabbit IgG-polygold (10 nm). Dilute the gold probe 1:10 in MPBS immediately before use. Incubate for 1 h at room temperature.
6. Rinse the grids thoroughly in buffer (three times, 10 min each).
7. Rinse the grids in double glass-distilled water (four times, 3 min each).

3.2.2.4. STAINING OF SECTIONS ON GRIDS FOR ELECTRON MICROSCOPY

1. Stain sections on grids for 5–10 min in 0.5% aqueous uranyl acetate. Cover from light to prevent precipitation.
2. Rinse the grids by dipping (10–20 dips) in reagent quality water.
3. Stain sections on grids with lead citrate (1–2 min). Stain in a plastic dish with NaOH pellets to prevent CO₂ from causing precipitation. Lead citrate should be dispensed from the top of the solution. Do not breathe on the lead citrate at any stage, as insoluble lead carbonate will form, which produces dense spots over the sections.
4. Rinse grids by dipping (10–20 dips) in reagent grade water. *Note:* LR Gold resin is hydrophilic and takes up the uranyl and lead stains considerably more rapidly than the standard epoxy resins.
5. Dry overnight.
6. Examine grids in the transmission electron microscope. **Figure 5** illustrates the application of the immunogold method at the electron microscopy level for the identification of the human CB₂ as expressed in the envelope of a baculovirus construct (13).

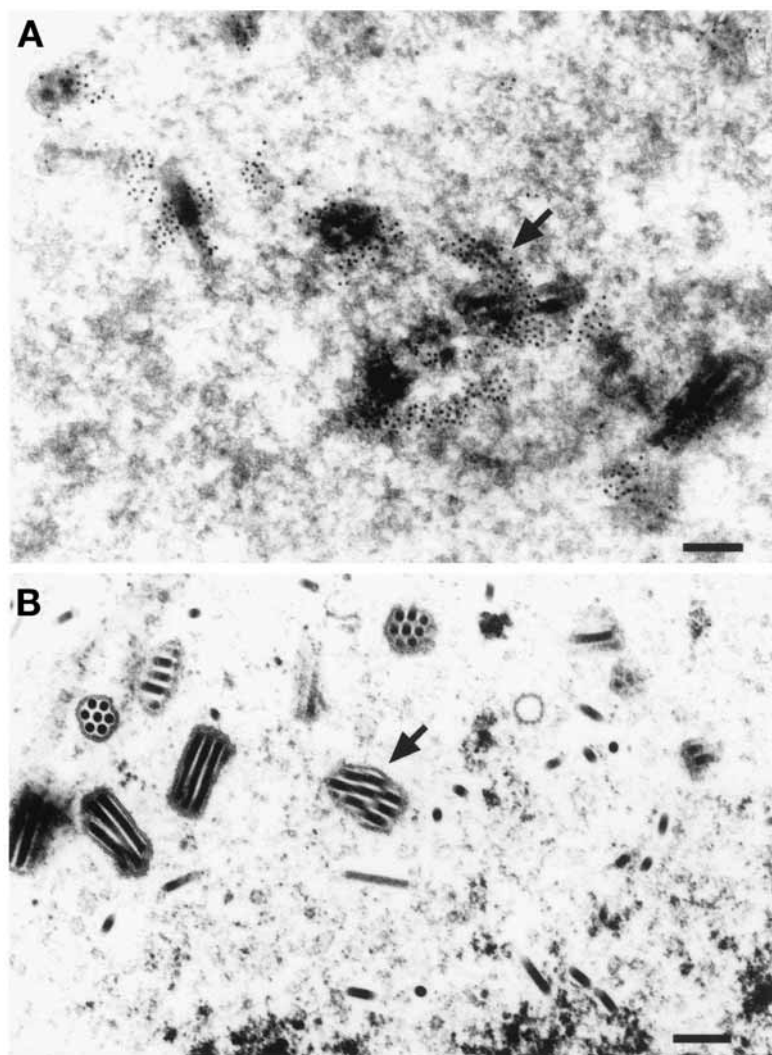


Fig. 5. Immunogold labeling for the demonstration of the human CB₂ cannabinoid receptor as expressed on the envelope of a baculovirus CB₂ expression vector in insect cells. (A) Intense immunogold label surrounds the envelope (arrow) of the baculovirus construct. (B) Control β -galactosidase recombinant baculovirus envelopes show no immunolabeling for the CB₂ cannabinoid receptor. Scale bars, A and B, 0.2 μ m.

4. Notes

1. For all subsequent steps do not use any solution containing sodium azide as this substance inhibits peroxidase activity.

2. Do not include normal serum or nonfat dried milk with ABC reagents as they may reduce activity.

Acknowledgments

The author thanks Dr. Denise Pettit for immunoperoxidase transmission electron microscopy and Dr. Kate Harmon for immunogold transmission electron microscopy. This work was supported by NIH/NIDA awards DA05832, DA09789, and DA15608.

References

1. Matsuda, L. A., Lolait, S. J., Brownstein, M. J., Young, A. C., and Bonner, T. I. (1990) Structure of a cannabinoid receptor and functional expression of the cloned cDNA. *Nature* **346** (6284), 561–564.
2. Gérard, C., Mollereau, C., Vassart, G., and Parmentier, M. (1990) Nucleotide sequence of a human cannabinoid receptor cDNA. *Nucleic Acids Res.* **18** (23), 7142.
3. Gérard, C. M., Mollereau, C., Vassart, G., and Parmentier, M. (1991) Molecular cloning of a human cannabinoid receptor which is also expressed in testis. *Biochem. J.* **279** (Pt 1), 129–134.
4. Chakrabarti, A., Onaivi, E. S., and Chaudhuri, G. (1995) Cloning and sequencing of a cDNA encoding the mouse brain-type cannabinoid receptor protein. *DNA Seq.* **5** (6), 385–388.
5. Galiégué, S., Mary, S., Marchand, J., et al. (1995) Expression of central and peripheral cannabinoid receptors in human immune tissues and leukocyte subpopulations. *Eur. J. Biochem.* **232** (1), 54–61.
6. Munro, S., Thomas, K. L., and Abu-Shaar, M. (1993) Molecular characterization of a peripheral receptor for cannabinoids. *Nature* **365** (6441), 61–65.
7. Kaminski, N. E., Abood, M. E., Kessler, F. K., Martin, and Schatz, A. R. (1992). Identification of a functionally relevant cannabinoid receptor on mouse spleen cells that is involved in cannabinoid-mediated immune modulation. *Mol. Pharmacol.* **42** (5), 736–742.
8. Bouaboula, M., Rinaldi, M., Carayon, P., et al. (1993) Cannabinoid-receptor expression in human leukocytes. *Eur. J. Biochem.* **214**(1), 173–180.
9. Noe, S. N., Newton, C., Widen, R., Friedman, H., and Klein, T. W. (2000) Anti-CD40, anti-CD3, and IL-2 stimulation induce contrasting changes in CB1 mRNA expression in mouse splenocytes. *J. Neuroimmunol.* **110** (1–2), 161–167.
10. Howlett, A. C., Barth, F., Bonner, T. I., et al. (2002) International Union of Pharmacology. XXVII. Classification of cannabinoid receptors. *Pharmacol. Rev.* **54** (2), 161–202.
11. Shire, D., Calandra, B., Rinaldi-Carmona, M., et al. (1996) Molecular cloning, expression and function of the murine CB2 peripheral cannabinoid receptor. *Biochim. Biophys. Acta* **1307** (2), 132–136.
12. Carlisle, S. J., Marciano-Cabral, F., Staab, A., Ludwick, C., and Cabral, G. A. (2002) Differential expression of the CB2 cannabinoid receptor by rodent

macrophages and macrophage-like cells in relation to cell activation. *Int. Immunopharmacol.* **2** (1), 69–82.

13. Nowell, K. W., Pettit, D. A., Cabral, W. A., Zimmerman, Jr., H. W., Abood, M. E., and Cabral, G. A. (1998) High-level expression of the human CB2 cannabinoid receptor using a baculovirus system. *Biochem. Pharmacol.* **55** (11), 1893–1905.

Localization of Cannabinoid CB₁ Receptor mRNA Using Ribonucleotide Probes

Methods for Double- and Single-Label In Situ Hybridization

Andrea G. Hohmann

Summary

This chapter presents a reliable, detailed method for performing double-label *in situ* hybridization (ISH) that has been validated for use in studies identifying the co-localization of cannabinoid CB₁ receptor mRNA with other distinct species of mRNAs. This method permits simultaneous detection of two different species of mRNA within the same tissue section. Double-label ISH may be accomplished by hybridizing tissue sections with a combination of radiolabeled and digoxigenin-labeled RNA probes that are complementary to their target mRNAs. Single-label ISH may be accomplished by following the procedures described for use with radioisotopic probes (here [³⁵S]-labeled) only. Silver grains derived from conventional emulsion autoradiography are used to detect the radiolabeled cRNA probe. An alkaline phosphatase-dependent chromogen reaction product is used to detect the nonisotopic (here, digoxigenin-labeled) cRNA probe. Necessary controls that are required to document the specificity of the labeling of the digoxigenin and radiolabeled probes are described. The methods detailed herein may be employed to detect even low levels of a target mRNA. These methods may be utilized to study co-localization and coregulation of expression of a particular gene within identified neurons in multiple systems.

Key Words: *In situ* hybridization; nonisotopic; digoxigenin; mRNA; riboprobe; CB₁; co-localization; emulsion; autoradiography.

1. Introduction

In situ hybridization (ISH) may be employed to localize cells containing messenger RNA (mRNA), for a particular gene of interest, thereby identifying those cells capable of synthesizing a protein of interest. The present chapter presents a simple method for performing double-label ISH that has been validated for use in studies identifying the co-localization of cannabinoid CB₁

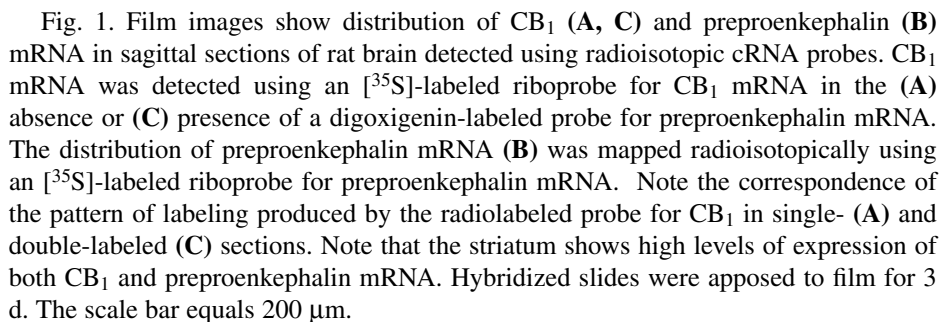
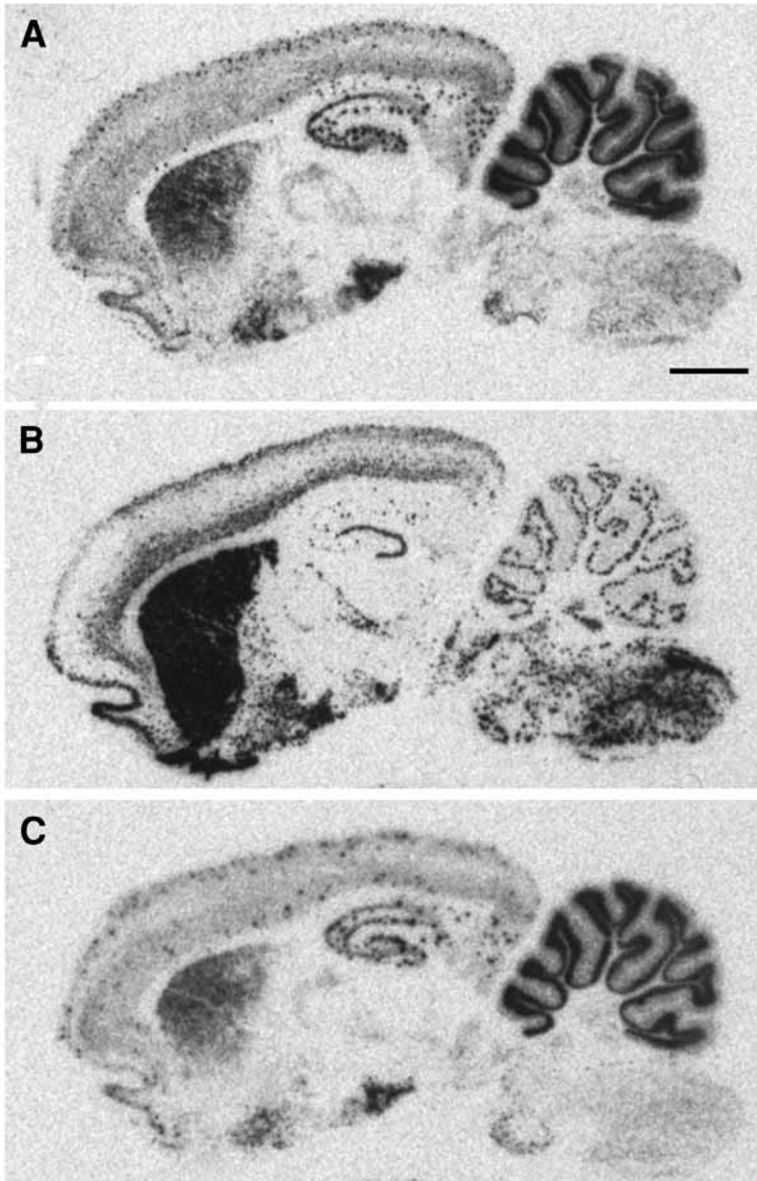


Fig. 1. Film images show distribution of CB₁ (A, C) and preproenkephalin (B) mRNA in sagittal sections of rat brain detected using radioisotopic cRNA probes. CB₁ mRNA was detected using an [³⁵S]-labeled riboprobe for CB₁ mRNA in the (A) absence or (C) presence of a digoxigenin-labeled probe for preproenkephalin mRNA. The distribution of preproenkephalin mRNA (B) was mapped radioisotopically using an [³⁵S]-labeled riboprobe for preproenkephalin mRNA. Note the correspondence of the pattern of labeling produced by the radiolabeled probe for CB₁ in single- (A) and double-labeled (C) sections. Note that the striatum shows high levels of expression of both CB₁ and preproenkephalin mRNA. Hybridized slides were apposed to film for 3 d. The scale bar equals 200 μm.

receptor mRNA with other distinct species of peptide mRNAs (1,2). This method permits simultaneous detection of two distinct species of mRNA within the same tissue section. Double-label ISH may be accomplished by hybridizing tissue sections with a cocktail of radiolabeled and digoxigenin-labeled cRNA probes. Single-label ISH may be accomplished by following the procedures detailed for use with radioisotopic probes (here [³⁵S]-labeled) only. Silver grains derived from conventional emulsion autoradiography are used to detect the radiolabeled cRNA probe (Fig. 1). An alkaline phosphatase (AP)-dependent chromagen reaction product is used to detect the nonisotopic (here, digoxigenin-labeled) cRNA probe. Thus, a co-localization of silver grains over cells marked by the colored reaction products identifies the double-labeled cell (Fig. 2). The specificity of the methods may be monitored by evaluating the correspondence of the radioisotopic and digoxigenin-labeled riboprobe for the same species of mRNA (see Note 1). These methods should be able to demonstrate identical patterns of mRNA co-localization when radioisotopic and digoxigenin-labeled mRNAs are substituted for each other in the same experiment. As an additional control, it is necessary to compare the pattern of mRNA expression produced by [³⁵S]-labeling of each riboprobe using single probes hybridized separately on adjacent tissue sections.

The distribution of cannabinoid CB₁ RNA in brain was first evaluated using oligonucleotide probes for CB₁ (3–5). The development of methods for ISH employing highly sensitive RNA probes, complementary to the mRNA of interest, has facilitated identification of neurons containing even low levels of expression of a target mRNA. The methods described here have been used to specifically evaluate co-localization of cannabinoid CB₁ receptor mRNA with other species of mRNA in rat striatum (2) and dorsal root ganglia (1) using highly sensitive cRNA probes. These methods were used to provide a direct demonstration of co-localization of CB₁ mRNA with mRNA markers of striatonigral (marked by prodynorphin or preprotachykinin A mRNAs) and stri-



atopallidal (marked by proenkephalin mRNAs) projection neurons (2). CB₁ mRNA was also localized to putative GABAergic interneurons that express high levels of GAD67 mRNA but not to cholinergic interneurons (expressing mRNAs for choline acetyltransferase or the vesicular acetylcholine transporter)

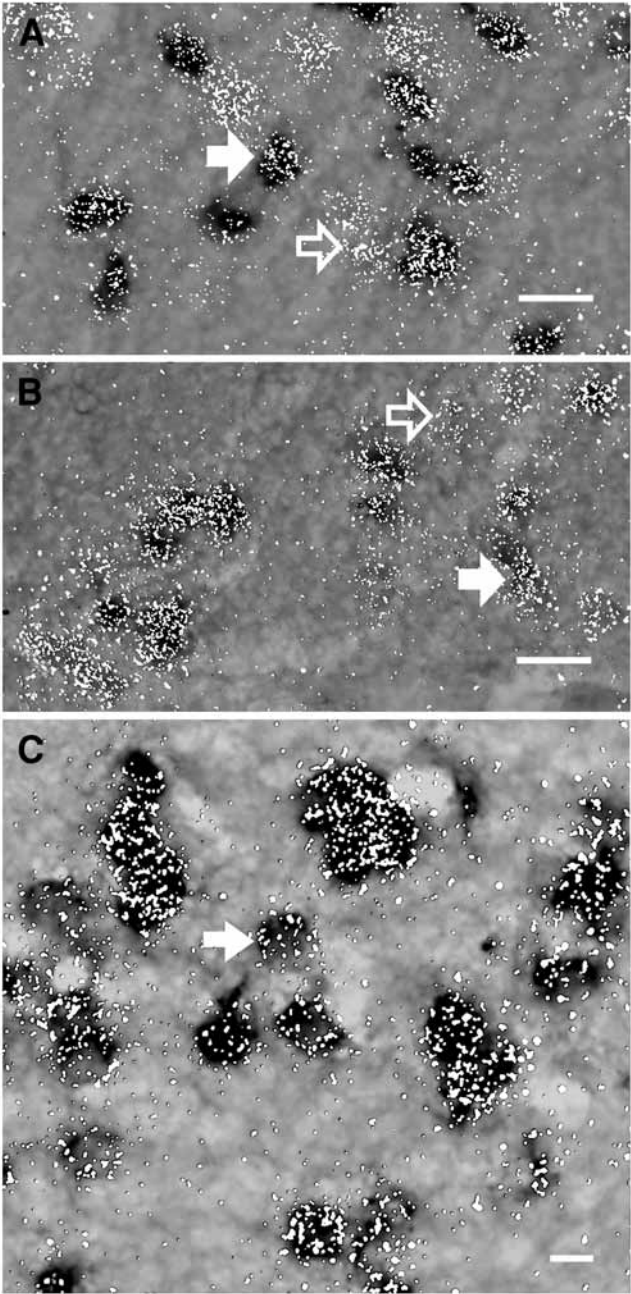




Fig. 2. Photomicrographs show co-localization of CB₁ mRNA with mRNAs for (A) preproenkephalin and (B) prodynorphin in rat striatum. CB₁ mRNA was detected radioisotopically using an [³⁵S]-labeled riboprobe. Preproenkephalin and prodynorphin mRNAs were detected nonisotopically using digoxigenin-labeled riboprobes for each species of mRNA. In all panels, the silver grains mark cells expressing CB₁ mRNA, whereas the colored reaction products mark cells expressing mRNAs for preproenkephalin and prodynorphin in A and B, respectively. The filled arrow shows a double-labeled cell whereas the open arrow shows a cell expressing CB₁ mRNA only. (C) Hybridization of the same tissue section with an [³⁵S]-labeled riboprobe for CB₁ and a combination of digoxigenin-labeled riboprobes for preproenkephalin and prodynorphin mRNAs revealed co-localization of CB₁ mRNA in striatal projection neurons. Striatopallidal neurons expressing preproenkephalin mRNA and striatonigral neurons expressing prodynorphin mRNA were detected using digoxigenin-labeled riboprobes for each respective species of mRNA. In all panels, the accumulation of silver grains over cells marked by the colored reaction product mark the double-labeled cells. Virtually all striatal projection neurons expressed CB₁ mRNA. The scale bar equals 20 μ m. (Adapted from [ref. 2.](#))

or interneurons expressing preprosomatostatin mRNA (2). In dorsal root ganglia, these methods were used to demonstrate co-localization of CB₁ mRNA in small subpopulations of neurons expressing mRNA for preprotachykinin A (a substance P precursor) and α -calcitonin gene related peptide (1). The present methods were adapted from procedures for double-label ISH described previously (6,7).

2. Materials

The supplies and reagents listed here include all materials required to perform single- and double-label ISH on slide-mounted sections using radioisotopic and nonradioisotopic ribonucleotide probes.

Required materials are listed below for each of six steps that are performed sequentially. These steps correspond directly to the methods described in **Subheading 3.**, including: (1) preparation of radioisotopic ([³⁵S]-radiolabeled) and nonisotopic (digoxigenin-labeled) probes by in vitro transcription, (2) preparation of tissue prior to hybridization, (3) riboprobe hybridization, (4) washing of tissue following hybridization, (5) visualization of digoxigenin-labeled probes (for double-label ISH only), (6) film exposure, development, and dipping of slides in autoradiographic emulsion, and (7) developing of slides for visualization of silver grains. This protocol thus permits both single- and double-label ISH to be performed, depending on the need. If only single-label ISH of ribonucleotide probes is required, the procedures pertaining to double-label

ISH only may be omitted (*see* column labeled digoxigenin). Procedures are described in **refs. 1** and **2**.

2.1. *In Vitro* Transcription

1. Δ NTP (final concentration 2.5 mM each):
 - a. 10 mM rATP, rCTP, rGTP.
(Promega no. P1132, P1142, P1152). 5 μ L of each
 - b. Diethylpyrocarbonate (DEPC)-treated water (*see* **Note 2**). 5 μ L
2. UTP (200 μ M final concentration):
 - a. 10 mM UTP. 3 μ L
 - b. DEPC water. 147 μ L
3. 5X transcription buffer (TSC buffer). Store at -70°C
4. Dithiothreitol (DTT; 100 mM) (*see* **Note 3**). Store at -70°C
5. RNasin ribonuclease inhibitor (Promega no. N2113; 40 U/ μ L). Store at -70°C
6. DNA of interest (1 μ g/ μ L).
7. [35 S]UTP (Dupont NEN no. NEG 039H; 50 μ Ci, NEN). Store at -70°C
8. Digoxigenin-11 UTP (Boehringer Mannheim no. 11209256; 400 μ M final conc).
9. RNA polymerase (Promega no. P2083, P2075, P1085; 15–20 U/ μ L). Store at -70°C
10. DEPC water.
11. RQ1 DNase (Promega no. M6101; 1 U/ μ g template). Store at -70°C
12. Tris EDTA (TE) pH 8.0.
13. 5 M DTT. Store at -70°C

2.2. *Tissue Preparation Prior to Hybridization*

1. Triethanolamine hydrochloride (TEA-HCl) solution (pH 8.0):

a.	TEA solution (Sigma T1377).	26.6 mL
b.	6 N HCl.	12 mL
c.	DEPC water.	<u>1961.4 mL</u>
	total volume	2000 mL
2. 4% formaldehyde in 1X phosphate-buffered saline (PBS):

a.	37% formaldehyde.	215 mL
b.	10X PBS.	200 mL
c.	DEPC water.	<u>1585 mL</u>
	total volume	2000 mL
3. Acetic anhydride (Sigma A6404).
4. 70%, 80%, 95%, 100% EtOH.
5. Chloroform.

2.3. Riboprobe Hybridization

1. Labeled riboprobe.
2. 2X riboprobe hybridization buffer (HB):

a. 5 M NaCl (1.2 M final concentration).	4.8 mL
b. 1 M Tris, pH 7.5 (20 mM final concentration).	400 μ L
c. 0.5 M EDTA, pH 8.0 (2 mM final concentration).	80 μ L
d. Sheared single-stranded (ss) DNA (0.02% final concentration, Sigma D7656).	400 μ L (10 mg/mL)
e. Yeast tRNA (0.02% final concentration; BRL/Gibco no. 5401SB).	80 μ L (25 mg/mL)
f. Total yeast RNA, Type X1 (Sigma R6750; 0.1% final concentration).	1 mL (20 mg/mL)
g. Denhardt's solution (50X Sigma D2532; 2X final concentration).	800 μ L (50X)
h. Dextran sulfate (20% final concentration).	8.0 ml (50%)
i. DEPC water.	<u>4.44 mL</u>
total volume	20 mL
- j. Add water, NaCl, Tris, EDTA, dextran, ss DNA, RNA, tRNA, Denhardt's solution.
- k. Tilt and agitate mildly to mix. Store aliquots at -70°C .
3. Formamide.
4. 10% sodium lauryl sulfate (SDS; Sigma L-4522).
5. 10% sodium thiosulfate.
6. 5 M DTT.
7. 4X SSC (sodium chloride containing sodium citrate)/50% formamide solution.
8. Fixed and delipidated tissue.

2.4. Washing of Tissue Following Hybridization

1. RNase A (final concentration: 20 μ g/mL):

a. RNase A (Boehringer Mannheim no. 109169; 20 mg/mL).	1 mL
b. RNase buffer.	1000 mL
2. 2X SSC buffer.
3. 0.2X SSC buffer (for [³⁵S]-labeled slides only).
4. 0.1X SSC buffer (for digoxigenin-labeled slides only).
5. 50% EtOH.
6. 70% EtOH.
7. 80% EtOH.
8. 90% EtOH with 0.3 M ammonium acetate.
9. 100% EtOH.

2.5. Visualization of Digoxigenin-Labeled Probes

1. Digoxigenin-labeling buffer (dig buffer 1):

a. 1 M Tris pH 7.4 (100 mM final concentration).	100 mL
b. 5 M NaCl (150 mM final concentration).	33 mL
c. Sterile water (dH ₂ O).	<u>867 mL</u>
total volume	1000 mL

2. Blocking solution (make fresh or keep refrigerated):

a. 3% normal goat serum (Sigma G-9023).	3 mL
b. 0.3% Triton X-100 (Sigma X-100).	300 µL
c. Dig buffer 1.	<u>97 mL</u>
total volume	100 mL

3. AP-anti-dig solution (10 mL/cytomailer):

a. AP conjugated anti-digoxigenin serum sheep polyclonal (Boehringer Mannheim no. 1093-274; dilute 1:1000).	10 µL
b. Blocking solution.	10 mL

4. AP reaction buffer:

a. 100 mM Trizma pH 9.1 (Sigma T-6128).	6.4 g
b. 5 M NaCl (100 mM final).	10 mL
c. MgCl ₂ · 6 H ₂ O.	5.0 g
d. Sterile dH ₂ O.	490 mL

5. Chromagen solution:

a. 5-Bromo-4-chloro-3-indoyl phosphate toluidinium salt (BCIP; Boehringer Mannheim no. 1585-002). 100% DMFO	9 mg in 500 µL
b. Nitroblue tetrazolium salt 70% DMFO (NBT; Boehringer Mannheim no. 1087-479).	17 mg in 500 µL
c. Levamisole (Sigma L9756).	12 mg
d. AP reaction buffer.	<u>49 mL</u>
total volume	50 mL

6. AP stop buffer (500 mL):

a. 1 M Tris pH 7.4 (100 mM final concentration).	100 mL
b. 5 M NaCl (100 mM final concentration).	10 mL
c. 0.5 M EDTA (10 mM final concentration).	10 mL
d. Sterile water.	380 mL

2.6. Film Exposure, Development, and Dipping of Hybridized Slides

1. Biomax MR film (Kodak)
2. Automatic x-ray film developing system (X-OMAT, Kodak) or appropriate manual alternative)
3. ARC165 standards (Amersham)
4. X-ray cassettes
5. LM-1 emulsion (Amersham)
6. NTB-2 emulsion (Kodak)
7. 0.1% Dreft detergent solution: (1) 0.50 mg Dreft in 50 mL dH₂O; (2) Sonicate to dissolve and filter into 50-mL plastic cylinder
8. D-19 developer (Kodak), prepared according to manufacturer's instructions
9. Rapid-fixer (Kodak; without hardener), prepared according to manufacturer's instructions
10. Sterile water

3. Methods

The methods described here outline the sequential steps involved in single- and double-label ISH using ribonucleotide probes including: (1) preparation of [³⁵S]-radiolabeled or digoxigenin-labeled probes by *in vitro* transcription, (2) preparation of tissue prior to hybridization, (3) riboprobe hybridization, (4) washing of tissue following hybridization, (5) visualization of digoxigenin-labeled probes (for double-label ISH only), (6) film exposure, development, and dipping of slides in autoradiographic emulsion, and (7) developing of slides.

The assay outlined here is conducted over a 3- to 4-d period. On d 1 slide-mounted sections are processed and hybridized. On d 2, slide-mounted sections are subjected to RNase treatment and washed. Slides treated with the radiolabeled probe only are dehydrated, dried, and are ready to be apposed to film. Digoxigenin-labeled sections are incubated in blocking solution (4 h to overnight, depending upon the number of slides processed). On d 3 (or d 2 if overnight incubation is not required), tissues are incubated with the antibody, followed by overnight incubation in chromagen solution. On d 4, the chromagen reaction is stopped and sections are dehydrated. Finally, all sections are exposed to film (for 3–4 d) and slides are coated with emulsion under darkroom conditions. After appropriate exposure times, slides are developed and cover slipped for microscopic localization of cells expressing mRNA markers of interest. An accumulation of silver grains over the colored reaction product marks the cells expressing the two distinct species of target mRNAs (Fig. 2).

3.1. In Vitro Transcription

In vitro transcription is used to synthesize radiolabeled cRNA probes from linearized plasmid DNA (1 μ g) and [35 S]-labeled UTP. An in vitro transcription reaction is also used to synthesize digoxigenin-labeled cRNA probes containing linearized plasmid DNA and digoxigenin-labeled UTP in combination with unlabeled UTP (4:1 digoxigenin-labeled UTP: unlabeled UTP, respectively). Briefly, the materials noted below are added to transcription buffer with DTT, RNase inhibitor (RNasin), sterile water, and RNA polymerase added. The transcription reaction is run at 37°C for 30 min for the radiolabeled riboprobes and 1 h for the digoxigenin-labeled riboprobes. At this time, the appropriate RNA polymerase is added, and the reaction proceeds at 37°C for the same time intervals. Sterile water is added to the [35 S] reaction. RNasin and RQ1 DNase are added to each reaction, and the incubation proceeds at 37°C for 10 min. The DNase reaction is terminated for the digoxigenin-labeled probe with the addition of Tris EDTA (TE pH 8.0). The probes are purified using Pharmacia Biotech Probequant columns. After purification, the optical density of the digoxigenin-labeled riboprobe is determined using a spectrophotometer. A reading of 1 at 260 nm corresponds to single-stranded RNA with a concentration of 40 μ g/mL. The concentration of the stock probe can be determined and diluted to obtain a concentration of 2 pmol digoxigenin-labeled riboprobe per 1 mL hybridization buffer (*see Note 4*). The in vitro transcription reaction for the radiolabeled probe is monitored by liquid scintillation counting to ensure that probes may be applied to tissue at 1 million cpm/30 mm cover slip (*see Note 4*).

	Digoxigenin	35 S
1. Mix at 25° C		
a. 5X transcription buffer	6 μ L	6 μ L
b. 100 mM DTT	3 μ L	3 μ L
c. RNasin (40 U/ μ L)	1 μ L	0.6 μ L
d. Δ NTP	6 μ L	5.5 μ L
e. DNA (1 μ g/ μ L)	1 μ L	1 μ L
f. [35 S]-UTP	—	15 μ L
g. Digoxigenin-11-UTP	1.2 μ L	—
h. 100 μ M UTP	3 μ L	—
i. RNA polymerase	1 μ L	1 μ L
j. DEPC water	7.8 μ L	—
total volume	30 μ L	32.1 μ L
2. Incubate at 37°C	1 h	30 min
3. Add RNA polymerase	1 μ L	1 μ L
4. Incubate at 37°C	1 h	30 min
5. Add sterile dH ₂ O	—	14.9 μ L

- | | | |
|---------------------|-----------------------------|-------------------|
| 6. Add RNasin | 1 μ L | 1 μ L |
| 7. Add RQ1 DNase | 1 μ L | 1 μ L |
| 8. Incubate at 37°C | 10 min | 10 min |
| 9. Add TE pH 8.0 | <u>17 μL</u> | <u> </u> |
| total volume | 50 μ L | 50 μ L |
10. Remove unincorporated NTPs
- a. Resuspend resin in Pharmacia Biotech ProbeQuant columns (Pharmacia no. 27-5335-01) by vortexing for 5 s
 - b. Loosen cap and snap off bottom of column
 - c. Prespin column in empty 1.5-mL Eppendorf tube in table top microfuge (speed 3 for 1 min)
 - d. Place column in new labeled 1.5-mL Eppendorf tube and apply 50- μ L sample to center of resin bed
 - e. Spin again at speed 3 for 2 min
 - f. Collect probe in Eppendorf tube labeled from **step d**
11. Determine probe concentration/labeling
- a. For dig: measure A₂₆₀ and A₂₈₀ of 2 μ L in 98 μ L TE pH 8.0
 $(A_{260} = 1.0 \text{ for RNA at } 40 \mu\text{g/mL})$

The desired concentration is approx 2 pM digoxigenin-labeled riboprobe/ mL hybridization buffer (usually this works out to be 2–6 μ L probe/50 μ L buffer)
 - b. For [³⁵S]: Add 1 μ L 5 M DTT and count 1 μ L in 10 mL cytoscent
12. Calculate required quantities of materials (i.e., probes, hybridization buffer, etc.) based upon number of slides and cover slip length required to hybridize all slide-mounted sections in the assay. This can be easily automated in Excel. Riboprobe hybridization buffer must be prepared with at least 20% more volume than would be calculated otherwise based on the number of slides.

3.2. Tissue Preparation Prior to Hybridization

Tissue sections are obtained from rats that are killed by decapitation. The brains (or other required tissue) are rapidly removed and frozen in isopentane that has been precooled (–30°C) on dry ice. Sections (14 μ M) are cryostat-cut and mounted (two sections per slide) under conditions that minimize RNase contamination. Mounting sections close to the bottom of the subbed slides will conserve reagents required for double-label ISH. Multiple adjacent series of sections are obtained, depending on need. For example, it is advisable to take a series for each [³⁵S]-labeled riboprobe both alone and in combination with each appropriate digoxigenin-labeled riboprobe. Slide-mounted sections are sorted at –20°C (in cryostat or cold room) prior to the assay to obtain the required number of near adjacent series. Slides brought to room temperature cannot be

returned to -80°C . Sagittal brain sections (or relevant positive control tissue) are included in each assay to verify that appropriate distribution of mRNA is obtained. Slide boxes containing tissue sections are stored in sealed plastic bags with sealed desiccant at -80°C . Gloves are worn during all procedures (including cutting of tissue and final stages for subbing of slides) and RNase-free solutions are employed in all prehybridization steps.

Prehybridization steps are identical for tissue hybridized with the $[^{35}\text{S}]$ -radiolabeled probe alone and tissue hybridized with the digoxigenin-labeled riboprobe applied in combination with the appropriate $[^{35}\text{S}]$ -radiolabeled probe. Slides are allowed to equilibrate to room temperature, are loaded into slide racks, fixed in formaldehyde-PBS buffer, rinsed in triethanolamine buffer (TEA-HCl), and incubated in TEA-HCl with fresh acetic anhydride added (10 min). Slides are subsequently dehydrated in ascending concentrations of ethanol, defatted by incubation in chloroform, rinsed in ethanol and air-dried. At this point, slides are now ready to be hybridized, although slides can also be stored at -80°C without loss of signal.

- | | |
|--|------------|
| 1. Fix tissue in 4% formaldehyde in 1X PBS | 1 min |
| 2. Rinse in TEA-HCl | |
| 3. Add 2.5 mL acetic anhydride to 1 L TEA-HCl, mix vigorously, and add to tissue | |
| 4. Incubate | 10 min |
| 5. Dehydrate/delipidate tissue by incubating in | |
| a. 70%, 80%, 95%, 100% EtOH | 1 min each |
| b. Chloroform | 5 min |
| c. 100% EtOH | 1 min |
| d. 95% EtOH | 1 min |
| 6. Air dry slides | 20 min |
| 7. Proceed with hybridization or box slides and store at -35°C in sealed bag with drierite | |

3.3. Riboprobe Hybridization

For double-label ISH, slide-mounted sections are hybridized with a cocktail of $[^{35}\text{S}]$ -labeled and digoxigenin-labeled riboprobes. We have found the greatest sensitivity (without additional steps for amplification) when the $[^{35}\text{S}]$ -labeled probe is used to label CB_1 mRNA and the digoxigenin-labeled probe is used to label typically more abundant peptide mRNAs of interest (e.g., prepro-tachykinin A, prodynorphin, and proenkephalin mRNA). In adjacent sections, the correspondence of the $[^{35}\text{S}]$ -labeled riboprobe with each digoxigenin-labeled riboprobe for the same species of mRNA should be examined in adja-

cent tissue sections. Riboprobe hybridization buffer is prepared in quantities required to cover slip all sections during hybridization procedures (based on 50 μL /30-mm cover slip). The concentration of radiolabeled probe is adjusted to yield 1 million cpm per 30-mm cover slip. The final concentration of digoxigenin-labeled probe is typically 2–6 μL /50 μL hybridization buffer (final volume). Probes are added to 2X riboprobe hybridization buffer, and probes are denatured by heating at 90°C for 5 min, and then quickly cooled on wet ice. Formamide, sodium dodecylsulfate (SDS), sodium thiosulfate, and DTT are added in the concentrations and volumes noted below.

Slides are placed in hybridization trays containing Whatman filter paper soaked in standard saline citrate (SSC)/formamide solution. Riboprobe hybridization buffer is applied to tissue using a repeater pipet, and slides are cover slipped. The cocktail of digoxigenin and [^{35}S]-labeled riboprobe hybridization buffer (or the [^{35}S]-labeled riboprobe hybridization buffer alone) is applied to tissue in fixed volumes determined by the size of the cover slip required to cover the sections (i.e., 50 μL per 30-mm cover slip for sections mounted one or two per slide or 100 μL per 5-mm cover slip for sections mounted three or four per slide). Slides are placed in a humidified chamber and incubated overnight at 52–55°C.

1. Prepare riboprobe hybridization buffer (ribo HB) mixture based on required quantities:

a. Total volume	50 μL /30-mm cover slip
b. Labeled riboprobe—digoxigenin	2–6 μL dig-probe/50 μL
—[^{35}S]	1 million cpm/30 mm cover slip
c. 2X ribo HB	0.5 \times total volume
d. Add probe to riboprobe HB	
e. Heat-denature probe and HB	5 min at 90°C
f. Cool in ice	5 min
g. Add formamide	0.5 \times total volume
h. Add 10% SDS	0.01 \times total volume
i. Add 10% sodium thiosulfate	0.01 \times total volume
j. Add 5 M DTT	0.02 \times total volume
2. Apply probe to tissue and cover slip:
 - a. Arrange slides on hybridization trays lined with filter paper saturated with 4X SSC/50% formamide
 - b. Use repeater pipette to deliver:
 - 50 μL HB mixture/30 mm cover slip (one to two sections) or
 - 100 μL HB mixture/50 mm cover slip (three to four sections)
 - c. Position small wells (e.g., caps taken from 60-mL conical tubes) of 4XSSC/50% formamide in each tray to prevent dehydration
3. Incubate tissue overnight in humidified incubator at 52–55°C

3.4. Washing of Tissue Following Hybridization

Following hybridization, cover slips are removed by soaking the cover slipped slides in disposable graduated cylinders containing 2X SSC buffer. Slides are loaded into racks, subjected to RNase treatment, and high-stringency washes are performed at the designated temperature in SSC buffers, as described below.

- 1. Remove cover slips and load into vertical racks submerged in 2X SSC. Soak cover slipped slides in 2X SSC until the cover slips slide off).
- 2. RNase treatment
 - a. Incubate in RNase buffer + RNase A 30 min
 - b. Rinse in RNase buffer 30 min
 - c. Rinse in 2XSSC
- 3. High-stringency washes. Transfer slides to buffers containing

	Digoxigenin	[³⁵ S]
a. 2X SSC	1h/50°C	1 h/50°C
b. 0.1X SSC	rinse/60 °C	
0.2X SSC		rinse/55°C
c. 0.1X SSC	1h/60°C	
0.2X SSC		1 h/55°C
d. 0.2X SSC		1 h/60°C
- 4. For [³⁵S] only: dehydrate tissue
 - a. 50, 70, 80, 90% EtOH with 0.3 M ammonium acetate 1 min each
 - b. 100% EtOH 1 min
 - c. Air-dry slides 20 min
 - d. [³⁵S]-labeled slides are ready to be put on film. Digoxigenin-labeled sections proceed to visualization step.

3.5. Visualization of Digoxigenin-Labeled mRNA

Slide-mounted sections are rinsed, incubated in blocking solution (1–2 h) and washed in Tris buffer (see Note 5). Slides are then transferred to cytomailers for incubation (3 h) in the diluted anti-digoxigenin-conjugated antibody, which is conjugated to alkaline phosphatase. Slides are subsequently rinsed in DIG buffer I and AP reaction buffer, respectively. Visualization of digoxigenin-labeled riboprobes is carried out by incubation in chromagen solution (see Note 6), followed by several washes. Cytomailers are wrapped in aluminum foil (see Note 6), and the reaction is allowed to proceed overnight in the refrigerator (4°C). Slides are transferred to slide racks or clean cytomailers, and the reaction is stopped by incubation in Tris buffer containing EDTA (AP stop buffer) for 30 min. Cells labeled by the AP-dependent chromagen reaction product are marked by a purple colored reac-

tion product (*see Note 7*). Cells will appear against a background that is a light creamy beige in tone (**6**).

1. Place slides in cytomailers to conserve materials. We typically use five-slide cytomailers for washes that can be autoclaved and reused.
2. Wash slides with dig buffer 1 on orbital shaker 3 × 5 min @ 150 rpm
3. Incubate with 5–10 mL blocking solution 1–2 h @ 150 rpm
4. Incubate with 10 mL AP-anti-dig solution 4 h to overnight
5. Wash in dig buffer 1 3 × 5 min @ 150 rpm
6. Wash in AP reaction buffer 3 × 5 min @ 150 rpm
7. Transfer slides to foil-wrapped cytomailers
8. Incubate in chromagen solution Overnight @ 4°C
9. Wash slides in AP stop buffer 3 × 5 min @ 150 rpm
10. Wash in distilled water 3 × 5 min @ 150 rpm
11. Air-dry slides 4 h to overnight
12. Load slides in cassette and expose to X-ray film for [³⁵S] for 1–7 d. Be sure to include a standard. (Amersham [¹⁴C] standards [ARC165] are appropriate for use with [³⁵S]).
13. Develop film (Kodak MR film) to produce film image of cells labeled by the [³⁵S]-labeled riboprobe (*see Note 8*). The film image is appropriate for quantifying mRNA densities using autoradiography and computer-assisted densitometry.

3.6. Dipping of Slides

To visualize silver grains that correspond to mRNAs labeled by the [³⁵S]-labeled riboprobe on single- and double-labeled slides, slide-mounted sections are dipped in emulsion under strict darkroom conditions. After emulsion has dried (2–4 h), slides are loaded into light tight boxes, exposed for several weeks under light-tight conditions and developed in Kodak D-19 developer.

1. In darkroom, turn on humidifier and set water bath to 42–44°C
2. Cover counter with absorbent material (e.g., Chix wipes) and set up drying racks on top of wipes. Pieces of angle iron can readily be used to support slides vertically during drying.
3. Under strict darkroom conditions, add NTB-2 and/or LM-1 emulsion (*see Note 9*) into their respective plastic cylinders and warm (along with 0.1% Dreft solution) in water bath. Allow emulsion to equilibrate for 45 min.
4. Dilute NTB-2 with Dreft solution (1:1) and stir with glass rod. Invert several times to disperse bubbles. LM-1 emulsion is not diluted. Allow emulsion to equilibrate for 1 h.
5. Stir each emulsion with clean glass rods and dip a clean subbed slide up and down (~50 times) to remove air bubbles. Check for a homogeneous coating of emulsions by dipping clean subbed slide in each respective emulsion.
6. Dip slides in emulsion slowly (a few seconds down, a few seconds up) and remove emulsion from the back of the slide with Kim-wipes. Slides are always boxed in the same orientation to avoid inadvertently touching the sections.

7. Place slides vertically against the drying racks and let dry for 2 h.
8. Place slides in light-tight boxes with enclosed desiccant. Slide boxes are wrapped (still under strict darkroom conditions) securely in aluminum foil and stored in -20°C for 1–12 wk.

3.7. Developing

Slides are developed in D-19 (Kodak). D-19 is prepared according to manufacturers instructions by slowly dissolving D-19 in distilled water (3.8 L final volume) at 52°C . To ensure that developer is at the proper temperature for developing slides, D-19 must be prepared at least 24 h in advance. Kodak Rapid Fixer is also prepared according to manufacturer's instructions, by diluting contents to 3.8 L (final volume) with distilled water. Following development, slides labeled with the [^{35}S] probe only (single-label) are lightly counterstained with cresyl violet. Digoxigenin-labeled sections (double-labeled) are typically not counterstained or dehydrated in ethanol to avoid bleaching of chromagen reaction product (*see Note 10*). Double-labeled cells may be visualized microscopically (*see ref. 2*) by evaluating co-localization of isotopic (silver grain-labeled) and nonisotopic (digoxigenin-labeled) markers of target mRNAs (*see Note 11*).

1. Allow foil-wrapped slide boxes to warm to room temperature (RT) and load slides into slide racks.
2. Prechill solutions by incubating staining dishes in wet ice slurry to bring solutions to $16\text{--}18^{\circ}\text{C}$
3. Develop slides under strict darkroom conditions. Ensure that safelight, if used, is appropriate for specific emulsion employed and that safelight veins are closed.
 - a. Submerge slides in D-19 with gentle agitation 2 min
 - b. Submerge in dH_2O 15 s
 - c. Submerge in fixer (without hardener) 2 min
 - d. Rinse in running tap water 20 min
 - e. Darkroom conditions are no longer required.
 - f. Rinse in dH_2O $3 \times 1 \text{ min}$
 - g. For [^{35}S] only: Proceed to Nissl stain
 1. Submerge in: Nissl stain 2 min
 2. 25% EtOH (short exposures of several s)
 3. 50% EtOH
 4. 70% EtOH
 5. 70% EtOH with 0.1% acetic acid
 6. 95% EtOH 1 min
 7. 100% EtOH 1 min
 8. Fresh 100% EtOH 1 min
 9. Xylene 5 min
 - h. For Digoxigenin-labeled slides: air dry 4 h to overnight

4. Cover slip slides

- a. Submerge slides in xylene 3 × 5 min
- b. Cover slip slides with permount

4. Notes

1. Controls must be performed to confirm that the radiolabeled and nonisotopic signals reflect specific hybridization signals for the targeted mRNAs. This is typically accomplished by (1) comparing the anatomical correspondence of the digoxigenin labeled probe with the [³⁵S] label for the same species of mRNA in adjacent tissue sections, (2) demonstrating co-localization of digoxigenin and [³⁵S]-labeled riboprobes for the same species of mRNA in the same section, (3) demonstrating that multiple probes labeling nonhomologous regions of the target mRNA show identical patterns, (4) demonstrating the absence of signal when sense rather than antisense probes are hybridized to adjacent tissue sections, and (5) demonstrating the absence of signal when tissues are pretreated with RNase.
2. For all prehybridization steps, we use strict RNase-free procedures both to minimize degradation of mRNAs within the tissue section and to produce a strong, specific hybridization signal. All solutions for prehybridization steps are prepared using molecular-biology-grade (18.2 MΩ) water that has been diethylpyrocarbonate (DEPC)-treated (1 mL/L) overnight and autoclaved. Slide carriers and containers used for incubations in the prehybridization steps are similarly treated with DEPC added to sterile water and incubated overnight prior to autoclaving. Gelatin-subbed slides are baked overnight in a convection oven (60°C) and handled with gloves. Gloves are worn during cutting of sections and throughout all procedures both to minimize contamination by RNase and/or exposure to radioligand. The stringent precautions involving autoclaved DEPC-treated water are eliminated during the wash steps.
3. Increasing the concentration of DTT in the hybridization mixture (to 200 mM DTT) has been employed to reduce background (i.e., nonspecific binding of probe) produced by radiolabeled probes (6). Background is typically extremely low with the methods described here, although the signal and specificity of the labeling of low abundance mRNAs or tissues presenting higher backgrounds (e.g., human brains) are reported to be optimized with such modifications (6). Reducing the ratio of unlabeled to radiolabeled UTP could also be expected to enhance the signal of low abundance mRNAs.
4. Digoxigenin-labeled probes are typically quite stable and may be stored at -20°C for several months with no apparent loss sensitivity. Radiolabeled probes typically show sufficient activity to be used over several days in the range of about 1 wk.
5. Slides are incubated with antibody in cytomailers (each holding five slides and approx 10 mL incubation volume) to conserve materials and ensure uniformity in incubation procedures. Sections should be mounted towards the bottom of the slides to conserve buffers and antibody required for various incubations.
6. The chromagen solution employed for visualization of digoxigenin-labeled mRNAs is sensitive to light, and is therefore prepared shortly before use.

Chromagen solution (per 50 mL) may be prepared by separately dissolving bromochloroindoyl phosphate (BCIP) (9 mg) in a small volume (500 μ L) of 100% *N,N*-dimethylformamide (DMFO) and nitroblue tetrazolium (NBT) (17 mg) in a small volume (500 μ L) of 70% DMFO and adding these to a foil-wrapped flask containing the AP reaction buffer. Levamisole can be dissolved directly in a small volume of AP reaction buffer and the mixture should be vortexed well. Chromagen solution is loaded into cytomailers just prior to adding slides. This solution may be filtered with a Millipore (0.22 μ m) to reduce crystalline artifacts in the background (6), but we have not found such measures necessary with the above methods. This buffer can readily be made during the second AP reaction buffer wash and stored at 4°C on the day of use.

7. The intensity of the colored reaction product of the digoxigenin-labeled cells will vary depending upon the amount of the targeted mRNA that is expressed in the cell. The darker the color of the labeled cells marked by the chromagen reaction product, the higher the level of target mRNA. This reaction is both time and temperature sensitive (6). Therefore, it is important to determine the optimal expression level for cells of interest in pilot studies; the intensity of the colored reaction product should not be so intense that it quenches the autoradiographic expression of silver grains produced by the radiolabeled probe in emulsion-coated sections. The intensity of the colored reaction product can also be monitored by removing test slides from the reaction for microscopic visualization to confirm that adequate labeling is obtained. The overnight incubation is used routinely as it eliminates variability and produces very consistent labeling. The amount of digoxigenin-labeled probe hybridized to slides should therefore be determined in pilot studies.
8. Digoxigenin-labeled test slides should be apposed to film to determine that radio-labeling has proceeded satisfactorily prior to dipping of slides. Test slides should also be collected, dipped, boxed, and developed separately to monitor that the duration of exposure of emulsion-coated sections is adequate and ensure that slides are not developed prematurely. It is especially important to confirm that the digoxigenin-labeling has not quenched the autoradiographic expression of silver grains, requiring longer exposure times than that required for radioisotopic (single-label) ISH alone.
9. Slides can be coated in 3% parlodion in isoamyl acetate to prevent negative chemography from occurring between the colored reaction product and NTB-2 emulsion (6). We have obtained good results using LM-1 emulsion (Amersham) without requiring the need for parlodion. Miller and colleagues (6) report that an additional benefit of the parlodion layer is that it prevents tissues from turning purple when exposed to the photographic fixer.
10. Digoxigenin-labeled slides are not counterstained to ensure that stain does not obscure detection of the digoxigenin signal. Nonetheless, sections exposed to the Kodak Rapid fixer turn a faint purple and may appear as if they have been Nissl-stained (6). The color of fiber tracts is not altered.
11. Reflected light darkfield microscopy (epifluorescence) can be used to visualize silver grains on darkly colored digoxigenin-labeled cells and obtain better contrast

than conventional darkfield microscopy (2). Silver grains can also be counted in conventional reflected light darkfield via automated image analysis (6).

Acknowledgments

Protocols for ISH using ribonucleotide probes ([³⁵S]-labeled) and procedures for dipping of slides were originally developed in the laboratory of Miles Herkenham. These protocols were adapted for double-label ISH (1,2) primarily based upon methods described by Miller and colleagues (6). Thus, several of the methods described here, especially those pertaining to single-label ISH and dipping, have evolved with contributions from several individuals. Special thanks go to Miles Herkenham, Michael Whiteside, Linda Brady, Ning Quan, and Eileen Briley.

References

1. Hohmann, A. G. and Herkenham, M. (1999) Localization of central cannabinoid CB₁ receptor messenger RNA in neuronal subpopulations of rat dorsal root ganglia: a double-label in situ hybridization study. *Neuroscience* **90**, 923–931.
2. Hohmann, A. G. and Herkenham, M. (2000) Localization of cannabinoid CB₁ receptor mRNA in neuronal subpopulations of rat striatum: a double-label in situ hybridization study. *Synapse* **37**, 71–80.
3. Mailleux, P. and Vanderhaeghen, J. J. (1992) Distribution of neuronal cannabinoid receptor in the adult rat brain: a comparative receptor binding radioautography and in situ hybridization histochemistry. *Neuroscience* **48**, 655–668.
4. Mailleux, P. and Vanderhaeghen, J. J. (1992) Localization of cannabinoid receptor in the human developing and adult basal ganglia. Higher levels in the striatonigral neurons. *Neurosci. Lett.* **148**, 173–176.
5. Matsuda, L. A., Bonner, T. I., and Lolait, S. J. (1993) Localization of cannabinoid receptor mRNA in rat brain. *J. Comp. Neurol.* **327**, 535–550.
6. Miller, M. A., Kolb, P. E., and Raskind, M. A. (1993) A method for simultaneous detection of multiple mRNAs using digoxigenin and radioisotopic cRNA probes. *J. Histochem. Cytochem.* **41**, 1741–1750.
7. Minami, M., Maekawa, K., Yabuuchi, K., and Satoh, M. (1995) Double in situ hybridization study on coexistence of μ -, δ - and κ -opioid receptor mRNAs with preprotachykinin A mRNA in the rat dorsal root ganglia. *Brain Res. Mol. Brain Res.* **30**, 203–210.

Morphometric Study on Cytoskeletal Components of Neuronal and Astroglial Cells After Chronic CB₁ Agonist Treatment

Patricia Tagliaferro, Alberto J. Ramos, Emmanuel S. Onaivi, Sergio G. Evrard, Maite Duhalde Vega, and Alicia Brusco

Summary

One of the major goals for the use of digital image analysis systems in neuroanatomy is to visualize structures, cells, or other tissue components in order to compare various populations. In addition, digital image analysis allows semi-quantification of cell labeling because it is capable of measuring simultaneously the staining intensity, location, size, and shape of labeled profiles. In the present work, the morphological changes in the CB₁ hippocampal area and corpus striatum induced by chronic treatment with the synthetic CB₁-receptor agonist WIN55,212-2 were analyzed as an example of digital image analysis application. Twice-daily treatment for 14 d with the CB₁-receptor agonist demonstrated significant changes in the expression of neuronal cytoskeletal proteins and in neuronal morphology, as evidenced by immunocytochemical and digital analysis studies. However, changes in the expression of astroglial cytoskeletal proteins were not found.

Key Words: Immunohistochemistry; digital image analysis; morphological parameters; cell area; optical density; cytoskeletal proteins.

1. Introduction

1.1. General Aspects

Since the 1960s, immunocytochemical techniques have become a major tool for mapping neurotransmitter pathways in the central nervous system (CNS) and have vastly expanded our knowledge about the anatomical location as well as the relationship among the neurotransmitter systems in the brain. The study of morphological alterations induced by pharmacological treatments, drugs, and toxicants exposure is an interesting field of neuroscience. Morphological

studies are an important tool to analyze neuronal plasticity, the expression of growth factors, receptors, and different intracellular molecules. All these morphological effects follow acute alterations in second messenger cascades and represent long-term effects. The combination of morphological studies with digital image analysis allows the observation of structural alterations but also the semi-quantification of different morphological parameters.

The human visual system is an efficient biological system that allows the qualitative evaluation of the image parameters, although the quantification of those parameters requires more exact tools. Digital image analysis was developed in the 1970s, but until the 1980s its use was very limited. After the appearance of smaller, faster, and less expensive personal computers, the image analysis has been in continuous expansion and development. The use of these techniques requires some basic knowledge of neuroanatomy to establish parameters and to measure and evaluate them in a precise way.

An image is an object representation and the first step in image analysis is to obtain a digitized image—the transformation of the given image into a discrete number of values with which mathematical transformations are able to be made. If the image is obtained by digital equipment (i.e., digital cameras or scanners), this step is made by the camera itself. The image units are pixels, which includes values of localization (X,Y), color, and intensity. Once the image has been digitized, it is easy to perform hundreds of mathematical transformations to change image appearance and to facilitate the evaluation.

In neuroscience studies, several parameters are useful to analyze the changes induced in CNS morphology by different drugs or toxicants (1–6). The analysis of cytoskeletal proteins by these morphometric methods using digital image analysis has been performed in our laboratory to study the relative area covered by cell cytoskeleton by means of the analysis of different cytoskeletal proteins and the structural changes of those components. Other transformations of these parameters, such as the introduction of a tissue section thickness, allow the stereological evaluation of volumetric variations, therefore rendering a three-dimensional (3D) study of the samples (1). Surface analysis is simple to perform, and the results are comparable to those obtained by volumetric analysis.

Endocannabinoids are present in the peripheral and CNS (7). In the CNS, endocannabinoids exert most of their pharmacological actions by activating the CB₁ receptor, which is expressed in neurons of specific brain regions (8,9). The CB₁ cannabinoid receptor is also expressed in astroglial cells (10,11), strengthening the importance of the neuron–astroglial relationship. The administration of endocannabinoids to experimental animals produces several of the pharmacological and behavioral actions associated with cannabinoids (12–15). Endocannabinoids may play a role as modulators of neurotransmitters release and action (10). On the other hand, the CB₁ receptor may be involved in synap-

tic plasticity (16) because cannabimimetic drugs are known to inhibit adenylyl cyclase and impair memory (17–19). Most of these effects of cannabimimetic drugs might be accompanied by morphological changes in different cellular populations. Cellular cytoskeleton is responsible for cellular morphology, and alterations in cytoskeletal components have been observed in many circumstances such as in synaptic plasticity, sprouting, and cellular damage. Digital image analysis offers us an important tool for estimating the type and size of these alterations.

In the present work, morphological changes were analyzed in the neuronal and astroglial cytoskeleton as well as the alterations in the area covered by neuronal processes induced by a chronic treatment with a classic synthetic CB₁ agonist, WIN55,212-2. Neurofilaments, microtubule-associated protein-2 (MAP-2), and glial fibrillary acidic protein (GFAP) expression were analyzed in the stratum radiatum of the hippocampal CA₁ area and in the corpus striatum. These areas were chosen because it has been reported that cannabinoids cause alterations in learning and memory in laboratory animals (17). Cannabinoids are also thought to decrease locomotor activity by inhibiting γ -aminobutyric acid (GABA) uptake at striatopallidal and striatonigral terminals and reducing dopamine uptake in the striatum (20). Morphological changes in neuronal and astroglial cytoskeleton as well as alterations in the area covered by neuronal cytoskeleton were studied by immunocytochemical techniques and digital image analysis.

1.2. Applications of Image Analysis in the Study of the CNS Morphology

One of the primary reasons for using digital image analysis in neuroanatomy is to statistically summarize and evaluate a structure to allow comparisons among populations. Digital image analysis offers a wide range of possibilities that are very useful when analyzing morphological changes. In this particular study, densitometry and morphometry, which are widely utilized functions of the digital image analysis, were used. Densitometry was employed to estimate the relative concentrations of different antigens detected by immunocytochemistry, while morphometry was used to study cell morphology and the relative area covered by cellular projections. Digital image analysis allows one to semi-quantify immunocytochemical experiments because it is capable of measuring simultaneously the labeling intensity, localization, size and shape of the labeled profiles.

1.2.1. Densitometry

Optical density measurements are those that read and evaluate the pixels' gray level in order to extract numerical information from the image (21). It is a very important parameter, because it allows the semi-quantification of

immunostaining intensity. The densities are proportional to the amount of antigen in the sample. It is possible to obtain a gray value either at any pixel. The gray value represents the intensity of pixel color in a numeric scale, usually 0–256 in 8-bit software. The computer software can also draw a line on the image and plot the gray value of the pixels along the line or the region of interest, which may also be a rectangle or even an irregularly shaped polygon. The main objective of semi-quantitative densitometry is to obtain measurements that can reflect the biological characteristics of the tissue. This is very useful, for example, when comparing variations in the immunostaining intensity of an antigen in a specific cellular population after a treatment that can induce alterations in its protein expression. Image analyzers based on cameras where the specimen is illuminated by diffuse light use parameters based on gray levels to measure optical densities. If the analyzer resolution is 8 bits, the possible maximum number of gray levels will be 256. The gray level transmittance (GLT) can be measured as follows:

$$\text{GLT} = \frac{\text{Observed gray levels}}{\text{Maximum number of gray levels (256)}}$$

or the observed gray levels can be converted to relative optical densities (RODs) by using the following formula:

$$\text{ROD} = \log_{10} \frac{\text{Maximum number of gray levels (256)}}{\text{Observed gray level}}$$

As described below, ROD values are used to compare the same cellular type from different tissue sections after experimental treatments. In this way, the immunostaining intensity of an antigen can be measured.

1.2.2. Morphometry

The measurement of morphometric parameters such as area, perimeter, centroid, angles, distance between structures, and maximum or minimum diameter can be used to obtain information about structures and their spatial relationship in a tissue section. These structures could be cells, cellular nuclei, cytoplasmic projections, fiber varicosities, cytoplasm inclusions, etc. All these parameters allow for the quantification of morphological data. Values obtained from these measurements can be read in different ways: through a table of values, a histogram (where different parameters can be analyzed), or graphics (where more than two parameters can be compared at the same time). The image analyzer can also offer statistical values such as mean, standard deviation, and standard error, or export the values to appropriate statistics software.

2. Materials

1. Male WISTAR rats (HSD: WI; weight: 150–160 g).
2. Dimethylsulfoxide (DMSO) (Merck, Darmstadt, Germany).
3. WIN55,212-2 mesylate (Research Biochemicals International, Natick, MA).
4. Chloral hydrate (Sigma Chemical Co, St. Louis, MO).
5. First washing solution: saline solution (0.9% w/v NaCl) containing 0.05% w/v NaNO₂ plus 50 IU of heparin (4°C).
6. Fixative solution, containing 4% w/v paraformaldehyde and 0.25% v/v glutaraldehyde in 0.1 M phosphate buffer, pH 7.4 (4°C).
7. Second washing solution, 0.1 M phosphate buffer pH 7.4 containing 5% w/v sucrose (4°C).
8. Oxford vibratome.
9. Cryoprotective solution, containing 25% w/v sucrose in 0.1 M phosphate buffer pH 7.0.
10. H₂O₂ 100 vol (30% v/v) (Merck, Darmstadt, Germany).
11. Methanol and ethanol (Merck, Darmstadt, Germany).
12. Normal goat serum.
13. 0.1 M phosphate-buffered saline (PBS), pH 7.4.
14. Primary antibodies: mouse monoclonal anti-neurofilaments—200 KDa (Nf-200) (diluted 1:2000), mouse monoclonal anti-MAP-2 (diluted 1:1000), rabbit polyclonal anti-GFAP (diluted 1:3000) (Sigma Chemical Co., St. Louis, MO) (GFAP, DAKO).
15. Biotinylated secondary antibodies diluted 1:200 (Sigma Chemical Co., St. Louis, MO).
16. Streptavidin–peroxidase complex diluted 1:400 (Sigma Chemical Co., St. Louis, MO).
17. Triton X-100 (Sigma Chemical Co., St. Louis, MO).
18. 0.1 M acetate buffer (AcB) pH 6.0.
19. 3,3'-Diaminobenzidine (Sigma Chemical Co., St. Louis, MO).
20. Nickel ammonium sulfate (Carlo Erba Reagenti, Milano, Italy).
21. Gelatin-coated slides.
22. Mounting medium (Permount).
23. Rotating-shaking apparatus (allowing to rotate at 180 rpm).
24. Axiophot Zeiss light microscope.
25. Zeiss-Kontron VIDAS image analyzer.
26. Adobe PhotoShop 6.0 computer program.

3. Methods

3.1. Treatment

Ten young male Wistar rats weighing 150–160 g were used. The model of CB₁ agonist treatment was modified from a previous report (22). One group of five rats were treated with WIN55,212-2 mesylate (4.0 mg/kg/d; injection volumes ranged from 0.2 to 0.3 mL) dissolved in DMSO (treated group) and another group of five rats were treated only with DMSO (control group) in

equivalent volume of 0.2–0.3 mL. The solution containing WIN55,212-2 was injected twice a day (every 12 h) subcutaneously (sc) for 14 d. During the treatment, no mortality of animals was observed. Control animals received the same volume of sterile DMSO and were kept in the same environment as the WIN-treated animals (12 h light–12 h dark cycle, controlled humidity and temperature, free access to standard laboratory rat food and water). The animal care for this experimental protocol was in accordance with the National Institutes of Health (NIH) Guidelines for the Care and Use of Laboratory Animals and the principles presented in the Guidelines for the Use of Animals in Neuroscience Research by the Society for Neuroscience.

3.2. Fixation

After twice-daily treatment for 14 d, animals were deeply anesthetized with 300 mg/kg of chloral hydrate (ip). They were perfused through the left ventricle, initially with a cold saline solution (first washing solution) and subsequently with a fixative solution. Brains were removed and kept in the same cold fixative solution for 4 h. Then, brains were washed three times in the second washing solution and left in this washing solution for 18 h at 4°C. Coronal and sagittal 40- μ m-thick brain sections were obtained using a vibratome. The sections were cryoprotected by immersing them in a cryoprotective solution and stored at –20°C until the immunohistochemical studies were performed.

3.3. Immunocytochemistry

Brain sections of both WIN-treated and control groups were processed simultaneously in the free floating state. In order to inhibit endogenous peroxidase activity, tissue sections were dehydrated by immersing them in graded ethanol (50–70–95–100%), treated with 0.5% v/v H₂O₂ in methanol for 30 min at room temperature and rehydrated. Free-floating brain sections were blocked for 1 h with 3% v/v normal goat serum in PBS. After two rinses in PBS, the sections were incubated for 48 h at 4°C in a rotating-shaking apparatus with anti-Nf-200, anti-MAP-2 or anti-GFAP primary antibodies. Following five rinses in PBS, sections were incubated for 1 h at room temperature with biotinylated secondary antibodies diluted 1:200. After further rinsing in PBS, sections were incubated for 1 h with streptavidin–peroxidase complex solution diluted 1:400. After rinsing again five times in PBS and two times in 0.1 AcB, development of peroxidase activity was carried out with a freshly prepared solution with 0.035% w/v 3,3'-diaminobenzidine plus 2.5% w/v nickel ammonium sulfate and 0.1% v/v H₂O₂ dissolved in AcB. Following the enzymatic incubation step, sections were rinsed in AcB three times and once in distilled water. Sections were mounted on gelatin-coated slides, dehydrated, and coverslipped using Permount for light microscopic observation.

All antibodies, as well as streptavidin complex, were dissolved in PBS containing 1% v/v normal goat serum and 0.3% v/v Triton X-100, pH 7.4.

3.4. Photomicrographs

Sections were observed and photographed in an Axiophot Zeiss light microscope, developed in black and white, scanned, and the final digital image plate was achieved by using the Adobe PhotoShop 6.0 computer program (Figs. 1 and 2).

3.5. Morphometric Measurement

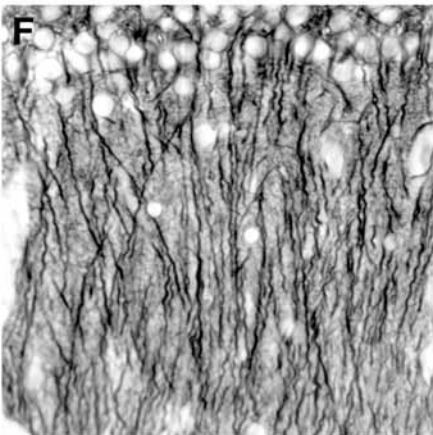
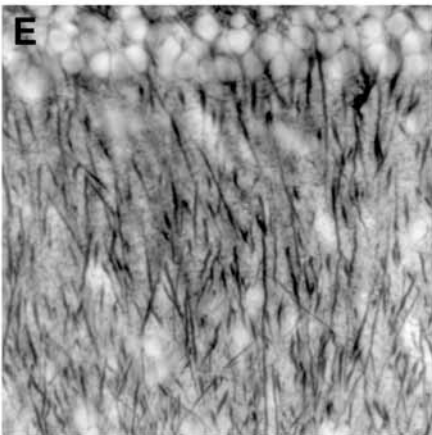
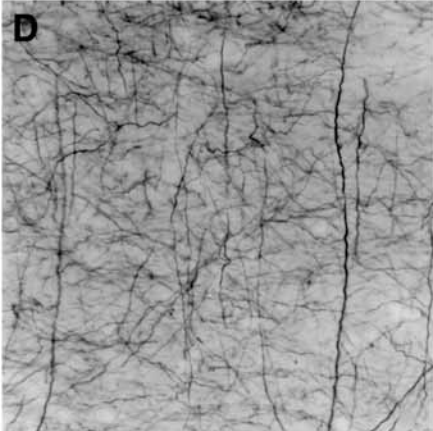
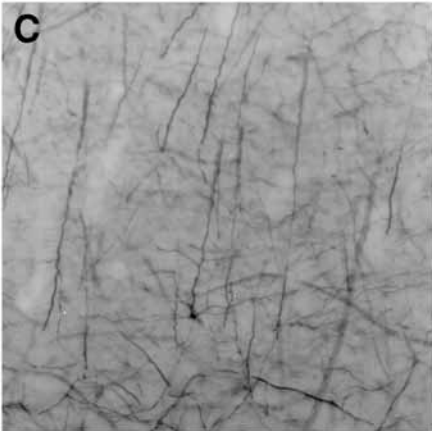
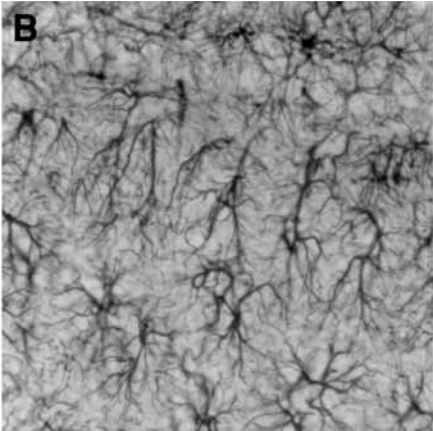
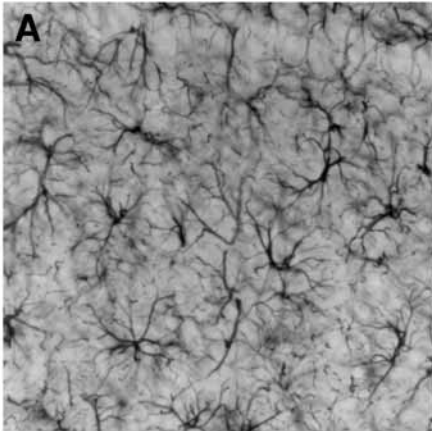
All measurements were performed on coded slides to ensure objectivity. Mean gray levels of GFAP immunostained astrocytes, astrocytic cell area, and the total area of immunostained neuronal cytoskeletal proteins (neurofilaments or microtubule-associated proteins) were measured in an Axiophot Zeiss light microscope equipped with a video camera on line with a Zeiss-Kontron VIDAS image analyzer. Images obtained with the light microscope were transferred to a video camera attached and connected to the interactive image analysis system on line. The images were digitized into an array of 512×512 pixels corresponding to $140 \times 140 \mu\text{m}$ (40X primary magnification). The resolution of each pixel was 256 gray levels (8 bits).

Immunostained cytoskeleton area was obtained after the normalization of the digitized images and the selection of an interactive threshold, a process called segmentation (i.e., interactively determining the studied object's limits). For the evaluation of cytoskeletal proteins, the total area of the immunolabeled cytoskeleton was related to the total area of the evaluated field, thus rendering a relative density parameter (Figs. 3 and 4). In GFAP-immunoreactive (GFAP-IR) astrocytes, the cell area was measured by interactively determining cell limits (Fig. 5).

ROD was obtained after a transformation of mean gray values by using the formula $\text{ROD} = \log(256/\text{mean gray})$, as was stated in **Subheading 1.2**. A background parameter was obtained from each section out of the labeled cells and subtracted from each cell ROD before statistically processing values (Fig. 6).

3.6. Statistics

Six to nine separate immunocytochemical experiments were run for each primary antibody. Individual experiments were composed of at least two or three tissue sections of each animal from each group. Ten to 14 fields were analyzed for each brain region. Interexperimental differences were not statistically significant. Values represent the mean \pm SD of experiments performed for each marker and treatment. The statistical study was performed by applying a two-tailed Student's *t*-test to the results of the quantitative analysis and by assuming



←
Fig. 1. Immunostaining for GFAP (*upper row*), Nf-200 (*middle row*), and MAP-2 (*lower row*) in the hippocampal CA₁ area of control (**A**, **C**, and **E**) and WIN-treated (**B**, **D**, and **F**) rats. In the WIN-treated animals, no changes in the morphology of GFAP-IR astrocytes or in the number or thickness of the cytoplasmic projections were observed. Note that in WIN-treated animals, Nf-200 expression was increased and cellular projections were thicker and presented an irregular morphology. Compared to control, WIN-treated animals showed changes in the morphology of MAP-2 immunoreactive dendrites. They appear as thicker, irregular, and waved neuronal processes. Primary magnification 400X.

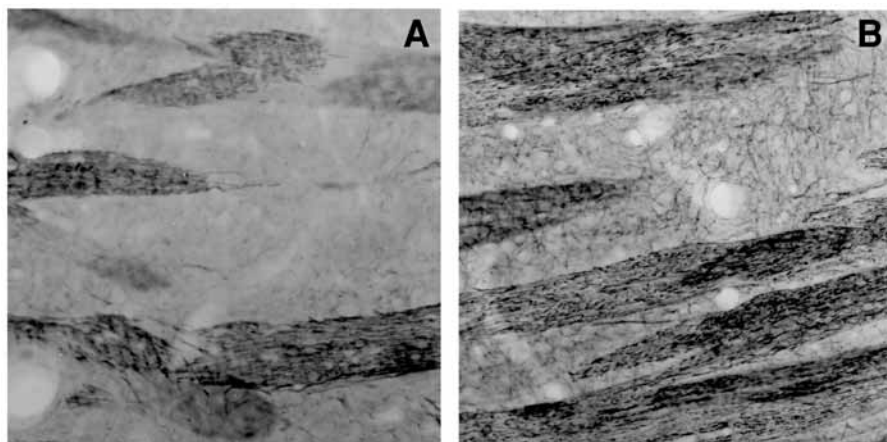


Fig. 2. Immunostaining for Nf-200 in the corpus striatum of control (**A**) and WIN-treated (**B**) rats. Note that in WIN-treated animals, there was an increase in Nf-200 expression in the two striatal areas. In the striatal patches these appeared as thicker and more irregular axons, while in the matrix these were observed as a fine network of neuronal processes. Primary magnification 400X.

that data were normally distributed. The equality of variance for control and treated values was analyzed by an F test. For the same group interanimal differences as well as interexperimental differences were not statistically significant. Statistical significance was set to $p < 0.05$.

4. Notes

1. Regarding the selection of the proper tissue-processing procedure, attention has to be focused on the preservation of immunoreactivity, as well as tissue structure. Therefore, compromise will be necessary in order to preserve both immunoreac-

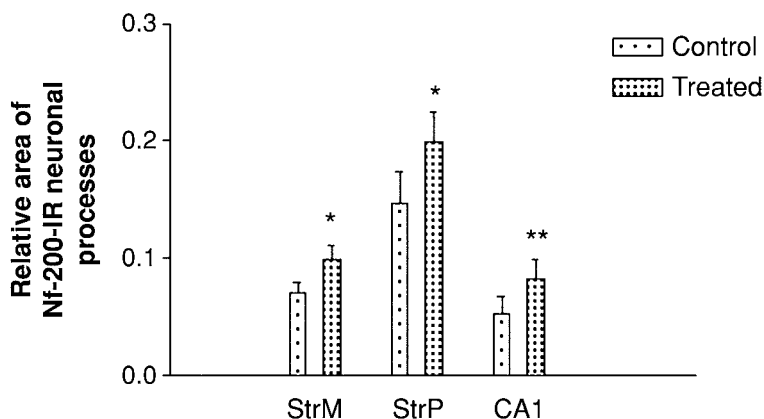


Fig. 3. Relative area of Nf-200-IR neuronal processes in two striatal areas: the matrix (StrM) (*left*) and the patches (StrP) (*middle*), and in the hippocampal CA₁ area (CA₁) (*right*). Data are expressed as area of Nf-200-IR neuronal processes per μm^2 of tissue. Note the increased area of Nf-200-IR processes in the three studied areas of WIN-treated animals. ** $p < 0.001$; * $p < 0.05$; after two-tailed Student's *t*-test. Bars represent mean \pm SD.

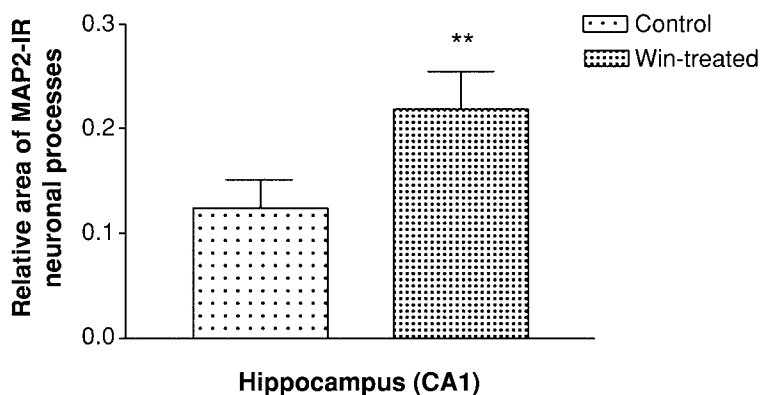


Fig. 4. Relative area of MAP2-IR neuronal processes in the hippocampal CA₁ area. Data are expressed as area of MAP2-IR neuronal processes per μm^2 of tissue. Note the increased area of MAP2-IR processes in this area. ** $p < 0.001$; after two-tailed Student's *t*-test. Bars represent mean \pm SD.

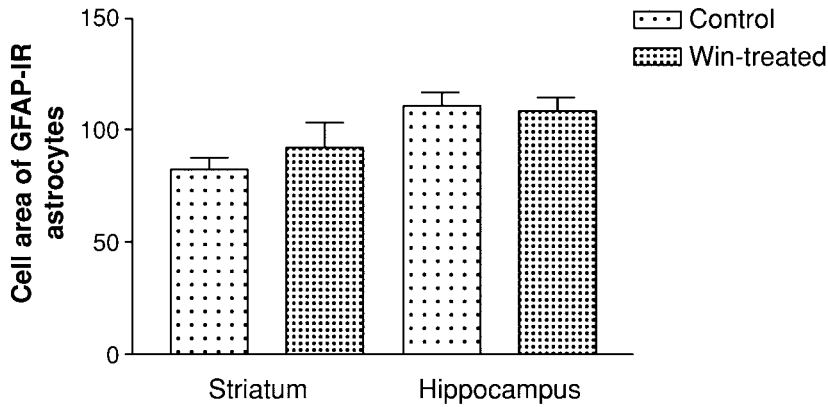


Fig. 5. Area of GFAP-IR astrocytes in striatum (*left*) and hippocampal CA₁ area (*right*). Data are expressed as area of GFAP-IR astrocytes in μm^2 . Note that there were no significant differences in the astrocytic cell area between control and WIN-treated rats after two-tailed Student's *t*-test. Bars represent mean \pm SD.

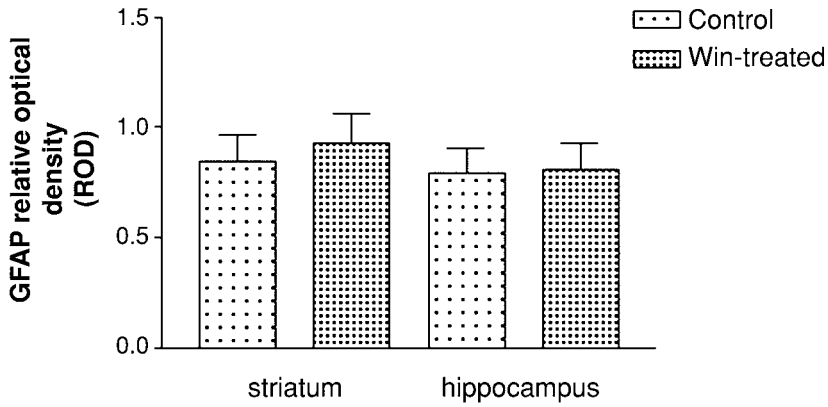


Fig. 6. Relative optical density (ROD) of GFAP-IR astrocytes in striatum (*left*) and in hippocampal CA₁ area (*right*). Data are expressed as ROD units. Note that there were no significant differences in the ROD values of GFAP-IR astrocytes between control and WIN-treated rats after two-tailed Student's *t*-test. Bars represent mean \pm SD.

tivity and tissue structure. The use of buffered fixatives based on paraformaldehyde with or without picric acid or glutaraldehyde renders good results for that purpose. The duration of the fixation, however, is also an important variable, since some antigens cannot be demonstrated in overfixed tissues (23).

2. Factors affecting labeling: To quantify immunocytochemical data, it is important to understand the kinetics involved in the labeling reaction (24). Different variables can affect the labeling intensity in immunocytochemistry. These variables include the concentration and exposure time to the antibody and other reagents, including the chromogen. All these variables are maintained as constant as possible to ensure reproducibility. Some variables will affect the optical density measurements of an immunocytochemically labeled section. Section thickness should be uniform in order to allow comparison of antibody labeling of different sections. Antibody penetration should also be equivalent in those sections. Reagent incubation times and dilutions should be identical in all experiments where data will be compared. The pH and temperature of the solutions should also be kept constant.
3. Another important point is the antibody specificity. In fixed tissues antibodies may bind nonspecific antigens (i.e., other than the specific antigen they were developed to recognize). This unspecific reaction could be produced by the conformational alteration of antigens in the fixed tissue. An immunocytochemistry protocol should always include appropriate control for antibody staining (i.e., omitting primary antibodies, absorbing the antibody with the appropriate antigen, etc.) (see, for example, ref. 23).
4. In order to obtain representative and reproducible values, it is important to take into account some methodological procedures. All sections obtained from the different experimental and control groups must be processed in parallel at the same time, under the same experimental conditions. Theoretically, the measurement of the density of a single specimen should always be the same value. Unfortunately, density values are only replicable under well-controlled conditions of measurement. All measurements should be performed by at least two independent observers in blind conditions.
5. In this chapter three different ways to measure immunocytochemically labeled nervous tissue have been described: the relative area covered by neuronal processes (dendrites and fibers), cell body area, and relative optical density. The relative area of cellular processes is the most difficult to achieve, the major problem involves the segmentation step (see **Subheading 3.5**). However, it can be resolved if the segmentation threshold is maintained from one field to another. On the contrary, it is easier to obtain the cell body area since it is usually less difficult to segment. Regarding ROD measures, it is important to remember that the background of the immunolabeled tissue section can affect the optical density values. Thus it is better to obtain the background parameter from each section out of the labeled cells and subtract this value from each cell ROD before statistically processing the values.
6. In the work presented in this chapter, the VIDAS-KONTRON image analyzer, which was a predecessor of the Zeiss KS-300 and KS-400 models that became available for the newest Windows versions (www.zeiss.de), was used. Our laboratory has used a Windows-based version of the Optimas (www.optimas.com) with excellent results. An image processing and analysis program for Macintosh or PC has been developed by the Research Services Branch (RSB) of the National

Institute for Mental Health (NIMH), part of the NIH, that can be downloaded at www.rsb.info.nih.gov. Most image analyzers do basically the same operations described in this chapter, with obvious speed differences according to the software–hardware combinations used. In the web pages of each image analyzer are also the necessary software modules for the different frame grabbers present in the market as well as very useful macros (small routines that can be loaded into the image analyzer for automatic operations). The experience of many scientists in different fields is available in the web sites of each image analyzer.

The results presented here show some interesting image analysis parameters that can be used for the morphological study in the CNS after drugs or toxicants exposure (*see*, for example, **refs. 3, 4, and 25**). In our experience these parameters (area, relative area, ROD, etc.) were extremely useful for the study of the effects of canabimimetic drugs on the young rat's CNS.

Acknowledgments

We thank Ms. Emérita Jorge Vilela de Bianchieri for her expert technical assistance. This work was supported by grant UBACYT M031 to A.B.

References

1. Tohyama, I., Kameyama, M., and Kimura, H. (1998) Quantitative morphometric analysis of two types of serotonin-immunoreactive nerve fibers differentially responding to p-chlorophenylalanine treatment in the rat brain. *Neuroscience* **26** (3), 971–991.
2. Brusco, A., Pecci Saavedra, J., García, G., Tagliaferro, P., Evangelista de Duffard, A. M., and Duffard, R. (1997) 2,4-Dichlorophenoxyacetic acid through lactation induces astrogliosis in rat brain. *Mol. Chem. Neuropathol.* **30**, 175–185.
3. Tagliaferro, P., Ramos, A. J., López, E. M., Pecci Saavedra, J., and Brusco, A. (1997) Neural and astroglial effects of a chronic parachloro-phenylalanine-induced serotonin synthesis inhibition. *Mol. Chem. Neuropathol.* **32**, 195–211.
4. Ramos, A. J., Tagliaferro, P., López, E. M., Pecci Saavedra, J., and Brusco, A. (2000) Neuroglial interactions in a model of parachlorophenylalanine-induced serotonin depletion. *Brain Res.* **883**, 1–14.
5. Hutcheon, B., Brown, L. A., and Poulter, M. O. (2000) Digital analysis of light microscope immunofluorescence: high-resolution co-localization of synaptic proteins in cultured neurons. *J. Neurosci Methods* **96** (1), 1–9.
6. Reilly, J. F., Games, D., Rydel, R. E., et al. (2003) *Proc. Natl. Acad. Sci USA* **100** (8), 4837–4842.
7. Onaivi, E. S., Leonard, C. M., Ishiguro, H., et al. (2002) Endocannabinoids and cannabinoid receptor genetics. *Prog. Neurobiol.* **66**, 307–344.
8. Dove Pettit, D. A., Harrison, M. P., Olson, J. M., Spencer, R. F., and Cabral, G. A. (1998) Immunohistochemical localization of the neural cannabinoid receptor in rat brain. *J. Neurosci. Res.* **51**, 391–402.
9. Pertwee, R. G. (1997) Pharmacology of cannabinoid CB1 and CB2 receptors. *Pharmacol. Ther.* **74**, 129–180.

10. Di Marzo, V., Meck, D., Bisogno, T., and De Petrocellis, L. (1998) Endocannabinoids: endogenous cannabinoid receptor ligands with neuromodulatory actions. *TINS* **21** (12), 521–528.
11. Salio, C., Doly, S., Fischer, J., Franzoni, M. F., and Conrath, M. (2002) Neuronal and astrocytic localization of the cannabinoid receptor-1 in the dorsal horn of the rat spinal cord. *Neurosci. Lett.* **329**, 13–16.
12. Onaivi, E. S., Chakrabarti, A., Gwebu, E. T., and Chaudhuri, G. (1995) Neurobehavioral effects of delta-9-THC and cannabinoid receptor gene expression in mice. *Behav. Brain Res.* **72**, 115–125.
13. Onaivi, E. S., Chakrabarti, A., and Chaudhuri, G. (1996) Cannabinoid receptor genes. *Prog. Neurobiol.* **48**, 275–305.
14. Martin, B. R., Mechoulam, R., and Razdan, R. K. (1999) Discovery and characterization of endogenous cannabinoids. *Life Sci.* **65**, 573–595.
15. Salzet, M., Breton, C., Bisogno, T., and Di Marzo, V. (2000) Comparative biology of the endocannabinoid system. Possible role in the immune response. *Eur. J. Biochem.* **267**, 4917–4927.
16. Kim, D. and Thayer, S. A. (2001) Cannabinoids inhibit the formation of new synapses between hippocampal neurons in culture. *J. Neurosci.* **21** (10): RC146.
17. Hampson, R. E. and Deadwyler, S. A. (1998) Role of cannabinoid receptors in memory storage. *Neurobiol. Dis.* **5**, 474–482.
18. Heyser, C. J., Hampson, R. E., and Deadwyler, S. A. (1993) Effects of delta-9-tetrahydrocannabinol on delayed match to sample performance in rats: alterations in short-term memory associated with changes in task specific firing of hippocampal cells. *J. Pharmacol. Exp. Ther.* **264**, 294–307.
19. Lichtman, A. H., Dimen, K. R., and Martin, B. R. (1995) Systemic or intrahippocampal cannabinoid administration impairs spatial memory in rats. *Psychopharmacology* **119**, 282–290.
20. Ameri, A. (1999) The effects of cannabinoids on the brain. *Prog. Neurobiol.* **58**, 315–348.
21. Capowski, J. J. (1989) Video input techniques, in *Computer Techniques in Neuroanatomy*, Plenum Press, New York, pp. 129–146.
22. Lawston, J., Borella, A., Robinson, J. D., and Whitaker-Azmitia, P. M. (2000) Changes in hippocampal morphology following chronic treatment with the synthetic cannabinoid WIN 55,212-2. *Brain Res.* **877**, 407–410.
23. Pool, C. W., Buijs, R. M., Swaab, D. F., Boer, G. J., and Van Leeuwen, F. W. (1983) On the way to a specific immunocytochemical localization, in *Immunohistochemistry* (Cuello, A. C., ed.), IBRO, a Wiley-Interscience Publication, New York, pp. 1–46.
24. Ranney Mize, R. (1989) The analysis of immunohistochemical data, in *Computer techniques in Neuroanatomy*. Plenum Press, New York, pp. 33–371.
25. Evrard, S. G., Vega, M. D., Ramos, A. J., Tagliaferro, P., and Brusco, A. (2003) Altered neuron-glia interactions in a low, chronic prenatal ethanol exposure. *Brain Res Dev Brain Res.* **147**(1–2), 119–133.

Visualizing Cannabinoid Effects Using Brain Slice Imaging and Electrophysiological Approaches

Alexander F. Hoffman and Carl R. Lupica

Summary

The use of electrophysiological recordings in brain slices is now routinely used to assess the actions of cannabinoid ligands within various central nervous system nuclei. In this chapter we describe common protocols involving both intracellular and extracellular recording techniques in the hippocampus, where the presynaptic modulatory effects of cannabinoid receptor activation have been studied in detail. In addition to describing the basic electrophysiological setup needed for these recordings, we will address common technical problems and limitations involved in working with highly lipophilic compounds, such as the cannabinoid ligands, in brain slices.

Key Words: Electrophysiology; brain slice; marijuana; drugs of abuse; intracellular; extracellular; hippocampus; synaptic transmission.

1. Introduction

The brain slice preparation has long enhanced our ability to study the fundamental synaptic targets for a variety of drugs (1), including those abused by humans. Intracellular and extracellular recording techniques, in combination with appropriate pharmacological tools, have elucidated the cellular substrates of many drugs of abuse, including nicotine (2), opiates (3,4), alcohol (5), and cocaine (6,7). Recently, the availability of selective ligands has allowed for the application of these traditional approaches to the study of cannabinoid receptors. In this chapter, we discuss the methods routinely used in our laboratory to study the synaptic effects of cannabinoid receptor activation in the hippocampus (8,9). We will first describe preparation and storage of hippocampal brain slices, and then separately describe intracellular and extracellular recording setups, including preparation of cannabinoid ligands routinely used in these studies.

2. Materials

1. Artificial cerebrospinal fluid (aCSF): 126 mM NaCl, 3 mM KCl, 1.5 mM MgCl₂, 2.4 mM CaCl₂, 1.2 mM NaH₂PO₄, 11 mM glucose, 26 mM NaHCO₃. This can be prepared as a stock (10X) solution and diluted fresh daily as needed.
2. 1% Tween-80, 2% dimethylsulfoxide (DMSO), dissolved in physiological saline.
3. DMSO (for preparation of stock solutions of cannabinoid ligands).
4. “Injector-style” stainless steel razor blades (Ted Pella Inc.)
5. Wecprep single-edge razor blades.
6. Whatman no. 3 qualitative filters.
7. Loctite tissue adhesive (Ted Pella Inc., Redding CA).
8. 10-cc syringe, 23 G needle.
9. Polyethylene PE-50 tubing.
10. 1 mL glass Pasteur pipets + rubber bulbs.
11. Intracellular electrode filling solution (composition varies according to experiment).
12. Borosilicate glass electrodes (1.5 mm O.D., 0.86 mm I.D.; Sutter Instrument Corp., Novato, CA).

3. Methods

3.1. Preparation of Hippocampal Slices

1. Rats are rapidly decapitated, and the brains are removed within 1 min and placed into a chilled aCSF solution. After 1–2 min, the brain is transferred to the filter paper that is kept on a chilled petri dish and is blocked using a single-edge Wecprep razor blade. One blocking cut is made just anterior to the cerebellum, and the other block is made approx 3 mm posterior to the anterior tip of the brain. A small piece of filter paper is then used to transfer the brain, anterior side up (e.g., the filter paper adheres to the anterior surface), to the cutting chamber. A drop of Loctite glue is placed on the stage of the chamber, and the brain is gently placed on the glue. Applying gentle downward pressure on the brain with an index finger, ice-cold (0–4°C) aCSF is then poured into the chamber to completely immerse the brain in solution. Sections are then taken at 300–400 μ m thickness (thinner sections are preferred for visualized whole-cell recordings; slightly thicker sections are appropriate for “blind patch” or extracellular recordings).
2. Slices are transferred to a holding chamber using a broken-back Pasteur pipet (the tip is broken off and a bulb is placed over this end). Numerous holding chambers are commercially available through suppliers, including Warner Instruments (Hamden, CT). However, we have found that homemade Gibb chambers (10) work well for maintaining the tissue. The holding chamber may be maintained at room temperature (~22°C) with no detrimental effect on slice viability. However, continuous saturation of the solution with a 95% O₂/5% CO₂ mixture is absolutely critical.
3. Slices are incubated for at least 90 min prior to being transferred to the recording chamber. This allows for equilibration of the tissue, and recovery of synaptic activity, following the cutting procedure.

3.2. Preparation of Cannabinoid Solutions

1. Stock solutions of WIN55,212-2, AM251, SR141716A, and most other ligands are prepared as 10 mM in DMSO. These stocks should be stable for many weeks when stored cold in a lab refrigerator or freezer.
2. Drugs are diluted to 100X the desired final bath concentration in a solvent consisting of 1% Tween-80, 2% DMSO, and 97% physiological saline. Thus, for a 1- μ M bath concentration, 100 μ L of stock would be dissolved in 9.9 mL of solvent to produce a 100- μ M solution.
3. Drugs are added to a 10-cc syringe. A 23 G needle is cut roughly in half using a Dremel tool, and the ends filed to allow for PE50 tubing to cleanly fit over the blunt ends. The tubing will thus lead from the nonsharp (Luer-fitting) end attached to the syringe to the sharp (beveled) end, which will be inserted into a rubber septum near the superfusion inlet of the slice chamber.
4. Following experiments, drug syringes may be kept cold in a lab refrigerator for 24–72 h. Thereafter, old drug solutions should be discarded, the syringes and tubing rinsed several times in EtOH and distilled H₂O, and fresh drug solutions prepared from stocks.

3.3. Electrophysiology Configuration/Setup

1. Acquisition software/hardware: We have found that Dr. John Dempster's WCP and EDR programs, freely available for download at <http://spider.science.strath.ac.uk/PhysPharm>, are highly versatile programs that are designed to work with a number of different A/D boards, amplifiers, etc. National Instruments (Austin, TX) provides low-cost boards and accessories (e.g., 6024E board and BNC-2090 interface) that may be used to acquire data to a Windows-based PC.
2. Amplifiers: Axopatch 200B (Axon Instruments, Foster City CA) for intracellular recordings; Model 1700 Differential A-C amplifier (A-M Systems, Carlsborg, WA) for extracellular recordings.
3. Stimulus isolation units: Iso-Flex (A.M.P.I., Jerusalem, Israel) provides either constant current or constant voltage stimulation.
4. Timer/pulse delivery: Master-8 (A.M.P.I., Jerusalem, Israel) readily interfaces with both the Axopatch 200B and Iso-Flex to allow for alternating stimulation/voltage step protocols.
5. Perfusion chambers: Warner Instruments (Hamden, CT) Series 20 platforms and chambers are ideally suited to maintaining slice superfusion in a relatively low bath volume (150–200 μ L). Slices are perfused at 2 mL/min. A flow-meter (Fisher Scientific) can be used to calibrate solution flow rate, and an in-line solution heater (Warner, SH-27B) can be used to maintain slices at 30–32°C during recordings.
6. Microscopes: A low-power stereomicroscope is sufficient for visualizing tissue and electrode placement for extracellular recordings. A Zeiss Axioscope or other similar microscope equipped with differential interference contrast/infrared (DIC-IR) optics is necessary for visualized whole-cell recordings.

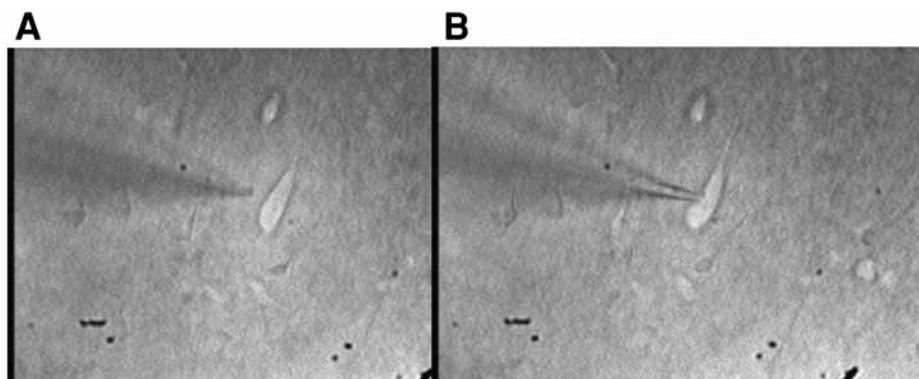


Fig. 1. DIC-IR image of a stratum radiatum interneuron in a hippocampal brain slice. The slice was cut at 300 μm , and the depth of the recorded cell was approx 175 μm from the surface of the slice. (A) The recording electrode is visible on the left as it approaches the cell. (B) Note the slight dimpling of the cell as the recording electrode makes contact.

7. Razel infusion pumps (Model A-99, Razel Scientific, Stamford, CT) provide an easy means to apply drugs via a 10 cc syringe, as described in **Subheading 3.2**.

3.4. Intracellular Recordings

1. Internal solution composition will vary according to the desired experiment (*see Note 2*). Osmolarity should be approx 270–290 mOsm/L and pH should be adjusted to 7.2–7.4. Addition of QX-314, a lidocaine derivative, to the internal solution (1–2 mg/mL) will prevent direct activation of Na^+ channels in the postsynaptic cell during electrical stimulation of the slice.
2. Electrodes are pulled on a Sutter P-97 Flaming/Brown micropipet puller. Tips are generally 2–3 μm in diameter, and resistances are 3–6 $\text{M}\Omega$.
3. Stimulating electrodes can be purchased from a variety of sources, including Frederick Haer Co. (FHC, Bowdoinham, ME). Alternatively, electrodes can be fabricated by running two strands of formvar-insulated nichrome wire into a 22G spinal needle (or other suitable cannula), then twisting the strands together tightly with a hemostat.
4. Recording electrodes are slowly lowered into the tissue, while applying slight positive pressure to keep the tip free of debris. The targeted cell should dimple slightly as the electrode encounters the membrane. At this point, pressure is released and slight suction can be used to facilitate sealing. **Figure 1** shows a hippocampal interneuron prior to, and following, impalement with the electrode.
5. A hyperpolarizing step (10–20 mV) is given every 30 s (alternating with electrical stimulation of the tissue) in order to ensure that whole-cell access is stable.
6. Stimulus intensity is set to elicit a response that is 30–40% of the maximum response amplitude.

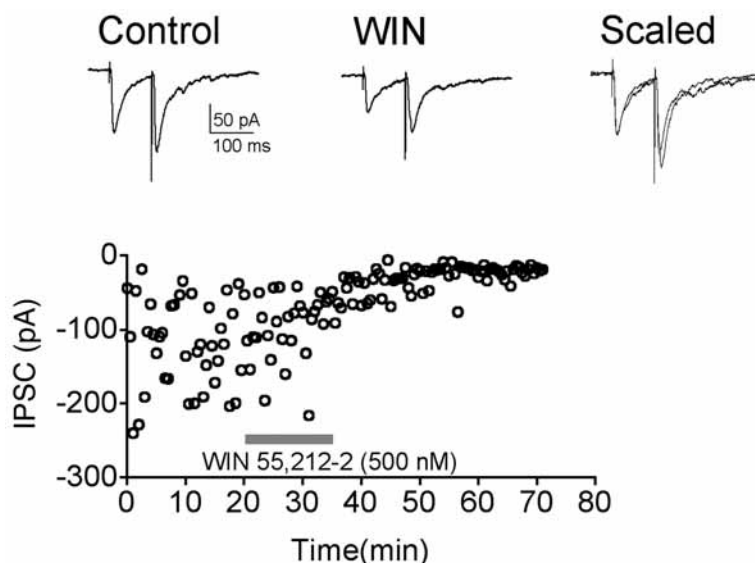


Fig. 2. Inhibition of GABAergic transmission in a stratum radiatum interneuron by WIN55,212-2. IPSCs were evoked by paired (100 ms) stimuli every 30 s. Under control conditions, the response showed paired-pulse facilitation ($\text{IPSC2} > \text{IPSC1}$). After application of 500 nM WIN55,212-2, the first response of the pair showed slightly greater inhibition than the second, resulting in an enhancement of facilitation. This is highlighted by the scaled trace on the right, where the first responses have been scaled to match. The increase in paired-pulse facilitation is one indication of the presynaptic inhibition of GABA release by CB_1 receptor activation. Note that the response does not spontaneously recover or reverse following the application of the agonist.

7. After a 10-min period to allow for stabilization of the response, cannabinoid agonists are added to the bath using the Razel pump described in **Subheading 3.3**. Pumps are initially set to deliver drugs at 20 $\mu\text{L}/\text{min}$, a 1:100 dilution into the flowing perfusate. This will reduce the solvent to 0.01% Tween-80 and 0.02% DMSO. Increasing the pump speed will result in a linear increase in drug concentration to the bath, but this will also increase the solvent concentration. Always run vehicle controls when higher concentrations are used to ensure the stability of the response in the presence of higher solvent concentrations (*see Note 4*).
8. Peak drug effects are generally observed within 10–12 min of drug application, although longer (20–25 min) time periods may be required for lower concentrations (<100 nM). Since spontaneous recovery/washout of the cannabinoid agonists is not observed (*see Fig. 2*), antagonists may be applied to reverse the effect of the drug. This may require an additional 30–45 min for complete reversal. Since whole-cell recordings may become unstable by this time, an alternative approach

Fig. 3. Concentration-dependent inhibition of hippocampal CA1 field EPSPs by WIN55,212-2. **(A)** Time course shows a cumulative concentration–response experiment where increasing bath concentrations of WIN55,212-2 were applied as indicated by the bars. Inset shows individual traces taken at the peak effect of each concentration. **(B)** Dose–response curve for fEPSP inhibition by WIN55,212-2. Each data point on the graph represents three to six slices. The calculated EC₅₀ was 465 nM. **(C)** Inhibition by 1 μ M WIN55,212-2 is blocked by co-application of the CB₁ receptor antagonist AM251 (2 μ M). fEPSP traces were taken at the points indicated prior to and after application of the agonist.

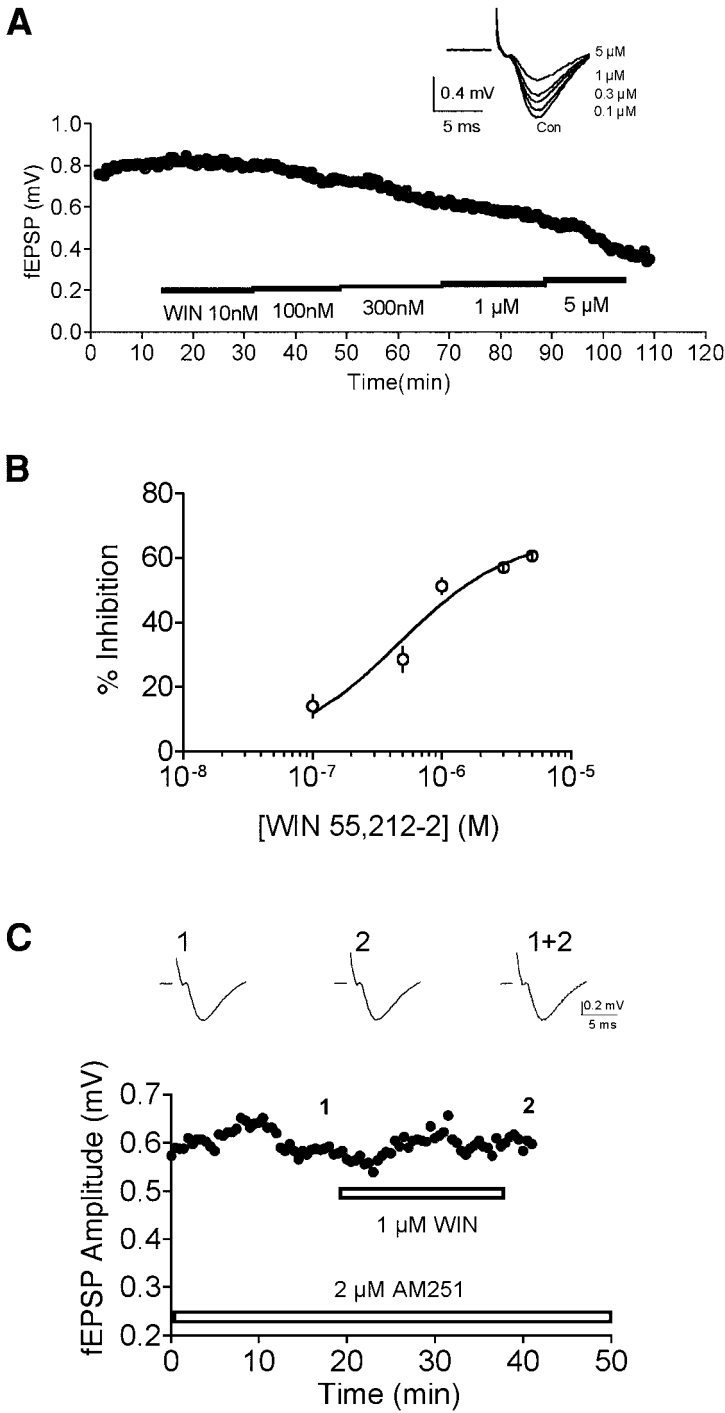
is to pretreat slices for 10–15 min with the antagonist or to incubate the tissue with the antagonist prior to recordings.

3.5. Extracellular Recordings

1. Extracellular electrodes are filled with 3M NaCl.
2. The stimulating electrode is placed in the stratum radiatum layer of CA1.
3. The recording electrode is lowered towards the tissue using coarse movement of the micromanipulator. As the electrode touches the surface of the tissue, there will be an obvious deflection when monitored on an oscilloscope. The electrode should be in the dendritic field of CA1, below the pyramidal cell layer, in order to avoid population spike contamination of the field response.
4. Stimuli are given every 5 s as the recording electrode is lowered in small steps (10–20 μ m) using the fine control on the manipulator. This movement is continued until an optimal field potential response (~0.5–1 mV) is achieved. Again, the stimulus intensity should be set to evoke a response that is 30–40% of the maximum.
5. Baseline responses are taken every 30 s for at least 10 min to ensure stability of the response.
6. Because the extracellular responses are more stable than intracellular responses, cumulative concentration–response curves (see **Note 5**) and antagonist reversal of responses are often easier to obtain (**Fig. 3**).

4. Notes

1. Picrotoxin (100 μ M) and DL-2-Amino-5-phosphonopentanoic acid (APV) (40 μ M) are included in the buffer when isolating (RS)- α -Amino-3-hydroxy-5-methyl-4-isoxazolepropionic acid (AMPA)-mediated excitatory postsynaptic current (EPSCs). APV and 6,7-Dinitroquinoxaline-2,3-dione (DNQX) (10 μ M) are included when isolating GABA_A-mediated IPSCs.
2. Typical internal solution for isolation of inhibitory postsynaptic currents (IPSCs): 125 mM CsCl, 10 mM *N*-2-hydroxyethyl-piperazine-*N'*-2-ethane-sulfonate (HEPES), 1 mM ethylene glycol tetraacetic acid (EGTA), 0.1 mM CaCl₂, 2.0 mM Mg²⁺-ATP, 0.2 mM Na⁺-Guanosine 5-triphosphate (GTP). For isolation of AMPA-



mediated EPSCs: 100 mM CsCH₃SO₃, 60 mM CsCl, 0.2 mM EGTA, 10 mM HEPES, 1.0 mM MgCl₂, 1.0 mM Mg²⁺-ATP, 0.3 mM Na⁺-GTP.

3. Recording chambers and all tubing should be flushed well with distilled, deionized H₂O at the end of each day, and with 70% EtOH solution (followed by H₂O) on a weekly basis.
4. Although many of the cannabinoid ligands have affinities in the low nM range for the CB₁ receptor, it is not uncommon in slice studies to utilize bath concentrations in excess of 1 μ M. This probably reflects the ability of the drug to partition from bath to tissue, and specifically to receptor sites within the tissue.
5. Concentration–response curves are readily constructed using any curve-fitting software, such as Prism (GraphPad Scientific, San Diego CA). Typically 4–10 slices per concentration will be used, and slices should be obtained from several animals, rather than from a single subject. We have not routinely observed desensitization of responses using a cumulative concentration protocol, and therefore find this approach to be useful, especially in extracellular recordings that can be maintained for several hours.

References

1. Dunwiddie, T. V. (1986) The use of in vitro brain slices in neuropharmacology, in *Electrophysiological Techniques in Pharmacology* (Geller, H. M., ed), Alan R. Liss, Inc., New York, pp. 65–90.
2. Pidoplichko, V. I., DeBiasi, M., Williams, J. T., and Dani, J. A. (1997) Nicotine activates and desensitizes midbrain dopamine neurons. *Nature* **390**, 401–404.
3. Brundage, J. M. and Williams, J. T. (2002) Differential modulation of nucleus accumbens synapses. *J. Neurophysiol.* **88**, 142–151.
4. Johnson, S. W. and North, R. A. (1992) Opioids excite dopamine neurons by hyperpolarization of local interneurons. *J. Neurosci.* **12**, 483–488.
5. Weiner, J. L., Gu, C., and Dunwiddie, T. V. (1997) Differential ethanol sensitivity of subpopulations of GABA_A synapses onto rat hippocampal CA1 pyramidal neurons. *J. Neurophysiol.* **77**, 1306–1312.
6. Nicola, S. M., Kumbian, S. B., and Malenka, R. C. (1996) Psychostimulants depress excitatory synaptic transmission in the nucleus accumbens via presynaptic D1-like dopamine receptors. *J. Neurosci.* **16**, 1591–1604.
7. Zhang, X. F., Hu, X. T., and White, F. J. (1998) Whole-cell plasticity in cocaine withdrawal: Reduced sodium currents in nucleus accumbens neurons. *J. Neurosci.* **18**, 488–498.
8. Hoffman, A. F. and Lupica, C. R. (2000) Mechanisms of cannabinoid inhibition of GABA(A) synaptic transmission in the hippocampus. *J. Neurosci.* **20**, 2470–2479.
9. Hoffman, A. F., Riegel, A. C., and Lupica, C. R. (2003) Functional localization of cannabinoid receptors and endogenous cannabinoid production in distinct neuron populations of the hippocampus. *Eur. J. Neurosci.* **18**, 524–534.
10. Edwards, F. A. and Konnerth, A. (1992) Patch-clamping cells in sliced tissue preparations. *Methods Enzymol.* **207**, 208–222.

Methods for the Synthesis of Cannabinergic Ligands

Ganesh A. Thakur, Spyros P. Nikas, Richard I. Duclos, Jr.,
and Alexandros Makriyannis

Summary

During the last decade, numerous cannabinergic ligands with high affinity and selectivity profiles for cannabinoid receptors (CB₁ and CB₂) emerged from rigorously pursued structure–activity relationship studies. This chapter focuses on the synthetic aspects of key cannabinoid receptor probes representing the different classes of cannabinergic ligands that encompasses classical cannabinoids (CCs) including some covalent binding derivatives, nonclassical cannabinoids (NCCs), hybrid cannabinoids, aminoalkylindoles (AAIs), diarylpyrazoles, and the endocannabinoids.

Key Words: Cannabinoid, CB₁, CB₂, aminoalkylindole, diarylpyrazole, endocannabinoid.

1. Introduction

The long history of worldwide self-medication by a mixture of cannabinoids present in *Cannabis sativa* generated the first wave of interest among synthetic and medicinal chemists in conjunction with the co-developments of modern separation, spectroscopic, and synthetic methods during the last half century. The identification of the family of C₂₁ tricyclic cannabinoids led to the chiro-specific partial syntheses of these classical cannabinoids from more readily available monoterpenes, and to the total syntheses of these plant constituents, as well as an expanding list of cannabimimetic compounds. However, only a few efficacious drugs, which include Marinol (Dronabinol, (-)- Δ^9 -THC from Roxane Labs), Cesamet (Nabilone, developed by Eli Lilly) and Sativex (Δ^9 -THC and cannabidiol, developed by GW Pharmaceuticals), have resulted. Cannabinoid synthesis has seen a renewed wave of interest with the discovery and cloning of the CB₁ and CB₂ cannabinoid receptors and the characterizations of the two endogenous cannabinoid ligands *N*-arachidonoyl ethanolamine

(AEA; anandamide) and 2-arachidonoylglycerol (2-AG). The synthesis and evaluation of ligands for the two cannabinoid receptors thus now includes six general classes of compounds. The first class is the classical cannabinoids (CCs), which have the benzopyran ABC-tricyclic framework. The second class of cannabinergic ligands was initially developed at Pfizer and includes both AC bicyclic and ACD-tricyclic compounds lacking the pyran B-ring, characteristic of the classical cannabinoids. A third class of analogs is a hybrid cannabinoid class (CC/NCC hybrid) combining the ABC-tricyclic structural framework of the classical cannabinoids with the additional chiral center at C6 in the B-ring. The fourth chemical class of cannabinoid receptor ligands is the aminoalkyl indoles, initially developed at Sterling Winthrop, of which WIN55,212-2 is perhaps the benchmark compound. The fifth chemical class of ligands is the diarylpyrazoles. This class includes the highly CB₁-selective SR141716A (Rimonabant) from Sanofi, which has currently passed phase III clinical trials for the treatment of obesity and smoking cessation, as well as the highly CB₂-selective SR144528 from Sanofi. The sixth class of cannabinoid receptor ligands includes the endogenous lipids AEA, 2-AG, noladin ether, as well as their synthetic analogs. While the preponderance of the literature relates to the classical cannabinoids, this discussion of the chemical methods and selected synthetic approaches is a more balanced discussion covering the six classes of CB₁ and CB₂ receptor ligands and covalent binding probes.

Discovery of the endocannabinoids and the biochemical systems involved in their inactivation, namely fatty acid amide hydrolase (FAAH) and monoglyceride lipase (MAGL), as well as the anandamide transporter (AT) system, has also prompted the synthesis of several substrates capable of modulating the endocannabinoid system. Ligands for FAAH, MAGL, and compounds targeting the AT system will not be discussed, however.

2. Materials

Standard laboratory practices and procedures were followed. Eye protection and a functioning fume hood, glassware, magnetic and mechanical stirrers, chromatography columns and column materials, rotary evaporator, and vacuum pump were required. Chemicals for syntheses were either commercially available or synthesized by following the standard reported procedures. Compounds were routinely checked by solution nuclear magnetic resonance spectroscopy (NMR) and other appropriate spectroscopic and analytical methods.

3. Synthesis of Cannabinoid Receptor Ligands: Approaches and Methods

3.1. Classical Cannabinoids and Covalent Binding Probes

The medicinal advantages of marijuana have been recognized for many centuries, but it was the characterization and synthesis ([1](#)) of its major active prin-

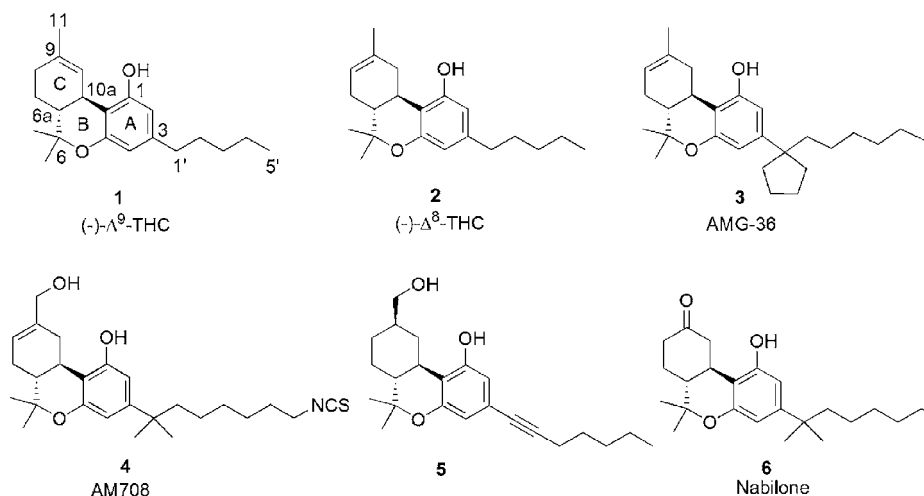


Fig. 1. Structures of representative classical cannabinoids.

ciple, $(-)\text{-}\Delta^9\text{-tetrahydrocannabinol}$ ($(-)\text{-}\Delta^9\text{-THC}$, **1**, Fig. 1) that began a new era for synthetic cannabinoids as pharmacological agents. The active constituents of the *Cannabis* plant, as well as numerous synthetic analogs, are the stereo-specific $(-)$ -enantiomers, i.e., the $(6aR,10aR)$ -configuration, of THC (Fig. 1).

$(-)\text{-}\Delta^9\text{-THC}$ (**1**) and its Δ^8 -isomer (**2**, Fig. 1) are the first members of a class of cannabinergic ligands referred to as classical cannabinoids. In general, these are ABC-tricyclic terpenoid compounds bearing a benzopyran moiety. Many CC analogs have been synthesized and evaluated pharmacologically and biochemically (for reviews, see refs. 2–8). Structure–activity relationship (SAR) studies recognize four pharmacophores within the cannabinoid prototype: a phenolic hydroxyl (PH), a lipophilic alkyl side chain (SC), a northern aliphatic hydroxyl (NAH), and a southern aliphatic hydroxyl (SAH). The first two are encompassed in the plant-derived cannabinoids, while all four pharmacophores are represented in some of the synthetic non-classical cannabinoids developed by Pfizer (e.g., **27**, Fig. 2).

Syntheses of $(-)\text{-}\Delta^9\text{-THC}$ have utilized the acid-catalyzed condensation of olivetol (**9**, Scheme 1) with suitable chiral monoterpenes, such as $(+)\text{-cis-}$ or $\text{trans-}p\text{-mentha-2,8-dien-1-ol}$ (**9,10**), $(+)\text{-trans-2-carene}$ epoxide (**11,12**), $p\text{-mentha-2-ene-1,8-diol}$ (**13,14**), and $(-)\text{-cis-}$ or trans-verbenol (**15**). Other successful approaches to $\Delta^9\text{-THCs}$ are also known (**16–21**), but a problem common to these methods is created by the fact that a variety of by-products results. “Normal” and “abnormal” THCs, *bis*-adducts, open-chain intermediates, starting materials, degradation products as well as double-bond isomers complicate work-up procedures and purifications. Although an improved method has

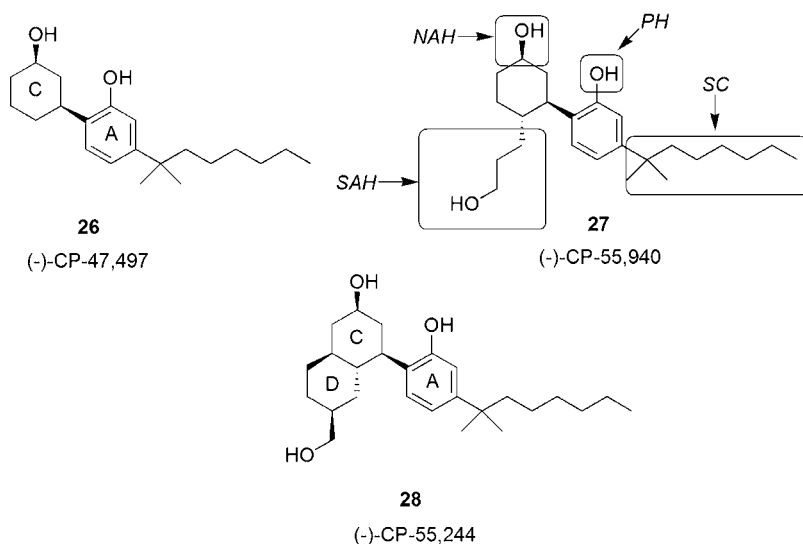
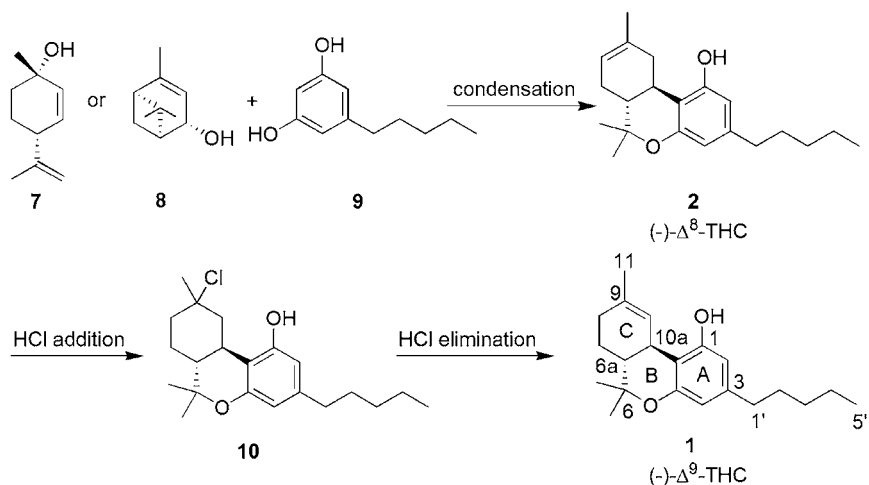
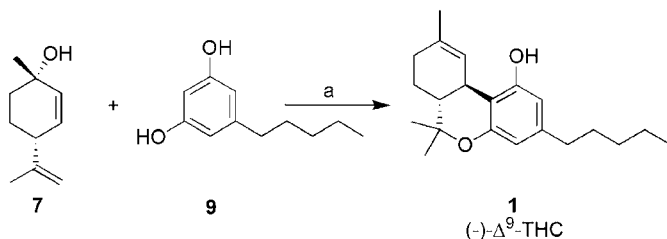


Fig. 2. Representative nonclassical cannabinoids.

Scheme 1. Syntheses of (*-*)- Δ^9 -THC.

recently been reported (14), the most popular syntheses of (*-*)- Δ^9 -THC employ either (+)-*cis*- or *trans*-*p*-mentha-2,8-dien-1-ol (7, Scheme 1) or (*-*)-*trans*- or *cis*-verbenol (8, Scheme 1). Neither method avoids double-bond isomerization of the thermodynamically less stable (*-*)- Δ^9 -THC to the more stable (*-*)- Δ^8 -iso-



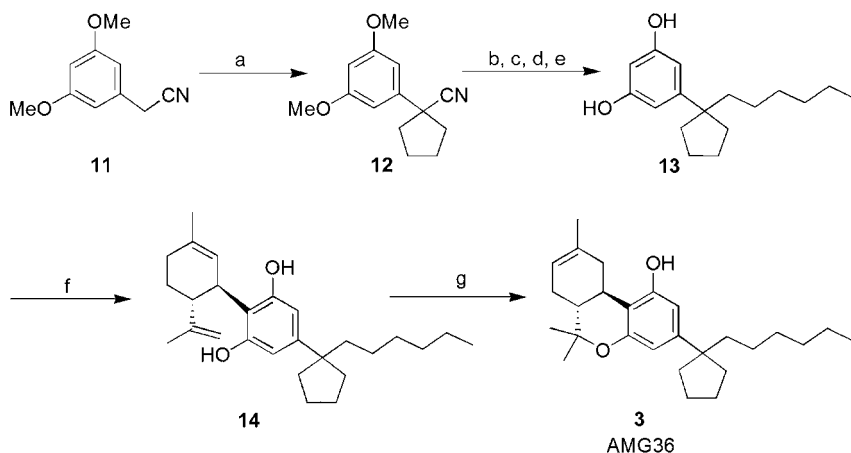
Scheme 2. Single-step synthesis of (-)- Δ^9 -THC (**10**). Reagents and conditions: (a) MgSO_4 , $\text{BF}_3\text{-Et}_2\text{O}$, CH_2Cl_2 , 0°C , 1.5 h, 31%.

(-)-*trans*- Δ^9 -THC (**1**). A mixture of 2.88 g (16.0 mmol) of olivetol (**9**), 2.45 g (16.1 mmol) of (+)-*cis/trans*-*p*-mentha-2,8-dien-1-ol (**7**), and 2 g of anhydrous magnesium sulfate was stirred with 100 mL of methylene chloride under a N_2 atmosphere. After cooling in an ice bath, 1 mL of freshly distilled $\text{BF}_3\text{-Et}_2\text{O}$ was added. The mixture was stirred for 1.5 h at 0°C , and 5 g of anhydrous sodium bicarbonate was added. Stirring continued until the color faded, and the reaction mixture was then filtered and evaporated to give a colorless gum (5 g). On the basis of gas-liquid chromatography it contained 50% Δ^9 -THC. One half of this material was chromatographed on 150 g of Florisil (100–200 mesh) packed in a 1 in \times 3 ft column in petroleum ether (30– 40°C). It was eluted with petroleum ether followed by graded mixtures up to 2:98 of ethyl ether:petroleum ether. Fractions containing pure **1** (TLC) were combined and evaporated to give 0.77 g (31%) of (-)- Δ^9 -THC.

mer. Addition of hydrogen chloride to the double bond of (-)- Δ^8 -THC, followed by phenolate-anion-assisted dehydrochlorination leads to (-)- Δ^9 -THC.

Razdan and coworkers (**10**) have reported a modification of the Petrzilka (**9**) cannabinoid synthesis. Thus, condensation of olivetol with (+)-*cis*- or *trans*-*p*-mentha-2,8-dien-1-ol in the presence of boron trifluoride-etherate and anhydrous magnesium sulfate at 0°C yielded (-)- Δ^9 -THC, and practically no Δ^8 -isomer was formed (**Scheme 2**). This modification represents a useful direct route to (-)- Δ^9 -THCs, (-)- Δ^9 -tetrahydrocannabivarin, and their regiospecifically deuterated analogs (**22–24**). It was recently reported that the synthesis of a (-)- Δ^9 -THC derivative was accomplished without the presence of a drying agent by keeping the reaction temperature at 0°C (**25**).

(-)- Δ^8 -THC has a pharmacological profile similar to (-)- Δ^9 -THC and has been used as a template since the early days of cannabinoid structure–activity correlations because of its greater chemical stability. In general, syntheses of (-)- Δ^8 -THC congeners does not differ from those reported for (-)- Δ^9 -THC, involving condensation of a resorcinol with a suitable chiral monoterpene, which affords the (6a*R*,10a*R*)-configuration. However, the initially formed (-)- Δ^9 -THC is subsequently allowed to isomerize to (-)- Δ^8 -THC. Over the years, numerous (-)- Δ^8 -THC analogs were synthesized and tested, providing substantial information

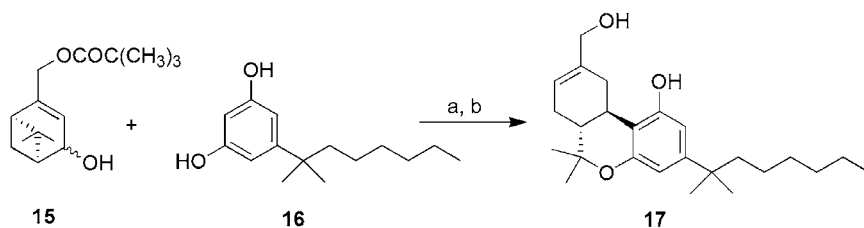


Scheme 3. Synthesis of a representative (-)- Δ^8 -THC analog (**34**). Reagents and conditions: (a) $(\text{Me}_3\text{Si})_2\text{N}^-\text{K}^+$, $\text{Br}(\text{CH}_2)_4\text{Br}$, THF, 0°C , 17 min, 88%; (b) DIBAL-H, CH_2Cl_2 , -78°C , 1 h, 87%; (c) $\text{Br}^-\text{Ph}_3\text{P}^+(\text{CH}_2)_4\text{CH}_3$, $(\text{Me}_3\text{Si})_2\text{N}^-\text{K}^+$, THF, 10°C , 1.5 h, 96%; (d) H_2 , 10% Pd/C, AcOEt, room temperature, overnight, 95%; (e) BBr_3 , CH_2Cl_2 , -78 to -20°C , 5 d, 90%; (f) (+)-*cis/trans*-*p*-mentha-2,8-dien-1-ol, *p*-TSA, C_6H_6 , 10 to 20°C , 1 h, 85%; (g) $\text{BF}_3\cdot\text{Et}_2\text{O}$, CH_2Cl_2 , 0°C to room temperature, 7 h, 79%.

1-(3,5-Dimethoxyphenyl)cyclopentanecarbonitrile (**12**). To a solution of **11** (2.0 g, 11.3 mmol) in dry tetrahydrofuran (THF) (99 mL) at 0°C , under an argon atmosphere, was added potassium bis(trimethylsilyl)amide (6.77 g, 34.0 mmol). The mixture was stirred at the same temperature for 3 min, and then a solution of 1,4-dibromobutane (2.7 g, 12.5 mmol) in dry THF (14 mL) was added over a period of 10 min. Following the addition, the reaction was stirred for 5 min at 0°C and then quenched by the addition of saturated aqueous NH_4Cl . The mixture was diluted with EtOAc, the organic layer separated, and the aqueous phase was extracted with EtOAc. The combined organic layer was washed with brine, dried over MgSO_4 , and the solvent evaporated under reduced pressure to give an oily residue. Purification by flash column chromatography (diethyl ether:petroleum ether 30:70) afforded 2.3 g (88% yield) of the compound **12** as a colorless oil.

(-)-2-[3-(3,4-*trans*-*p*-Menthadien-(1,8))-yl]-5-(1-hexylcyclopentyl)resorcinol (**14**). To a solution of **13** (571 mg, 2.18 mmol) in dry benzene (22 mL) at 10°C under an argon atmosphere was added *p*-toluenesulfonic acid (79 mg, 0.42 mmol) followed by the addition of a solution of (+)-*cis/trans*-*p*-mentha-2,8-dien-1-ol (464 mg, 3.05 mmol) in dry benzene (6 mL). The reaction mixture was stirred at 10 – 20°C for 1 h, at which time thin-layer chromatography (TLC) indicated the complete consumption of starting material. The reaction mixture was diluted with diethyl ether, and the ether solution was washed with saturated NaHCO_3 solution, water, and brine. The organic layer was dried over MgSO_4 , filtered, and concentrated under reduced pressure. Purification by flash column chromatography (diethyl ether:petroleum ether 7:93) afforded 736 mg (85% yield) of the title compound **14** as colorless viscous oil.

(see bottom of page 119)



Scheme 4. Synthesis of (-)-11-hydroxydimethylheptyl- Δ^8 -THC. Reagents and conditions: (a) $\text{BF}_3\cdot\text{Et}_2\text{O}$, CH_2Cl_2 ; (b) LiAlH_4 , THF.

about the phenolic hydroxyl (PH) and the lipophilic side chain (SC) pharmacophores (**2–7,26,27**). The latter has been recognized as the most critical pharmacophoric group. Variation of the *n*-pentyl group of natural cannabinoids can lead to wide variations in potency and selectivity. Optimal activity is obtained with a seven or eight carbon length substituted with 1',1'- or 1',2'-dimethyl groups, as was first demonstrated by Adams (**28–30**). More recent studies have focused on novel side chains bearing 1',1'-cyclic moieties (**31–34**). One of the most successful compounds to result from this work was the C1'-cyclopentyl analog **3** (**Fig. 1**), chosen here to represent the side-chain-modified (-)- Δ^8 -tetrahydrocannabinols. The one-pot cyclobisalkylation of **11** to give cyclopentane carbonitrile **12**, the terpenylation of resorcinol **13** with (+)-*cis/trans*-*p*-mentha-2,8-dien-1-ol, and the cyclization of the cannabidiol intermediate **14** in which the initially formed (-)- Δ^9 -THC derivative is converted to the respective (-)- Δ^8 -isomer are the key steps leading to **3** (**Scheme 3**).

Structural modifications of the tetrahydrocannabinol framework identified one further pharmacophore: a northern aliphatic hydroxyl (NAH) at the C-9 or C-11 position of the classical cannabinoids. Thus, introduction of a hydroxyl group at the C-11 position in tetrahydrocannabinols (e.g., (-)-11-hydroxydimethylheptyl- Δ^8 -THC, **17**, **Scheme 4**) leads to significant enhancement in affin-

(6a*R*)-(trans)-3-(1-Hexylcyclopentyl)-6a,7,10,10a-tetrahydro-6,6,9-trimethyl-6*H*-dibenzo[*b,d*]pyran-1-ol (**3**). To a solution of **14** (601 mg, 1.52 mmol) in anhydrous CH_2Cl_2 (43 mL) at 0°C under an argon atmosphere was added boron trifluoride-etherate (1.32 mL 10.6 mmol). Following the addition, the mixture was stirred at 0°C for 1 h and then at room temperature for 7 h. The reaction was quenched by the addition of saturated NaHCO_3 solution, and the volatiles were removed under reduced pressure. The crude residue was diluted with EtOAc, and the organic layer was washed with water, brine, and dried over MgSO_4 . Solvent evaporation and purification by flash column chromatography on silica gel (diethyl ether:petroleum ether 6:94) afforded 476 mg (79% yield) of the title compound **3** as white foam.

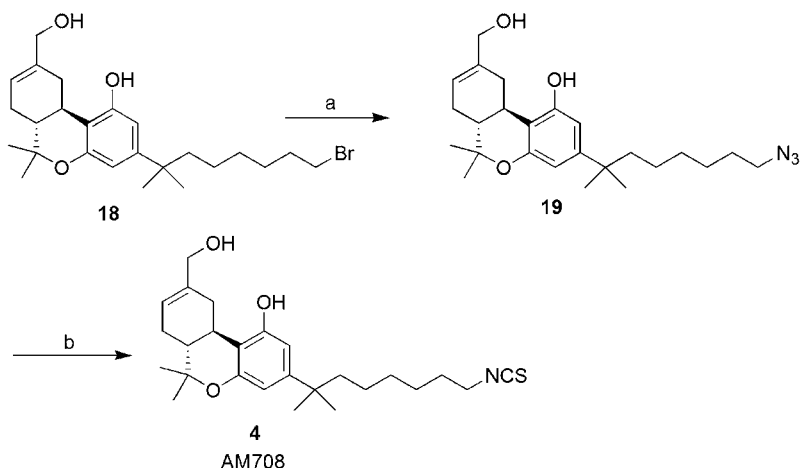
ity and potency for CB₁ and CB₂ (35,36). This is also the case for the hexahydrocannabinols (HHC, e.g., 5, Fig. 1) in which the C-ring is fully saturated. Based on the relative configuration at the C-9 position, hexahydrocannabinol encompasses two types of isomers (9 α and 9 β). Although both isomers are biologically active, the β -epimers in which the C-9 hydroxyl or hydroxymethyl group is equatorial (e.g., 5) have been shown to be more potent than the α -axial counterparts (37–39).

In general, synthesis of 11-hydroxy- Δ^8 -THC derivatives (e.g., 17, Scheme 4) follows a strategy used for the preparation of (-)- Δ^8 -THCs. Thus, verbenol (8, Scheme 1) is replaced by optically active 4-hydroxymyrtenyl pivalate (15, Scheme 4) in a Lewis-acid-catalyzed condensation with the appropriate resorcinol (15,30,40–42).

For example, the highly potent (-)-11-hydroxydimethylheptyl- Δ^8 -THC (17) was synthesized following this method and has served as a template for the design of the high affinity covalent binding probes 19 and 4 (Scheme 5). Development of these ligands was directed at obtaining information on the receptor-binding domain. The electrophilic isothiocyanato group (NCS) targets nucleophilic amino acid residues such as lysine, histidine, and cysteine at or near the active site, and the photoactivatable aliphatic azido group (N₃) is capable of labeling amino acid residues at the active site via a highly reactive nitrene intermediate. Both probes were shown to successfully label the cannabinoid receptors (43). The C-7' bromo analog 18 is the starting point for the synthesis of 19 and 4. Thus, displacement of the bromide in 18 by tetramethylguanidinium azide (TMGA) led to C-7' azide 19, which was converted to the respective isothiocyanate 4 by the triphenylphosphine/carbon disulfide method (41).

Introduction of the more potent equatorial hydroxymethyl group for the hexahydrocannabinol series can be accomplished either by catalytic hydrogenation of the Δ^8 -double bond followed by chromatographic separation of the resulting mixture of isomers (44) or preferably, by utilizing a Wittig–Horner–Emmons process starting from the appropriate keto-precursor (38,45–47). The synthesis of the analog 5, a representative hexahydrocannabinol derivative, is shown in Scheme 6. Protection of the free phenolic hydroxyl in 20 followed by Wittig olefination using (methoxymethylene)triphenylphosphorane produced a mixture of methyl enol ethers, which were hydrolyzed to aldehyde diastereomers 21 and 22. Epimerization (38,45–48) gave the thermodynamically more stable equatorial aldehyde 22. This was followed by carbonyl reduction and deprotection of the phenolic hydroxyl to give 5.

It is also known that presence of a C-9 carbonyl group significantly enhances cannabinergic activity (49). Thus, nabilone (6) (developed at Eli Lilly) represents a successful modification at the northern end of the tricyclic ABC-cannabinoid. This ligand was synthesized (50) from the corresponding

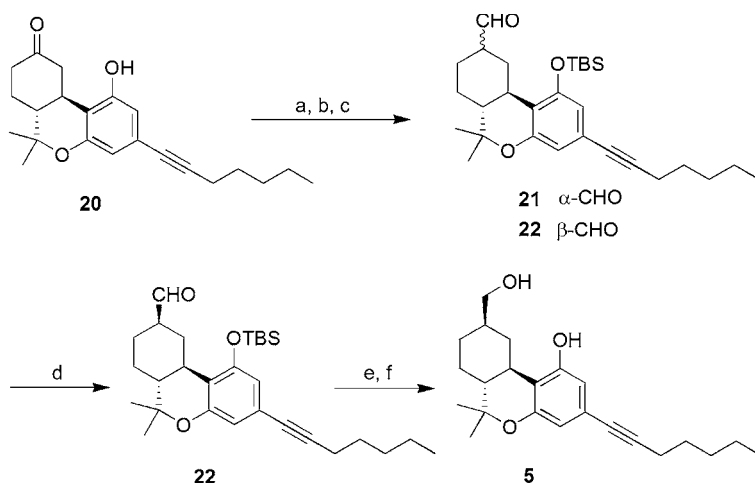


Scheme 5. Synthesis of representative covalent probes for cannabinoid receptors (**41**). Reagents and conditions: (a) TMGA, CHCl_3 , reflux, overnight, 92%; (b) CS_2 , PPh_3 , THF, room temperature, 3 d, 73%.

(-)-11-Hydroxy-7'-azido-1',1'-dimethylheptyl- Δ^8 -THC (**19**). A solution of 11-hydroxy-7'-bromo-1',1'-dimethylheptyl- Δ^8 -THC (**18**) (138.2 mg, 0.297 mmol) in 10 mL of dry chloroform was added dropwise to a solution of TMGA (94 mg, 0.594 mmol) in 5 mL of dry chloroform at 0°C under nitrogen. The resulting mixture was allowed to reach room temperature and refluxed overnight. Subsequently, the solvent was removed under a flow of nitrogen, and ethyl ether was added until no more precipitate was formed. The precipitate was filtered out, and the filtrate was dried over sodium sulfate. Removal of the solvent yielded 124.8 mg of crude product, which was purified by column chromatography (ethyl ether:petroleum ether 70:30). The desired product (**19**), 117.3 mg (light yellow oil), was obtained in 92% yield.

(-)-11-Hydroxy-7'-isothiocyanato-1',1'-dimethylheptyl- Δ^8 -THC (**4**). (-)-11-Hydroxy-7'-azido-1',1'-dimethylheptyl- Δ^8 -THC (**19**) (100 mg, 0.23 mmol) and carbon disulfide (0.4 mL, 6.6 mmol) were dissolved in 10 mL of anhydrous THF. The mixture was stirred at room temperature, and triphenylphosphine (92 mg, 0.35 mmol) was added. After 3 d, the solvent was evaporated under vacuum, and the residue was purified by column chromatography (ethyl ether:petroleum ether 70:30). After purification 74.4 mg of **4** (white solid) was obtained in 73% yield.

resorcinol **16** and either of the acetates **23** or **24** (Scheme 7), which were in turn obtained from commercially available (1*R*,5*S*)-(+)-nopinone in two steps (**46,50,51**). Coupling of **16** with **23** or **24** in the presence of *p*-toluenesulfonic acid afforded the key intermediate **25** (**50**). A useful modification of this method was reported later (**46**). Norpinanone **25** was then treated with stannic chloride in chloroform at room temperature to give ketone **6** not free from its respective *cis*-isomer. However, nabilone (**6**) was purified by column chro-

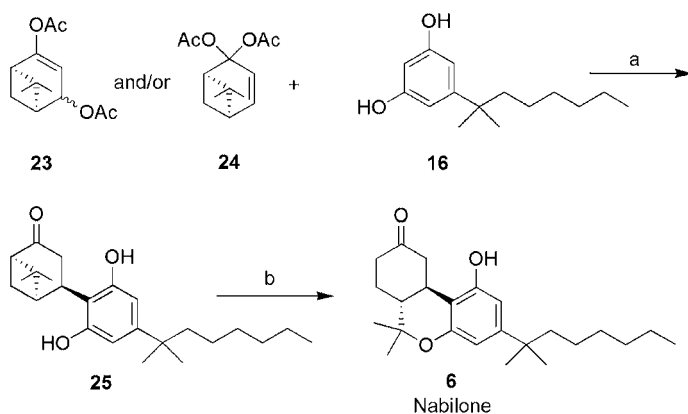


Scheme 6. Synthesis of 3-hept-1-ynyl-11-hydroxyhexahydrocannabinol (**45**). Reagents and conditions: (a) $t\text{-Bu}(\text{CH}_3)_2\text{SiCl}$, imidazole, DMF, 25°C , 92%; (b) $\text{Ph}_3\text{P}=\text{CHOMe}$, PhH, 70°C , 1.5 h; (c) Cl_3CCOOH , $\text{CH}_2\text{Cl}_2/\text{H}_2\text{O}$, 25°C ; (d) K_2CO_3 , EtOH, 25°C , 85% (three steps); (e) NaBH_4 , EtOH, 0°C ; (f) $n\text{-Bu}_4\text{NF}$, THF, 0°C , 95% (two steps).

Aldehyde **22**. (Methoxymethyl)triphenylphosphonium chloride (247 mg, 0.72 mmol) was suspended in 6 mL of dry benzene. Sodium *tert*-amylate (1.24 M in benzene, 0.58 mL, 0.72 mmol), from NaH and *tert*-amyl alcohol, was added, and the reaction mixture was stirred for 5 min at 25°C . The TBS derivative of ketone **20** (107 mg, 0.24 mmol) was dissolved in the minimum amount of benzene and transferred to the solution of the ylide via cannula. The reaction mixture was stirred at 70°C for 1.5 h. Quenching with saturated aqueous NH_4Cl , dilution with ether, and extraction with 3×10 mL of ethyl ether produced an organic phase, which was washed with brine, dried (MgSO_4), and evaporated. The residue was dissolved in 16 mL of dichloromethane, 155 mg (0.9 mmol) of wet trichloroacetic acid was added, and the mixture was stirred at 25°C for 30 min. The reaction was quenched with saturated aqueous NaHCO_3 :brine 50:50, and the mixture was diluted with dichloromethane. The aqueous phase was extracted with 3×20 mL of dichloromethane, and the combined organic extract was washed with brine, dried (MgSO_4), and evaporated. The residue, which consisted of a mixture of aldehydes **21** and **22**, was dissolved in 10 mL of ethanol and added to 71 mg (0.54 mmol) of powdered potassium carbonate suspended in 10 mL of ethanol. The heterogeneous mixture was stirred at 25°C for 4 h. Then the reaction was quenched with saturated aqueous NaH_2PO_4 and the mixture diluted with ether. The aqueous phase was extracted with 4×20 mL of ether. The combined organic extracts were dried (MgSO_4), evaporated, and purified by flash column chromatography (ethyl acetate:hexane 5:95) to produce 94 mg (85% overall yield) of **22** as an oil.

(continues on top of page 123)

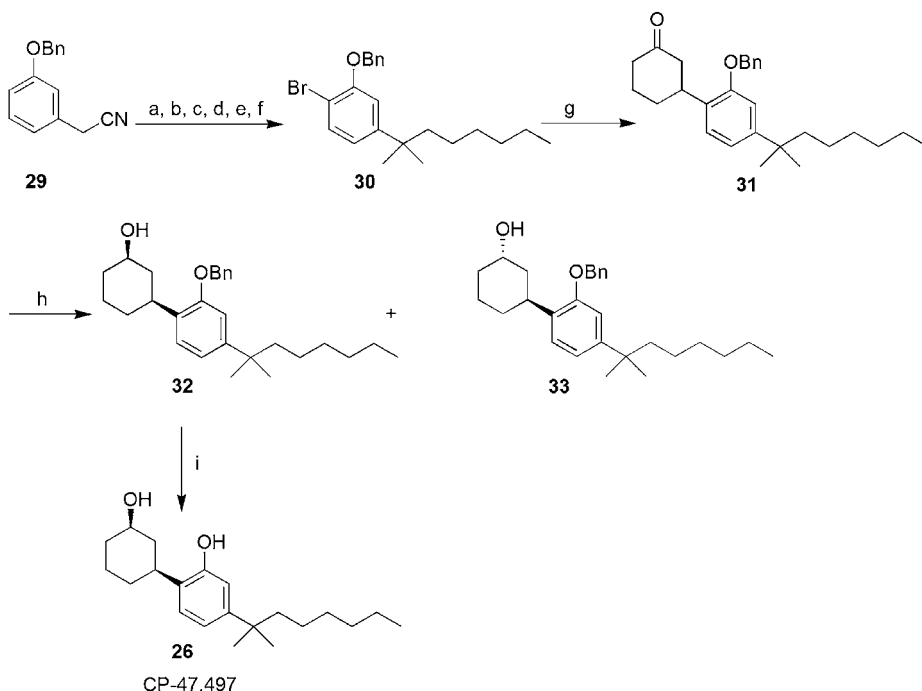
Diol **5**. Aldehyde **22** (45 mg, 0.124 mmol) was dissolved in 1.5 mL of EtOH and cooled to 0°C. A solution of 11 mg (0.289 mmol) of NaBH₄ dissolved in 0.5 mL of EtOH was added via cannula. The reaction mixture was stirred at 0°C for 30 min, the reaction quenched with water, and the mixture diluted with ether. The aqueous phase was extracted twice with ether, and the combined organic extracts were washed with brine and dried (MgSO₄). The solvent was evaporated, and the crude product was dissolved in 3 mL of THF and cooled to 0°C. Tetrabutylammonium fluoride (48 mg, 0.188 mmol) in 0.7 mL of THF was added, the mixture was stirred at 0°C for 45 min, and then the reaction was quenched with water. Ether was added (5 mL), and the aqueous phase was extracted with 2 × 10 mL of ether. The combined organic extracts were washed with brine, dried (MgSO₄), evaporated, and purified by flash chromatography (ethyl acetate:hexane 35:65) to produce 34 mg of **5** (95% overall yield) as an oil.



Scheme 7. Synthesis of nabilone (**50**). Reagents and conditions: (a) *p*-TSA-H₂O, CHCl₃, room temperature, 4 h, 70%; (b) SnCl₄, CHCl₃, room temperature, 16 h, 82%.

(+)-4-[4-(1,1-Dimethylheptyl)-2,6-dihydroxyphenyl]-6,6-dimethyl-2-norpinanone (**25**). A mixture of 1.19 g (5 mmol) of either **23** or **24**, 1.18 g (5 mmol) of **16**, and 0.95 g (5 mmol) of *p*-TSA-H₂O in 50 mL of CHCl₃ was permitted to stand at room temperature for 4 h. Ether was added, and the organic extracts were washed with 10% aqueous NaHCO₃, water, dried over Na₂SO₄, and concentrated to give a semicrystalline residue. The residue was triturated with 25 mL of *n*-hexane and filtered to provide 1.30 g (70% yield) of **25** as a white, crystalline solid.

(-)-*trans*-3-(1,1-Dimethylheptyl)-6,6a,7,8,10,10a-hexahydro-1-hydroxy-6,6-dimethyl-9*H*-dibenzo[*b,d*]pyran-9-one (**6**, nabilone). To a solution of 372 mg (1 mmol) of **25** in 25 mL of CHCl₃ was added 1.0 mL of SnCl₄. The resulting mixture was stirred at room temperature for 16 h and then poured onto ice and extracted with Et₂O. The organic extracts were combined, washed with 2 *N* HCl, water, 5% aqueous NaHCO₃, dried over Na₂SO₄, filtered, and concentrated to afford 378 mg of a foam. Chromatography (Woelm activity II, silica gel; benzene) yielded 305 mg (82% yield) of **6** and 55 mg (14% yield) of its corresponding *cis*-isomer.



Scheme 8. Synthesis of CP-47,497 (**54**). Reagents and conditions: (a) MeBr, NaOH, DMSO/H₂O, 98%; (b) DIBAL-H, THF, 99%; (c) Ph₃P=CH(CH₂)₃CH₃, DMSO, 57%; (d) Pd/C, H₂, EtOH, 78%; (e) Br₂, CCl₄, 100%; (f) KH, PhCH₂Br, DMF, 100%; (g) Mg, CuI, 2-cyclohexen-1-one, THF, 79%; (h) NaBH₄, MeOH, 51% of **32** and 12% of **33**; (i) Pd/C, EtOH, H₂, 77%.

3-[2-(Benzyloxy)-4-(1,1-dimethylheptyl)phenyl]cyclohexanone (**31**). A solution of **30** (75.0 g, 0.193 mol) in 200 mL of THF was slowly added to 70–80 mesh Mg (9.25 g, 0.386 mol). The resultant mixture was refluxed for 20 min and then cooled to -18°C . CuI (1.84 g, 9.7 mmol) was added, and stirring was continued for 10 min. To the resultant mixture was slowly added a solution of 2-cyclohexen-1-one (18.5 g, 0.193 mol) in 40 mL of THF at such a rate that the reaction temperature was maintained at $< -3^{\circ}\text{C}$ with NaCl–ice cooling. The reaction was stirred an additional 30 min, and then added to 500 mL of 2 *N* HCl and 2 L of ice water. The quenched reaction was extracted with 3×500 mL portions of ether. The combined extracts were washed with 2×100 mL of water and with 2×100 mL of saturated aqueous NaCl, dried (MgSO₄), and evaporated to give an oil. The oil was purified via column chromatography on 1.6 kg of silica gel (ethyl ether:cyclohexane 20:80) to yield 62.5 g (79%) of **31** as an oil.

(*cis*)- and (*trans*)-3-[2-(Benzyloxy)-4-(1,1-dimethylheptyl)phenyl] cyclohexanol (**32** and **33**). To a -40°C solution of **31** (4.30 g, 0.106 mol) in 500 mL of MeOH and 15 mL of THF was added NaBH₄ (8.05 g, 0.212 mol). The reaction mixture was stirred for 1 h at -40°C , allowed to warm to -10°C , and then quenched by the addition of 100 mL

(continues on top of page 125)

of saturated aqueous NaCl. The quenched reaction was diluted with 1.5 L of H₂O and extracted with 3 × 450 mL portions of Et₂O. The combined extracts were washed with 3 × 100 mL of H₂O and with 2 × 200 mL of saturated aqueous NaCl, dried (MgSO₄), and evaporated to give an oil. The oil was purified via column chromatography on 400 g of silica gel (ethyl ether:cyclohexane 20:80) to yield, in order of elution, 5.0 g of **33** (12%) as an oil and 22.2 g of **32** (51%) as a solid.

(*cis*)-3-[4-(1,1-Dimethylheptyl)-2-hydroxyphenyl]cyclohexanol (**26**, CP-47,497). A mixture of **32** (2.20 g, 5.39 mmol), NaHCO₃ (12 g), and 10% Pd/C (2.0 g) in 100 mL of EtOH was stirred under 1 atm of H₂ for 2 h. The reaction mixture was filtered through diatomaceous earth, and the filtrate was evaporated to give a solid. The solid was recrystallized from hexane to yield 1.32 g (77%) of **26**.

matography. It should be mentioned that in closely related systems, a clean and rapid cyclization resulted when trimethylsilyl triflate was used in place of stannic chloride (45).

3.2. Nonclassical Cannabinoids

A second class of cannabinergic ligands possessing close similarity with CCs was developed at Pfizer in an effort to simplify the CC structure, while maintaining or improving biological activity (52–56). This group of compounds is generally designated as nonclassical cannabinoids and includes AC-bicyclic (e.g., **26** and **27**, Fig. 2) and ACD-tricyclic (e.g., **28**, Fig. 2) ligands lacking the pyran B-ring of CCs. NCCs share some of the key pharmacophores of the CCs, namely, the phenolic hydroxyl, the side chain, and the northern aliphatic hydroxyl groups. Additionally, this class of cannabinergics has a hydroxypropyl chain on the cyclohexyl ring contiguous and *trans* to the aromatic phenolic group (e.g., (-)-CP-55,940, **27**, Fig. 2). This important new pharmacophore was designated as the southern aliphatic hydroxyl group (3) and has been subjected to extensive investigation by the Makriyannis and Tius groups (46,47,57–60). Synthetic approaches for the SAH group are given in hybrid cannabinoids (Subheading 3.3).

Synthesis of CP-47,497, a ligand that represents the simplest structure in this series, is shown in Scheme 8. The AC-bicyclic nucleus of CP-47,497 was constructed via a cuprous-ion-catalyzed conjugate addition of the Grignard reagent generated from **30** with cyclohexenone. Sodium borohydride reduction of ketone **31** in methanol at low temperature gave a 4:1 ratio of epimeric alcohols **32** and **33**. Chromatographic separation of **32** followed by deprotection of the phenolic hydroxyl group led to racemic **26**.

3.3. Hybrid Cannabinoids

Hybrid cannabinoids, as the name indicates, were generated by combining the pharmacophoric features of classical and nonclassical cannabinoids (Fig. 3). The

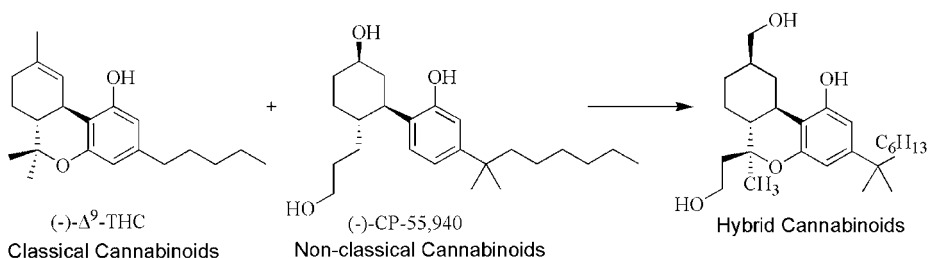


Fig. 3. Evolution of hybrid cannabinoids.

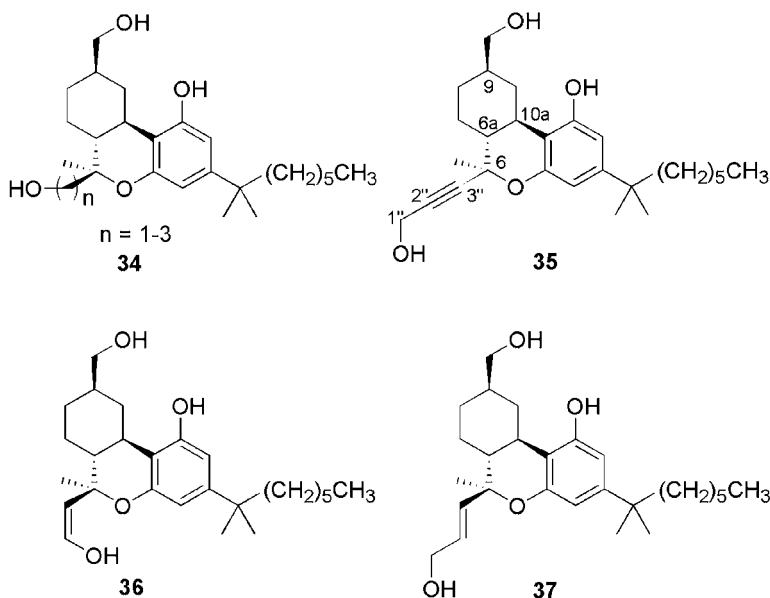
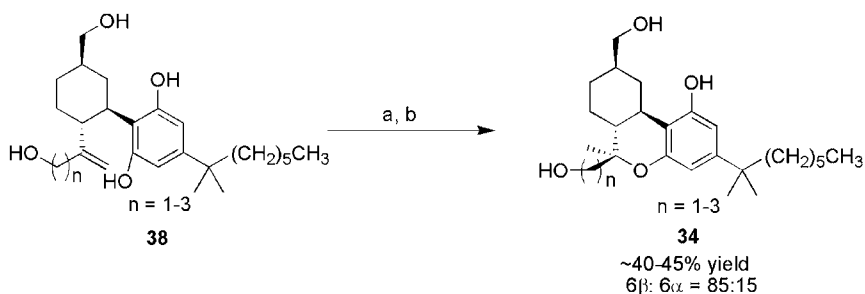


Fig. 4. Novel CC/NCC hybrid ligands.

objective behind their design was to study more precisely the stereochemical requirements of the SAH pharmacophore, which was discovered during the development of NCCs. These hybrid cannabinoids had the added advantage of serving as conformationally more defined three-dimensional probes for the CB₁ and CB₂ active sites than their nonclassical counterparts.

First-generation hybrid cannabinoids (**34**, Fig. 4) were designed to find a correlation between the stereochemistry of the SAH group (6 α or 6 β), the chain length, and the affinity of the compounds for CB₁ and CB₂ receptors (**46,58**),

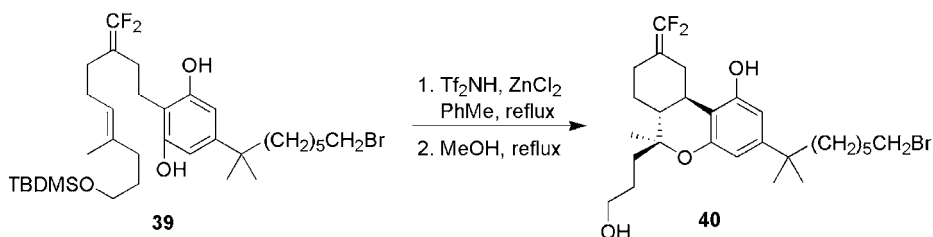


Scheme 9. Stereoselective intramolecular oxymercuration–demercuration approach (**46**). Reagents and conditions: (a) $\text{Hg}(\text{OAc})_2$; (b) aq. NaOH ; NaBH_4 , $n\text{-Bu}_4\text{NOH}$.

3-(1,1-Dimethylheptyl)-12 β -hydroxy-9-nor-9 β -(hydroxymethyl)hexahydrocannabinol (**34**, $n = 1$). To a solution of 25 mg of **38** ($n = 1$) (0.06 mmol) in THF was added 38 mg of mercuric acetate (0.12 mmol), and the solution was stirred for 20 h at room temperature. The reaction was cooled to -78°C , and 36 mg of NaBH_4 (0.94 mmol) in 1 M sodium methoxide/methanol (3 mL) was added in a single portion. The mixture was stirred at -78°C for 15 min, quenched with degassed saturated aqueous NH_4Cl , and allowed to warm to room temperature. The reaction was diluted with ether and washed with brine, and the aqueous phase extracted with ether. The combined ether phases were dried (MgSO_4), and the solvent was evaporated to give a yellow oily solid. Elution through a short column of silica gel (EtOAc:hexane 50:50) followed by purification by HPLC (10×250 mm Phenomenex silica gel column, EtOAc:hexane 50:50, 1.5 mL/min, RI detection) gave **34** as a white foam (15 mg, 62% yield) with a retention time of 12 min. Chiral HPLC (1×25 cm Chiracel OD column, 2-propanol:hexane 10:90, 2.5 mL/min, UV detection at 254 nm) showed **34** (16.30 min retention time, 92.66%) and the enantiomer of **34** (22.71 min retention time, 4.12%), 92% ee; $R_f = 0.20$ (EtOAc:hexane 50:50).

whereas the second-generation hybrid cannabinoids (**35–37**, **Fig. 4**) were designed to obtain additional information on the stereochemical preferences of the SAH group with respect to its ability to interact with the CB_1 and CB_2 binding sites (**47**). A systematic study in which C6 stereochemistry and the chain length of the derivatives at this carbon were varied, revealed that the C6- β -hydroxypropyl analog had a high affinity for both CB_1 and CB_2 receptors.

The challenge to the synthetic chemist that was posed by these structures was the control of C6 stereochemistry. An early solution to this problem involved the intramolecular oxymercuration–demercuration approach, as illustrated in **Scheme 9** (**46,58**). Thus, the stereoselective cyclization of **38** to the tricyclic cannabinoid skeleton by means of the intramolecular oxymercuration–demercuration reaction (**58,61**) gave the 6 β -isomer predominantly (6 β :6 α = 85:15). The enantiomers were separated by chiral high-performance liquid chromatography (HPLC) using Chiralpak OD columns. The probable



Scheme 10. Stereoselective intramolecular cyclization approach.

origin of this stereoselectivity has been discussed (62). Although the yield for this dihydrobenzopyran ring-forming step was modest, this approach was successfully applied to the synthesis of several SAH ligands (46). Several analogs synthesized by the above-mentioned approaches exhibited modest to good receptor affinities. Another approach is shown in **Scheme 10**, wherein the cyclization of **39** leads to formation of two rings of **40** and also determines the stereochemistry at carbon atoms 10a, 6a, and 6 in a single process (59). However, the reaction suffered from a low yield.

The synthesis of second-generation hybrid cannabinoids **35–37** was carried out using a modified approach as depicted in **Scheme 11** (on page 130) (47).

Aldol condensation of aromatic fragment **41** and aliphatic fragment **42** (63) produced **43** (**Scheme 11**). Reduction of **43** with sodium borohydride followed by exposure of the resulting diastereomeric mixture of alcohols to trifluoroacetic acid in dry chloroform at 0°C produced tricyclic alcohol **44** as an approx 1:1 mixture of C9 diastereomers. Oxidation of the diastereomers of **44** with the Dess–Martin periodinane gave ketone **45**, which was converted to β -equatorial alcohol **47** by following a sequence involving the Wittig–Horner–Emmonds reaction (see **Subheading 3.2**). Palladium-catalyzed reductive cleavage of the phenolic allyl ether function, followed by silyl ether removal, gave **35**. Semihydrogenation of **35** in the presence of Lindlar’s catalyst gave **36**. Isomerization of an irradiated (tungsten filament lamp) solution of **36** in benzene in the presence of phenyl disulfide produced **37**.

It should be noted that hybrid cannabinoids obtained by following these procedures were racemic and the enantiomers were separated by chiral HPLC using a method developed with chiral AD columns (60).

3.4. Aminoalkylindoles

The fourth chemical class of cannabinergic compounds, the aminoalkylindoles (AAIs), were initially developed at Sterling Winthrop as potential

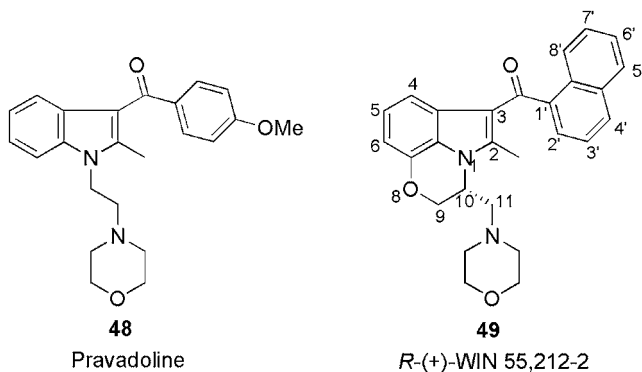


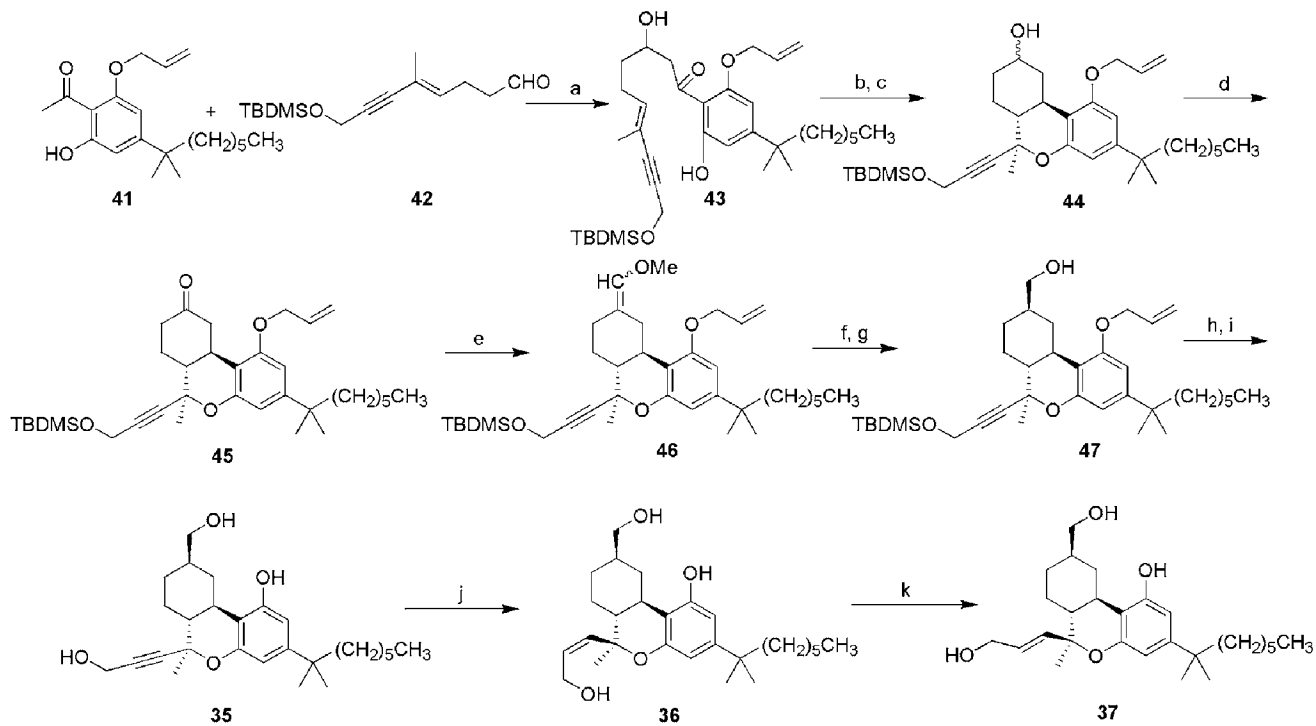
Fig. 5. Representative aminoalkylindoles.

nonulcerogenic analogs of nonsteroidal anti-inflammatory drugs (NSAIDs) (**64**) and bear no structural relationship to the cannabinoids (e.g., **48**, **49**, Fig. 5). These analogs also exhibited antinociceptive properties that eventually were attributed to their interactions with the cannabinoid receptors (**65,66**). The most widely studied compound of this series is WIN55,212-2 (**49**), a potent CB₁ and CB₂ agonist with a slight preference for CB₂. Cannabinergic activity resides principally with only one optical antipode and is more potent than Δ^9 -THC in several pharmacological and behavioral assays. WIN55,212-2 has played an important role in the identification and characterization of cannabinoid receptors and their associated functions and is now in standard use as a CB₁/CB₂ radioligand.

Aminoalkylindoles are generally synthesized by following either Method A or Method B as depicted in **Scheme 12** (**65,66**). An appropriately functionalized indole was aroylated in the first step followed by *N*-alkylation (Method A). Alternatively, *N*-alkylation could be accomplished first, followed by aroylation of the resulting indole derivative at C3 (Method B). For acid-sensitive analogs, EtAlCl₂ is used in place of AlCl₃ in Friedel–Crafts acylation.

WIN55,212-2 (**49**) has been synthesized as shown in **Scheme 13** (**65**). Swern oxidation of **50** afforded the very sensitive α -amino ketone **51**. Reductive cyclization of **51** with Raney-Ni provided the key intermediate **52**. The enantiomers of **52** were obtained by crystallization with (+)- and (-)-dibenzoyltartaric acid (DBT). Hydrazine **54** obtained from enantiomerically pure **53** was then converted to enamino ketone **55**, which when refluxed in the presence of acetic acid yielded (*R*)-(+)-WIN55,212-2 (**49**) in 44% yield.

[³H]WIN55,212-2 has served as an important probe in the discovery of cannabinoid receptors. It was synthesized by catalytic tritium dehalogenation of



Scheme 11. Stereoselective synthesis of conformationally restricted hybrid cannabinoids (**47**). Reagents and conditions: (a) (i) LDA, THF, -78°C , 30 min, (ii) **41**, -78°C , 30 min, (iii) AcOH, 68%; (b) NaBH_4 , MeOH, room temperature, 5 min, 97%; (c) TFA, CHCl_3 , 0.02 M, 0°C , 3.5 h, 76%; (d) Dess-Martin periodinane, CH_2Cl_2 , 0°C to room temperature, 2.5 h, 69%; (e) $\text{Ph}_3\text{PCH}_2\text{OMe}^+\text{Cl}^-$, Na *tert*-amylate, PhH, room temperature, 15 min, 88%; (f) wet $\text{Cl}_3\text{CCO}_2\text{H}$, CH_2Cl_2 , room temperature, 45 min; (g) (i) K_2CO_3 , MeOH, room temperature, 2 h, (ii) NaBH_4 , room temperature, 15 min, 91% from **46**; (h) NaBH_4 , 6 mol % $\text{Pd}(\text{PPh}_3)_4$, THF, room temperature, 23 h, 94%; (i) triethylamine trihydrofluoride, Et_3N , CH_2Cl_2 , room temperature, 18 h, 96%; (j) 8 mol % Lindlar's catalyst, quinoline, 1 atm H_2 , PhH, room temperature, 2 h, 91%; (k) PhSSPh , PhH, hv, room temperature, 22 h, 64%.

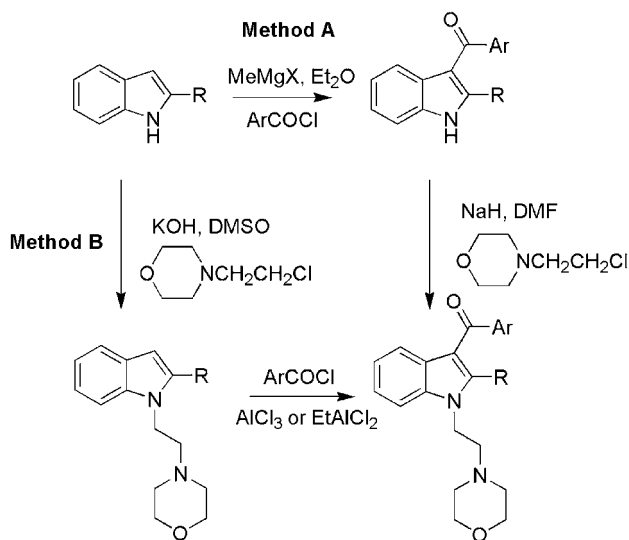
(6*E*)-1-[4-(1,1-Dimethylheptyl)-2-hydroxy-6-prop-2-en-yloxyphenyl]-3-hydroxy-10-*tert*-butyldimethylsilyloxy-7-methyldec-6-en-8-yn-1-one (**43**). To a solution of diisopropylamine (1.80 mL, 1.30 g, 12.8 mmol) in 24 mL of THF at -78°C was added *n*-BuLi (5.45 mL, 2.37 M in hexanes, 12.9 mmol). After 20 min, a solution of ketone **41** (1.97 g, 6.20 mmol) in 8 mL of THF at -78°C was added via cannula. After 30 min, a solution of aldehyde **42** (1.53 g, 5.75 mmol) in 8 mL of THF at -78°C was added via cannula. After 30 min, the reaction mixture was quenched with acetic acid (1.40 mL, 1.47 g, 24.5 mmol) warmed to room temperature and diluted with ether and water. The aqueous phase was extracted thrice with ether, and the combined organic extracts were washed with brine and dried (MgSO_4). Purification by flash column chromatography on silica gel (2.5% to 5% to 10% EtOAc in hexanes) gave ketone **43** (2.28 g, 68% yield) as a pale yellow oil: $R_f = 0.27$ (EtOAc:hexanes 10:90).

Tricyclic C9 Alcohol **44**. To a solution of diol (2.00 g, 3.41 mmol) derived from NaBH_4 reduction of **43** in 175 mL of CHCl_3 at 0°C was added TFA (290 μL , 429 mg, 3.76 mmol). After 3.5 h, the reaction mixture was quenched with saturated aqueous NaHCO_3 and diluted with water. The aqueous phase was extracted twice with CH_2Cl_2 , and the combined organic extracts were washed with brine and dried (MgSO_4). Purification by flash column chromatography on silica gel (5% to 10% to 20% EtOAc in hexanes) gave alcohol **44** (1.48 g, 76% yield) as a colorless oil as a 1:1 mixture of diastereomers: $R_f = 0.29$ and 0.21 (EtOAc:hexanes 20:80).

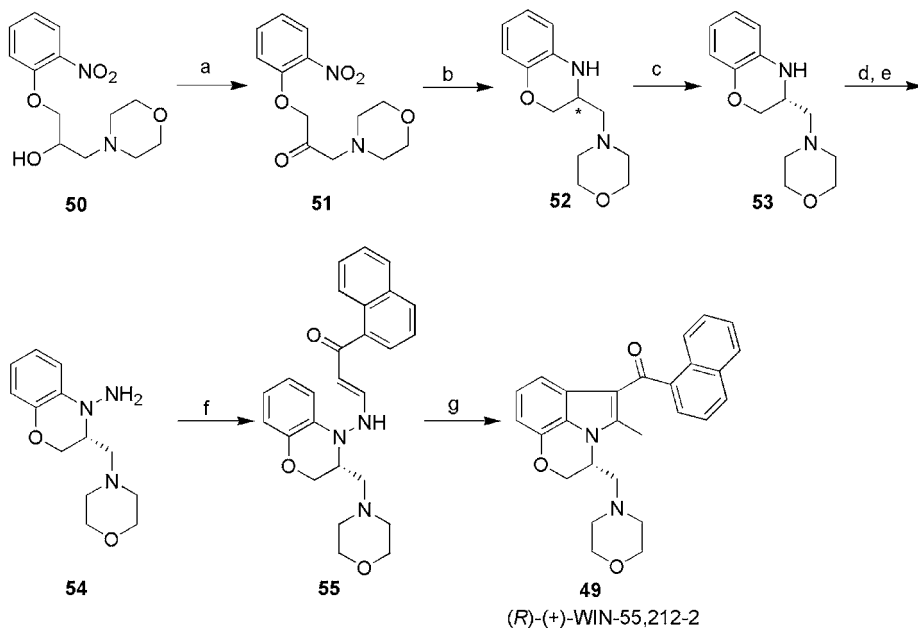
Alkyne **35**. To a solution of phenol obtained after deallylation of **47** (159 mg, 0.29 mmol) in 15 mL of CH_2Cl_2 at room temperature was added triethylamine trihydrofluoride (500 μL , 495 mg, 3.07 mmol) and triethylamine (50 μL , 36 mmol, 0.36 mmol). The reaction mixture was stirred at room temperature for 18 h and diluted with water. The aqueous phase was extracted four times with CH_2Cl_2 , and the combined organic extracts were washed with brine and dried (MgSO_4). Purification by flash column chromatography on silica gel (3% to 4% to 5% EtOH in CH_2Cl_2) gave **35** (120 mg, 96% yield) as a white foam: MP $87\text{--}88^{\circ}\text{C}$; $R_f = 0.18$ (EtOH: CH_2Cl_2 5:95).

(*Z*)-Alkene **36**. To a solution of quinoline (31 mg, 0.24 mmol) in 5 mL of benzene at room temperature was added Lindlar catalyst (27 mg, 2.5% on CaCO_3 , 6.3 μmol) and a solution of alkyne **35** (35 mg, 0.082 mmol) in 20 mL of benzene. The static nitrogen atmosphere was replaced by hydrogen from a double balloon, and the reaction mixture was stirred at room temperature for 2 h, filtered through celite, and concentrated. Purification by flash column chromatography on silica gel (2% to 3% EtOH in CH_2Cl_2) gave (*Z*)-alkene **36** (32 mg, 91% yield) as a white foam: MP $68\text{--}69^{\circ}\text{C}$; $R_f = 0.26$ (EtOH: CH_2Cl_2 6:94).

(*E*)-Alkene **37**. A solution of (*Z*)-alkene **36** (33 mg, 0.077 mmol) and diphenyl disulfide (4 mg, 0.02 mmol) in 12 mL of benzene was irradiated with a 50 W incandescent flood lamp at room temperature for 12 h, at which time additional diphenyl disulfide (3 mg, 0.01 mmol) was added. Irradiation was continued for 10 h, and the reaction mixture was concentrated. Purification by flash column chromatography on silica gel (30% to 50% EtOAc in hexanes) gave alcohol **37** (21 mg, 64% yield) as a white foam: MP $82\text{--}83^{\circ}\text{C}$; $R_f = 0.14$ (EtOAc:hexanes 50:50).



Scheme 12. Synthetic approaches for aminoalkylindoles.

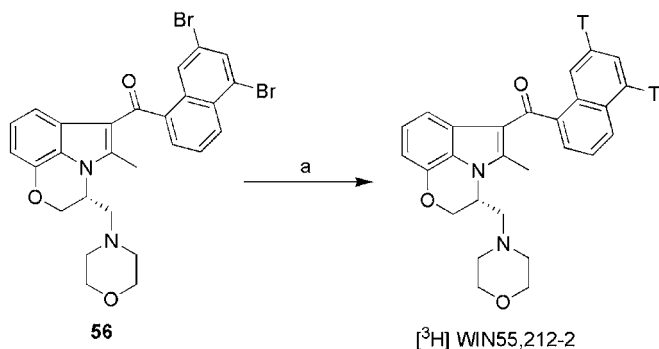


Scheme 13 (*Bottom of facing page*). Synthesis of WIN55,212-2 (**65**). Reagents and conditions: (a) (i) TFAA, DMSO, CH₂Cl₂, -78°C, (ii) Et₃N; (b) H₂, Ra-Ni, EtOAc; (c) dibenzoyl tartaric acid, MeOH; (d) NaNO₂, HCl; (e) LiAlH₄, THF; (f) 1-naphthoylacetone, C₆H₅CH₃, H⁺, reflux; (g) AcOH, reflux.

(*R*)-(+)-3,4-Dihydro-3-[(4-morpholinyl)methyl]-2*H*-1,4-benzoxazine (**53**). Many initial attempts to resolve either enantiomer of **52** as the dibenzoyltartaric acid salts crystallizing from acetone/hexane mixtures only resulted in modest enantiomeric enhancements in ratios of approximately 45:55. Resolution was ultimately achieved on these mixtures by crystallization from CH₃OH. Thus, 23.5 g of the (-)-dibenzoyltartrate salt of **52** was recrystallized twice from CH₃OH to afford an off-white solid containing enantiomerically pure (*R*)-(+)-**53** by gas chromatographic (GC) analysis. Characterization revealed this salt to be a 2:1 complex with **53**:dibenzoyltartaric acid, respectively. The free base of (*R*)-(+)-**53** was made by partitioning the salt between EtOAc and saturated aqueous Na₂CO₃. An analytical sample was prepared by recrystallization from EtOAc/hexane: MP 94–96°C, [α]_D = -28.0° (c = 1, CHCl₃).

1-Amino-3,4-dihydro-3-[(4-morpholinyl)methyl]-2*H*-1,4-benzoxazine (**54**). To a mechanically stirred solution of 55.6 g (0.24 mol) of **53** in 1 L of 2 *N* HCl at 0°C was added over 10 min to an aqueous solution of 18 g (0.26 mol) of NaNO₂. The mixture was stirred for 1 h at 0°C, then diluted with 1 L of H₂O and 1 L of EtOAc, and was made neutral by the cautious addition of solid NaHCO₃. The organic phase was washed with 1 L of saturated aqueous NaCl, dried over MgSO₄, and filtered. Concentration under reduced pressure afforded nitrosamine, which was reduced directly as follows. To 1.5 L of THF under N₂ at 0°C in a 3-L, three-neck flask fitted with a mechanical stirrer was cautiously (Caution!! *see Note 3*) added ~16 g (0.4 mol) of powdered LiAlH₄. The nitrosamine was added as a solution in ~200 mL of THF. After the addition was complete, the mixture was refluxed for 1 h. The reaction mixture was then cooled in an ice bath, and ~60 mL of saturated aqueous Na₂SO₄ was cautiously added dropwise. The resulting thick suspension was stirred for a few minutes and then filtered through a plug of celite, and the filter cake was washed thoroughly with EtOAc. The filtrate was concentrated under reduced pressure to afford 58.4 g of the hydrazine **54**.

WIN55, 212-2 (**49**). A solution of 5.8 g of **54**, (0.026 mol) of 1-naphthoylacetone and 0.5 g of pyridinium 3-nitrobenzenesulfonic acid in 300 mL of H₂O was refluxed for 3 h using a Dean-Stark water trap connected to a reflux condenser. The cooled solution was filtered and concentrated under reduced pressure. The concentrate was dissolved in 250 mL of AcOH and refluxed for 1 h. The cooled solution was then concentrated under reduced pressure, and the residue was partitioned between H₂O and EtOAc. Concentrated aqueous NH₄OH was added until the aqueous phase was alkaline. The organics were dried over MgSO₄, filtered, and concentrated under reduced pressure. Chromatography followed by crystallization from CH₃OH/Et₂O afforded **49** in 51% yield from **54**: MP 256–259°C.



Scheme 14. Synthesis of ^[3H]WIN55,212-2 (**67**). Reagents and conditions: (a) 10% Pd/C, Et₃N, tritium gas.

^[3H]WIN55,212-2. A solution of 25 mg (0.044 mmol) of precursor **56** in 2 mL of ethanol with 25 mg of 10% Pd/C and 0.025 mL of triethylamine was vigorously stirred with 80 Ci of tritium gas at ambient temperature and atmospheric pressure for 4 h. After this time the catalyst was filtered, labile tritium was removed by several evaporations of methanol, and the crude product (1960 mCi) was dissolved in 20 mL of ethanol. Purification was accomplished on two 500-mm silica gel plates eluted with hexane:ethyl acetate 50:50 to afford 988 mCi (a 37% radiochemical yield based on precursor **56**) of product that was found to be >98% radiochemically pure and to coelute with authentic WIN55,212-2 (**49**) both on silica gel TLC (hexane:ethyl acetate 50:50) and reverse-phase HPLC (water:acetonitrile 35:65). The specific activity of product ^[3H]WIN55,212-2 was measured to be 60 Ci/mmol by UV assay (where E246 = 20,958) and the UV of product was superimposable on that of unlabeled compound. A proton-decoupled tritium NMR (CDCl₃) of product **49** showed two peaks at 7.49 and 7.98 ppm.

56, as shown in **Scheme 14** (**67**). The starting compound **56** was prepared analogously to the synthesis of **49**.

In 1996, the Sterling Winthrop and Makriyannis laboratories further explored structural requirements at the N-1 position of aminoalkylindoles by synthesizing novel analogs in which the aminoalkyl chain of the indole ring is attached to a heterocyclic amine through a C-C bond (**68**). These analogs are generally more potent than the C-N analogs and exhibit more favorable physicochemical properties. Potency was optimum for *N*-methylpiperidinyl-2-methyl substitution at the N-1 position (**57**, **58**, **Fig. 6**), while activity resided predominantly in the *R*-enantiomer.

AM1241 (**58**, **Fig. 6**), a highly CB₂-selective and potent agonist, was recently developed by Makriyannis. Design of this molecule incorporated *N*-methylpiperidinyl-2-methyl substituent at the N-1 position and a novel 2-iodo-5-nitrobenzoyl group at C-3.

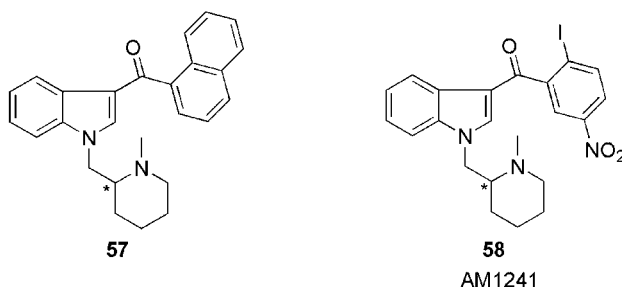


Fig. 6. C-Attached aminoalkylindoles.

A standard approach utilized for the synthesis of these C-attached AAIs involves arylation of indole using MeMgX and ArCOCl followed by *N*-alkylation using 1-methyl-2-chloromethylpiperidine. The racemic compounds were then resolved either by forming diastomeric salts with chiral acids or by HPLC using a semi-preparative Chiracel AD column using ethanol:hexane 20:80.

3.5. Diarylpyrazoles

The most widely studied compound of the diarylpyrazole class is SR141716A (Rimonabant) (**59**, **Fig. 7**), developed by Rinaldi-Carmona and co-workers at Sanofi, which has passed phase III clinical trials for the treatment of obesity and smoking cessation (**69**). This highly potent and selective CB_1 receptor ligand has served as a unique pharmacological and biochemical tool for further characterization of the CB_1 receptor (**70,71**). Other diarylpyrazole ligands that have contributed to our understanding of CB_1 pharmacology are AM251 and AM281 (**60** and **61**, respectively, **Fig. 7**). Both AM251 and AM281 are CB_1 antagonist/inverse agonists capable of displacing [^3H]SR141716A and [^3H]CP-55,940 in CB_1 receptor membrane preparations and share the ability of SR141716A to attenuate the responses to established cannabinoid receptor agonists like WIN55,212-2 or CP-55,940. However, recent evidence indicates that AM251 may have a more “ CB_1 -selective” role than SR141716A. The most notable CB_2 receptor antagonist/inverse agonist is SR144528, a diarylpyrazole (**62**, **Fig. 7**) developed by Sanofi, exhibiting 700-fold selectivity for the CB_2 receptor over CB_1 .

The synthesis of AM281 [*N*-(morpholin-4-yl)-1-(2,4-dichlorophenyl)-5-(4-iodophenyl)-4-methyl-1*H*-pyrazole-3-carboxamide] (**61**) is outlined in **Scheme 15**. 4'-Bromopropiophenone was reacted with diethyl oxalate in anhydrous diethyl ether under basic conditions to afford the lithium salt of ethyl 2,4-dioxo-3-methyl-4-(4-bromophenyl) butanoate **63**, which was further reacted with 2,4-

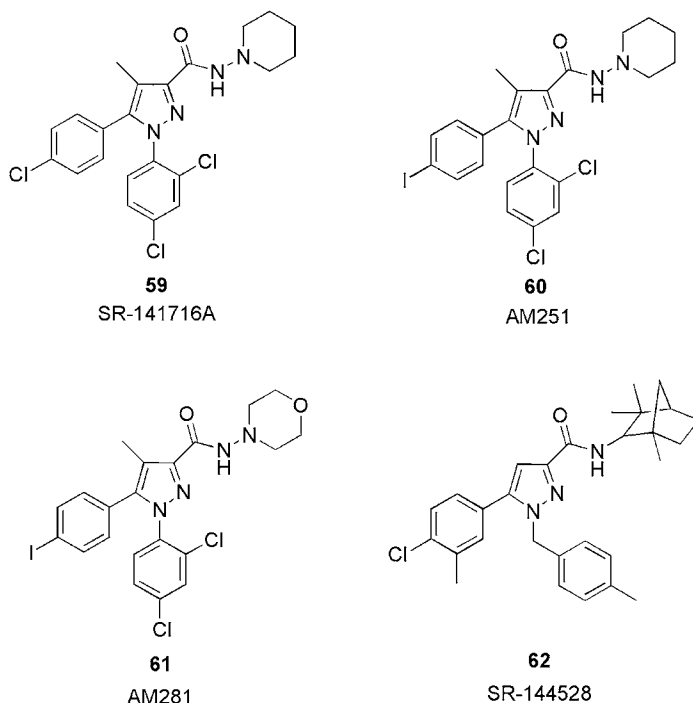
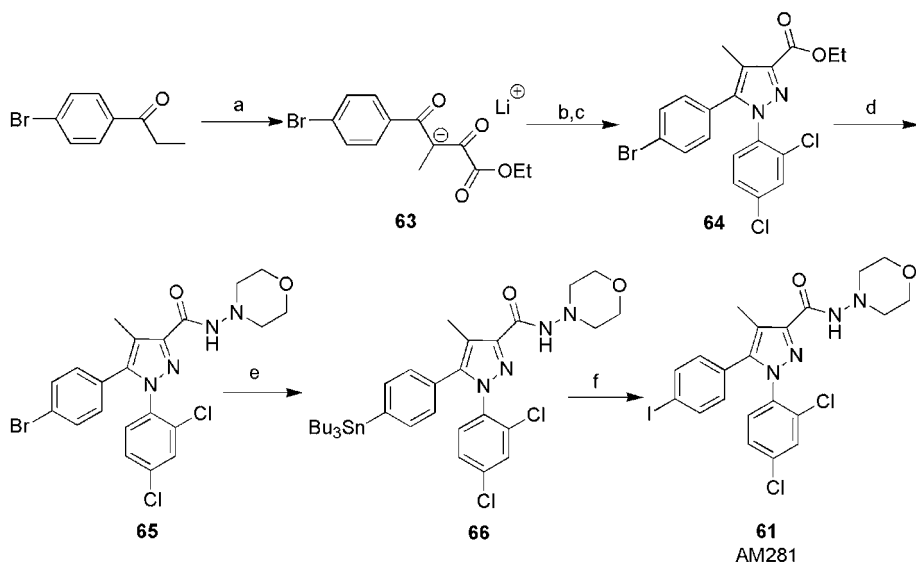


Fig. 7. Representative diarylpyrazole ligands.

dichlorophenylhydrazine hydrochloride to provide 5-(4-bromophenyl)-1-(2,4-dichlorophenyl)-4-methyl-1*H*-pyrazole-3-carboxylic acid ethyl ester **64**. The procedure (*see also* [ref. 72](#)) for the conversion of ester **64** to amide **65** via three steps analogously to the synthesis of AM251 ([73](#)) was now shortened to a single step in which ester **64** was allowed to react with 4-aminomorpholine under basic conditions ([74](#)). Subsequently, the bromo derivative **65** reacted with bis(tributyltin) in the presence of a catalytic amount of tetrakis(triphenylphosphine)palladium to afford the tributyltin derivative **66**. Iododestannylation of compound **66** using iodine in a carbon tetrachloride solution gave AM281 (**61**) in almost quantitative yield.

3.6. Endocannabinoids

In 1992 an arachidonic acid ethanolamide derivative (**67**, [Fig. 8](#)) isolated from porcine brain and characterized as an endogenous ligand for the cannabinoid receptors was named anandamide ([75](#)). It was then followed by the discovery of two other endocannabinoids 2-AG ([76–78](#)) (**68**, [Fig. 8](#)) and 2-arachidonoylglycerol ether ([79](#)) (noladin ether, **69**, [Fig. 8](#)). Anandamide is a highly



Scheme 15. Synthesis of AM281 (**74**). Reagents and conditions: (a) (i) LiHMDS, THF (ii) EtO₂CCO₂Et; (b) 2,4-dichlorophenylhydrazine hydrochloride, EtOH; (c) AcOH; (d) 4-aminomorpholine, LiHMDS, THF; (e) Bu₃Sn₂, Pd(PPh₃)₄, Et₃N; (f) I₂, CCl₄.

N-(Morpholin-4-yl)-5-(4-bromophenyl)-1-(2,4-dichlorophenyl)-4-methyl-1*H*-pyrazole-3-carboxamide (**65**). To a magnetically stirred solution of ester **64** (3.00 g, 6.60 mmol) and 4-aminomorpholine (772 μ L, 7.90 mmol) in dry tetrahydrofuran (25 mL) was added a 1.0 *M* solution of lithium bis(trimethylsilyl)amide in hexane (10.0 mL, 10.0 mmol). The resulting mixture was stirred at room temperature for 2 h and then quenched with saturated aqueous ammonium chloride and extracted with 3 \times 50 mL of chloroform. The combined extracts were washed with brine, dried over anhydrous sodium sulfate, filtered, and evaporated. Purification by flash column chromatography on silica gel with chloroform:ethyl acetate 50:50 afforded amide **65** as a white solid (3.30 g, 98% yield): MP 255–257°C (dec.).

N-(Morpholin-4-yl)-1-(2,4-dichlorophenyl)-5-(4-tributyltinphenyl)-4-methyl-1*H*-pyrazole-3-carboxamide (**66**). To a magnetically stirred suspension of **65** (2.40 g, 4.70 mmol) in freshly distilled triethylamine (150 mL) was added bis(tributyltin) (3.16 mL, 6.25 mmol) followed by tetrakis(triphenylphosphine)palladium(0) (272 mg, 0.23 mmol) at room temperature under an argon atmosphere, and the reaction mixture was heated to reflux for 30 h. After cooling to room temperature, the precipitate was removed by filtration. The filtrate was then concentrated under reduced pressure and purified by flash column chromatography on silica gel with petroleum ether:acetone 80:20 to give the tributyltin derivative **66** (470 mg, 21% yield based on the recovery of starting material): MP 64–68°C.

N-(Morpholin-4-yl)-1-(2,4-dichlorophenyl)-5-(4-iodophenyl)-4-methyl-1*H*-pyrazole-3-carboxamide (**61**). To a magnetically stirred solution of organotin compound **66** (290 mg, 0.40 mmol) in carbon tetrachloride (15 mL) was added dropwise a 0.02 *M* solution of iodine in carbon tetrachloride (25 mL, 0.50 mmol) at room temperature. After TLC showed that the reaction was completed, carbon tetrachloride was removed under reduced pressure. The residue was purified by flash column chromatography on silica gel (petroleum ether:ethyl acetate 50:50) to afford the desired product **61** as a white solid (215 mg, 97% yield): MP 265–268°C (dec.).

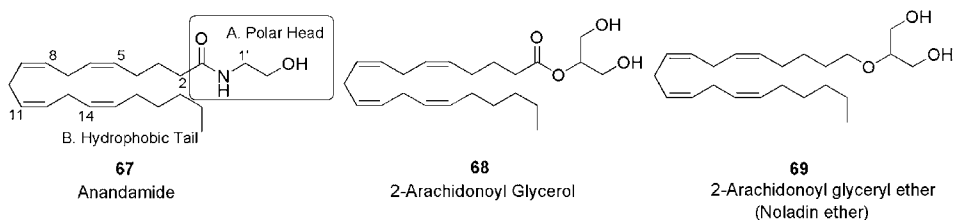


Fig. 8. Endogenous cannabinoid receptor agonists.

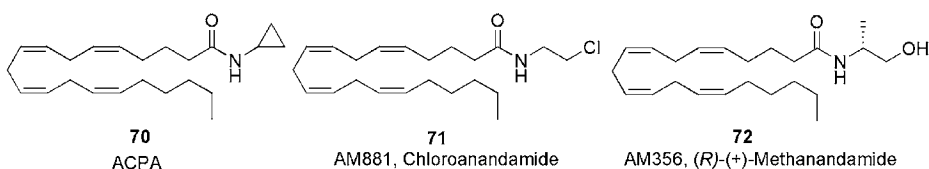


Fig. 9. Head-group-modified analogs of anandamide.

lipophilic compound with four nonconjugated *cis* double bonds and is sensitive to both oxidation and hydrolysis. It was shown to bind to the CB₁ receptor with moderate affinity ($K_i = 61$ nM), has low affinity for the CB₂ receptor ($K_i = 1930$ nM), and behaves as a partial agonist in the biochemical and pharmacological tests used to characterize cannabinoid activity. Its role as a neurotransmitter or neuromodulator is supported by its pharmacological profile as well as by the biochemical mechanisms involved in its biosynthesis and bioinactivation.

The SAR studies of endocannabinoids have been reviewed (80–83). The chemical structure of anandamide can be divided into two major molecular fragments (67, Fig. 8): a polar ethanolamido head group and a hydrophobic arachidonoyl chain. The polar head group is comprised of a secondary amide functionality with an *N*-hydroxyalkyl substituent, while the hydrophobic fragment is a nonconjugated all-*cis* tetraolefinic chain and an *n*-pentyl tail reminiscent of the lipophilic side chain found in the classical cannabinoids.

Anandamide and its head-group-modified analogs (70–72, Fig. 9) were prepared by reaction of the appropriate amino alcohols or aminophenols with arachidonic acid chloride. Alternatively, direct transformation of the methyl ester of arachidonic acid to the corresponding amides was achieved by cyanide-catalyzed amidation (84).

The general procedure for the synthesis of head group modified analogs is as follows (85,86).

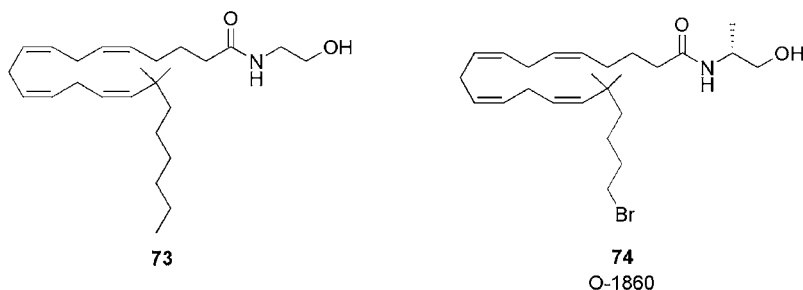
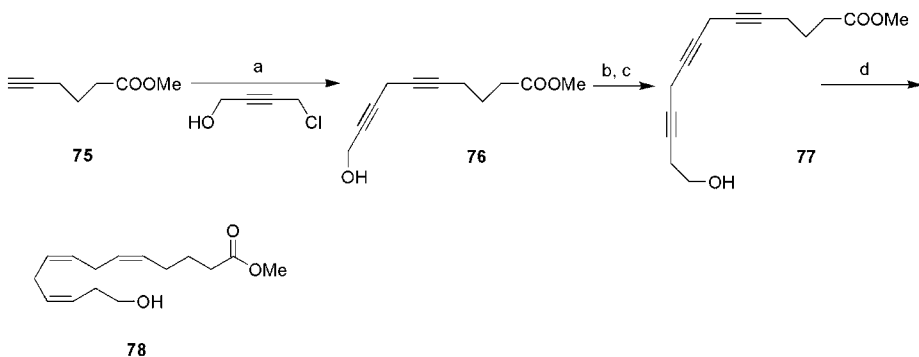


Fig. 10. Tail-modified analogs of anandamide and methanandamide.

N-Arachidonoylamine analogs. A solution of arachidonic acid (200 mg, 0.66 mmol) and dry dimethylformamide (0.05 mL, 0.66 mmol) in 5 mL of dry benzene was cooled in an ice bath, and oxalyl chloride (0.12 mL, 1.32 mmol) was added dropwise under nitrogen. The reaction mixture was stirred at 25°C for an additional hour when 5 mL of anhydrous THF was added, and the mixture was cooled in an ice bath. Subsequently, a solution of the appropriate amino alcohol (10-fold excess) in 5 mL of anhydrous THF was added. After further stirring at room temperature for 15 min, the reaction mixture was diluted with chloroform (15 mL), washed successively with 10% HCl and NaOH solutions, and dried (MgSO₄). The solvent was removed under vacuum, and the residue purified by column chromatography on silica gel.

Although there is very little structural similarity between the classical cannabinoids and anandamide, there is considerable evidence suggesting that these two classes of cannabimimetic agents bind similarly to the CB₁-active site (87). It was thus assumed that incorporation of the 1',1'-dimethylalkyl side chain (from classical cannabinoids) in AEA structure would lead to potent analogs. Indeed, tail-chain-modified anandamide analogs (73,74, Fig. 10) bearing a dimethylalkyl chain exhibited marked increases in receptor affinities and *in vivo* potencies (88–90).

For the synthesis of tail-modified analogs, methyl 14-hydroxy-(all-*cis*)-5,8,11-tetradecatrienoate (78, Scheme 16) is the key intermediate. It can be synthesized either starting from arachidonic acid (86,91–94) or through a reaction sequence (95) depicted in Scheme 16. In this procedure, alcohol 78 was synthesized starting from hex-5-ynoic acid, which was converted into its methyl ester 75 by treatment with *p*-TSA in MeOH. The ester 75 was then coupled with 4-chloro-but-2-yn-1-ol (96) in the presence of CuI as a catalyst to give 10-hydroxy-deca-5,8-diyynoic acid methyl ester 76. Bromination with CBr₄/Ph₃P gave the propargylic bromide, which was then coupled with but-3-yn-1-ol in the presence of CuI as a catalyst to provide the triynoic acid methyl ester 77 (97).



Scheme 16. Preparation of 14-hydroxy-(all-*cis*)-5,8,11-tetradecatrienoate (**78**)⁽⁹⁵⁾. Reagents and conditions: (a) CuI, NaI, K₂CO₃, 4-chlorobut-2-yn-1-ol, DMF, 18 h, 23°C, 87%; (b) CBr₄, PPh₃, CH₂Cl₂, -20 to 23°C, 1 h, 92%; (c) CuI, NaI, K₂CO₃, but-3-yn-1-ol, DMF, 18 h, 23°C, 85%; (d) P-2 Ni, ethanol, 3 h, 23°C, 50%.

Methyl hex-5-ynoate (**75**). A stirred solution of hex-5-ynoic acid (5 g, 44.6 mmol), *p*-TSA (58 mg, 0.3 mmol) in MeOH (8 mL) and CH₂Cl₂ (17 mL) was refluxed for 24 h. The mixture was quenched with saturated aqueous NaHCO₃ and the organic layer was separated. The aqueous layer was extracted with CH₂Cl₂. The combined organic layers were dried over MgSO₄ and evaporated under reduced pressure to yield the methyl ester **75** (5.46 g, 97%).

10-Hydroxydeca-5,8-diyneic acid methyl ester (**76**). A mixture of K₂CO₃ (5.94 g, 43 mmol), CuI (4.1 g, 22 mmol), 4-chlorobut-2-yn-1-ol (4.47 g, 43 mmol), NaI (6.44 g, 43 mmol), and methyl hex-5-ynoate (5.46 g, 43 mmol) in dimethyl formamide (DMF) (86 mL) was stirred overnight at 25°C. The mixture was diluted with ethyl acetate and filtered through a pad of celite. It was washed with saturated aqueous NH₄Cl followed by brine. The solution was dried over MgSO₄, and the solvent was evaporated under vacuum. The oily residue was dissolved in hexanes:ethyl acetate 50:50 and filtered through a pad of silica gel to provide a yellowish oil (7.2 g, 87%), which was used in the subsequent step without further purification since some of the diyne decomposed upon flash chromatography.

14-Hydroxytetradeca-5,8,11-triynoic acid methyl ester (**77**). To a stirred solution of diyne **76** (8.65 g, 44.6 mmol) and CBr₄ (17.74 g, 53.5 mmol) in CH₂Cl₂ (80 mL) cooled to -20°C, a solution of triphenylphosphine (14.6 g, 55.7 mmol) in CH₂Cl₂ (40 mL) was added dropwise. After the addition, the cooling bath was removed and the mixture was stirred for an additional 1 h. Hexanes:ethyl acetate 80:20 was then added until triphenylphosphine oxide precipitated. The mixture was filtered through a pad of silica gel to yield methyl 10-bromodeca-5,8-diyneate as a colorless oil (10.54 g, 92%). Attempts to further purify it by flash chromatography resulted in partial decomposition of the bromide. Hence, it was used as such in the subsequent reaction. A mixture of K₂CO₃ (9.67 g, 70 mmol), CuI (6.66 g, 35 mmol), but-3-yn-1-ol (5.3 mL, 70 mmol), NaI (10.50 g, 70 mmol) and methyl 10-bromodeca-5,8-diyneate (17.99 g, 70 mmol) in DMF (140

(continues on top of page 141)

mL) was stirred overnight at 25°C. The mixture was diluted with ethyl acetate and filtered through a pad of celite. It was washed with saturated aqueous NH_4Cl followed by brine. The solution was dried over MgSO_4 and the solvent was evaporated under vacuum. The oily residue was dissolved in hexanes:ethyl acetate 50:50 and filtered through a pad of silica gel to provide compound **77** as a yellowish oil (14.63 g, 85%), which was used in the subsequent step without further purification. Attempts to purify **77** by flash chromatography resulted in partial decomposition of the triyne.

14-Hydroxytetradeca-(all-*cis*)-5,8,11-trienoic acid methyl ester (**78**). To a stirred solution of $\text{Ni}(\text{OAc})_2$ (14.93 g, 60 mmol) in EtOH (450 mL) was added ethylenediamine (4 mL, 60 mmol) followed by a 1 *M* solution of NaBH_4 (60 mL). The mixture was stirred at 25°C for 0.5 h. The triyne **77** (6.6 g, 26.8 mmol) was added to the reaction mixture and a H_2 atmosphere (balloon) was kept over the reaction mixture. It was stirred for 3 h at 25°C, and the solvent was removed in vacuo. The residue was dissolved in hexanes:ethyl acetate 50:50 and filtered through a pad of silica gel. Purification by flash chromatography (hexanes:ethyl acetate 65:35) provided the desired triene **78** as a colorless oil (3.38 g, 50%).

Partial reduction of the triyne **77** over nickel boride catalyst (**98**) provided the key intermediate **78**.

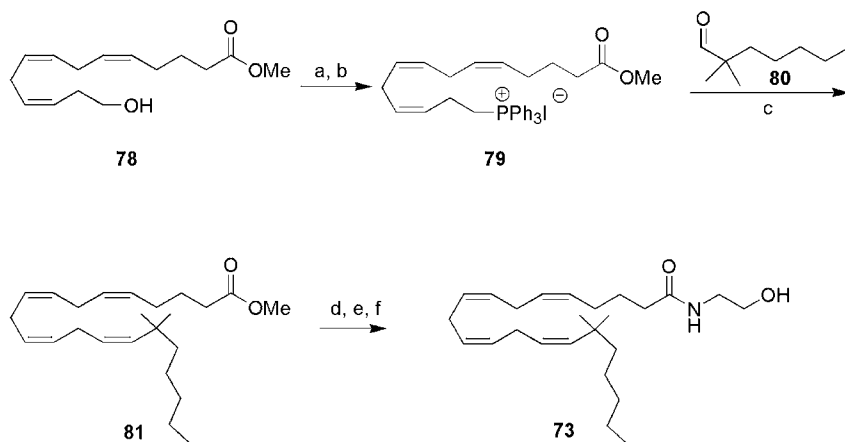
The alcohol **78** was then converted to tail-modified analog **73**, as shown in **Scheme 17**. Phosphonium iodide **79**, obtained from **78**, was treated with NaHMDS to give the ylide, which was then allowed to react with the aldehyde **80** in a Wittig reaction to give the ester derivative **81**. Hydrolysis of the ester **81** with LiOH , followed by treatment with oxalyl chloride (**85,88**) and a suitable amine gave the tail-modified analog **73** (**Scheme 17**).

4. Notes

1. All chemical manipulations should be conducted in a fume hood by qualified personnel.
2. All anhydrous reactions should be performed under a static argon or nitrogen atmosphere in flame-dried glassware using scrupulously dry solvents.
3. In the LiAlH_4 reduction of the nitroso derivative of **53** (see **Scheme 13**) and related nitrosamines, an induction period may occur. The out-of-control refluxing and frothing that have resulted can be controlled by using oversized glassware and cautiously warming the mixture to reflux.

Acknowledgments

Supported by grants from National Institutes on Drug Abuse (DA9158, DA03801, and DA07215).



Scheme 17. Synthesis of tail-modified analog **73** (**95**). Reagents and conditions: (a) I_2 , PPh_3 , imidazole, Et_2O/CH_3CN , 0 to $23^\circ C$, 1 h, 98%; (b) PPh_3 , CH_3CN , reflux, 18 h, 90%; (c) NaHMDS, THF/HMPA, **80**, -78 to $23^\circ C$, 2 h, 61%; (d) LiOH, MeOH/ H_2O , $23^\circ C$, 18 h, 94%; (e) oxalyl chloride, CH_2Cl_2 , $0^\circ C$, 2 h, 100%; (f) 2-ethanolamine, CH_2Cl_2 , 0 to $23^\circ C$.

Methyl 14-(triphenylphosphonio)tetradeca-(all-*cis*)-5,8,11-trienoate iodide (**79**). To a stirred solution of triphenylphosphine (456 mg, 1.74 mmol) and imidazole (118 mg, 1.74 mmol) in $Et_2O:CH_3CN$ 5:1.7, cooled to $0^\circ C$, I_2 was added (441 mg, 1.74 mmol) in several portions. The resulting slurry was warmed to $25^\circ C$ and stirred for 20 min. It was again cooled to $0^\circ C$, and the alcohol **78** was added slowly. The mixture was warmed to $25^\circ C$ after the addition and stirred for 1 h. It was diluted with pentane:ether 80:40 and filtered through a pad of silica gel to yield the iodide as a colorless oil (562 mg, 98%). A solution of triphenylphosphine (2.25 g, 8.6 mmol) and the above iodide (2.83 g, 7.82 mmol) in acetonitrile (50 mL) was refluxed overnight. The solvent was removed under reduced pressure, and the oily residue was purified by washing and decanting with 80 mL of hexanes:benzene 50:50. The solvent was removed and the oily residue was heated in a vacuum oven overnight at $60^\circ C$ to yield **79** as a yellow gum (90%), which was used in the subsequent step without further purification.

16,16-Dimethyldocosa-5,8,11,14-(all-*cis*)-tetraenoic acid methyl ester (**81**). To a stirred solution of the phosphonium salt **79** (686 mg, 1.1 mmol) in THF:hexamethylphosphoramide (HMPA) 6:1 cooled to $-10^\circ C$ was added dropwise a 1 M solution of NaHMDS in THF (1.1 mL). The mixture was stirred at $0^\circ C$ for 30 min and cooled to $-78^\circ C$. The aldehyde **80** (171 mg, 1.1 mmol) (**88**) was added dropwise in THF (1.5 mL) to the reaction mixture. The cooling bath was removed and left to warm to $25^\circ C$ over 2 h. It was quenched with hexanes, and the mixture was filtered through a pad of silica gel (ethyl acetate:hexanes 20:80). The filtrate was dried over $MgSO_4$, and the solvent was removed under reduced pressure. The oily residue was purified by flash chromatography (EtOAc:hexanes 3:97) to yield the tetraene **81** as a colorless oil (0.25 g, 61%).

References

1. Gaoni, Y. and Mechoulam, R. (1964) Hashish. III. Isolation, structure, and partial synthesis of an active constituent of hashish. *J. Am. Chem. Soc.* **86**, 1646–1647.
2. Razdan, R. K. (1986). Structure-activity relationships in cannabinoids. *Pharmacol. Rev.* **38**, 75–149.
3. Makriyannis, A. and Rapaka, R. S. (1990) The molecular basis of cannabinoid activity. *Life Sci.* **47**, 2173–2184.
4. Mechoulam, R., Devane, W. A., and Glaser, R. (1999) Cannabinoid geometry and biological activity, in *Marijuana and Medicine* (Nahas, G. G., Sutin, K. M., and Agurell, S., eds.), Humana Press, Totowa, NJ, pp. 65–90.
5. Khanolkar, A. D., Palmer, S. L., and Makriyannis, A. (2000) Molecular probes for the cannabinoid receptors. *Chem. Phys. Lipids* **108**, 37–52.
6. Palmer, S. L., Thakur, G. A., and Makriyannis, A. (2002) Cannabinergic ligands. *Chem. Phys. Lipids* **121**, 3–19.
7. Goutopoulos, A. and Makriyannis, A. (2002) From cannabis to cannabinergics: new therapeutic opportunities. *Pharmacol. Ther.* **95**, 103–117.
8. Makriyannis, A. and Goutopoulos, A. (2004) Cannabinergics: old and new therapeutic possibilities, in *Drug Discovery Strategies and Methods* (Makriyannis, A. and Biegel, D., eds.), Marcel Dekker, Inc., New York, pp. 89–128.
9. Petrzilka, T., Haefliger, W., and Sikemeier, C. (1969) Synthesis of hashish components. IV. *Helv. Chim. Acta* **52**, 1102–1134.
10. Razdan, R. K., Dalzell, H. C., and Handrick, G. R. (1974) Hashish. X. Simple one-step synthesis of (-)- Δ^1 -tetrahydrocannabinol (THC) from *p*-mentha-2,8-dien-1-ol and olivetol. *J. Am. Chem. Soc.* **96**, 5860–5865.
11. Crombie, L., Crombie, W. M. L., Jamieson, S. V., and Palmer, C. J. (1988) Acid catalyzed terpenylations of olivetol in the synthesis of cannabinoids. *J. Chem. Soc., Perkin Trans. 1* **5**, 1243–1250.
12. Razdan, R. K. and Handrick, G. R. (1970) Hashish. V. A stereospecific synthesis of (-)- Δ^1 - and (-)- $\Delta^{1(6)}$ -tetrahydrocannabinols. *J. Am. Chem. Soc.* **92**, 6061–6062.
13. Handrick, G. R., Uliss, D. B., Dalzell, H. C., and Razdan, R. K. (1979) Hashish. Part 24. Synthesis of (-)- Δ^9 -tetrahydrocannabinol (THC) and its biologically potent metabolite 3'-hydroxy- Δ^9 -THC. *Tetrahedron Lett.* **8**, 681–684.
14. Stoss, P. and Merrath, P. (1991) A useful approach towards Δ^9 -tetrahydrocannabinol. *Synlett*, 553–554.
15. Mechoulam, R., Braun, P., and Gaoni, Y. (1972) Syntheses of Δ^1 -tetrahydrocannabinol and related cannabinoids. *J. Am. Chem. Soc.* **94**, 6159–6165.
16. Childers, W. E., Jr. and Pinnick, H. W. (1984). A novel approach to the synthesis of the cannabinoids. *J. Org. Chem.* **49**, 5276–5277.
17. Chan, T. H. and Chaly, T. (1982) A biomimetic synthesis of Δ^1 -tetrahydrocannabinol. *Tetrahedron Lett.* **23**, 2935–2938.
18. Moore, M., Rickards, R. W., and Ronneberg, H. (1984) Cannabinoid studies. IV. Stereoselective and regiospecific syntheses of (\pm)- Δ^9 -*trans*- and (\pm)- Δ^9 -*cis*-6a,10a-tetrahydrocannabinol. *Aust. J. Chem.* **37**, 2339–2348.

19. Rickards, R. W. and Roenneberg, H. (1984) Synthesis of (-)- Δ^9 -6a,10a-trans-tetrahydrocannabinol. Boron trifluoride catalyzed arylation by a homocuprate. *J. Org. Chem.* **49**, 572–573.
20. Evans, D. A., Shaughnessy, E. A., and Barnes, D. M. (1997) Cationic bis(oxazoline)Cu(II) Lewis acid catalysts. Application to the asymmetric synthesis of ent- Δ^1 -tetrahydrocannabinol. *Tetrahedron Lett.* **38**, 3193–3194.
21. Evans, D. A., Barnes, D. M., Johnson, J. S., et al. (1999) Bis(oxazoline) and bis(oxazoliny)pyridine copper complexes as enantioselective Diels-Alder catalysts: reaction scope and synthetic applications. *J. Am. Chem. Soc.* **121**, 7582–7594.
22. Nikas, S. P., Thakur, G. A., and Makriyannis, A. (2002) Synthesis of side chain specifically deuterated (-)- Δ^9 -tetrahydrocannabinols. *J. Labelled Compd. Radiopharm.* **45**, 1065–1076.
23. Nikas, S. P., Thakur, G. A., and Makriyannis, A. (2002) Regiospecifically deuterated (-)- Δ^9 -tetrahydrocannabivarin. *J. Chem. Soc., Perkin Trans. 1* **22**, 2544–2548.
24. Nikas, S. P., Thakur, G. A., and Makriyannis, A. (2002) A convenient and effective synthesis of 3-(3,5-dimethoxyphenyl)propanal. *Synth. Commun.* **32**, 1751–1756.
25. Nikas, S. P., Grzybovska, J., Papahatjis, D. P., et al. (2004) The role of halogen substitution in classical cannabinoids: a CB1 pharmacophore model. *AAPS J.* **6**, Article 30 (<http://www.aapsj.org>).
26. Thakur, G. A., Nikas, S. P., Li, C., and Makriyannis, A. (2005) Structural Requirements for cannabinoid receptor probes, in *Handbook of Experimental Pharmacology* (Pertwee, R. G., ed.), Springer Verlag, New York, Vol. 168, pp. 210–246.
27. Thakur, G. A., Nikas, S. P., and Makriyannis, A. (2005) CB1 cannabinoid receptor ligands. *Mini-Rev. Med. Chem.* **5**, 631–640.
28. Adams, R., Harfenist, M., and Loewe, S. (1949) New analogs of tetrahydrocannabinol. XIX. *J. Am. Chem. Soc.* **71**, 1624–1628.
29. Huffman, J. W., Miller, J. R. A., Liddle, J., et al. (2003) Structure-activity relationships for 1',1'-dimethylalkyl- Δ^8 -tetrahydrocannabinols. *Bioorg. Med. Chem.* **11**, 1397–1410.
30. Liddle, J. and Huffman, J. W. (2001). Enantioselective synthesis of 11-hydroxy-(1'S,2'R)-dimethylheptyl- Δ^8 -THC, a very potent CB1 agonist. *Tetrahedron* **57**, 7607–7612.
31. Papahatjis, D. P., Kourouli, T., Abadji, V., Goutopoulos, A., and Makriyannis, A. (1998) Pharmacophoric requirements for cannabinoid side chains: multiple bond and C1'-substituted Δ^8 -tetrahydrocannabinols. *J. Med. Chem.* **41**, 1195–1200.
32. Papahatjis, D. P., Nikas, S., Tsotinis, A., Vlachou, M., and Makriyannis, A. (2001) A new ring-forming methodology for the synthesis of conformationally constrained bioactive molecules. *Chem. Lett.* **3**, 192–193.
33. Papahatjis, D. P., Nikas, S. P., Andreou, T., and Makriyannis, A. (2002) Novel 1',1'-chain substituted Δ^8 -tetrahydrocannabinols. *Bioorg. Med. Chem. Lett.* **12**, 3583–3586.
34. Papahatjis, D. P., Nikas, S. P., Kourouli, T., et al. (2003) Pharmacophoric requirements for the cannabinoid side chain. Probing the cannabinoid receptor subsite at C1'. *J. Med. Chem.* **46**, 3221–3229.

35. Mechoulam, R., Lander, N., Srebnik, M., et al. (1987) Stereochemical requirements for cannabimimetic activity. *NIDA Res. Monogr.* **79**, 15–30.
36. Mechoulam, R., Feigenbaum, J. J., Lander, N., et al. (1988) Enantiomeric cannabinoids: stereospecificity of psychotropic activity. *Experientia* **44**, 762–764.
37. Devane, W. A., Breuer, A., Sheskin, T., Jarbe, T. U., Eisen, M. S., and Mechoulam, R. (1992) A novel probe for the cannabinoid receptor. *J. Med. Chem.* **35**, 2065–2069.
38. Yan, G., Yin, D., Khanolkar, A. D., Compton, D. R., Martin, B. R., and Makriyannis, A. (1994) Synthesis and pharmacological properties of 11-hydroxy-3-(1',1'-dimethylheptyl)hexahydrocannabinol: a high-affinity cannabinoid agonist. *J. Med. Chem.* **37**, 2619–2622.
39. Wilson, R. S., May, E. L., Martin, B. R., and Dewey, W. L. (1976) 9-Nor-9-hydroxyhexahydrocannabinols. Synthesis, some behavioral and analgesic properties, and comparison with the tetrahydrocannabinols. *J. Med. Chem.* **19**, 1165–1167.
40. Mechoulam, R., Lander, N., Breuer, A., and Zahalka, J. (1990) Synthesis of the individual, pharmacologically distinct enantiomers of a tetrahydrocannabinol derivative. *Tetrahedron: Asymmetry* **1**, 315–318.
41. Guo, Y., Abadji, V., Morse, K. L., Fournier, D. J., Li, X., and Makriyannis, A. (1994) (-)-11-Hydroxy-7'-isothiocyanato-1',1'-dimethylheptyl- Δ^8 -THC: a novel, high-affinity irreversible probe for the cannabinoid receptor in the brain. *J. Med. Chem.* **37**, 3867–3870.
42. Pop, E., Rachwal, B., Rachwal, S., Vlasak, J., Brewster, M. E., and Prokai, L. (1998) Synthesis of deuterated dextranabinol, a nonpsychotropic cannabinoid with neuroprotective properties. *J. Labelled Compd. Pharm.* **41**, 885–897.
43. Picone, R. P., Fournier, D. J., and Makriyannis, A. (2002) Ligand based structural studies of the CB1 cannabinoid receptor. *J. Pept. Res.* **60**, 348–356.
44. Mechoulam, R., Lander, N., Varkony, T. H., et al. (1980) Stereochemical requirements for cannabinoid activity. *J. Med. Chem.* **23**, 1068–1072.
45. Busch-Petersen, J., Hill, W. A., Fan, P., et al. (1996) Unsaturated side chain β -11-hydroxyhexahydrocannabinol analogs. *J. Med. Chem.* **39**, 3790–3796.
46. Drake, D. J., Jensen, R. S., Busch-Petersen, J., et al. (1998) Classical/nonclassical hybrid cannabinoids: southern aliphatic chain-functionalized C-6 β methyl, ethyl and propyl analogues. *J. Med. Chem.* **41**, 3596–3608.
47. Harrington, P. E., Stergiades, I. A., Erickson, J., Makriyannis, A., and Tius, M. A. (2000) Synthesis of functionalized cannabinoids. *J. Org. Chem.* **65**, 6576–6582.
48. Edery, H., Porath, G., Mechoulam, R., Lander, N., Srebnik, M., and Lewis, N. (1984) Activity of novel aminocannabinoids in baboons. *J. Med. Chem.* **27**, 1370–1373.
49. Archer, R. A., Stark, P., and Lemberger, L. (1986) Nabilone, in *Cannabinoids as Therapeutic Agents* (Mechoulam, R., ed.), CRC Press, Boca Raton, FL, pp. 85–103.
50. Archer, R. A., Blanchard, W. B., Day, W. A., et al. (1977) Cannabinoids. 3. Synthetic approaches to 9-ketocannabinoids. Total synthesis of nabilone. *J. Org. Chem.* **42**, 2277–2284.
51. Coxon, J. M., Garland, R. P., and Hartshorn, M. P. (1970) Derivatives of nopinone. *Aust. J. Chem.* **23**, 1069–1071.

52. Johnson, M. R. and Melvin, L. S. (1986) The discovery of non-classical cannabinoid analgesics, in *Cannabinoids as Therapeutic Agents* (Mechoulam, R., ed.), CRC Press, Boca Raton, FL, pp. 121–145.
53. Little, P. J., Compton, D. R., Johnson, M. R., Melvin, L. S., and Martin, B. R. (1988) Pharmacology and stereoselectivity of structurally novel cannabinoids in mice. *J. Pharmacol. Exp. Ther.* **247**, 1046–1051.
54. Melvin, L. S., Johnson, M. R., Harbert, C. A., Milne, G. M., and Weissman, A. (1984) A cannabinoid derived prototypical analgesic. *J. Med. Chem.* **27**, 67–71.
55. Melvin, L. S., Milne, G. M., Johnson, M. R., Subramaniam, B., Wilken, G. H., and Howlett, A. C. (1993) Structure-activity relationships for cannabinoid receptor-binding and analgesic activity: studies of bicyclic cannabinoid analogs. *Mol. Pharmacol.* **44**, 1008–1015.
56. Melvin, L. S., Milne, G. M., Johnson, M. R., Wilken, G. H., and Howlett, A. C. (1995) Structure-activity relationships defining the ACD-tricyclic cannabinoids: cannabinoid receptor binding and analgesic activity. *Drug Des. Discov.* **13**, 155–166.
57. Chu, C., Ramamurthy, A., Makriyannis, A., and Tius, M. A. (2003) Synthesis of covalent probes for the radiolabeling of the cannabinoid receptor. *J. Org. Chem.* **68**, 55–61.
58. Tius, M. A., Makriyannis, A., Long Zou, X., and Abadji, V. (1994) Conformationally restricted hybrids of CP-55,940 and HHC: stereoselective synthesis and activity. *Tetrahedron* **50**, 2671–2680.
59. Tius, M. A., Busch-Petersen, J., and Marris, A. R. (1997) Synthesis of a bifunctional cannabinoid ligand. *J. Chem. Soc. Chem. Commun.* **19**, 1867–1868.
60. Thakur, G. A., Palmer, S. L., Harrington, P. E., Stergiades, I. A., Tius, M. A., and Makriyannis, A. (2002) Enantiomeric resolution of a novel chiral cannabinoid receptor ligand. *J. Biochem. Biophys. Methods* **54**, 415–422.
61. Brown, H. C. and Geoghegan, P. J., Jr. (1970) Solvomercuration-demercuration. I. Oxymercuration-demercuration of representative olefins in an aqueous system. Mild procedure for the Markovnikov hydration of the carbon-carbon double bond. *J. Org. Chem.* **35**, 1844–1850.
62. Tius, M. A. and Busch-Petersen, J. (1994) Stereochemical control in the oxymercuration of 5-alken-1-ols. *Tetrahedron Lett.* **35**, 5181–5184.
63. Trost, B. M., Sorum, M. T., Chan, C., and Ruehter, G. (1997) Palladium-catalyzed additions of terminal alkynes to acceptor alkynes. *J. Am. Chem. Soc.* **119**, 698–708.
64. Bell, M. R., D'Ambra, T. E., Kumar, V., et al. (1991) Antinociceptive (aminoalkyl)indoles. *J. Med. Chem.* **34**, 1099–1110.
65. D'Ambra, T. E., Estep, K. G., Bell, M. R., et al. (1992) Conformationally restrained analogues of pravadoline: nanomolar potent, enantioselective, (aminoalkyl) indole agonists of the cannabinoid receptor. *J. Med. Chem.* **35**, 124–135.
66. Eissenstat, M. A., Bell, M. R., D'Ambra, T. E., et al. (1995) Aminoalkylindoles: structure-activity relationships of novel cannabinoid mimetics. *J. Med. Chem.* **38**, 3094–3105.
67. Seguin, R. J. and Filer, C. N. (2003) Synthesis and characterization of the potent cannabinoid agonist [naphthyl-³H]WIN55212-2 at high specific activity. *J. Labelled Compd. Pharm.* **46**, 67–71.

68. D'Ambra, T. E., Eissenstat, M. A., Abt, J., et al. (1996) C-attached aminoalkylindoles: potent cannabinoid mimetics. *Bioorg. Med. Chem. Lett.* **6**, 17–22.
69. Rinaldi-Carmona, M., Barth, F., Heaulme, M., et al. (1994). SR141716A, a potent and selective antagonist of the brain cannabinoid receptor. *FEBS Lett.* **350**, 240–244.
70. Lan, R., Liu, Q., Fan, P., et al. (1999) Structure-activity relationship of pyrazole derivatives as cannabinoid receptor antagonists. *J. Med. Chem.* **42**, 776–779.
71. Nakamura-Palacios, E. M., Moerschbaecher, J. M., and Barker, L. A. (1999). The pharmacology of SR 141716A: a review. *CNS Drug Rev.* **5**, 43–58.
72. Seltzman, H. H., Carroll, F. I., Burgess, J. P., Wyrick, C. D., and Burch, D. F. (1995) Synthesis, spectral studies and tritiation of the cannabinoid antagonist SR141716A. *J. Chem. Soc., Chem. Commun.* **15**, 1549–1550.
73. Lan, R., Gatley, S. J., and Makriyannis, A. (1996) Preparation of iodine-123 labeled AM251: a potential SPECT radioligand for the brain cannabinoid CB1 receptor. *J. Labelled Compd. Radiopharm.* **38**, 875–881.
74. Lan, R., Gatley, J., Lu, Q., et al. (1999) Design and synthesis of the CB1 selective cannabinoid antagonist AM281: a potential human SPECT ligand. *AAPS J.* **1**, Article 4 (<http://www.aapsj.org>).
75. Devane, W. A., Hanus, L., Brewer, A., et al. (1992) Isolation and structure of a brain constituent that binds to the cannabinoid receptor. *Science* **258**, 1946–1949.
76. Mechoulam, R., Ben-Shabat, S., Hanus, L., et al. (1995) Identification of an endogenous 2-monoglyceride, present in canine gut, that binds to cannabinoid receptors. *Biochem. Pharmacol.* **50**, 83–90.
77. Mechoulam, R., Ben Shabat, S., Hanus, L., et al. (1996) Endogenous cannabinoid ligands—chemical and biological studies. *J. Lipid Mediat. Cell Signal.* **14**, 45–49.
78. Stella, N., Schweitzer, P., and Piomelli, D. (1997) A second endogenous cannabinoid that modulates long-term potentiation. *Nature* **388**, 773–778.
79. Hanus, L., Abu-Lafi, S., Fride, E., et al. (2001) 2-Arachidonyl glyceryl ether, an endogenous agonist of the cannabinoid CB1 receptor. *Proc. Natl. Acad. Sci. USA* **98**, 3662–3665.
80. Khanolkar, A. D. and Makriyannis, A. (1999) Structure-activity relationships of anandamide, an endogenous cannabinoid ligand. *Life Sci.* **65**, 607–616.
81. Palmer, S. L., Khanolkar, A. D., and Makriyannis, A. (2000) Natural and synthetic endocannabinoids and their structure-activity relationships. *Curr. Pharm. Des.* **6**, 1381–1397.
82. Reggio, P. H. (2002) Endocannabinoid structure-activity relationships for interaction at the cannabinoid receptors. *Prostaglandins Leukot. Essent. Fatty Acids* **66**, 143–160.
83. Thomas, B. F., Adams, I. B., Mascarella, S. W., Martin, B. R., and Razdan, R. K. (1996) Structure-activity analysis of anandamide analogs: relationship to a cannabinoid pharmacophore. *J. Med. Chem.* **39**, 471–479.
84. Hoegberg, T., Stroem, P., Ebner, M., and Raembsby, S. (1987) Cyanide as an efficient and mild catalyst in the aminolysis of esters. *J. Org. Chem.* **52**, 2033–2036.
85. Abadji, V., Lin, S., Taha, G., et al. (1994) (R)-Methanandamide: a chiral novel anandamide possessing higher potency and metabolic stability. *J. Med. Chem.* **37**, 1889–1893.

86. Corey, E. J., Cashman, J. R., Kantner, S. S., and Wright, S. W. (1984) Rationally designed, potent competitive inhibitors of leukotriene biosynthesis. *J. Am. Chem. Soc.* **106**, 1503–1504.
87. Barnett-Norris, J., Guarnieri, F., Hurst, D. P., and Reggio, P. H. (1998) Exploration of biologically relevant conformations of anandamide, 2-arachidonylglycerol, and their analogues using conformational memories. *J. Med. Chem.* **41**, 4861–4872.
88. Ryan, W. J., Banner, W. K., Wiley, J. L., Martin, B. R., and Razdan, R. K. (1997) Potent anandamide analogs: the effect of changing the length and branching of the end pentyl chain. *J. Med. Chem.* **40**, 3617–3625.
89. Seltzman, H. H., Fleming, D. N., Thomas, B. F., et al. (1997) Synthesis and pharmacological comparison of dimethylheptyl and pentyl analogs of anandamide. *J. Med. Chem.* **40**, 3626–3634.
90. Di Marzo, V., Bisogno, T., De Petrocellis, L., et al. (2001) Highly selective CB1 cannabinoid receptor ligands and novel CB1/VR1 vanilloid receptor “hybrid” ligands. *Biochem. Biophys. Res. Commun.* **281**, 444–451.
91. Manna, S., Falck, J. R., Chacos, N., and Capdevila, J. (1983) Synthesis of arachidonic acid metabolites produced by purified kidney cortex microsomal cytochrome P-450. *Tetrahedron Lett.* **24**, 33–36.
92. Falck, J. R., Lumin, S., Blair, I., et al. (1990) Cytochrome P-450-dependent oxidation of arachidonic acid to 16-, 17-, and 18-hydroxyeicosatetraenoic acids. *J. Biol. Chem.* **265**, 10244–10249.
93. Falck, J. R., Sun, L., Lee, S. G., et al. (1992) Enantiospecific synthesis of 17- and 18-hydroxyeicosatetraenoic acids, cytochrome P450 arachidonate metabolites. *Tetrahedron Lett.* **33**, 4893–4896.
94. Heckmann, B., Mioskowski, C., Lumin, S., Falck, J. R., Wei, S., and Capdevila, J. H. (1996) Chiral acetals: stereocontrolled syntheses of 16-, 17-, and 18-hydroxyeicosatetraenoic acids, cytochrome P-450 arachidonate metabolites. *Tetrahedron Lett.* **37**, 1425–1428.
95. Dasse, O., Mahadevan, A., Han, L., Martin, B. R., Marzo, V. D., and Razdan, R. K. (2000) The synthesis of *N*-vanillyl-arachidonoyl-amide (Arvanil) and its analogs: an improved procedure for the synthesis of the key Synthons methyl 14-hydroxy-(all-*cis*)-5,8,11-tetradecatrienoate. *Tetrahedron* **56**, 9195–9202.
96. Crombie, L., Haigh, D., Jones, R. C. F., and Mat-Zin, A. R. (1993) Synthesis of the alkaloid homaline in (\pm) and natural (*S,S*)-(-) forms, using amination and transamidative ring expansion in liquid ammonia. *J. Chem. Soc., Perkin Trans. 1* **17**, 2047–2054.
97. Durand, S., Parrain, J.-L., and Santelli, M. (1998) A large-scale and concise synthesis of g-linolenic acid from 4-chlorobut-2-yn-1-ol. *Synthesis* **7**, 1015–1018.
98. Brown, H. C. and Brown, C. A. (1963) Reaction of sodium borohydride with nickel acetate in ethanol solution; a highly selective nickel hydrogenation catalyst. *J. Am. Chem. Soc.* **85**, 1005–1006.

Cannabinoid Receptor Binding to Membrane Homogenates and Cannabinoid-Stimulated [³⁵S]GTPγS Binding to Membrane Homogenates or Intact Cultured Cells

Christopher Breivogel

Summary

Radioligand-binding assays can be used to obtain information about the binding characteristics of a ligand to its receptor or the general location of binding sites within a tissue or even provide evidence for the existence of a specific receptor. In the case of the cannabinoid receptor system, radioligand binding has been instrumental for each of these applications. While receptor binding can provide the above information, it says little about the efficacy of the ligand interacting with it. Binding assays that assess the effect of an unlabeled receptor ligand on the binding of the radiolabeled guanosine triphosphate (GTP) analog [³⁵S]GTPγS provide such information and may be the most sensitive assays available for determining the relative efficacies of ligands that act through G protein-coupled receptors, like the CB₁ cannabinoid receptor. Herein are described methods for radioligand binding to both brain membrane homogenates and membrane homogenates of cultured cells, as well as a recently developed protocol for assessing agonist-stimulated [³⁵S]GTPγS binding to intact cultured cells.

Key Words: [³⁵S]GTPγS; cannabinoid; cannabinoid CB₁ receptor; cell culture; intact cells; brain membranes; radioligand binding; efficacy.

1. Introduction

The very existence of a receptor for cannabinoids like Δ⁹-tetrahydrocannabinol (THC) was debated prior to 1990, but compelling evidence for this receptor was reported in the late 1980s by the laboratory of Dr. Allyn Howlett. They demonstrated cell-specific inhibition of cyclic adenosine monophosphate (cAMP) accumulation (1) and guanylylimidodiphosphate (GPP-NH-P)-sensitive binding of a tritium-labeled CP55940 to rat brain membranes (2), implying

a G protein-coupled receptor (GPCR) target. Upon the cloning of CB₁, the seven-transmembrane (7TM) spanning domain structure of a GPCR was confirmed (3). Since that time, a second GPCR for cannabinoids, CB₂, has been cloned (4), and evidence for additional receptor subtypes is growing (5–7).

The binding of a radiolabeled ligand to its receptor, while providing data on the affinity of a ligand for its receptor and the number of binding sites, yields little information about activation of the receptor by that ligand. A somewhat newer radioligand-binding technique, agonist-stimulated [³⁵S]GTPγS binding (8–11) can determine the efficacy of ligands acting at a wide range of GPCRs and is probably the most sensitive technique for determining relative agonist efficacies at GPCRs. Some of the earliest reports of this method were in the cannabinoid receptor system (12), and some of the most recent lines of evidence for additional cannabinoid receptor subtypes have been obtained using agonist-stimulated [³⁵S]GTPγS binding (6).

Radioligand receptor binding is based on the law of mass action that assumes that if $L + R \rightarrow LR$, then $[LR] = k[L][R]$ at equilibrium. Thus, if one adds known concentrations of L* (radiolabeled ligand) to a solution or suspension containing R, allows the mixture to come to equilibrium, separates L* from L*R, and measures the quantity of L*R, the amount of R present and the equilibrium dissociation constant for L*R can be determined. In the cannabinoid field there is a variety of commercially available radioligands from which to choose, including agonists and antagonists that are nonselective or selective for the two known subtypes of cannabinoid receptors.

Seven-transmembrane spanning domain GPCRs exert most (but perhaps not all) of their effects via activation of G proteins, which are heterotrimeric proteins composed of α, β and γ subunits. Binding of an agonist to a GPCR induces the Gα subunit to lose affinity for guanosine diphosphate (GDP), which is bound to the inactive subunit, allowing a molecule for GTP to bind to Gα thus activating it. Binding of GTP to Gα causes the Gβγ subunit complex to dissociate from Gα, resulting in activation of Gβγ. The activity of Gα is terminated when the intrinsic GTPase activity of Gα cleaves the terminal (or γ) phosphate from GTP to form GDP plus phosphate. GDP remains bound to the inactive Gα, which then couples a free Gβγ, thereby inactivating that Gβγ subunit complex as well. The heterotrimeric G protein may then reassociate with a GPCR, preparing it for another round of activation.

In the agonist-stimulated [³⁵S]GTPγS binding assay, what is being measured is the activity of a ligand for the activation of G proteins, acting via GPCRs. Substitution of [³⁵S]GTPγS for GTP in the G protein cycle has two effects: (1) GTPγS binds to Gα with high affinity, but cannot be cleaved by the intrinsic GTPase of Gα, meaning that it remains bound to Gα and thus the cell membrane for ease of separation from the unbound ligand; and (2)

radiolabeled [^{35}S]GTP γ S can be detected by liquid scintillation spectrophotometry. In a membrane-binding assay, the assay can be incubated as for receptor radioligand binding, and bound can be separated from free [^{35}S]GTP γ S as in receptor binding. While this method does not give specific information about the type of G protein activated, it can be used to determine the potency and efficacy of ligands at a GPCR, the relative quantity of G proteins activated, and the affinity of the agonist-activated G proteins for [^{35}S]GTP γ S. This technique has recently been modified to assess receptor-stimulated binding of [^{35}S]GTP γ S by a number of receptors to either an immortalized cell line or a primary culture of neuronal cells. It was shown that μ agonist stimulated [^{35}S]GTP γ S binding to C6 glioma cells transfected with human μ opioid receptors and that adenosine and cannabinoid agonists stimulated [^{35}S]GTP γ S binding to primary cultures of rat cerebellar granule cells (13).

2. Materials

1. [^{35}S]Guanosine-5'-O-(3-thiotriphosphate) ([^{35}S]GTP γ S) (Perkin Elmer; Boston, MA).
2. GTP γ S (Roche Molecular Biochemicals; Indianapolis, IN).
3. GDP (Sigma Chemical Co; St. Louis, MO).
4. Assay buffer: 50 mM Tris-HCl, pH 7.4, 3.0 mM MgCl₂, 0.2 mM ethylene glycol tetraacetic acid (EGTA), 100 mM NaCl.
5. Membrane buffer: (50 mM Tris-HCl, pH 7.4, 3.0 mM MgCl₂, 0.2 mM EGTA).
6. Bovine serum albumin (BSA).
7. Adenosine deaminase (Type X; EC 3.5.4.4).
8. Ethanol and/or dimethyl sulfoxide (DMSO) (vehicles for dissolving cannabinoid ligands).
9. Cannabinoid ligands (BioMol Research Laboratories, Plymouth Meeting, PA; Tocris Cookson, Inc., Ellisville, MO; Cayman Chemical Co., Ann Arbor, MI).
10. Scintillation fluid (ScintiSafe Econo 1, Fisher Scientific).
11. Whatmann GF/B glass fiber filters.
12. Scintillation vials.
13. Phenylmethylsulfonyl fluoride (PMSF) and *n*-butanol for endocannabinoids.
14. Saponin solution (140 mM potassium glutamate-HCl, pH 6.8, with 1 mg/mL ATP and 0.1 mg/mL saponin) for the intact cell-binding assay.

3. Methods

The methods describe preparation of membranes from central nervous system (CNS) tissue or cultured cells, radioligand binding to cell membrane homogenates, agonist-stimulated [^{35}S]GTP γ S binding to cell membrane homogenates, and agonist-stimulated [^{35}S]GTP γ S binding to intact cultured cells.

3.1. Preparation of Cell Membrane Homogenates

The membrane homogenate preparation procedure isolates cell membranes and membrane-associated macromolecules and assures their homogeneity for assaying small fractions of the preparation in each of many test tubes. It removes the majority of soluble macromolecules, small molecules (including endogenous receptor ligands), and minerals via multiple centrifugation steps each followed by resuspension in fresh buffer containing the divalent ion chelator ethylenediamine tetraacetic acid (EDTA). Some prefer a P2 preparation, which involves discarding an initial pellet generated by a low-speed centrifugation step, but this appears to be unnecessary for these assays.

In the case that the membranes will be assayed for agonist-stimulated [^{35}S]GTP γ S binding, a preincubation step to remove endogenous adenosine is useful. It has been noted that a significant quantity of endogenous adenosine remains in membrane preparations of brain tissue, which causes elevation of basal [^{35}S]GTP γ S binding, thereby reducing the signal-to-noise ratio for agonist-stimulated [^{35}S]GTP γ S binding for other agonists. To eliminate this complication, membranes can be routinely pretreated with adenosine deaminase to remove this adenosine and its accompanying activity. A stock of adenosine deaminase of 1–2 U/mL can be kept in 1 mg/mL BSA at -4°C for months at a time.

For either agonist-stimulated [^{35}S]GTP γ S binding or receptor binding when endocannabinoids, like 2-arachidonyl glycerol (2-AG) or anandamide, are to be assayed, pretreatment of the membranes with phenylmethylsulfonyl fluoride (PMSF) is advisable. PMSF irreversibly inhibits amidase enzymes, including fatty acid amide hydrolase (FAAH), the enzyme that degrades endocannabinoids. This treatment has been shown to greatly increase the potency of endocannabinoids in such assays. A stock solution of PMSF is prepared immediately before use at 100 mM in *n*-butanol.

Specific CNS regions of interest or whole brain and/or spinal cord are dissected from freshly sacrificed animals on ice. The preparation can be handled in one of two ways: tissue can be frozen at -80°C at this point until the day it is to be assayed, or membrane homogenates may be prepared prior to freezing and the homogenate separated into aliquots and frozen until the day they are to be assayed (*see Note 1*). To prepare membrane homogenates from cultured cells, cell media is replaced with cold membrane buffer (50 mM Tris, pH 7.4, 3.0 mM MgCl_2 , 0.2 mM EGTA), and the cells are scraped or triturated from their growing surface and transferred to centrifuge tubes. In any case (whether preparing tissue or cultured cells and whether the tissue is prepared immediately after dissection or after frozen storage), each sample is placed in a centrifuge tube with 3–15 mL of cold membrane buffer. Samples are kept on ice or in the refrigerated centrifuge throughout the membrane preparation procedure.

3.1.1. Membrane Homogenization Procedure

1. Pulverize each sample with an electric tissue grinder for 30 s until homogeneous. As an alternative to the electric grinder, a ground glass homogenizer can be used and is especially useful for very small samples, since a small but significant amount of tissue is lost each time the electric grinder is used.
2. Centrifuge samples at 40,000*g* for 10 min at 4°C.
3. Discard the supernatant, then resuspend the pellet with the tissue grinder for 10 s in 3–15 mL of cold membrane buffer.
4. Centrifuge and resuspend the pellet again as before.
5. Repeat **Steps 2 and 3**. If endocannabinoids are being assayed, the membrane homogenate should be treated by adding PMSF to a final concentration of 50 μM and thoroughly mixing (*see above*). No additional incubation should be necessary, so the homogenate can undergo the final centrifugation (same conditions as before) almost immediately.
6. The final resuspension should be in a volume calculated to give an appropriate protein concentration; approx 100 mg of membrane protein is obtained for every gram of brain tissue prepared. After the final resuspension, a sample of the homogenate is taken for determination of protein content by Bradford or Lowry assays.
7. If the sample was not frozen prior to membrane preparation, it may now be separated into aliquots for storage at -80°C . On the day of the binding assay, thawed aliquots are resuspended with the tissue grinder for 10 s in the desired amount of buffer and the protein content determined.
8. If the membranes are to be assayed for [^{35}S]GTP γ S binding, add adenosine deaminase from a stock solution to give a final concentration of 0.004 U/mL, and incubate the membranes for 10 min at 30°C.
9. The membrane homogenate is now ready to be added to a binding assay.

3.2. Cannabinoid CB $_1$ Receptor Radioligand Binding

Cannabinoid receptor ligands are generally highly lipophilic, and the concentrations that can be used are limited by this fact (*see also Notes 2 and 3*). A sample saturation assay of the commonly used CB $_1$ -selective antagonist SR141716A is illustrated in **Fig. 1**. The figure shows how concentrations of this ligand above 5 nM result in more nonspecific binding than specific binding, and thus rarely yield usable results. This is true even in rat cortex membranes where CB $_1$ is expressed at very high levels (compared to other GPCRs in brain); in this assay, the B_{max} of [^3H]SR141716A binding was around 5 pmol/mg. The ratio of specific to nonspecific binding can be improved by increasing the amount of membrane protein in the assay, but doing so also increases the chances of ligand depletion; in fact, in the assay shown in **Fig. 1**, more than 10% of total ligand was bound at the four lowest concentrations. Decreasing the amount of protein to avoid this complication will limit the useful maximum concentration of ligand further.

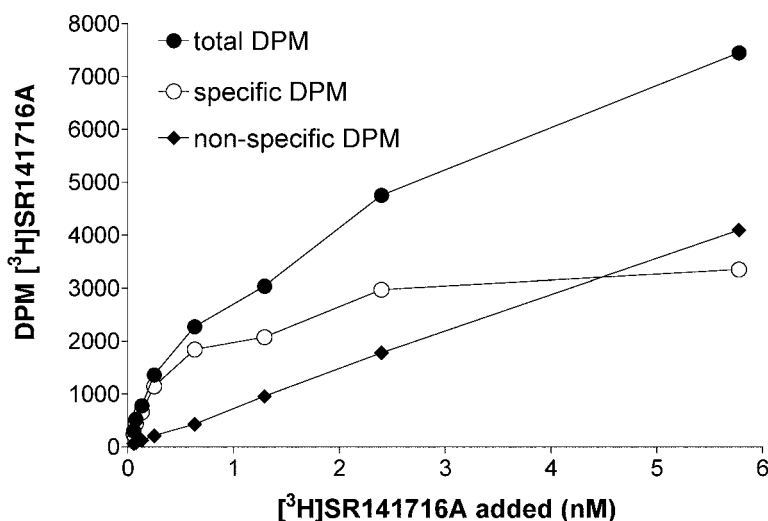


Fig. 1. Saturation binding of a cannabinoid receptor ligand to brain membranes. Shown are the results of a typical saturation assay of [³H]SR141716A (a CB₁-selective antagonist) in rat cortex membranes. Various concentrations (0.05–5.5 nM) of radioligand were incubated in assay buffer with 0.1% BSA and rat cortex membrane homogenates (20 µg/tube) for 1 h at 30°C in the absence (total DPM) and presence (nonspecific DPM) of 5 µM unlabeled SR141716A. Specific DPM and nonspecific DPM shown are the mean of three values measured in consecutive assay tubes in the same rack. Specific DPM were calculated by subtracting mean nonspecific DPM from mean total DPM at each concentration of [³H]SR141716A.

3.2.1. Receptor Binding Procedure

1. Tris buffer (50 mM Tris-HCl, pH 7.4) with 0.2% (w/v) BSA is added to test tubes on ice. To duplicate the conditions of the [³⁵S]GTPγS binding assay, assay buffer (50 mM Tris, pH 7.4, 3 mM MgCl₂, 0.2 mM EGTA, 100 mM NaCl) with the same concentration of GDP and GTPγS as used in the [³⁵S]GTPγS-binding assay could be used with antagonist radioligands. This does not work very well with agonist radioligands, since NaCl and GTPγS decrease specific binding of GPCR agonists.
2. Unlabeled cannabinoid ligands (for nonspecific binding) are added to the assay tubes. Nonspecific binding is determined in the presence of unlabeled ligand approx 1000-fold higher than that of the labeled ligand (usually 1 µM; *see Note 2*).
3. Membrane homogenates (prepared as above) from CNS tissues (10–50 µg/tube) or cultured cells expressing cannabinoid receptors (5–100 µg/tube, depending on the level of expression) are added to the assay tubes.
4. Add approx 0.01–5 nM cannabinoid receptor radioligand (*see Notes 2 and 3*) for a final volume of 1.0 mL.
5. Initiate the assay by incubating (typically in a temperature-controlled, shaking water bath) for 1–2 h at 30°C, depending on the ligand.

6. Terminate by rapid filtration onto Whatmann GF/B glass fiber filters that have been soaked for at least 1 h in 50mM Tris-HCl, pH 7.4, containing 0.5% BSA. Filters are then rinsed seven times with approx 3 mL/tube Tris-HCl, pH 7.4, containing 0.05% BSA.
7. Place filters in scintillation vials with several milliliters of scintillation fluid, and allow the samples to extract into the scintillation fluid overnight (or shake for 1 h).
8. Determine radioactivity by liquid scintillation spectrophotometry.

Each condition in this assay is repeated in triplicate. Mean values \pm SD are calculated for each triplicate, and triplicates for which the SD is greater than 10% of the mean are inspected for values that are outliers.

3.3. Agonist-Stimulated [^{35}S]GTP γ S Binding to Cell Membrane Homogenates

When performing these assays in a new tissue for the first time, it is helpful to first perform an assay to optimize assay conditions by determining nonspecific, basal, and agonist-stimulated (using a maximally effective concentration of agonist) with different amounts of membrane protein (*see Fig. 2*). Typically, using brain homogenates, 3–20 μg of membrane protein per test tube yields good results. With cultured cells, the amount of protein required depends on the receptor expression level and, perhaps more importantly, the G protein expression level, which is often not as high as in brain, where the amount of G $_o$ -type G protein is estimated to make up nearly 1% of total brain protein. Experience has shown that even in a cell line in which cannabinoid inhibition of adenylyl cyclase has been observed, there may be no significant activity of cannabinoids for [^{35}S]GTP γ S binding. In tissues in which cannabinoid-stimulated [^{35}S]GTP γ S is observed (including brain tissue), the percent stimulation by agonist increases with decreasing protein (up to a point), but specific binding and total disintegrations per minute (DPM) decreases (*see Fig. 2*). A protein concentration that yields approx 1000–2000 DPM of basal [^{35}S]GTP γ S binding has been found to work well (using 0.05–0.1 nM [^{35}S]GTP γ S).

Next, using the previously determined protein concentration, the optimal concentration of GDP is determined by assaying the amount of basal and agonist-stimulated [^{35}S]GTP γ S binding using a maximally effective concentration of agonist (*see Fig. 3*). In this assay, nonspecific binding need only be determined once, including the highest concentration of GDP and 30 μM unlabeled GTP γ S. Concentrations of GDP from 0.1 to 300 μM typically give a full range of effects. Generally, total and specific DPM decrease with increasing GDP, but percent stimulation increases up to approx 100 μM , where specific DPM are quite low. Ten to fifty μM GDP appears to give the best results (*see Fig. 3*).

Finally, using the optimal concentrations of membrane protein and GDP, a time-course could be performed to determine optimal incubation time. At each time point, nonspecific, basal, and agonist-stimulated binding should be determined.

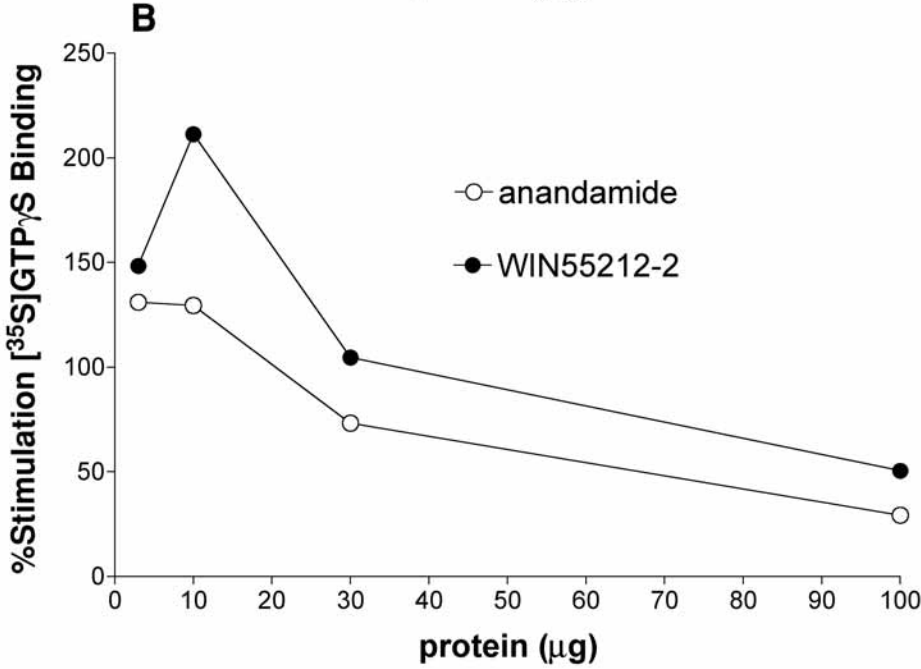
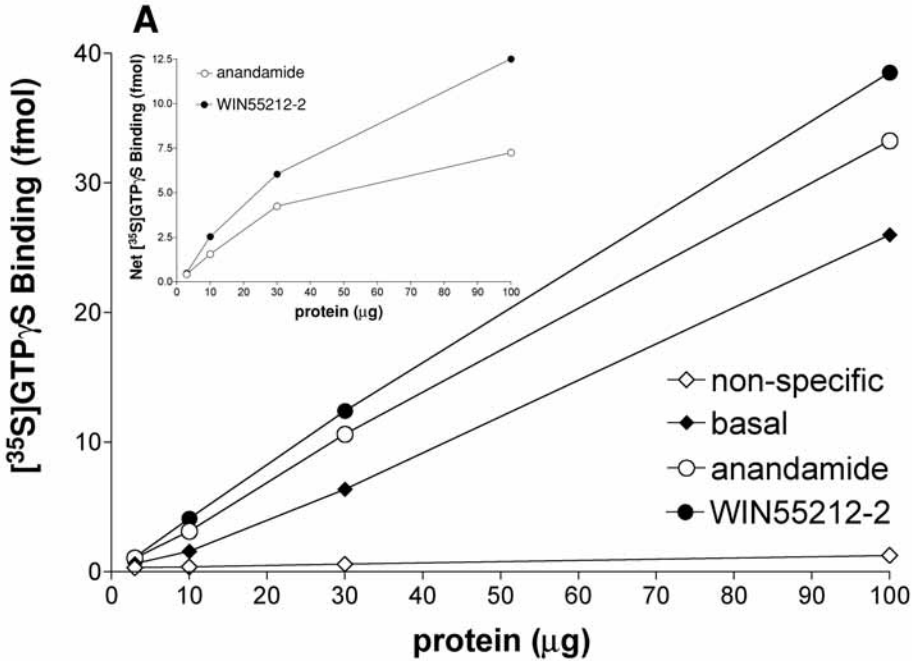


Fig. 2. Effect of protein content on [^{35}S]GTP γ S binding to brain membranes. The figure shows an assay typical of varying amounts of membrane protein. In particular, non-specific, basal, anandamide-stimulated, and WIN55,212-2-stimulated [^{35}S]GTP γ S binding to whole mouse brain membranes is depicted. Membranes were incubated in assay buffer with 0.1% BSA for 1 h at 30°C. Values shown are the mean of three values measured in consecutive assay tubes in the same rack. Nonspecific binding was determined in the presence of 25 μM unlabeled GTP γ S, basal in the absence of GTP γ S or agonists, and anandamide and WIN55,212-2 with 30 μM and 10 μM of these agonists, respectively (**A**). Net binding (**A**, inset) was calculated by subtracting mean basal values from mean values obtained in the presence of anandamide or WIN55,212-2 at each amount of protein. Percent stimulation (**B**) was determined by dividing net binding values by basal binding values obtained at each amount of protein. Notice that though overall and net-agonist-stimulated binding increase with increasing protein, due to the concurrent increase in basal binding, percent stimulation (i.e., the signal-to-noise ratio) is optimal at lower amounts of membrane protein.

Incubations are typically 1 or 2 h. Using brain tissue and cannabinoid agonist, it was found that increasing incubation time from 1 to 2 h increased both basal and total binding somewhat, decreasing percent stimulation to a degree, but at 2 h the assay was at a steady state, where there was little further increase in binding beyond that time (**14**). Times between 0.5 and 4 h give a full range of effects in brain tissue (from very little specific binding to a steady-state condition).

3.3.1. [^{35}S]GTP γ S Membrane Binding Procedure

1. Assay buffer: 50 mM Tris-HCl, pH 7.4, 3 mM MgCl_2 , 0.2 mM EGTA, 100 mM NaCl with 0.1% (w/v) BSA is added to test tubes on ice.
2. GDP is added to all test tubes (*see Note 4*).
3. GTP γ S is added to triplicate(s) of nonspecific binding (*see Note 4*).
4. Cannabinoid ligands are added to the assay tubes (*see Note 2*).
5. Membrane homogenate is added to the test tubes: from CNS tissues (5–10 $\mu\text{g}/\text{tube}$) or cultured cells expressing cannabinoid receptors (3–50 $\mu\text{g}/\text{tube}$, depending on the level of expression).
6. Add 0.05–0.2 nM [^{35}S]GTP γ S (*see Note 4*) for a final volume of 0.2–1.0 mL.
7. Initiate the assay by transferring to a temperature-controlled, shaking water bath at 30°C; incubate for 1–2 h.
8. Assays are terminated by rapid filtration onto Whatmann GF/B glass fiber filters, followed by three rinses with 50 mM cold Tris-HCl, pH 7.4.
9. Filters are placed in scintillation vials with several milliliters of scintillation fluid and are allowed to remain so overnight (or for 1 h of vigorous shaking); either will allow extraction of the sample into the scintillation fluid.
10. Determine the amount of binding by liquid scintillation spectrophotometry at 95% efficiency for ^{35}S .

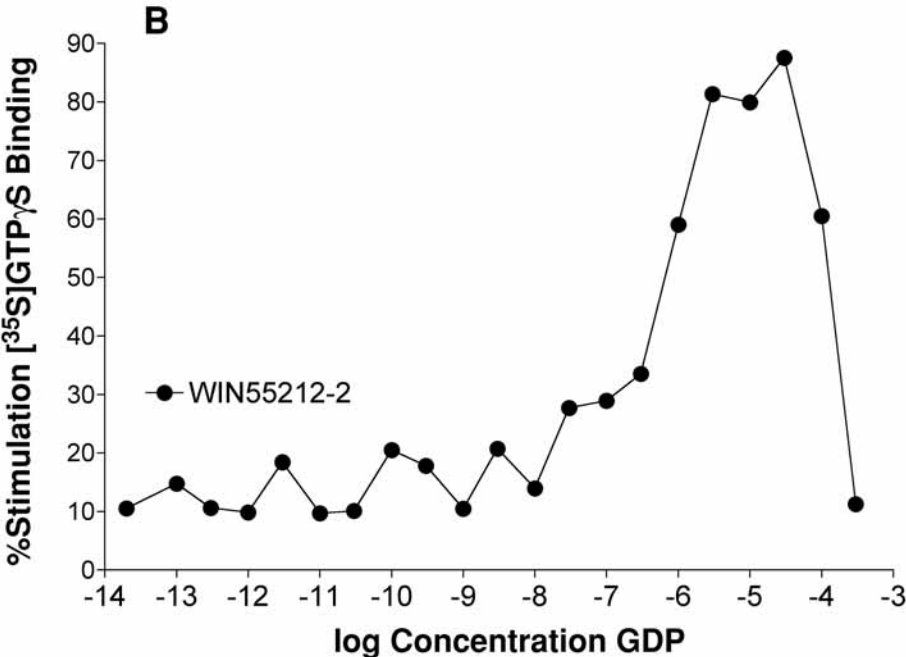
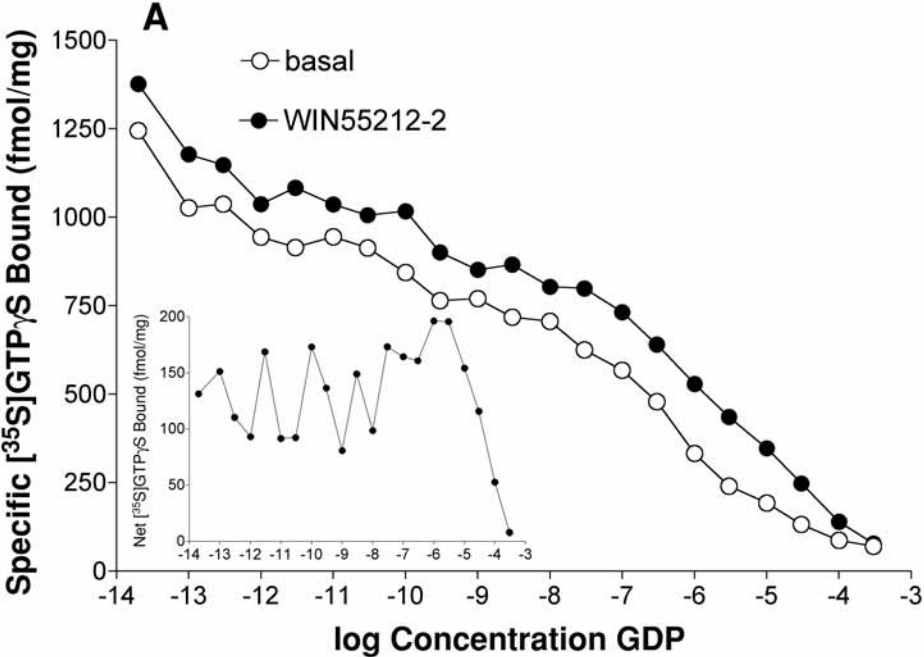


Fig. 3. Effect of GDP concentration on [^{35}S]GTP γ S binding to brain membranes. The figure shows an assay typical of varying amounts of GDP. In particular, basal and WIN55,212-2-stimulated [^{35}S]GTP γ S binding to rat cerebellar membranes is depicted. Membranes were incubated in assay buffer with 0.1% BSA for 1 h at 30°C. Values shown are the mean of three values measured in consecutive assay tubes in the same rack. Binding was determined in the absence (basal) and presence of 30 μM WIN55,212-2 (A). Net binding (A, inset) was calculated by subtracting mean basal values from mean values obtained in the presence of WIN55,212-2 at each concentration of GDP. Percent stimulation (B) was determined by dividing net binding values by basal binding values obtained at each concentration of GDP. While basal and agonist-stimulated binding decrease with increasing GDP (A), net agonist-stimulated binding (A, inset) and percent stimulation (B) do not change much at GDP concentrations below 10^{-6} M (1 μM). Above 1 μM GDP, net agonist-stimulated binding decreases sharply, but is accompanied by a more rapid decrease in basal binding, leading to optimal percent stimulation values. Above 10^{-4} M (100 μM), binding values are too low and the difference between agonist-stimulated and basal values are too small to yield usable results.

3.3.2. Data Analysis

Each condition in the assay is repeated in triplicate. Basal [^{35}S]GTP γ S binding is determined in the absence of receptor ligands, and nonspecific binding is determined in the absence of receptor ligands and the presence of 10 μM unlabeled GTP γ S. Mean values \pm SD are calculated for each triplicate, and triplicates for which the SD is greater than 10% of the mean are inspected for values that are outliers. The mean value obtained for nonspecific binding in each assay is subtracted from every other mean value to obtain specific binding values, which are used for all further calculations. Net-agonist-stimulated binding is calculated by subtracting basal values from each value obtained in the presence of ligand. Percent stimulation by agonist is calculated by dividing each net-agonist-stimulated value by the basal value. Concentration-effect is determined by nonlinear regression using an appropriate model in Prism (GraphPad Software, San Diego, CA) to determine EC_{50} (the concentration producing half-maximal effect) and E_{max} (the theoretical maximal value obtained with each ligand) values for each agonist in each assay.

3.4. [^{35}S]GTP γ S Binding to Intact Cultured Cells

[^{35}S]GTP γ S binding to whole intact cultured cells is a new technique, only recently published (13). The method was made possible by using saponin to permeabilize the cells prior to the binding assay; thus the term “intact” is used rather than “live,” since the cells may no longer be viable even though the cells that remained following saponin treatment were clearly intact (as determined

by microscopic examination). In the cultured rat cerebellar granule cells that were used to develop this assay, agonist stimulation of [^{35}S]GTP γ S binding to the intact cells was similar to that observed in membrane homogenates prepared from the cultured cells. However, binding to the intact cells exhibited decreased [^{35}S]GTP γ S binding in response to the antagonist, SR141716A, which was apparently due to antagonism of endogenous cannabinoid ligand activity. In homogenized cell membranes, SR141716A exhibited only antagonist activity. Thus, taken together with several other lines of evidence, it appeared that the intact cell [^{35}S]GTP γ S-binding assay is useful for investigating the endogenous signaling system.

3.4.1. [^{35}S]GTP γ S Cell Binding Procedure

1. Rinse adherent cultured cells twice for 5 min at 37°C with 0.5 mL/well assay buffer.
2. Incubate cells for 2 min at room temperature in 0.5 mL/well saponin solution (140 mM potassium glutamate-HCl, pH 6.8, with 1 mg/mL ATP and 0.1 mg/mL saponin) to permeabilize the cell membranes. Optionally, 50 μM PMSF can be added to the saponin solution to irreversibly inhibit amidase enzymes if endocannabinoids are to be added or their endogenous activity is to be studied.
3. Rinse cells again two times with assay buffer.
4. Preincubate cells in assay buffer for 10 min at 37°C with 100 μM GDP and 0.004 units/mL adenosine deaminase (220 U/mg protein, Sigma Chemical Co.) in the presence and absence of the ligand(s) of interest.
5. Initiate the binding assay by adding 0.1 nM [^{35}S]GTP γ S and incubate for 1 h.
7. Terminate the assay by triturating or scraping the cells from the culture wells and transferring the cells and buffer to glass test tubes on ice. Each well should be rinsed with a few milliliters of cold buffer, which are added to the respective test tubes.
8. Mix test tubes thoroughly, then transfer a fraction of each sample to another set of test tubes to be assayed for protein content by the Bradford or Lowry assays. The fraction of the total sample must be adequate to obtain good results with the protein assay.
9. Filter the samples under vacuum through Whatman GF/B glass fiber filters.
10. Rinse each test tube three times with approx 3 mL cold 50 mM Tris-HCl, pH 7.4, each rinse should be used to wash the filter.
11. Transfer each filter to a scintillation vial and add several milliliters of scintillation fluid.
12. Allow the samples to extract overnight in the scintillation fluid (or for 1 h with vigorous shaking).
13. Determine bound radioactivity by liquid scintillation spectrophotometry.

3.4.2. Data Analysis

Nonspecific binding is determined in the absence of ligands and the presence of 10 μM unlabeled GTP γ S. Normalize all data to the amount of protein recovered from each well prior to other calculations (which are the same as above for binding to membrane homogenates).

4. Notes

1. For cases where the same tissue preparation may be assayed multiple times, several like tissues (i.e., the cerebellum from several animals) may be combined and homogenized together prior to freezing the tissue for storage. In cases where each piece of tissue will be assayed only once or the number of samples to be taken is too large to be able to prepare in a reasonable amount of time, each piece of tissue must be frozen separately and prepared on the day it is to be assayed. In either case, for agonist-stimulated [^{35}S]GTP γ S binding, the tissue may be frozen only once before or after making a membrane preparation; multiple freezing and thawing destroys the activity.
2. Cannabinoid ligands must be dissolved in an organic solvent prior to addition to any aqueous solutions, and all aqueous solutions of cannabinoid ligands (radio-labeled or unlabeled) should contain at least 1 mg/mL BSA. For the most part ethanol can be used to dissolve ligands at 10–100 mM to keep the highest concentration of ethanol in the assay at or below 0.1%. High-affinity/high-potency ligands, such as CP55940 and HU-210, that are maximally effective at 1 μM can be dissolved at 1–10 mM. Lower-affinity/low-potency ligands such as methanandamide or WIN55,212-2, which are maximally effective at 30–100 μM , should be dissolved at 30–100 mM. Note also that WIN55,212-2 mesylate is not adequately soluble in ethanol and should be dissolved in DMSO. All dissolved ligands can be stored at -20°C , but DMSO freezes even in the refrigerator, so only small quantities of ligands in DMSO should be made or it should be separated into aliquots to avoid excessive freezing and thawing of the drug. Also, when making aqueous solutions it is best to avoid concentrations of cannabinoid ligands $>20 \mu\text{M}$, when possible, as solutions over this concentration will be cloudy. To accomplish this, one can make the ligand solution one half of the total assay volume, so that the concentration of cannabinoid ligand in aqueous solution is never over twice the desired final concentration. Remember that any aqueous solution used to dissolve cannabinoid ligands must contain at least 1 mg/mL BSA.
3. The concentration of radiolabeled cannabinoid ligand that can be used is severely limited by lipophilicity. Concentrations above approx 2–5 nM (depending on the ligand) display much more nonspecific binding than specific binding, and values obtained at such concentrations are usually unusable (see Fig. 1).
4. GDP and GTP γ S are rather unstable and should be stored at -80°C both in powder form and in solution. Radiolabeled [^{35}S]GTP γ S is thawed and diluted 20 times with ddH $_2\text{O}$ before the first use and separated into aliquots of approx 3 μCi each, or enough for an assay of 50 test tubes with a final volume of 0.5 mL at 0.1 nM with a comfortable excess. Unlabeled GTP γ S is made up at 6 mM in ddH $_2\text{O}$ and stored in 25- μL aliquots; after 975 μL of assay buffer is added, this is sufficient for 10 test tubes of 100 μL each (30 μM final concentration). GDP is made up at 20 mM in ddH $_2\text{O}$ and stored in aliquots of 45 μL , enough for 60 test tubes at 30 μM final concentration after dilution with 2.955 mL of assay buffer.

References

1. Howlett, A. C., and Fleming, R. M. (1984) Cannabinoid inhibition of adenylate cyclase: Pharmacology of the response in neuroblastoma cell membranes. *Mol. Pharmacol.* **26**, 532–538.

2. Devane, W. A., Dysarz, F. A. I., Johnson, M. R., Melvin, L. S., and Howlett, A. C. (1988) Determination and characterization of a cannabinoid receptor in rat brain. *Mol. Pharmacol.* **34**, 605–613.
3. Matsuda, L. A., Lolait, S. J., Brownstein, M. J., Young, A. L., and Bonner, T. I. (1990) Structure of a cannabinoid receptor and functional expression of the cloned cDNA. *Nature* **346**, 561–564.
4. Munro, S., Thomas, K. L., and Abu-Shaar, M. (1993) Molecular characterization of a peripheral receptor for cannabinoids. *Nature* **365**, 61–65.
5. Di Marzo, V., Breivogel, C. S., Tao, Q., Bridgen, D. T., Razdan, R. K., Zimmer, A. M., Zimmer, A., and Martin, B. R. (2000) Evidence of non-CB₁, non-CB₂ receptor-mediated actions of anandamide in mouse brain: Levels, metabolism and pharmacological activity of anandamide in CB1 receptor knock-out mice. *J. Neurochem.* **75**, 2434–2444.
6. Breivogel, C. S., Griffin, G., Di Marzo, V., and Martin, B. R. (2001) Evidence for a new G protein-coupled cannabinoid receptor in mouse brain. *Mol. Pharmacol.* **60**, 155–163.
7. Hajos, N., Ledent, C., and Freund, T. F. (2001) Novel cannabinoid-sensitive receptor mediates inhibition of glutamatergic synaptic transmission in the hippocampus. *Neuroscience* **106**, 1–4.
8. Asano, T., Pedersen, S. E., Scott, C. W., and Ross, E. M. (1984) Reconstitution of catecholamine-stimulated binding of guanosine 5'-O-(3-thiotriphosphate) to the stimulatory GTP-binding protein of adenylate cyclase. *Biochemistry* **23**, 5460–5467.
9. Lorenzen, A., Fuss, M., Vogt, H., and Schwabe, U. (1993) Measurement of guanine nucleotide-binding protein activation by A1 adenosine receptor agonists in bovine brain membranes: stimulation of guanosine-5'-O-(3-[³⁵S]thio)triphosphate binding. *Mol. Pharmacol.* **44**, 115–123.
10. Traynor, J. R., and Nahorski, S. R. (1995) Modulation by μ -opioid agonists of guanosine-5'-O-(3-[³⁵S]thio)triphosphate binding to membranes from human neuroblastoma SH-SY5Y cells. *Mol. Pharmacol.* **47**, 848–854.
11. Breivogel, C. S., Selley, D. E., and Childers, S. R. (1997) Acute and chronic effects of opioids on delta and mu receptor activation of G-proteins in NG108-15 and SK-N-SH cell membranes. *J. Neurochem.* **68**, 1462–1472.
12. Selley, D. E., Stark, S., Sim, L. J., and Childers, S. R. (1996) Cannabinoid receptor stimulation of guanosine-5'-O-(3-[³⁵S]thio)triphosphate binding in rat brain membranes. *Life Sci.* **59**, 659–668.
13. Breivogel, C. S., Walker, J. M., Huang, S. M., Roy, M. B., and Childers, S. R. (2004) Cannabinoid signaling in rat cerebellar granule cells: G-protein activation, inhibition of glutamate release and endogenous cannabinoids. *Neuropharmacology* **47**, 81–91.
14. Breivogel, C. S., Selley, D. E., and Childers, S. R. (1998) Cannabinoid receptor agonist efficacy for stimulating [³⁵S]GTP γ S binding to rat cerebellar membranes correlates with agonist-induced decreases in GDP affinity. *J. Biol. Chem.* **273**, 16865–16873.

Methods to Assay Anandamide Hydrolysis and Transport in Synaptosomes

Filomena Fezza, Natalia Battista, Monica Bari, and Mauro Maccarrone

Summary

Anandamide (AEA) is the most studied member of a new class of lipid mediators, collectively called endocannabinoids. The biological activity of AEA at cannabinoid and noncannabinoid receptors depends on its life span in the extracellular space, which is regulated by a rapid cellular uptake, followed by intracellular degradation by the enzyme AEA hydrolase (fatty acid amide hydrolase). Here, we present the methodological details of the procedures that we have developed to assay fatty acid amide hydrolase activity and to characterize AEA transport through cell membranes in a new ideal *ex vivo* system like brain synaptosomes.

Key Words: Anandamide; brain; fatty acid amide hydrolase; synaptosomes; uptake.

1. Introduction

The discovery of anandamide (arachidonoyl ethanolamide, AEA) and of its manifold roles in the central nervous system and in the periphery (reviewed in **refs. 1** and **2**) prompted several researchers to develop analytical methods to assay and characterize the activity of the enzymes responsible for AEA metabolism in various cells and tissues. Fatty acid amide hydrolase (arachidonoyl ethanolamide amidohydrolase, EC 3.5.1.4; FAAH) has emerged as the key AEA hydrolase, showing a molecular mass of approx 64 kDa and an optimum pH of around 9.0 (**3**). Recently, FAAH has been crystallized, and its three dimensional structure has been determined at 2.8Å resolution (**4**). This enzyme cleaves the amide bond and releases arachidonic acid and ethanolamine. High-performance liquid chromatography (HPLC) is the most widely used method to determine FAAH activity from different sources. We developed a new method (**5**) based on reversed-phase (RP)-HPLC and on-line scintillation counting, which combines the need for high resolution, reproducibility, and sensitivity

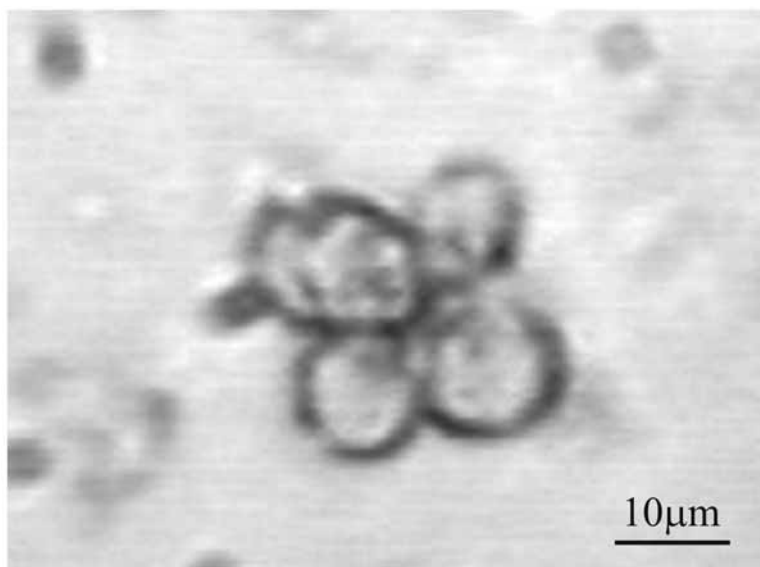


Fig. 1. Synaptosomes from mouse brain. Synaptosomes were prepared from freshly isolated mouse brain, and were photographed at a magnification of 100 \times . The bar corresponds to 10 μ m.

with the convenience of a handy and fast manipulation of several samples at once. Overall, this method allows both significant time and reagent saving, and overcomes the sensitivity problems implied by a direct ultraviolet (UV) detection. Moreover, our procedure is suitable to detect FAAH activity in minute cerebral tissues ([Table 1](#)) or in samples available in tiny amounts or with a very low enzymatic activity. On the other hand, the cellular uptake of AEA seems to be mediated by a specific AEA membrane transporter (AMT), which works according to a saturable, selective, and temperature-dependent mechanism. The molecular properties of AMT are still elusive, and even the existence of a transporter has been questioned ([6](#)). However, AMT activity has been demonstrated in a variety of *in vitro* systems ([7](#)) as well as in *ex vivo* systems like cortical areas and striatum of rats ([8](#)). Recently, we isolated synaptosomes ([9](#)) from human, mouse ([Fig. 1](#)), and rat brain and were able to show that this system is suitable to investigate presence and activity of AMT *ex vivo* ([10](#)). The results of AMT activity in synaptosomes isolated from different areas of mouse brain are reported in [Table 1](#).

2. Materials

1. Buffer 1: 50 mM Tris-HCl, 1 mM ethylenediamine tetraacetic acid (EDTA) at pH 7.4.

Table 1
Anandamide Hydrolysis by FAAH and Uptake by AMT in Synaptosomes From Different Areas of Mouse Brain

Area of mouse brain	FAAH activity ^a	AMT activity ^a
Cerebellum	1020 ± 215	82 ± 8
Cortex	950 ± 203	93 ± 12
Hippocampus	1660 ± 209	100 ± 10
Striatum	832 ± 195	20 ± 15

^aExpressed as pmol/min/mg protein.

2. Buffer 2: 50 mM Tris-HCl at pH 9.0.
3. Buffer A (extraction): 0.32 M sucrose, 5 mM Tris-HCl at pH 7.4 and ice-cold. It is important to make it fresh as required.
4. Buffer B (resuspension): 136 mM NaCl, 5 mM KCl, 0.16 mM CaCl₂, 0.1 mM ethylene glycol tetraacetic acid (EGTA), 1.3 mM MgCl₂, 10 mM glucose, 10 mM Tris-HCl, at pH 7.4 and ice-cold. It is important to make it fresh as required.
5. Phosphate-buffered saline.
6. Bovine serum albumin.
7. Sigma FluorTM high-performance liquid scintillation counter (LSC) cocktail for non-aqueous solution.
8. [³H]AEA (205 Ci/mmol; Perkin Elmer Life Sciences, Inc., Boston, MA).
9. Teflon-glass homogenizer.
10. UltraTurrax T 25.
11. DNA MINI speedvac.
12. Radio-HPLC instrument (*see Note 1*).
13. Liquid scintillation β -counter.

3. Methods

3.1. Radiochromatographic Assay of FAAH Activity

This radiochromatographic method, joining the resolution and reproducibility of HPLC with the sensitivity of scintillation counting, allows the detection of FAAH at the femtomolar level in specimens available not only in large amounts, but also in small quantities, such as brain areas or primary cells in culture. The method involves the procedure for both extraction of the proteins from samples and enzyme assay, performed by measuring the release of [³H]arachidonic acid from [³H]anandamide.

3.1.1. Preparation of Tissue and Cellular Samples

1. Homogenize fresh tissue or cells in buffer 1 (weight/volume ratio = 1:10 for tissues and 30 × 10⁶ cells/ mL for cells) with UltraTurrax T 25 (*see Note 2*).

2. Centrifuge the homogenate at 11000g at 4°C for 20 min.
3. Resuspend the final pellet, containing most of FAAH activity, in ice-cold buffer 1 at a protein concentration of 1 mg/mL and store at -80°C for no longer than 1 wk.

3.1.2. FAAH Activity Assay

1. In 2-mL Eppendorf tube, add [³H]AEA (at the final concentration of 5 μM) to a total volume of 200 μL buffer 2 and initiate the reaction by the addition of 20 μg of tissue or cell homogenates.
2. Incubate for 15 min at 37°C. The pH of the solution should remain at a value of 9.0.
3. Stop the reaction by the addition of 800 μL ice-cold methanol/chloroform (2:1, v/v) and vortex the mixture.
4. Incubate at room temperature for 30 min and then add 240 μL chloroform and 240 μL water, with vortexing.
5. After 10 min at room temperature, centrifuge the mixture at 3000g for 5 min.
6. The upper aqueous layer is removed by suction (*see Note 3*), and the lower organic phase is dried by spinning in a DNA MINI speedvac (*see Note 4*) at 100 mbar and 30°C for 30 min.
7. Dissolve the dried lipids into 50 μL methanol.
8. This sample is directly used for analysis by RP-HPLC.

3.2. Anandamide Uptake Assay

This procedure describes how to prepare synaptosomes from freshly isolated human, mouse, and rat brain and how to determine the activity of anandamide membrane transporter (AMT) in this ex vivo model.

3.2.1. Preparation of Synaptosomes

1. Resuspend fresh tissues in buffer A (weight/volume ratio = 1:20) and gently disrupt by 10 up-and-down strokes in a Teflon-glass homogenizer.
2. Centrifuge the homogenate at 1000g for 5 min at 4°C.
3. Take the supernatant and then centrifuge again at 17,000g for 15 min at 4°C.
4. Resuspend the final pellet in buffer B at a protein concentration of 3 mg/mL using the Bradford's colorimetric assay.

3.2.2. Determination of Anandamide Uptake

1. For each assay, incubate 100 μL of synaptosomes, equivalent to 300 μg of protein, with 300 nM [³H]AEA for different time intervals at 37°C or 4°C to discriminate carrier-mediated from non-carrier-mediated transport of AEA through cell membranes. Alternatively, to determine the kinetic constants of AMT, incubate for 15 min with different concentrations of [³H]AEA, in the range 0–1000 nM (in this case the uptake at 4°C has to be subtracted from that at 37°C).
2. Centrifuge at 10000g for 5 min and discard the supernatant by suction.

3. Resuspend the pellet in 1 mL of PBS containing 1% bovine serum albumin and centrifuge again at 10000g.
4. Discard the supernatant and wash the pellet in 1 mL of PBS.
5. Repellet by centrifugation as in **step 3**.
6. Discard the supernatant and, finally, resuspend the pellet in 0.5 mL of methanol.
7. Transfer to a scintillation counter vial and add 4.5 mL of liquid scintillation cocktail.
8. Cap the vials and mix the content of each vial thoroughly.
9. Determine the radioactivity by counting in a liquid scintillation β -counter for 5 min.

4. Notes

1. The HPLC equipment is a Perkin-Elmer Nelson Model 1022 Plus Chromatograph, connected to a Perkin-Elmer series 200 LC Pump, a LC295 UV/VIS detector, a 7125 BIO injector with a 20- μ L loop, and a Canberra Packard Flow Scintillation Analyzer 500 TR Series, with a 0.5-mL flow cell. The system is interfaced with a Compaq Prolinea 5100 computer, using a Canberra Packard FLO-ONE software for system control and data processing. The RP-HPLC columns are Pecosphere C₁₈, 5 μ m, 30 \times 3 mm i.d. (SGE Inc.), with a 5- μ m C18 guard column (SGE Inc.). Mobile phase is a mixture of methanol:water:acetic acid (85:15:0.1), and the elution of metabolites is done at a constant flow rate of 0.8 mL/min. Absorbance values are measured at 204 nm. Liquid scintillation cocktail (Ultima Flo M, Canberra Packard) is mixed with the eluent at a 1:2 (eluent/LSC) ratio. Retention times of AEA and arachidonic acid (AA) are 3.2 and 4.5 min, respectively. The concentration of AA is calculated from radioactivity of peak area, and FAAH specific activity is expressed as pmol AA released/min/mg protein.
2. An alternative procedure to prepare the cellular homogenates include treatment with a Vibracell sonifier, where samples are sonicated on ice three times for 10 s, with 10-s intervals.
3. It has been observed that to optimize the final result, the organic phase should be withdrawn by means of a Gilson pipet and transferred into an Eppendorf tube. In this way you can be sure to take the same volume from each sample, thus ensuring the highest reproducibility.
4. If a DNA MINI speedvac is not available, you can still remove the organic solvent under a nitrogen stream, keeping your samples on ice throughout the procedure.

Acknowledgments

This study was partly supported by Istituto Superiore di Sanità (III AIDS project) and by Ministero dell'Istruzione, dell'Università e della Ricerca (Cofin 2002), Rome. F. Fezza and N. Battista participated equally in the preparation of the chapter, and they were responsible with M. Bari for the assays of anandamide hydrolase activity and uptake. M. Maccarrone conceived and coordinated the study.

References

1. Frider, E. (2002) Endocannabinoids in the central nervous system—an overview. *Prostaglandins Leukot. Essent. Fatty Acids* **66**, 221–233.
2. Maccarrone, M., and Finazzi-Agrò, A. (2002) Endocannabinoids and their actions. *Vitam. Horm.* **65**, 225–255.
3. Ueda, N., Puffenberger, R. A., Yamamoto, S., and Deutsch, D.G. (2000) The fatty acid amide hydrolase (FAAH). *Chem. Phys. Lipids* **108**, 107–121.
4. Bracey, M. H., Hanson, M. A., Masuda, K. R., Stevens, R. C., and Cravatt, B. F. (2002) Structural adaptations in a membrane enzyme that terminates endocannabinoid signaling. *Science* **298**, 1793–1796.
5. Maccarrone, M., Bari, M., and Finazzi Agrò A. (1999) A sensitivity and specific radiochromatographic assay of fatty acid amide hydrolase activity *Anal. Biochem.* **267**, 314–318.
6. Glaser, S. T., Abumrad, N. A., Fatade, F., Kaczocha, M., Studholme, K. M., and Deutsch, D. G. (2003) Evidence against the presence of an anandamide transporter. *Proc. Natl. Acad. Sci. USA* **100**, 4269–4274.
7. Hillard, C. J. and Jarrahian, A. (2000) The movement of *N*-arachidonylethanolamine (anandamide) across cellular membranes. *Chem. Phys. Lipids* **108**:123–134.
8. Giuffrida, A., Beltramo, M., and Piomelli, D. (2001) Mechanism of endocannabinoid inactivation. *J. Pharmacol. Exp. Ther.* **298**, 7–14.
9. Barbaccia, M. L., Gandolfi, O., Chuang, D. M., and Costa, E. (1983) Modulation of neuronal serotonin uptake by the imipramine recognition site: evidence for an endogenous ligand. *Proc. Natl. Acad. Sci. USA* **80**, 5134–5138.
10. Battista, N., Bari, M., Finazzi-Agrò, A., and Maccarrone, M. (2002) Anandamide uptake by synaptosomes from human, mouse and rat brain: inhibition by glutamine and glutamate. *Lipids Health Dis.* **I**, 1–3.

Methods Evaluating Cannabinoid and Endocannabinoid Effects on Gastrointestinal Functions

Nissar A. Darmani

Summary

This chapter briefly describes the physiological neural mechanisms by which diverse neurotransmitter receptor systems control several aspects of gastrointestinal functions such as motility, secretion, feeding, and emesis. The current techniques used to study the effects of cannabinoids on these gastrointestinal functions are then sequentially described, starting with isolated gastrointestinal muscle preparations and ultimately evolving to whole animal models. Both Δ^9 -tetrahydrocannabinol (Δ^9 -THC) and well-studied representatives of other classes of exogenous cannabinoid CB_1/CB_2 receptor agonists inhibit gastrointestinal motility, peristalsis, defecation, and secretions via cannabinoid CB_1 receptors since the CB_1 (SR141716A)- and not the CB_2 (SR144528)-receptor antagonist reverses these effects in a dose-dependent manner. In addition, exogenous cannabinoids inhibit vomiting produced by diverse emetic stimuli in a SR141716A-sensitive manner in different animal models of emesis. Often these cannabinoids produce hyperphagic effects under laboratory conditions in most human and animal models of feeding. Administration of SR141716A by itself can produce effects opposite to cannabinoid agonists (e.g., increases in gastrointestinal motility and secretions, hyperphagia and vomiting), which suggests an important role for endocannabinoids in these gastrointestinal functions. Indeed, the presence of cannabinoid CB_1 receptor markers, endocannabinoids such as anandamide and 2-arachidonoylglycerol (2-AG), their metabolic enzymes, and an endocannabinoid reuptake system have been confirmed in the gastrointestinal tract (GIT). The well-studied endocannabinoid anandamide also seems to reduce both gastrointestinal motility and secretion while producing hyperphagia. On the other hand, while the less well-investigated endocannabinoid 2-AG is a potent emetogen, anandamide may possess weak antiemetic activity.

Key Words: Gastrointestinal; stomach; intestine; in vivo; in vitro; emesis; feeding cannabinoid; Δ^9 -THC; endocannabinoid; anandamide; 2-arachidonoylglycerol; peristalsis; SR141716A; techniques.

1. Introduction

The gastrointestinal effects of cannabinoids have recently been reviewed by a number of researchers (1–4). It appears that the endocannabinoid anandamide

and the well-investigated representatives of structurally diverse exogenous cannabinoids (Δ^9 -THC, WIN55,212-2, and CP 55, 940) inhibit gastrointestinal motility in several *in vitro* and *in vivo* models and delay gastric emptying in different animal species. Accumulating evidence also suggests that exogenous cannabinoids inhibit both basal and evoked fluid accumulation in the gastrointestinal tract (GIT). While exogenous cannabinoids possess antiemetic effects, peripheral administration of the less well-investigated endocannabinoid 2-AG potentially induces emesis in a dose-dependent fashion, whereas anandamide has weak antiemetic activity. In addition, both endogenous and exogenous cannabinoids are orexigenic. The discussed cannabimimetic effects are mediated via cannabinoid CB₁ receptors. These basic findings in animals seem to support the anecdotal and published clinical findings that cannabis products can be useful in several gastrointestinal disorders including nausea, vomiting, and diarrhea (1,5).

Numerous *in vitro* and *in vivo* techniques have been developed over the past three decades to investigate the underlying mechanisms by which cannabinoids affect the gastrointestinal system. Prior to describing specific research techniques that have led to the current understanding of gastrointestinal mechanisms of cannabinoid action, it is helpful to briefly consider the physiological neurotransmitter systems by which the discussed gastrointestinal activities are normally controlled. To varying degrees, both central and peripheral neural mechanisms control gastrointestinal functions such as motility (6,7), secretion (8,9), feeding (10,11), and emesis (12,13). Although several components of gastrointestinal functions are autonomic and are largely controlled by the enteric nervous system (ENS) in the gut, these activities are also modulated in part by the central nervous system (CNS) via both autonomic (sympathetic and parasympathetic) and somatic innervations as well as humoral pathways.

In the GIT, the ENS is organized into two plexi: the myenteric plexus, which is situated between the circular and longitudinal muscle layers of the GIT and regulates motor activity; and the submucosal plexus, found below the epithelium, which controls secretion. The vagus and pelvic nerves arise from the dorsal vagal complex of the medulla oblongata and the sacral region of the spinal cord, respectively, and primarily constitute the parasympathetic innervation of the GIT. Enhancements in parasympathetic nerve activity cause a general increase in both motor and secretory activities of the entire enteric system. The sympathetic innervation is supplied by nerves running between the spinal cord and the prevertebral ganglia and between these ganglia and the organs of the gut. The postganglionic projections from sympathetic prevertebral ganglia release norepinephrine (NE) and terminate as synapses in myenteric and submucosal plexi and inhibit their activity. Increased sympathetic activity inhibits motor activity and has dual effects on secretion: (1) sympathetic stimulation alone usually increases secretion, and (2) if parasympathetic or hormonal stimulation is

already causing copious secretion, then sympathetic activation often leads to a reduction in secretion (8). Several neurotransmitters are involved in gut motility. The primary motor neurotransmitter to smooth muscle in the GIT is acetylcholine. Both substance P and neurokinin A are also excitatory neurotransmitters and are co-released with acetylcholine following depolarization of enteric neurons. Another excitatory motor transmitter in the myenteric plexus is serotonin. Once released, these agents act via their specific receptors to increase gastrointestinal motility (2). Nitric oxide is a major inhibitory motor neurotransmitter in the GIT and can also mediate the inhibitory effects of γ -aminobutyric acid (GABA) and ATP (6). The catecholamine dopamine also suppresses GIT motility, as it lowers both esophageal sphincter and intragastric pressure. These effects are caused by suppression of acetylcholine release from myenteric motor neurons, which occurs via the activation of dopamine D₂ receptors. Thus, dopamine D₂ receptor antagonists are clinically used as prokinetic agents.

Gastric emptying is partially controlled by stomach factors such as degree of filling and the excitatory effect of gastrin on gastric peristalsis. The more important control of stomach emptying is via inhibitory feedback signals from the duodenum, including both enterogastric nervous feedback reflexes and hormonal feedback (14). Secretomotor neurons are excitatory neurons in the submucous plexus that innervate the crypts of Lieberkühn in the small and large intestine. When activated, they evoke secretion of water, electrolyte, and mucus into the intestinal lumen. Acetylcholine and vasoactive intestinal polypeptide (VIP) are primary neurotransmitters released by these neurons. Acetylcholine via M₃ receptors causes endothelial release of nitric oxide, which leads to vasodilation of submucosal arterioles and thus enhanced secretion. A significant component of vasodilation of submucosal arterioles in the colon is noncholinergic. Substance P, calcitonin gene-related peptide, and VIP are prime candidate neurotransmitters for these noncholinergic vasodilatory responses (8).

Classical emetic neurotransmitters include acetylcholine, dopamine, histamine, serotonin and substance P. Selective activation of muscarinic M₁, histamine H₁, serotonin 5-HT₃, and 5-HT₄ and neurokinin NK₁ receptors by the cited respective neurotransmitters either in the CNS, in the periphery, or at both sites induces emesis (12,13). A number of less well-recognized mediators such as arachidonic acid and some of its downstream metabolites (prostaglandins PGE₂ and PGF_{2 α} , and leukotriene B₄) are also emetic (1,2). Moreover, activation of vanilloid VR1 receptors can induce vomiting, whereas their rapid desensitization following the initial exposure of animals to VR1 agonists (e.g., resiniferatoxin) produce antiemetic effects (15–17). With respect to emetic mediators, it is important to note that 2-AG, by itself, is a potent emetogen (18). Furthermore, both 2-AG and anandamide can be metabolized to arachidonic acid, and anandamide activates VR1 receptors (19). In general, both endo-

cannabinoids as well as exogenous cannabinoids produce hyperphagic effects in several species under laboratory conditions (2). In addition, elevated levels of both 2-AG and anandamide are found in brain sites that control feeding (hypothalamic nuclei) in genetically obese rodents (19).

Several mechanisms may account for the inhibitory actions of cannabinoids on the GIT. Exogenously administered cannabinoids modify gastrointestinal functions via inhibition of release of both excitatory and inhibitory neurotransmitters from their corresponding nerve terminals. Indeed, the cannabinoid CB₁ receptor is often preferentially located on the presynaptic terminals in the brain, spinal cord, and peripheral neurons (e.g., cholinergic terminals in the myenteric plexus). One important function of these receptors is to reduce the release of neurotransmitters such as acetylcholine, norepinephrine, dopamine, serotonin, GABA, and ATP (20,21), most of which are significantly found in the GIT. Interaction between different receptor systems is apparent when both receptors are expressed within the same neurons. In this respect, at least in the CNS, CB₁ receptors are co-localized with dopamine D₁ and D₂ as well as serotonin 5-HT_{1B} and 5-HT₃ receptors (22). Thus, cannabinoids could modulate activity of co-localized receptors and vice versa (23,24). Retrograde signaling is used by the nervous system to convey information about the activity of neurons back to cells that innervate them. Endocannabinoids are considered to function as diffusible and short-lived modulators that may transmit signals retrogradely from postsynaptic to presynaptic neurons and thus alter transmitter release via presynaptic CB₁ receptors, as described earlier (25). Cannabinoids can alter the binding of serotonin 5-HT₂ receptor ligands (26), which leads to alteration of their function (27,28). More recently, it has been shown that cannabinoids stereoselectively inhibit currents through serotonin 5-HT₃ receptors independently of currently recognized cannabinoid receptors (29). In the latter case cannabinoids failed to alter the binding kinetics of the 5-HT₃ receptor ligand ³H-GR6530 but caused a concentration-dependent inhibition of currents through the 5-HT₃ ion channel, probably via an allosteric modulatory site on the 5-HT_{3A} receptor. This mechanism can account for the ability of exogenous cannabinoids suppressing the Bezold–Jarisch reflex produced by selective 5-HT₃ receptor agonists in anesthetized rats (30).

2. Techniques for the Investigation of Gastrointestinal Effects of Cannabinoids

Numerous *in vitro* and *in vivo* techniques have been employed for the study of cannabinoid agonists and antagonists on gastrointestinal functions. These include *in vitro* studies on isolated gastrointestinal muscle preparations, *in vitro* peristalsis studies, *in vivo* gastrointestinal motility studies, *in vitro* and *in vivo*

gastrointestinal secretion studies, orexigenic (appetite-stimulating) and anorexigenic (appetite-reducing) studies, and emesis studies.

2.1. *In Vitro* Studies on Isolated Gastrointestinal Muscle Preparations

Contractions of the intestine are affected by the activities of two layers of smooth muscle cells: an outer layer with the long axis of the cells arranged longitudinally and an inner layer with the long axis of the cells arranged circularly. The study of inhibitory effects of cannabinoids on the contraction of isolated gastrointestinal tissue began over three decades ago in the laboratory of Paton (31). These experiments involved the utilization of guinea pig ileum in which contractions were produced indirectly via electrical stimulation of pre-junctional neurons rather than by direct stimulation of intestinal smooth muscle. This preparation is generally referred to as the myenteric plexus-longitudinal muscle preparation (MPLM), which has been mainly utilized in the laboratories of Pertwee for more than 35 yr for the *in vitro* study of cannabinoids on intestinal contractility (3). This muscle preparation is obtained by stretching a 7- to 10- cm length of guinea pig ileum on a 6- to 8- mm-wide glass rod and removing the mesentery. By stroking tangentially away from the mesenteric attachment at one end of the strip with a wisp of cotton wool, the longitudinal muscle layer can be separated from the underlying circular muscle. This preparation yields a longitudinal muscle strip with Auerbach's plexus attached (32). To obtain plexus-free longitudinal strips, the ileum is gently pulled upwards on the supporting glass rod by applying traction to the proximal end. Human MPLM (33) as well as rat gastric stripe (34) and guinea pig ileal circular muscle (as 2- to 3-cm-wide rings) (35) preparations have also been utilized for the study of cannabinoids. These isolated tissues are normally suspended in organ baths containing Krebs solution. Once mounted in organ baths, each tissue is subjected to an electrical field stimulation (EFS) via platinum electrodes (0.1–10 Hz for 0.3–0.5 s). Depending upon the intensity and duration of EFS, cholinergic and nonadrenergic noncholinergic contractions can be obtained (35,36). In addition, pharmacological agents such as acetylcholine can be directly added to the organ bath to induce contractions (37). The contractions are now routinely monitored by computerized data capturing and analysis systems that are linked via amplifiers to transducers. The inhibitory actions of cannabinoids on these tissue preparations have recently been reviewed (2–4). The main conclusions are:

1. At low EFS intensities, MPLM, circular ileal and gastric stripe muscle preparations produce contractions in response to electrically induced release of acetylcholine from presynaptic enteric cholinergic nerves (34–37).
2. Both 2-AG and anandamide are found in relatively high concentrations throughout the GIT, and the cannabinoid CB₁ receptor or its markers are differentially distrib-

uted on neurons supplying the stomach to colon in several species, including humans (2–4,49).

3. Structurally diverse cannabinoids attenuate the EFS-induced contractions with a potency order (CP 55, 940 > WIN55, 212-2 > nabilone > Δ^9 -THC > cannabinol > anandamide), similar to their affinity rank order for cannabinoid CB₁ receptors. In addition, the selective cannabinoid CB₁ receptor antagonist/inverse agonist SR141716A counters the inhibitory effects of cannabinoid agonists (4).
4. Synthetic cannabinoid agonists reduce electrically evoked acetylcholine release from myenteric nerves of the guinea pig ileum in a SR141716A-sensitive manner (37). However, cannabinoid agonists do not reduce contractions in these muscle preparations produced in response to exogenously added contractile agents such as acetylcholine or substance P (3). Thus, cannabinoid agonists do not modify contractions produced by a direct action on muscarinic receptors located on intestinal smooth muscle but inhibit acetylcholine release from presynaptic cholinergic nerves. Indeed, the presence of presynaptic CB₁ receptor markers in the myenteric and submucosal plexuses have been confirmed.
5. In addition to being an endocannabinoid, anandamide is also an endovanilloid. Anandamide appears to act on both CB₁ and non-CB₁ receptors to inhibit the electrically evoked intestinal contractions. Furthermore, it stimulates both basal acetylcholine release and basal MPLM tone in the guinea pig ileum via the activation of vanilloid VR1 receptors (38).
6. Although 2-AG was the first endocannabinoid to be discovered in the GIT, virtually nothing has been published on its effects in the gastrointestinal system. However, a recent study suggests that both 2-AG and anandamide induce contractions of longitudinal muscle preparations of guinea pig colon via stimulation of myenteric cholinergic neurons, and neither cannabinoid CB₁/CB₂ or vanilloid VR1 receptors contribute to the contractile response, but the effect is mediated by one or more lipoxygenase metabolites of these endocannabinoids (39). Analogs of these products also cause contractions in gastric fundus preparations (40).

2.2. *In Vitro* Peristalsis Studies in Isolated Intestine

Peristalsis is a coordinated motor process that allows the intestine to propel its content toward the anus. It consists of a preparatory phase in which longitudinal muscles contract in response to effluent infusion and a subsequent emptying phase in which coordinated contractions of circular muscles expel the effluent from the stomach to the anal end. Peristalsis is induced in 5- to 10-cm isolated segments of guinea pig ileum by either a constant fluid perfusion (41,42) or electrical field stimulation in a constant intraluminal perfusion system (43). Ileal segments are secured horizontally in organ baths containing 30–80 mL of Krebs solution. Peristalsis is elicited by delivering Krebs solution into the oral end of the intestinal lumen at a rate of 0.5–0.85 mL/min. In the case of electrically induced peristalsis, the rate of Krebs solution entering the intestinal lumen is low enough that it does not induce peristalsis. Depending on

the experimenter's laboratory equipment, a number of peristaltic parameters are recorded. For example, (1) the intraluminal pressure at the aboral end of the segments as well as peristaltic pressure threshold, the residual baseline pressure, the amplitude of peristaltic waves, and the maximal acceleration of peristaltic waves can be measured with a pressure transducer whose signal is fed via an analog/digital converter into a computer and is then analyzed by appropriate software (42), (2) the volume expelled at the end of each contraction can be measured with a use of a cylinder (41), and (3) mechanical events during peristalsis and changes in intestinal wall morphology can be recorded by a camera synchronized with polygraphic traces, which can be analyzed by specialized software (43). Several recent reviews (2–4) have summarized the effects of cannabinoids on peristalsis:

1. Structurally diverse cannabinoid CB₁/CB₂ agonists inhibit peristalsis induced in segments of isolated intestine (ileum or colon) by continuous luminal fluid infusion (41) or electrical field stimulation (43). Indeed, these agonists seem to reduce both the preparatory phase of peristalsis (i.e., longitudinal muscle contractions in response to fluid or electrical field stimulation) as well as the subsequent emptying phase in which intestinal circular muscles contract towards the aboral end. Overall, cannabinoids increase the threshold pressure and the volume for triggering peristalsis but decrease compliance and ejection pressure.
2. The discussed cannabinoid-induced effects on intestinal peristalsis are reportedly completely countered by SR141716A, suggesting they are CB₁ receptor mediated (41,43,44). However, the inhibitory action of methanandamide on distension-induced propulsive motility is also sensitive to the presence of L-NAME (a nitric oxide synthase inhibitor) and apamine (an inhibitor of Ca²⁺-dependent potassium channels) (44).
3. The effect of 2-AG on peristaltic activity has not yet been reported. However, downstream metabolites of endocannabinoids affect propulsive peristalsis in fluid-perfused segments of the guinea pig small intestine (42).

2.3. In Vivo Gastrointestinal Motility Studies

In vivo studies utilized to investigate the effects of cannabinoid agonists on gastrointestinal motility generally employ techniques which measure either the discharge of fecal pellets (45), the passage of a nonadsorbable marker such as a charcoal suspension in gum arabic (46) or a carmine solution containing methylcellulose (47), a nonadsorbable radioactive marker such as ⁵¹Cr as sodium chromate (48), or glass beads (49) in the GIT of several rodent species. These markers are administered either orally, intraduodenally, or in distal colon prior to cannabinoid treatment. At the end of experimental drug exposure and following sacrifice, the animal intestine is removed from the stomach to the anus. The distance traveled by the glass bead or the head of the marker in isolated intestine is then measured and often expressed as percent

of total length of the intestine. Fecal pellet excretion is assessed in mice by placing individual animals in grid-floor cages, with food and water ad libitum. Two to 3 h later, the food is withdrawn and different groups of animals are treated with varying doses of a cannabinoid. The pellets discharged during the next 3 h are collected and weighed immediately and after drying (20 h at 50°C dry weight). An action on secretion or reabsorption of fluids is assessed from the ratio of wet to dry fecal weights (46). Other studies have also measured intragastric pressure and pyloric contractility (50) and transient lower esophageal sphincter relaxations (TLESRs) (51). TLESRs are the major cause of gastroesophageal acid reflux and are triggered by postprandial gastric retention. The intragastric pressure is recorded via a latex balloon placed in the rat stomach, while circular smooth muscle contractility of the pyloric region is recorded via strain gauges mounted on the surface of the rat stomach. TLESRs are stimulated by intragastric infusion of an acidified nutrient soup followed by air insufflation in dogs. Manometric recordings of TLESRs are then made via water-perfused Dentsleeve multilumen assemblies. Recent reviews (2–4) on the effects of cannabinoids on in vivo gastrointestinal motility indicate:

1. Exogenous cannabinoids delay gastric emptying in diverse species (45,48,50,52,53) with an ED₅₀ potency order (CP 55, 940 > WIN55,212-2 > Δ⁹-THC > cannabidiol) that is similar to their potency rank order in attenuating electrically evoked contractions of isolated ileum preparations, and their affinity rank order for cannabinoid CB₁ receptors. The latter studies also show that SR141716A counters the inhibitory effects of the CB₁/CB₂ receptor agonists in a dose-dependent manner. These cannabinoid agonists also reduce intragastric pressure, pyloric contractility, transient lower esophageal sphincter relaxation, and gastroesophageal reflux via cannabinoid CB₁ receptors (51). To date, the effect of endocannabinoids on in vivo models of gastric emptying has not been reported.
2. In line with the discussed in vitro studies, in vivo findings also show that structurally diverse exogenous cannabinoids (Δ⁸-THC, Δ⁹-THC, nabilone, cannabinal, WIN55,212-2, CP 55, 940, HU-210, and *N*-[2-chloroethyl]-5Z,8Z,11Z,14Z-eicosatetraenamide [ACEA]) attenuate intestinal motility and transit in several species in an SR141716A-sensitive manner.
3. The endocannabinoid anandamide also inhibits intestinal motility since it was shown to reduce both charcoal transit in the upper GIT (46) and glass bead transit in distal colon (49) via cannabinoid CB₁ receptors. In addition, a selective inhibitor of anandamide cellular uptake, VDMII, can inhibit colonic propulsion in a SR141716A-sensitive manner. However, a less selective anandamide uptake inhibitor, AM404, appears to be inactive on small intestine motility in mice (4,49).
4. Noladin ether (2-arachidonoyl glycerol ether) is another putative endocannabinoid that also possesses intestinal antitransit properties. Although 2-AG is also present both in small intestine and colon, its in vivo effects on intestinal motility have not yet been investigated.

2.4. *In Vitro and In Vivo Gastrointestinal Secretion Studies*

In addition to mucus-secreting cells that line the entire surface of the stomach and small intestine, the stomach mucosa contains oxyntic glands, which secrete gastric HCl and pyloric glands that secrete mainly mucus but also pepsinogen and gastrin. Located within the first few centimeters of the duodenum are the Brunner's glands, which secrete large amounts of alkaline mucus in response to vagal and tactile stimulation. The crypts of Lieberkühn, located over the entire surface of the small intestine, secrete large quantities of water and electrolytes in addition to mucus. The great preponderance of secretion in the large intestine is mucus, which contains moderate amounts of bicarbonate ions.

The gastric antisecretory effects of cannabinoids have been studied in *in vitro* models via rat isolated gastric preparations (54) or *in vivo* models via perfusion of stomach with saline through an esophageal cannula and collection of the perfusate with a duodenal cannula in anesthetized rats (55,56). Gastric acid is often expressed as absolute values in $\mu\text{Eq HCl/kg/min}$. Acid response to different secretagogues (e.g., histamine, pentagastrin, or 2-de-oxy-D-glucose) are calculated for each rat by subtracting the basal output from peak acid secretion (plateau response) obtained after a stimulant administration ($\mu\text{Eq HCl/kg/min}$). The inhibitory effect of cannabinoid agonists is expressed as percent inhibition of the stimulated acid plateau secretion, which is considered as 100%. Both isolated intestinal preparations (57) and *ex vivo* intestinal preparations are used for the study of the inhibitory effects of cannabinoids on intestinal secretions (58). For ileal tissue preparations, the longitudinal muscle layer and the attached myenteric plexus are peeled off, and then mucosal sheets are mounted in a Ussing chamber system bathed in Krebs buffer at 37°C. Measurement of electrogenic ion transport is made by measuring short currents (ISC) continuously in the mucosal sheet via a pair of agar salt bridge electrodes connected to a multiple channel voltage/current clamp apparatus. The ISC is continuously recorded by a Maclab Data Acquisition System. The effect of cannabinoids on ISC is measured as peak changes from baseline values and is expressed as $\mu\text{A/cm}^2$. *Ex vivo* measurement of changes induced by cannabinoids on intraluminal fluid accumulation is often determined by enteropooling method in rats (59). Thus, following a 30- to 60-min exposure to a cannabinoid, rats are sacrificed and the entire small intestine is removed and its contents squeezed into a test tube. The intestinal contents are weighed immediately and after drying (36 h at 50°C) in order to determine water content. Changes in water content is expressed as intestinal fluid volume (mL/rat). Samples of intestinal fluid content are analyzed for Na^+ concentration by using high-performance liquid chromatography. The effects of cannabinoids have also been studied in castor-oil-induced diar-

rhea in rats (45) and in croton-oil-induced inflammation in mice (60). Evidence for the *in vitro* and *in vivo* inhibitory effects of cannabinoids on gastrointestinal secretions is summarized (2–4) as:

1. Structurally diverse cannabinoids (Δ^9 -THC; WIN55,212-2; HU-210) inhibit stimulated but not basal gastric acid secretions and also reduce the volume of gastric juice (54–56). The inhibition appears to occur presynaptically involving cholinergic and noncholinergic excitatory neurons. The inhibition is cannabinoid CB₁ receptor mediated since it is reversed by SR141716A. Cannabinoids generally do not inhibit acid secretion produced by direct-acting secretagogues such as histamine, but they do prevent the action of prosecretory agents such as pentagastrin, which in part act indirectly to release histamine.
2. Cannabinoid agonists also inhibit both neurally evoked ileal secretion in mucosal preparation of isolated sheets of rat small intestine and *in vivo* fluid accumulation and diarrhea via cannabinoid CB₁ receptors (45,46,57,58).
3. The cannabinoid CB₁ (SR141716A) but not the CB₂ (SR144528) receptor antagonist by itself increases intestinal fluid volume and fecal water content in rats, which indicates a possible role of endocannabinoids in the control of gastrointestinal functions (45,46). However, SR141716A by itself does not affect gastric acid secretion.
4. Inflammation of the gut increases both the potency of cannabinoid agonists (probably via upregulation of CB₁ receptor expression) and the turnover of intestinal endocannabinoids.

2.5. *Orexigenic and Anorexigenic Studies*

A combination of central and peripheral mechanisms control food intake. Indeed, hypothalamic nuclei and the brainstem act as input stations for hormonal and gastrointestinal information (10,11). Furthermore, peripheral satiety factors such as cholecystokinin (CCK) activate CCK₁ receptors on vagal afferents, which transmit signals to hindbrain nuclei such as the nucleus tractus solitarius (NTS). The NTS in turn communicates with several hypothalamic nuclei, which play critical roles in appetite regulation. In addition, adipose tissue secretes the hormone leptin, which enters the CNS and stimulates the arcuate nucleus within the hypothalamus. Leptin appears to be the main signal via which the hypothalamus senses nutritional states and modulates food intake. Leptin directly affects neurons in which either the anorexigenic (appetite-reducing) peptides proopiomelanocortin (POMC) and cocaine- and amphetamine-regulated transcript (CART) or the orexigenic (appetite-stimulating) peptides neuropeptide Y (NPY) and agouti-related protein (AGRP) are co-localized. The NPY/AGRP-expressing neurons increase feeding, while those expressing POMC/CART inhibit feeding.

The stimulatory effects of cannabis extracts on human appetite have been anecdotally known for over hundreds of years. Δ^9 -THC and other exogenous

cannabinoid agonists also induce hyperphagic effects under laboratory conditions in most human and animal models (61–64), but no effect (65) or a reduction in food intake (66) has also been reported. In addition, the cannabinoid CB₁ receptor antagonist SR141716A (Rimonabant) suppresses feeding in animals (67,68) and is currently under phase II clinical trials as an appetite-suppressing agent. The design of acute food-intake studies generally includes feeding rodents (e.g., rats) for 1 h at the onset of dark period in their home cages. Thereafter, any remaining food is removed and different groups of animals are treated with varying doses of a cannabinoid agonist or antagonist. Approximately an hour or so later, each animal is placed in an observation chamber with access to preweighed food and water, and its feeding and other behaviors are recorded. At the end of the test, each animal is returned to its home cage and food and water intake are determined by weighing the remaining food (plus spillage) and water (69). Cannabinoid agonists or antagonists are administered either peripherally (e.g., orally [69] or subcutaneously [67]) or via central injections through implanted cannulae in specific brain loci such as the ventromedial hypothalamus (70) or the nucleus accumbens shell (71). Although earlier studies have mainly been confined to direct measurement of food and water intakes, more recent published studies have additionally utilized video recording techniques to measure several aspects of feeding behavior followed by their subsequent analysis via commercial software (e.g., the Observer, Noldus InformationTechnology). Thus, these studies have recorded numerous additional behaviors such as eating (may consist of biting, gnawing, or swallowing food), drinking (licking at the water bottle spout), rearing, grooming (scratching, licking or biting of coat), sniffing, locomotion, resting/inactive, or sleeping (69). On the other hand, in chronic cannabinoid exposure studies, only measurement of daily food and water intake is generally carried out (e.g., **ref.** 67). The effects of cannabinoid CB₁ receptor ligands on feeding are summarized (2) as:

1. Δ^9 -THC and other synthetic cannabinoids reliably induce hyperphagia and increase food intake in laboratory animals (61–64). These hyperphagic actions are mediated via cannabinoid CB₁ receptors since they are selectively blocked by the cannabinoid CB₁ receptor antagonist SR141716A but not with the CB₂ antagonist SR144258 (71).
2. Most studies indicate that SR141716A by itself suppresses appetite and food intake in rodents (e.g., **refs.** 73 and 74), which can lead to a reduction in body weight (67). In addition, CB₁ receptor knockout mice eat less and are leaner than their wild-type littermates (19,75). These findings indicate an important role for endocannabinoids in the control of feeding.
3. Administration of either endocannabinoids (2-AG or anandamide) induces overeating in laboratory animals in a SR141716A-sensitive manner (70–72,76–78). Endocannabinoids are implicated in appetite and body weight regulation.

4. Leptin administration suppresses hypothalamic endocannabinoid levels in normal rats, while genetically obese, chronically hyperphagic rodents express leptin-reversible, elevated hypothalamic anandamide and 2-AG levels (19). Moreover, fasting seems to increase levels of both anandamide and 2-AG in the limbic fore-brain and, to a lesser extent, of 2-AG in the hypothalamus, whereas in fed animals the hypothalamic content of 2-AG declines (72). However, another study has shown that while food deprivation failed to alter anandamide levels in whole brain, hunger did increase intestinal anandamide content, which normalized following feeding (79).
5. Cannabinoid CB₁ receptor markers are found in epididymal fat pads (75) and are co-expressed in hypothalamic neurons that contain neuropeptides known to modulate food intake such as CART (75). The cannabinoid system appears to be an essential endogenous regulator of appetite and energy balance, which acts via both central orexigenic as well as peripheral lipogenic mechanisms (72,75,79).
6. Both cannabinoid CB₁/CB₂ receptor agonists (Δ^9 -THC [Dronabinol] and nabilone [Cesamet]) and selective cannabinoid CB₁ receptor antagonists (e.g., SR141716A [Rimonabant]) can be clinically used to respectively increase and decrease appetite (1).

2.6. Vomiting Studies

In the past two decades there have been important basic and clinical advances in the understanding of the mechanisms by which chemo- and radio-therapy produce emesis. These findings led to the introduction of clinically useful antiemetics such as serotonin 5-HT₃ receptor antagonists in the early 1990s, which revolutionized the treatment of both radiotherapy- and the initial phase of chemotherapy-induced nausea and vomiting. However, 5-HT₃ receptor antagonists by themselves are ineffective in the treatment of the delayed phase of emesis (80). Although more broad-spectrum antiemetics such as tachykinin NK₁ receptor antagonists appear to be effective in both early and delayed phases of chemotherapy-induced emesis in animals, these agents are only employed as combination antiemetics in conjunction with a 5-HT₃ receptor antagonist and dexamethasone (80). In the latter antiemetic regimen, NK₁ antagonists significantly improve the antiemetic effects of the standard dual therapy in the clinic (i.e., use of a 5-HT₃ antagonist plus dexamethasone). Limited clinical studies also suggest broad-spectrum antiemetic activity for Δ^9 -THC (1). The broad-spectrum antiemetic activity of Δ^9 -THC has also been confirmed in animal models of emesis (1,2).

The antiemetic activity of Δ^9 -THC was initially investigated in the dog following clinical observations that it may possess antiemetic potential against chemotherapy-induced emesis. However, both Δ^9 -THC and its analog nabilone failed to prevent vomiting in dogs produced by cisplatin (81) or apomorphine (82,83). On the other hand, both agents were effectively shown to prevent cis-

platin-induced vomiting in the cat (84,85). Since then, the antiemetic potential of both Δ^9 -THC and representatives of other classes of synthetic cannabinoids (CP 55, 940; WIN55,212-2, or HU 210) against cisplatin-induced emesis has been confirmed in several other emetic species, including the pigeon (86,87), the ferret (88), the house musk shrew (89), and the least shrew (90–92).

In addition, Δ^9 -THC appears to possess broad-spectrum antiemetic activity since it also suppresses emesis produced by the opiate morphine (93,94), the endocannabinoid 2-AG (18), the serotonin precursor 5-hydroxytryptophan and direct-acting serotonin 5-HT₃ receptor agonists (95), and various selective and nonselective dopamine D₂/D₃ receptor agonists such as apomorphine, quinpirole, quinlorane, and 7-OH DPAT (96). The receptor mechanism by which cannabinoid CB₁/CB₂ receptor agonists prevent emesis produced by diverse emetic stimuli remained unknown until recently. The first dose-dependent indication that cannabinoids may prevent emesis via stimulation of cannabinoid CB₁ receptors was given when Δ^9 -THC was shown to block emesis produced by large doses of the cannabinoid CB₁ receptor antagonist SR141716A (90). Since then, most of the cited studies have shown that SR141716A pretreatment can reverse the ability of an effective antiemetic dose of Δ^9 -THC (or other CB₁/CB₂ agonists) against diverse emetic stimuli. Some investigators have utilized only a single SR141716A dose to reverse the antiemetic activity of cannabinoid agonists, while others have carried out full dose-response studies. Nonemetic animal species (e.g., rats) have also been used for the study of antiemetic potential of Δ^9 -THC and other cannabinoids (98,99). In this case, the ability of a cannabinoid CB₁/CB₂ agonist to interfere with the expression of conditioned rejection reactions produced by chemotherapeutic agents is taken as an index of antiemetic potential of CB₁/CB₂ receptor agonists.

The introduction of newer and smaller animal models of emesis has led to a renaissance in the fields of cannabinoids and emesis. It is quite clear from the above discussion that dogs are not a suitable animal model for the study of antiemetic effects of cannabinoids since Δ^9 -THC at relatively low doses cause profound emesis by itself in this species (82,100). In recent published cannabinoid studies, the ferret (900–1500 g), the house musk shrew (*Suncus murinus*, 30–80 g), and the least shrew (*Cryptotis parva*, 3–6 g) have been mainly utilized as models of emesis. In these studies a cannabinoid CB₁/CB₂ receptor agonist is administered either intraperitoneally or subcutaneously 0–30 min prior to injection of an effective dose of an emetic agent. Depending on the emetic agent, vomiting parameters are scored 30–60 min after the administration of the emetogen. The mean frequency of vomiting, the frequency of retches, the percentage of animals that vomit or retch, the onset latency to first vomits or retch, and/or vomits or retches per animal are recorded (1,18,89,93,94). Since some clinical studies have suggested that Δ^9 -THC prevents emesis at

sedative doses (1), some investigators have determined the motor-suppressive effects of the corresponding antiemetic as well as larger doses of cannabinoid agonists in separate groups of the employed vomiting species. However, in earlier studies an emetic species was used for the vomiting component of the study, and rodents were used for motor suppressing effects of cannabinoids (87). More recently, with the introduction of a new shrew model of vomiting, the least shrew has been used for both purposes in such studies (91,92,96,97). These studies have shown that both Δ^9 -THC and WIN55,212-2 possess effective antiemetic activity at nonsedative doses (91,96,97), whereas CP 55, 940 prevents emesis at doses that significantly depress motor activity (92). The antiemetic activity of cannabinoid is currently summarized as (1,2):

1. Structurally diverse cannabinoid CB₁/CB₂ receptor agonists potently block emesis produced by diverse emetic stimuli with an ID₅₀ order (CP 55, 940 > WIN55,212-2 > Δ^9 -THC) that is highly correlated to their rank affinity order for cannabinoid CB₁ receptors in shrew brain homogenates and EC₅₀ potency order for GTP γ S stimulation (92).
2. Large doses (10–40 mg/kg, ip) of the well-investigated CB₁ receptor antagonist SR141716A produces emesis by itself (90). Although a 5 mg/kg dose of another CB₁ receptor antagonist, AM251, by itself does not evoke either retching or vomiting, it does potentiate the emetic action of morphine (93). These findings suggest an important role for endocannabinoids in emetic circuits.
3. Exogenously administered 2-AG is a potent emetic agent, whereas peripheral administration of the other endocannabinoid, anandamide, causes a non-dose-dependent emetic effect (18). The more stable analog of anandamide, methanandamide, may also induce vomiting or retching in a few animals (18,93). In addition, both anandamide and methanandamide possess weak antiemetic activity against some emetic stimuli. The major metabolite of endocannabinoids, arachidonic acid (AA), is a potent emetogen (18). Emesis can be also produced by downstream metabolites of AA such as prostaglandins (2).
4. Exogenously administered cannabinoids act via both central and peripheral mechanisms to prevent emesis produced by emetic stimuli such as serotonin or chemotherapeutic agents (8,95).

Acknowledgments

This work was supported by grants from the National Cancer Institute (CA 115331) and Solvay Pharmaceuticals Inc. The author would like to thank Professor L. Towns for proofing and helpful suggestions and R. Chronister for typing the manuscript.

References

1. Darmani, N. A. (2002) Antiemetic action of Δ^9 -tetrahydrocannabinoid and synthetic cannabinoids in chemotherapy-induced nausea and vomiting, in *Biology of*

- Marijuana: From Gene to Behavior* (Onaivi, E. S., ed.), Taylor and Francis Books Ltd., London, pp. 356–389.
2. Darmani, N. A. (2005) Endocannabinoids and gastrointestinal function, in: *Endocannabinoids: The Brain and Body's Marijuana and Beyond* (Onaivi, E. S., Sugiura, T., and Di Marzo, V.), Taylor and Francis Books Ltd, London, 377–401.
 3. Pertwee, R. G. (2001) Cannabinoids and the gastrointestinal tract. *Gut* **48**, 859–867.
 4. Pinto, L., Capasso, R., Di Carlo, G., and Izzo, A.A. (2002) Endocannabinoids and the gut. *Prostag. Leukotr. Essent. Fatty Acids* **66**, 333–341.
 5. Mechoulam, R. (1986) The pharmaco-history of *Cannabis sativa*, in *Cannabinoids as Therapeutic Agents* (Mechoulam, R., ed.), CRC Press, Boca Raton, FL, pp. 1–20.
 6. Olsson, C. and Holmgren, S. (2001) The control of gut motility. *Compar. Biochem. Physiol.* **128**, 481–503.
 7. Kunze, W. A. A. and Furness, J. B. (1999) The enteric nervous system and regulation of intestinal motility. *Ann. Rev. Physiol.* **61**, 117–142.
 8. Wood, J. D. (1999) Neurotransmission at the interface of sympathetic and enteric divisions of autonomic nervous system. *Clin J. Physiol.* **42**, 201–10.
 9. Brown, D. R. and O'Grady, S. M. (1997) Regulation of iontransport in the porcine intestinal tract by enteric neurotransmitters and hormones. *Comp. Biochem. Physiol.* **118**, 309–317.
 10. Halford, J. C. G. and Blundell, J. E. (2000) Separate systems for serotonin and leptin in appetite control. *Ann. Med.* **32**, 222–232.
 11. Chiesi, M., Huppertz, C., and Hofbauer, K.G. (2001) Pharmacotherapy of obesity: targets and prospectives. *Trends Pharmacol. Sci.* **22**, 247–254.
 12. Mitchelson, F. (1992) Pharmacological agents affecting emesis: a review (part 1). *Drugs* **43**, 295–315.
 13. Veyrat-Follet, C., Farinoti, R., and Palmer, J. L. (1997) Physiology of chemotherapy-induced emesis and antiemetic therapy. Predictive models for evaluation of new compounds. *Drugs* **53**, 206–234.
 14. Guyton, A. C. and Hall, J. E. (2000) Propulsion and mixing of food in the alimentary tract, in *Textbook of Medical Physiology*, 10th ed., Saunders Company, St. Louis, pp. 728–737.
 15. Andrews, P. L. R. and Bhandari, P. (1993) Resiniferatoxin, an ultra potent capsaicin analogue, has antiemetic properties in the ferret. *Neuropharmacology* **32**, 799–806.
 16. Andrews, P. L. R., Okada, F., Woods, A. J., Hagiwara, H., Kakimoto, S., Toyoda, M., and Matsuki, N. (2000) The emetic and antiemetic effects of the capsaicin analog resiniferatoxin in *Suncus murinus*, the house musk shrew. *Br. J. Pharmacol.* **130**, 1247–1254.
 17. Rudd, J. A. and Wai, M. K. (2001) Genital grooming and emesis induced by vanilloids in *Suncus murinus*, the house musk shrew. *Eur. J. Pharmacol.* **422**, 185–195.
 18. Darmani, N. A. (2002) The potent emetogenic effects of the endocannabinoid, 2-AG (2- arachidonoylglycerol) are blocked by Δ^9 -tetrahydrocannabinol and other cannabinoids. *J. Pharmacol. Exp. Ther.* **300**, 34–42.

19. Di Marzo, V., Goparaju, S. K., Wang, L., et al. (2001) Leptin-regulated endo-cannabinoids are involved in maintaining food intake. *Nature* **410**, 822–825.
20. Schlicker, E. and Kathman, M. (2001) Modulation of transmitter release via presynaptic cannabinoid receptors. *Trends Pharmacol. Sci.* **22**, 565–572.
21. Ralevic, V. (2003) Cannabinoid modulation of peripheral autonomic and sensory neurotransmission. *Eur. J. Pharmacol.* **472**, 1–21.
22. Hermann, H., Marsicano, G., and Lutz, B. (2000) Coexpression of the cannabinoid receptor type 1 with dopamine and serotonin receptors in distinct neuronal subpopulations of the adult mouse forebrain. *Neuroscience* **109**, 451–460.
23. Glass, M. and Felder, C. C. (1997) Concurrent stimulation of cannabinoid CB₁ and dopamine D₂ receptors augments cAMP accumulation in striatal neurons: evidence for a Gs linkage to the CB₁ receptor. *J. Neurosci.* **17**, 5327–5333.
24. Jarrahian, A., Watts, V. J., and Barker, E. J. (2004) D₂ dopamine receptors modulate G_α- subunit coupling of the CB₁ cannabinoid receptor. *J. Pharmacol. Exp. Ther.* **308**, 880–886.
25. Ohno-Shosaku, T., Maejima, T., and Kano, M. (2001) Endogenous cannabinoids mediate retrograde signals from depolarized postsynaptic neurons to presynaptic terminals. *Neuron* **29**, 729–738.
26. Kimura, T., Ohta, T., Watanabe, K., Yoshimura, H., and Yamamoto, I. (1998) Anandamide, an endogenous cannabinoid receptor ligand, also interacts with 5-hydroxytryptamine (5-HT) receptor. *Biol. Pharm. Bull.* **21**, 224–226.
27. Damani, N. A. (2001) Cannabinoids of diverse structure inhibit two DOI-induced 5-HT_{2A} receptor mediated behaviors in mice. *Pharmacol. Biochem. Behav.* **68**, 311–317.
28. Cheer, U. F., Cadogan, A.-K., Marsden, C. A., Fone, K. C. F., and Kendall, D. A. (1999) Modification of 5-HT₂ receptor mediated behavior in the rat by oleamide and the role of cannabinoid receptors. *Neuropharmacology* **38**, 533–541.
29. Barann, M., Molderings, G., Brüss, M., Bönisch, H., Urban, B. W., and Göthert, M. (2002) Direct inhibition by cannabinoids of human 5-HT_{3A} receptors: probable involvement of an allosteric modulatory site. *Br. J. Pharmacol.* **137**, 589–596.
30. Godlewski, G., Göthert, M., and Malinowska, B. (2003) Cannabinoid receptor-independent inhibition by cannabinoid agonists of the peripheral 5-HT₃ receptor-mediated von Bezold- Jarish reflex. *Br. J. Pharmacol.* **138**, 767–774.
31. Gill, E. W., Paton, W. D. M., and Pertwee, R. G. (1970) Preliminary experiments in the chemistry and pharmacology of cannabis. *Nature* **228**, 134–136.
32. Paton, W. D. M. and Zar, M. A. (1968) The origin of acetylcholine released from guinea-pig intestine and longitudinal muscle strips. *J. Physiol.* **194**, 13–33.
33. Croci, T., Manara, L., Aureggi, G., et al. (1998) In vitro functional evidence of neuronal cannabinoid CB₁ receptors in human ileum. *Br. J. Pharmacol.* **125**, 1393–1395.
34. Storr, M., Gaffal, E., Saur, D., Schusdziarra, V., and Allescher, H. D. (2002) Effect of cannabinoids on neural transmission in rat gastric fundus. *Can. J. Physiol.* **80**, 67–76.

35. Izzo, A. A., Mascolo, N., Borelli, F., and Capasso, F. (1998) Excitatory transmission to the circular muscle of the guinea-pig ileum: evidence for the involvement of cannabinoid CB₁ receptors. *Br. J. Pharmacol.* **124**, 1363–1368.
36. Pertwee, R. G., Fernando, S. R., Nash, J. E., and Coutts, A. A. (1996) Further evidence for the presence of cannabinoid CB₁ receptors in guinea-pig small intestine. *Br. J. Pharmacol.* **118**, 2199–2205.
37. Coutts, A. A. and Pertwee, R. G. (1997) Inhibition by cannabinoid receptor agonists of acetylcholine release from the guinea-pig myenteric plexus. *Br. J. Pharmacol.* **121**, 1557–1566.
38. Mang, C. F., Erbelding, D., and Kilbinger, H. (2001) Different effects of anandamide on acetylcholine release in the guinea-pig ileum mediated via vanilloid non-CB₁ cannabinoid receptors. *Br. J. Pharmacol.* **134**, 161–167.
39. Kojima, S.-I., Sugiura, T., Waku, D., and Kamikawa, Y. (2002) Contractile response to a cannabimimetic eicosanoid, 2-arachidonoylglycerol, of longitudinal smooth muscle from the guinea-pig distal colon in vitro. *Eur. J. Pharmacol.* **444**, 203–207.
40. Sametz, W., Hennerbichler, S., Glaser, S., Wintersteiger, R., and Juan, H. (2000) Characterization of prostanoid receptors mediating actions of the isoprostanes, 8-iso-PGE₂ and 8-iso-PGE_{2α}, in some isolated smooth muscle preparations. *Br. J. Pharmacol.* **130**, 1903–1910.
41. Izzo, A. A., Mascolo, N., Tonini, M., and Capasso, F. (2000) Modulation of peristalsis by cannabinoid CB₁ ligands in the isolated guinea-pig ileum. *Br. J. Pharmacol.* **129**, 984–990.
42. Shahbazian, A., Heinemann A., Peskar, B. A., and Holzer, P. (2002) Differential peristaltic motor effects of prostanoid (DP, EP, IP, TP) and leukotriene receptor agonists in guinea-pig isolated small intestine. *Br. J. Pharmacol.* **137**, 1047–1054.
43. Mancinelli, R., Fabrizi, A., Del Monaco, S., et al. (2001) Inhibition of peristaltic activity of cannabinoids in the isolated distal colon of mouse. *Life Sci.* **69**, 101–111.
44. Heinemann, A., Shabazian, A., and Holzer, P. (1999) Cannabinoid inhibition of guinea-pig intestinal peristalsis via inhibition of excitatory and activation of inhibitory neural pathways. *Neuropharmacology* **38**, 1289–1297.
45. Izzo, A. A., Moscolo, N., Pinto, L., Capasso, R., and Capasso, F. (1999) The role of cannabinoid receptor in intestinal motility, defaecation and diarrhea in rats. *Eur. J. Pharmacol.* **384**, 37–42.
46. Izzo, A. A., Mascolo, N., Borrelli, F., and Capasso, F. (1999) Defaecation, intestinal fluid accumulation and motility in rodents: implications of cannabinoid CB₁ receptors. *Naunyn-Schmied. Arch. Pharmacol.* **359**, 65–70.
47. Colombo, G., Agabio, R., Lobina, C., Reali, R., and Gessa, G. L. (1998) Cannabinoid modulation of intestinal propulsion in mice. *Eur. J. Pharmacol.* **344**, 67–69.
48. Shook, J. E. and Burks, T. F. (1989) Psychoactive cannabinoids reduce gastrointestinal propulsion and motility in rodents. *J. Pharmacol. Exp. Ther.* **249**, 444–449.

49. Pinto, L., Izzo, A., Cascio, M., et al. (2002) Endocannabinoids as physiological regulators of colonic propulsion in mice. *Gastroenterology* **123**, 227–234.
50. Krowicki, Z. K., Moerchbaecher, J. M., Winsauer, P. J., Digavalli, S. V., and Hornby, P. J. (1999) Δ^9 -Tetrahydrocannabinol inhibits gastric motility in the rat through cannabinoid CB₁ receptors. *Eur. J. Pharmacol.* **371**, 187–196.
51. Lehmann, A., Blackshaw, L. A., Brändén, L., et al. (2002) Cannabinoid receptor agonism inhibits transient lower esophageal sphincter relaxations and reflux in dogs. *Gastroenterology* **123**, 1129–1134.
52. Izzo, A. A., Mascolo, N., Capasso, R., Germano, M. P., De Pasquale, R., and Capasso, F. (1999) Inhibitory effect of cannabinoid agonists on gastric emptying in the rat. *Naunyn-Schmied. Arch. Pharmacol.* **360**, 221–223.
53. Landi, M., Croci, T., Rinaldi-Carmona, M., Maffrand, J.-P., Le Fur, G., and Manara, L. (2002) Modulation of gastric emptying and gastrointestinal transit in rats through intestinal cannabinoid CB₁ receptors. *Eur. J. Pharmacol.* **450**, 77–83.
54. Rivas, V. I. F. and Garcia, R. (1980) Inhibition of histamine-stimulated gastric acid secretion by Δ^9 -tetrahydrocannabinol in rat isolated stomach. *Eur. J. Pharmacol.* **65**, 317–318.
55. Adami, M., Frati, P., Bertini, S., et al. (2002) Gastric antisecretory role and immunohistochemical localization of cannabinoid receptors in the rat stomach. *Br. J. Pharmacol.* **135**, 1598–1606.
56. Coruzzi, G., Adami, M., Coppelli, G., Frati, P., and Soldani, G. (1999) Inhibitory effect of the cannabinoid receptor agonist WIN 55, 212-2 on pentagastrin-induced acid secretion in the anesthetized rat. *Naunyn-Schmied. Arch. Pharmacol.* **360**, 715–718.
57. Tyler, L., Hilland, C. J., and Greenwood-Van Meerveld, B. (2000) Inhibition of small intestinal secretion by cannabinoids is CB₁ receptor-mediated in rats. *Eur. J. Pharmacol.* **409**, 207–211.
58. Mascolo, N., Izzo, A. A., Babato, F., and Capasso, F. (1993) Inhibitors of nitric oxide synthetase prevent castor-oil-induced diarrhea in the rat. *Br. J. Pharmacol.* **108**, 861–864.
59. Robert, A., Nezamis, J. E., Lancaster, C., Hanchar, A.-J., and Klepper, M. S. (1976) Enteropooling assay: a test for diarrhea produced by prostaglandins. *Prostaglandins* **11**, 809–828.
60. Izzo, A. A., Capasso, R., Pinto, L., Di Carlo, G., Mascolo, N., and Capasso, F. (2001) Effect of vanilloid drugs on gastrointestinal transit in mice. *Br. J. Pharmacol.* **132**, 1411–1416.
61. Kirkham, T. C. and Williams, C. M. (2001) Endogenous cannabinoids and appetite. *Nutr. Res. Rev.* **14**, 65–86.
62. Croxford, J. L. (2003) Therapeutic potential of cannabinoids in CNS disease. *CNS Drugs* **17**, 179–202.
63. Berry, E. M. and Mechoulam, R. (2002) Tetrahydrocannabinol and endocannabinoids in feeding and appetite. *Pharmacol. Ther.* **95**, 185–190.
64. Mattes, R. D., Engelman, K., Shaw, L. M., and Elsohly, M. A. (1994) Cannabinoids and appetite stimulation. *Pharmacol. Biochem. Behav.* **49**, 187–195.

65. Graceffo, T. J. and Robinson, J. K. (1998) Delta-9-tetrahydrocannabinol (THC) fails to stimulate consumption of a highly palatable food in the rat. *Life Sci.* **62**, PL85–PL88.
66. Miczek, K. A. and Dixit, B. N. (1980) Behavioral and biochemical effects of chronic delta-9- tetrahydrocannabinol in rats. *Psychopharmacology* **67**, 195–202.
67. Colombo, G., Agabio, R., Diaz, G., Lobina, C., Reali, R., and Gessa, G.L. (1998) Appetite suppression and weight loss after the cannabinoid antagonist SR 141716A. *Life Sci.* **63**, 113–117.
68. Kirkham, T. C. and Williams, C. M. (2001) Synergistic effects of opioid and cannabinoid antagonists on food intake. *Psychopharmacology* **153**, 267–270.
69. Williams, C. M. and Kirkham, T. C. (2002) Observational analysis of feeding induced by Δ^9 - THC and anandamide. *Physiol. Behav.* **76**, 241–250.
70. Jamshidi, N. and Taylor, D. A. (2001) Anandamide administration into the ventro-medial hypothalamus stimulates appetite in rats. *Br. J. Pharmacol.* **134**, 1151–1154.
71. Williams, C. M. and Kirkham, T. C. (2002) Reversal of Δ^9 -THC hyperphagia by SR 141716A and naloxone but not dexfenfluramine. *Pharmacol. Biochem. Behav.* **71**, 333–340.
72. Kirkham, T. C., Williams, C. M., Fezza, F., and Di Marzo, V. (2002) Endocannabinoid levels in rat limbic forebrain and hypothalamus in relation to fasting, feeding and satiation: stimulation of eating by 2-arachidonoylglycerol. *Br. J. Pharmacol.* **136**, 550–557.
73. Arnone, M., Maruani, J., Chaperon, F., et al. (1997) Selective inhibition of sucrose and ethanol intake by SR 141716A, an antagonist of central cannabinoid (CB1) receptors. *Psychopharmacology* **132**, 104–106.
74. Simiand, J., Keane, M., Keane, P. E., and Soubrie, P. (1998) SR 141716A, a CB1 cannabinoid receptor antagonist, selectively reduces sweet food intake in marmoset. *Behav. Pharmacol.* **9**, 179–181.
75. Cota, D., Mariscano, G, Tschöp, M, et al. (2003) The endogenous cannabinoid system affects energy balance via central orexigenic drive and peripheral lipogenesis. *J. Clin. Invest.* **112**, 423–431.
76. Williams, C. M. and Kirkham, T.C. (1999) Anandamide induces overeating: mediation by central cannabinoid (CB1) receptors. *Psychopharmacology* **143**, 315–317.
77. Williams, C. M. and Kirkham, T. C. (2001) Hyperphagia induced by intra-accumbens injection of 2-arachidonoylglycerol. Symposium on the cannabinoids, Burlington, VT, *International Cannabinoid Res. Soc.*, p. 103.
78. Hao, S., Avraham, Y., Mechoulam, R., and Berry, E. M. (2000) Low dose anandamide affects food intake, cognitive function, neurotransmitter and corticosterone levels in diet-restricted mice. *Eur. J. Pharmacol.* **392**, 147–156.
79. Gomez, R., Navarro, M., Ferrer, B., et al. (2002) A peripheral mechanism for CB1 cannabinoid receptor-dependent modulation of feeding. *J. Neurosci.* **22**, 9612–9617.
80. Hesketh, P. K., Van Belle, S., Aapro, M., et al. (2003) Differential involvement of neurotransmitters through the time course of cisplatin-induced emesis as revealed by therapy with specific receptor antagonists. *Eur. J. Cancer* **39**, 1074–1080.

81. Gylys, J. A., Doram, K. M., and Buyniski, J. P. (1979) Antagonism of cisplatin induced emesis in the dog. *Res. Commun. Chem. Pathol. Pharmacol.* **23**, 61–67.
82. Shannon, H. E., Martin, W. R., and Silcox, D. (1978) Lack of antiemetic effects of Δ^9 - tetrahydrocannabinol in apomorphine-induced emesis in the dog. *Life Sci.* **23**, 49–54.
83. Stark, P. (1982) The pharmacologic profile of nabilone: anew antiemetic agent. *Cancer Treatment Rev.* 9 (Suppl. B) **11**, 1–6.
84. London, S. W., McCarthy, L. E., and Borison, H. L. (1979) Suppression of cancer chemotherapy-induced vomiting in the cat by nabilone, a synthetic cannabinoid. *Proc. Soc. Exp. Biol. Med.* **160**, 437–440.
85. McCarthy, L. E. and Borison, H. L. (1981) Antiemetic activity of N-methyllevonantradol and nabilone in cisplatin-treated cats. *J. Clin. Pharmacol.* **21**, 30S–37S.
86. Feigenbaum, J. J., Richmond, S. A., Weissman, Y., and Mechoulam, R. (1989) Inhibition of cisplatin-induced emesis in the pigeon by a non-psychotropic synthetic cannabinoid. *Eur. J. Pharmacol.* **169**, 159–165.
87. Ferrari, F., Ottani, A., and Giuliani, D. (1999) Cannabimimetic activity in rats and pigeons of HU 210, a potent antiemetic drug. *Pharmacol. Biochem. Behav.* **62**, 75–80.
88. Van Sickle, M. D., Oland, L. D., Mackie, K., Divison, J. S., and Sharkey, K. A. (2003) Δ^9 - Tetrahydrocannabinol selectively acts on CB₁ receptors in specific regions of dorsal vagal complex to inhibit emesis in ferrets. *Am. J. Physiol. Gastrointest. Liver Physiol.* **285**, G566–G576.
89. Kwiatkowska, G., Parker, L. A., Burton, P., and Mechoulam, R. (2004) A comparative analysis of the potential of cannabinoids and ondansetron to suppress cisplatin-induced emesis in the *Suncus murinus* (house musk shrew). *Psychopharmacology (Berl.)*, **174**, 254–259.
90. Darmani, N. A. (2001) Δ^9 -Tetrahydrocannabinol and synthetic cannabinoids prevent emesis produced by the cannabinoid CB₁ receptor antagonist/inverse agonist SR 141716A. *Neuropsychopharmacology* **24**, 198–203.
91. Darmani, N. A. (2001) Delta-9-tetrahydrocannabinol differentially suppresses cisplatin- induced emesis and indeces of motor function via cannabinoid CB₁ receptors in the least shrew. *Pharmacol. Biochem. Behav.* **69**, 239–249.
92. Darmani, N. A., Sim-Selly, L. J., Martin, B. R., Janoyan, J. J., Crim, J. L., and Breivogel, C. S. (2003) Antiemetic and motor depressive actions of CP55, 940: cannabinoid CB₁ receptor characterization, distribution and G-protein activation. *Eur. J. Pharmacol.* **459**, 83–95.
93. Van Sickle, M. D., Oland, L. D., Ho, W., et al. (2001) Cannabinoids inhibit emesis through CB₁ receptors in the brainstem of the ferret. *Gastroenterology* **121**, 767–774.
94. Simoneau, I. I., Hamza, M. S., Mata, H. P., et al. (2001) The cannabinoid agonist WIN 55, 212-2 suppresses opioid-induced emesis in ferrets. *Anesthesiology* **94**, 882–887.
95. Darmani, N. A. and Johnson, J. C. (2004) Central and peripheral mechanisms contribute to the antiemetic actions of delta-9-tetrahydrocannabinol against 5-hydroxytryptophan-induced emesis. *Eur. J. Pharmacol.* **488**, 201–212.

96. Darmani, N. A. and Crim, J .L. (2005) Delta-9-tetrahydrocannabinol prevents emesis more potently than enhanced locomotor activity produced by chemically diverse dopamine D₂/D₃ receptor agonists in the least shrew (*Cryptotis parva*), *Pharmacol. Biochem. Behav.* **80**, 35–44.
97. Darmani, N. A. (2001) The cannabinoid antagonist/inverse agonist SR 141716A reverses the antiemetic and motor depressant action of WIN 55, 212-2 in the least shrew. *Eur. J. Pharmacol.* **430**, 49–58.
98. Limebeer, C. L. and Parker, L. A. (1999) Delta-9-tetrahydrocannabinol interferes with the establishment and the expression of conditioned rejection reactions produced by cyclophosphamide: a rat model of nausea. *Neuroreport.* **10**, 3769–3772.
99. Parker, L. A., Mechoulam, R., and Schlievert, C. (2002) Cannabidiol, a nonpsychoactive component of cannabis and its synthetic dimethylheptyl homolog suppress nausea in an experimental model with rats. *Neuroreport.* **13**, 1–4.
100. Lowe, S. (1946) Studies on the pharmacology and acute toxicity of compounds with marijuana activity. *J. Pharmacol. Exp. Ther.* **88**, 154–161.

The Bioassay of Cannabinoids Using the Mouse Isolated Vas Deferens

Adèle Thomas and Roger G. Pertwee

Summary

The mouse isolated vas deferens is a nerve–smooth muscle preparation that serves as a highly sensitive and quantitative functional *in vitro* bioassay for cannabinoid CB₁ receptor agonists. Additionally, it is commonly used as a bioassay for competitive surmountable CB₁ receptor antagonists, and also provides a means for distinguishing neutral CB₁ antagonists from CB₁ inverse agonists. The bioassay of CB₁ receptor agonists relies on the ability of these ligands to produce concentration-related decreases in the amplitude of electrically evoked contractions of the vas deferens. This they do by acting on naturally expressed prejunctional neuronal CB₁ receptors to inhibit release of the contractile neurotransmitters, noradrenaline and ATP, that is provoked by the electrical stimulation. The bioassay of competitive surmountable CB₁ receptor antagonists involves determining the ability of these compounds to produce parallel dextral shifts in CB₁ receptor agonist log concentration–response curves in electrically stimulated tissues. The mouse vas deferens has also been used to measure the ability of anandamide to activate vanilloid (TRPV1) receptors, to monitor modulation by cannabinoids such as 6''-azido-2''-yne-cannabidiol and abnormal cannabidiol of contractions elicited in electrically unstimulated tissues by agonists for P2X purinoceptors or α_1 -adrenoceptors, and as a bioassay for the nonpsychoactive plant cannabinoid cannabidiol.

Key Words: CB₁ receptor agonists; CB₁ receptor antagonists; cannabidiol; 6''-azido-2''-yne-cannabidiol; abnormal-cannabidiol; P2X purinoceptors; α_1 -adrenoceptors; vanilloid (TRPV1) receptors; SR141716A; R-(+)-WIN55212; CP55940; anandamide; ATP; phenylephrine.

1. Introduction

One *in vitro* preparation that has been widely used as a bioassay for characterizing the pharmacological properties of CB₁ receptor agonists is the mouse isolated vas deferens. This bioassay relies on the presence in this tissue of native neuronal CB₁ receptors and on the ability of CB₁ agonists to interact with these receptors to produce a concentration-related decrease in the amplitude of

electrically evoked smooth muscle contractions by inhibiting contractile neurotransmitter release (1–6). These neurotransmitters are ATP, acting on P2X purinoceptors, and noradrenaline, acting on α_1 -adrenoceptors (7). The mouse isolated vas deferens has also been used to investigate the properties of competitive, surmountable CB₁ receptor antagonists: their ability to oppose the inhibitory effects of CB₁ receptor agonists and the ability of some of these antagonists to behave as inverse agonists when administered alone. For such a ligand, antagonistic potency is usually calculated from the size of the parallel dextral shift it produces in the log concentration–response curve of an established CB₁ receptor agonist such as *R*-(+)-WIN55212 or CP55940 (8). The presence of inverse agonism is indicated by the statistically significant increase in the amplitude of electrically evoked contractions that occurs when an inverse agonist such as SR141716A is added by itself (9), there being no evidence that endocannabinoids are released by the mouse isolated vas deferens when this is electrically stimulated (10,11). The nonpsychoactive plant cannabinoid cannabidiol shares the ability of competitive, surmountable CB₁ receptor antagonists to produce parallel dextral shifts in the log concentration–response curves of *R*-(+)-WIN55212 and CP55940 (12). Although the mechanism that underlies this effect seems to be CB₁ receptor independent, the effect can still be exploited for the bioassay of cannabidiol and related compounds. The mouse isolated vas deferens has also been used to investigate the ability of the endogenous cannabinoid anandamide to activate vanilloid (TRPV1) receptors (13) and of certain cannabinoids such as 6''-azido-2''-yne-cannabidiol and abnormal-cannabidiol to modulate contractile responses elicited by agonists for P2X purinoceptors or α_1 -adrenoceptors in electrically unstimulated tissues (11,12).

2. Materials

Because cannabinoids generally have very low water solubility, a non aqueous vehicle is required. Cannabinoids are generally stored at –20°C in ethanol (usually 1 mg/mL) or in dimethyl sulfoxide (DMSO; for more details see **Note 1**). If, like anandamide, a compound is particularly prone to oxidation, its ethanolic stock solution is stored under argon. For addition to organ baths in this laboratory, any ethanol is removed by evaporation, and cannabinoids are dispersed in Tween-80 and saline (14) or dissolved in DMSO (see **Note 1** and **Table 1**).

3. Methods

The following sections describe the dissection of the mouse vas deferens (**Subheading 3.1.**), the procedure for tissue set-up (**Subheading 3.2.**) and for the production and measurement of electrically induced contractions (**Subheadings 3.2.1.** and **3.2.2.**), the method for conducting field-stimulation experiments (**Subheadings 3.2.3.** and **3.3.**), and methods for performing exper-

Table 1
The Preparation Procedure for Some Common Cannabinoids, Stored at a Concentration of 1 mg/mL in Ethanol

Compound	Molecular weight	Volume ^a of stock solution evaporated (μL)	Vehicle ^b
Δ ⁹ -THC	314.47	188.68	DMSO
R-(+)-WIN55,212	522.61	313.57	DMSO/Saline (1:1 v/v)
CP55940	376.58	225.95	DMSO
Anandamide	347.54	208.52	DMSO
SR141716A	463.79	278.28	DMSO

^a This is the volume required to prepare a final organ bath concentration of 10 μM, assuming that 10 μL of cannabinoid is added to a 4-mL bath.

^b Once the ethanol has been completely evaporated, the cannabinoid is diluted in 150 μL of the vehicle.

iments with electrically unstimulated tissues (**Subheading 3.4.**). Data analysis is also discussed (**Subheadings 3.3.3.** and **3.4.3.**), as are some potential interpretational difficulties together with possible solutions (**Subheading 3.5.**).

3.1. Dissection

The animals used in this laboratory are albino MF1 mice that are at least 4 wk old (30–50 g). Each mouse is stunned by a blow to the head and killed by cervical dislocation. A vertical cut is made through the lower abdominal wall. Removal of the fatty tissue reveals the testes. These can be used to identify the vasa deferentia, each of which is attached to a testis via the epididymis. Gripping the epididymis with forceps, each vas deferens is cut free first from the testis and then from the connective tissue. The vas deferens is then removed from the mouse by cutting through its prostatic end. The isolated vas deferens should now be kept moist in physiological salt solution (solution A). This consists of modified Mg²⁺-free Krebs solution (118.2 mM NaCl, 4.75 mM KCl, 1.19 mM KH₂PO₄, 25.0 mM NaHCO₃, 11.0 mM glucose, and 2.54 mM CaCl₂). Before setting the tissue up in an organ bath, further removal of connective tissue, mesentery, and the epididymis is performed. Thread is attached to both ends of the vas deferens and the tissue mounted in an organ bath. The tissue is attached to a transducer under 0.5g of tension. In the organ bath the tissue is kept in solution A, which is maintained at 33–35°C and continuously bubbled with 95% O₂/5% CO₂ (*see* **Notes 2** and **3**). In this laboratory, 4-mL organ baths are used and vasa deferentia are mounted vertically (**Fig. 1**).

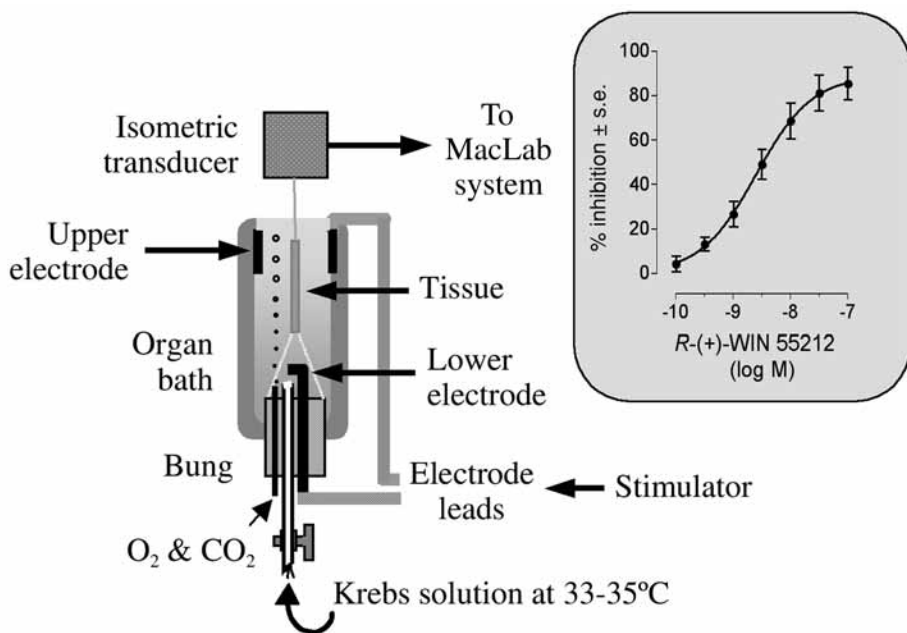


Fig. 1. Representation of the tissue set-up in the organ bath.

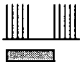
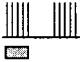



3.2. Tissue Set-Up

The next two sections describe the electrical stimulation procedures used in this laboratory (**Subheadings 3.2.1.** and **3.2.2.**). Whether cannabinoids are to be assayed using electrically stimulated tissue (**Subheading 3.3.**) or not (**Subheading 3.4.**), vasa deferentia are first subjected to an equilibration procedure that always involves electrical stimulation, as described in **Subheading 3.2.3.**

3.2.1. Electrical Stimulation Conditions

Contractions are usually evoked by applying 0.5-s trains of pulses of 110% maximal voltage (train frequency 0.1 Hz; pulse frequency 5 Hz; pulse duration 0.5 ms) (see **Note 4** and **Table 2** for more details). The amplitude of each monophasic contraction so induced appears to be determined more by released ATP than noradrenaline (**Subheading 1.**), as we have found that twitch amplitude is attenuated to a significantly greater extent by PPADS (a P2 receptor antagonist) than by prazosin (an α_1 -adrenoceptor antagonist) (**12**). Different stimulation conditions have been described by another laboratory (see **Note 5**).

Table 2
Simplified Electrical Stimulation Conditions on Grass S48 Stimulator (Grass Medical Instruments, Quincy, MA)

Parameter		Setting
Train rate		0.1 train/s
Train duration		500 ms
Stimulation rate		5 pulse/s
Delay		0.01 ms
Pulse duration		0.5 ms
Pulse size (Volts)		6×10 (25 Ω)

3.2.2. Electrically Induced Contractions

Tissue contractions are usually monitored by computer (Apple Macintosh or PC) connected to a data recording and analysis system (MacLab or PowerLab). These are linked via preamplifiers to Pioden UF1 isometric transducers (Harvard Apparatus), to which the tissue is attached. Electrical stimuli are generated by a Grass S48 stimulator, are amplified (channel attenuator; MedLab Instruments), and then divided to yield separate outputs to four organ baths (StimuSplitter; MedLab Instruments). As this laboratory sets up eight organ baths, two four-organ bath set-ups are employed. The stimuli are applied through a stainless steel electrode attached to the lower end of each bath and a platinum electrode attached to the upper end. Although this laboratory prefers to monitor tissue contractions by computer (*see also* **Note 6**), it is also possible to use flatbed recorders.

3.2.3. Equilibration Procedure

Each tissue is electrically stimulated over a period of 10 min, starting with a submaximal voltage and systematically increasing this output until a supra-maximal voltage is achieved (110% maximal). Electrical stimulation is then

Table 3
Dose Cycles and Typical Concentrations for Some Common Cannabinoids

Compound	Dose cycle (minutes) ^a	Typical concentrations (nM)
Δ^9 -THC	30	1 → 1000
R-(+)-WIN55,212	15	0.1 → 1000
CP55940	15	0.1 → 1000
Anandamide	15	1 → 10,000
SR141716A	— ^b	32, 100

^a The dose cycle (interval between doses) is dependent on the length of time taken for the cannabinoid to produce the maximum effect.

^b SR141716A is usually incubated for 30 min before the construction of a cannabinoid concentration–response curve is commenced (*see Subheading 3.3.2*).

stopped and the tissue rested for 10 min before subjecting it to further electrical stimulation for 2 min. This cycle of 10 min of rest followed by 2 min of stimulation is repeated until the tissue contractions exhibit a constant amplitude.

3.3. Assays Using Electrically Stimulated Tissues

One common feature of all these experiments is that tissues are not stimulated continuously but only for 2-min periods separated by periods in which no electrical stimuli are applied (*see Note 7*). These assays can be used to construct agonist concentration–response curves in the absence (**Subheading 3.3.1.**) or presence of an antagonist (**Subheading 3.3.2.**) or to follow the time course of the response to a single dose of agonist (*see Note 8*). Typical concentrations or concentration ranges used for a selection of cannabinoid receptor ligands can be found in **Table 3**. Only one cannabinoid concentration–response curve is constructed per experiment (*see Note 9*). How data from such experiments are analyzed is discussed in **Subheading 3.3.3.**

3.3.1. Agonist Concentration–Response Curves

Ideally the time required for the agonist under investigation to produce its full effect should be predetermined (*see Note 8*). For the construction of a concentration–response curve, the tissue is electrically stimulated to produce contractions 2 min prior to the addition of the lowest dose of agonist. The stimulator is then turned off and the tissue allowed to rest for the time, Y, required for the agonist to produce its full effect. After this time has elapsed, the tissue is once again electrically stimulated for 2 min prior to the addition of the second dose of agonist. This cycle is repeated until the concentration–response curve has been completed. This protocol is illustrated in **Fig. 2**. Concentration–

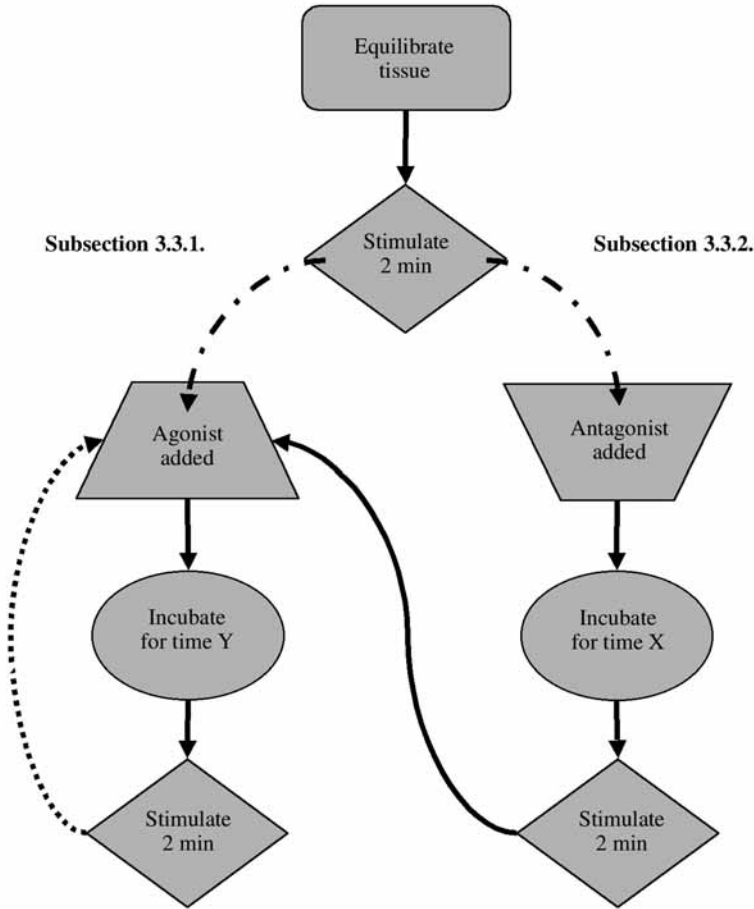


Fig. 2. Some protocols for assays using electrically stimulated tissues (*see Subheading 3.3.*).

response curves are constructed without bath wash-out between successive additions (*see Note 9* for explanation). [Table 3](#) shows dose cycles employed in this laboratory for some commonly used cannabinoid receptor agonists.

3.3.2. Agonist Concentration–Response Curves in the Presence of an Antagonist

Each tissue is electrically stimulated 2 min prior to the addition of the antagonist or its vehicle. After sufficient time, X, has elapsed for the antagonist to reach its pharmacological target (e.g., 30 min for the CB₁ receptor antagonist, SR141716A), the tissue is once again stimulated and the heights of the con-

tractions recorded for 2 min before a concentration–response curve of the agonist is constructed as described in **Subheading 3.3.1.** and portrayed in **Fig. 2.**

3.3.3. Data Analysis for Assays Using Electrically Stimulated Tissues

Analysis of the recorded data involves measuring the height of the last six contractions produced during each 2-min stimulation period. This includes the period immediately before the first addition of agonist, antagonist, or vehicle is made. For experiments with antagonists (**Subheading 3.3.2.**), any change in contraction height produced by the antagonist is monitored to establish whether the antagonist itself has any direct effect on the amplitude of electrically evoked contractions. SR141716A and cannabidiol are both ligands that can significantly enhance the height of electrically evoked contractions in the mouse vas deferens (**9,12**). The contraction amplitudes measured just prior to the addition of the first (lowest) dose of agonist serve as the baseline amplitudes with which each subsequent set of contraction heights is compared when calculating the percentage change in contraction height produced by the agonist.

For agonists, values for EC_{50} , for maximal effects (E_{max}) and for the SEM or 95% confidence limits of these values can be calculated by nonlinear regression analysis using the equation for a sigmoid concentration–response curve (GraphPad Prism; GraphPad Software, San Diego, CA). It is usually sufficient to replicate each concentration–response curve six times. The dissociation constant (K_B) of a competitive surmountable antagonist can be obtained by constructing agonist dose response curves in the presence of more than one concentration of the antagonist and then determining the slope ($1/K_B$) of the best-fit straight line of a plot of $(x-1)$ against B , constructed by linear regression analysis and constrained to pass through the origin (GraphPad Prism) (**15**). The equation for this graph is $(x-1) = B/K_B$, where x (the concentration ratio) is the concentration of a twitch inhibitor that produces a particular degree of inhibition in the presence of a competitive reversible antagonist at a concentration, B , divided by the concentration of the same twitch inhibitor that produces an identical degree of inhibition in the absence of the antagonist. K_B values of competitive surmountable antagonists can also be calculated by substituting a single concentration ratio value into the above equation. Values of the concentration ratio and its 95% confidence limits can be determined by symmetrical ($2 + 2$) dose parallel line assays (**16**), using responses to pairs of agonist concentrations located on the steepest part of each log concentration–response curve. This method can also be used to establish whether 2-point log concentration–response plots deviate significantly from parallelism.

3.4. Assays Using Electrically Unstimulated Tissue

As stated in **Subheading 3.2.**, even when bioassays are to be performed without electrical stimulation, all tissues are first subjected to an equilibration procedure that involves electrical stimulation (**Subheading 3.2.3.**). Bioassays without electrical stimulation are used, for example, to measure the ability of cannabinoids to modulate responses to α_1 -adrenoceptor and P2X receptor agonists that act directly on the smooth muscle to induce contractions. Care must be taken in such experiments to avoid the tissues becoming desensitized to these agents, particularly when high concentrations are used. Two protocols have been used in this laboratory to investigate interactions between cannabinoids and an α_1 -adrenoceptor agonist (phenylephrine, methoxamine or norepinephrine) or a P2X receptor agonist (β , γ -methyleneadenosine 5'-triphosphate) as described in **Subheadings 3.4.1.** and **3.4.2.** Both protocols initially involve the addition of a submaximal dose, A, of the selected agonist to the organ bath after which the resultant contractile response of the tissue is recorded. The agonist is then quickly washed out to avoid tissue desensitization. This procedure serves to identify responsive tissues, since occasionally a tissue will fail to contract in response to an α_1 -adrenoceptor or P2X receptor agonist. Additionally, in Protocol 2 (**Subheading 3.4.2.**) this initial response is compared with a subsequent contractile response induced by a second addition of this agonist (dose A) that on this occasion is made in the presence of a cannabinoid. How data from electrically unstimulated experiments are analyzed is discussed in **Subheading 3.4.3.** Examples of results obtained from such experiments can be found elsewhere ([11,12](#)).

3.4.1. Protocol 1

After establishing whether the tissues are responding to the α_1 -adrenoceptor or P2X receptor agonist (*see Subheading 3.4.*), either a cannabinoid or its vehicle is added to the organ bath, after which (time interval Y) a cumulative concentration–response curve is constructed for the chosen α_1 -adrenoceptor or P2X receptor agonist. This is achieved by adding the next dose to the bath as soon as the contractile response to the previous dose is complete, a protocol that reduces the risk of desensitization and that results in a dose cycle of about 2 min and in the production of a complete concentration–response curve within about 10 min (*see also Fig. 3*). To avoid desensitization problems, it is advisable not to attempt to obtain more than one concentration–response curve from any one tissue.

3.4.2. Protocol 2

The objective of this protocol is to establish the effect of a cannabinoid on the contractile response to a dose, A, of an α_1 -adrenoceptor or P2X receptor

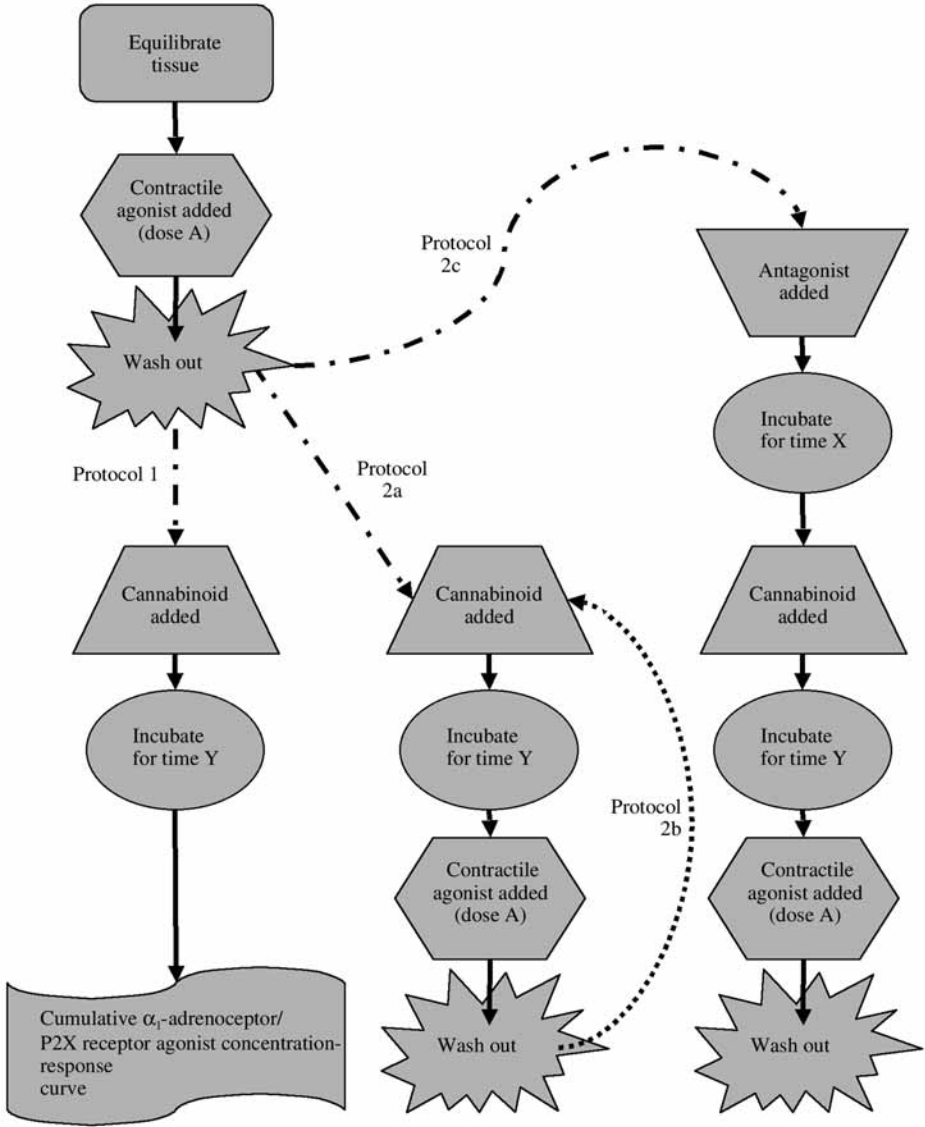


Fig. 3. The electrically unstimulated protocols described in **Subheading 3.4.**

agonist. This involves measuring either the effect of a single dose of a cannabinoid (Protocol 2a; *see Subheading 3.4.2.1.*) or the effects of a range of cannabinoid doses (Protocol 2b; *see Subheading 3.4.2.2.*) on the contractile response

to dose A of the α_1 -adrenoceptor or P2X receptor agonist. Additionally, the effect of a cannabinoid can be measured in the presence of an antagonist (Protocol 2c; *see Subheading 3.4.2.3.*). Protocols 2a, 2b, and 2c are depicted in **Fig. 3**.

3.4.2.1. PROTOCOL 2A

The first step is to add the submaximal dose, A, of the selected contractile agonist. This is washed out as soon as a full contraction has been induced. One dose of the cannabinoid under investigation (or its vehicle) is now added and, after the period of time Y the submaximal dose A of the agonist is once again applied. The resultant contractile response is compared with the response that was elicited at the beginning of the experiment.

3.4.2.2. PROTOCOL 2B

This section describes the protocol for investigating a range of cannabinoid doses on the contractile response to the submaximal dose A of the α_1 -adrenoceptor or P2X receptor agonist. As can be seen from **Fig. 3**, this protocol is an extended version of protocol 2a, described in **Subheading 3.4.2.1**. Thus, after the second contractile response to dose A of the α_1 -adrenoceptor or P2X receptor agonist has been determined, the cannabinoid and the contractile agonist are immediately washed out and another (higher) dose of cannabinoid then added. After the period of time Y dose A of the contractile agonist is once again applied to the organ bath, the response measured, and the bath contents immediately washed out. This cycle can be continued with progressively higher doses of cannabinoid.

3.4.2.3. PROTOCOL 2C

This protocol is used to determine the ability of an antagonist to oppose cannabinoid-induced alterations of α_1 -adrenoceptor or P2X receptor agonist-induced contractions. As in Protocols 2a and 2b, the response to a submaximal dose, A, of the selected contractile agent is first determined. Then, a cannabinoid antagonist or its vehicle is added to the organ bath. After sufficient time, X, has elapsed for the antagonist to reach its pharmacological target, a cannabinoid or its vehicle is added to the organ bath. As shown in **Fig. 3**, dose A of the α_1 -adrenoceptor or P2X receptor agonist is applied again after the period of time Y has elapsed and its contractile effect measured. This is followed by a bath wash-out. If required, further additions can now be made of the selected contractile agent and of progressively higher doses of cannabinoid as described for Protocol 2b (*see Subheading 3.4.2.2.*). The antagonist must then be replaced after each bath wash-out.

3.4.3. Data Analysis of Assays Using Electrically Unstimulated Tissues

Using a 0.5-g weight to calibrate the system, the amplitudes of evoked contractions are converted into the amount of applied tension that would be required in order to produce an equivalent increase. How the data are then analyzed depends on whether Protocol 1 or 2 was used. **Subheading 3.4.3.1.** discusses data analysis for Protocol 1, and **Subheadings 3.4.3.2. to 3.4.3.4.** data analysis for protocols 2a, 2b, and 2c.

3.4.3.1. DATA ANALYSIS FOR PROTOCOL 1

This involves measuring the height of the contraction induced by each dose of the α_1 -adrenoceptor or P2X receptor agonist in the presence of a cannabinoid or its vehicle. In the mouse vas deferens, the addition of either an α_1 -adrenoceptor or P2X receptor agonist results in a transient contraction followed by relaxation, even when there is no wash-out. Extra care is therefore needed to ensure that a measure is obtained of the maximal increase in tension produced by each dose of the contractile agonist. The size of each contraction should be measured from a point on the baseline just prior to the start of the induced contraction. Contractile responses are expressed in g tension, as discussed in **Subheading 3.4.3.**

3.4.3.2. DATA ANALYSIS OF PROTOCOL 2A

The initial contraction produced by the submaximal dose A of the chosen contractile agonist is determined. This is then compared to the contraction produced by a second addition of dose A of the same contractile agent, performed after addition to the organ bath of the cannabinoid (or its vehicle). Contractile responses are expressed in g tension (**Subheading 3.4.3.**), and comparisons can be made using Student's two-tailed *t*-test for paired data.

3.4.3.3. DATA ANALYSIS OF PROTOCOL 2B

When the effects of multiple doses of a cannabinoid on the response to the single dose A of the contractile agent are investigated, the size of each contraction produced in the presence of the cannabinoid can be compared to the size of the initial contraction evoked in the absence of the cannabinoid. This may be achieved by normalizing the data such that, for example, each contractile response elicited in the presence of the cannabinoid is expressed as a percentage of the initial contractile response, normalized to 100%. The effects of different cannabinoid doses can be compared with the initial contraction by performing a one-way analysis of variance (ANOVA) followed by a *post hoc* test such as Dunnett's test.

3.4.3.4. DATA ANALYSIS OF PROTOCOL 2C

The method used for analyzing the effect of a cannabinoid in the presence of an antagonist in electrically unstimulated tissues is essentially the same as the method used to analyze data obtained from experiments performed using Protocol 2a (**Subheading 3.4.3.2.**).

3.5. Some Interpretational Difficulties

Although there is good evidence that cannabinoids can act via neuronal cannabinoid CB₁ receptors to inhibit electrically evoked contractions of the mouse isolated vas deferens (**Subheading 1.**), there is also evidence that this tissue contains additional pharmacological targets with which some cannabinoids can interact to produce this inhibitory response. Thus, the endocannabinoid anandamide appears to inhibit electrically evoked contractions of the vas deferens by acting not only on CB₁ receptors but also on neuronal vanilloid (TRPV1) receptors (**Subheading 1.**). There is also evidence that anandamide and several other established CB₁/CB₂ receptor agonists can act through a “CB₂-like” cannabinoid receptor to inhibit electrically evoked contractions of this tissue preparation ([17](#)). In addition, other as yet uncharacterized neuronal and non neuronal targets for cannabinoids may be present in the mouse vas deferens ([11,12](#)). A further complication is that some cannabinoids, including the nonpsychoactive plant cannabinoid cannabidiol may affect the amplitude of electrically evoked contractions or modulate the ability of CB₁ receptor agonists to inhibit the twitch response by acting on more than one pharmacological target. Such cannabinoids may, for example, not only act on neuronal targets but also affect the ability of endogenously released ATP and/or noradrenaline to induce contractions ([11,12](#)).

For the characterization of a putative cannabinoid CB₁ receptor agonist, these problems can be addressed to some extent by determining the K_B value of a selective competitive surmountable cannabinoid receptor antagonist for antagonism of the agonist under investigation (**Subheadings 3.3.2. and 3.3.3.**). This K_B value can then be compared with the CB₁ K_i value of the antagonist determined in binding experiments and with its K_B value for antagonism in the vas deferens of one or more established cannabinoid receptor agonists such as CP55940 or R-(+)-WIN55212. Similarly, for the characterization of a putative cannabinoid receptor antagonist, its K_B value for antagonism of an established cannabinoid receptor agonist in the vas deferens can be compared with its CB₁ K_i value. Twitch inhibition through TRPV1 receptors can be prevented by adding a TRPV1 receptor antagonist such as capsazepine or iodoresiniferatoxin to the organ bath or by using capsaicin to desensitize these receptors ([13](#); Thomas and Pertwee, unpublished). It should also be possible to determine the

extent to which a cannabinoid twitch inhibitor is acting on a non-CB₁ target by performing experiments with vasa deferentia obtained from CB₁ receptor knockout mice. Finally, the ability of cannabinoids to act on prejunctional neurons rather than on the smooth muscle of the mouse vas deferens can be investigated by directly monitoring noradrenaline release from isolated vasa deferentia (3,6).

4. Notes

1. When cannabinoids are stored in ethanol, this solvent must be removed by evaporation and replaced with the chosen vehicle (e.g., DMSO, but *see* Table 1 for more details). This can be achieved by using a rotary evaporator (as in this laboratory) or by bubbling the ethanolic solution with argon or nitrogen.
2. The vas deferens has been described as the most robust and hardiest of a range of isolated smooth muscle-containing preparations (18). Even so, it is still essential to ensure that the tissue is kept moist and that overstretching of the tissue is avoided during dissection. The tissue is set up under a tension of 0.5 g, using a 0.5-g weight for calibration; exerting a greater force than this could result in failure of the tissue to contract in response to field stimulation or to an α_1 -adrenoceptor or P2X receptor agonist. Care must also be taken to ensure that the vas deferens is set up in the center of the bath and that neither the tissue nor the thread is touching any part of the organ bath.
3. Tissues occasionally fail to contract in response to electrical stimulation. Such failure can arise from errors made during the preparation of the modified Krebs solution. If after setting up tissues in the organ baths it is found that they are not responding to electrical stimulation, it may be possible to revive the tissues by immediately replacing the fluid in the baths with some freshly prepared modified Krebs solution.
4. To set up the stimulation conditions described in Subheading 3.2.1. on a Grass S48 Stimulator (Grass Medical Instruments, Quincy, MA), the settings on the apparatus should be positioned as detailed in Table 2. Additionally it should be noted that train mode is set at "repeat," pulses at "single," and stimulation mode repeat at "off."
5. An Organon research group has recently published optimal stimulation data for the bioassay of cannabinoid receptor agonists using the mouse isolated vas deferens (19,20). The stimulation conditions described in Subheading 3.2.1. approximate closely these optimal conditions.
6. The advantage of using the computer-based method for monitoring tissue contractions becomes apparent on completion of experiments involving many concentrations of an agonist. Use of the computer and the associated MacLab/PowerLab program allows quick and accurate measurement of the size of the contractions produced by the tissue. By clicking on the baseline and then the peakline, the computer program is able to calculate the contraction height. Even so, some laboratories still prefer to use flatbed recorders since these provide an instant and permanent hard copy of the experimental traces. Additionally, the use of flatbed recorders facilitates performance of data analysis while the experiment is running.

7. When the mouse isolated vas deferens is stimulated continuously, the size of the evoked contractions tends to lessen significantly with time. However, when the tissues are subjected to alternate periods of stimulation and rest (**Subheading 3.3.**), this effect is less marked, allowing bioassays to be performed over a reasonable length of time (about 6 h).
8. One method for establishing the dose cycle to be used for constructing the concentration–response curve of a particular twitch inhibitor is to perform a time-course experiment with a single dose of the inhibitor. This dose is added to the tissue in the organ bath and then at particular times after this addition (e.g., 5, 10, 15, 30, 45, 60, 90, 120, and 150 min), the tissue is stimulated for 2 min and the height of resulting contractions recorded. The time taken for inhibition of the electrically evoked contractions to reach a plateau is indicative of the time required for the test dose to produce its full effect. Time-course experiments can be repeated with other doses of the same twitch inhibitor. For some cannabinoids it can take more than 60 min for the response to a particular dose to develop fully in the vas deferens (**14**). Typical dose cycles for some commonly used cannabinoids are shown in **Table 3**.
9. As most cannabinoids are highly lipophilic, it is not possible to reverse their effects by washing them out of the vas deferens. Consequently, all cannabinoid concentration–response curves are constructed cumulatively with no wash-out between additions, and no more than one such concentration–response curve is constructed per tissue. This high lipophilicity also necessitates the use of a special washing procedure between experiments. Thus, after each experiment, the organ bath set-up is washed through with warm acidified water (an approx 1% solution of 1 *N* hydrochloric acid in water), followed by distilled water. Each bath is then filled with ethanol, which is left in the bath overnight. On the day of the next experiment, it is important to eliminate all traces of this ethanol not only by draining it off but also by subjecting each bath to a thorough wash-out with modified Krebs solution. Periodically, the whole organ bath set-up is dismantled and sonicated in distilled water and detergent (Camtox, Camlab Limited, Cambridge, UK) to ensure that cannabinoids do not accumulate in the system.

References

1. Pertwee, R. G. (1997) Pharmacology of cannabinoid CB₁ and CB₂ receptors. *Pharmacol. Ther.* **74**, 129–180.
2. Pertwee, R. G., Coutts, A. A., Griffin, G., Fernando, S. R., McCallion, D., and Stevenson, L. (1996) Presence of cannabinoid CB₁ receptors on prejunctional neurones of certain isolated tissue preparations: a brief review. *Med. Sci. Monit.* **2**, 840–848.
3. Trendelenburg, A. U., Cox, S. L., Schelb, V., Klebroff, W., Khairallah, L., and Starke, K. (2000) Modulation of ³H-noradrenaline release by presynaptic opioid, cannabinoid and bradykinin receptors and β -adrenoceptors in mouse tissues. *Br. J. Pharmacol.* **130**, 321–330.
4. Schlicker, E. and Kathman, M. (2001) Modulation of transmitter release via presynaptic cannabinoid receptors. *Trends Pharmacol. Sci.* **22**, 565–572.

5. Howlett, A. C., Barth, F., Bonner, T. I., Cabral, G., Casellas, P., Devane, W. A., Felder, C. C., Herkenham, M., Mackie, K., Martin, B. R., Mechoulam, R., and Pertwee, R. G. (2002) International Union of Pharmacology. XXVII. Classification of cannabinoid receptors. *Pharmacol. Rev.* **54**, 161–202.
6. Schlicker, E., Redmer, A., Werner, A., and Kathmann, M. (2003) Lack of CB₁ receptors increases noradrenaline release in vas deferens without affecting atrial noradrenaline release or cortical acetylcholine. *Br. J. Pharmacol.* **140**, 323–328.
7. von Kügelgen, I. and Starke, K. (1991) Noradrenaline-ATP co-transmission in the sympathetic nervous system. *Trends Pharmacol. Sci.* **12**, 319–324.
8. Pertwee, R. G., Griffin, G., Lainton, J. A. H., and Huffman, J. W. (1995) Pharmacological characterization of three novel cannabinoid receptor agonists in the mouse isolated vas deferens. *Eur. J. Pharmacol.* **284**, 241–247.
9. Pertwee, R. G., Fernando, S. R., Griffin, G., Ryan, W., Razdan, R. K., Compton, D. R., and Martin, B. R. (1996) Agonist-antagonist characterization of 6'-cyanohept-2'-yne- Δ^8 -tetrahydrocannabinol in two isolated tissue preparations. *Eur. J. Pharmacol.* **315**, 195–201.
10. Pertwee, R. G., Fernando, S. R., Griffin, G., Abadji, V., and Makriyannis, A. (1995) Effect of phenylmethylsulphonyl fluoride on the potency of anandamide as an inhibitor of electrically evoked contractions in two isolated tissue preparations. *Eur. J. Pharmacol.* **272**, 73–78.
11. Thomas, A., Ross, R. A., Saha, B., Mahadevan, A., Razdan, R. K., and Pertwee, R. G. (2004) 6''-Azidohept-2''-yne-cannabidiol: a potential neutral, competitive cannabinoid CB₁ receptor antagonist. *Eur. J. Pharmacol.* **487**, 213–221.
12. Pertwee, R. G., Ross, R. A., Craib, S. J., and Thomas, A. (2002) (–)-Cannabidiol antagonizes cannabinoid receptor agonists and noradrenaline in the mouse vas deferens. *Eur. J. Pharmacol.* **456**, 99–106.
13. Ross, R. A., Gibson, T. M., Brockie, H. C., Leslie, M., Pashmi, G., Craib, S. J., Di Marzo, V., and Pertwee, R. G. (2001) Structure-activity relationship for the endogenous cannabinoid, anandamide, and certain of its analogues at vanilloid receptors in transfected cells and vas deferens. *Br. J. Pharmacol.* **132**, 631–640.
14. Pertwee, R. G., Stevenson, L. A., Elrick, D. B., Mechoulam, R., and Corbett, A. D. (1992) Inhibitory effects of certain enantiomeric cannabinoids in the mouse vas deferens and the myenteric plexus preparation of guinea-pig small intestine. *Br. J. Pharmacol.* **105**, 980–984.
15. Tallarida, R. J., Cowan, A., and Adler, M. W. (1979) pA₂ and receptor differentiation: a statistical analysis of competitive antagonism. *Life Sci.* **25**, 637–654.
16. Colquhoun, D. (1971) *Lectures on Biostatistics*, Oxford University Press, Oxford.
17. Griffin, G., Fernando, S. R., Ross, R. A., McKay, N. G., Ashford, M. L. J., Shire, D., Huffman, J. W., Yu, S., Lainton, J. A. H., and Pertwee, R. G. (1997) Evidence for the presence of CB₂-like cannabinoid receptors on peripheral nerve terminals. *Eur. J. Pharmacol.* **339**, 53–61.
18. Westfall, T. D. and Westfall, D. P. (2001) Pharmacological techniques for the in vitro study of the vas deferens. *J. Pharmacol. Toxicol. Methods* **45**, 109–122.

19. McMillan, K., Jolly, N., Bom, A., and Cottney, J. (2003) Effect of electrical field stimulation parameters on the potency of two cannabinoid agonists in the mouse vas deferens. *Proc. Br. Pharmacol. Soc.* at <http://www.pa2online.org/Vol1Issue3abst043P.html>.
20. Campbell, C., Jolly, N., Bom, A., and Cottney, J. (2003) The actions of six cannabinoid agonists in mouse vas deferens preparations under two different stimulation conditions. *Proc. Br. Pharmacol. Soc.* at <http://www.pa2online.org/Vol1Issue3abst044P.html>.

Assessment of Cannabis Craving Using the Marijuana Craving Questionnaire

Stephen J. Heishman and Edward G. Singleton

Summary

Cannabis is the most widely used illicit drug in the United States, with 14.6 million current users. Cannabis-dependent individuals presenting for treatment typically report cannabis craving; however, the phenomenon has received little research attention. In the absence of a valid, multidimensional questionnaire to assess cannabis craving, we developed the Marijuana Craving Questionnaire (MCQ). The MCQ consists of four constructs or factors that characterize cannabis craving: compulsivity, emotionality, expectancy, and purposefulness. A separate score is calculated for each factor. The MCQ can be used to measure cue-elicited craving in a research setting or natural craving in cannabis-dependent individuals presenting for treatment. Either the 47-item or 12-item version can be used, and standardized instructions for completion of the MCQ should be given. The MCQ can be administered using a paper and pencil form or a computerized version. In a research setting, the MCQ should be administered immediately after cue presentation and repeated frequently to capture the full time course. In a treatment setting, the MCQ should be administered at intake and during and at the end of treatment.

Key Words: Cannabis; marijuana; craving; desire; urge; questionnaire; human; self-report.

1. Introduction

Cannabis is the most widely used illicit drug in the United States, accounting for 75% of all reported illicit drug use in 2002, and national surveys estimate 14.6 million current (past month) cannabis users (1). However, little research has been conducted on cannabis craving. Drug craving is typically described as one component of drug dependence, leading to continued drug use and relapse after treatment or during periods of drug abstinence (2). For example, craving for cannabis was reported by 93% of cannabis-dependent adults seeking treatment (3), and craving intensity increased significantly during periods of cannabis abstinence (4).

Given the absence of a psychometrically valid instrument with which to measure cannabis craving, we developed a multidimensional questionnaire (5). The full version of the Marijuana Craving Questionnaire (MCQ) contains 47 items and was administered to 217 current cannabis smokers not seeking treatment. Exploratory and confirmatory factor analyses indicated that four constructs characterized marijuana craving: (1) *compulsivity*, an inability to control marijuana use; (2) *emotionality*, use of marijuana in anticipation of relief from withdrawal or negative mood; (3) *expectancy*, anticipation of positive outcomes from smoking marijuana; and (4) *purposefulness*, intention and planning to use marijuana for positive outcomes. Further testing indicated that the MCQ is a reliable and valid measure of cannabis craving (6). The length of the 47-item MCQ could limit its use in clinic settings and in research studies in which measures are repeated frequently. Thus, we constructed a 12-item version of the MCQ by selecting the three items from each factor that exhibited optimal within-factor reliability (Cronbach's α coefficient) and interitem correlation.

2. Materials

2.1. Assessing Cannabis Craving in a Research Setting

1. Approved study protocol and consent form.
2. Cannabis use history form.
3. Craving cues.
4. 47-item or 12-item MCQ.
5. Physiological equipment to record heart rate and skin conductance (Coulbourn Instruments, Lehigh Valley, PA).

2.2. Assessing Cannabis Craving in a Treatment Setting

1. Cannabis use history form.
2. 12-item MCQ.

3. Methods

The methods described below outline the assessment of cue-elicited cannabis craving in a research setting and natural craving in a treatment or clinic setting.

3.1. Assessing Cannabis Craving in a Research Setting

The measurement of cue-elicited cannabis craving in studies testing human research volunteers is described in **Subheadings 3.1.1.–3.1.7.** This includes (1) recruiting cannabis users who are not seeking treatment for their cannabis use, (2) obtaining written informed consent from research participants, (3) training participants in completion of the MCQ, (4) cue presentation to elicit a craving response, (5) measuring the craving response with the MCQ and physiological

recording devices, and (6) debriefing participants before they are discharged from the laboratory.

3.1.1. Recruiting Research Volunteers

The use of cannabis-experienced participants who are not seeking treatment for their cannabis use is critical. There are no proven methods for long-lasting craving reduction; thus, it would be unethical to elicit craving in individuals who were trying to reduce or quit using cannabis. A thorough screening procedure, including a history of cannabis use (*see Note 1*), will generally ensure that appropriate participants are enrolled in the study.

3.1.2. Obtaining Informed Consent

As in any study involving human research volunteers, an Institutional Review Board (IRB) must approve the study protocol and consent form. When the IRB office has released the stamped consent form to the investigator, participants can be enrolled in the study. The consent form consists of a description of study procedures, any risks that are involved, monetary compensation if any, and investigators' contact information should participants have questions or concerns. When a participant understands all aspects of the study and potential risks, the investigator and participant sign the consent form; a copy is given to the participant.

3.1.3. Training in Completion of MCQ

The only aspect of the MCQ with which participants might be unfamiliar is the 7-point Likert scale that is used to record responses to each statement of the MCQ. For this reason, it is important that all participants be given standard instructions before the study begins (*see Note 2*). [Table 1](#) presents the 12-item MCQ; its scoring is discussed in [Note 3](#).

3.1.4. Craving Induction

Various types of cues have been used to elicit craving in drug users ([7](#)). We have recently used imagery scripts that were recorded on compact disc and presented auditorially to participants via headphones ([6](#)). Scripts described situations that depicted a person experiencing either a desire to smoke cannabis (low-craving script), a strong desire to smoke (high-craving script), or made no mention of smoking cannabis (no-craving script). All scripts were written with positive emotional tone (*see Note 4* for sample scripts). Participants are instructed to close their eyes while they listen to the scripts, to imagine themselves in the scene, and to continue imagining until they hear a tone. Each imagery trial consists of 120 s of baseline physiological recording, 60 s of script presentation, and 30 s of continued imagery. A rest period of 5–10 min should

Table 1
12-Item Marijuana Craving Questionnaire

1. Smoking marijuana would be pleasant right now.
STRONGLY DISAGREE ____ : ____ : ____ : ____ : ____ : ____ : ____ STRONGLY AGREE
2. I could not easily limit how much marijuana I smoked right now.
STRONGLY DISAGREE ____ : ____ : ____ : ____ : ____ : ____ : ____ STRONGLY AGREE
3. Right now, I am making plans to use marijuana.
STRONGLY DISAGREE ____ : ____ : ____ : ____ : ____ : ____ : ____ STRONGLY AGREE
4. I would feel more in control of things right now if I could smoke marijuana.
STRONGLY DISAGREE ____ : ____ : ____ : ____ : ____ : ____ : ____ STRONGLY AGREE
5. Smoking marijuana would help me sleep better at night.
STRONGLY DISAGREE ____ : ____ : ____ : ____ : ____ : ____ : ____ STRONGLY AGREE
6. If I smoked marijuana right now, I would feel less tense.
STRONGLY DISAGREE ____ : ____ : ____ : ____ : ____ : ____ : ____ STRONGLY AGREE
7. I would not be able to control how much marijuana I smoked if I had some here.
STRONGLY DISAGREE ____ : ____ : ____ : ____ : ____ : ____ : ____ STRONGLY AGREE
8. It would be great to smoke marijuana right now.
STRONGLY DISAGREE ____ : ____ : ____ : ____ : ____ : ____ : ____ STRONGLY AGREE
9. I would feel less anxious if I smoked marijuana right now.
STRONGLY DISAGREE ____ : ____ : ____ : ____ : ____ : ____ : ____ STRONGLY AGREE
10. I need to smoke marijuana now.
STRONGLY DISAGREE ____ : ____ : ____ : ____ : ____ : ____ : ____ STRONGLY AGREE
11. If I were smoking marijuana right now, I would feel less nervous.
STRONGLY DISAGREE ____ : ____ : ____ : ____ : ____ : ____ : ____ STRONGLY AGREE
12. Smoking marijuana would make me content.
STRONGLY DISAGREE ____ : ____ : ____ : ____ : ____ : ____ : ____ STRONGLY AGREE

separate each imagery trial, and the three imagery conditions (no, low, and high craving) should be randomized across participants to avoid the confounding of a condition order effect.

3.1.5. Measurement of Craving

The MCQ should be administered before the study begins (baseline) and immediately after the imagery trial because craving levels peak at this time.

The MCQ can be administered using paper and pencil forms or using a computerized version. Advantages to the paper and pencil method are that it requires no equipment other than the form, a pencil, and perhaps a clipboard; however, it will have to be scored by hand, which introduces the possibility of human error. A computerized version presents the MCQ items one at a time, and participants respond using the mouse or keyboard to move a cursor to indicate their response. Repeated administration of the MCQ should continue for sufficient time to observe a complete time course. Responses to tobacco imagery cues have been shown to remain at peak levels for at least 15 min (8).

3.1.6. Physiological Recording (Optional)

Typically, the primary measure in craving studies is self-reported responses on questionnaires such as the MCQ. However, certain physiological measures have reliably shown changes during cue-elicited craving episodes in the laboratory. Heart rate and skin conductance are two of the most reliable effects (7). Participants should be connected to any physiological recording devices during a training session to allow them to become familiar with the equipment. Experimental sessions should begin by connecting participants to the equipment, which can then record responses during the entire session.

3.1.7. Debriefing

At the conclusion of a session, participants should undergo a debriefing session to reduce potentially heightened craving. The debriefing session entails 10–15 min of guided progressive relaxation. This procedure involves alternatively tensing and relaxing the major muscle groups of the body (e.g., neck, shoulders, arms, legs). As the various muscle groups are tensed and relaxed, the person is encouraged to note the difference between muscle tension and relaxation. Relaxation has been shown to reduce craving in the laboratory (6,9,10). Participants should not be released from the laboratory until their self-reported cravings at the end of the relaxation session are less than or equal to their craving levels at the start of the session.

3.2. Assessing Cannabis Craving in a Treatment Setting

In a treatment or clinic setting, patients are typically assessed with numerous forms, questionnaires, and interviews. To reduce burden on patients, we suggest using the 12-item MCQ rather than the full version.

3.2.1. Training on Completion of MCQ

As discussed above (**Subheading 3.1.3.**), patients should be given instructions before completing the MCQ (*see Note 2*).

3.2.2. Measurement of Craving

The use of the MCQ in a treatment setting may be more flexible than in a research setting. A patient's level of craving may be assessed at initial intake or at baseline before entering treatment. Craving can then be measured periodically during and at the end of treatment to determine treatment outcome. Presumably, craving levels will decrease as a person reduces cannabis use or achieves abstinence.

4. Notes

1. At a minimum, a history of cannabis use should include the following: age of first use, age when use became regular (e.g., weekly, monthly), lifetime estimate of number of times using cannabis, frequency of use in past 6 mo, frequency of use in past 30 d, amount (e.g., number of joints) typically used at one time, and type of cannabis preparation typically used.
2. Each item of the MCQ is rated on a 7-point Likert scale from *strongly disagree* to *strongly agree*. The following instructions should appear at the top of the MCQ form or on the computer monitor if using a computerized version and should be read aloud to the participant the first time it is completed: "Indicate how strongly you agree or disagree with each of the following statements by placing a check mark in one of the spaces between *strongly disagree* and *strongly agree*. The closer you place your check mark to one end or the other indicates the strength of your agreement or disagreement. If you don't agree or disagree with a statement, place your check mark in the middle space. Please complete every item. We are interested in how you are thinking or feeling right now as you are filling out the questionnaire."
3. All items are scored on a scale ranging from 1 (*strongly disagree*) to 7 (*strongly agree*). For the 12-item MCQ, the scores of the three items in each factor should be summed for a total factor scale score (range 3–21). Factor 1 (*compulsivity*) consists of items 2, 7, and 10; factor 2 (*emotionality*) consists of items 4, 6, and 9; factor 3 (*expectancy*) consists of items 5, 11, and 12; and factor 4 (*purposefulness*) consists of items 1, 3, and 8 (see [Table 1](#)).
4. *No-Craving Script*: You're at the beach lying on a blanket. The warm sun penetrates your skin and relaxes you thoroughly. A fresh breeze blows over your body as you run your hands through the clean white sand and let the grains fall through your fingers. You're feeling refreshed and at ease, and pleasant thoughts run through your mind. You can hear the sounds of waves splashing rhythmically against the shore. Nearby some children are playing a game. A bright red beach ball lands near your blanket. You look up and see two of the children running toward you to get their ball. You stand up, pick up the ball and toss it to them. They laugh and giggle and run back to their game. You go to the blanket and lie down. You're enjoying this day completely.

Low-Urge Script: You're on the phone talking to friend you haven't seen in a year. This is a long distance call and the phone connection is not very good; there's

a lot of static on the line and you can hear other voices faintly in the background. Your friend just told you that he's making plans to visit you in a couple of weeks. You're happy and excited. The two of you always had great times in the past, and you know that it's going to be a fantastic visit. The static gets worse and it's hard to hear your friend. You suggest that you hang up and call right back so the two of you can make definite plans. As you hang up the phone you remember the bag of marijuana that you bought earlier and think about smoking a joint. A smile comes to your face as you think how much fun the two of you will have together.

High-Urge Script: You're at a friend's house sitting in a big comfortable chair. You're with people you've known for a long time and you're enjoying yourself very much. You're feeling relaxed and totally at ease. Many of your friends are smoking marijuana. As you sit there listening to the conversation and music, you begin to think about how enjoyable a joint would be. The smoke begins to fill the room and you think about how satisfying it would be to hold a joint between your fingers. The more you think about smoking marijuana, the stronger your desire becomes. Maybe tonight when you're with your friends and having a good time, it would be okay to get stoned. How could you really enjoy yourself fully unless you were smoking pot? Your desire to smoke becomes really intense and you know that there's no good reason not to smoke any of the joints being passed around.

References

1. Substance Abuse and Mental Health Services Administration. (2003) *Overview of Findings from the 2002 National Survey on Drug Use and Health* (DHHS Publication No. SMA 03-3836), Rockville, MD.
2. American Psychiatric Association. (2000) *Diagnostic and Statistical Manual of Mental Disorders* (4th ed., text rev.), American Psychiatric Association, Washington, DC.
3. Budney, A. J., Novy, P. L., and Hughes, J. R. (1999) Marijuana withdrawal among adults seeking treatment for marijuana dependence. *Addiction* **94**, 1311-1321.
4. Budney, A. J., Hughes, J. R., Moore, B. A., and Novy, P. L. (2001) Marijuana abstinence effects in marijuana smokers maintained in their home environment. *Arch. Gen. Psychiatry* **58**, 917-924.
5. Heishman, S. J., Singleton, E. G., and Liguori, A. (2001) Marijuana Craving Questionnaire: development and initial validation of a self-report instrument. *Addiction* **96**, 1023-1034.
6. Singleton, E. G., Trotman, A. J.-M., Zavahir, M., Taylor, R. C., and Heishman, S. J. (2002) Determination of the reliability and validity of the Marijuana Craving Questionnaire using imagery scripts. *Exp. Clin. Psychopharmacol.* **10**, 47-53.
7. Carter, B. L. and Tiffany, S. T. (1999) Meta-analysis of cue-reactivity in addiction research. *Addiction* **94**, 327-340.
8. Heishman, S. J., Saha, S., and Singleton, E. G. Imagery-induced tobacco craving: duration and lack of assessment reactivity bias. *Psychol. Addict. Behav.*, **18**, 284-288.
9. Singleton, E. G., Anderson, L. M., and Heishman, S. J. (2003) Reliability and validity of the Tobacco Craving Questionnaire and validation of a craving-

- induction procedure using multiple measures of craving and mood. *Addiction* **98**, 1537–1546.
10. Ehrman, R. N., Robbins, S. J., Childress, A. R., Goehl, L., Hole, A. V., and O'Brien, C. P. (1998) Laboratory exposure to cocaine cues does not increase cocaine use by outpatient subjects. *J. Subst. Abuse Treat.* **15**, 431–435.

Methods for Studying Acute and Chronic Effects of Marijuana on Human Associative Processes and Memory

Robert I. Block

Summary

This chapter summarizes the methods and results of studies in which the author examined the acute or chronic effects of marijuana on human associative processes and memory. Eleven tests used to assess marijuana's effects on associative processes, semantic memory, and episodic memory are described.

Key Words: Δ^9 -tetrahydrocannabinol; acute effects; associative processes; chronic effects; constrained associations; episodic memory; free associations; free recall; human; learning; marijuana; memory; paired-associate learning; reaction time; recall; retrieval; semantic memory; THC.

1. Introduction

This chapter summarizes the methods and results of seven studies (1–7) in which the author examined the acute or chronic effects of marijuana on human associative processes and memory. Both semantic and episodic memory were examined. Semantic memory refers to memory for meanings of words, concepts, rules, abstract ideas, and so on, whereas episodic memory refers to memory for temporally dated episodes or events in a person's life, e.g., “autobiographical” information (8). Associative processes, semantic memory, and episodic memory were examined using three, three, and five different tests, respectively. The tests of associative processes, semantic memory, and episodic memory are listed in Tables 1–3, respectively, along with information about the results, the type of marijuana effects studied (i.e., acute or chronic), characteristics of subjects, periods of abstinence from marijuana use prior to testing, and doses of marijuana that were administered, if any. The results and other information in the tables may pro-

vide some indication of the potential utility of the different tests for future studies. The methodological details of each test are provided in the **Notes** section. This chapter is restricted to methodology and results. Theoretical issues are considered in the original articles and are not addressed here.

In the studies of acute effects (*1–5*), marijuana was administered by smoking under double-blind conditions. The research assistant guided the subject in paced smoking procedures. Cigarettes that contained either 10 mg or 19 mg of Δ^9 -tetrahydrocannabinol (THC) were compared with placebo cigarettes that contained inactive, cannabinoid-extracted marijuana with only trace amounts of THC. In the studies of chronic effects (*6,7*), chronic marijuana users were compared with nonusers, i.e., control subjects. In the initial study of chronic marijuana users (*6*), these users were also grouped according to frequency of marijuana use.

2. Associative Processes

Associative processes can be studied with free or constrained associations. With free associations, for example, the subject might be presented with a stimulus word and asked to respond with the first word of any kind that comes to mind as an association. With constrained associations, for example, the subject might be presented with a category name and asked to respond with an example of that category. The response must relate to the stimulus word in some specified way with constrained associations, whereas no required relationship is specified for free associations.

2.1. Acute Effects

As indicated in **Table 1**, smoking a marijuana cigarette containing 10 mg of THC produced changes in subjects' responses in constrained association tests in which they were presented with a category name (e.g., CLOTHING) and provided examples of that category for 2 min or were presented with a category name followed by a letter (e.g., WEAPON — G) and provided an instance of that category beginning with that letter (e.g., GUN) (*3*). In both tests marijuana produced changes in the direction of giving more uncommon associations. Changes in the direction of giving more uncommon associations were likewise produced by smoking a marijuana cigarette containing a higher dose of THC (19 mg) in a test in which subjects were presented with a word and cued to give either a free association or one of five types of constrained associations (*5*).

2.2. Chronic Effects

As indicated in **Table 1**, the test in which subjects were presented with a word and cued to give either a free association or one of five types of constrained associations was also used to study the effects of chronic marijuana use. No effects were observed.

Table 1
Studies of Associative Processes

Reference	MJ effects studied	MJ Users— <i>n</i> , gender, mean age	MJ Users—MJ usage characteristics	Non-users— <i>n</i> , gender, mean age	Non-users—MJ usage characteristics	Abstinence period	Acute dose	Cognitive test	Results
3, Exp 1	Acute	48 men. 23 yr	Min = 2/mo in last 6 mo, median = 2/wk in last 6 mo	None	—	Min = 24 h	10 mg THC vs 0 mg THC	Giving examples of categories (Note 1)	During middle 40 s period of 2 min allowed per category, MJ altered normative frequency and rated typicality of instances given in direction of more uncommon associations.
3, Exp 2	Acute	36 men. 24 yr	Min = 2/mo in last 6 mo, median = 3/wk in last 6 mo	None	—	Min = 24 h	10 mg THC vs 0 mg THC	Giving examples of categories beginning with specified letters (Note 2)	MJ altered the content of responses, i.e., response rate and percent of targets, in direction of more uncommon associations, but did not alter RT in an analogous manner.

(continues)

Table 1
(Continued)

Reference	MJ effects studied	MJ Users— <i>n</i> , gender, mean age	MJ Users—MJ usage characteristics	Non-users— <i>n</i> , gender, mean age	Non-users—MJ usage characteristics	Abstinence period	Acute dose	Cognitive test	Results
5	Acute	48 men. 21 yr	88% current, 12% experienced (but not current) users; median for current users = 1–4/wk	None	—	Min = day of session and preceding 3 d	19 mg THC vs 0 mg THC	Free and constrained associations (Note 3)	MJ altered normative frequency of responses given in direction of more uncommon associations and slowed response time
6	Chronic	144 (112 men, 32 women). 23 yr	64 1–4/wk, 28 5–6/wk, 52 ≥7/wk on average for min = 2 yr (means at these frequencies = 5.5 yr, 5.8 yr, and 6.2 yr, respectively)	72 (57 men, 15 women). 23 yr	0–2/lifetime	Min = 24 h	None	Free and constrained associations (Note 3)	No effect of MJ use

Note: Abbreviations are as follows: Exp = Experiment; min = minimum; MJ = marijuana; RT = reaction time; THC = Δ^9 -tetrahydrocannabinol.

3. Semantic Memory

Although tests of associative processes involve retrieval from semantic memory, the structure of semantic memory and the processes involved in retrieving information from it have typically been studied with tests that involve measurement of reaction times (RTs) for making simple decisions. Such tests are considered in this section.

3.1. Acute Effects

As indicated in [Table 2](#), the studies examined the effects of smoking a marijuana cigarette containing 10 mg of THC on RTs for deciding if an item belonged to a specified category (with trials such as FRUIT — APPLE and FRUIT — CROWN) ([1](#)); deciding if two items belonged to the same category (with trials such as APPLE APPLE, APPLE PEACH, and APPLE BLUEBIRD) ([1](#)); and letter-matching, i.e., deciding whether two letters had the same name (with trials such as AA, Aa, and Ab) ([4](#)). Although marijuana slowed overall RT in some tests, this slowing did not appear to be specific to memory, i.e., marijuana did not influence the RT effects produced by several within-test experimental manipulations, suggesting that it did not slow semantic memory-retrieval mechanisms or alter them in a manner promoting access to uncommon associations. Thus, the changes in the direction of giving more uncommon associations that were observed as acute effects of marijuana in the tests of associative processes ([Subheading 2.1.](#)) did not appear to be directly attributable to underlying, general alterations of semantic memory retrieval mechanisms.

3.2. Chronic Effects

Effects of chronic marijuana use on semantic memory were not assessed because the studies of acute effects, which were conducted earlier, did not show any marijuana-induced changes in semantic memory-retrieval mechanisms.

4. Episodic Memory

Episodic memory ([8](#)) is commonly studied by presenting some information such as a list of words one or more times and testing the subject's ability to remember it. A conceptual distinction is made between the processes of storing information in relatively persisting form in long-term memory and retrieving this information once it has been stored. Various experimental methods have been developed in efforts to assess these processes.

4.1. Acute Effects

As indicated in [Table 3](#), smoking a marijuana cigarette containing 10 mg of THC did not affect recall in a paired-associate learning test in which subjects were presented with a list of pairs of words ([2](#)). Memory was assessed by pre-

Table 2
Studies of Semantic Memory

Reference	MJ effects studied	MJ Users— <i>n</i> , gender, mean age	MJ Users—MJ usage characteristics	Non-users— <i>n</i> , gender, mean age	Non-users—MJ usage characteristics	Abstinence period	Acute dose	Cognitive test	Results
1, Exp 1	Acute	36 men. 24 yr	Min = 2/mo in last 6 mo, median = 3/wk in last 6 mo	None	—	Min = 24 h	10 mg THC vs 0 mg THC	Deciding if item belongs to specified category (Note 4)	MJ slowed overall RT. MJ did not influence the RT advantage of common instances over uncommon instances, suggesting that it did not alter semantic memory retrieval mechanisms in a manner promoting access to uncommon associations.
1, Exp 2	Acute	40 men. 23 yr	Min = 2/mo in last 6 mo, median = 3.5/wk in last 6 mo	None	—	Min = 24 h	10 mg THC vs 0 mg THC	Deciding if two items belong to same category (Note 5)	MJ did not slow overall RT. MJ did not influence the RT effects produced by varying the type of trial, the type of instance, or the priming condition, suggesting that it did not slow semantic memory retrieval mechanisms or alter them in a manner promoting access to uncommon associations.
4	Acute	24 men. 23 yr	Min = 2/mo in last 6 mo, median = 2.5/wk in last 6 mo	None	—	Min = 24 h	10 mg THC vs 0 mg THC	Letter-matching (Note 6)	MJ slowed overall RT, but slowing was uninfluenced by test manipulations and, therefore, apparently unrelated to memory retrieval.

Note: For abbreviations, see [Table 1](#).

Table 3
Studies of Episodic Memory

Reference	MJ effects studied	MJ Users— <i>n</i> , gender, mean age	MJ Users—MJ usage characteristics	Non-users— <i>n</i> , gender, mean age	Non-users—MJ usage characteristics	Abstinence period	Acute dose	Cognitive test	Results
2	Acute	48 men. 22 yr	Min = 2/mo in last 6 mo, median = 2.3/wk in last 6 mo	None	—	Min = 24 h	10 mg THC vs 0 mg THC	Paired-associate learning (Note 7)	MJ did not affect overall recall or the improvement in recall produced by visual imagery instructions. MJ decreased the rated vividness of described images.
5	Acute	48 men. 21 yr	88% current, 12% experienced (but not current) users; median for current users = 1–4/wk	None	—	Min = day of session and preceding 3 d	19 mg THC vs 0 mg THC	Text learning (Note 8)	MJ reduced both immediate and delayed recall and slowed RT.
5	Acute	48 men. 21 yr	88% current, 12% experienced (but not current) users; median for current users = 1–4/wk	None	—	Min = day of session and preceding 3 d	19 mg THC vs 0 mg THC	Paired associate learning of associated and unassociated words (Note 9)	MJ reduced overall recall of associations; this effect varied for different types of associations

(continues)

Table 3
(Continued)

Reference	MJ effects studied	MJ Users— <i>n</i> , gender, mean age	MJ Users—MJ usage characteristics	Non-users— <i>n</i> , gender, mean age	Non-users—MJ usage characteristics	Abstinence period	Acute dose	Cognitive test	Results
5	Acute	48 men. 21 yr	88% current, 12% experienced (but not current) users; median for current users = 1–4/wk	None	—	Min = day of session and preceding 3 d	19 mg THC vs 0 mg THC	Buschke's Test (Note 10)	MJ reduced overall recall, long-term retrieval, and consistent long-term retrieval
6	Chronic	144 (112 men, 32 women). 23 yr	64 1–4/wk, 28 5–6/wk, 52 ≥7/wk on average for min = 2 yr (means at these frequencies = 5.5 yr, 5.8 yr, and 6.2 yr, respectively)	72 (57 men, 15 women). 23 yr	0–2/lifetime	Min = 24 h	None	Text learning (Note 8)	No effect of MJ use
6	Chronic	144 (112 men, 32 women). 23 yr	64 1–4/wk, 28 5–6/wk, 52 ≥7/wk on average for min = 2 yr (means at these frequencies = 5.5 yr, 5.8 yr, and 6.2 yr, respectively)	72 (57 men, 15 women). 23 yr	0–2/lifetime	Min = 24 h	None	Paired associate learning of associated and unassociated words (Note 9)	No effect of MJ use

Table 3
(Continued)

Reference	MJ effects studied	MJ Users— <i>n</i> , gender, mean age	MJ Users—MJ usage characteristics	Non-users— <i>n</i> , gender, mean age	Non-users—MJ usage characteristics	Abstinence period	Acute dose	Cognitive test	Results
6	Chronic	144 (112 men, 32 women). 23 yr	64 1-4/wk, 28 5-6/wk, 52 ≥ 7/wk on average for min = 2 yr (means at these frequencies = 5.5 yr, 5.8 yr, and 6.2 yr, respectively)	72 (57 men, 15 women). 23 yr	0-2/lifetime	Min = 24 h	None	Buschke's Test (Note 10)	Individuals who used MJ ≥ 7/wk (relative to non-users) impaired in long-term retrieval and consistent long-term retrieval for high-imagery (but not low-imagery) words.
7	Chronic	18 (9 men, 9 women). 22 yr.	≥ 7/wk on average (mean = 18/wk); using at this rate for min = 2 yr, mean = 3.9 yr	13 (6 men, 7 women). 23 yr.	Never (<i>n</i> = 10) or 1-2/lifetime (<i>n</i> = 3)	Min = 24 h of monitored preceded by 7 h of unmonitored abstinence (means = 27.8 h and 15.7 h, respectively, for free recall)	None	Buschke's Test and subsequent free recall (Note 11)	MJ users needed more presentations to learn and relearn list to criterion before neuroimaging. During neuroimaging, they showed no overall recall impairment, but for new list showed a stronger recency effect.

Note: For abbreviations, see Table 1.

senting the initial word from each pair, with subjects instructed to supply the second word in each pair. Smoking a marijuana cigarette containing a higher dose of THC (19 mg) impaired recall in a different paired-associate learning test administered in a subsequent study (5). The drug effect on recall was influenced by the types of associative relationships between pairs of words (*see Note 9*) and by the length of time that subjects held the smoke in their lungs. These influences are illustrated in **Fig. 1**. In this study (5), smoking a marijuana cigarette containing 19 mg of THC also impaired recall of paragraphs in a text learning test and a list of words in Buschke's Test (9). The latter test involves a "selective reminding" technique during the learning process (*see Note 10*) that allows scoring several aspects of memory in addition to total recall. Results with this technique indicated that marijuana impaired long-term retrieval and consistent long-term retrieval (5).

4.2. Chronic Effects

As indicated in **Table 3**, effects of chronic marijuana use were examined with the three tests of episodic memory used to examine effects of smoking a marijuana cigarette containing 19 mg of THC. In Buschke's Test, chronic marijuana users who used seven or more times weekly on average for the previous 2 yr or more (the heaviest usage group) showed deficits, in comparison to nonusers, for long-term retrieval and consistent long-term retrieval of high-imagery (but not low imagery) words (*see Note 10*) (6). These effects are illustrated in **Fig. 2**, as is a more equivocal difference among the user groups in effects of imagery on short-term retrieval. No effects of chronic marijuana use were observed in the paired-associate learning test or the text learning test. In a later study that also used Buschke's Test (7), subjects learned a list of words to a criterion of two consecutive perfect recalls during an initial session, followed by relearning of the same list, again to a criterion of two consecutive perfect recalls, during a subsequent session. As illustrated in **Fig. 3**, chronic marijuana users who used seven or more times weekly on average for the last 2 yr required more presentations than nonusers in learning and relearning the list to criterion during these two sessions. In a subsequent functional neuroimaging session, when subjects were presented with a different list of words a single time and asked to recall the words, the chronic marijuana users showed an increased recency effect, i.e., better recall for the words at the end of the list than those in the middle, relative to nonusers. This pattern suggests greater reliance on short-term memory by the chronic marijuana users.

5. Notes

1. *Giving examples of categories:* Eight common categories like CLOTHING with a large number of concrete instances were used. Normative data were available on

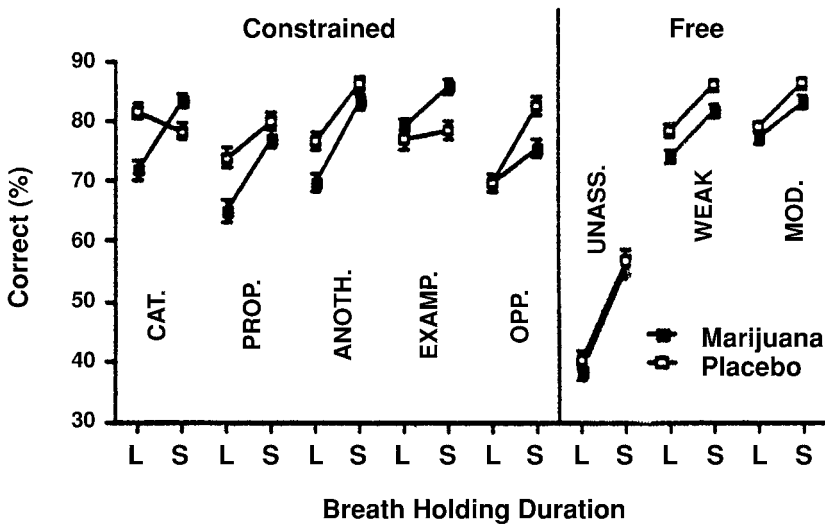


Fig. 1. Acute effects of marijuana on paired-associate learning. Significant impairments produced by marijuana containing 19 mg of THC (relative to placebo) and long (relative to short) breath-holding duration, and drug \times associative type and drug \times breath-holding duration \times associative type interactions, for percentage correct. The research assistant guided the subjects in paced smoking procedures, which involved long or short breath-holding durations for different subjects. The drug \times breath-holding duration interaction is shown separately for each of five associative types of constrained associations (**left**) and three associative types of free associations (**right**) (see **Note 9**). The drug \times associative type and drug \times breath-holding duration \times associative type interactions were attributable solely to constrained associations. The “example” associative type was primarily responsible for the drug \times associative type interaction for constrained associations. The overall impairment in learning produced by marijuana was shown by all the other associative types, but was reversed for the “example” associative type. The drug \times breath-holding duration \times associative type interaction for constrained associations partly reflected greater marijuana effects when the breath-holding duration was long rather than short for three associative types (“category,” “property,” and “another”), but not the others. The error bars indicate standard errors. Abbreviations: ANOTH. = another; CAT. = category; EXAMP. = example; L = long breath-holding duration; MOD. = moderately strong free associates; OPP. = opposite; PROP. = property; S = short breath-holding duration; UNASS. = unassociated words; WEAK = weak free associates. (From **ref. 5**.)

the frequency with which various instances are given as examples of the categories (10). Each subject was tested individually. The subject was instructed to give as many instances of each category as he or she could, in whatever order they came to mind. The experimenter spoke a category name and the subject gave instances

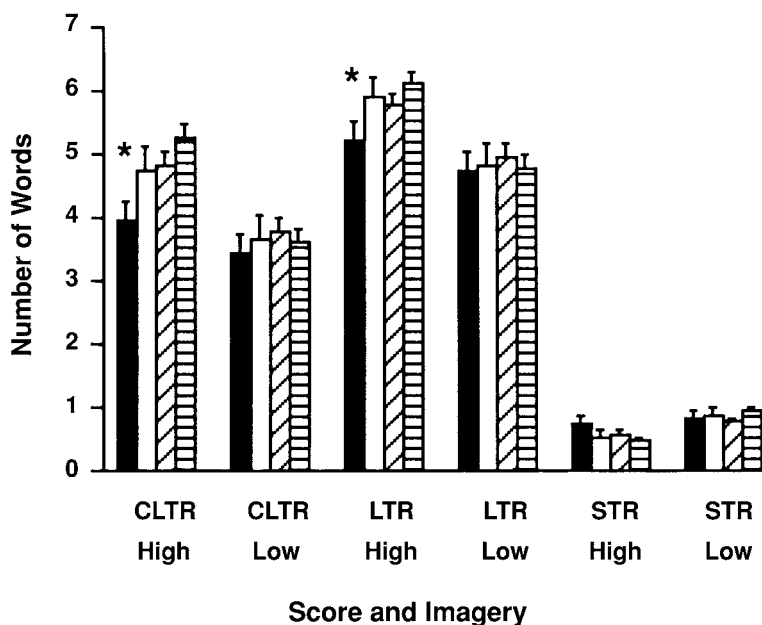


Fig. 2. Effects of chronic marijuana use on retrieval in Buschke's Test. Significant user group \times imagery interactions for consistent long-term retrieval, long-term retrieval, and short-term retrieval scores. The chronic marijuana users were classified as heavy, intermediate, or light users. These groups were defined by usage seven or more times, five to six times, or one to four times weekly on average for the previous 2 yr or more, respectively; and are represented by black bars, white bars, and bars with diagonal lines, respectively. Nonusers are represented by bars with horizontal lines. The scores, which are averaged over trials, are based on eight high-imagery words and eight low-imagery words (see **Note 10**). The error bars indicate standard errors. Heavy users showed impairment relative to nonusers in long-term retrieval for high-imagery but not low-imagery words (**center**). Consistent long-term retrieval, which measured the numbers of words reliably recalled from trial to trial without omission, showed a similar pattern, i.e., impairment in heavy users relative to nonusers for high-imagery but not low-imagery words (**left**). The data for short-term retrieval suggested a slight, opposite, compensatory tendency, but were equivocal (**right**); although the user group \times imagery interaction was significant, nonusers did not differ from heavy users (or from intermediate or light users). Significance is indicated as follows: * heavy users differed from nonusers by Dunnett's test, $p < 0.05$. Abbreviations are as follows: CLTR = consistent long-term retrieval; High = high-imagery words; Low = low-imagery words; LTR = long-term retrieval; STR = short-term retrieval. (From **ref. 6**.)

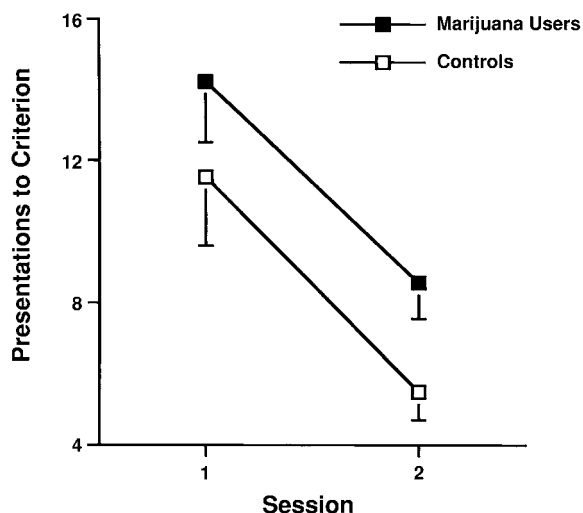


Fig. 3. Effects of chronic marijuana use on presentations to criterion in Buschke's Test. Learning a list of words to a criterion of two consecutive perfect recalls during an initial session, followed by relearning of the same list, again to a criterion of two consecutive perfect recalls, during a subsequent session (*see Note 11*). Numbers of presentations of the list required to reach the criterion are shown. Abbreviations: 1 = initial session; 2 = subsequent session. Chronic marijuana users performed more poorly than control subjects (nonusers), i.e., they required more presentations in learning and relearning the list to criterion during these two sessions. Not surprisingly, far fewer presentations were necessary to relearn the list during the second session than to learn it initially during the first session. Despite this, the impairment in the chronic marijuana users did not vary between sessions, i.e., the number of extra presentations required by chronic marijuana users, relative to control subjects, was similar for initial learning and relearning, $F < 1$ for the interaction of group and session. (From *ref. 7*.)

for 2 min. The responses were tape-recorded. Subjects rested for 1 min between categories. The order in which the categories were presented was counterbalanced over subjects. In scoring, exact repetitions of instances given previously were deleted. Subsequently, ratings of typicality were obtained for all instances given by subjects from a separate group of college students.

2. *Giving examples of categories beginning with specified letters:* On each of a series of trials, subjects were presented with a category name followed by a letter (e.g., WEAPON — G), and had to name an instance of that category beginning with that letter (e.g., GUN). The “target” for each category–letter combination was defined as the most frequently given instance of the category beginning with the specified letter according to frequency norms (*10–11*). Some trials used category–letter combinations with “common targets,” while others had “uncommon targets.” For

instance, WEAPON — G had a common target (GUN), whereas WEAPON — B had an uncommon target (BOMB), because when people give examples of WEAPONS, GUN is a more common example than BOMB. The experiment provided three measures for analysis: “response rate,” the percentage of trials in which any response was given; the RT for those responses; and “percent of targets,” the percentage of the subject’s responses that were the expected targets. Each category was used on two trials with different letters (e.g., WEAPON — G, then WEAPON — B). One third of the categories were tested at “long lags” and the remainder at “short lags,” the lag being defined as the number of trials on other, unrelated categories that intervened between the two trials on a given category. A series of 126 trials was formed using 63 categories and two letters for each category. The experimenter spoke a category name, following which a letter was presented by a tachistoscope. The subject responded orally. RT was measured by a voice-operated relay.

3. *Free and constrained associations.* For each of 100 words presented at a 10-s rate on a computer monitor, the subject gave a single word as an association. Response times were measured by a voice-activated relay. For 50 words, the subject was cued to provide a “free association,” i.e., any kind of association that came to mind; for 10 words each, the subject was to provide one of five types of “constrained associations,” i.e., a response that related to the stimulus in a specified way, cued by the words “another,” “category,” “example,” “opposite,” or “property.” Examples of these types are “book–magazine,” “aluminum–metal,” “fruit–apple,” “night–day,” and “banana–yellow,” respectively. The words were drawn from those used in a pilot study (12) involving other subjects, so that for each response in the present study the number of pilot subjects giving that response (“dominance”) could be scored, e.g., eight pilot subjects gave “sandal” in response to “shoe.”
4. *Deciding if item belongs to specified category:* Subjects saw a category name followed by an instance, and decided whether the instance was an example of the category as fast as possible. The correct response was “yes” for half the trials (e.g., FRUIT — APPLE) and “no” for the others (e.g., FRUIT — CROWN). The instance was a common example of the category on half of the “yes” trials, an uncommon example on the other half. Categories and instances were selected using normative data (10). Each of 32 categories appeared on two “yes” trials (one with a common instance and one with an uncommon instance) and on two “no” trials (with two different noninstances, i.e., items belonging to other categories). For each trial the category and, 2 s later, the instance were presented by a tachistoscope. The subject responded by pressing one of two switches labeled YES and NO to indicate whether or not the instance belong to the specified category. RT was measured.
5. *Deciding if two items belong to same category:* Subjects viewed two instances and decided whether they belonged to the same category (e.g., APPLE PEACH) or to different categories (e.g., APPLE BLUEBIRD). Half the trials were primed, half unprimed. On primed trials only, before seeing the two instances, subjects heard a prime, i.e., a category name like FRUIT, which informed them that one or both of

the forthcoming instances would come from that category. Half of the primed and unprimed trials involved common examples of categories; the other trials involved uncommon examples. For each combination of priming condition and type of instance (common vs uncommon), the correct response was "same" for half the trials and "different" for the rest, and the "same" trials were evenly divided between "same category" trials like APPLE PEACH, involving two distinct instances from the same category; and "same instance" trials like APPLE APPLE, on which a single instance appeared twice. To form 80 primed trials, 10 categories were chosen. Each category was used as the prime on eight trials, which were allocated in the required proportions to "same category," "same instance," and "different" trials with common vs uncommon instances. Each specific instance was used in only one primed trial. For each primed trial formed in this way, there was a corresponding unprimed trial using the identical pair of instances. On each trial, the experimenter spoke the category name on primed trials or the word "blank" (as a warning signal) on unprimed trials, following which the pair of instances was presented by a tachistoscope. The subject responded by pressing one of two switches labeled SAME and DIFFERENT to indicate whether or not the two instances belonged to the same category. RT was measured.

6. *Letter-matching*: On each trial, subjects saw two letters and decided whether or not they had the same name. Three kinds of trials were mixed together: "same-case" trials like "AA," on which the letters were physically identical; "same-name" trials like "Aa," on which the letters had the same name but appeared in opposite cases; and "different" trials like "Ab," on which the letters had different names. There were 80 "primed" trials and 80 "unprimed" trials. On primed trials only, before seeing the pair of letters, subjects heard a prime (i.e., a letter name like "A"), which informed them that one or both of the forthcoming letters would have that name (e.g., would be "A" or "a"). For each priming condition, the correct response was "same" for half the trials and "different" for the remainder, and the "same" trials were evenly divided between "same case" and "same name" trials. Ten letter names were used with equal frequencies as the prime on primed trials. The experimenter spoke a letter name on primed trials or the word "blank" (as a warning signal) on unprimed trials, following which a pair of letters was presented by a tachistoscope. The subject responded by pressing one of two switches labeled SAME and DIFFERENT to indicate whether the two letters had the same name. RT was measured.
7. *Paired-associate learning*: Three lists of high-imagery nouns, each consisting of 20 pairs of words, were tape-recorded. For each list, the tape contained two study trials (the 20 word pairs read sequentially) and two test trials (the 20 initial words read sequentially, with subjects instructed to orally supply the second word in each pair). The interval between successive pairs was 8 s. All subjects were given standard paired-associate learning instructions. Half the subjects were instructed to use visual imagery during learning—to try to learn by forming a vivid, detailed visual image of the two items in each pair in some interactive relationship. The other subjects were not instructed in any specific learning technique. Each subject received the two study and test trials on one list, then two on a second list, then two on a

third list, with a rest between lists. After the testing, subjects who were given imagery instructions were asked to describe their images for each word pair. Subsequently, a separate group of college students rated the vividness of the described images.

8. *Text learning*: The subject read a paragraph from an article in *Reader's Digest* on a computer monitor at his or her own pace, pressed a button when finished, and then recalled as much as possible in 3 min. The subject then reread the paragraph and recalled it again. Following this, the entire procedure was repeated with a different paragraph. In addition, delayed recall was tested 15 min before the end of the session. The subject's recall was tape-recorded for later scoring of the propositions recalled (13). Reading times were determined based on the subject's button presses.
9. *Paired-associate learning of associated and unassociated words*: A list of 30 pairs of words was presented at a 3-s rate on a computer monitor. Following this study trial, the initial word from each pair was presented in a test trial at a 5-s rate (with subjects instructed to orally supply the second word in each pair). Response times were measured by a voice-activated relay. These study and test trials were then repeated. Following this, two study and test trials were administered on a second list, consisting of different pairs of words. Each list consisted of three pairs representing each of the five types of constrained associations used in the free and constrained associations test (see Note 3), mixed with 15 other pairs, of which equal numbers involved moderately strong free associates, weak free associates, and unassociated words, e.g., "plumber-pipe," "tell-secret," and "carpet-laughter," respectively (12).
10. *Buschke's Test*. A list of 16 nouns, half "high-imagery" words that were easy to visualize (e.g., "bouquet") and the remainder "low-imagery" words that were difficult to visualize (e.g., "replacement") (14), was presented on a computer monitor at a rate of 3 s per word. The subject tried to recall as many words as possible. Seven learning and test trials were given consecutively. The subject tried to recall the whole list on each test trial, but, on learning trials after the first, was reminded only of the words missed on the immediately preceding test trial. This "selective reminding" technique allowed scoring several aspects of memory in addition to total recall (9). In essence, recall of a word without an immediately preceding reminder (i.e., recall on two successive trials) indicated that the word had entered (and presumably remained in) long-term storage. Recall of the word before this occurrence was attributed to short-term retrieval; after it, to long-term retrieval. Long-term retrieval was designated "consistent" when the word was never subsequently omitted.
11. *Buschke's Test and subsequent free recall*. The subject learned a list of 15 common words, such as "drum," "curtain," etc., to a criterion of two consecutive perfect recalls, using Buschke's "selective reminding" technique (9) (see Note 10). The subject's recall was oral. In a subsequent session, the subject relearned the same list, again to a criterion of two consecutive perfect recalls. Next, the subject was played a recording of the list and recalled it according to slightly different proce-

dures to be used in a functional neuroimaging session on the following day (e.g., computerized presentation of a digitized recording of the list), and again relearned it. During the neuroimaging session, the subject tried to orally recall the list relearned on the previous day, without any prompting. The subject then heard the computerized presentation of this list again and immediately tried to recall it. Subsequently, the subject heard a list of 15 different common words and immediately tried to recall them. These three tests differed in their relative demands on episodic memory encoding and retrieval. During each test, the subject recalled the words for 40 s and was asked to repeat them if he or she could not think of any more. The two lists were from the Rey Auditory Verbal Learning Test (15).

Acknowledgments

The research was supported in part by grants DA03988 and DA10554, NIDA, NIH, and RR00059, General Clinical Research Centers Program, NCRR, NIH.

References

1. Block, R. I. and Wittenborn, J. R. (1984) Marijuana effects on semantic memory: Verification of common and uncommon category members. *Psychol. Rep.* **55**, 503–512.
2. Block, R. I. and Wittenborn, J. R. (1984) Marijuana effects on visual imagery in a paired-associate task. *Percept. Mot. Skills* **58**, 759–766.
3. Block, R. I. and Wittenborn, J. R. (1985) Marijuana effects on associative processes. *Psychopharmacology* **85**, 426–430.
4. Block, R. I. and Wittenborn, J. R. (1986) Marijuana effects on the speed of memory retrieval in the letter- matching task. *Int. J. Addict.* **21**, 281–285.
5. Block, R. I., Farinpour, R., and Braverman, K. (1992) Acute effects of marijuana on cognition: Relationships to chronic effects and smoking techniques. *Pharmacol. Biochem. Behav.* **43**, 907–917.
6. Block, R. I. and Ghoneim, M. M. (1993) Effects of chronic marijuana use on human cognition. *Psychopharmacology* **110**, 219–228.
7. Block, R. I., O’Leary, D. S., Hichwa, R. D., et al. (2002) Effects of frequent marijuana use on memory-related regional cerebral blood flow. *Pharmacol. Biochem. Behav.* **72**, 237–250.
8. Tulving, E. (1972) Episodic and semantic memory, in *Organization of Memory* (Tulving, E. and Donaldson, W., eds.), Academic Press, New York, pp. 381–403.
9. Buschke, H. (1973) Selective reminding for analysis of memory and learning. *J. Verbal Learn. Verbal Behav.* **12**, 543–550.
10. Battig, W. F. and Montague, W. E. (1969) Category norms for verbal items in 56 categories: a replication and extension of the Connecticut category norms. *J. Exp. Psychol. Monogr.* **80**, 3, Pt. 2.
11. Shapiro, S. I., and Palermo, D. S. (1970) Conceptual organization and class membership: normative data for representatives of 100 categories. *Psychonom. Monogr.* (Suppl 3) (11, Whole No. 43).

12. Block, R. I., Farnham, S., Braverman, K., Hinrichs, J. V., and Ghoneim, M. M. (1989) Norms for free associations and five types of constrained associations. *Psychol. Rep.* **64**, 1065–1066.
13. Miller, J. R. and Kintsch, W. (1980) Readability and recall of short prose passages: a theoretical analysis. *J. Exp. Psychol. Hum. Learn. Mem.* **6**, 335–354.
14. Paivio, A., Yuille, J. C., and Madigan, S. A. (1968) Concreteness, imagery, and meaningfulness values for 925 nouns. *J. Exp. Psychol.* **76**, 1–25.
15. Rey, A. (1964) *L'examen Clinique en Psychologie*, Presses Universitaires de France, Paris.

Methods for Clinical Research Involving Cannabis Administration

David A. Gorelick and Stephen J. Heishman

Summary

Better scientific understanding of cannabis effects and the development of treatments for cannabis dependence require clinical studies involving cannabis administration. Cannabis can be administered by smoking a plant-derived cigarette or by oral or intravenous administration of Δ^9 -tetrahydrocannabinol (THC), the primary psychoactive chemical in cannabis. The smoked route is most commonly used outside the laboratory, but is subject to wide variation in absorbed dose. Oral synthetic THC is a legally marketed medication (dronabinol), also subject to wide pharmacokinetic variation, but offering a greater safety margin because of slower onset of action and lower potency. Intravenous THC offers precise investigator control of dose and timing. Acute adverse effects of cannabis administration include tachycardia, orthostatic hypotension, pulmonary irritation (if smoked), motor incoordination, cognitive impairment, anxiety, paranoia, and psychosis. Screening of research subjects should identify and exclude those with risk factors for such events, e.g., a history of significant cardiovascular, pulmonary, or psychiatric disorders.

Monitoring of subjects during cannabis administration should include heart rate, blood pressure, and mental status. Subjects should not be discharged from research participation until reevaluation has shown that they have returned to baseline status.

Key Words: Cannabis; marijuana; dronabinol; human; smoked; adverse events; cardiovascular; neurological; cognition; performance; subjective effects.

1. Introduction

Cannabis is the generic term for preparations derived from the hemp plant *Cannabis sativa*. The most commonly used preparations outside the laboratory are marijuana (combined leaves, stems, and flowering tops) and hashish (resin from the female flower). Cannabis is the most widely used illegal psychoactive drug, with an estimated 163 million current users worldwide (1) and 14.5 million in the United States (2). Cannabis contains more than 400

identified chemicals, including cannabinoids and terpenoids (3). The primary psychoactive constituent is Δ^9 -tetrahydrocannabinol (THC).

Some scientific issues related to cannabis use and abuse can be adequately addressed only by studies that involve experimental administration of cannabis to human research subjects (4–6). This type of study design may be necessary for valid attribution of putative cannabis effects (or abnormalities observed in those who use cannabis) to the actual pharmacological action of the drug and for controlled studies of cannabis interactions with other drugs and medications. In the natural environment, numerous confounding factors may be present when cannabis is taken. Possible confounding factors include pharmacological factors such as cannabis dose, purity, and rate of administration, subject factors such as physical and psychological condition at the time of cannabis intake, and environmental factors such as setting and time of day. Cannabis administration studies in a controlled research setting allow direct evaluation and manipulation of cannabis effects, which can elucidate mechanisms of action and further the development of new diagnostic tests or treatments (7).

Research involving experimental administration of cannabis requires research methods and poses risks to subjects little different, in principle, from other drug administration research, with two exceptions. Because cannabis is a psychoactive drug, psychological drug effects are often a prime scientific focus, and psychological adverse effects may be a prime concern. Because cannabis is an illegal drug in the United States and most countries worldwide, special legal and ethical considerations come into play.

This chapter reviews common research methods used to recruit, screen, and enroll research subjects, to administer cannabis to them, and to measure its physiological and psychological (including both subjective and cognitive) effects. Methods of monitoring for and minimizing possible adverse effects of cannabis (both physical and psychological) will also be described.

2. Materials

Cannabis or THC has been administered for human research purposes via the smoked, oral, and intravenous routes of administration. Each route of administration has experimental advantages and disadvantages. The smoked route mimics the most common way that cannabis is used outside the laboratory, but it can cause pulmonary adverse effects (see **Subheading 3.3.1.3.**) and is subject to wide individual variation in effective dose and time of onset because of differences in absorption, which depend on such factors as puff frequency, depth of inhalation, and retention of inhaled smoke (8,9) (see **Note 1**). Smoking or ingesting the cannabis plant material administers a large number of active chemicals in addition to THC, potentially causing a different range of effects

than does pure THC (3). Oral cannabis and THC also are associated with great individual variability in absorption and with reduced dose potency because of first-pass metabolism in the liver. The slower onset of effect and lower potency might be considered advantages from a safety perspective. Intravenous THC offers uniform absorption and precise investigator control of dosage and timing. Regardless of route of administration, maintenance of a double-blind design is important because significant expectancy effects are associated with cannabis administration (10,11).

The vast majority of recent US laboratory studies administering smoked cannabis have used standardized marijuana cigarettes provided by the US National Institute on Drug Abuse (NIDA) (*see Note 2*). These marijuana cigarettes resemble in size an unfiltered tobacco cigarette, weigh 700–1000 mg, and contain approx 1–4% of THC by weight, yielding maximum THC doses of 7–40 mg. (The actual effective dose will be up to 70% less because of pyrolysis of THC, loss in side-stream smoke, incomplete absorption, and metabolism in the lung.) The THC concentration in NIDA cigarettes is less than the typical THC content of marijuana available in the community, which may range from 4 to 10% or higher. THC dose for research purposes can be manipulated by using cigarettes that differ in THC content and/or by varying the number of puffs administered to subjects (one cigarette is usually completely consumed with five to eight puffs). NIDA also provides placebo cigarettes from which the THC has been chemically extracted. These cigarettes burn and smell the same as active marijuana cigarettes, but the plant material may differ somewhat in color (12) (*see Note 3*).

Cigarettes are typically held by the subject in a clip or plastic holder in order to allow smoking of the entire cigarette without risk of burning the fingers. Plastic holders offer the advantage of hiding the end of the cigarette, minimizing the chance of subjects getting clues to dosage from the appearance of the plant material (although this appears unlikely unless subjects have prior experience with NIDA-provided cigarettes). Cigarettes are usually smoked according to a paced procedure, such that the investigator dictates the duration of an inhalation (typically 5 s), the duration of breath-holding (typically 5–10 s), and the interpuff interval (typically 40–120 s) (e.g., *ref. 13*). This provides greater dosing consistency across subjects and reduces the chance of subjects exceeding study dose limits by smoking more than intended. Subjects should always have the opportunity to end a smoking session at any time if they experience adverse effects.

Cannabis can also be administered orally, although this route of administration is now rarely used experimentally. Marijuana plant material is crushed into a powder, which then is baked into a brownie or similar easily consumed food (14).

Oral synthetic THC is available in the United States as dronabinol (brand name Marinol®; Unimed Pharmaceuticals, Marietta, GA, a medication legally marketed as an appetite stimulant to treat weight loss due to acquired immunodeficiency syndrome (AIDS) and to treat nausea and vomiting due to cancer chemotherapy. It comes as soft gelatin capsules containing 2.5, 5, or 10 mg of dronabinol dissolved in sesame oil. The recommended doses are up to 20 mg/d for appetite stimulation and up to 15 mg/m² (of body surface area) up to six times a day for nausea and vomiting. Use of dronabinol offers several practical advantages to investigators. First, as a legal medication classified in Schedule III of the Controlled Substances Act (whereas cannabis and THC are in Schedule I), there are fewer complicated regulatory requirements for acquiring and storing the research medication. Second, dronabinol capsules can be stored in a cool environment or refrigerator, whereas cannabis cigarettes must be stored frozen. Third, use of dronabinol within the Food and Drug Administration (FDA)-recommended doses may reassure institutional review boards and potential subjects as to the safety of the study. These practical advantages must be weighed against the scientific disadvantages mentioned above.

THC has been administered intravenously in doses up to 5 mg (15). Because THC is poorly soluble in water, it must be mixed with human albumin or other solubilizing agents.

3. Methods

3.1. Research Subjects

3.1.1 Recruiting Subjects

The ethical principle of distributive justice requires that the burdens and benefits of research be distributed fairly across the population with the condition under study. The external validity (generalizability) of a study is enhanced when the study sample is representative of the population with the condition under study. Thus, for both ethical and scientific reasons, recruiting of subjects for cannabis-administration studies should involve the broadest possible population. Such studies will almost certainly enroll only subjects with some prior cannabis use (for reasons described below). Cannabis use and abuse occur in all US population groups, but is greatest among young adults 18–25 yr of age. The 2002 National Survey on Drug Use and Health (NSDUH) found that 17.3% of this age group were current (past month) cannabis users (2). Recruiting efforts could efficiently include sites with large concentrations of young adults, such as college campuses. However, individuals younger than the age of legal adulthood (18 or 21 yr) should not be recruited because legal and ethical considerations generally preclude the administration to minors of an illegal psychoactive drug such as cannabis.

Women comprise about 37% of current (past month) cannabis users in the United States (2), and should not be excluded *a priori* from cannabis administration studies. However, certain subgroups of women can be validly excluded on ethical and safety grounds. Oral synthetic THC (dronabinol) is rated in pregnancy category C (risk cannot be ruled out because adequate human studies are lacking and animal studies have shown a risk to the fetus) by FDA. Rodent studies show dose-dependent increases in fetal mortality. There are no controlled studies of cannabis or THC in pregnant women. Therefore, the unfavorable risk:benefit ratio for the fetus justifies excluding pregnant women from cannabis-administration studies (see **Note 4**).

THC is concentrated in and secreted in human breast milk and absorbed by the nursing infant. Thus, it is not appropriate to include nursing women in cannabis-administration studies. Because of the health advantages to the infant of breast feeding over bottle feeding, care should be taken to avoid research participation becoming an incentive for the mother to stop nursing. This can be done by eliciting nursing status early in the screening process, before potential subjects are aware of the exclusion of nursing women.

3.1.2. Screening Subjects

Screening of potential subjects should evaluate for any medical or psychological condition that might put them at increased risk from cannabis administration. Study eligibility criteria should exclude potential subjects with any such risk factor. Research volunteers may underreport health information that might exclude them from a study (16,17). Thus, the status of any risk factor should be objectively evaluated as much as possible by obtaining past medical records and/or contemporaneous examination and laboratory testing.

Many investigators would also require that subjects have used cannabis in the past, with no reported clinically significant adverse experiences. This allows subjects' own use of cannabis prior to research participation to serve as a pre-screen for adverse effects, including potential idiosyncratic reactions. The assumption is that adverse effects are unlikely to appear during research administration of cannabis if they have not occurred during the subjects' prior use (see **Note 5**).

The major adverse medical effects of cannabis include increased heart rate, orthostatic hypotension, and respiratory irritation (from smoked cannabis). Thus, medical screening should include evaluation of the cardiovascular and respiratory systems. Individuals with a past or current condition that makes them less tolerant of increased heart rate (e.g., a cardiac arrhythmia, coronary artery disease), decreased blood pressure (e.g., history of syncope), or respiratory irritation (e.g., asthma, bronchitis) should be excluded.

The major psychological adverse effects of cannabis include anxiety, paranoia, and psychosis. Thus, psychological screening should include a detailed psychiatric evaluation to identify individuals with a history of anxiety, paranoia, psychosis, or psychiatric disorders such as depression, manic depression (bipolar), panic disorder, or schizophrenia, which may be exacerbated by cannabis.

3.1.3. *Consenting Subjects*

To be considered legally and ethically valid, informed consent to research participation should not be obtained while subjects are under the influence of a psychoactive drug such as cannabis. Cannabis intoxication can impair memory, attention, and judgment in ways that compromise the ability of the individual to understand and appropriately judge the risks and benefits of research participation (*see* **Note 6**).

Another consent issue for cannabis administration studies is the voluntariness of consent for subjects who are cannabis users. Users who are abusing or dependent on cannabis can be considered as having lost some control over their cannabis use, in that they continue to use the drug despite experiencing adverse consequences from such use (Diagnostic and Statistical Manual of Mental Disorders [DSM]-IV criterion A.4 for substance abuse; criterion 7 for substance dependence), are unable to control their drug use (criterion 4 for substance dependence), and/or often take more drug than was intended (criterion 3 for substance dependence) (*18*). Some have argued that, because of diminished control, such individuals are not fully voluntary when accepting an offer to participate in a cannabis-administration study (*19,20*). Others have argued that loss of control in addiction is not an all-or-none phenomenon, and that even dependent drug users can make valid judgments regarding the relative risks and benefits of a drug-administration research study (*21*). To minimize the chance that the offer of cannabis administration would exert an undue influence on the decision to participate, subject eligibility criteria often require that subjects' prior cannabis use be at a dose, duration, and frequency at least as great as that offered in the research study. In this way, a decision to participate in research is a decision by the individual to decrease their cannabis use, which presumably would not be unduly influenced by the offer of cannabis administration.

3.1.4. *Discharging Subjects*

Subjects should not be discharged from a cannabis-administration research study until they have been evaluated for any unresolved or residual adverse effects from study participation. Adverse physical and psychological effects from acute cannabis administration, such as tachycardia, orthostatic hypotension, impaired motor coordination, and drowsiness, usually resolve completely within hours. Thus, subjects can usually be safely discharged a few hours to a

day after the last cannabis administration, depending on the dose and frequency of cannabis administration. A predischarge medical and psychological evaluation, similar to the screening evaluation, serves to document the resolution of any adverse effects and detect any clinically significant residual effects. Ethical and legal considerations require that subjects be informed of any abnormalities detected, and be referred for appropriate diagnosis and treatment (when this will not be done by the research team itself).

Subjects may face sociolegal risks even after discharge from a cannabis administration research study. Cannabis constituents such as THC are stored in body fat and can appear in the urine for several weeks after the last use of cannabis (22,23). Former research subjects who undergo urine drug testing at work or in forensic settings (e.g., on probation or parole) could test positive for cannabis because of their research participation, with serious adverse employment, insurance, or legal consequences. This is probably not a significant risk in practice, because research administration is likely to involve relatively low amounts of THC, which would not be long detectable by commonly used drug-screening tests. In addition, subjects in a relatively short study may test positive after research participation because of their preresearch cannabis use, regardless of any cannabis administration during the study (unless a negative cannabinoid test was a criterion for study entry).

The risk of postdischarge detection can be eliminated by not discharging subjects until their urine samples test negative for cannabinoids at the commonly used detection threshold of 50 ng/mL. This is likely to occur within 1 d of smoking a low-dose cannabinoid cigarette (17–20 mg THC), within 2 d of smoking a high-dose cigarette (30–35 mg THC) (22), and within 6 d of oral ingestion of marijuana (14). One could also give subjects a statement of research participation to confirm that they have been legally exposed to cannabis (although, of course, this does not exclude the illegal use of cannabis).

3.1.5. Follow-Up of Subjects

There are no known delayed adverse effects of cannabis administration. Assuming that the above precautions have been taken, there is little need for further follow-up of research subjects after their discharge from a cannabis-administration study.

3.2. Measurement of Cannabis Effects

3.2.1. Physiological

3.2.1.1. CARDIOVASCULAR

Periodic monitoring of heart rate and blood pressure during cannabis administration is recommended because of the expected effects of tachycardia and

orthostatic hypotension. Monitoring should begin before cannabis administration, to provide a baseline, and continue until values have returned to baseline levels. Measurements should be obtained more frequently during periods of expected maximum cannabis effect (which will vary by route of administration), then less frequently as the cannabis effect subsides. Heart rate can be efficiently monitored using an electrocardiographic (ECG) chest lead. This also provides information about heart rhythm (although cannabis administration is not commonly associated with cardiac arrhythmia). Blood pressure can be measured with a standard clinical sphygmomanometer.

3.2.1.2. NEUROLOGICAL

Gross motor coordination can be assessed with standard clinical neurological tests, such as finger-to-nose, one-leg stand, and observation of gait, and by computerized body sway devices. Tremor can be assessed by observation using standardized rating scales, or with electronic devices (accelerometers).

3.2.2. *Psychological*

3.2.2.1. SUBJECTIVE EFFECTS

Cannabis and other drugs of abuse produce psychoactive effects, i.e., drug-induced changes in mood and feelings mediated by the central nervous system. Such changes in mood and feelings are termed subjective because they are not directly observable. Because of common verbal learning histories, subjects can generally agree in their responses on validated questionnaires when describing subjective states produced by psychoactive drugs. Subjective effects are also termed self-report effects because they can only be inferred from subjects' responses to questionnaires or other measurement instruments.

The acute subjective effect most commonly reported by experienced cannabis users is the pleasant, euphoric state known as the drug "high." The intensity of this and other subjective effects (e.g., sedation, hunger, anxiety, clarity of thinking) can be assessed by two different types of questions. Visual analog scales (VAS) require subjects to place a vertical mark along a 100-mm line anchored by "not at all" on the left and "extremely" on the right. Responses are measured in mm from 0 to 100. A Likert scale requires subjects to choose from among several categories of intensity, e.g., "not at all," "mild," "moderate," and "severe." Responses are scored as ascending integers starting with 0. The simplest scale is dichotomous, i.e., the effect is scored as either present (1) or absent (0). For both types of questions, the higher the score, the greater the intensity of the subjective effect. Cannabis-specific questions should be interspersed with nonspecific questions to minimize response bias (*see Note 7*).

The marijuana (M) scale is a self-report instrument specifically designed to measure cannabis intoxication. It is a subscale (12 true–false statements) of the

larger Addiction Research Center Inventory (ARCI) (24,25) (see **Note 8**). Higher scores indicate greater intensity of cannabis intoxication. The ARCI contains several other subscales that are less reliably sensitive to acute cannabis effects (see **Note 9**).

Peak subjective effects typically occur during or immediately after smoking a single cannabis cigarette and gradually decline over several hours. To capture the complete time course of subjective effects, measurements should be repeated every 10 to 15 min during the first hour after smoking and every 20 to 30 min thereafter.

3.2.2.2. PSYCHOMOTOR PERFORMANCE

Psychomotor performance refers to motor (movement) skills, eye–hand coordination, and speed of response to visual or auditory stimuli (often referred to as reaction time). Acute cannabis administration typically impairs psychomotor performance, with higher doses producing greater impairment (for reviews, see refs. 26–28). Numerous standardized tests measure various aspects of psychomotor performance (see **Note 10**). Impaired performance is observed within 30–45 min after smoking cannabis and persists for several hours. Some studies have documented performance decrements 12–24 h after smoking cannabis (29).

3.2.2.3. ATTENTION AND COGNITION

Attention and cognition are broad psychological terms that include many specific functions involving higher order cognitive processing. Attentional processes involve searching, scanning, and detecting visual or auditory stimuli for brief or extended periods of time. These can be categorized as focused, selective, divided, or sustained attention (30). Cognitive processes involve learning, memory, problem solving, and reasoning skills. Such distinctions are somewhat arbitrary because any memory task requires attention and memory skills, as well as other cognitive resources. Acute cannabis administration impairs many aspects of attention and cognition, as described below and reviewed elsewhere (26–28) (see **Note 11**). As with psychomotor performance, cognitive impairment can last for up to 24 h after smoking cannabis (31).

3.3. Adverse Events From Cannabis Administration

3.3.1. Physiological

3.3.1.1. CARDIOVASCULAR

Acute cardiovascular effects of cannabis administration include tachycardia, slightly increased blood pressure when supine, orthostatic hypotension, increased cardiac output, and decreased left ventricular ejection fraction (32,33). These effects increase myocardial oxygen demand at the same time

that oxygen delivery to tissues may be decreased because of the increased carboxyhemoglobin from smoking. As a result, smoking one marijuana cigarette significantly reduces maximal exercise performance and exercise tolerance of physically healthy subjects (34) and patients with angina (35). However, in healthy subjects the acute cardiovascular effects of cannabis are mild, self-limiting, and rarely cause clinically significant adverse events (32,36–38).

Orthostatic hypotension may be associated with light-headedness and syncope (39). This may be minimized by ensuring that subjects are well hydrated (including encouraging fluid intake during cannabis administration), avoiding sudden changes in position, and keeping subjects seated with legs elevated during cannabis administration.

Acute cannabis administration is rarely associated with clinically significant ECG changes (32). Changes associated with tachycardia may be seen during monitoring, such as nonspecific, transient S-T segment or T-wave changes.

3.3.1.2. NEUROLOGICAL

Acute neurological effects of cannabis administration include headache, tremor, impaired balance, and impaired gross and fine motor coordination (37,38,40). The latter, especially in conjunction with drowsiness, increases the risk of motor vehicle accidents, falls, and other unintended injuries (41). Physical activity by subjects under the influence of cannabis should be limited and performed only in a protected environment that minimizes the risk of injury. Subjects should be advised not to drive, operate machinery, or engage in other potentially hazardous activities until it is clear that their coordination (and mental alertness) has returned to normal.

3.3.1.3. PULMONARY

Smoked cannabis causes bronchodilation (probably by THC) (42), pulmonary irritation from inhalation of the smoke, and increased absorption of carbon monoxide (43,44). The latter leads to elevated blood carboxyhemoglobin levels, resulting in decreased oxygen delivery to tissues. These effects rarely cause clinically significant adverse events with the limited exposure usually involved in cannabis administration research studies (45). However, even a single cannabis cigarette may trigger coughing or breathing difficulty (dyspnea) in a susceptible subject, e.g., one with active asthma or bronchitis.

Oral and intravenous THC cause bronchodilation (42) but are not associated with pulmonary adverse events.

3.3.1.4. OTHER PHYSIOLOGICAL EFFECTS

Acute cannabis administration may cause pupil constriction, conjunctival injection (“red eye”), and dry mouth. These effects are mild and self-limiting

and do not require treatment (37). Dry mouth may be worsened by the smoked route of administration. It can be relieved by providing subjects with fluid to drink, sucking candy, or chewing gum.

3.3.2. Psychological

3.3.2.1. ANXIETY, PSYCHOSIS

Acute cannabis administration can cause a spectrum of adverse psychological effects, ranging from hypervigilance and anxiety, to panic, agitation, paranoid thinking, and psychosis (38,40). These are rare at the doses commonly used in research studies but are more likely to occur in susceptible individuals (46,47). Although controlled studies have not been done, susceptible subjects include those with preexisting psychopathology or a history of a psychiatric illness such as schizophrenia, schizoaffective disorder, major depression, manic depression (bipolar disorder), or anxiety disorder. Screening for these conditions relies largely on subject self-report and so may not always be completely reliable. Thus, it is prudent to conduct cannabis-administration studies in a setting where appropriate psychiatric intervention is promptly available. This should include facilities for safe physical restraint of agitated subjects and administration of parenteral medication. Cannabis-induced psychological effects usually subside within several hours and respond well to supportive reassurance and placement in a quiet environment. Severe agitation that makes the subject a danger to himself or others can be controlled with a benzodiazepine sedative such as lorazepam (effective by both oral and intramuscular administration). Psychosis can be controlled with standard doses of antipsychotic (neuroleptics) medication.

3.3.2.2. PSYCHOMOTOR PERFORMANCE

Acute psychomotor effects of cannabis administration include decreased postural balance (48,49), increased body sway (due to impaired equilibrium) (50), and increased tremor. Effects on simple and complex reaction time tasks are mixed, with some studies reporting impaired performance (51,52) and others showing no effect (50,53). Acute cannabis administration can also impair performance on the digit symbol substitution test (DSST) (9,13,49),

3.3.2.3. ATTENTION AND COGNITION

Cannabis administration acutely disrupts performance of complex tasks requiring continuous monitoring and the ability to shift attention rapidly between various stimuli (54,55). These same attentional abilities are required when operating a motor vehicle. Cannabis administration impairs performance on laboratory tests that model various components of driving (56) and increas-

es braking latency in a driving simulator (50). It also impairs performance on standardized tests used by law enforcement personnel to determine whether a person can safely drive (57,58). In tests of on-road driving, cannabis moderately increases lateral movement of the vehicle within the driving lane on a highway (59).

One of the most reliable effects of acute cannabis administration is the impairment of memory processes. Numerous studies have found that smoked marijuana decreased the number of words or digits recalled and/or increased the number of intrusion errors in either immediate or delayed tests of free recall (9,53,55,60). Using an extensive battery of cognitive tests, Block et al. (51) found that cannabis slowed response time for producing word associations, slowed reading of prose, and impaired tests of reading comprehension, verbal expression, and mathematics. Heishman et al. (31) also found that simple addition and subtraction skills were impaired by smoking one, two, or four cannabis cigarettes.

3.3.3. Addictive Risk

Addictive risk refers to the risk that cannabis administration during a research study might trigger or worsen cannabis abuse or dependence (6). It seems unlikely that the brief cannabis exposure involved with most research studies would be sufficient to have such an effect, especially in view of the fact that only 10% of regular cannabis users develop cannabis dependence (61,62). However, several steps can be taken to minimize whatever risk does exist. First, subjects with a history of abuse or dependence can be excluded on the grounds that they would be most susceptible (*see Note 12*). Second, the dose, frequency, and duration of cannabis administration in the research study should be no greater (and preferably less) than what subjects were using on their own prior to study participation. This removes any incentive to enter a study to gain more access to cannabis. Third, smoked cannabis, because it is considered to have the greatest abuse potential, should only be given to subjects with prior smoked cannabis experience.

4. Notes

1. To avoid some of the problems associated with the smoked route of administration (i.e., with inhalation of burning plant material), methods are being developed for inhalation of pure THC via either nebulizer or metered dose inhaler (63).
2. NIDA cigarettes can be ordered in writing from the Chemistry & Physiological Systems Research Branch, Division of Neuroscience & Behavioral Research, 6001 Executive Boulevard, MSC 9555, Bethesda, MD 20892-9555 (301 443-6275). US investigators must hold a valid Schedule I research license from the US Drug Enforcement Administration and have an approved IND from the US Food and Drug Administration.

3. The marijuana for NIDA cigarettes is grown under contract at the University of Mississippi, Oxford, MS. The plant material is sent to the Research Triangle Institute (RTI), Research Triangle Park, NC, where the marijuana leaves are stripped, cleaned, and rolled into cigarettes. RTI assays the cigarettes for THC content. Cigarettes are stored freeze-dried until shipped to an investigator. Cigarettes should be kept frozen in an air-tight container in order to maintain potency. Their moisture content prior to use should be raised by placing them above a saturated sodium chloride solution in a closed humidifier for 12–48 h.
4. Some investigators may accept a woman's self-report of reproductive status (e.g., hysterectomy, tubal ligation), abstinence from sexual activity, or use of contraception. However, it is prudent to confirm reproductive status with medical records and to have women with reproductive potential undergo pregnancy testing prior to study participation. Periodic pregnancy testing may be needed if the study extends over a period of time.
5. The validity of this prescreen approach depends on at least three factors. First, subjects' prior cannabis use should be by the same route of administration as used in the research study, e.g., a subject whose only prior cannabis was oral would not participate in a smoked cannabis study. This avoids exposing subjects to a route of administration that might produce more intense effects than they are used to. One concern in this regard is a route of administration, such as smoking, that produces rapid onset of positive psychological effects, thus increasing abuse liability and the potential for engendering or worsening cannabis abuse (64).

Second, the dosage, duration, and frequency of cannabis administration during research should not exceed that previously used by subjects. Obviously, the absence of adverse events following a single, low-dose use is not very reassuring with regard to the possibility of adverse events following higher-dose or more frequent cannabis administration.

Third, subjects must provide honest and accurate self-report about their prior experience with cannabis. Accuracy of self-report about illegal drug use is enhanced when subjects are aware that there will be objective confirmation by drug testing and when there are no adverse consequences for honest reporting (65–67). In the case of screening for a cannabis administration study, the adverse consequence for honest reporting may be exclusion from the study. Therefore, potential subjects who are aware of this connection may have a powerful incentive to withhold information. Thus, it is important to elicit the history of prior cannabis use and its adverse effects early in the screening process and without giving potential subjects clues, either overt or covert, about what types of responses will lead to inclusion or exclusion from the study. This can be done by collecting relevant information from questions embedded throughout larger questionnaires (rather than grouping all relevant questions together) and by couching questions broadly in terms of learning what to expect from cannabis administration in a particular subject.

6. There are no standardized measures of cannabis intoxication that have been used to assess the ability to give informed consent. The marijuana (M) scale of the Addiction Research Center Inventory (ARCI) has been used to measure the acute

intoxicating effects of cannabis in research settings (e.g., [ref. 25](#)), but not as part of the subject consent process. In the latter setting, decisions about intoxication are based on clinical interview and judgment.

7. Typical questions measuring acute subjective effects of cannabis include “How high do you feel?”, “How much of a good drug effect do you feel?”, or “How stoned are you?” Questions can be presented either on paper (with subjects responding by marking with a pen) or on a computer screen (with responding by moving a cursor on the screen). Computer presentation is usually more efficient in terms of time and staff resources and eliminates data-entry errors. Subjects’ attention and response to each question can be ensured by requiring that the cursor be moved slightly before any answer is recorded.
8. The M scale is scored by assigning one point for each “true” response and summing the points to obtain a total scale score. The 12 true–false statements that comprise the M scale are as follows: Things around me seem more pleasing than usual. I feel as if something pleasant had just happened to me. I have difficulty in remembering. I feel a very pleasant emptiness. My mouth feels very dry. Some parts of my body are tingling. I have a weird feeling. My movements seem slower than usual. I notice that my heart is beating faster. My thoughts seem to come and go. I notice my hand shakes when I try to write. I have an increasing awareness of bodily sensations.
9. The ARCI consists of 550 true–false statements comprising many empirically derived scales sensitive to the subjective effects of various psychoactive drugs. A widely used short form of the ARCI consists of 40 true–false statements that comprise three scales: morphine–benzedrine group (MBG), a measure of euphoria; pentobarbital–chlorpromazine–alcohol group (PCAG), a measure of sedation; and lysergic acid diethylamide (LSD), a measure of dysphoria and psychotomimetic changes ([68](#)).
10. Domains of psychomotor performance and tests shown to be sensitive to the acute effects of cannabis administration include (1) gross and fine motor abilities: body sway, one leg stand, hand steadiness, finger tapping; (2) eye–hand coordination: digit–symbol substitution, circular lights, rotary pursuit, pegboard, card sorting; (3) reaction time: visual or auditory simple (one stimulus) and choice (multiple stimuli). (For details about the tests and the effects of cannabis, see [refs. 26–28](#).)
11. Domains of attention and cognition and tests shown to be sensitive to the acute effects of cannabis administration include (1) focused attention: simple and choice reaction time, digit–symbol substitution; (2) selective attention: letter search, Stroop color naming; (3) divided attention: various tests requiring simultaneous performance of a central and peripheral task, driving and flying simulators; (4) sustained attention: visual or auditory signal detection, continuous performance, vigilance; (5) learning: repeated acquisition and performance of response sequences, paired–associate learning, Buschke selective reminding; (6) memory: digit span, free recall, recognition memory, prose recall; (7) problem solving: mental arithmetic, spatial orientation, embedded figures; (8) reasoning: logical reasoning, creativity. (For details about the tests and the effects of cannabis, see [refs. 26–28](#).)

12. In the absence of relevant data or controlled studies, there is a spectrum of practice regarding excluding subjects with a history of abuse or dependence. At one end are investigators who would exclude any subject with a family or lifetime personal history of any substance abuse or dependence (perhaps with the exception of nicotine dependence). At the other end are investigators who would exclude only subjects with current substance dependence. As with many other subject eligibility criteria for clinical research, there is usually an inverse relationship between strictness of the criterion and the availability of eligible subjects to enroll.

Acknowledgment

This work was supported by National Institute on Drug Abuse intramural funds.

References

1. United Nations Office on Drugs and Crime. (2003) *Global Illicit Drug Trends, 2003*, United Nations Office on Drugs and Crime, New York.
2. Substance Abuse & Mental Health Services Administration. (2002) *National Survey on Drug Use and Health, 2002*, Substance Abuse & Mental Health Services Administration, Rockville MD.
3. McPartland J. M. and Pruitt P. L. (1999) Side effects of pharmaceuticals not elicited by comparable herbal medicines: the case of tetrahydrocannabinol and marijuana. *Altern. Ther. Health Med.* **5**, 57–62.
4. College on Problems of Drug Dependence. (1995) Human subject issues in drug abuse research. College on Problems of Drug Dependence. *Drug Alcohol Depend.* **37**, 167–175.
5. Fischman M. W. and Johanson C. E. (1998) Ethical and practical issues involved in behavioral pharmacology research that administers drugs of abuse to human volunteers. *Behav. Pharmacol.* **9**, 479–498.
6. Gorelick D. A., Pickens R., and Bonkovsky F. (1999) Clinical research in substance abuse: human subjects issues, in *Ethics in Psychiatric Research: A Resource Manual for Human Subject Protection* (Pincus, H. A., Lieberman, J. A., and Ferris, S., eds.) American Psychiatric Press, Washington, DC, pp. 177–218.
7. Miller F. G. and Rosenstein D. L. (1997) Psychiatric symptom-provoking studies: an ethical appraisal. *Biol. Psychiatry.* **42**, 403–409.
8. Azorlosa J. L., Heishman S. J., Stitzer M. L., and Mahaffey J. M. (1992) Marijuana smoking: effect of varying delta 9-tetrahydrocannabinol content and number of puffs. *J. Pharmacol Exp Ther.* **261**, 114–122.
9. Heishman S. J., Stitzer M., and Yingling J. E. (1989) Effects of tetrahydrocannabinol content on marijuana smoking behavior, subjective reports, and performance. *Pharmacol Biochem. Behav.* **34**, 173–179.
10. Chait L. D. and Perry J. L. (1992) Factors influencing self-administration of, and subjective response to, placebo marijuana. *Behav. Pharmacol.* **3**, 545–552.
11. Kirk J. M., Doty P., and de Wit H. (1998) Effects of expectancies on subjective responses to oral delta9-tetrahydrocannabinol. *Pharmacol. Biochem. Behav.* **59**, 287–293.

12. Chait L. D. and Pierri J. (1989) Some physical characteristics of NIDA marijuana cigarettes. *Addict. Behav.* **14**,61–67.
13. Heishman S. J., Stitzer M. L., and Bigelow G. E. (1988) Alcohol and marijuana: comparative dose effect profiles in humans. *Pharmacol. Biochem. Behav.* **31**, 649–655.
14. Cone, E. J., Johnson, R. E., Paul, B. D., Mell, L. D., and Mitchell, J. (1988) Marijuana-laced brownies: behavioral effects, physiologic effects, and urinalysis in humans following ingestion. *J. Anal. Toxicol.* **12**, 169–175.
15. Mathew, R. J., Wilson, W. H., Turkington, T. G., and Coleman, R. E. (1998) Cerebellar activity and disturbed time sense after THC. *Brain Res.* **797**,183–189.
16. Apseloff, G., Swayne, J. K., and Gerber, N. (1996) Medical histories may be unreliable in screening volunteers for clinical trials. *Clin. Pharmacol. Ther.* **60**,353–356.
17. Struve, F. A., Straumanis, J. J., Manno, J. E., Fitzgerald, M. J., Patrick, G., and Leavitt, J. (2000) Inadequacies of self-report data for exclusion criteria detection in marijuana research: an empirical case for multi-method direct examination screening. *J. Addict. Dis.* **19**,71–87.
18. American Psychiatric Association. (2000) *Diagnostic and Statistical Manual of Mental Disorders*, 4th text revision ed., American Psychiatric Association, Washington, DC.
19. Charland, L. C. (2002) Cynthia's dilemma: consenting to heroin prescription. *Am. J. Bioeth.* **2**,37–47.
20. Cohen, P. J. (2002) Untreated addiction imposes an ethical bar to recruiting addicts for non-therapeutic studies of addictive drugs. *J. Law Med. Ethics* **30**, 73–81.
21. Ling, W. (2002) Cynthia's dilemma. *Am. J. Bioeth.* **2**, 55–56.
22. Huestis, M. A., Mitchell, J. M., and Cone, E. J. (1995) Detection times of marijuana metabolites in urine by immunoassay and GC-MS. *J. Anal. Toxicol.* **19**,443–449.
23. Verstraete, A. G. (2004) Detection times of drugs of abuse in blood, urine, and oral fluid. *Ther. Drug Monit.* **26**, 200–205.
24. Chait, L. D., Fischman, M. W., and Schuster, C. R. (1985) 'Hangover' effects the morning after marijuana smoking. *Drug Alcohol Depend.* **15**, 229–238.
25. Huestis, M. A., Gorelick, D. A., Heishman, S. J., et al. (2001) Blockade of effects of smoked marijuana by the CB1-selective cannabinoid receptor antagonist SR141716. *Arch. Gen. Psychiatry* **58**,322–328.
26. Beardsley, P. M. and Kelly, T. H. (1999) Acute effects of cannabis on human behavior and central nervous system function, in *The Health Effects of Cannabis* (Kalant, H., Corrigan, W., Hall, W., and Smart, R., eds.), Addiction Research Foundation, Toronto, pp. 127–169.
27. Chait, L. D. and Pierri, J. (1992) Effects of smoked marijuana on human performance: a critical review, in *Marijuana/Cannabinoids: Neurobiology and Neurophysiology* (Murphy, L. and Bartke, A., eds.), CRC Press, Boca Raton, FL, pp. 387–424.
28. Heishman, S. J. and Myers, C. S. (2005) Effects of abused drugs on human performance: Laboratory assessment, in *Drug Abuse Handbook* (Karch S. B., ed.), CRC Press, Boca Raton, FL, in press.

29. Pope, H. G., Jr., Grube, A. J., and Yurgelun-Todd, D. (1995) The residual neuropsychological effects of cannabis: the current status of research. *Drug Alcohol Depend.* **38**, 25–34.
30. Heishman, S. J., Taylor, R. C., and Henningfield, J. E. (1994) Nicotine and smoking: a review of effects on human performance. *Exp. Clin. Psychopharmacol.* **2**, 345–395.
31. Heishman, S. J., Huestis, M., Henningfield, J. E., and Cone, E. J. (1990) Acute and residual effects of marijuana: profiles of plasma THC levels, physiological, subjective, and performance measures. *Pharmacol. Biochem. Behav.* **37**, 561–565.
32. Jones, R. T. (2002) Cardiovascular system effects of marijuana. *J. Clin. Pharmacol.* **42**, 58S–63S.
33. Prakash, R., Aronow, W. S., Warren, M., Laverty, W., and Gottschalk, L. A. (1975) Effects of marihuana and placebo marihuana smoking on hemodynamics in coronary disease. *Clin. Pharmacol. Ther.* **18**, 90–95.
34. Renaud, A. M. and Cormier, Y. (1986) Acute effects of marihuana smoking on maximal exercise performance. *Med. Sci. Sports Exerc.* **18**, 685–689.
35. Aronow, W. S. and Cassidy, J. (1974) Effect of marihuana and placebo-marihuana smoking on angina pectoris. *N. Engl. J. Med.* **291**, 65–67.
36. Frishman, W. H., Del Vecchio, A., Sanal, S., and Ismail, A. (2003) Cardiovascular manifestations of substance abuse: part 2: alcohol, amphetamines, heroin, cannabis, and caffeine. *Heart Dis.* **5**, 253–271.
37. Selden, B. S., Clark, R. F., and Curry, S. C. (1990) Marijuana. *Emerg. Med. Clin. North Am.* **8**, 527–539.
38. Wilkins, J. N., Mellott, K. G., Markvitsa, R., and Gorelick, D. A. (2003) Management of stimulant, hallucinogen, marijuana, phencyclidine, and club drug intoxication and withdrawal, in *Principles of Addiction Medicine* (Graham, A. W., Schultz, T. K., Mayo-Smith, M. F., Ries, R. K., and Wilford, B. B., eds.), American Society of Addiction Medicine, Chevy Chase, MD, pp. 671–695..
39. Mathew, R. J., Wilson, W. H., and Davis, R. (2003) Postural syncope after marijuana: a transcranial Doppler study of the hemodynamics. *Pharmacol. Biochem. Behav.* **75**, 309–318.
40. Brust, J. C. M. (1998) Acute neurologic complications of drug and alcohol abuse. *Neurol. Clin. North Am.* **16**, 503–519.
41. Macdonald, S., Anglin-Bodrug, K., Mann, R. E., Erickson, P., Hathaway, A., Chipman, M., and Rylett, M. (2003) Injury risk associated with cannabis and cocaine use. *Drug Alcohol Depend.* **72**, 99–115.
42. Tashkin, D. P., Shapiro, B. J., and Frank, I. M. (1973) Acute pulmonary physiologic effects of smoked marijuana and oral Δ^9 -tetrahydrocannabinol in healthy young men. *N. Engl. J. Med.* **289**, 336–341.
43. Tilles, D. S., Goldenheim, P. D., Johnson, D. C., Mendelson, J. H., Mello, N. K., and Hales C. A. (1986) Marijuana smoking as cause of reduction in single-breath carbon monoxide diffusing capacity. *Am. J. Med.* **80**, 601–606.
44. Wu, T. C., Tashkin, D. P., Djahed, B., and Rose, J. E. (1988) Pulmonary hazards of smoking marijuana as compared with tobacco. *N. Engl. J. Med.* **318**, 347–351.

45. Taylor, D. R., Fergusson, D. M., Milne, B. J., et al. (2002) A longitudinal study of the effects of tobacco and cannabis exposure on lung function in young adults. *Addiction* **97**, 1055–1061.
46. Hurlbut, K. M. (1991) Drug-induced psychoses. *Emerg. Med. Clin. North Am.* **9**, 31–52.
47. Szuster, R. R., Pontius, E. B., and Campos, P. E. (1988) Marijuana sensitivity and panic anxiety. *J. Clin. Psychiatry* **49**, 427–429.
48. Greenberg, H. S., Werness, S. A., Pugh, J. E., Andrus, R. O., Anderson, D. J., and Domino, E. F. (1994) Short-term effects of smoking marijuana on balance in patients with multiple sclerosis and normal volunteers. *Clin. Pharmacol. Ther.* **55**, 324–328.
49. Greenwald, M. K. and Stitzer, M. L. (2000) Antinociceptive, subjective and behavioral effects of smoked marijuana in humans. *Drug Alcohol Depend.* **59**, 261–275.
50. Liguori, A., Gatto, C. P., and Robinson, J. H. (1998) Effects of marijuana on equilibrium, psychomotor performance, and simulated driving. *Behav. Pharmacol.* **9**, 599–609.
51. Block, R. I., Farinpour, R., and Braverman, K. (1992) Acute effects of marijuana on cognition: relationships to chronic effects and smoking techniques. *Pharmacol. Biochem. Behav.* **43**, 907–917.
52. Wilson, W. H., Ellinwood, E. H., Mathew, R. J., and Johnson, K. (1994) Effects of marijuana on performance of a computerized cognitive-neuromotor test battery. *Psychiatry Res.* **51**, 115–125.
53. Heishman, S. J., Arasteh, K., and Stitzer, M. L. (1997) Comparative effects of alcohol and marijuana on mood, memory, and performance. *Pharmacol. Biochem. Behav.* **58**, 93–101.
54. Hart, C. L., Ward, A. S., Haney, M., Comer, S. D., Foltin, R. W., and Fischman, M. W. (2002) Comparison of smoked marijuana and oral delta(9)-tetrahydrocannabinol in humans. *Psychopharmacology (Berl.)* **164**, 407–415.
55. Kelly, T. H., Foltin, R. W., Emurian, C. S., and Fischman, M. W. (1993) Performance-based testing for drugs of abuse: dose and time profiles of marijuana, amphetamine, alcohol, and diazepam. *J. Anal. Toxicol.* **17**, 264–272.
56. Kurzthaler, I., Hummer, M., Miller, C., et al. (1999) Effect of cannabis use on cognitive functions and driving ability. *J. Clin. Psychiatry* **60**, 395–399.
57. Heishman, S. J., Singleton, E. G., and Crouch, D. J. (1996) Laboratory validation study of drug evaluation and classification program: ethanol, cocaine, and marijuana. *J. Anal. Toxicol.* **20**, 468–483.
58. Heishman, S. J., Singleton, E. G., and Crouch, D. J. (1998) Laboratory validation study of drug evaluation and classification program: alprazolam, d-amphetamine, codeine, and marijuana. *J. Anal. Toxicol.* **22**, 503–514.
59. Ramaekers, J. G., Robbe, H. W., and O'Hanlon, J. F. (2000) Marijuana, alcohol and actual driving performance. *Hum. Psychopharmacol.* **15**, 551–558.
60. Curran, H. V., Brignell, C., Fletcher, S., Middleton, P., and Henry, J. (2002) Cognitive and subjective dose-response effects of acute oral delta 9-tetrahydro-

- cannabinol (THC) in infrequent cannabis users. *Psychopharmacology (Berl.)* **164**, 61–70.
61. Chen, K., Kandel, D. B., and Davies, M. (1997) Relationships between frequency and quantity of marijuana use and last year proxy dependence among adolescents and adults in the United States. *Drug Alcohol Depend.* **46**, 53–67.
 62. Wagner, F. A. and Anthony, J. C. (2002) From first drug use to drug dependence: developmental periods of risk for dependence upon marijuana, cocaine, and alcohol. *Neuropsychopharmacology* **26**, 479–488.
 63. Wilson, D. M., Peart, J., Martin, B. R., Bridgen, D. T., Byron, P. R., and Lichtman, A. H. (2002) Physiochemical and pharmacological characterization of a delta(9)-THC aerosol generated by a metered dose inhaler. *Drug Alcohol Depend.* **67**, 259–267.
 64. Gorelick, D. A. (1998) The rate hypothesis and agonist substitution approaches to cocaine abuse treatment. *Adv. Pharmacol.* **42**, 995–997.
 65. Brown, J., Kranzler, H. R., and Del Boca, F. K. (1992) Self-reports by alcohol and drug abuse inpatients: factors affecting reliability and validity. *Br. J. Addict.* **87**, 1013–1024.
 66. Harrison, L. (1997) The validity of self-reported drug use in survey research: an overview and critique of research methods. *NIDA Res. Monogr.* **167**, 17–36.
 67. Martin, G. W., Wilkinson, D. A., and Kapur, B. M. (1988) Validation of self-reported cannabis use by urine analysis. *Addict. Behav.* **13**, 147–150.
 68. Jasinski, D. R., Martin, W. R., and Sapiro, J. D. (1968) Antagonism of the subjective, behavioral, pupillary, and respiratory depressant effects of cyclazocine by naloxone. *Clin. Pharmacol. Ther.* **9**, 215–222.

Neurological Assessments of Marijuana Users

Jean Lud Cadet, Karen Bolla, and Ronald I. Herning

Summary

This chapter summarizes the neurological approaches used to assess the potential long-term effects of drugs on the nervous system of drug abusers. These include the use of neuropsychological assessments, transcranial Doppler (TCD) sonography, and electroencephalographic (EEG) recordings. Neuropsychological procedures are used in an effort to provide an unbiased estimate of the individual's cognitive capacity, and included tests of language skills, attention, memory, and motor skills. TCD allows for the measurements of blood flow in the anterior cerebral and middle cerebral arteries, which supply blood to the cortex. An EEG recording was included in our assessment on marijuana abusers using a sound-attenuated, electronically shielded chamber. These neurological approaches have allowed the detection of various neurological and neurovascular deficits that are associated with the abuse of marijuana.

Key Words: Neurology; neuropsychiatry; EEG; TCD; neuropsychological testing; neurophysiology; blood flow; cognition.

1. Introduction

The use of marijuana has continued unabated among the US population and worldwide. Its use is often associated with acute neuropsychiatric signs and symptoms, which include euphoria, altered levels of consciousness, and drug intoxication ([1](#)). It has also been shown that the drug can affect an individual's equilibrium and psychomotor performance to such an extent as to impair his or her ability to function in a test of simulated driving ([2](#)). Moreover, abstinent marijuana abusers have been reported to suffer from (1) various patterns of cognitive differences in comparison to control populations who do not abuse illicit drugs ([3–8](#)) and (2) poor motor skills ([9](#)). Reduced cerebral blood flow has been observed in abstinent chronic marijuana abusers in studies using $^{133}\text{Xenon}$ imaging ([10,11](#)), single photon emission-coupled tomography (SPECT) imaging ([12](#)), or ^{15}O positron emission tomography (PET) imaging ([13](#)). In addition, there have been reports of strokes in rela-

tively young marijuana users (14–24). Although the basic mechanisms for the cerebrovascular accidents remain to be clarified, it is possible that they might be related to neurobiological changes that form the basis for the reported changes in cerebral perfusion found in similar patient populations with the use of various modern imaging techniques.

We thus reasoned that approaches that address the clinical neurobiology of marijuana might offer a window to the neuropathological substrates responsible for the neurological signs and symptoms encountered in some of these individuals. The purpose of this chapter is to present the neurological approaches that we have taken in clinical research focusing on this patient population. These include neuropsychological assessments, transcranial Doppler (TCD) sonography, and electroencephalographic (EEG) recordings.

2. Materials

1. Marijuana and non-marijuana users.
2. Black and white letter/visual blocks.
3. Vision naming tasks.
4. Computerized test systems.
5. Pegs and holes.
6. Various drawing and line drawings.
7. Complex figure tasks.
8. Playing cards.
9. Ultrasound transducer for TCD.
10. Blood pressure (BP)-measuring devices.
11. Kits to assay cholesterol, hemoglobin, hematocrit.
12. EEG apparatus and electrodes.

3. Methods

The methods described below in human marijuana users and respective non-marijuana users outline (1) neuropsychological assessment of marijuana users, (2) transcranial doppler sonography, and (3) EEG recordings and analysis.

3.1. Neuropsychological Assessment of Marijuana Users

Neuropsychological procedures are used in an effort to provide an unbiased estimate of the individual's cognitive capacity. In neurology and psychiatry, these tests have been used to help clinicians to better diagnose patients and to provide them with better treatments. We chose to use a fixed battery in our effort to assess neurobehavioral changes that might be associated with the chronic use of marijuana. That battery included tests of language skills, visual and spatial memory, attention, concentration, executive function, visuo-constructive skills, manual dexterity, simple reaction time, and complex reaction time in subjects in our studies. The various tests used are listed below.

3.1.1. Block Design (25)

This is a subtest of the Wechsler Adult Intelligence Scales–Revised (WAIS-R). Participants are required to arrange red and white blocks to copy the visual presentation of a printed design. There are time limits for each of the problems; and subjects receive points for each design depending on the time to perfect completion. This is a test of visuoconstructional assembly ability and visuomotor coordination. It is sensitive to cortical dysfunction, but primarily parietal lobe dysfunction.

3.1.2. Boston Naming Test (Short Form)

This is a 30-item version of the Boston Naming Task from the Boston Diagnostic Aphasia Battery. In this test, the participant has to name the picture, which is presented.

3.1.3. Controlled Oral Word Association Test (COWAT) (26)

The participant is required to generate as many words as possible that begin with the letters, F, A, and S and animal names within 60 s. This task involves the function of the frontal cortex and is also a test of verbal fluency (language).

3.1.4. California Computerized Assessment Package (Short Form) (CALCAP)

The CALCAP (27) is used to measure simple and choice reaction time and speed of information processing. This test has proven to be sensitive in detecting central nervous system (CNS) changes in studies of acquired immunodeficiency syndrome (AIDS) dementia. This computerized test consists of four individual tests (one test of simple visual reaction time and three tests of choice reaction time) and takes only 10 min to administer.

3.1.5. Clock Drawing (28)

This is another test of visuoconstruction. The subject is asked to draw the face of the clock, put in all the numbers, and set the hands to 11:10. The drawing is scored for accuracy.

3.1.6. Digital Symbol (25)

This test is from the WAIS-R digit symbol. It requires the subject to fill in blank spaces with symbols under the numbers 1 to 9. The key of numbers and symbols is in full view. After instruction and a brief practice session, the time allotment is 90 s and the score is the maximum correct in this time period. The task involves several functions: visual memory, learning of nonverbal associates, sustained attention, speed of visual scanning, and visual motor planning

and motor coordination. This test was chosen because it has been shown to be very sensitive to neurotoxic-related cognitive change. (test–retest reliability is 0.81).

3.1.7. *Finger Tapping (29)*

This is a measure of simple motor speed. The participant is instructed to tap a key with the index finger as rapidly as possible for 10 s. Three trials are obtained for each hand and the mean is used for the analyses. This is a sensitive measure of CNS motor dysfunction.

3.1.8. *Grooved Pegboard (30)*

Participants are required to place pegs into holes first with their dominant hand and then with their nondominant hand. The amount of time it takes to place all the pegs is the dependent measure.

3.1.9. *Immediate Logical Memory (Immediate/Delayed Recall) (31)*

A single-paragraph story is read by the examiner, and the subject is asked to recall as many of the details as possible. This tests immediate recall of logical verbal material. Following 30 min of further testing, the participant is asked to recall the previously presented story. The difference between the initial score and the delayed recall score indicates the amount of verbal material that was retained after the delay.

3.1.10. *Line Orientation (32)*

Participants are presented with the picture of two lines placed at varying angles and required to choose from an array of 11 items that angle the two lines match. This test measures visuospatial ability.

3.1.11. *Rey Auditory Verbal Learning Task (RAVLT) (33)*

A list of 15 common nouns is read to the subject, who is required to recall as many words as possible, in any order, for five trials. The entire list of words is repeated for each trial. The first trial provides a measure of immediate memory span; the fifth trial provides a measure of the total amount of information that is learned. A total score across all five trial measures the amount of immediate recall and total amount of information learned. Learning curves can be generated over the five trials. The number of perseverations, intrusions, and confabulations are noted (all are types of inaccurate responses). After a 30-min delay, delayed free recall of the list is required. Finally, a recognition form where the original 15 items are visually identified from a list of 50 words completes the test. Specific characteristics of memory such as verbal learning and memory, retention, and recall can be evaluated using the different parts of the RAVLT.

3.1.12. Rey Osterreith Complex Figure (34)

The complex figure task assesses visual memory and visuoconstruction. The subject is shown a complex figure and asked to draw a copy of the figure on a blank piece of paper. Thirty minutes later she or he is asked to reproduce the figure from memory. The drawing is scored for accuracy.

3.1.13. Shipley IQ

This is a brief test that estimates general reasoning and intelligence. It correlates 0.79 with WAIS-R full-scale IQ. It assesses vocabulary, abstract reasoning, and mathematical abilities. As in our pilot data, this score was useful for controlling for individual differences in pre-morbid intellectual ability.

3.1.14. Stroop Test (35)

The Stroop task also tests executive function. Words with the names of colors are listed on a page. First, the subject is asked to read the words (names of colors) that are printed in black as fast as he can during a specific time period. Second, the subject is asked to say the color of the ink in which a series of \times s are printed with as fast as possible within 45 s. Third, the subject is asked to say name of the color of the ink that the words (color names that do not match the words) are printed with as fast as possible. The number of words correctly read or colors correctly named in the time period is the score.

3.1.15. Symbol Digit-Paired Associate Learning (36)

The subject is shown seven cards, each with an unfamiliar symbol and a single digit, for 3 s each. The symbol is then presented as a cue, and the subject is asked for the corresponding digit. After each response the symbol digit pair is displayed for another 3 s. The test consists of three trials and generates a total score out of 21. It is a test of nonverbal associative learning.

3.1.16. Trails A and B (29)

Subjects are required to connect a series of numbers (Trails A) or letters alternating with numbers (Trails B) in order with paper and pencil in timed trials. The time for perfect completion (the administrator of the test corrects any inaccuracies as the test proceeds) is the score on this test. This task assesses speed of visuomotor integration and visuomotor scanning, planning (Trails A and B), and cognitive flexibility (Trails B).

3.1.17. Verbal and Nonverbal Cancellation Test (37)

This is a test of attention and concentration. The participant is required to identify targets (the letter A for verbal, and a specific symbol for nonverbal)

among 374 distractor items. Time to completion and number of missed targets will be analyzed.

3.1.18. WRAT-Reading Test (38)

The test measures language skills. The subject is asked to read a series of 64 words. The correctness of the pronunciation of each word is determined.

3.1.19. WAIS-R-Vocabulary (31)

This is a subtest of the WAIS-R. It correlates highly ($r = 0.81$) with the full-scale IQ (a composite of 11 individual subtests) and is therefore the single best subtest to estimate general intelligence. Therefore, the WAIS-R vocabulary score is a reasonable choice to control for pre-morbid intellectual capacity. The vocabulary score is resistant to the effects of age and mild brain injury and has been found to control for the effects of educational level and is a reproducible and quantitative test. We have repeatedly shown that this measure is a better predictor than years of education for performance on neurocognitive tests (39).

3.1.20. Wisconsin Card Sorting Test (40)

This test measures complex problem-solving ability, planning, cognitive flexibility, and the ability to use external feedback to monitor decisions. These tests have been shown to be especially sensitive in detecting dysfunction of the dorsolateral portion of the prefrontal lobes.

3.2 TCD Sonography

3.2.1. TCD Methodology

The routine TCD evaluation of cerebral blood flow velocity began in the 1980s (41). TCD provides clinically useful information in assessing abnormal hemodynamics in cerebral arteries. Current clinical applications of TCD include screening children 2–16 yr of age with sickle cell disease for stroke risk, the detection and monitoring vasospasm after subarachnoid hemorrhage, detection of intracranial steno-occlusive disease, monitoring vasomotor reactivity, detection cerebral circulatory arrest, monitoring carotid endarterectomy, monitoring cerebral thrombosis, and monitoring coronary artery bypass operations (42). TCD differs from other methodologies such as $^{133}\text{Xenon}$, SPECT, and ^{15}O PET imaging in that TCD measures blood flow velocity directly in large arteries rather than cerebral perfusion in small vessels in different areas of the brain using radioligands. In addition, similar to TCD, fMRI methodology does not use radioligands, although the clinical application of fMRI might be prohibitive due to its relatively cost of operations.

Because of its relative ease of use, its low cost of operation, and the important information weaned from TCD, we have used it extensively to assess the

prolonged effects of marijuana on cerebral hemodynamics in marijuana users. Blood flow velocity is measured by using a temporal window (zygomatic arch) middle (MCA) and anterior (ACA) cerebral arteries by using pulsed transcranial Doppler sonography. The temporal window may also be used for the posterior cerebral artery. The transorbital window is used for the ophthalmic artery and the carotid siphon. The foramen window (suboccipital) is used to determine blood flow velocity in the vertebral and basilar arteries. We have chosen the ACA and MCA because they supply blood to the cortex. Recording of both the ACA and MCA is possible via the temporal window because of the anatomy of the brain and these blood vessels. The carotid artery in the neck splits into the external and internal carotid arteries. As the internal carotid artery enters the base of the brain near the optic chiasm, it bifurcates into the ACA and MCA. The MCA then travels toward the outside of the cortex via the Sylvian fissure or toward the temporal window. It supplies blood to the external surface of the frontal, central, parietal, and temporal cortices. The ACA travels toward the medial surface of the cortex or away from the temporal window. It supplies blood to medial surface of the cortex.

TCD uses a hand-held ultrasound transducer directed at the cerebral artery of interest using the correct placement on the skull, angle and depth setting while the subject is lying down. For the ACA, blood is flowing away from the transducer, and for the MCA, blood is flowing toward the transducer. Thus, the Doppler effect comes into play. The shift in emitted ultrasound frequency (usually 2 MHz) in the reflected sound flowing either toward or away from the transducer indicates the blood flow velocity in that artery. Blood flowing toward the transducer results in a higher recorded frequency, and blood flowing away from the transducer results in a lower recorded frequency. A fast Fourier transform is used to analyze the frequencies of the incoming signal and provides a continuous recording of velocity changes. Signal depth is determined by recording the reflected sound at a time window from the emitted signal specific to the depth of interest. Blood flow velocities from the other cerebral arteries can be obtained by changing transducer to the appropriate window, angle, and depth setting. The evaluation of these four arteries takes 15–20 min. Three successive readings along the artery from the continuous recording are saved and averaged together for the velocity estimate for each middle cerebral artery. Two successive readings along the artery from the continuous recording are saved and averaged together for the velocity estimate for each anterior cerebral artery. The following measurements are obtained: systolic velocity (V_s : cm/s); diastolic velocity (V_d : cm/s); and mean velocity (V_m : cm/s). The pulsatility index ($PI = (V_s - V_d)/V_m$) is a derived number, which is a composite of the other values.

Differences in blood flow velocity in large arteries can represent constriction, partial obstruction, or dilation of these vessels (43–45). A decrease in blood

flow velocity, for example, in a patient population in comparison to control subjects might indicate a dilation in that artery (46). In contrast, an increase in blood flow velocity in one patient population in comparison to control subjects might indicate a constriction or partial obstruction in that artery. The pulsatility index (PI), which is obtained mathematically from TCD velocity (41,46, 47), reflects changes in cerebral resistance distal to the recording site or changes in cerebral perfusion pressure in the comparison groups (48,49). Thus, changes in cerebral resistance of small cortical blood vessels are inferred from blood velocity values recorded in large arteries, with increases in PI measurements indicating increases in cerebral resistance in smaller vessels more distal from the recording site. While normative values for velocity and PI are available (41,43,50), an age-matched control group collected concurrently is recommended for research studies. As mentioned above, because the use of TCD is noninvasive, economical, and rapid, this technique allows for repeated assessments of large samples of subjects. Thus, we use a test that is easily available in clinical neurology settings in order to study the effects of drugs on cerebral vessels and to determine the vascular risks potentially associated with these drugs.

3.2.2. Cardiovascular and Blood Viscosity Considerations

Cardiovascular or blood viscosity measures may differ between the control subjects and marijuana abusers and thereby confound the results of TCD studies. Resting heart rate and BP are recorded in all subjects at times when TCD measurements are made. Measurements are made within 72 h of admission and at 28–30 d after admission to the clinical unit for the substance abusers. These cardiovascular measures are also recorded on an outpatient visit for the control subjects as a comparison. Cholesterol, hemoglobin, and hematocrit are measured on an outpatient visit for control subjects and within 72 h of last use for substance abusers as indirect measures of blood viscosity.

3.3. Electroencephalographic

3.3.1. EEG Recordings and Analyses

The EEG has been used extensively in attempts to establish brain–behavior correlations. Changes in EEG can reflect changes in the electrophysiological or metabolic activities of neurons located within a certain radius of the electrodes that are recording these changes. These activities are thought to represent the summation of postsynaptic potentials of many neurons. Thus, the EEG might reflect both normal and pathological changes that occur within the individual's brain. Although the EEG was originally used extensively in the clinical neurosciences, clinicians are aware mostly of its use to diagnose seizure disorders and in the follow-up care of these patients. Nevertheless, there is a significant

literature of the use of the EEG to evaluate the acute and chronic effects of drug abuse (51).

In our studies, participants are seated in a reclining chair in a sound-attenuated, electronically shielded chamber. A 3-min eyes-closed and 3-min eyes-open recording is obtained. Additional tasks can include photic driving and hyperventilation. The EEG is recorded from the following 16 International 10/20 scalp sites: Fp1, F₃, C₃, P₃, O₁, F₇, T₃, T₅, F_{p2}, F₄, C₄, P₄, O₂, F₈, T₄, and T₆. Additional recording sites can include: F_z, C_z, P_z, and O_z. The EEG recording uses the ear tips as reference. Eye movement is recorded from above and to the side of the left eye. Silver/silver chloride electrodes are used at all locations. The EEG is amplified with Grass (Model 7P511) amplifiers and processed with a 1- to 50-Hz half-amplitude band pass and notch filter at 60 Hz. The EEG is sampled rates from 100 to 200 samples per second per channel. EEG power is then determined for δ (0.4–3.9 Hz), θ (4.0–7.9 Hz), α_1 (8.0–9.9 Hz), α_2 (10.0–13.9 Hz), β_1 (14.0–24.9 Hz), and β_2 (25.0–40.0 Hz) EEG bands using the fast Fourier transform using 256 points per epoch and averaging the spectra over epoches. The logarithm (log) of EEG power is calculated for each EEG band. Relative power (percentage) is also calculated for each band.

EEG records can suffer from artifacts caused by subject or equipment variables. These include pen or amplifier misadjustments, head movements, or eye blinks. Therefore, artifacts in the EEG are removed by computer assisted visual inspection by an operator blind to the test day and subject.

4. Conclusions

The approaches described in the present chapter have formed the bases for our neurological and neuropsychiatric evaluation of patients who use a number of illegal drugs. As with marijuana users, we have documented the cognitive changes that are present in cocaine abusers (8,57,58). We have reported on blood flow velocity observed in cocaine and opiate abusers to determine the effects of these substances cerebrovasculature (53–55). As mentioned above, all these studies were carried out in the same populations of patients who were observed under identical conditions. It is our hope that a more widespread adaptation of these approaches will help to clarify the pathobiological substrates for the neuropsychiatric disturbances observed in a large number of patients who abuse illicit drugs.

5. Notes

1. Subject and experimental considerations in studies of abstinence: Exclusion criteria that applied to all of our subjects include: (1) major medical and psychiatric illnesses; (2) head injuries with loss of consciousness for more than 5 min; (3) evidence of any neurological abnormalities by history or examination; (4) human immunodeficiency virus (HIV) seropositivity; and (5) excessive illicit drug or alco-

hol use other than marijuana use. Demographic information and drug use history information in our lab are obtained from the Addiction Severity Index (ASI) (52). The metric, joints per week, is determined from the subjects self-reported drug history. Since the number of marijuana joints per week varied widely, marijuana abusers are divided into three groups using the procedure described by Bolla and associates (8). In that procedure, a blunt (cigar-size marijuana smoking material) was equal to four joints (small-diameter cigarette-size smoking material). The light marijuana users smoke 2–15 joints per week. The moderate marijuana users smoke 17–70 joints per week. The heavy marijuana users smoke between 78 and 350 joints per week. Subjects with illicit drug use other than marijuana use are screened out.

2. The neurological assessments are made within 72 h of admission to our closed clinical research ward. A second measurement is made after 28–30 d of monitored abstinence. Random urine samples are collected for drug testing. This approach allows us to determine changes that might be consequent to subacute residual effects of the drug or to a withdrawal state as well as determine if drug-related changes are more chronic or permanent. The relationship between the magnitude and duration of these deficits and current drug use can also be determined.
3. Summary of findings: The main findings of our studies of cerebral blood flow of marijuana abusers (53,54) are that, in comparison to control subjects, marijuana abusers have (1) elevated systolic and mean blood flow velocity in the MCA and ACA; (2) higher PI values in both the MCA and ACA; (3) no significant improvements in systolic velocity and PI values during a month of monitored abstinence in marijuana abusers with daily use. The present measurements, obtained during a month of observed abstinence from marijuana abusers, document potentially long-lasting marijuana-mediated changes in vascular hemodynamics.
4. The changes in blood flow velocity observed in our study of marijuana abusers may be due to abuse of substances other than marijuana, since cocaine abusers also show abnormalities in TCD measurements (55). However, the marijuana abusers we recruit for our studies report no substance abuse except for alcohol and nicotine. In fact, prospective subjects who reported other substance abuse or had urine tests positive for other substance were rejected from our marijuana studies. Subjects with excessive use of alcohol are also screened out of our studies.
5. Our studies using EEG and neuropsychological testing also report that prolonged abuse of marijuana results in EEG alterations and poor performance on a number of cognitive tests over a month of monitored abstinence. As joints per week smoked increased, performance decreased on tests measuring memory, executive functioning, psychomotor speed, and manual dexterity. When marijuana users are divided into light, middle, and heavy user groups, the heavy group performed significantly below the light group on 5/35 measures, and the size of the effect ranged from 3.00 to 4.20 standard deviation units. Duration of use had little effect on neurocognitive performance. Heavy use of marijuana is associated with persistent decrements in neurocognitive performance even after 28 d of abstinence (8). It is unclear if these decrements will resolve with continued abstinence or became progressively worse

with continued heavy marijuana use (8). Log EEG θ and α_1 power in recently abstinent marijuana abusers were reduced compared to control subjects, and the reductions persisted over a month of monitored abstinence (56). Thus, this neurological approach has identified persistent impairments in cognitive performance, deficits in blood flow velocity, and alterations in EEG power frequencies in a sample heavy marijuana abusers. Because these various abnormalities were observed within the same group of marijuana users, attempts will be made to relate the observed cerebrovascular abnormalities to neurocognitive deficits in order to test the possibility that cerebrovascular perfusion deficits are the substrates for various degrees of subclinical abnormalities in tests of executive and memory functions.

Acknowledgment

This work was supported by NIDA-NIH, DHSS, USA.

References

1. Webb, E., Ashton, C. H., Kelly, P., and Kamali, F. (1996) Alcohol and drug use in UK university students. *Lancet* **348**, 922–925.
2. Liguori, A., Gatto, C. P., and Robinson, J. H. (1998) Effects of marijuana on equilibrium, psychomotor performance, and simulated driving. *Behav. Pharmacol.* **9**, 599–609.
3. Fletcher, J. M., Page, J. B., Franci, D. J., et al. (1996) Cognitive correlates of long-term cannabis use in Costa Rican men. *Arch. Gen. Psychiatry* **31**, 1051–1057.
4. Pope, H. G. and Yurgelun-Todd, D. (1996) The residual cognitive effects of heavy marijuana use in college students. *JAMA* **275**, 521–527.
5. Pope, H. G., Gruber, A. J., Hudson, J. I., Huestis, M. A., and Yurgelun-Todd, D. (2001) Neuropsychological performance in long-term cannabis users. *Arch. Gen. Psychiatry* **58**, 909–915.
6. Ehrenreich, H., Rinn, T., Kunert, H. J. et al. (1999) Specific attentional dysfunction in adults following early start of cannabis use. *Psychopharmacology* **142**, 295–301.
7. Solowij, N., Stephens, R. S., Roffman, R. A., et al. (2002) Cognitive functioning of long-term heavy cannabis user seeking treatment. *JAMA* **287**, 1123–1131.
8. Bolla, K. I., Brown, K., Eldreth, D., Tate, K., and Cade, J. L. (2002) Dose-related neurocognitive effects of marijuana use. *Neurology* **59**, 1337–1343.
9. Reeves, V. C., Grant, J. D., Robertson, W., Gillespie, H. K., and Hollister, L. E. (1983) Plasma concentrations of delta-9-tetrahydrocannabinol and impaired motor function. *Drug Alcohol Depend.* **11**, 167–175.
10. Tunving, K., Thulin, S. O., Risberg, J., and Warkentin, S. (1986) Regional cerebral blood flow in long-term heavy cannabis use. *Psychiatry Res.* **17**, 15–21.
11. Lundqvist, T., Jonsson, S., and Warkentin, S. (2001) Frontal lobe dysfunction in long-term cannabis users. *Neurotoxicol. Teratol.* **23**, 437–443.
12. Amen, D. G. and Waugh, M. (1998) High resolution brain SPECT imaging of marijuana smokers with AD/AD. *J. Psychoactive Drugs* **30**, 209–214.
13. Block, R. I., O'Leary, D. S., Hichwa, R. D., et al. (2002) Effects of frequent marijuana use on memory-related regional cerebral blood flow. *Pharmacol. Biochem. Behav.* **72**, 237–250.

14. Cooles, P., and Michaud, R. (1987) Stroke after heavy cannabis smoking. *Postgrad. Med. J.* **63**, 511.
15. Zarchariah, S. B. (1991) Stroke after heavy marijuana smoking. *Stroke* **22**, 406–409.
16. Barnes, D., Palace, J., and O'Brien, M. D. (1992) Stroke following marijuana smoking. *Stroke* **23**, 1381.
17. Lawson, T. M., and Rees, A. (1996) Stroke and transient ischemic attacks in association with substance abuse in a young man. *Postgrad. Med. J* **72**, 693–693.
18. MacCarron, M. O., and Thomas, A. M. (1997) Cannabis and alcohol in stroke. *Postgrad. Med. J.* **73**, 448.
19. White, D., Martin, D., Gellar, T., and Pittmann, T., (2000) Stroke associated with marijuana abuse. *Pediatr. Neurosurg.* **32**, 92–94.
20. Marinella, M. A. (2001) Stroke after marijuana smoking in a teenager with factor V Leiden mutation. *South. Med. J.* **72**, 692–693.
21. Mesec, A., Rot, U., and Grad, A. (2001) Cerebrovascular disease associated with marijuana abuse: a case report. *Cerebrovasc Dis.* **11**, 284–285.
22. Alvaro, L., Iriondo, C. I., and Villaverde, F. J. (2002) Sexual headache and stroke in a heavy cannabis smoker. *Headache* **42**, 224–226.
23. Geller, T., Loftis, L., and Brink, D. S. (2004) Cerebellar infarction in adolescent males associated with acute marijuana use. *Pediatrics* **113**, e365–370.
24. Mouzak, A., Agathos, P., Kerezoudi, E., Mantas, A., and Vourdeli-Yiannakoura, E. (2004) Transient ischemic attack in heavy cannabis smokers—how 'safe' is it? *Eur. Neurol.* **44**, 42–44.
25. Wechsler, D. (1981) *Wechsler Adult Intelligence Scale Revised (WAIS-R)*, The Psychological Corporation, New York.
26. Benton, A. L., and Hamsher, K. (1978) *Multilingual Aphasia Examination Manual*, University of Iowa, Iowa City.
27. Miller, E. N., Statz, P., and Visscher, B. V. (1991) Computerized and conventional neuropsychological assessment of HIV-1 infected homosexual men. *Neurology* **41**, 1608–1616.
28. Butterley, W. S., Bender, M. B., Pollack, N., and Kahn, R. L. (1956) Unilateral spacial-agnosia in patient with cortical lesions. *Brain* **78**, 68–99.
29. Reitan, R. M. (1977) *Manual for Administration of Neuropsychological Test Batteries for Adults and Children*, NM Neuropsychology Laboratory, Tucson, AZ.
30. Klove, H. (1963) Clinical neuropsychology, in *The Medical Clinics of North America*, WB Saunders, New York, pp. 1647–1658.
31. Wechsler, D. (1987) *Wechsler Memory Scale—Revised*, Psychological Corporation, San Antonio, TX.
32. Benton, A. L., Hamsher, K., and Varney, N. (1983) *Contributions to Neuropsychological Assessment*, Oxford University Press, New York.
33. Rey, A. (1964) *L'Examen Clinique en Psychologie*, Presses de Universitaires de France, Paris.
34. Talyor, L. B. (1969) Localization of cerebral lesions by psychological testing. *Clin. Neurosurg.* **16**, 269–287.

35. Stroop, Z. B. (1935) Studies of interference in verbal reactions. *J. Exp. Psychol.* **18**, 643–662.
36. Kapur, N., and Butters, N. (1977). An analysis of visuoperceptual deficits in alcohol. *J. Stud. Alcoholism* **38**, 2025–2055.
37. Mesulam, M. M. (1985) *Principles of Behavioral Neurology*, FA Davis, Philadelphia.
38. Johnstone, B., Callahan, D., Kapila, C. J., and Bouman, D. E. (1996) The comparability of the WRAT-R Reading Test and NAART as estimates of premorbid intelligence in neurologically impaired patients. *Arch. Clin. Neuropsychol.* **11**, 513–519.
39. Bolla, K. I., Rothman, R., and Cadet, J. L. (1999) Dose-related neurobehavioral effects of chronic cocaine use. *J. Neuropsychiatry Clin. Neurosci.* **11**, 361–369.
40. Heaton, R. K. (1981) *Wisconsin Card Sorting Test Manual*, Psychological Assessment Resources, Odessa, FL.
41. Arnolds, B. J. and von Reutern, G. M. (1986) Transcranial Doppler sonography: examination technique and normal reference values. *Ultrasound Med. Biol.* **12**, 115–123.
42. Sloan, M. A., Alexandrov, A. V., Tegeler, C. H., et al. (2004) Therapeutics and Technology Assessment Subcommittee of the American Academy of Neurology. Assessment: transcranial Doppler ultrasonography: report of the Therapeutics and Technology Assessment Subcommittee of the American Academy of Neurology. *Neurology* **62**, 1468–1481.
43. Martin, P. J., Evans, D. H., and Naylor, A. (1994) Transcranial color-coded sonography of basal cerebral circulation: reference data from 115 volunteers. *Stroke* **25**, 390–396.
44. Silvestrini, M., Troisi, E., Matteis, M., Cupini, L. M., and Caltagirone, C. (1996) Transcranial Doppler assessment of cerebrovascular reactivity in symptomatic and asymptomatic severe carotid stenosis. *Stroke* **27**, 970–973.
45. Howard, G., Baker, W. H., Chambless, L. E., Howard, V. J., Jones, A. M., and Toole, J. T. (1999) An approach for the use of Doppler ultrasound as a screening tool for hemodynamically significant stenosis. *Stroke* **27**: 1951–1957.
46. Cho, S., Kim, G. W., and Sohn, Y. H. (1997) Blood flow velocity changes in the middle cerebral artery as an index of chronicity of hypertension. *J. Neurol. Sci.* **50**, 77–80.
47. Czosnyka, M., Pickard, J., Whitehouse, H. E., and Richards, H. K. (1996) Relationship between transcranial Doppler-determined pulsatility index and cerebrovascular resistance: an experimental study. *J. Neurosurg.* **84**, 79–84.
48. Reinhard, M., Roth, M., Miller, T., Czosnyka, M., Timmer, J., and Hertz, A. (2003) Cerebral autoregulation in carotid artery occlusive disease assessed from spontaneous blood pressure fluctuations by correlation coefficient index. *Stroke* **34**, 2138–2144.
49. Ursino, M., and Giulioni, M. (2003) Quantitative assessment of cerebral autoregulation from transcranial Doppler pulsatility: a computer simulation study. *Med. Eng. Phys.* **25**, 655–666.

50. Steinmeier, R., Laumer, R., Bondar, I., Priem, R., and Fahlbush, R. (1993) Cerebral hemodynamics in subarachnoid hemorrhage evaluated by transcranial Doppler sonography. Part 2. Pulsatility index: normal reference values and characteristics in subarachnoid hemorrhage. *Neurosurgery* **31**, 10–19.
51. Bauer, L. (1999) Electroencephalographic studies of the effects of substance use and abuse, in *Brain Imaging in Substance Abuse: Research, Clinical, and Forensic Applications* (Kaufman, M. J., ed.), Humana Press, Totowa, NJ.
52. McLellan, A. T., Luborsky, L., Cacciola, J., Griffith, J. McGaham, P., and O'Brien, C. P. (1986) *Guide to the Addiction Severity Index: Background, Administration, and Field Testing Results*, National Institute on Drug Abuse, Treatment Research Reports, Rockville, MD.
53. Herning, R. I., Better, W. E., Tate, K., and Cadet, J. L. (2005) Cerebrovascular perfusion in marijuana users during a month of monitored abstinence. *Neurology*, **44**, 488–493.
54. Herning, R. I., Better, W., Tate, K. Y., and Cadet, J. L. (2001) Marijuana abusers are at risk for stroke: preliminary evidence from cerebrovascular perfusion data. *Ann. NY Acad. Sci.* **939**, 413–415.
55. Herning, R. I., King, D. E., Better, W. E., and Cadet, J. L. (1999) Neurovascular deficits in cocaine abusers. *Neuropsychopharmacology* **21**, 110–118.
56. Herning, R. I., Better, W. E., Tate, K., Umbricht, A., Preston, K. L., and Cadet, J. L. (2003) Methadone treatment induces attenuation of cerebrovascular deficits associated with the prolonged abuse of cocaine and heroin. *Neuropsychopharmacology* **28**, 562–568.
57. Herning, R. I., Better, W., Tate, K. Y., and Cadet, J. L. (2003) EEG deficits in chronic marijuana abusers are during monitored abstinence *Ann. NY Acad. Sci.* **993**, 75–78.
58. Bolla, K. I., Funderburk, F. R., and Cadet, J. L. (2000) Differential effects of cocaine and cocaine alcohol on neurocognitive performance. *Neurology* **54**, 2285–2292.
59. Herning, R. I., Tate, K. Y., Better, W., and Cadet, J. L. (2002) Cerebral blood flow pulsatility deficits in HIV+ poly substance abusers: Differences associated with antiviral medications. *Drug Alcohol Depend.* **65**, 129–135.
60. Robins, L. N., Cottler, L. Bucholz, K., and Compton, W. (1995) *Diagnostic Interview Schedule for DSM-IV*, Washington University Press, St Louis, MO.

Behavioral Methods in Cannabinoid Research

Ester Fride, Alex Perchuk, F. Scott Hall, George R. Uhl,
and Emmanuel S. Onaivi

Summary

In the absence of any specific behavioral assay for cannabinoids or endocannabinoids, a cannabinoid-induced profile in a series of four *in vivo* assays in mice is most commonly used to assess a specific cannabinoid activity at the behavioral level. Thus, when a given compound produces motor depression in an open field, catalepsy on an elevated ring, analgesia on a hot plate, as well as hypothermia, cannabinoid CB₁ receptor activation is assumed, although exceptions are possible. The full cannabinoid profile, however, includes for example ataxia in dogs and discrimination learning in rats. In view of (1) the addictive/reward potential of cannabis and the cannabinoids and (2) the multiple roles of the endocannabinoid physiological control system (EPCS) in behavioral functions, including memory, emotionality, and feeding, a number of behavioral techniques have been used to assess the effects of cannabinoids in these functions. In this chapter we will describe the tetrad of cannabinoid-induced effects as well as a series of behavioral assays used in the behavioral pharmacology of marijuana–cannabinoid research. Since the EPCS plays an important role in the developing organism, methods used in the assessment of physical and behavioral development will also be discussed. The techniques include the tetrad, drug discrimination, self-stimulation and self-administration, conditioned place preference/aversion, the plus-maze, chronic mild stress (CMS), ultrasonic vocalizations, cognitive behaviors, and developmental assessment in mouse (and rat) pups.

Key Words: Behavior; cannabinoids; endocannabinoids; newborn; learning/memory; Δ^9 -THC; appetite; ontogeny; reward.

1. INTRODUCTION

Behavioral testing of cannabinoids and endocannabinoids is performed in order to assess psychoactive drug potential, central side effects, as well as medicinal potential. Medicinal effects include central effects (e.g., appetite stimulation, brain trauma, forgetting of traumatic memories) and peripherally

mediated medicinal potential (including inhibition of peripherally created pain, inflammation, and blood pressure regulation ([1,2](#))). This chapter will concentrate on techniques used to assess central effects of cannabinoids.

No behavioral parameter is specifically influenced by cannabinoids. By comparison, entrance onto the open arms of an “elevated plus-maze” reflects benzodiazepine-mediated antianxiety effects or, at least, the effects of anxiolytic agents across chemical classes ([3](#)). In the absence of a specific behavioral or physiological response for cannabinoids, Martin and colleagues ([4](#)) have developed a multiple in vivo assay for the evaluation of cannabinomimetic effects. These procedures have been shown to be predictive of psychoactive cannabinoid activity and to highly correlate with affinity for centrally located cannabinoid CB receptors ([4–7](#)). The full battery includes a fourfold evaluation in mice (the tetrad), a drug discrimination test and catalepsy test in rats, an evaluation of static ataxia in dogs, and operant suppression in monkeys ([4](#)). However, often only parts of the battery are used, such as the mouse tetrad and the two tests in rats ([4](#)) or the mouse tetrad and the dog ataxia test ([8](#)), or the mouse tetrad and the rat discrimination learning ([6](#)) or the mouse tetrad only ([9–11](#)). Sometimes only two of the components of the mouse tetrad are used, for example, for structure–activity relationship studies ([10](#)). Whether employed in full or in part, the test battery produces a characteristic pharmacological profile for exogenous ([4,6,12](#)) as well as for endogenous cannabinoids (endocannabinoids) ([11](#)).

2. Materials

1. Activity meters.
2. Pertwee ring.
3. Rectal temperature probe.
4. Tailflick apparatus and hotplate.
5. Operant-conditioning apparatus.
6. Drug-discrimination setup.
7. Two-chamber conditioned place preference apparatus.
8. Elevated plus-maze test apparatus.
9. Water maze consisting of circular pool with white platform.
10. Computer-operated radial maze with hoppers.
11. Bat detector.
12. Strobe lights.
13. Cages for mice or rat strains.
14. Drugs: alcohol, cocaine, and cannabinoids, e.g., WIN55,212-2 and capsaicin, imipramine, haloperidol, fluoxetine.
15. Sucrose.
16. Rodent chow.
17. Stereotaxic surgery set up with frame, cannulae, injection units, drill, and surgical materials.

18. Weighing balance.
19. Human volunteers.
20. Marijuana cigarettes and placebo cigarettes.

3. Methods

3.1. The Mouse Tetrad Test

The mouse tetrad consists of four simple evaluations, which may be measured in sequence in the same animal.

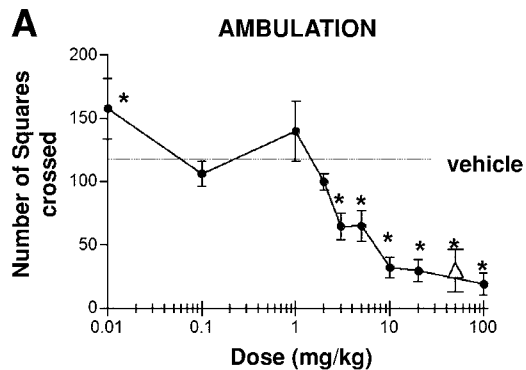
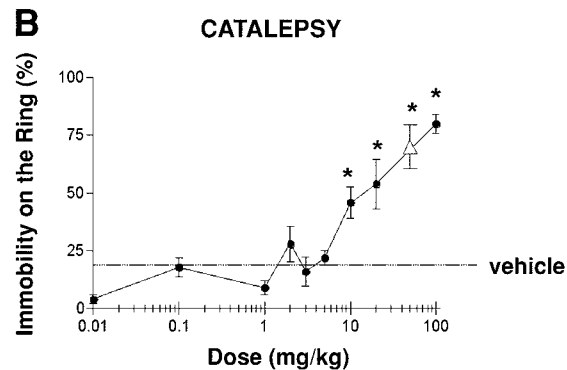
1. Motor activity in an open field is measured for various lengths of time, but typically for 10 min, by digitized or manual observation.
2. The amount of time in which the mouse is immobile after placement on a metal ring of 5.5 cm diameter, fixed at approx 16 cm above a table top, is recorded for 4–5 min. This method was developed by Pertwee (13) and is taken as a measure of catalepsy. Although an automated version of the ring-catalepsy test has been developed (14), this assay is usually performed manually.
3. Rectal temperature is measured by a telethermometer.
4. Analgesic (pain-reducing) effects of cannabinoids are measured by the tailflick (e.g., ref. 12) or hot plate method (e.g., refs. 11 and 15; see also ref. 16). In the tailflick test, radiant heat is focused on the tail, and the latency is measured until the animal flicks its tail away, which is taken as a measure of nociceptive sensitivity (17). In the hot plate test, the mouse is placed on a hot plate with temperature usually fixed at 54–55°C. The latency to responses such as jumping or licking a hindpaw is taken as the nociceptive response (18). The tailflick test is considered a reflex response at the spinal level, while the hot plate tests pain perception at higher (supraspinal) levels (17). In general, both tests are sensitive to cannabinoids (see Note 1, Fig. 1).

3.1.1. Biphasic Effects of Cannabinoids in Tetrad Tests

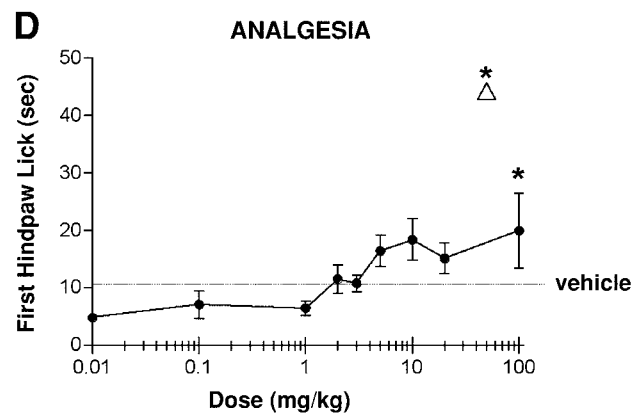
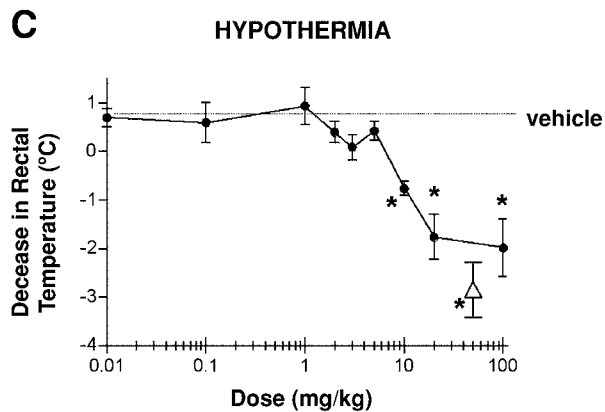
1. Very low doses of anandamide and the synthetic endocannabinoid-like docosahexaenylethanolamide, but not of Δ^9 -tetrahydrocannabinol (THC), inhibited pharmacological effects of conventional doses of Δ^9 -THC (27).
2. Low doses (0.01 mg/kg) of anandamide by itself produced pharmacological effects entirely unlike those found with moderate or high doses (26,32) (see Note 2).

3.2. Drug Discrimination

1. Rodents are trained to discriminate cannabinoids from drugs of other classes, and they will generalize responses to other cannabinoids.
2. In the drug-discrimination paradigm (see ref. 19 and Note 3), laboratory animals learn to recognize the presence of a certain drug (such as nicotine, morphine, LSD, Δ^9 -THC) and express the discrimination between the drug under investigation and a control substance (placebo) in a two-choice situation, where the correct choice is rewarded.

 Δ THC

● anandamide



← Fig. 1. Dose–response curves of anandamide in the mouse tetrad; comparison with Δ^8 -THC. Performance of Sabra mice in the tetrad test for cannabinoid activity. Female Sabra mice were injected ip with anandamide (0.01–100 mg/kg) or with Δ^8 -THC (50 mg/kg) and were tested in the tetrad for cannabinoid-induced effects after 15 or 30 min, respectively. Mice were tested for ambulation (**A**) and rearing (not shown) in an open field; catalepsy on a ring (**B**); rectal temperature (**C**); and analgesia on a hot plate (**D**). $n = 5$ –8. *Significantly different from vehicle control, $p < 0.05$.

3.2.1. Endocannabinoids and Drug Discrimination

1. Anandamide was tested for its ability to substitute for Δ^9 -THC or other cannabinoids in the rat drug-discrimination test.
2. Initially it was reported that anandamide substituted for Δ^9 -THC, but only at high doses (30–45 mg/kg), which also produced severe immobility (35). However, this lack of generalization to anandamide could be ascribed to the facile breakdown of anandamide (36).
3. Dose-dependent generalization to Δ^9 -THC was observed upon administration of the metabolically stable analogs of anandamide, (R)-methanandamide (37,38), or 2-methyl-arachidonyl-2'-fluoroethylamide (39).

3.3. Reward and Reinforcement

3.3.1. Intracranial Self-Stimulation: Self-Delivered Electrical Stimulation of CNS Reward Circuits

1. Electrodes are placed in the reward pathway at the level of the medial forebrain bundle of the animal's (most frequently rat) brain (see Note 4).
2. Thus, when microelectrodes were implanted in the medial forebrain bundle, a low dose of Δ^9 -THC (1.5 mg/kg ip) decreased the electrophysiological threshold for the delivery of intracranial self-stimulation (ICSS) (40,41).
3. The rat is placed in an operant chamber, and after an initial priming current, a current is applied each time the animal performs an operant response such as a lever press or turning of a wheel manipulandum.
4. The response threshold is determined by the midpoint in μ A between the current intensity at which the animal made two or more positive responses to three stimuli (or three out of five) and where the animal made less than the criterion (42).

3.3.2. Self-Administration of Δ^9 -THC

1. Animals are surgically or stereotactically prepared for subsequent intravenous or intracerebral self-administration of cannabinoids and other abused substance (see Note 5).
2. The drug is administered either intravenously into a cannulated vein or directly into the brain through an implanted cannula placed in the lateral ventricle or into a limbic structure such as the nucleus accumbens (43).

3. The catheter is connected to a drug reservoir (usually a syringe).
4. Thus with each operant response (such as a lever press for a rat or a nose poke for a mouse), a bolus of the drug is delivered through the cannula. Usually, a noncontingent priming dose is required to initiate the response.
5. Subsequently, drug intake gradually escalates over a number of test days (43,44).

3.3.3. Conditioned Place Preference/Aversion

1. The cannabinoid agonist or antagonist is administered either ip or sc. Drugs are dissolved in an ethanol:alkamuls–emulphor:saline solution (1:1:18) for the cannabinoids.
2. Prior to the experiment, the animals are habituated to handling.
3. The experimental design consists of four phases: priming, pretesting, conditioning, and testing.
4. Mice receive a priming THC injection 24 h prior to conditioning to avoid the possible dysphoric consequences of the first drug exposure (49).
5. In the pretesting phase, animals are placed in the middle of the chamber with the guillotine door raised approx 12 cm and allowed 10 min to explore both chambers of the conditioned place preference (CPP) apparatus.
6. The conditioning phase consists of two pairings of one of the distinctive compartments with either Δ^9 -THC or SR141716, alternated with two pairings of the other compartment with the vehicle.
7. Animals in each drug group are randomly assigned to compartments and injection orders, both of which are counterbalanced.
8. Each animal is placed in the appropriate compartment immediately after receiving an ip. injection of the drug or vehicle. The guillotine door is closed to confine the animal to the compartment for 30 min.
9. Test sessions are separated by 48 h to allow clearance of the drugs.
10. In the testing phase, no drug or vehicle is injected and the guillotine door is raised 12 cm to allow access to either chamber. The animals are placed in the middle and allowed to move about freely for 20 min. The amount of time spent in each compartment is recorded (see Note 6).

3.4. Anxiety and Stress

3.4.1. Chronic Mild Stress

1. Rats or mice, males or females, are used in this paradigm.
2. For each species there will be a control group and an experimental group. The control groups will be given food and drink at all times, as well as comfortable cage surroundings.
3. The experimental groups will be subjected to different kinds of timed stressors such as tilting and wetting their cages, fasting, and discomforts for 4 wk.
4. These stressors are applied alternately and unpredictably for 4 wk. The CMS animals are housed separately from the controls. Weight changes are monitored throughout the studies in both controls and CMS animals.



Fig 2. Setup of the elevated plus-maze test of anxiety. A computerized setup that automatically monitors the time spent and number of entries into the open, center, and closed arm of the plus-maze.

4. These stressors are applied alternately and unpredictably for 4 wk. The CMS animals are housed separately from the controls. Weight changes are monitored throughout the studies in both controls and CMS animals.
5. Once a week a measure of anhedonia is obtained by monitoring consumption of 2% sucrose for a defined time.
6. After exposure to the CMS procedure, the pharmacological effects of cannabinoid ligands are investigated in this animal model of depression to test the hypothesis that depression may play a role in substance abuse. Other animals of varying genetic background can be subjected to CMS for the determination of novel targets that are involved in depression and cannabinoid action, for example, using the CB₁r and CB₂r and VR₁r mutant mice in the CMS model.

3.4.2. Elevated Plus-Maze Test of Anxiety

1. The mouse is placed in the central platform and allowed to freely explore the maze for 5 min (see **Note 7**).
2. The behavior can be videotaped or scored by one or two observers, or automated versions are computer linked for data acquisition, storage, and retrieval (**Fig. 2**).

3.4.3. Ultrasonic Vocalizations (USVs)

1. After the application of the stress stimulus and/or the drug under study (*see Note 8*), the animal is placed in a small test chamber ($6.5 \times 10 \times 7$ cm high).
2. The bat detector output is digitized and may be recorded by various devices. We have used the Ultravox hardware and software (Noldus, Wageningen, the Netherlands), alternatingly (every 3 min) recording at 25, 30, 60, and 70 kHz, starting before stress, for a duration of 65 min.
3. After experimenting with various types of bedding of the test chamber (sawdust, cotton, rubber, sponge), we now use cotton wool as bedding because it creates the least amount of interference.

3.5. Cognition Tests

3.5.1. Radial-Arm Maze Task

1. Initial training of all rats or mice to search for food at the end of the eight arms for 3 consecutive days until criteria of no more than two errors.
2. Delay training for assessment of information and retention phases.
3. For the information phase, the rat is placed on the central platform with access to all the alleys blocked, but the gates to four randomly selected, baited arms raised. This last until all four alleys are entered or 5 min has elapsed.
4. The retention phase immediately follows the information phase, and the rat is placed on the center and the four previously blocked alleys are baited and all doors raised, until all four alleys are entered or 5 min has elapsed.
5. During the testing phase, the rat is injected with the vehicle first, the selected doses of the cannabinoids after the information phase, and then vehicle once more.

Morris Water-Maze Task

1. Initially, before beginning acquisition training, rats or mice used are given a pre-training session to swim in the circular pool for a fixed time of 5–10 min.
2. Animals are trained in the Morris water-maze task to locate a hidden escape platform in the pool.
3. Each animal is given 8 trials a day in blocks of 4 trials for 4 consecutive days for a total of 32 trials.
4. The time taken to locate the escape platform (escape latency) and the distance traveled are determined. Once the animal locates the platform, it is allowed to stay there for 30 s before removal from the pool.
5. After a set number of acquisition training sessions, animals are subjected to various manipulations, e.g., the platform could be moved to the opposite side of the pool.
6. The amount of time that each animal spent in each quadrant is recorded (quadrant search time).
7. For both reference and working memory tasks, with placement of the platform in different locations, if the animal failed to locate the platform within 120 s it is guided to it.

8. Vehicle and drug tests and combination of drugs, agonist–antagonist combination, or drug interactions is conducted similar to training sessions (see **Note 9**)

3.6. Appetite and Food Intake

3.6.1. Human Studies (see Note 10)

1. In open pilot studies, dronabinol (Δ^9 -THC) treatment caused weight gain in the majority of subjects (58).
2. A relatively low dose of dronabinol, 2.5 mg twice daily, enhanced appetite and stabilized body weight in acquired immunodeficiency syndrome (AIDS) patients suffering from anorexia (59) for at least 7 mo, although in another study, dronabinol was not effective (60).
3. When dronabinol was administered to healthy volunteers, an increase in caloric intake was recorded after twice-daily administrations for 3 d, when rectal suppositories were used, rather than the oral route (62).
4. When the effects of marijuana smoking by healthy volunteers on the intake of various types of food were compared, a selective increase in snack foods was observed (62).

3.6.2. Animal Studies

3.6.2.1. HYPERPHAGIA IN PREFED ANIMALS

1. A comprehensive dose–response study (68) has shown that acute low doses of Δ^9 -THC (0.5–2.0 mg/kg *per/os*) induce hyperphagia for the first 2 h after administration to prefed rats.
2. At the beginning of the dark cycle, individually housed rats were given free access to 30 g of a wet mash diet (200 mL of ground chow plus 250 mL of tap water) for 2 h.
3. After removal of the remaining food including spillage, Δ^9 -THC was administered.
4. Starting 1 h after drug treatment, regular preweighed chow was introduced to the cage and food intake was recorded after 1, 2, 3, 4, 5, and 24 h, taking spillage into account.

3.6.2.2. INCENTIVE VALUE OF FOOD: OBSERVATIONAL ANALYSIS OF CANNABINOID-INDUCED FEEDING

1. Rats are prefed with 30 g of a wet mash diet (200 mL of ground chow plus 250 mL of tap water) for 2 h. This procedure (69) establishes the cannabinoid-induced increase in the incentive value of food.
2. After sc injections of Δ^9 -THC (0.5–2 mg/kg) or anandamide (1–10 mg/kg), the rat is transferred to a transparent open field (30 × 75 × 40 cm), provided with a dish with regular lab chow and water.
3. A number of behaviors, including eating (gnawing, biting, or swallowing), are recorded and scored digitally (using e.g., the Observer, Noldus Information Technology, the Netherlands).

3.6.2.3. FOOD-REINFORCED OPERANT BEHAVIOR

1. The appetitive aspect of food intake is more specifically assessed by operant food-reinforced behavior. De Vry et al. (70) suggest that a short-duration reinforcement schedule (10 min, fixed ratio 1—operant food reinforcement) is especially sensitive to the appetitive process.
2. After initial shaping to press the correct lever for food reinforcement, rats are trained to achieve a stable baseline of operant behavior on the predetermined reinforcement schedule (70).
3. Whether food-restricted rats or those with unlimited access to food, rats can be trained to press the correct lever for dispensing of a food pellet.
4. Using a 30-min fixed ratio 15 (FR 15) reinforcement schedule, both the CB₁ receptor WIN55,212 and the CB₁ receptor antagonist SR141716 dose-dependently suppressed response rate (71) (see Note 11).

3.7. Postnatal Development

3.7.1. Physical Development and Milkbands

1. Pups are separated each day from their mothers only for the duration of injection and/or weighing and scoring of the presence of milkbands. As the stomach area in mouse pups is transparent, due to lack of hair and the thinness of the skin, the amount of milk consumed can be observed as a milkband.
2. The dam is kept in a holding cage in a separate room. Pups are kept at an environmental temperature of 28–30°C. Injections of SR141716 (20 mg/kg, sc in the neck or flank) are performed on a single day only. However, pups are examined daily during the first 2 wk of life.
3. Pups are injected in the neck using 26–27G needles (injection volume: 100 µL/10 g). SR141716 is dissolved in a mixture of ethanol, cremophor EL, and saline (1:1:18, the vehicle), as described previously (11).
4. Experiments in our laboratory have indicated that cannabinoid CB₁ receptors are critically important for survival of newborn mice. Thus, when CB₁ receptors are blocked (with 20 mg/kg SR141716), during the first 24 h of life, the pup does not ingest milk during the next 24 h (77).
5. Timing is critical for this effect since SR141716 injection on the second day only affects 50% of the pups and SR141716 administration on a later day (d 5) has no effect at all (77).
6. The response is dose-dependent (see Note 12; Table 1). Thus a relatively high dose (20 mg/kg) is required to see the full effect, while a half dose produces half the effect and 5 mg/kg has no effect on suckling and growth (77).

3.7.2. Ultrasonic Vocalizations

1. Adult USVs emitted are usually measured at lower frequencies (20–30 kHz) than separation/anxiety call emitted by neonates (50–70 kHz) (43), although USVs emitted by pups have also been measured at frequencies 30 and 50 kHz (3).

Table 1
Milk Ingestion by Newborn Mice: Strain Differences in Response to Inhibition by SR141716 and in CB₁^{-/-} Receptor Knockout Mice

Strain	Mortality rate (%)	Milkbands d 1 (before SR141716)	Milkbands d 2 (24 h after SR141716)
Vehicle C57Bl/6 ^a	100	100	100
<i>SR141716:</i>			
C57Bl/6	80	90	10 ^b
Sabra	80–92	100	0 ^b
ICR	26	100	20 ^b
<i>Without SR141716:</i>			
CB1 ^{-/-}	25	18 ^c	75 ^c

^aVehicle controls were included for C57Bl/6 and Sabra strains too (not shown), with similar results.

^bDifferent from vehicle-treated controls.

^cDifferent from C57BL/6 on the same day.

2. We have found similar results in pups when recording at the lower frequency (25–30 kHz) compared to the higher range (60–70 kHz). Recording at even higher frequencies (80 kHz) yielded unreliable results (Fride et al., unpublished).
3. We either test all pups or randomly select four pups from each litter and place them in a observation cage (6.5 × 10 × 7 cm high), which is prewarmed and maintained at 30°C.
4. A bat detector is positioned above the observation cage and the output is digitized. A variety of devices have been used. We have used the Ultravoxhardware and software (Noldus Information Technology, the Netherlands), recording every 3 min at 25, 30, 60, and 70 kHz. After experimenting with various types of bedding (sawdust, cotton, rubber, and sponge), we now use cotton wool as bedding, since it creates the least amount of interference.
5. Using a four-channel Ultravox, pups can be tested simultaneously, one pup at each frequency (see **Note 13**).

3.7.3. Central Cannabinoid Activity (Motor Behavior, Body Temperature, and Analgesia)

1. Mouse pups from the age of 6 d are exposed every 3 d to an open field (we have used the same size as used for adult mice, i.e., 20 × 30 cm divided into 12 squares of equal size).
2. The number of squares crossed is recorded for 4 min. From d 18 of age, hot plate analgesia is measured immediately after open field exposure as the latency until the first hindpaw lick or jump from the hot plate, which is maintained at 54–55°C. The maximal time allowed on the hot plate is 54 s (84). (See **Note 14** for general discussion.)

3.8. Future Directions

This chapter has described methods for the assessment of cannabinoid-induced behavioral changes. In view of the widespread presence of cannabinoid receptors and their ligands (*see* for example refs. 84a, 84b), it is hardly surprising that the cannabinoids are involved in virtually every mode of behavior. Moreover, it has recently become evident that the endocannabinoids play a pivotal role as the retrograde messengers in glutamatergic and GABA-ergic synapses in a number of brain structures (84b–84d). With new technologies, in this era of the genome, the creation and availability of transgenics and knockout and knockin mice will allow the determination of the mechanisms associated with specific behaviors induced by cannabinoids. As the identity of previously unknown components of the EPCS become available, these behavioral tests and new methods to tease out the contribution of cannabinoid genetics in mediating the behavioral effects of cannabinoids will be needed. Although several decades of irrational prejudice may have hampered basic and clinical research on the therapeutic potential of cannabinoids, new knowledge of the evolutionary conservation of the components of the EPCS and high copy number of cannabinoid receptors in the brain underscores the numerous behaviors induced by cannabinoids. Undoubtedly future research will uncover the role of cannabinoids in diverse pathways associated with apoptosis, neurogenesis, epigenesis, neuroinflammation, and neuroprotection and how these processes affect behavior and how such behaviors can be evaluated. Thus, cannabinoid research has experienced major breakthroughs over the last 25 yr since the discovery of the CB₁ and CB₂ receptors for the plant-derived Δ^9 -THC and their endogenous ligands. No specific behavioral methods have been devised to capture cannabinoid-induced behaviors except for the “tetrad,” which describes a relatively selective “cannabinoid profile.” This is not surprising, however, in view of the ubiquitous presence of CB₁ receptors and their ligands in the central nervous system and the rich interactions between the EPCS system and other neurotransmitter/modulator systems such as the opiates and dopamine. We therefore envision progress in behavioral cannabinoid research as going in tandem with the progress made in neurobehavioral techniques designed to measure the endocannabinoid as interacting with a variety of other neurochemical systems. When the smoke clears, the influence of the EPCS in feeding behaviors for example, may be exploited in the treatment of obesity and other disturbances regulated by endocannabinoid signaling.

4. Notes

1. Compton et al. (6) have shown a high degree of correlation between performance in the mouse tetrad and cannabinoid receptor (CB₁) binding in rat brain membranes. These authors also described a high degree of correlation between CB₁ receptor binding and cannabinoid potencies in the rat drug discrimination test,

which is taken to be predictive of cannabimimetic effects in humans (19). Because they also found a significant correlation between CB₁ receptor binding and psychoactive effect in humans, they suggested that the mouse model might be used to investigate potential abuse potential of cannabinoids (6). The endogenous ligands for the cannabinoid receptors discovered thus far (the endocannabinoids) include the anandamides (20,21), 2-arachidonoyl glycerol (2-AG) (22), noladin (arachidonoyl glyceryl ether) (23), the antagonist/partial agonist virodhamine (24), and *N*-arachidonoyl-dopamine (NADA) (25). Thus far, the prototypical anandamide, arachidonoyl ethanolamide (20), and 2-AG are the most thoroughly studied endocannabinoids. Although the overall pharmacological activity is similar to the psychoactive plant constituent Δ^8 -THC (11,26), there are clear differences between anandamide and plant-derived and synthetic cannabinoids (26–30). Behaviorally, it was clear from the initial description of anandamide's effects in the tetrad that it has partial effects for some of its components (hypothermia and analgesia) (see Fig. 1) (11,26). Moreover, when different routes of anandamide administration were compared, a complex pattern of full and partial activities was observed (29). Furthermore, Δ^9 -THC but not anandamide produced conditioned place avoidance (31). Additional behavioral differences include the effects of very low doses of anandamides (0.0001–0.01 mg/kg).

2. These biphasic effects of anandamide suggest the possibility that the physiological functions of the endocannabinoids may be opposite those depicted by many of the experimental, pharmacological observations performed with high doses of cannabinoids. A speculative explanation was offered as a linkage of the CB₁ receptor to G_s proteins at different levels of CB₁ receptor activation. Thus, when agonist concentrations are high (which is usually the case in pharmacological experiments or after intake of high amounts of cannabis), only G_i protein activation is observable, resulting overall in behavioral depression. In contrast, when agonist concentrations are low, activation of G_s proteins become apparent (27), in an analogous fashion to what has been found for opiate receptors (33). Direct evidence for such G_s linkage to the CB₁ receptor has been demonstrated, at least in neurons from the corpus striatum and in CB₁-transfected cells (34).
3. These observations are compatible with the assessments (see above) that cannabinoids, although they are not associated with one unique type of behavior, produce a characteristic pattern of effects on the central nervous system. Moreover, both discriminative stimulus effects of various cannabinoids and marijuana-intoxication symptoms in humans were found to highly correlate with CB₁ receptor binding. Consequently it was suggested that the rat model of drug discrimination may be used to predict cannabinoid intoxication in humans (19).
4. ICSS was discovered in the 1950s, and a wide variety of ICSS techniques have been developed since then. In 1988 Gardner's group showed that Δ^9 -THC enhances brain stimulation reward in rats (40,41).
5. Although early attempts to induce THC self-administration failed (40), more recent studies, using more potent and specific CB₁ agonists and the CB₁ antagonist SR141716, have unequivocally shown that cannabinoids are readily self-adminis-

tered and that SR141716 will block this behavior in mice (45,46), rats (47) and monkeys (48). The latter study in monkeys was performed using Δ^9 -THC, which makes these data even more pertinent to the human condition.

6. Conditioned place preference is a behavioral model currently used to measure the rewarding or aversive properties induced by the administration of various drugs. The administration of cannabinoid agonists is known to produce variable rewarding and aversive responses in the place-conditioning paradigm, while the endogenous cannabinoid anandamide does not induce any behavioral response. Conditioned place aversion induced by cannabinoid agonists is abolished by the co-administration of SR141716. SR141716 administration can produce some intrinsic motivational responses in this conditioned paradigm. Thus, some specific doses of SR141716 are able to produce conditioned place preference in rats and conditioned place aversion in mice.
7. The plus-maze test was developed in 1984 (50) as a behavioral assay for testing antianxiety effects in benzodiazepine drugs. Indeed, this test has been associated most specifically with this class of drugs. However, it can also be used to assess the level of anxiety influenced by other agents such as antidepressants (3) or to assess levels of anxiety as affected by prenatal stress, (51), isolation rearing (93), or to determine differences in basal levels of anxiety in rat strains (94). Δ^9 -THC (52), HU210 (53), and anandamide (54) all have been shown to cause anxiety-like behavior in the plus-maze, depending on the dose administered. The involvement of the EPCS in anxiety and the response to stress has been documented thoroughly. For example, intracerebroventricular injections of anandamide or Δ^9 -THC activated the hypothalamic–pituitary–adrenal stress axis in rats (55), while the potent cannabinoid receptor agonist HU210 produced a stress-like behavioral response in the defensive withdrawal test, which was accompanied by a rise in plasma corticosterone (56).
8. In rodents USVs are interpreted as distress calls and are therefore used to assess anxiety (57). Benzodiazepines and antidepressants effectively inhibit stress-induced USVs in rodents (57). We have observed in mice that although swim stress increases USVs in normal C57BL/6, the response in CB1^{-/-} knockout mice is blunted (92).
9. The Morris water-maze task with the hidden platform is widely accepted for examining spatial learning and memory, and a number of studies have shown that some phytocannabinoids and cannabinoids can impair memory (89) or enhance memory (89) function in rodent models. Genetic and pharmacological manipulation have been used to evaluate the CB₁ mutant mice in the Morris water maze and the antagonist SR141716 in a delayed radial maze task (90,91).
10. Cannabis is well known to stimulate appetite (61–64). There is evidence that suggests that cannabinoid-induced enhancement of appetite is selective for snack foods (62,65). Thus, in human studies the use of higher doses of cannabinoids as well as different routes of administration, including the rectal (66) or the sublingual (67) route, should be further investigated.
11. Studies in laboratory animals have confirmed observations in humans and unequivocally shown that cannabinoid CB₁ receptors mediate cannabinoid-induced

increase in food ingestion (72), especially of highly palatable foods (73). Thus, both exogenous cannabinoids (Δ^9 -THC) and the endocannabinoid anandamide-induced enhancement of appetite were reversed by the specific CB₁ antagonist SR141716A (68,72). SR141716A injected by itself reduced appetite and body weight. Whether palatability is required for the antagonist's anorectic effect is controversial (71,74,75). In a chronic study in mice, very low doses of anandamide (0.001 mg/kg) were effective in enhancing food intake (76), in accordance with a stimulatory effect of very low doses of anandamide in a series of cannabimimetic assays (32).

12. These findings were replicated in three strains of mice (Table 1). Interestingly, the strain greatly influences the size of the antagonist-induced effect. A large majority of Sabra and C57BL/6 mice perish as a result of SR141716 application on d 1 of life, while more than 75% of ICR pups survive. It is not clear whether the strain differences are related to CB₁ receptor distributions and/or to strain differences in general development. Interestingly, *uninjected* CB₁^{-/-} pups only start milk suckling on d 2–3 (78,87) (Table 1) and display an overall greater mortality and depressed growth curve compared to wild-type C57BL/6 pups (Table 1). The possibility of a compensatory role of a putative “CB₃” receptor has been discussed (78). Taken together, the poor development of CB₁ receptor knockout mice supports a role for differential CB₁ receptor development in explaining the strain differences in the effects of SR141716 on pup suckling and development.
13. Ultrasonic vocalizations in rodent pups are increased after maternal separation, suggesting that the neonates emit USVs to attract retrieval and maternal care. USVs emitted by pups have also been anthropomorphically described as “separation cries,” homologous to those of human infants (79,80). However, more severe stress suppresses USVs (80). Cannabinoid receptors have been linked to stress (55,81) and to USV emission (82). Thus, SR141716 injected into 12-d-old rat pups increased ultrasonic vocalizations without effect on body temperature (82). We have observed that ultrasonic vocalizations in pups treated with SR141716 on the first day of life are inhibited (a preliminary report of these data was presented in ref. 83). Untreated CB₁^{-/-} knockout pups had lower USVs compared to wild-type mouse pups (92). Thus, in agreement with Morgan et al. (80), there seems to be a bimodal USV response to stress: moderate stress increases USV rates, severe stress suppresses the emission of USVs. Perhaps when the organism is faced with a life and death danger, it is more beneficial for survival not to be heard at all.
14. Behavioral effects of cannabinoids are usually assessed in adult rodents. However, in vivo assessment of cannabinoid effects in developing animals is important in order to assess the correlation between CB₁ receptor development with age and their functional (in vivo) expression (84). In addition, in vivo developmental studies help evaluate therapeutic and/or side effects of putative cannabinoid-based (medicinal) drugs in children (85,86). The tetrad developed for assessment of cannabinoid-like activity in adult mice is not suitable for assaying cannabinoid effects in immature rodents. However, several aspects of such function do develop sufficiently that valid assessments of cannabinoid-induced behaviors may be meas-

ured before puberty (86). Thus, although newborn rodents do not rear and cannot balance themselves on an elevated ring, we found that significant locomotion is expressed by d 6 and gradually increases over the next 2 wk, while analgesia on a hot plate is present from d 18. Moreover, using an external thermocouple probe (TES 1307 k/J thermometer, Bioseb, France), axillary temperature can be reliably measured in newborns (87). Thus, we have found that suppression of locomotion and the analgesic response to anandamide and Δ^9 -THC is not present at least until 3 wk of age. Because these parameters are indices of central cannabinoid activity, this finding has important implications for the therapeutic use of cannabinoids in children (85,88).

Acknowledgments

EF acknowledges the National Institute for Psychobiology and the Danone Institute for the advancement of nutrition in Israel, while ESO acknowledges support from William Paterson University and Center for Research and also as a guest scientist at NIDA-NIH. Work from Dr. Uhl's lab is supported by NIDA-NIH.

References

1. Fride, E. and Shohami, E. (2002) The endocannabinoid system: function in survival of the embryo, the newborn and the neuron.. *Neuroreport* **13**, 1833–1841.
2. Mechoulam, R., Hanus, L. and Fride, E. (1998) Towards cannabinoid drugs—revisited. *Prog. Med. Chem.* **35**, 199–243.
3. Treit, D. and Menard, J. (1998) Animal models of anxiety and depression, in *In Vivo Neuromethods* (Boulton, E., Baker, G., and Bateson, A., eds.), Humana Press, Totowa, NJ.
4. Martin, B. R., Compton, D. R., Thomas, B. F., et al. (1991) Behavioral, biochemical, and molecular modeling evaluations of cannabinoid analogs. *Pharmacol. Biochem. Behav.* **40**, 471–478.
5. Abood, M. E. and Martin, B. R. (1992) Neurobiology of marijuana abuse. *Trends Pharmacol. Sci.* **13**, 201–206.
6. Compton, D. R., Rice, K. C., De Costa, B. R., Razdan, R. K., Melvin, L. S., Johnson, M. R., and Martin, B. R. (1993) Cannabinoid structure-activity relationships: correlation of receptor binding and in vivo activities. *J. Pharmacol. Exp. Ther.* **265**, 218–226.
7. Razdan, R. K. (1986) Structure-activity relationships in cannabinoids. *Pharmacol. Rev.* **38**, 75–149.
8. Little, P. J. and Martin, B. R. (1991) The effects of delta 9-tetrahydrocannabinol and other cannabinoids on cAMP accumulation in synaptosomes. *Life Sci.* **48**, 1133–1141.
9. Adams, I. B., Compton, D. R., and Martin, B. R. (1998) Assessment of anandamide interaction with the cannabinoid brain receptor: SR 141716A antagonism studies in mice and autoradiographic analysis of receptor binding in rat brain. *J. Pharmacol. Exp. Ther.* **284**, 1209–1217.

10. Adams, I. B., Ryan, W., Singer, M., Thomas, B. F., Compton, D. R., Razdan, R. K., and Martin, B. R. (1995) Evaluation of cannabinoid receptor binding and in vivo activities for anandamide analogs. *J. Pharmacol. Exp. Ther.* **273**, 1172–1181.
11. Frider, E. and Mechoulam, R. (1993) Pharmacological activity of the cannabinoid receptor agonist, anandamide, a brain constituent. *Eur. J. Pharmacol.* **231**, 313–314.
12. Little, P. J., Compton, D. R., Mechoulam, R., and Martin, B. R. (1989) Stereochemical effects of 11-OH-delta 8-THC-dimethylheptyl in mice and dogs. *Pharmacol. Biochem. Behav.* **32**, 661–666.
13. Pertwee, R. G. (1972) The ring test: a quantitative method for assessing the 'cataleptic' effect of cannabis in mice. *Br J. Pharmacol.* **46**, 753–763.
14. Martin, B. R., Prescott, W. R., and Zhu, M. (1992) Quantitation of rodent catalepsy by a computer-imaging technique. *Pharmacol. Biochem. Behav.* **43**, 381–386.
15. Frider, E. (1995) Anandamides: tolerance and cross-tolerance to delta 9-tetrahydrocannabinol. *Brain Res.* **697**, 83–90.
16. Segal, M. (1986) Cannabinoids and analgesia, in *Cannabinoids as Therapeutic Agents* (Mechoulam, R., ed.), CRC Press, Boca Raton, FL, pp. 106–120.
17. Tjolsen, A. and Hole, K. (1997) Animal models of analgesia., in *The Pharmacology of Pain* (Dickenson, L., and Bessing, J., eds.), Springer, Heidelberg, pp. 1–20.
18. Ankier, S. I. (1974) New hot plate tests to quantify antinociceptive and narcotic antagonist activities. *Eur J Pharmacol* **27**, 1–4.
19. Balster, R. L. and Prescott, W. R. (1992) Delta 9-tetrahydrocannabinol discrimination in rats as a model for cannabis intoxication. *Neurosci. Biobehav. Rev.* **16**, 55–62.
20. Devane, W. A., Hanus, L., Breuer, A., et al. (1992) Isolation and structure of a brain constituent that binds to the cannabinoid receptor. *Science* **258**, 1946–1949.
21. Hanus, L., Gopher, A., Almog, S., and Mechoulam, R. (1993) Two new unsaturated fatty acid ethanolamides in brain that bind to the cannabinoid receptor. *J. Med. Chem.* **36**, 3032–3034.
22. Mechoulam, R., Ben-Shabat, S., Hanus, L., et al. (1995) Identification of an endogenous 2-monoglyceride, present in canine gut, that binds to cannabinoid receptors. *Biochem. Pharmacol.* **50**, 83–90.
23. Hanus, L., Abu-Lafi, S., Frider, E., et al. (2001) 2-Arachidonyl glyceryl ether, an endogenous agonist of the cannabinoid CB₁ receptor. *Proc. Natl. Acad. Sci. USA* **98**, 3662–3665.
24. Porter, A. C., Sauer, J. M., Knierman, M. D., et al. (2002) Characterization of a novel endocannabinoid, virodhamine, with antagonist activity at the CB₁ receptor. *J. Pharmacol. Exp. Ther.* **301**, 1020–1024.
25. Walker, J. M., Krey, J. F., Chu, C. J., and Huang, S. M. (2002) Endocannabinoids and related fatty acid derivatives in pain modulation. *Chem. Phys. Lipids* **121**, 159–172.
26. Mechoulam, R. and Frider, E. (1995) The unpaved road to the endogenous brain cannabinoid ligands, the anandamides, in *Cannabinoid Receptors* (Pertwee, R. G., ed), Academic Press, London, pp. 233–258.

27. Fride, E., Barg, J., Levy, R., Saya, D., Heldman, E., Mechoulam, R., and Vogel, Z. (1995) Low doses of anandamides inhibit pharmacological effects of delta 9-tetrahydrocannabinol. *J. Pharmacol. Exp. Ther.* **272**, 699–707.
28. Mackie, K., Devane, W. A., and Hille, B. (1993) Anandamide, an endogenous cannabinoid, inhibits calcium currents as a partial agonist in N18 neuroblastoma cells. *Mol. Pharmacol.* **44**, 498–503.
29. Smith, P. B., Compton, D. R., Welch, S. P., Razdan, R. K., Mechoulam, R., and Martin, B. R. (1994) The pharmacological activity of anandamide, a putative endogenous cannabinoid, in mice. *J. Pharmacol. Exp. Ther.* **270**, 219–227.
30. Welch, S. P., Dunlow, L. D., Patrick, G. S., and Razdan, R. K. (1995) Characterization of anandamide- and fluoroanandamide-induced antinociception and cross-tolerance to delta 9-THC after intrathecal administration to mice: blockade of delta 9-THC-induced antinociception. *J. Pharmacol. Exp. Ther.* **273**, 1235–1244.
31. Mallet, P. E. and Beninger, R. J. (1998) The cannabinoid CB1 receptor antagonist SR141716A attenuates the memory impairment produced by delta 9-tetrahydrocannabinol or anandamide. *Psychopharmacology (Berl.)* **140**, 11–19.
32. Sulcova, E., Mechoulam, R., and Fride, E. (1998) Biphasic effects of anandamide. *Pharmacol. Biochem. Behav.* **59**, 347–352.
33. Cruciani, R. A., Dvorkin, B., Morris, S. A., Crain, S. M., and Makman, M. H. (1993) Direct coupling of opioid receptors to both stimulatory and inhibitory guanine nucleotide-binding proteins in F-11 neuroblastoma-sensory neuron hybrid cells. *Proc. Natl. Acad. Sci. USA* **90**, 3019–3023.
34. Glass, M. and Felder, C. C. (1997) Concurrent stimulation of cannabinoid CB1 and dopamine D2 receptors augments cAMP accumulation in striatal neurons: evidence for a Gs linkage to the CB1 receptor. *J. Neurosci.* **17**, 5327–5333.
35. Wiley, J. L., Huffman, J. W., Balster, R. L., and Martin, B. R. (1995) Pharmacological specificity of the discriminative stimulus effects of delta 9-tetrahydrocannabinol in rhesus monkeys. *Drug Alcohol Depend.* **40**, 81–86.
36. Di Marzo, V., Melck, D., Bisogno, T., and De Petrocellis, L. (1998) Endocannabinoids: endogenous cannabinoid receptor ligands with neuromodulatory action. *Trends Neurosci.* **21**, 521–528.
37. Burkey, R. T. and Nation, J. R. (1997) (R)-methanandamide, but not anandamide, substitutes for delta 9-THC in a drug-discrimination procedure. *Exp. Clin. Psychopharmacol.* **5**, 195–202.
38. Jarbe, T. U., Lamb, R. J., Makriyannis, A., Lin, S., and Goutopoulos, A. (1998) Delta 9-THC training dose as a determinant for (R)-methanandamide generalization in rats. *Psychopharmacology (Berl.)* **140**, 519–522.
39. Wiley, J. L., Golden, K. M., Ryan, W. J., Balster, R. L., Razdan, R. K., and Martin, B. R. (1997) Evaluation of cannabimimetic discriminative stimulus effects of anandamide and methylated fluoroanandamide in rhesus monkeys. *Pharmacol. Biochem. Behav.* **58**, 1139–1143.
40. Gardner, E. L. (2002) Marijuana addiction and CNS reward-related events, in *The Biology of Marijuana* (Onaivi, E., ed.), Harwood Academic Publishers, Reading, pp. 75–109.

41. Gardner, E. L. and Lowinson, J. H. (1991) Marijuana's interaction with brain reward systems: update 1991. *Pharmacol. Biochem. Behav.* **40**, 571–580.
42. Markou, A. and Koob, G. (1993) Intracranial self-stimulation threshold as a measure of reward, in: *Behavioral Neuroscience: A Practical Approach*, Vol. 2 (Sahgal, A., ed.), IRL Press, Oxford, pp. 93–115.
43. Crawley, J. N., (2000) *What's Wrong with My Mouse? Behavioral Phenotyping of Transgenic and Knockout Mice*, Wiley-Liss, New York.
44. Cain, S., Lintz, R., and Koob, G.F. (1993) Intravenous drug self-administration techniques in animals, in *Behavioral Neuroscience: A Practical Approach*, Vol. 2 ed. A. Sahgal, A., ed.), IRL Press, Oxford, pp. 93–115.
45. Ledent, C., Valverde, O., Cossu, G., Petitet, F., Aubert, J. F., Beslot, F., Bohme, G. A., Imperato, A., Pedrazzini, T., Roques, B. P., Vassart, G., Fratta, W., and Parmentier, M. (1999) Unresponsiveness to cannabinoids and reduced addictive effects of opiates in CB1 receptor knockout mice. *Science* **283**, 401–404.
46. Martellotta, M. C., Cossu, G., Fattore, L., Gessa, G. L., and Fratta, W. (1998) Self-administration of the cannabinoid receptor agonist WIN 55,212-2 in drug-naïve mice. *Neuroscience* **85**, 327–330.
47. Braida, D., Pozzi, M., Parolaro, D., and Sala, M.. (2001) Intracerebral self-administration of the cannabinoid receptor agonist CP 55,940 in the rat: interaction with the opioid system, *Eur. J. Pharmacol.* **413**, 227–234.
48. Tanda, G., Munzar, P., and Goldberg, S. R. (2000) Self-administration behavior is maintained by the psychoactive ingredient of marijuana in squirrel monkeys. *Nat. Neurosci.* **3**, 1073–1074.
49. Valjent, E. and Maldonado, R. (2000). A behavioural model to reveal place preference to 9-tetrahydrocannabinol in mice. *Psychopharmacology* **147**, 436–438.
50. Pellow, S., Chopin, P., File, S. E., and Briley, M. (1985) Validation of open:closed arm entries in an elevated plus-maze as a measure of anxiety in the rat. *J. Neurosci. Methods* **14**, 149–167.
51. Fride, E. and Weinstock, M.. (1988) Prenatal stress increases anxiety related behavior and alters cerebral lateralization of dopamine activity. *Life Sci.* **42**, 1059–1065.
52. Onaivi, E. S., Green, M. R., and Martin, B. R. (1990) Pharmacological characterization of cannabinoids in the elevated plus maze. *J. Pharmacol. Exp. Ther.* **253**, 1002–1009.
53. Giuliani, D., Ferrari, F., and Ottani, A. (2000) The cannabinoid agonist HU 210 modifies rat behavioural responses to novelty and stress. *Pharmacol. Res.* **41**, 47–53.
54. Chakrabarti, A., Ekuta, J. E., and Onaivi, E. S. (1998) Neurobehavioral effects of anandamide and cannabinoid receptor gene expression in mice. *Brain Res. Bull.* **45**, 67–74.
55. Weidenfeld, J., Feldman, S., and Mechoulam, R. (1994) Effect of the brain constituent anandamide, a cannabinoid receptor agonist, on the hypothalamo-pituitary-adrenal axis in the rat. *Neuroendocrinology* **59**, 110–112.
56. Rodriguez de Fonseca, F., Rubio, P., Menzaghi, F., Merlo-Pich, E., Rivier, J., Koob, G. F., and Navarro, M. (1996) Corticotropin-releasing factor (CRF) antagonist [D-

- Phe12,Nle21,38,C alpha MeLeu37]CRF attenuates the acute actions of the highly potent cannabinoid receptor agonist HU-210 on defensive-withdrawal behavior in rats, *J Pharmacol. Exp. Ther.* **276**, 56–64.
57. Sanchez, C. (2003) Stress-induced vocalisation in adult animals. A valid model of anxiety? *Eur. J. Pharmacol.* **463**,133–143.
58. Plasse, T. F., Gorter, R. W., Krasnow, S. H., Lane, M., Shepard, K. V., and Wadleigh, R. G. (1991) Recent clinical experience with dronabinol. *Pharmacol. Biochem. Behav.* **40**, 695–700.
59. Beal, J. E., Olson, R., Lefkowitz, L., Laubenstein, L., Bellman, P., Yangco, B., Morales, J. O., Murphy, R., Powderly, W., Plasse, T. F., Mosdell, K. W., and Shepard, K. V. (1997) Long-term efficacy and safety of dronabinol for acquired immunodeficiency syndrome-associated anorexia. *J. Pain Symptom Manage.* **14**, 7–14.
60. Timpone, J. G., Wright, D. J., Li, N., Egorin, M. J., Enama, M. E., Mayers, J., and Galeto, G. (1997). The safety and pharmacokinetics of single-agent and combination therapy with megestrol acetate and dronabinol for the treatment of HIV wasting syndrome. The DATRI 0004 Study Group. Division of AIDS Treatment Research Initiative. *AIDS Res. Hum. Retrovirus* **13**, 305–315.
61. Mattes, R. D., Engelman, K., Shaw, L. M., and Elsohly, M. A. (1994) Cannabinoids and appetite stimulation. *Pharmacol. Biochem. Behav.* **49**, 187–195.
62. Foltin, R. W., Brady, J. V., and Fischman, M. W. (1986) Behavioral analysis of marijuana effects on food intake in humans. *Pharmacol. Biochem. Behav.* **25**, 577–582.
63. Abel, E. L. (1971) Effects of marihuana on the solution of anagrams, memory and appetite. *Nature* **231**, 260–261.
64. Fride, E. (2002) Endocannabinoids in the central nervous system—an overview. *Prostaglandins Leukot Essent Fatty Acids* **66**, 221–233.
65. Mattes, R. D., Shaw, L. M., and Engelman, K. (1994) Effects of cannabinoids (marijuana) on taste intensity and hedonic ratings and salivary flow of adults. *Chem. Senses* **19**, 125–140.
66. Bennet, W. and Bennet, S. (1999) Marihuana for AIDS wasting: a critique of the data, in *Marihuana and Medicine* (Nahas, G., Sutin, K., Harvey, D., and Agurell, S., eds.), Humana Press, Totowa, NJ, pp. 717–721.
67. Whittle, B., Guy, G., and Robson, P. (2001) Prospects for new cannabis-based prescription drugs. *J. Cannabis Therapeut.* **1**, 183–205.
68. Williams, C. M., Rogers, P. J., and Kirkham, T. C. (1998) Hyperphagia in pre-fed rats following oral delta9-THC. *Physiol. Behav.* **65**, 343–346.
69. Williams, C. M and Kirkham, T. C. (2002) Observational analysis of feeding induced by Delta9-THC and anandamide. *Physiol. Behav.* **76**, 241–250.
70. De Vry, J., Schreiber, R., Eckel, G., and Jentsch, K. R. (2004) Behavioral mechanisms underlying inhibition of food-maintained responding by the cannabinoid receptor antagonist/inverse agonist SR141716A. *Eur. J. Pharmacol.* **483**, 55–63.
71. Freedland, C. S., Poston, J. S. and Porrino, L. J. (2000) Effects of SR141716A, a central cannabinoid receptor antagonist, on food-maintained responding. *Pharmacol. Biochem. Behav.* **67**, 265–270.

72. Williams, C. M. Kirkham, T. C. (2002) Reversal of delta 9-THC hyperphagia by SR141716 and naloxone but not dexfenfluramine. *Pharmacol. Biochem. Behav.* **71**, 333–340.
73. Koch, J. E. and Matthews, S. M.. (2001) Delta9-tetrahydrocannabinol stimulates palatable food intake in Lewis rats: effects of peripheral and central administration. *Nutr. Neurosci.* **4**, 179–187.
74. Arnone, M., Maruani, J., Chaperon, F., Thiebot, M. H., Poncelet, M., Soubrie, P., and Le Fur, G. (1997) Selective inhibition of sucrose and ethanol intake by SR 141716, an antagonist of central cannabinoid (CB1) receptors. *Psychopharmacology (Berl.)* **132**, 104–106.
75. Colombo, G., Agabio, R., Diaz, G., Lobina, C., Reali, R., and Gessa, G.L. (1998) Appetite suppression and weight loss after the cannabinoid antagonist SR 141716. *Life Sci.* **63**, PL113–117.
76. Hao, S., Avraham, Y., Mechoulam, R., and Berry, E. M. (2000) Low dose anandamide affects food intake, cognitive function, neurotransmitter and corticosterone levels in diet-restricted mice. *Eur. J. Pharmacol.* **392**, 147–156.
77. Fride, E., Ginzburg, Y., Breuer, A., Bisogno, T., Di Marzo, V., and Mechoulam, R. (2001) Critical role of the endogenous cannabinoid system in mouse pup suckling and growth. *Eur. J. Pharmacol.* **419**, 207–214.
78. Fride, E., Foxx, A., Rosenberg, E., Faigenboim, M., Cohen, V., Barda, L., Blau, H., and Mechoulam, R. (2003) Milk intake and survival in newborn cannabinoid CB1 receptor knockout mice: evidence for a “CB3” receptor. *Eur. J. Pharmacol.* **461**, 27–34.
79. Hofer, M. A. (1996) On the nature and consequences of early loss. *Psychosom. Med.* **58**, 570–581.
80. Morgan, K. N., Thayer, J. E., and Frye, C. A. (1999) Prenatal stress suppresses rat pup ultrasonic vocalization and myoclonic twitching in response to separation., *Dev. Psychobiol.* **34**, 205–215.
81. Rodriguez de Fonseca, F., Rubio, P., Menzaghi, F., Merlo-Pich, E., Rivier, J., Koob, G. F., and Navarro, M. (1996) Corticotropin-releasing factor (CRF) antagonist [D-Phe12,Nle21,38,C alpha MeLeu37]CRF attenuates the acute actions of the highly potent cannabinoid receptor agonist HU-210 on defensive-withdrawal behavior in rats. *J.Pharmacol. Exp. Ther.* **276**, 56–64.
82. McGregor, I. S., Dastur, F. N., McLellan, R. A., and Brown, R. E. (1996) Cannabinoid modulation of rat pup ultrasonic vocalizations. *Eur. J. Pharmacol.* **313**, 43–49.
83. Fride, E., Ezra, D., Suris, R., Weisblum, R., Blau, H., and Feigin, C. (2003) Role of CB1 receptors in newborn feeding and survival: maintenance of ultrasonic distress calls and body temperature, *Symposium on the Cannabinoids*, International Cannabinoids Research Society, Cornwall, Canada, 37.
84. Fride, E. and Mechoulam, R. (1996b) Ontogenetic development of the response to anandamide and delta 9-tetrahydrocannabinol in mice. *Brain Res. Dev. Brain Res.* **95**, 131–134.

- 84a. Fride E. (2005) Endocannabinoid networks in the central nervous system. In: *The Endocannabinoid System in the Brain: From Biology to Therapy*, ed. Maccarrone M (editor), in press.
- 84b. Howlett A. C., Breivogel C. S., Childers, S. R., Deadwyler S. A., Hampson, R. E., Porrino, L. J. (2004) Cannabinoid physiology and pharmacology: 30 years of progress. *Neuropharmacology* **47 Suppl. 1**, 345–358.
- 84c. Freund T. F., Katona I. Piomelli D. (2003) Role of endogenous cannabinoids in synaptic signaling. *Physiol. Rev.* **83**, 1017–1066.
- 84d. Gerdeman G. L., Lovinger D. M. (2003) Emerging roles for endocannabinoids in long-term synaptic plasticity. *Br. J. Pharmacol.* **140**, 781–789.
85. Fride, E. (2004) The endocannabinoid-CB receptor system: importance during development and in pediatric disease. *Neuroendocrine Lett.* in press.
86. Fride, E. and Mechoulam, R. (1996) Developmental aspects of anandamide: ontogeny of response and prenatal exposure. *Psychoneuroendocrinology* **21**, 157–172.
87. Fride, E., Ezra, D., Suris, R., Weisblum, R., Blau, H., and Feigin, C. (2003) Role of CB1 receptors in newborn feeding and survival: maintenance of ultrasonic distress calls and body temperature, *2003 Symposium on the Cannabinoids*, International Cannabinoids Research Society, Cornwall, Canada, 37.
88. Fride, E., (2004) Developmental aspects of the endocannabinoid receptor system, in *Pharmacology and Physiology of Exogenous and Endogenous Cannabinoids* (Wenger, T. ed.) (Research Signpost).
89. Castellano, C., Rossi-Arnaud, C., Cestari, V., and Costanzi, M. (2003) Cannabinoids and memory: animal studies. *Curr. Drug Target-CNS Neurol. Disord.* **2**, 389–402.
90. Varvel, S. A. and Lichtman, A. H. (2002) Evaluation of CB1 receptor knockout mice in the Morris water maze. *J. Pharmacol. Exp. Ther.* **301**, 915–924.
91. Wolff, M. C. and Leander J. D. (2003) SR141716A, a cannabinoid CB1 receptor antagonist, improves memory in a delayed radial maze task. *Eur. J. Pharmacol.* **477**, 213–217.
92. Fride, E., Suris, R., Weidenfeld, J., and Mechoulam, R (2004) The endocannabinoid system lowers stress response, *2004 Symposium on the Cannabinoids*, ICRS, Paestum, Italy 200.
93. Hall, F. S., Humby, T., Wilkinson, L. S., and Robbins, T. W. (1997) The effects of isolation-rearing on sucrose consumption in rats. *Physiol. Behav.* **62**, 291–297.
94. Hall, F. S., Humby, T., Wilkinson, L. S., and Robbins, T. W. (1997) The effects of isolation-rearing of rats on behavioral responses to food and environmental novelty. *Physiol. Behav.* **62**, 281–290.

Methods to Study the Behavioral Effects and Expression of CB₂ Cannabinoid Receptor and Its Gene Transcripts in the Chronic Mild Stress Model of Depression

Emmanuel S. Onaivi, Hiroki Ishiguro, Patel Sejal, Paul A. Meozzi, Lester Myers, Patricia Tagliaferro, Bruce Hope, Claire M. Leonard, George R. Uhl, Alicia Brusco, and Eileen Gardner

Summary

Behavioral and molecular methods were used to study and determine whether there is a link between depression that may be a factor in drug/alcohol addiction, and the endocannabinoid hypothesis of substance abuse. Depression is a lack of interest in the pleasurable things of life (termed anhedonia) and depressed mood. It is unknown whether CB₂ cannabinoid receptors are expressed in the brain and whether they are involved in depression and substance abuse. Therefore, mice were subjected daily for 4 wk to chronic mild stress (CMS), and anhedonia was measured by the consumption of 2% sucrose solution. Behavioral and rewarding effects of abused substances were determined in the CMS and control animals. The expression of CB₂ receptors and their gene transcripts was compared in the brains of CMS and control animals by Western blotting using CB₂ receptor antibody and reverse transcriptase-polymerase chain reaction (RT-PCR). Furthermore, the expression and immunocytochemical identification of CB₂ cannabinoid receptor in the rat brain were determined. CMS induced gender-specific aversions, which were blocked by WIN55,212-2, a nonspecific CB₁ and CB₂ cannabinoid receptor agonist. Direct CB₂ antisense oligonucleotide microinjection into the mouse brain induced anxiolysis, indicating that CB₂ or CB₂-like receptors are present in the brain and may influence behavior. The major finding from these studies was the expression of CB₂ receptor and its gene transcript in the mouse brain, which was enhanced by CMS. These preliminary results, if confirmed, suggest that the CB₂ receptors are expressed in the mammalian brain and may be involved in depression and substance abuse.

Key Words: Antisense oligonucleotide; chronic mild stress; neuroinflammation; neuro-immunocannabinoid; depression; CB₂ cannabinoid receptor; immunoblots.

1. Introduction

Depression is a mental disorder that is characterized by feelings of hopelessness, uselessness, unhappiness, and anhedonia. Anhedonia is defined as a lack of interest in the pleasurable things of life and can be studied using the chronic mild stress (CMS) model of depression in rodents. In the CMS model, mice were exposed to different mild stressors and decreased consumption of sucrose solution was used as a measure of anhedonia. The previously unknown but ubiquitous endocannabinoid physiological control system (EPCS) exerts a modulatory action in synaptic transmission and in biological systems in the body and brain. The components of the EPCS include CB₁, CB₂ cannabinoid receptor subtypes, endocannabinoids, metabolizing enzymes, and perhaps associated uptake system(s). The CB₁ receptor is known to be abundantly present in the brain and peripheral tissues and has often been called brain-type cannabinoid receptor (1–4). The EPCS is known to play a role in the stress response, development, and substance abuse (5–7). The CB₂ receptor has been found primarily in cells of the immune system and has been generally referred to as the peripheral cannabinoid receptor. Although a number of laboratories have not been able to detect the presence of this so-called peripheral CB₂ cannabinoid receptor in the brain, there has been demonstration of CB₂ expression in the rat microglial cells (8), in cerebral granule cells (9,10), and in mast cells (11), which are all part of the central nervous system (CNS). New reports indicate that CB₂ receptors are expressed by a limited population of microglial cells in normal healthy and in neuritic plaque-associated glia in Alzheimer's disease brain (10–13). We investigated whether the so-called peripheral CB₂ cannabinoid receptors are present in naïve and CMS mouse brain and therefore play a role in depression and substance abuse.

2. Materials

1. Elevated plus-maze test apparatus.
2. Activity meters.
3. Strobe lights.
4. Cages for rodents mice or rat strains.
5. Drugs: alcohol, and cannabinoids, e.g., WIN55,212-2.
6. Sucrose.
7. Rodent chow.
8. Stereotaxic surgery set up with frame, cannulae, injection units, drill, and surgical materials.
9. Weighing balance.
10. CB₂ polyclonal antibodies and peptide.
11. Mice and rat brain tissue.
12. TaqMan real-time PCR system (ABI 7900).
13. PCR and RT-PCR, real-time PCR reagents.

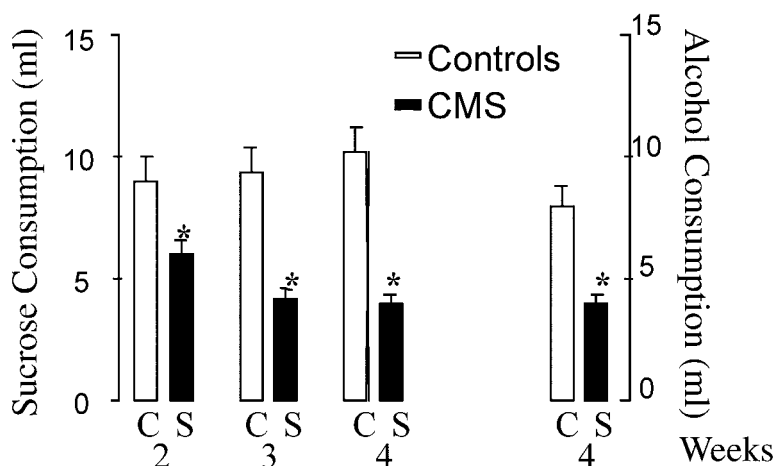


Fig. 1. Animals were subjected to the CMS protocol as described, and their weekly sucrose consumption was used as a measure of anhedonia. On the fourth week the intake of alcohol was also measured. *Sucrose or alcohol intake by CMS animals significantly different from controls; $p < 0.05$.

3. Methods

3.1. The CMS Model of Depression

We have now set up the CMS model to evaluate the presence of CB₂ cannabinoid receptors in the brain and whether or not they play a role in depression. This was achieved as follows:

1. Male and female BALBc mice were exposed to mild stressors every day for 4 wk to simulate the symptoms of anhedonia, a major feature in depression.
2. The experimental animals were subjected to a weekly CMS regime consisting of three 10-h periods of 45° cage tilt; three periods of overnight stroboscopic illumination; two 10-h periods of empty water bottle; two periods of overnight food or water deprivation; two 10-h periods of damp bedding.
3. The control animals were housed in a separate room. Anhedonia and weight changes were measured weekly in both the CMS and control animals.
4. Behavioral and rewarding effects of abused substances were also determined in the CMS and control animals.
5. The effect of depression in reward showed that the data obtained are consistent with anhedonia, a lack of pleasure in sucrose consumption, as demonstrated by the CMS animals.
6. We were surprised that the CMS animals also consumed less alcohol compared to control animals (Fig. 1).

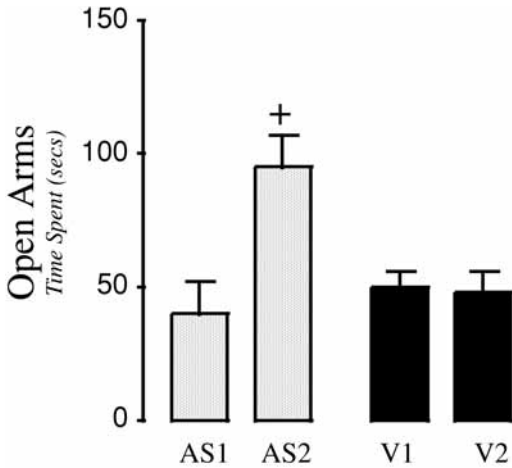


Fig. 2. The intracerebroventricular (ICV) administration of CB₂ antisense oligos, 20 µg twice daily for 3 d, and the performance of mice in time spent in the open arms of the plus-maze is shown compared to controls injected with sense and mismatch oligos (V1 and V2). AS1 and AS2 was time spent in open arms before and after treatment with the antisense oligos. +Significantly different from controls is indicated; $p < 0.5$.

7. The CMS animals demonstrated anhedonia because of their lack of interest in reward, whereas the control animals that were not exposed to CMS consumed more sucrose solution, as shown in [Fig 1](#).

3.2. Elevated Plus-Maze Test of Anxiety

1. The influence of CMS with or without challenge with WIN55,212-2, a nonspecific cannabinoid agonist in male and female mice, was evaluated in the plus-maze test.
2. CMS induced gender-specific aversions, which were blocked by WIN55,212-2, 1.0 mg/kg (data not shown).
3. The intracerebroventricular (ICV) administration of CB₂ antisense oligos, 20 µg, on the performance of mice was assessed before and after 3 d of twice-daily microinjection and compared to mice injected with sense and mismatched oligos ([Fig. 2](#)).
4. Direct CB₂ antisense oligonucleotide microinjection into the mouse brain induced anxiolysis, indicating that CB₂ or CB₂-like receptors may influence behavior ([Fig. 2](#)). The CB₂ antisense oligonucleotide used is 5'-TGTCTCCCGGATCCTC-3', CB₂ sense is 5'-GAGGGATGCCGGGAGACA-3', and CB₂ mismatch is 5'-TCTATCCGGTCTTGCGTC-3'.

3.3. Western Blotting

1. Equal amounts of protein 20 µg obtained from the brains of stressed and control mice were loaded and separated by 10% sodium dodecylsulfate–polyacrylamide gel electrophoresis (SDS-PAGE) and then transferred onto PVD membrane.

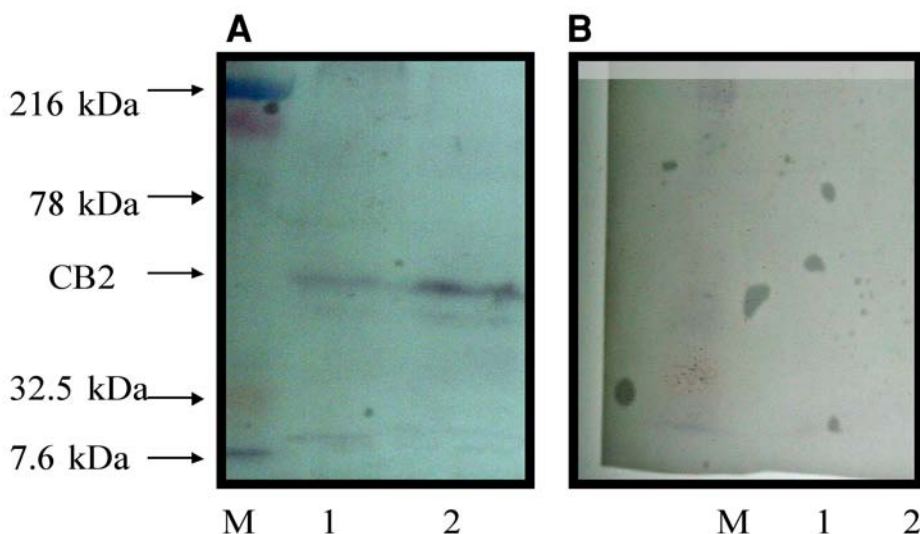


Fig. 3. Western blots of CB₂ cannabinoid receptor immunoreactivities with CB₂ receptor antibody (**A**) and postincubation with CB₂ blocking peptide (**B**) in mouse brain from CMS and control mice. M is the marker, lane 1 is control brain, and lane 2 is CMS brain. No immunoreactivities were detected when primary antibodies were preincubated with the CB₂- blocking peptide.

2. The membrane was washed and blocked in Tris buffered saline containing 5% bovine serum albumin and incubated with the CB₂ antibody overnight. The membranes were washed and incubated with a conjugated goat anti-rabbit secondary antibody and processed for immunoreactivities with and without preincubation of the primary antibodies with CB₂ peptide.
3. The CB₂ antibody used in these studies has been raised against a sequence between the N-terminus and the first transmembrane domain of the protein of the human CB₂ receptor (Cayman Chemicals, MI), which is claimed to be used for Western blotting and immunohistochemical applications as utilized in these studies.
4. There were CB₂ immunoreactivities with enhanced expression in the whole brains of CMS animals in comparison to controls (**Fig. 3A**) and no detectable immunoreactivities postincubation with CB₂ blocking peptide (**Fig. 3B**).

3.4. Mouse CB₂ Gene Expression and Rat CB₂ Brain Immunohistochemistry

1. CMS and control mice in-groups of 5–10 were sacrificed and brains removed immediately to extract RNA. The expression of CB₂ RNA was compared by real-time PCR system (TaqMan, ABI) using the CB₂ cannabinoid receptor gene-specific probe and primers.

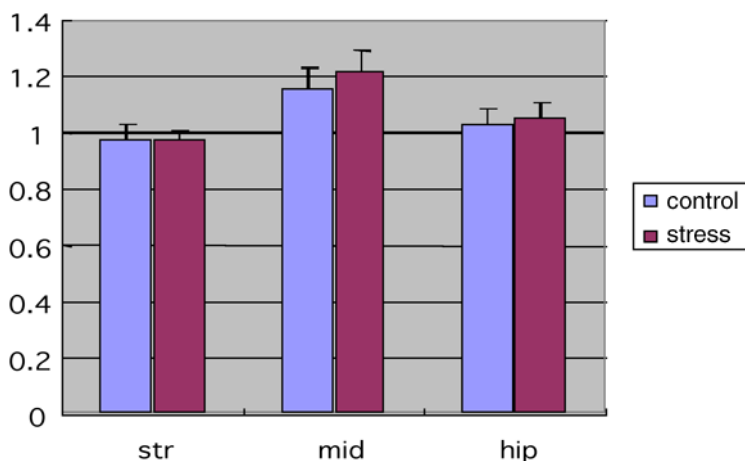


Fig. 4. C57Bl/6 mice were subjected to acute and chronic mild stress and assessed for anhedonia (CMS animals) by weekly sucrose consumption. Mice were sacrificed at the end of wk 4 or following acute stress, and the brains were quickly dissected to extract RNA for CB₂ cannabinoid receptor gene expression by real-time PCR system using the gene-specific probe and primers (TaqMan real-time PCR system, ABI 7900). CB₂ gene expression was detected in the acute and chronic mild stress mice in the striatum (str), midbrain (mid), and the hippocampus (hip).

2. CB₂ cannabinoid gene transcripts are expressed in the striatum (str), midbrain (mid), and hippocampus (hip) in naïve and stressed mice (Fig. 4).
3. For immunohistochemical studies, animals were anesthetized and perfused through the left ventricle with 4% paraformaldehyde dissolved in 0.1 M phosphate buffer (PB) pH 7.4. The brains were removed, post-fixed in the same fixative solution for 2 h, and cryoprotected in 30% sucrose in PB at 4°C overnight, then frozen on dry ice. Serial 30-μm sagittal sections were cut on a cryostat. Standard immunohistochemical protocol, as described previously (10–13), was used. Briefly, sections were prepared, and after incubation overnight with the CB₂ polyclonal antibody, the sections were washed and incubated with biotinylated goat anti-rabbit antibody, followed by avidin–biotin complex. Treating the sections with diaminobenzidine and hydrogen peroxide produced visible reaction. Mounted sections were observed and photographed. Dense CB₂ cannabinoid receptors are abundantly expressed in the rat hippocampus, striatum and cerebral cortex (data not shown).

3.5. Future Directions

The preliminary results obtained and presented here will help us to lay the foundation to continue these exciting studies. The preliminary result indicating that CB₂ or some form of CB₂ cannabinoid receptor subtype may be present in the

mouse brain with an enhanced expression in CMS model of depression may open new areas and approaches in our understanding of depression and addictive disorders, which may be associated with neuroinflammation, since CB₂ cannabinoid receptors have traditionally been known to be present in immune cells.

4. Notes

1. Previous study of the distribution of rat CB₂ receptor mRNA was assessed by Northern blot analysis, and CB₂ gene expression was detected only in the spleen and not in the brain, which led the investigators to conclude that CB₂ receptor was absent in the CNS (14). Our preliminary data using real-time PCR system (TaqMan, ABI) with CB₂ cannabinoid-receptor-gene-specific probe and primers indicated abundant expression of CB₂ mRNA in the striatum, cortex, and hippocampus in naïve and stressed mice.
2. Other previous studies have also demonstrated the presence of CB₂ expression in the rat microglial cells (7), in cerebral granule cells (8,11), and in mast cells (9). Furthermore, new research indicates that CB₂ receptors are expressed by a limited population of microglial cells in normal healthy and in neuritic plaque-associated glia in Alzheimer's disease brain (10–13).
3. We provide evidence for the first time, that one of the cannabinoid receptors (CB₂), activated by smoking marijuana, which was previously thought to be expressed in peripheral immune cells is also expressed in the brain using the mouse CMS model and in rats. We also found that not only is this receptor present in the brain, but that the expression of the receptor is regulated in the CMS model of depression. If this is confirmed in humans, it will revolutionize what we know about depression and how we treat depression, which may be caused in part by neuroinflammation

Acknowledgments

This work was funded in part by a faculty summer research award from the WPUNJ center of research to ESO and WPUNJ-SURP grants to Paul Meozzi, Sejal Patel, and Lester Myers. ESO also acknowledges the guest scientist support by NIDA-NIH. Dr. George Uhl's Molecular Neurobiology Branch is supported by NIDA-NIH.

References

1. Matsuda, L. A., Lolait, S. J., Brownstein, M. J., Young, A. C., and Bonner, T. I. (1990) Structure of a cannabinoid receptor and functional expression of the cloned cDNA. *Nature* **346** (6284), 561–564.
2. Gérard, C., Mollereau, C., Vassart, G., and Parmentier, M. (1990) Nucleotide sequence of a human cannabinoid receptor cDNA. *Nucleic Acids Res.* **18** (23), 7142.
3. Gérard, C. M., Mollereau, C., Vassart, G., and Parmentier, M. (1991) Molecular cloning of a human cannabinoid receptor which is also expressed in testis. *Biochem. J.* **279** (Pt. 1), 129–134.

4. Chakrabarti, A., Ekuta, J. E., and Onaivi, E. S. (1998) Neurobehavioral effects of anandamide and cannabinoid receptor gene expression in mice. *Brain Res. Bull.* **45**, 67–74.
5. Arnone, M., Maruani, J., Chaperon, F., Thiebot, M.H., Poncelet, M., Soubrie, P., and Le Fur, G. (1997) Selective inhibition of sucrose and ethanol intake by SR 141716, an antagonist of central cannabinoid (CB1) receptors. *Psychopharmacology (Berl.)* **132**, 104–106.
6. Frider, E. (2004) The endocannabinoid-CB receptor system: importance for development and in pediatric disease. *Neuro. Endocrinol. Lett.* **25**, 24–30.
7. Frider, E., Suris, R., Weidenfeld, J., and Mechoulam, R. (2004) The endocannabinoid system lowers stress response. *2004 Symposium on the Cannabinoids*, ICRS, Paestum, Italy 200.
8. Kearn, C. S. and Hilliard, C. J. (1997) Rat microglial cell express the peripheral-type cannabinoid receptor (CB2) which is negatively coupled to adenylyl cyclase. *ICRS 1997 Symposium on Cannabinoids*, p. 61.
9. Facci, L., Dal Toso, R., Romanello, S., Buriani, A., Skaper, S. D., and Leona, A. (1995) Mast cells express a peripheral cannabinoid receptor with differential sensitivity to anandamide and palmitoylethanolamide. *PNAS* **92**, 3376–3380.
10. Pazos, M. R., Nunez, E., Benito, C., Tolon, R. M., and Romero, J. (2004). Role of the endocannabinoid system in Alzheimer's disease: new perspectives. *Life Sci.* **75**, 1907–1915.
11. Skaper, S. D., Buriani, A., Dal Toso, R., Petrelli, L., Rimanello, S., Facci, L., and Leon, A. The AliAmide palmitoylethanolamide and cannabinoids, but not anandamide are protective in a delayed postglutamate paradigm of excitotoxic death in cerebellar granule neurons. *PNAS* **93**, 3984–3989.
12. Benito, C., Nunez, E., Tolon, R. M., Carrier, E. J., Rabano, A., Hillard, C. J., and Romero, J. (2003) Cannabinoid CB2 receptors and fatty acid amide hydrolase are selectively overexpressed in neurite plaque-associated glia in Alzheimers's disease brains. *J. Neurosci.* **23**, 11136–11141.
13. Nunez, E., Benito, C., Pazos, M. R., Barbachano, A., Fajardo, O., Gonzalez, S., Tolon, R. M., and Romero, J. (2004) Cannabinoid CB2 receptors are expressed by perivascular microglia cells in the human brain: an immunohistochemical study. *Synapse* **53**, 208–213.
14. Griffin G., Wray, E. J., Tao, Q., McAllister S. D., Rorrer, W. K., Aung, M., Martin, B. R., and Abood, M. E. (1999) Evaluation of the cannabinoid CB2 receptor-selective antagonist, SR144528: further evidence for cannabinoid CB2 receptor absence in the rat central nervous system. *Eur. J. Pharmacol.* **377**, 117–125.

Index

A

2-AG, *see* 2-Arachidonoylglycerol

AM251, synthesis, 136

AM281, synthesis, 135–137

AM708, synthesis, 121

AM1241, synthesis, 134, 135

Aminoalkylindoles, cannabinoid
synthesis, 128–135

Anandamide,

analog synthesis, 138–142

cannabinoid receptor subtype
affinity, 138

COS cell uptake assay, 12, 16

gastrointestinal effects, 174, 180

metabolism, *see* Fatty acid amide
hydrolase

structure–activity relationship
studies, 138

synaptosome transporter,
assay,

materials, 164, 165, 167

synaptosome preparation, 166

uptake assay, 166, 167

brain distribution, 165

overview, 164

Anxiety,

marijuana induction, 245

rodent behavior studies of
cannabinoids,

chronic mild stress, 274, 275

chronic mild stress model, 294

elevated plus-maze test, 275, 282,
294

ultrasonic vocalizations, 276, 282

Appetite,

human studies of marijuana effects,
178–180, 277, 282

rodent behavior studies of

cannabinoids,

food-reinforced operant behavior,
278, 279

hyperphagia in prefed animals,
277

incentive value of food, 277

Arachidonoyl ethanolamide, *see*
Anandamide

2-Arachidonoylglycerol (2-AG),
gastrointestinal effects, 175,
176, 180, 181

2-Arachidonoylglycerol ether,
discovery, 136

Associative processes, marijuana
effects, *see also*

Neuropsychological

assessment, marijuana users,

acute, 218–220, 226, 227, 229, 230

chronic, 218, 220, 230

B

Behavior models, *see* Mouse behavior
models

Boston Naming Task,

neuropsychological assessment
of marijuana users, 257

Brain slice, *see* Hippocampal slice

C

California Computerized Assessment
Package, neuropsychological
assessment of marijuana users,
257

Cannabidiol,

gastrointestinal effects, 176

vas deferens bioassays, 192, 198

- Cannabinoid receptors, *see also* CB₁; CB₂
immunocytochemistry, *see*
Immunocytochemistry,
cannabinoid receptors,
ligands, *see also* specific
compounds,
classification, 114
synthesis,
aminoalkylindoles, 128–135
classical cannabinoids, 114–
125
diarylpyrazoles, 135, 136
endocannabinoids, 136–141
hybrid cannabinoids, 125–128
nonclassical cannabinoids, 125
signaling, 20
transcript localization, *see In situ*
hybridization
Western blot, *see* Western blot,
cannabinoid receptors
- Cannabis, *see* Marijuana
- Cannabis craving, *see* Marijuana
Craving Questionnaire
- CB₁,
agonist-stimulated GTP-binding
assays, *see* GTP-binding assays
brain-region-specific isoform
expression pattern analysis, 12
colocalization with neurotransmitter
receptors, 172
DNA microarray analysis,
expression, 9
single nucleotide polymorphism
genome scanning and
analysis, 5, 7
endocannabinoid binding and
function, 92, 93
gene variation analysis in
polysubstance abusers,
association study, 4
bioinformatics, 3
haplotype determination, 4
human subjects, 3
linkage analysis, 4
opiate regulation of expression, 5
RNA analysis, 4, 5
sequencing and genotyping, 3, 4
statistical analysis, 4
history of study, 20
immunocytochemistry, *see*
Immunocytochemistry,
cannabinoid receptors
promoter analysis, 11, 12
radioligand binding, 153–155, 161
sequence homology studies, 41, 42
tissue distribution, 2, 41, 42
transcript localization, *see In situ*
hybridization
Western blot, *see* Western blot
- CB₂,
expression analysis in chronic mild
stress model,
brain distribution, 296, 297
immunohistochemistry, 296
real-time polymerase chain
reaction, 295–297
Western blot, 294, 295
history of study, 20
immune function studies,
cell culture,
macrophages, 23, 30, 31
proliferation assays, 23, 31
splenocytes, 21, 22, 27, 28
T-cells, 22, 23, 28–30
cytokine assays,
splenocytes, 24, 31–33
T-cells, 24, 25, 34
macrophage phagocytosis assay,
foreign antigens, 25, 34, 35
microscopy, 25, 26, 35, 36
materials, 21–27, 37, 38
mitogen-activated protein kinase
assay,
cell lysis and treatment, 26, 36,
37
enzyme-linked immunosorbent
assay, 26, 27, 37, 38
overview, 20, 21

- immunocytochemistry, *see*
 - Immunocytochemistry, cannabinoid receptors
- knockout mouse studies, 20, 21
- sequence homology studies, 41, 42
- tissue distribution, 2, 41, 42
- Western blot, *see* Western blot
- Chronic mild stress (CMS) model,
 - CB₂ expression analysis,
 - brain distribution, 296, 297
 - immunohistochemistry, 296
 - real-time polymerase chain reaction, 295–297
 - Western blot, 294, 295
 - depression model, 292
 - induction, 293, 294
 - materials, 292
- CMS model, *see* Chronic mild stress model
- Conditioned place preference/aversion,
 - rodent behavior studies of cannabinoids, 274, 282
- Controlled Oral Word Association Test,
 - neuropsychological assessment of marijuana users, 257
- CP-47,497, synthesis, 124, 125
- CP55940
 - gastrointestinal effects, 174, 176, 182
 - vas deferens bioassays, 192, 203
- Craving, *see* Marijuana Craving Questionnaire
- Cytoskeleton, *see*
 - Immunocytochemistry, cannabinoid receptors
- D**
- Dependence, marijuana, 246, 249
- Depression, *see* Chronic mild stress model
- Diarylpyrazoles, cannabinoid synthesis, 135, 136
- Digital image analysis, *see*
 - Immunocytochemistry, cannabinoid receptors
- 3-(1,1-Dimethylheptyl)-12 β -hydroxy-9-nor-9 β -hydroxymethyl) hexahydrocannabinol,
 - synthesis, 127, 138
- Drug discrimination tests, rodent behavior studies of cannabinoids, 271, 273, 281
- E**
- EEG, *see* Electroencephalography
- Electroencephalography (EEG),
 - marijuana studies, 262–265
- Electron microscopy, *see*
 - Immunocytochemistry, cannabinoid receptors
- Electrophysiology, *see* Hippocampal slice; *Xenopus* oocyte, cannabinoid receptor studies
- ELISA, *see* Enzyme-linked immunosorbent assay
- Emesis,
 - cannabinoid inhibition and assays, 170, 180–182
 - neurotransmission, 171
- Endocannabinoids, *see* specific compounds
- Enteric nervous system,
 - anatomy, 170
 - neurotransmission, 171
- Enzyme-linked immunosorbent assay (ELISA), mitogen-activated protein kinase, 26, 27, 36–38
- Episodic memory, *see* Memory
- F**
- FAAH, *see* Fatty acid amide hydrolase
- Fatty acid amide hydrolase (FAAH),
 - anandamide hydrolysis, 163
 - assay,
 - materials, 164, 165, 167
 - overview, 163, 164
 - radiochromatographic assay, 166, 167
 - sample preparation, 165–167
 - brain distribution, 165

G

- Gastric emptying,
 - animal studies, 175, 176
 - cannabinoid inhibition, 170
 - regulation, 171
- Gastric secretion, cannabinoid
 - inhibition studies, 177, 178
- GTP-binding assays,
 - cell membrane homogenates,
 - preparation, 152, 153
 - [35S]GTP γ S binding, 155, 157, 159, 161
 - cultured cells, 159, 160
- G protein cycle, 150
- materials, 151
- overview of cannabinoid receptor-stimulated binding, 149–151

H

- 3-Heptyl-1-ynyl-11-hydroxyhexahydrocannabinol, synthesis, 120, 122, 123
- Hippocampal slice,
 - cannabinoid studies,
 - electrophysiology,
 - extracellular recording, 110
 - intracellular recording, 108–110, 112
 - setup, 107, 108
 - materials, 106, 110
 - overview, 105
 - solution preparation, 107
 - preparation, 106

I

- Immunocytochemistry, cannabinoid receptors,
 - antibodies,
 - CB₁, 42, 43
 - CB₂, 42–44
 - CB₂ expression in chronic mild stress model, 297
 - cytoskeleton component changes after chronic CB₁ agonist treatment,

- digital image analysis,
 - densitometry, 93, 94
 - morphometry, 94, 97
 - overview, 92, 93
 - photomicrography, 97
- fixation of tissues, 96, 99, 101
- immunostaining, 96, 97, 102
- instrumentation, 102, 103
- materials, 95
- neuronal and astroglial proteins, 93
- rat treatment, 95, 96
- statistical analysis, 97, 99
- immunoelectron microscopy,
 - immunogold labeling,
 - labeling, 66
 - resin embedding, 63, 66
 - staining, 66
 - tissue preparation, 63
 - immunoperoxidase staining,
 - fixation, 59
 - secondary antibody incubation and color development, 60–63, 68
 - sectioning, 59, 60, 67
- overview, 46
- light microscopy,
 - cell cultures,
 - intracellular receptor staining, 55, 57, 58
 - surface receptor staining, 58
 - cryosections, 51–53
 - formalin-fixed, paraffin-embedded tissue, 53–55
- materials, 47–51
- resources, 45
- Informed consent, marijuana clinical studies, 211, 240, 247, 248
- In situ* hybridization (ISH),
 - CB₁ transcripts,
 - developing, 86–88
 - double-labeling for transcript colocalization, 71–73, 75
 - hybridization, 82, 83

- materials, 75–79, 87
- probe synthesis with in vitro transcription, 80, 81, 87
- slide dipping in emulsion, 85, 86, 88
- time requirements, 79
- tissue preparation, 81, 82
- visualization of digoxigenin-labeled probe, 84, 85, 87, 88
- washing, 84
- principles, 71, 72, 87
- Intestinal motility,
 - animal studies, 175, 176
 - cannabinoid inhibition, 173, 174
 - peristalsis studies in vitro, 174, 175
- ISH, *see In situ* hybridization
- L,M**
- Linkage analysis, gene variation
 - analysis in polysubstance abusers, 4
- Macrophage,
 - cell culture, 23, 30, 31
 - phagocytosis assay,
 - foreign antigens, 25, 34, 35
 - microscopy, 25, 26, 35, 36
- MAPK, *see* Mitogen-activated protein kinase
- Marijuana,
 - adverse effects,
 - anxiety, 245
 - attention and cognition, 245, 246
 - cardiovascular, 243, 244
 - dependence, 246, 249
 - dry mouth, 244, 245
 - neurological, 244
 - psychomotor performance, 245, 255
 - pulmonary, 244
 - associative process studies, *see* Associative processes
 - CB₁ gene variation analysis in polysubstance abusers, *see* CB₁
 - clinical trial design considerations,
 - administration routes and materials, 236–238, 246, 247
 - cardiovascular measurements, 241, 242
 - discharging of subjects, 241
 - follow-up, 241
 - informed consent, 240, 247, 248
 - neurological measurements, 242
 - psychological measurements,
 - attention and cognition, 243, 248
 - psychomotor performance, 243, 248
 - subjective effects, 242, 243, 248
 - recruiting of subjects, 238, 239, 247
 - screening of subjects, 239, 240, 247
 - memory effects, *see* Memory
 - neuropsychological assessment, *see* Neuropsychological assessment, marijuana users
 - popularity of use, 235
- Marijuana Craving Questionnaire (MCQ),
 - assessment,
 - debriefing, 213
 - induction of craving, 211, 212, 214, 215
 - informed consent, 211
 - measurement of craving, 212, 213
 - physiological recording, 213
 - subject recruitment, 211, 214
 - training, 211, 213, 214
 - treatment settings, 213, 214
 - intensity of craving, 209
 - overview, 210
 - sample, 212
- MCQ, *see* Marijuana Craving Questionnaire
- Memory,
 - episodic memory,
 - definition, 217

- marijuana effects,
 - acute, 221, 223, 224, 226, 231, 232
 - chronic, 224, 226, 232, 233
 - semantic memory,
 - definition, 217
 - marijuana effects,
 - acute, 221, 222, 230–232
 - chronic, 221
 - Mitogen-activated protein kinase (MAPK), enzyme-linked immunosorbent assay, 26, 27, 36–38
 - Morris water-maze task, rodent
 - behavior studies of
 - cannabinoids, 276, 277, 282
 - Mouse behavior models,
 - anxiety,
 - chronic mild stress, 274, 275
 - elevated plus-maze test, 275, 282
 - ultrasonic vocalizations, 276, 282
 - appetite studies,
 - food-reinforced operant behavior, 278, 279
 - hyperphagia in prefed animals, 277
 - incentive value of food, 277
 - cognition tests,
 - Morris water-maze task, 276, 277, 282
 - radial-arm maze task, 276
 - depression, *see* Chronic mild stress model
 - drug discrimination tests, 271, 273, 281
 - materials, 270, 251
 - overview, 269, 270
 - postnatal development studies,
 - central cannabinoid activity, 279, 283, 284
 - milk intake, 278, 283
 - ultrasonic vocalizations, 278, 279, 283
 - prospects, 280
 - reward and reinforcement,
 - conditioned place preference/aversion, 274, 282
 - intracranial self-stimulation, 273, 281
 - self-administration of
 - cannabinoid, 273, 274, 281, 282
 - tetrad tests, 271, 280, 281
 - MPLM, *see* Myenteric plexus-longitudinal muscle preparation
 - Myenteric plexus-longitudinal muscle preparation (MPLM),
 - cannabinoid inhibition studies, 173, 174
- N**
- Nabilone,
 - gastrointestinal effects, 174, 176, 180
 - synthesis, 120, 121, 123, 125
 - Neuropsychological assessment,
 - marijuana users,
 - associative processes and marijuana effects,
 - acute, 218–220, 226, 227, 229
 - chronic, 218, 220, 230
 - block design, 256
 - Boston Naming Task, 257
 - California Computerized Assessment Package, 257
 - clock drawing, 257
 - Controlled Oral Word Association Test, 257
 - digital symbol test, 257, 258
 - finger tapping, 258
 - grooved pegboard, 258
 - immediate logical memory, 258
 - line orientation, 258
 - materials, 256
 - overview, 255, 256
 - Rey Auditory Verbal Learning Task, 258
 - Rey Osterreith Complex Figure Task, 259

Shipley IQ test, 259
Stroop task, 259
symbol digit-paired associate
 learning, 259
Trails A and B task, 259
verbal and nonverbal cancellation
 test, 259, 260
WAIS-R vocabulary, 260
Wisconsin Card Sorting Test, 260
WRAT-Reading Test, 260

P,R

Purine P2X receptor, vas deferens
 bioassays, 199, 201, 202
Radial-arm maze task, rodent behavior
 studies of cannabinoids, 276
Rey Auditory Verbal Learning Task,
 neuropsychological assessment
 of marijuana users, 258
Rey Osterreith Complex Figure Task,
 neuropsychological assessment
 of marijuana users, 259
Rodent behavior models, *see* Mouse
 behavior models

S

Semantic memory, *see* Memory
Serotonin receptors, cannabinoid effects
 on ligand binding, 172
Shipley IQ test, neuropsychological
 assessment of marijuana users,
 259

Splenocyte,

 cell culture, 21, 22, 27, 28
 cytokine assays, 24, 31–33
 proliferation assays, 23, 31
SR144528, synthesis, 135, 136
SR141716A,
 gastrointestinal effects, 175, 176,
 178, 180, 182
 radioligand binding to CB₁, 153–
 155, 161
 synthesis, 135
 vas deferens bioassays, 198

Stroop task, neuropsychological
 assessment of marijuana users,
 259

Synaptosome, *see* Anandamide

T

T-cell,

 cell culture, 22, 23, 28–30
 cytokine assays, 24, 25, 34
 proliferation assays, 23, 31

Tetrad tests, rodent behavior studies of
 cannabinoids, 271, 280, 281

(-)- Δ^8 -Tetrahydrocannabinol,
 11-hydroxy derivatives, 119, 120
 synthesis, 117–119

(-)- Δ^9 -Tetrahydrocannabinol,
 structure, 115
 synthesis, 115–117

THC, *see* (-)- Δ^9 -Tetrahydrocannabinol

Transcranial Doppler sonography,
 marijuana studies, 260–262, 264
 principles, 260

U

Ultrasonic vocalizations, rodent
 behavior studies of
 cannabinoids,

 anxiety, 276, 282
 development, 278, 279, 283

Ultrasonography, *see* Transcranial
 Doppler sonography

V

Vas deferens cannabinoid bioassays,
 dissection, 193, 204
 electrical stimulation,
 cannabinoid agonist
 concentration-response curve
 studies,
 antagonist incubation, 197, 198
 dose cycle, 196, 205
 wash-out inability, 197, 205
 data analysis, 198
 duration of stimulation, 196, 205

- equilibration, 196, 197
- set-up, 194, 204
- tissue contraction monitoring, 195, 204
- electrically unstimulated tissue assays, 199–203
- interpretation difficulty, 203, 204
- materials, 192, 200, 204
- overview, 191, 192
- Vomiting, *see* Emesis
- W,X**
- Western blot, cannabinoid receptors, CB₂ expression in chronic mild stress model, 294, 295
- electrophoresis and blotting, 13, 16
- protein extraction, 12, 13
- WIN55,2212-2,
 - brain slice electrophysiology studies, *see* Hippocampal brain slice
 - gastrointestinal effects, 174, 176, 178, 182
 - synthesis, 129, 132–134
 - vas deferens bioassays, 192, 203
- Wisconsin Card Sorting Test,
 - neuropsychological assessment of marijuana users, 260
- WRAT-Reading Test,
 - neuropsychological assessment of marijuana users, 260
- Xenopus* oocyte, cannabinoid receptor studies,
 - complementary RNA synthesis and microinjection, 14
 - electrophysiology studies, 14

Series Editor: John M. Walker

Marijuana and Cannabinoid Research

Methods and Protocols

Edited by

Emmanuel S. Onaivi, PhD

Department of Biology, William Paterson University, Wayne, NJ

The revolutionary discovery that the human body and brain make their own marijuana-like substances called endocannabinoids has transformed marijuana–cannabinoid research into a mainstream science impacting our understanding of reproduction, development, and cell death. In *Marijuana and Cannabinoid Research: Methods and Protocols*, prominent researchers and clinicians from around the world detail the cutting-edge in vitro and in vivo methods they are using to elucidate the mechanisms associated with cannabinoid function in health and disease. The techniques can be used in studies across the board from genes to behavior. The molecular neurobiological methods are invaluable in analyzing the structure, the polymorphisms, and the molecular expression of the cannabinoid receptors (CBRs), as well as their association with polysubstance abuse. Other chapters describe methods to study the role of CBRs in immune function, the morphometric cytoskeletal components of neuronal and astroglial cells after cannabinoid treatment, and the in vitro and in vivo effects of cannabinoids in animals, including humans. There are also methods for localizing cannabinoid receptors in different systems, visualizing cannabinoid effects using brain slice imaging and electrophysiological approaches, and designing and synthesizing cannabinoids and endocannabinoids. The protocols follow the successful *Methods in Molecular Medicine*™ series format, each offering step-by-step laboratory instructions, an introduction outlining the principles behind the technique, lists of the necessary equipment and reagents, and tips on troubleshooting and avoiding known pitfalls.

Cutting-edge and highly practical, *Marijuana and Cannabinoid Research: Methods and Protocols* will help both basic and clinical investigators unravel the specific mechanisms of the marijuana–cannabinoid actions that are of central importance in biological and therapeutic research today.

Features

- **Cutting-edge techniques for marijuana–cannabinoid research from genes to behavior**
- **Bioassay of cannabinoids using mouse-isolated vas deferens**
- **Design and synthesis of cannabinoids and endocannabinoids**
- **Gene expression studies using rodent and human samples**
- **Versatile techniques that can be applied to studying mental and neurological disorders**
- **Synthesis of novel cannabinoids as targets for CNS disorders**
- **Focus on human genes that encode cannabinoid receptors and contribute to addiction**
- **Step-by-step instructions to ensure successful results**
- **Tricks of the trade and notes on troubleshooting and avoiding known pitfalls**

Methods in Molecular Medicine™ • 123

ISSN 1543-1894

Marijuana and Cannabinoid Research: Methods and Protocols

ISBN: 1-58829-350-5 E-ISBN: 1-59259-999-0

humanapress.com

ISBN 1-58829-350-5



9 0000